A

THESIS

entitled

GEOCHEMICAL PROSPECTING TECHNIQUES
FOR PRIMARY NICKEL ORE
IN CENTRAL AFRICA

SUBMITTED FOR THE

DEGREE OF

DOCTOR OF PHILOSOPHY

IN THE

FACULTY OF SCIENCE OF THE UNIVERSITY OF LONDON

BY

MARTIN HALE

ROYAL SCHOOL OF MINES

IMPERIAL COLLEGE OF SCIENCE AND TECHNOLOGY

LONDON SW7 2BP

JANUARY 1978

ABSTRACT

Research into geochemical prospecting for sulphide nickel ore has been undertaken by studying eight mafic and ultra-mafic intrusives in Zambia and Rhodesia. Two intrusives have economic or sub-economic mineralization, while the remainder are considered non-mineralized, following their detailed commercial exploration.

Analysis of random diamond drillhole core samples of visibly non-mineralized intrusive rocks for S, by combustion, and for metals in sulphide minerals, using a bromine attack, yields multi-variate data which discriminates between mineralized and non-mineralized intrusives. Applying the same techniques to random outcrop samples produces poorer discrimination because of the the varying degree of weathering in different field areas, but S values rank the two mineralized intrusives third and fourth among those seven intrusives examined in this way.

In soils, underlying mineralization is indicated by Ni values in excess of 5000 ppm, accompanied by lower Cr, high Cu and S concentrations and moderate F enrichment. Nickel anomalies derived from nickel-rich silicates at depth are accompanied by high Cr and possibly Mg, and, in the C horizon in particular, low F. Simultaneous multi-variate evaluation of these elements using their summed standard normal deviates (Zsums) gives a simple quantitative anomaly assessment, which is a convenient prospecting tool.

In the sediments of streams draining intrusives, high Cu concentrations are the most characteristic feature of mineral-ization, but in regional drainage reconnaissance the Ni, Cu, Fe, Mg and Co dispersion patterns are relevant to distinguishing mineralized intrusives from non-mineralized intrusives and other non-significant Ni anomalies, and a Zsum screening procedure efficiently performs optimum prospecting target selection.

Analysis of leaf samples of Diplorynchus condylocarpon and Combretum ghasalense show that these trees take up most metals in a controlled manner, but they may accumulate unusually high

concentrations of Ni where the soil Ni content exceeds the threshold level at which the exclusion mechanism in the roots breaks down. The source of Ni in the soil, whether sulphide mineralization or nickel-rich silicates, does not influence Ni uptake, and hence a biogeochemical Ni anomaly does not necessarily reflect mineralization.

The determination of sulphur dioxide in soil gas shows little promise as a nickel exploration method.

On the basis of the research, recommendations for improved nickel prospecting include the multi-element analysis of reconnaissance stream sediment samples; early elimination of mafic and ultramafic intrusives with a low S content; and the interpretation of Ni soil anomalies using multi-element data.

A number of potentially profitable avenues for further geochemical prospecting research are identified, such as the analytical speciation of S in soils, the biogeochemistry of S and the application of sulphur gases in soils to mineral exploration.

TABLE OF CONTENTS

LIST OF FIGURES

+ Denotes figure follows the page given.

+ Denotes figure follows the page given

+ Denotes figure follows the page given.

LIST OF TABLES

+ Denotes table follows the page given.

ACKNOWLEDGEMENTS

1. INTRODUCTION

1.1. Aims of the research project

The research was undertaken with the objective of optimizing geochemical prospecting for primary nickel ore in Central Africa and other regions of comparable climate. The principal problems in geochemical prospecting for nickel sulphides are the masking of Ni anomalies related to mineralization, and the existence of Ni anomalies not indicative of mineralization.

Nickel sulphides are usually clearly associated with mafic or ultramafic intrusive rocks which are themselves comprised of silicate minerals comparatively enriched in nickel. At the regional level of prospecting, such as drainage reconnaissance, the intrusive body almost invariably furnishes a substantial Ni anomaly which can camouflage any Ni dispersion from associated mineralization.

Detailed geochemical surveys of intrusive bodies, usually by soil sampling, reveal Ni anomalies within the area of outcrop of the intrusive, but these may be derived from either zones of nickel sulphides, lenses of nickel-rich silicate rock (such as a dunite lens within a gabbro body), or localized secondary enrichment of nickel in the B soil horizon.

The aims of the research are to attempt to resolve these nickel prospecting problems by establishing geochemical parameters diagnostic for a Ni anomaly derived from sulphide mineralization. To this end the distribution of both nickel and associated elements in several sampling media, including rock, soil, vegetation, and stream sediments is examined. Selective analysis for that mineral phase most closely related to, and indicative of, mineralization is only adopted when the proposed method is sufficiently rapid and convenient to constitute a viable commercial approach. Since a comprehensive study of all variables is impracticable, the course of research was guided by previous research in the same fields, the availability of sample material, and the initial promise of proposed analytical techniques when tested on samples.

The final objective is to formulate the results of the research into an overall scheme for geochemical prospecting for primary nickel ores in tropical climates.

1.2   Previous research

Research theses on nickel geochemistry with particular reference to primary nickel ore prospecting have been written on two previous occasions (Coope, 1958; Wilding,1965).

Coope (1958) studied the nickel geochemistry of mafic-ultramafic intrusives in Botswana and Tanzania and noted that secondary dispersion of nickel is mainly mechanical, but chemical dispersion may be significant below pH 6.5. Chemical dispersion may be enhanced where the parent rocks are easily oxidized, as in shear zones. However, soluble nickel is fixed by co-precipitation with manganese and iron colloids, by decaying organic matter, and by colloidal silica to form garnierite. Nickel sulphide mineralization is always indicated by a Ni soil anomaly which is normally weak, but Ni values increase with depth in the soil profile. In both soils and stream sediments the presence of mineralization is characterized by coincident Ni and Cu anomalies. This is ascribed to the primary dispersion of the metals in that copper, by its chalcophile nature, concentrates in the sulphide phase whenever this separates from a mafic-ultramafic melt.

Wilding (1965) undertook research into the secondary dispersion of nickel using field areas in Rhodesia and Zambia. His findings affirm and supplement those of Coope (1958). Wilding noted that sulphide minerals weather more rapidly than silicates owing to the lower pH created in their weathering environment. Once nickel passes into solution and undergoes chemical dispersion, metal derived from sulphides behaves in the same way as that derived from silicates, and the origin of chemically dispersed nickel cannot be distinguished. In the C soil horizon exposed in pits, anomalous concentrations of exchangeable Ni adsorbed in the clay fraction can be indicative of sulphide mineralization, but physico-chemical factors, in particular pH, must be taken into account. This feature of exchangeable Ni enrichment does not persist into the higher soil horizons and cannot be applied

in soil surveys. There are good As and less consistent Sb
anomalies accompanying Ni anomalies in the C soil horizon
overlying mineralization, and significant Hg anomalies
traceable into the upper soil. In general, Ni mobility
increases as pH decreases, and hydrolysis occurs at about pH 6.7.
However, nickel is sorbed by organic matter, especially in
dambos and vleis, in environments as acid as pH 5.2. In stream
waters iron and manganese hydroxides co-precipitate nickel;
clear waters from field area streams were found to contain a
maximum of 10 ppb Ni,whereas turbid waters with suspended
colloids contained up to 200 ppb. Copper anomalies are always
found with Ni anomalies related to mineralization in weathered
rock, soils and stream sediments. Biogeochemical sampling of
several genera and species of trees showed that leaves are
the most nickel-rich tissues and exhibit strong Ni anomalies
over mineralization. In some areas of high soil nickel content
there are negative geobotanical anomalies of scant or stunted tree
growth, because excessive nickel is toxic to plants. Another
study in Rhodesia (Cole, 1971) further demonstrated the validity
of biogeochemical sampling and analysis for identifying locations
of primary nickel ore.

Other researchers have selectively determined the
Ni, Cu, Co and S content of sulphide minerals in non-mineralized
specimens of mafic and ultramafic rocks from Canadian intrusives,
and shown that discriminant analysis of the data is useful in
identifying those intrusives with economic or sub-economic nickel
sulphide concentrations (Cameron, Siddeley and Durham, 1971). The
S:Ni ratios of serpentinite core specimens have been used as a
means of identifying serpentinite units (Hausen,
Ahlrichs and Odekirk,1973). The multi-element characteristics,
or signatures, of ferruginous outcrops in Australia have been
shown to distinguish nickel sulphide gossans from other ironstones
(Clema and Stevens-Hoare, 1973). Also in Australia at the Kambalda
nickel deposits, the distribution of nickel and copper in the -180 μm
fraction of soils is found to be controlled by a strong association
with secondary iron oxides, with enrichment of nickel in the coarse
fraction of soils overlying mineralization (Mazzucchelli, 1972).

1.3.   The primary and secondary distribution of nickel

The average content of 8.49% Ni in meteorites
indicates a cosmic abundance of 270 parts Ni per 10,000 parts
Si. The bulk composition of the Earth includes 2.39% Ni, mainly
concentrated in the iron-nickel core. The igneous rocks of the
crust contain an average of only 78 ppm Ni, and this is mainly
found in mafic and ultramafic rocks which contain typically 150
to 2000 ppm Ni   (Ginzburg, 1960; Mason, 1966).

The magma from which mafic and ultramafic igneous
rocks crystallize is derived from molten rock in the lower crust
forced upward during periods of deep-seated crustal movement. As
the magma cools, minerals crystallize in descending order of their
melting points. When sulphur is present in the melt, sulphides
separate as an immiscible liquid, and begin to crystallize at a
comparatively late stage in cooling, probably about $600^{\circ}C$. At
this temperature silicate minerals are already crystalline. The
sulphide minerals therefore often occur as disseminations scattered
throughout the silicate matrix of the rock. However, sulphides may
be closely associated with water and other volatiles which remain
liquid to a late stage of magmatic crystallization. As the
crystalline silicate mass cools it may fracture, typically along
contacts, and the volatile fluids and sulphides migrate down the
pressure gradient into these fractures, so forming concentrations
of massive sulphides.

Where the entire cooling process takes place below
the crustal surface, plutonic mafic and ultramafic rocks are formed.
If crystallization occurs in a relatively undisturbed environment,
the plutonic rocks form a layered intrusion, characterized by
rhythmic mineral layering and cryptic chemical layering. If the
crystallizing melt is disturbed by orogenic deformation, possibly
accompanied by syntectonic intrusions of fresh magma, layering may
be poor or absent and the plutonic rocks are semi-homogeneous.
Clearly the layered intrusive is pre-disposed to the evolution of
disseminated sulphides whereas deformation is condusive to fracturing
and sulphide concentration. A third type of plutonic ultramafic
rock, the alpine-type intrusive, is recognised as characteristic of

a semi-crystalline, olivine-rich, magma mush intruded into water-bearing geosynclinal sediments of orogenic belts, producing a comparatively low-temperature intrusive rock with extensive incipicient hydration of olivine to serpentine. The alpine-type intrusive may bear disseminated or massive sulphides in the same way as other mafic and ultramafic rocks (Bowen, 1956; Turner and Verhoogen, 1960).

Where a semi-molten mafic-ultramafic magma is forced out of the chamber onto the crustal surface, extrusive rocks of the komatiitic series are formed. These cool rapidly without layering, but may contain disseminated sulphides and even massive sulphide concentrations along the basal contact (Naldrett and Arndt, 1975).

The silicate minerals formed in the cooling magma possess mainly ionic bonding, while the sulphides have more covalent character. Nickel has a divalent ionic radius of $0.78\overset{o}{A}$, the same as that for magnesium, and nickel substitutes for magnesium in the lattice of silicate minerals, particularly olivines, $(Mg,Fe,Ni)_2SiO_4$, and also pyroxenes and amphiboles. Nickel is not chalcophile and rarely forms its own sulphides such as millerite, NiS. However, it exhibits siderophile character, and with an atomic radius of $1.24\overset{o}{A}$ in a state of twelve-coordination, similar to that of Fe at $1.27\overset{o}{A}$, readily enters into the structure of iron sulphides such as pyrrhotite $(Fe, Ni)_7S_8$, pentlandite $(Fe,Ni)_9S_8$, and violarite, Ni_2FeS_4 (Ginzburg, 1960; Goldschmidt, 1954).

Many mafic and ultramafic intrusives are partially serpentinized. Serpentinization occurs at a late stage of crystallization, at temperatures of less than $500^{o}C$, and involves the hydration of olivine to serpentine. The water for this process can be magmatic water related to the intrusive, or extraneously introduced (unrelated) magmatic water, or can be water contained in sediments into which the intrusive was emplaced. The equation illustrating this process is as follows:-

$$5(Mg,Ni)_2SiO_4 + 4H_2O \rightarrow 2H_4(Mg,Ni)_3Si_2O_9 + 4MgO + SiO_2$$
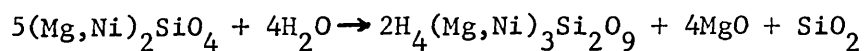
Since some magnesia and silica are removed in solution, but no nickel is lost, serpentinization results in a slight nickel enrichment in serpentine compared with olivine (Turner and Verhoogen, 1960).

When mafic and ultramafic rocks are exposed to the atomsphere, mechanical and chemical weathering break down the outcropping rocks and, in all but the most arid climites, living organisms occupy the degraded material and assist in forming soil. Chemical weathering of mechanically fragmented rock is promoted by the mild acidity of soil water due to dissolved atmospheric carbon dioxide and the organic acids produced by decaying vegetation and micro-organisms. As mineral grains are attacked, their constituents pass into solution as ions and colloids. In general, chemical attack is greatest at the surface, where fresh rainwater charged with carbon dioxide is received and where plant, animal and bacterial life is most abundant. As rainwater percolates downwards it becomes saturated with the soluble products of mineral breakdown and the rate of further mineral dissolution decreases, while the contribution made by living organisms becomes less as their numbers decrease with depth. Of the primary silicate minerals in mafic and ultramafic rocks, olivine breaks down most easily, because iron and magnesium which bond silica tetrahedra in the mineral are readily soluble and their loss causes the ready release of individual tetrahedral units, thereby exposing fresh surfaces to attack. However, silica does not pass into solution so readily, and residual silica may polymerize into sheets, fixing some magnesium (and nickel) to form serpentine. Pyroxenes and amphiboles are more resistant chain silicates bonded mainly by iron, magnesium and aluminium. The bonding cations are dissolved when water penetrates the cleavages, and the released silica chains tend to polymerize into sheets, and, with residual alumina and magnesia, form chlorite and montmorillonite (Loughnan, 1969). Most soluble products of weathering are leached downward out of the upper soil, or A horizon. Some marginally soluble elements and colloids tend to precipitate further down the profile, and absorb and adsorb other soluble elements to form a zone of

accumulation, or B horizon. Beneath this is a C horizon of less intensively weathered rock, merging below the water table with unweathered rock.

Where sulphide minerals in the rock are dissolved, the sulphate ions passing into solution further increase acidity and accelerate the breakdown of minerals. The weathering of massive sulphides and rich disseminations creates a highly acidic environment which promotes leaching of trace elements in solution, while iron hydroxides and sometimes silica precipitate to form a predominantly ferruginous gossan. The gossan is usually characterized by a cellular boxwork or sponge texture, but this can be masked by excessive silicification and formation of a cherty gossan (McKinstry, 1948).

Nickel is highly mobile in acid solution of less than pH 6.5 and is generally readily leached from both silicate and sulphide minerals of mafic and ultramafic rocks. Nickel removed from the A soil horizon is to some extent co-precipitated with iron hydroxides in the B horizon. Nickel in solution may also combine with colloidal silica to precipitate as hydrated nickel silicates, collectively known as garnierite, $(Mg,Ni)SiO_3.nH_2O$. Over ultramafic rocks in particular, substantial secondary enrichment of nickel can occur by these mechanisms, forming a nickeliferous laterite. However, in the highly acid environment created by oxidizing sulphide mineralization, nickel is commonly intensively leached, and if a gossan is formed it is not necessarily nickel-rich.

1.4. Economic geology of nickel

The world annual consumption of nickel is presently about 700,000 tonnes, and this is used mainly in stainless and other steels, copper–nickel alloys and electroplating. The nickel is obtained from two types of ore both closely associated with mafic and ultramafic rocks: pyrrhotite-pentlandite sulphide deposits, mined in Australia, Botswana, Canada, Finland, Rhodesia, South Africa, the U.S.A. and the U.S.S.R.; and lateritic nickel oxide ores exploited in Albania, Cuba, Greece, Guatemala, New Caledonia, the Philippines, the U.S.A. and the U.S.S.R. Canadian production provides 37% of world requirements, the USSR 19%, New Caledonia 18%, Cuba 6%, Australia 5%

and other countries less than 2% each. The grade of mineralization found to be economic is usually about 1.5% Ni or better.

The sulphide ores are mainly massive sulphide concentrations along the contacts, joints and fissures of mafic and ultramafic intrusives (and occasionally extrusives) and their adjacent country rocks. Their evolution depends solely on geological processes, and there is no geographical constraint on their distribution. The lateritic desposits are developed over serpentinites with no evidence of sulphide mineralization. The richest nickeliferous laterite ores are found in very hot and wet tropical climates, and are therefore never far from sea level and ocean water-masses. Chemical weathering and laterite formation are strongly favoured in such climates. In addition a relatively flat land surface minimizes mechanical erosion of the laterite, and gradual uplift of the land surface promotes continued lateritization. The ideal climate and physiography for nickeliferous laterite formation is found in New Caledonia, the Philippines and Cuba, with a mean annual temperatures of about $25^{o}C$, annual rainfall over 3500 mm and alternating wet and dry seasons.

1.4.1.   The search for nickel in Central Africa

In the period 1969-1970 nickel shortages and high prices encouraged nickel prospecting in many parts of the world, notably in Australia. The known existence of nickel sulphide ores in Botswana, South Africa and Rhodesia also stimulated increased nickel prospecting throughout Central Africa.

In Central Africa the high mobility of nickel in the secondary environment commends geochemical prospecting in the search for nickel deposits. However mineralization is invariably associated with mafic and ultramafic rocks which themselves furnish an elevated and variable Ni background. On a regional scale this constitutes a non-significant Ni anomaly which may camouflage a significant anomaly. The detailed soil geochemical investigations may be confused by non-significant Ni anomalies derived from lenses or bands of nickel-rich primary silicates in parts of the mafic-ultramafic body. Finally secondary enrichment of Ni in lateritic soil horizons, unlikely to be
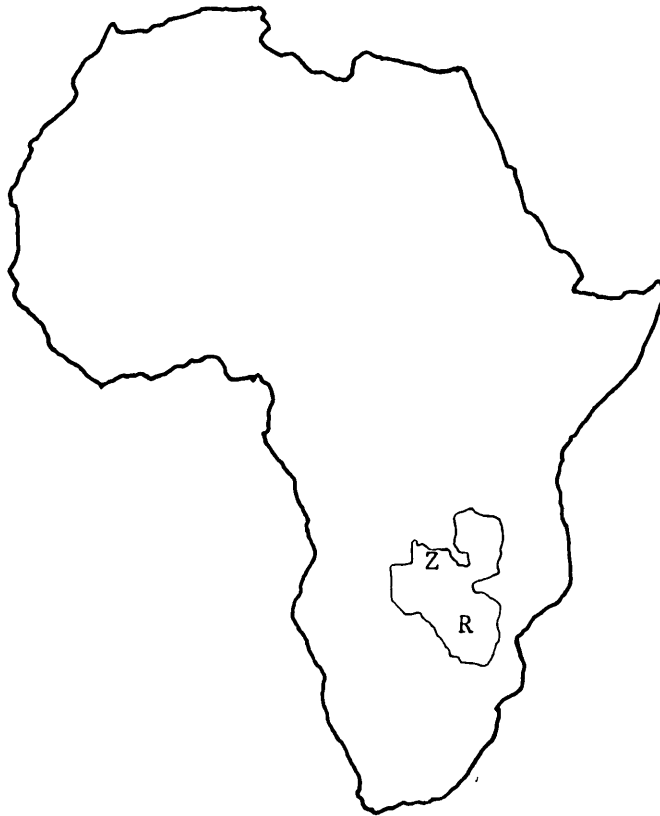
Figure 1: Africa, the location of Zambia and Rhodesia.

| | Rainfall (mm) | Average maximum daily temperatures (^{o}C) | | |
		January	July	October
Kabwe	818	26	25	31
Livingstone	749	29	25	34
Salisbury	792	26	21	28

Table 1: Climatic features of towns of the Central African Plateau

of nickeliferous laterite ore-grade in the non-ideal climate of
Central Africa, may hinder interpretation from soil geochemistry
of the primary distribution of nickel in the underlying mafic
and ultramafic rocks.

In the early 1970s, geochemical prospecting in Zambia
led to the discovery of one nickel orebody and several detailed
investigations of mafic and ultramafic bodies which proved to be
non-mineralized. This prompted research into improving geochemical
prospecting techniques for primary nickel ore in Central Africa.

1.5.   Physical features of the Central African Plateau

The Central African Plateau is the land surface at
about 1300 m above sea level bounded by the rift valleys of lakes
Tanganyika and Malawi in the east, the Limpopo depression, or lowvelt
in the south and the upper Zambesi and Upembe rift in the east and
north. This region includes Zambia, Malawi,most of Rhodesia except
the extreme south, southeastern Zaire and northwestern Mozambique
(figure 1). Within this region the Plateau is dissected by two major
rift valleys, the Luangwa rift in Zambia and the central Zambesi rift
separating Zambia and Rhodesia.

1.5.1.   Geology

According to Brock, the geology of Central Africa is
controlled by the pattern of vertical uplift. The two principal
structural features are the Northern Rhodesian Block to the north
and the Southern Rhodesian Crustal Fragment in the south, both
bounded by rifts and depressed blocks, and separated by the Zambesi
rift. Brock suggested that the Northern Rhodesian Block was divided
by a zone of weakness into an eastern Bangweulu Block and western
Kasempa Block (Mendelsohn, 1961; figure 2).

The Bangweulu Block comprises granitic and gneissose
basement rocks some 1800 million years of age, while the Kasempa Block
is entirely overlain by younger rocks. Rocks around the southern
boundaries of these blocks were in part remobilized during the Kibaran
orogeny of 1300 million years ago and constitute the Basement Complex.
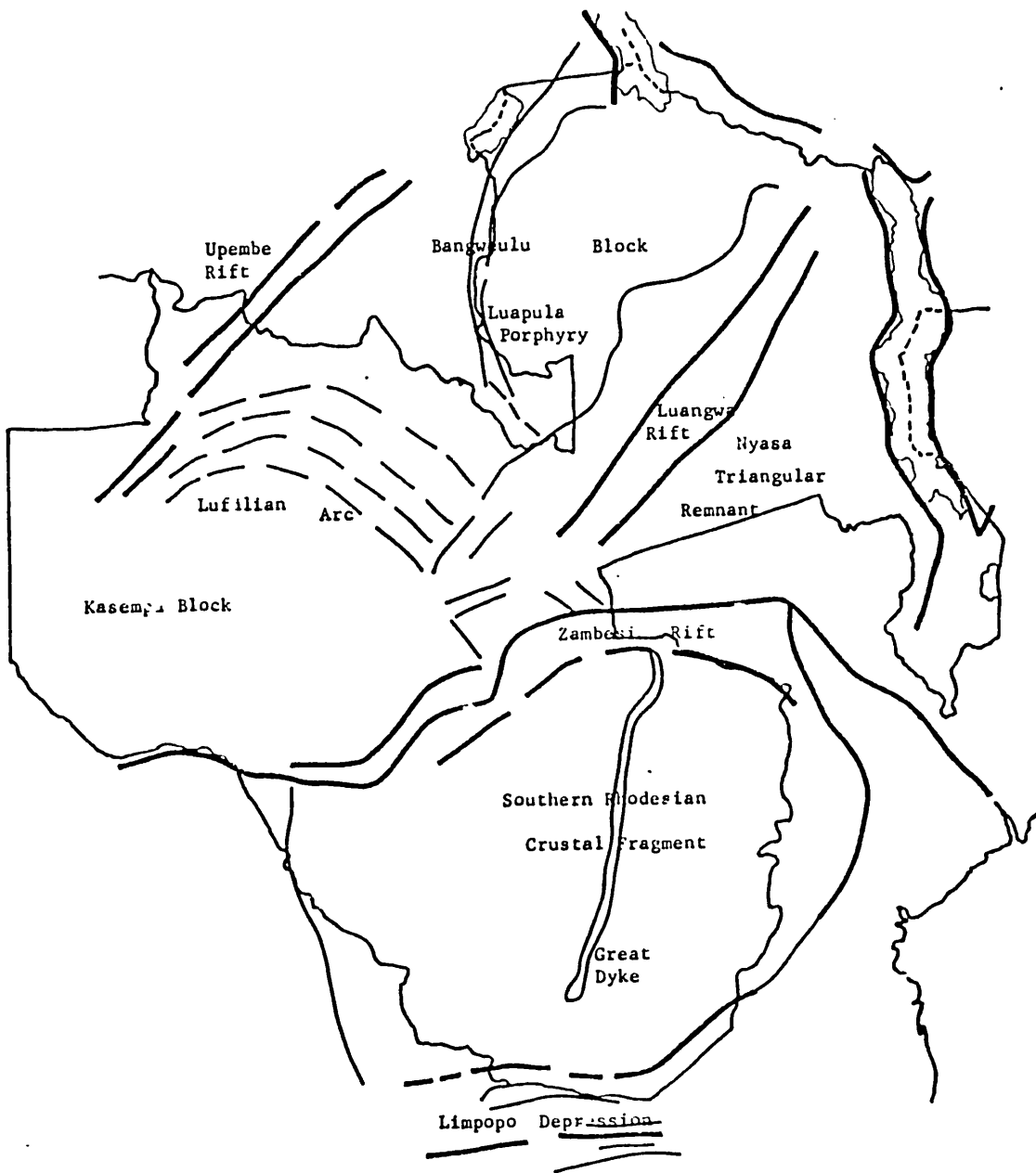
Figure 2: The structural features of Central Africa. (after Brock, in
Mendelsohn, 1961; approximate scale 1:10,000,000).

The ancient crystalline rocks of the Bangweulu Block and Basement
Complex in Zambia are correlated with the Sebakwian, Bulawayan and
Shamvaian systems of Rhodesia. In both Zambia and Rhodesia these
rocks include a number of scattered mafic-ultramafic intrusive
complexes which are generally concordant with the country rocks,
regionally metamorphosed, and in some cases extensively serpentinized.
In the extreme east of Zambia and Malawi is another uplifted unit,
Brock's Nyasa Triangular Remnant, part of the Mozambique Belt. The
rocks comprise complex folded gneiss, charnokite and granite of
about 460 million years of age. The zone of weakness separating the
Bangweulu and Kasempa blocks is a fault-bounded crustal downwarp
occupied by geosynclinal sediments of the Katanga System. These
comprise conglomerates, quartzites, argillites and dolomite of late
pre-Cambrian and early Palaeozoic age. The rocks were folded and
slightly metamorphosed in the Lufilian Orogeny dated at 500 million
years ago. Middle Katanga beds are intruded by numerous stocks and
sills of mafic and ultramafic rocks of post-tectonic age. The
Katanga System rests unconformably on the Basement Complex in Zambia
and is correlated with the Lomagundi System in Rhodesia. In the
west of Zambia and in the rift valleys, the rocks are mainly continental
sediments and lavas of the Karroo System of Permian-Jurassic age. The
lithologies present comprise conglomerates,sandstones,arkoses,clays,shales
and coal, and basaltic lava flows. The extreme west of Zambia and
southeast Rhodesia are blanketed by aeolian sandstones and
unconsolidated sands of the Pleistocene Kalahari System (Drysdall,
Johnson, Moore and Thieme, 1972; figure 3).

1.5.2. Physiography

Most of the Central African Plateau comprises gently
rolling topography broken only by the valleys occupied by major rivers
and by isolated hills. The general elevation of the land is about
1300 m above sea level, and represents the African or mid-Tertiary
erosional surface. The mid-Tertiary erosion cycle began with a period
of late-Cretaceous uplift and terminated in late-Tertiary times with
further uplift. The late-Cretaceous Gondwana landscape is still present
as conspicuous monadnoks rising to 1400 m and more above sea level.
Since the late-Tertiary period, rivers have cut V-shaped valleys into
the African erosion surface down to about 1200 m above sea level
(Mendelsohn, 1961).

Legend:

- Kalahari
- Karoo
- Katanga and Lomagundi
- Kibaran
- Plateau sediments
- Granite and volacanics
- Undifferentiated pre-Katanga
- Grea: Dyke

Bangweulu Block

Bulawayan
Shamvaian
Sebakwian
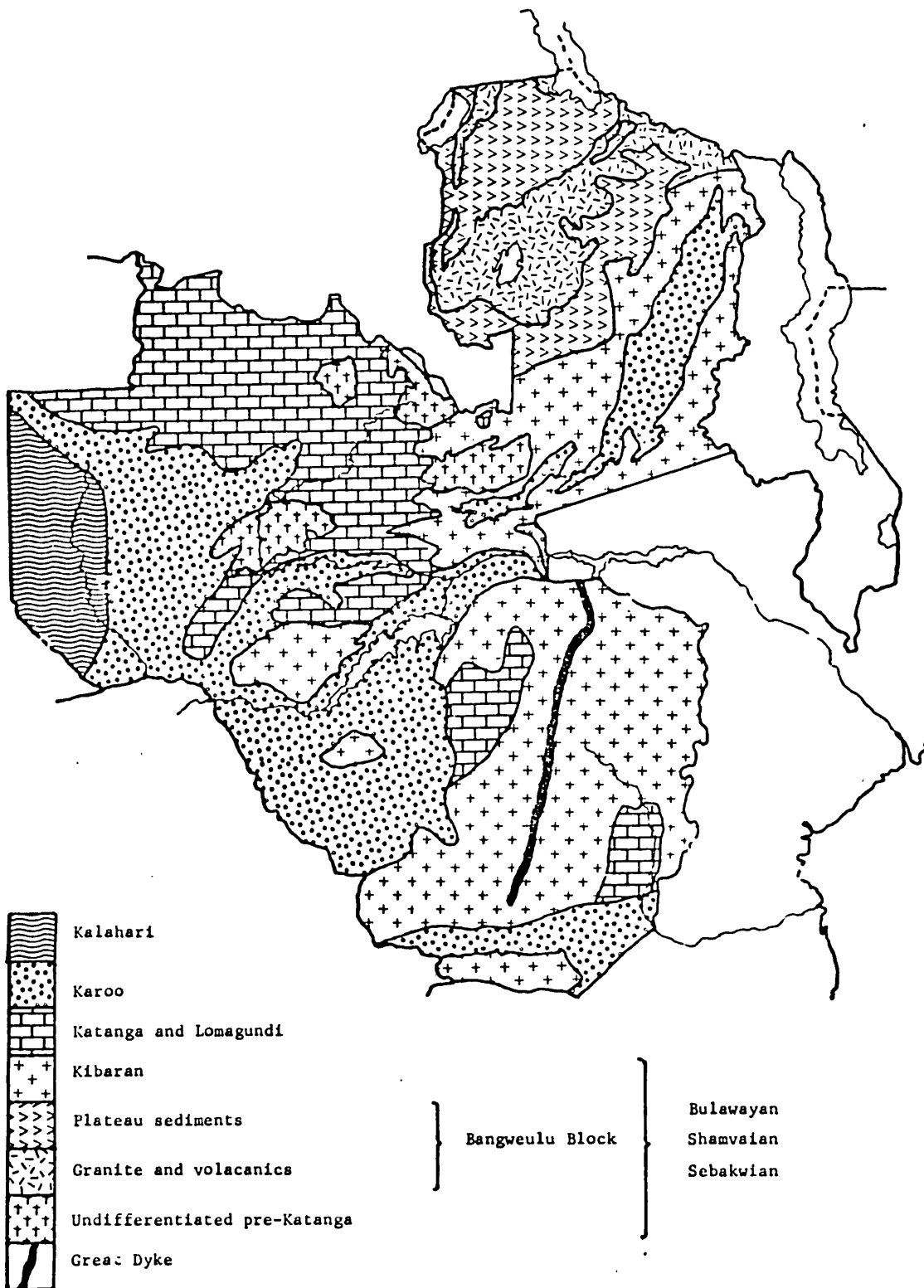
Figure 3: Outline geological map of Zambia and Rhodesia (approximate scale 1:10,000,000).

The region is drained by a dendritic network of streams which rise in broad shallow saucer-shaped treeless depressions termed dambos (in Zambia) or vleis (Rhodesia). These become water-logged and swampy during the rainy seasόn but are usually dry during the later part of the dry season. Dambos and vleis are characteristically headwater features, but may extend downstream as river meadows over great distances. There is little dissection of the land surface by minor streams, except in areas of rugged terrain. The streams feed the principal rivers of the region, such as the Kafue River, which have cut incised valleys with broad flood plains. Their waters drain into the Zambesi, Sabi and Limpopo rivers which occupy rift valleys and flow to the Indian Ocean.

1.5.3. Climate

The climate of Central Africa is tropical, but the elevation of the Plateau gives rise to lower temperatures than might otherwise be expected.

There is a clearly defined seasonal climatic cycle, with rainfall confined to the hot summer months of November to March, and warm dry winters from April to October. Rain falls as tropical thunderstorms which usually last for a few hours of each afternoon during the rainy season. There is generally little cloud except immediately prior to and during rainfall. The sun begins to warm the ground surface by 8 am each day and maximum temperatures are attained about 2 pm. The highest maximum daily temperatures are attained immediately before the onset of the rains in October, and lowest maximum daily temperatures are recorded in July. Most of the Central African Plateau has a climatic pattern similar to those of Kabwe, Livingstone and Salisbury (table 1). In the north of the region rainfall increases to about 1200 mm at Mpika, but temperatures are little changed. The rift valleys of the Limpopo, Zambesi and Lunangwa, at a lower elevation than the Plateau, are characterized by higher temperatures and lower rainfall. These features are seen to a small extent at Livingstone, which stands on the margin of the Zambesi valley.

1.5.4. <u>Soils</u>

The principal soils of the Central African Plateau, developed in freely drained, oxidizing conditions, vary from low-organic tropical podzols to latosols and poorly developed laterites (Wiik, 1969). The A horizon ranges from a few centimetres to several metres in thickness, and can be subdivided into an A_1 humic topsoil horizon, up to 10 cm thick, and a yellow-brown, sandy, leached A_2 horizon. The B horizon is up to 2 m thick and often comprises a coarse quartz rubble in an orange-brown ferruginous matrix. In many places this matrix is a hard, nodular cement, forming a lateritic horizon. Beneath the laterite is the B_2 horizon of red-brown or yellow-brown silty soil, up to 5 m thick. The B_2 horizon grades downwards into the C horizon of weathered rock fragments often in a mottled red-yellow soil matrix. This horizon lies between the seasonal maximum and minimum water-table levels and the mottled appearance of the matrix is derived from the accompanying alternations of oxidizing and reducing conditions.

In rugged terrain and on valley slopes, soils are more easily washed away by rainwater run-off, and immature, poorly profiled, thin, rubbly soils are present.

Dambos and vleis are characterized by poorly drained glei soils developed under waterlogged and reducing conditions. The glei soils possess a black, richly-organic, peaty A_1 horizon up to 1 m thick, with an underlying pale leached zone, but there is little further profile development.

1.5.5. <u>Termitaria</u>

Much of the freely-drained land area of the Plateau has a scattering of termitaries. The surface expression of these structures comprises mounds of cemented subsurface soil up to 8 m high, but they extend below ground to depths not ascertained with certainty, and are believed to reach the water table. Since grains of subsurface soil are brought from the lower parts of the termitary by the termite colony in building the mound, termitaria have been used as a useful sampling medium. However, soil sampling of the B horizon on a regular grid or traverse is generally more convenient.

Termitaria are absent from dambos and vleis, but small anthills, up to 50 cm high, are common.

1.5.6. Vegetation

The natural vegetation of the Central African Plateau is Brachystegia-Isoberlinia deciduous woodland, which takes its name from the two most abundant species, Brachystegia spiciformis and Isoberlinia globiflora. Other species of these genera are common along with species of Albizia, Combretum, Diplorynchus, Monotes, Strychnos, Uapaca and other genera. On freely drained soil the tree density varies from open grassland to near-forest, and fully grown trees range from 5 to 15 m high. At ground level there is a cover of grasses and shrubs. In dambos and vleis there are no trees, but dense growth of grass and reeds is common.

In the warmer and drier rift valleys below the level of the Plateau, the Brachystegia woodland gives way to Mopani woodland.
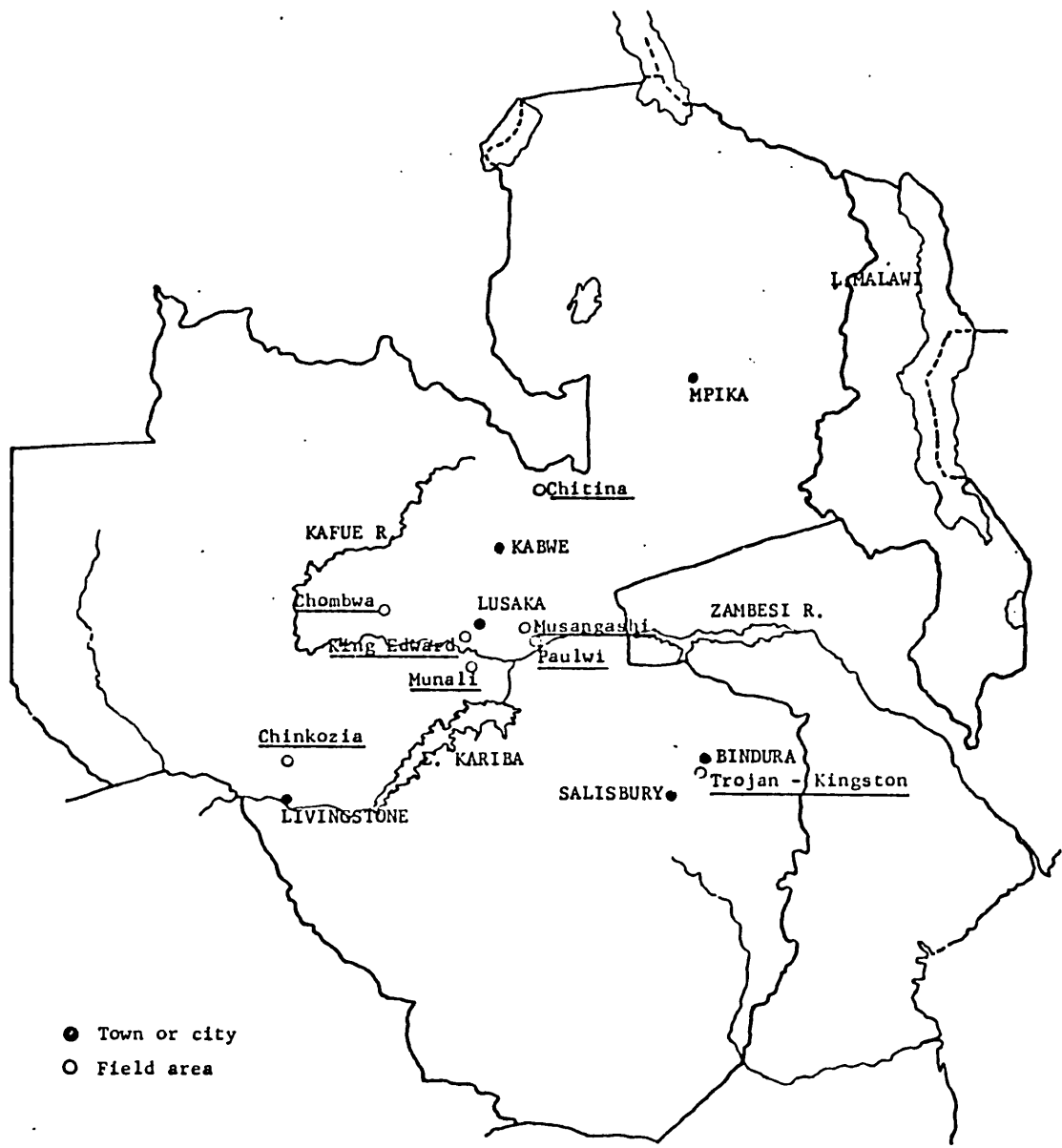
Figure 4: Location of field areas (approximate scale 1:10,000,000)

2. FIELDWORK

2.1. Description of field areas

Mafic and ultramafic bodies located on the Central African Plateau were used as type field areas for research into geochemical prospecting for sulphide nickel ore (figure 4). The Chinkozia, Chitina and Musangashi bodies are metamorphosed mafic-ultramafic intrusives set in the Kibaran Basement Complex. The Paulwi and Kingston-Trojan bodies, also of Kibaran age, are ultramafic complexes exhibiting extensive serpentinization. At Chombwa, King Edward and Munali there are mafic-ultramafic stocks and sills in Katanga meta-sediments, and the intrusives are probably post-Lufilian in age. All of the areas have at some time been investigated for their nickel ore potential by prospecting subsidiaries of the Anglo American Corporation of South Africa and orebodies have been defined at Munali and Trojan . The relevant (unpublished) company reports provide most of the geological and geochemical background to the areas, supplemented by Geological Survey publications and thin section examination of rock specimens collected during the present research, and this is termed "prospecting data" in figures 5 to 13.

2.1.1. Chinkozia

The Chinkozia prospect is about 60 km north of Livingstone on the Central African Plateau. An intrusive about 14,000 m by 3000 m forms a prominent, low hill in an area of flat to undulating terrain. The elevated area occupied by the intrusive is open grassland with stunted trees while the slopes of the hill and surrounding countryside have a more typical woodland vegetation. On the elevated ground, streams rise in broad open dambos, and on the slopes stream courses become incised, with occasional waterfalls.

The Chinkozia body is a stock or large sill mainly of norite (Harden, 1962). The norite is folded into the surrounding gneiss of the Basement Complex and is enlongated parallel to the northeast-southwest strike of the country rocks (figure 5). The elevated outcrop forms a conspicuous remnant of the Gondwana surface.

N

Research sampling:

• Sample points

▲

Prospecting data:

Norite

Quartzite and
schist

Gneiss

+ 200 ppm Ni in soil
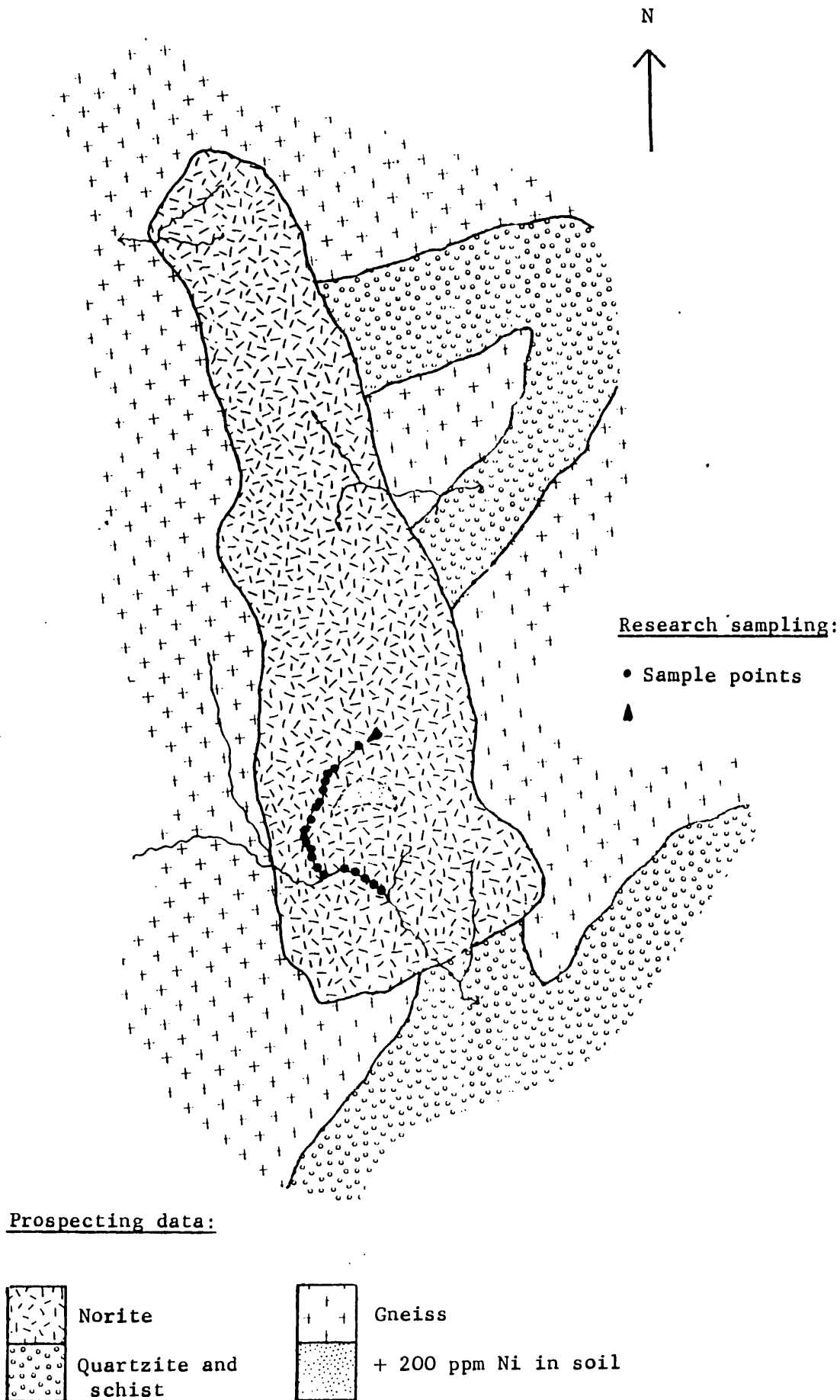
Figure 5: Chinkozia, outline geological map with Ni soil anomalies and
research sampling scheme; approx scale 1:100,000.

The norite comprises about 40% medium-grained hypersthene, 10% small augite crystals, 40% large twinned plagioclase, probably andesine, and a little fine-grained microcline. The texture is finer in marginal rocks, and the composition more anorthositic in the centre. There is some alteration of pyroxenes to amphiboles, but in general the rock is not severely altered and outcrops are not intensively weathered. Finely disseminated sulphides, mainly pyrite, are present in some outcrops.

In a stream sediment reconnaissance the intrusive is identified by samples containing up to 195 ppm Ni. A soil sampling grid covering the norite revealed a background of 70 to 150 ppm Ni with an arcuate anomaly of up to 550 ppm in the southwest.

2.1.2. Chitina

The Chitina area is 120 km northwest of Kabwe and 270 km southwest of Mpika. The terrain is flat to gently rolling with broad open dambos and a woodland natural vegetation.

The Chitina intrusive has a suboutcrop area of about 8000 m by 1500 m and is probably a single continuous body at depth although its surface expression is discontinuous. The intrusive rocks are recorded as mainly gabbro and peridotite, locally altered to serpentinite and talc schist, although much information is inferential due to scarcity of outcrop. The intrusive is folded into the northeast-southwest regional strike of the surrounding Basement Complex of quartz-mica schist and phyllite (Stillman, 1965; figure 6).

The peridotite comprises large olivines, often extensively altered to serpentine, in a matrix of fine-grained talc and sericite. There is up to 10% small pyroxenes partly altered to amphiboles, and up to 10% medium-sized crystals of carbonate minerals. Only a few specks of sulphides are present.

Coverage of the area by soil sampling revealed that background over the intrusive is about 100 ppm Ni and there are several anomalous zones with up to 950 ppm Ni . Vertical pits on these anomalies showed that the soil C horizon contains up to 1700 ppm Ni.

N

Research sampling:

Traverse line with
sample no. origin
and detailed zone.

+ Pit

• Other sample points

Prospecting data:

Gabbro and peridotite

Schist

Granite

+ 400 ppm Ni in soil
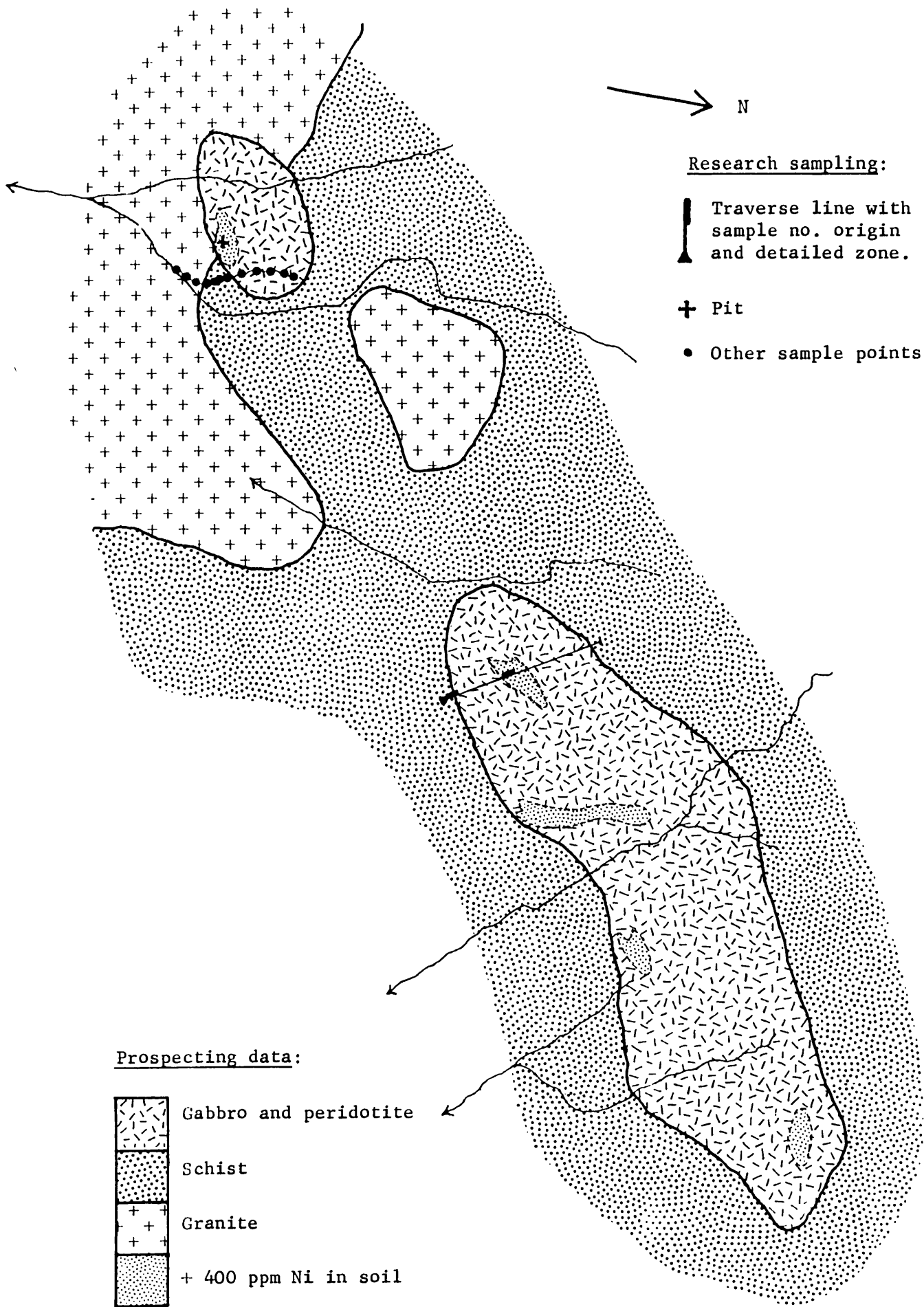
Figure 6: Chitina, outline geological map with Ni soil anomalies and
research sampling scheme; approx scale, 1:50,000.

2.1.3.   Chombwa

At Chombwa, some 170 km southwest of Kabwe, the
topography is flat with low hills and there are no streams.
There are brown to red-brown freely-drained soils and ill-defined
depressions with organic-rich semi-dambo soil. The natural
vegetation is woodland, but this has been extensively cleared
for farming.

The Chombwa intrusive is a sub-circular stock, about
5000 m in diameter, and was originally described as gabbro (Phillips,
1958). More recent work shows that the principal rock type is
metagabbro of ophitic texture, with lenses of peridotite and
meta-lherzolite. In places garnets are present in the metagabbro,
indicating retrogressive metamorphism (Prasad and Vrana,1972). The
country rocks of the area are quartz and limestone of the Katanga
System, and patches of limestone occur within the stock, which is
of late or post-Katanga age (figure 7).

The metagabbro comprises up to 50% hornblende, up to
50% andesine plagioclase partly replaced by scapolite, and usually
some olivine crystals with rims of pyroxene and fibrous serpentine.
Where alteration is most advanced the rock comprises a fine groundmass
of amphibole, plagioclase and fibrous minerals. The peridotite
comprises mainly olivine altering to chrysotile, plus pyroxene,
amphibole and a little chlorite. The meta-lherzolite consists of
a fine-grained, extensively altered groundmass of olivine, amphibole,
plagioclase and some fibrous chrysotile.

The Ni background in soils overlying the gabbro is
about 300 ppm, with anomalous zones of over 2000 ppm
In shallow pits in anomalous localities, values in the C horizon are
also in excess of 2000 ppm Ni. Diamond drilling at six sites located
only specks of disseminated sulphide minerals.

Research sampling:

Traverse line with
sample no. origin and
detailed zone.

+Pit

•Other sample points
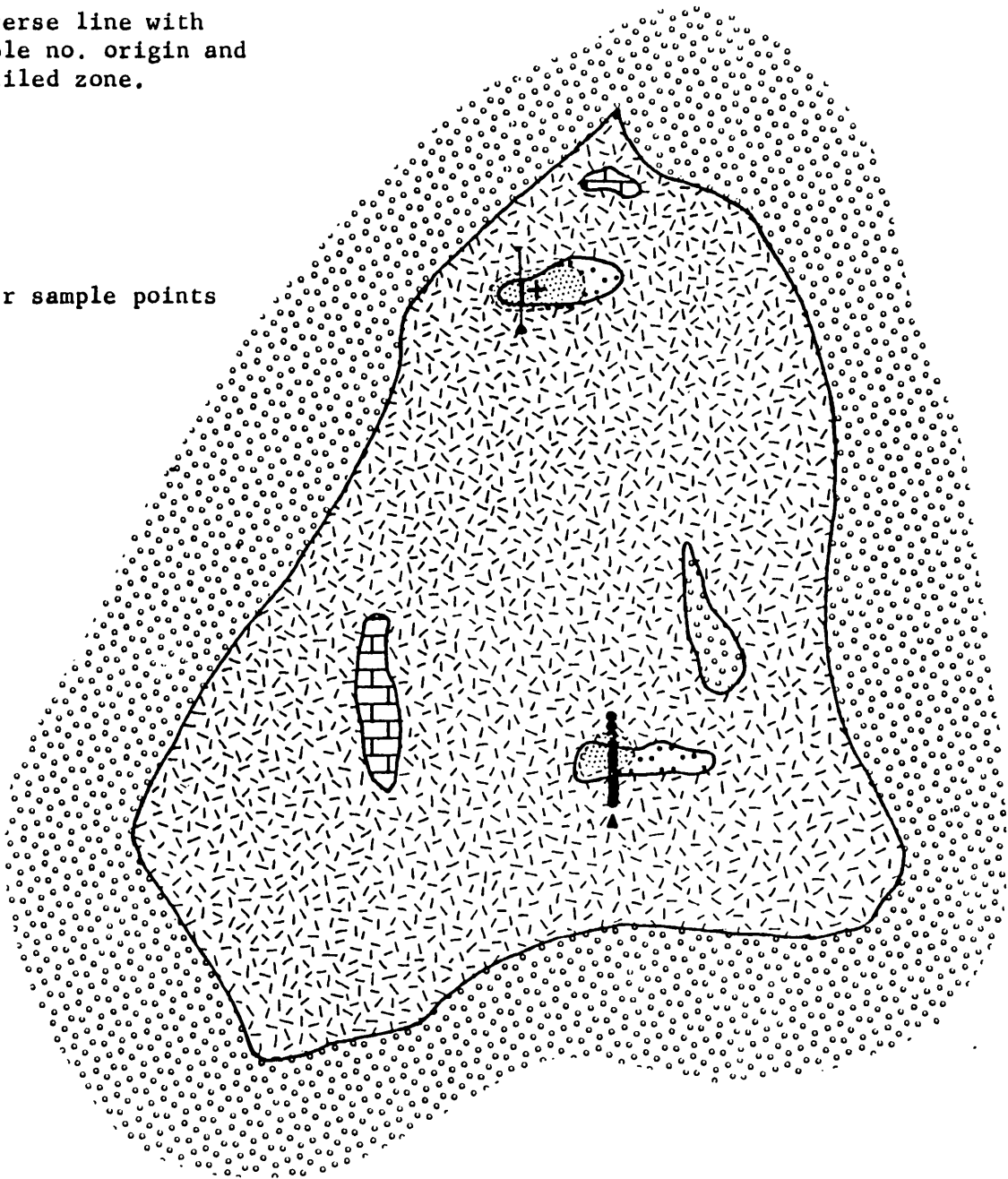
Prospecting
data:
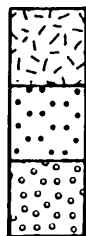
Meta-gabbro

Meta-lherzolite
and peridotite
Quartzite and
schist
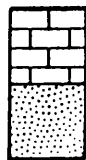
Limestone

+ 1000 ppm Ni in soil

Figure 7:   Chombwa, outline geological map with Ni soil anomalies and
research sampling scheme; approx scale, 1:50,000.

2.1.4. King Edward

The King Edward (KEX 6) prospect is 120 km south of Kabwe and 40 km west of Lusaka. The intrusive occupies a shallow, basin-shaped depression rimmed by a low ridge. A sandy stream drains the basin towards the southwest. The soil over the intrusive is red-brown and the vegetation cover is fairly open woodland.

The intrusive, about 800 m in diameter, is one of several small stocks in the area intruded into limestone, dolomite and shale beds of the Katanga System (Smith, 1963). The principal rock type of the King Edward stock is peridotite, but along the southern contact are zones of pyroxenite and gabbro, in places calcareous due to assimilation of country rocks (figure 8).

The peridotite comprises 75% large olivine crystals in varying degrees of serpentinization, about 10% of smaller amphiboles, a few plagioclase crystals, and up to 10% chlorite and phlogopite. Where severely altered the rock comprises remnants of olivine and amphibole in a fine chlorite-serpentine matrix.

The soils over the intrusive possess a high and variable Ni background in the range 1000 to 1500 ppm, with anomalies of over 3000 ppm associated with the southern contact zone. The C horizon samples from trenches in this vicinity contain up to 5500 ppm Ni. Two diamond drillholes in the southern contact zone intersected calcareous and brecciated peridotite and gabbro, with disseminations, clusters, grains and veinlets of pyrrhotite and pyrite of no economic worth.

2.1.5. Munali

The Munali prospect is 180 km south of Kabwe and 320 km northeast of Livingstone. The intrusive has little topographic expression and lies between a series of discontinuous low hills on the edge of the Kafue flats to the southwest and the Munali Hills to the northeast. Two sandy streams with slightly incised valleys drain the northwestern end of the intrusive. The intrusive is covered by brown to red-brown soils, and the natural vegetation is woodland.

N

Research sampling:

Traverse line with
sample no. origin
and detailed zone.

+ Pit

• Other sample
  points

Prospecting
data:

Gabbro

Peridotite

Limestone

Pyroxenite

Calcareous gabbro

+ 2300 ppm Ni in soil
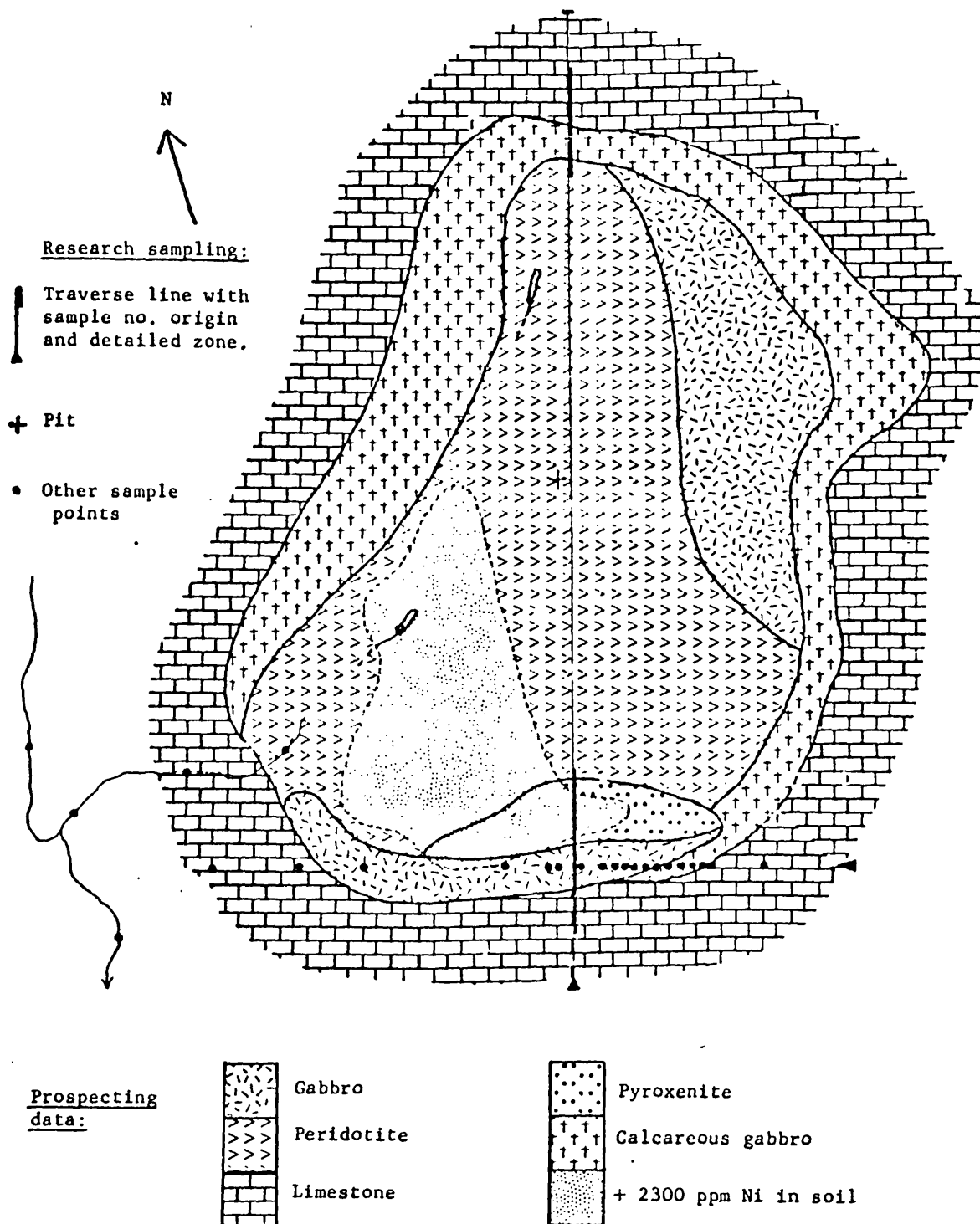
Figure 8: King Edward, outline geological map with Ni soil anomalies
           and research sampling scheme; approx scale, 1:6000

The Munali intrusive is a sub-vertical gabbro sill about 2300 m long and 500 m wide. The gabbro has replaced and assimilated northwest-southeast striking crystalline limestone and dolomite of the Katanga System (figure 9). In places the contact zone of the gabbro has been subjected to shearing and carbonatization. The country rocks of the area are meta-sedimentary limestone, dolomite, quartzite and schist of the Katanga System, and the Munali Hills granite (Smith, 1963). The gabbro has an ophitic texture and mineral composition of about 40% augite, 40% labradorite plagioclase and up to 10% sulphide minerals and magnetite.

The Munali gabbro was located by a low-order anomaly of 220 ppm Ni in stream sediment reconnaissance. Soil sampling showed that the Ni background over the intrusive is about 200 ppm and there are two elongate anomalous zones of over 5000 ppm. Trench and pit samples from these zones returned values of up to 2.3% Ni in gossan material. Diamond drilling intersected coarsely crystalline blobs, grains, veinlets and stringers of sulphide minerals which form massive replacements in places. The sulphides comprise pyrrhotite, pentlandite, violarite, pyrite and chalcopyrite, and are associated with zones of brecciation, chloritization, carbonatization, talcification and serpentinization developed within the gabbro along its southern contact with the limestone host rock. Both alteration and mineralization are probably related to late-stage injection of liquid-magma sulphide differentiates and carbonate-rich hydrothermal fluids into planes of weakness along the gabbro contact. A diamond drilling programme of more than 50 holes located several million tonnes of nickel mineralization in lenses and pods of variable grade, thickness and lateral extent, with an average grade of better than 1% Ni.

2.1.6. Musangashi

The Musangashi prospect is 120 km southeast of Kabwe. The area is flat, and much of the intrusive underlies a broad, treeless dambo and semi-dambo meadow clearing. The surrounding natural vegetation is fairly dense woodland. Two dambo watercourses in the north and south drain eastward from the intrusive. The well-drained soils over margins of the intrusive are brown to yellow-brown, while the dambo and semi-dambo soils are grey to black, organic-rich gleis.

Research sampling:

Traverse line with
sample no. origin
and detailed zone

+ Pit

• Other sample points
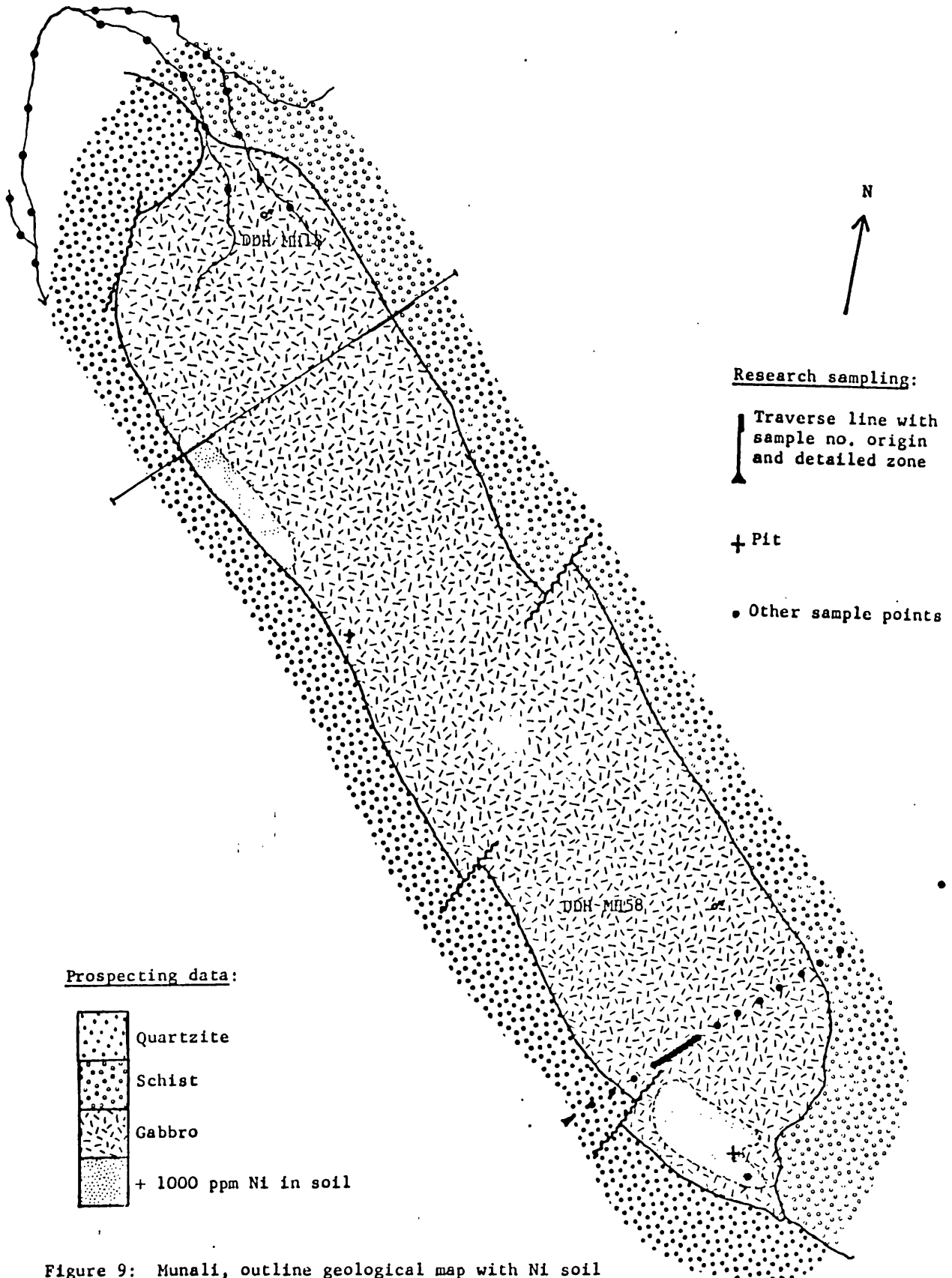
Prospecting data:

Quartzite

Schist

Gabbro

+ 1000 ppm Ni in soil

Figure 9: Munali, outline geological map with Ni soil
anomalies and research sampling scheme; approx scale, 1:12,000.

The Musangashi intrusive is a stock 6000 m by 2000 m emplaced into granite gneiss and quartz-biotite schist of the Basement Complex (figure 10). The principal rock types are amphibolitized norite, gabbro and pyroxenite, with minor shear zones of actinolite-chlorite schist (Simpson, 1967). The rocks possess a holocrystalline texture and comprise about 75% large crystals of hypersthene and augite altering to amphiboles, and 25% plagioclase crystals altering to sericite.

Soils overlying the intrusive contain a background level of about 100 ppm Ni while an anomalous zone in the west-central part of the gabbro has a peak value of 2200 ppm. Samples of C horizon material from trenches in the anomalous zone contain up to 3400 ppm Ni.

2.1.7. Paulwi

The Paulwi prospect is some 160 km southeast of Kabwe and is located in the extremely rugged terrain of the northern Zambesi escarpment. The intrusive forms a series of steep hills dissected by swift-flowing, sandy streams. The soils over the intrusive are mainly skeletal lithosols. The sub-outcrop of the intrusive is characterized by sparse and stunted tree growth within an area of dense bush.

The Paulwi intrusive complex is about 5000 m long and 1500 m wide and was emplaced into granite gneiss and schist of the Basement Complex (figure 11). The eastern sector of the complex is serpentinized peridotite, with patches of talc schist, tremolite-actinolite schist and anthophyllite schist along joints and contacts. The western sector comprises pyroxenite. The complex is slightly dissected by faulting (Barr, in print).

The serpentinized peridotite comprises up to 90% olivine crystals showing intense alteration to serpentine, with subsidiary enstatite and augite. The pyroxenite consists mainly of augite and enstatite altering to tremolite and other fibrous amphiboles. A few specks of sulphides are present in both rock types.
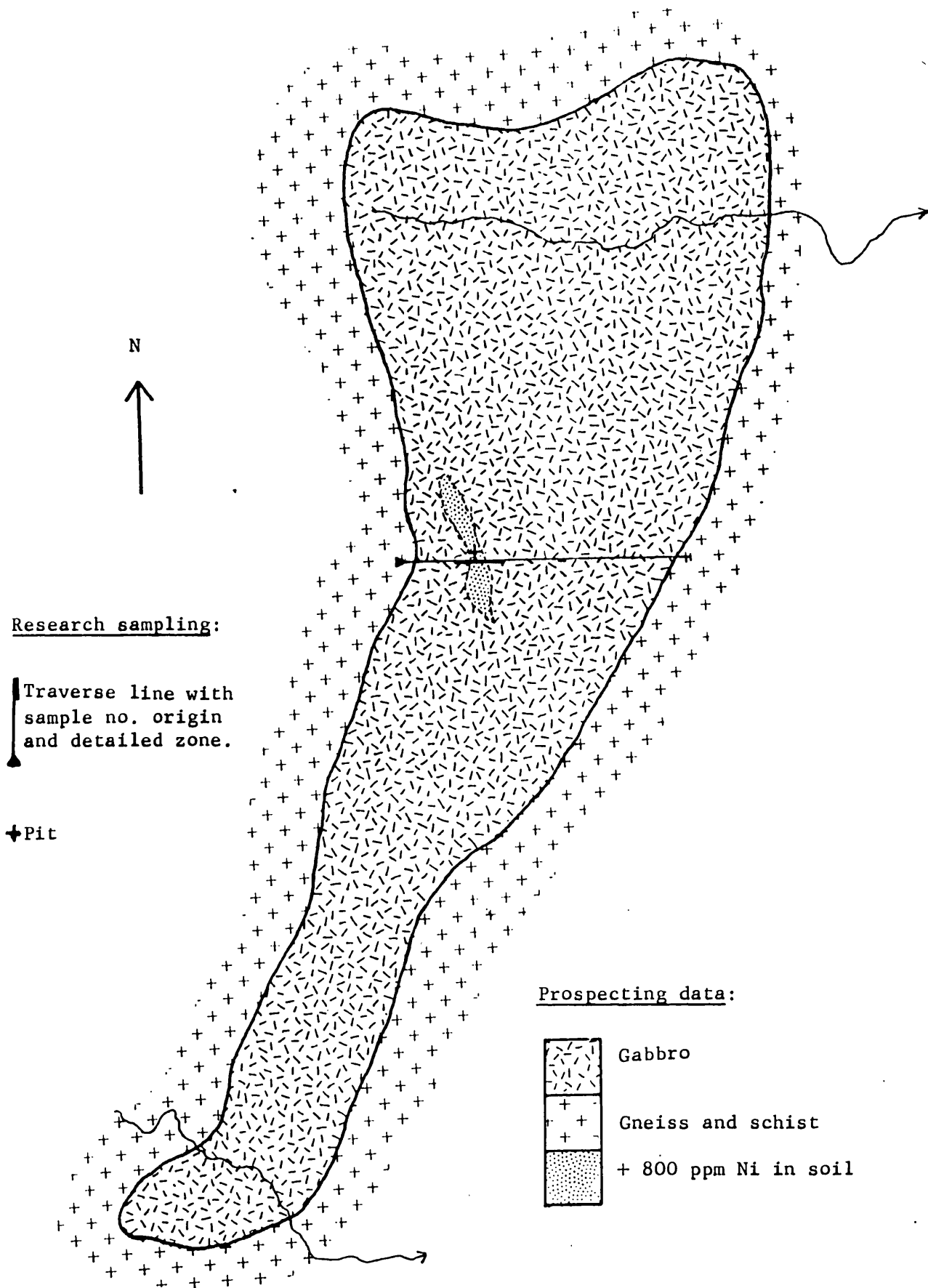
Figure 10:   Musangashi, outline geological map with Ni soil anomalies and research sampling scheme; approx scale, 1:25,000.

Several reconnaissance stream sediment samples reflect
the presence of the Paulwi intrusive with values of up to 3600 ppm Ni.
The soil background is about 500 ppm Ni over the pyroxenite and 3000
to 5000 ppm over the peridotite, with up to 9500 ppm in anomalous zones.
Trench samples of weathered rock typically contain over 4000 ppm Ni
and a trench section across a contact zone returned 20,800 ppm over
10.7 m. in serpentinized peridotite. Garnierite is seen on weathered
rock surfaces. Diamond drilling of 16 boreholes located only a few
specks of disseminated pyrite and pyrrhotite.

2.1.8. **Kingston and Trojan**

The Kingston and Trojan intrusives are about 60 km
northeast of Salisbury near the town of Bindura, and form a row
of steep hills set in otherwise flat country. Fast-flowing sandy
streams drain the hills, and dambos are found in the surrounding
countryside. The soil cover over the Trojan intrusive is skeletal,
but a more mature red-yellow soil is developed at Kingston. The
natural vegetation is woodland.

The complex outcrops over a length of 10,000 m and
is up to 1000 m wide. The intrusives were emplaced into east-west
striking and isoclinally folded arkose, greywacke and conglomerate of
the Shamvaian System and meta-sedimentary quartzite, argillite and
limestone and volcanics of the Bulawayan System. The host rocks
of the intrusives are pyritic argillite and quartzite of the
Bulawayan Banded Iron Formation. The intrusive rocks of the
western sectors of the complex, forming Cardiff Hill and Trojan Hill,
are serpentinite (figure 12). The eastern sector, forming Kingston
Hill,comprises peridotite (figure 13). The intrusive complex is cut
by a network of east-west strike faults which probably displaced
an originally continuous body. Within the serpentinite of Cardiff
Hill and Trojan Hill the faults break into wide shear zones of talc
schist, but shearing within the Kingston Hill peridotite is not
prevalent (Tyndale-Biscoe, 1933; Le Roex, 1964).

N

Research sampling:

Traverse line with
sample no. origin
and detailed zone.

• Other sample points

Prospecting data:

Amphibolite

Granite gneiss

Serpentinite

Pyroxenite

+ 6000 ppm Ni
in soil
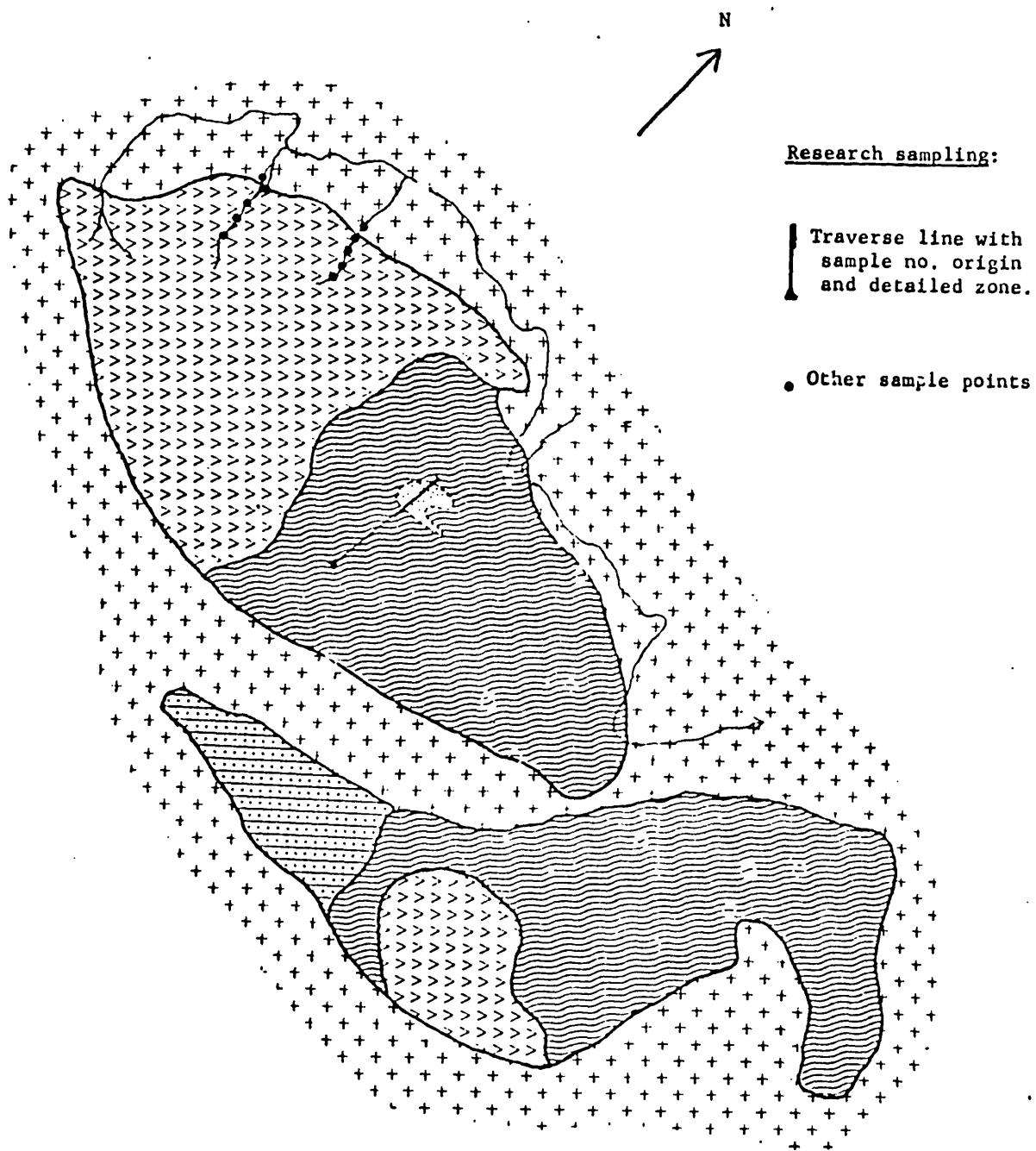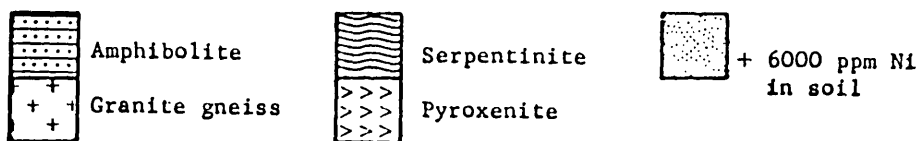
Figure 11: Paulwi, outline geological map with Ni soil anomalies and
research sampling scheme; approx scale, 1:30,000.

The peridotite comprises 90% olivine showing
incipient alteration to chrysotile, in a groundmass of fine
sericite. The serpentinite comprises a cryptocrystalline groundmass
of talc and sericite, with a few relic olivines and in places a
few carbonate minerals.

Sediment samples from streams flowing off the intrusives
contain up to 5050 ppm Ni. Soil sampling grids over Cardiff Hill
and Trojan Hill indicate a background of about 1500 ppm Ni. The
soils over Kingston Hill have a background of about 3000 ppm Ni and
anomalies reaching 20,000 ppm. A grid of shallow pits into the C soil
horizon   re-affirmed the soil Ni pattern. Initial diamond drilling
established that disseminations of pyrrhotite, pentlandite, pyrite,
chalcopyrite and millerite are scattered through the serpentinite and
peridotite, and located economic concentrations of disseminated
sulphides associated with talc schist shear zones within the Cardiff
Hill and Trojan Hill   serpentinite. Ore genesis remains a matter
of controversy, and either direct magmatic origin or silicate-nickel
leaching from olivines by sulphur-rich fluids during post-emplacement
regional metamorphism seems acceptable. An extensive diamond drilling
programme subsequently delineated orebodies at Cardiff Hill and Trojan
Hill of several million tonnes grading slightly less than 1% Ni. The
Cardiff Hill orebody is currently being mined.

2.2.   Sampling

Samples were collected in the field areas during the
period May to September 1973. During this time typical dry season
climatic conditions prevailed, although in the preceding wet season
less than average rainfall was recorded. In the various field areas
core, outcrop, pit profile, soil traverse, biogeochemical and stream
sediment samples were collected (table 2). The types of sample obtained
in each field area were determined by the local natural environment
and the prospecting history of the area. The fieldwork carried out
specifically for this project is referred to as "research sampling"
in figures 5 to 13.

Research sampling:

▮ Traverse line with
▮ sample no. origin
▲ and detailed zone.

✛ Pit

● Other sample points

Caved Area

Prospecting data:

≈≈≈ Serpentinite

∷∷ Meta-sediments

⋯⋯ Amphibolite

░░ + 6000 ppm Ni in soil
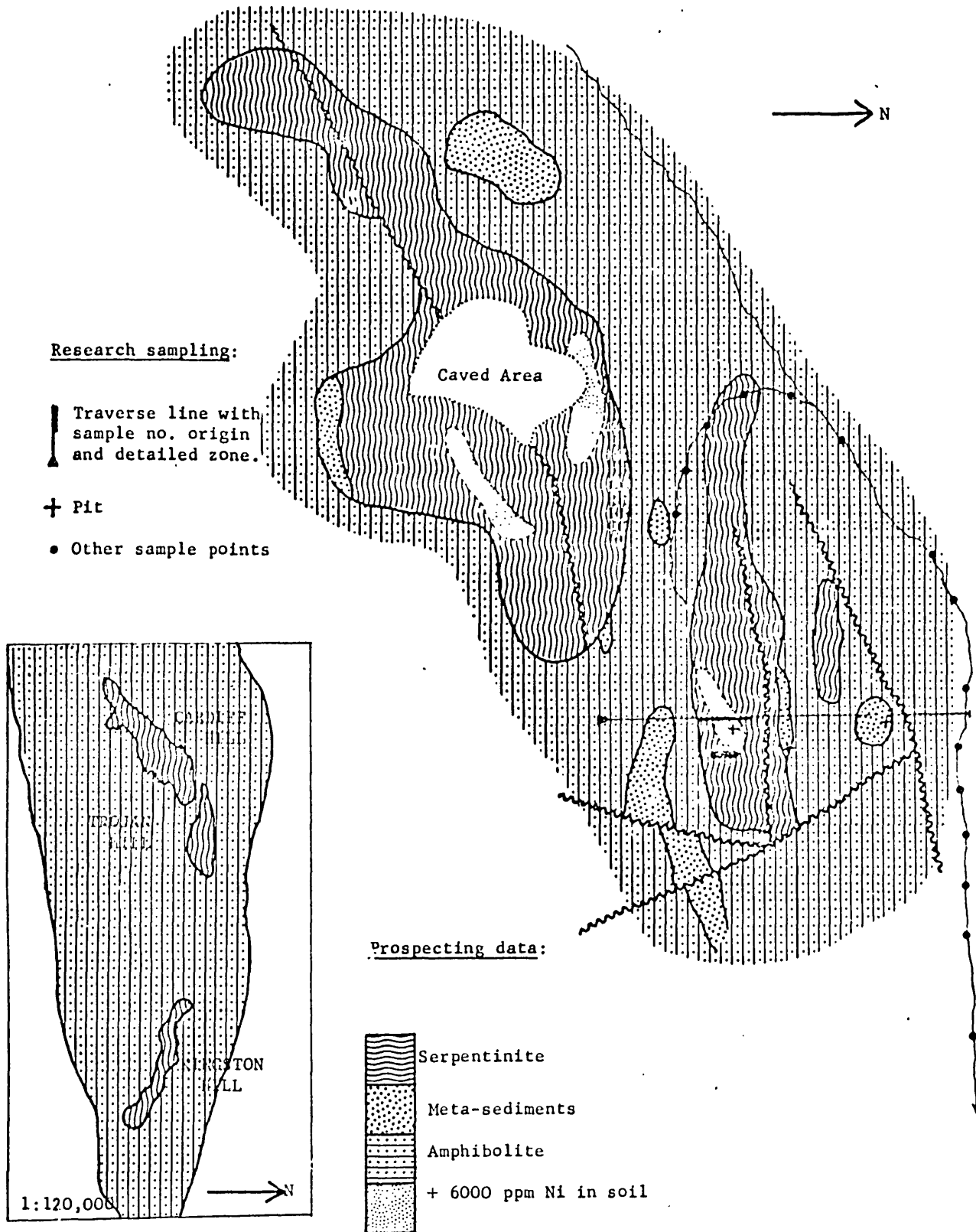
1:120,000

Figure 12: Trojan, outline geological map with Ni soil anomalies and
research sampling scheme; approx scale, 1:12,000

2.2.1.   Core and outcrop sampling

Diamond drillhole core specimens of mafic and ultramafic rocks were taken in those areas where drilling had been carried out. In each area up to 30 specimens were selected to provide the best spatial representivity of the intrusive, according to the extent of the diamond drilling programme. At Munali a further 65 specimens were acquired by sampling at 5 m intervals the full 320 m length of the core of diamond drillhole MH58.

Outcrop specimens of mafic and ultramafic rocks were taken to provide representative cover of the surface area of the intrusives, insofar as outcrop distribution would allow. Up to 32 outcrop specimens were collected in all field areas except Chitina, where paucity of outcrop precluded any systematic outcrop sampling.

Core and outcrop samples were pulverised to a particle size of less than 100 μm in diameter.

2.2.2.   Pit profile sampling

Vertical pits about 0.8 m in diameter were sited in locations of anomalous and background soils in most field areas. The pits were dug through the soil profile to reach semi-solid rock at depths ranging from 1.0 m in the immature, rubbly soils at Trojan to 5.1 m in the mature, thick soils of Chombwa. An annotated pictorial log of the vertical profile was made for each pit, with special reference to the depths at which soil horizon boundaries were identified. The pit was sampled by taking horizontal channel samples at depths from the surface of 7, 20, 35, 50, 100 cm and then every 1 m to the base of the pit, a sampling pattern designed to provide at least one sample representative of each major soil horizon.

Pit profile samples were air dried at temperatures not exceeding $30^{o}C$, lightly ground by pestle and mortar and sieved to give seven arbitrarily-selected fractions of different grain size (table 3). The coarse fraction of C horizon samples included all material obtained coarser than 2000 μm.

Research sampling:

▐ Traverse line with
sample no. origin
and detailed zone.

✛ Pit

● Other sample points

Prospecting data.

Amphibolite

Meta-sediments

Serpentinized peridotite

+ 6000 ppm Ni in soil
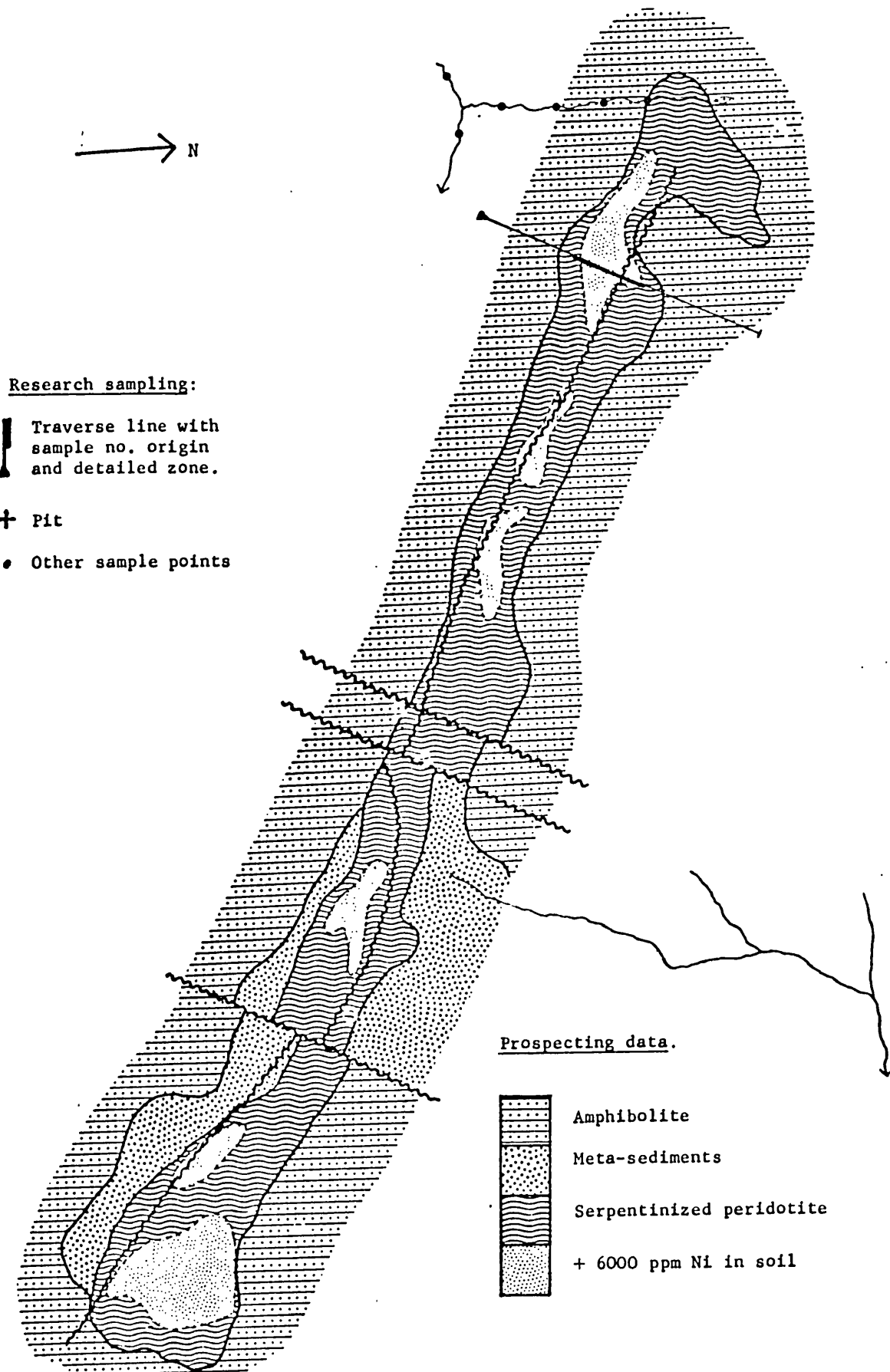
Figure 13:   Kingston, outline geological map with Ni soil anomalies and research
sampling scheme; approx scale, 1:12,000.

2.2.3.   Soil sampling

                 Soil samples were collected from the top of the
B horizon, the approximate depth of which was determined from
inspection of vertical pit profiles and generally found to be 20
to 30 cm. During soil sampling, the top of the B horizon could
usually be recognized by the presence of quartz rubble.

                 Soil samples were collected along traverse lines
over intrusive rocks and anomalous zones in all field areas except
Chinkozia. Wherever practicable the traverse lines extended the
full width of the intrusive body and onto the surrounding country
rocks, and the length of traverse lines varied from 600 to 1600 m.
The standard sampling interval was 50 m and this was closed to 10 m
across anomalous zones.

                 Soil samples were air dried at temperatures not
exceeding 30°C, lightly ground by pestle and mortar and sieved
into seven convenient fractions of various grain size range (table 3).

2.2.4.   Biogeochemical sampling

                 The relationship of the trace element content of the
natural vegetation to the underlying soil and rock was investigated
by leaf sampling. Leaves or two year old twigs are the usual
sampling media for biogeochemical surveys, and leaves were adopted
following the observation that leaves contain higher concentrations
of nickel and exhibit better anomaly contrast than twigs in several
Central African trees (Cole, 1971).

                 Preliminary field observations were made in central
Zambia to establish species of trees which were easily identified,
locally abundant, had readily accessible leaves, and were known to
have wide geographical distribution on the Central Africa Plateau.
The two apparently most suitable trees fulfilling these prerequisites
were Diplorynchus condylocarpon and Combretum ghasalense. Furthermore
these two trees tend to have a partially complementary local distribution,
Diplorynchus being more prolific on well-drained ground and on hills,
and Combretum on flat and poorly-drained land.

	Chinkozia	Chitina	Chombwa	King Edward	Munali	Musangashi	Paulwi	Kingston-Trojan
Core samples			*		*		*	*
Outcrops	*		*	*	*	*	*	*
Pit profiles		*	*	*	*	*		*
Soil traverse		*	*	*	*	*	*	*
Leaf samples		*	*	*	*	*		*
Stream sediments	*	*		*	*		*	*
Regional suite		*			*		*	

Table 2: Sampling programme, May-September 1973

Bolting cloth mesh range	Approximate particle size (ɥm)	Nomenclature
-¼"+10	-6300+2000	Coarse*
-10+20	-2000+850	
-20+40	-850+425	
-40+80	-425+180	Intermediate
-80+120	-180+125	
-120+160	-125+100	
-160	-100	Fine

*Use of the phrase "coarse fraction" in the text refers to this particle size pulverized to -100 ɥm.

Table 3: Particle size range of sieved pit profile, soil and stream sediment samples.

Diplorynchus condylocarpon is a small semi-deciduous, straggly, woodland tree. Specimens are often multi-stemmed, with a light, flat, narrow crown, and grade in size from small bushes less than 1 m tall to trees up to 30 cm in diameter and 10 m high. The bark is grey-brown, fissured and scaly. The leaves are opposite, simple oblong-elliptic, thin, leathery and glabrous (figure 14). The flowers are white and the pods brown and sickle-shaped. Copious white latex is found when twigs and leaves are broken off.

Combretum ghasalense is a small deciduous woodland tree with a heavy rounded crown. Specimens grade in size from small bushes less than 1 m tall to trees up to 25 cm in diameter and 8 m high. The bark is creamy-brown, vertically cracked, and scaly. The leaves are simple ovate, elliptic or obvate, glabrous, thick and chartaceous, and branch from the twigs in trees (figure 15). The flowers are creamy-yellow, and the fruits bronze-yellow and four-winged (Coates-Palgrave, 1957; Fanshawe, 1968).

Several leaf samples from both species were wet-ashed and analysed for Ni and other trace elements to ensure that leaves of these trees contained metals of interest in measurable concentrations. The results were satisfactory.

Biogeochemical traverses were made along soil traverse lines by collecting leaf samples from trees near soil sample points wherever possible. Sampling was confined to one species along any one traverse line. Leaf samples and nearby soil samples were also collected at other locations over intrusives. Diplorynchus samples were obtained at Chitina, King Edward, Munali, Musangashi, Trojan and Kingston and Combretum samples were taken at Chombwa, King Edward and Munali.

Leaves were dried in a cupboard at $40^{o}C$ for 12 hours and hand crushed in preparation for ashing and analysis (section 3.9.)

Figure 14: Sketch of Diplorynchus condylocarpon (Fanshawe, 1968)

2.2.5. Stream sediment sampling

Stream sediment samples were taken from stream and dambo courses draining intrusives and adjacent rocks in all field areas except Chombwa, where there were no streams, and Musangashi. Samples were collected from the centre of the drainage channel at approximately 100 m intervals along streams. All were dry when sampled.

Stream sediment samples were air dried, in the same way as pit profile and soil samples, lightly crushed, and sieved to provide seven size fractions (table 3).

Three regional drainage sample suites of -80 mesh (-180 μm) stream sediment samples collected during prospecting were obtained for the research project. These each comprised over 100 samples and covered areas of up to 80 km^2 including the mafic-ultramafic intrusives at Chitina, Munali and Paulwi.
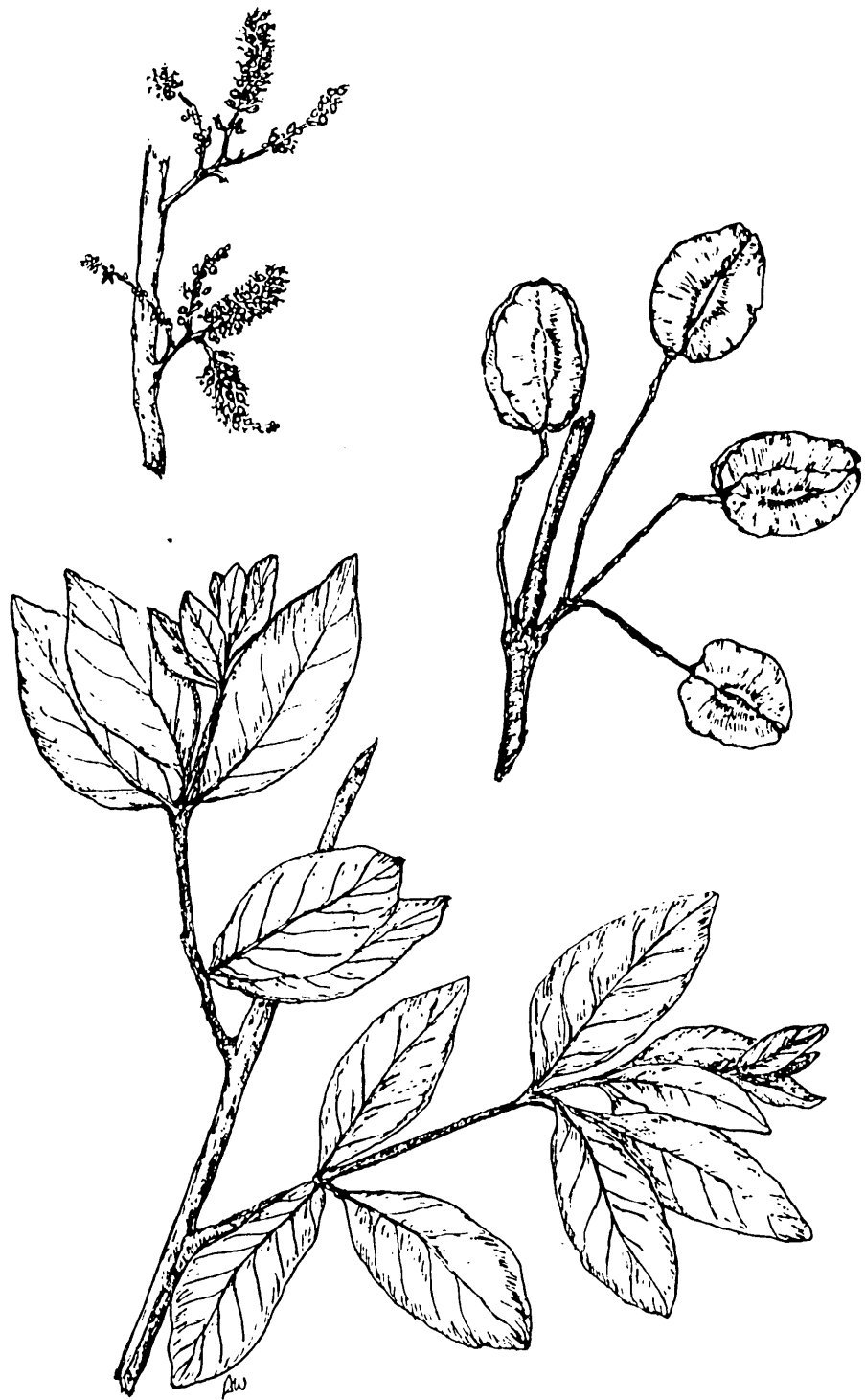
Figure 15: Sketch of Combretum ghasalense (Fanshawe, 1968)

3. ANALYTICAL TECHNIQUES

The elements selected for investigation in samples were those whose chemical characteristics indicated an association with primary nickel mineralization, such as Ni, Co, Cu, Fe, S and F, and those likely to be associated with Ni anomalies of silicate origin, such as Ni, Co, Al, Si, Cr, Ti and Mg. When multi-element techniques were used, such as emission spectrography which furnished analytical data for 25 elements simultaneously, the full data were retained for study.

Core and outcrop samples were analysed following sample pulverization to -100μm. In the case of pit profile, soil and stream sediment sample, orientation studies were first carried out to determine the most useful natural size fraction of sample material for general analysis. Biogeochemical samples were analysed as ash. Standard AGRG laboratory procedures were adopted for total metal analyses, but preliminary testwork was carried out on other techniques.

In the general analysis programme, samples were analysed in batches which included duplicate samples and standards. Within each batch the sample order, selection and location of duplicates, and location of standards was randomized by preliminary processing of batch sample numbers by a computer program RANDOM (Howarth, 1972). The sample composition of individual batches, and therefore the numerical sequence and selection of duplicates, was different for each analytical technique. The analysis of standards and duplicates provided analytical control and precision data, while randomization ensured the elimination of laboratory anomalies.

3.1. Pit profile, soil and stream sediment orientation studies

Prior to the general analysis of secondary environment samples, orientation studies were made to ensure the adoption of the grain-size fraction which would provide optimum total Ni (and other total metal) contrast between mineralized and non-mineralized localities. Pit profile, B horizon soil and stream sediment samples from mineralized localities at Munali and Trojan, and the non-mineralized Chombwa, King Edward and Paulwi areas were used in the orientation work.
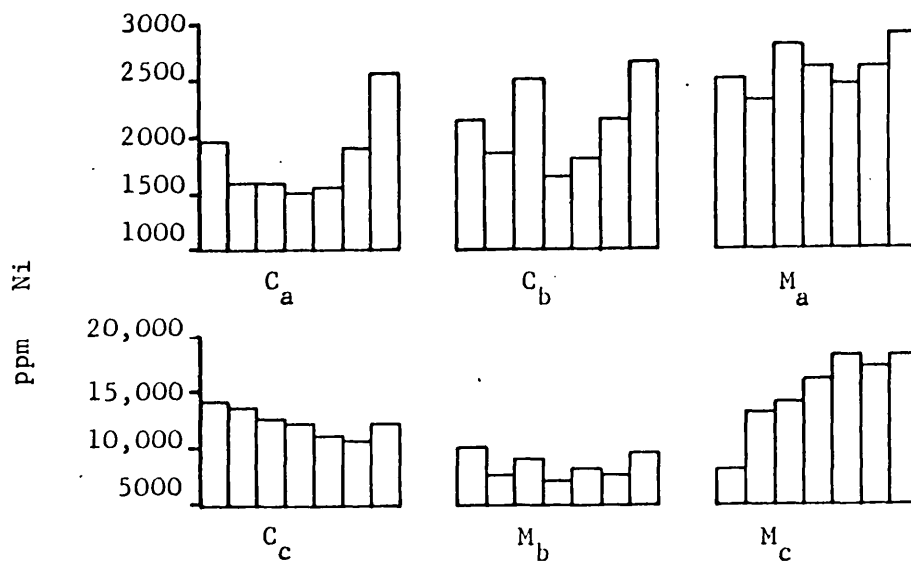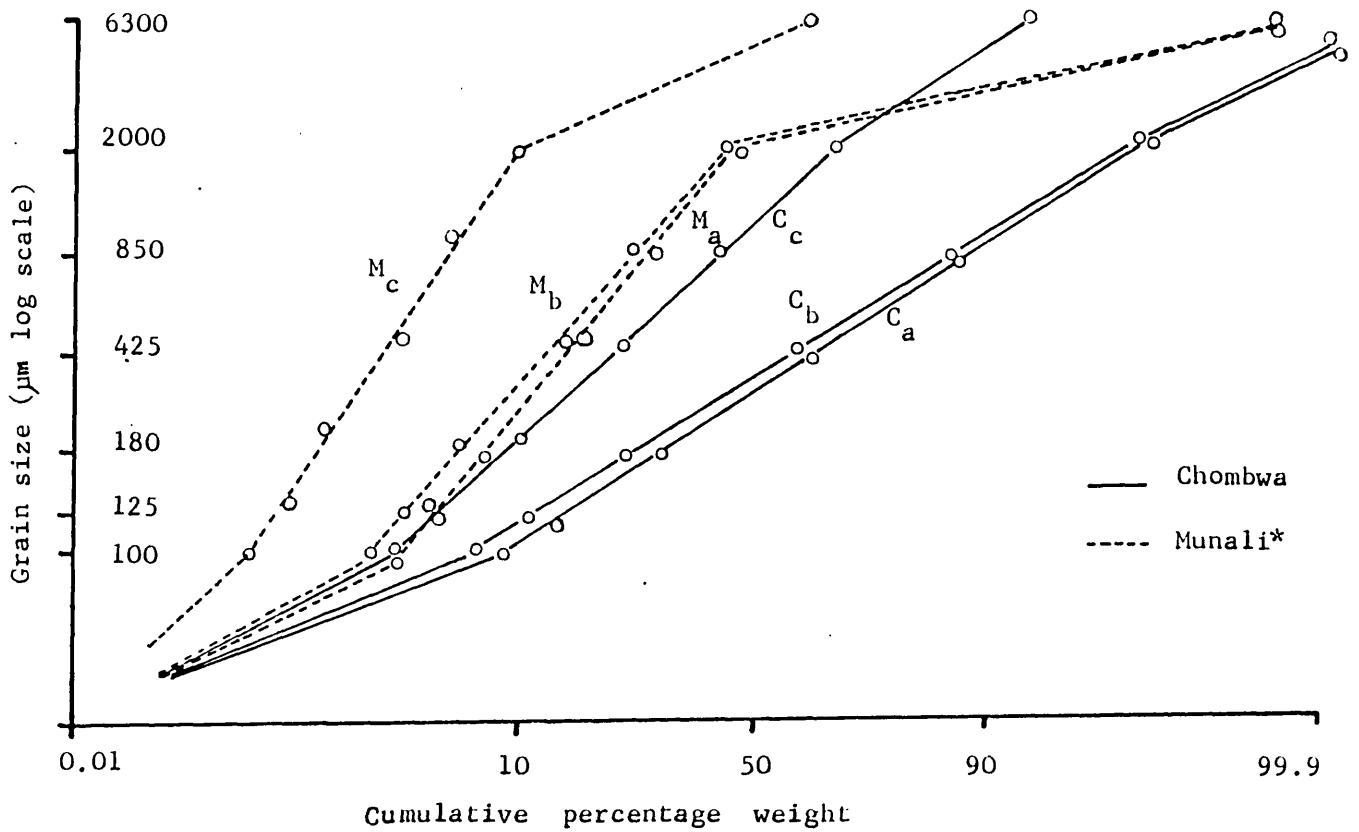
Ni content of size fractions (left to right = coarse to fine)

a = soil A horizon   b = soil B horizon   c = soil C horizon

*Pit sited on projected suboutcrop of mineralization

Figure 16:   Pit profile samples, cumulative frequency distribution
              by weight of grain size, and size fraction Ni content (ppm)
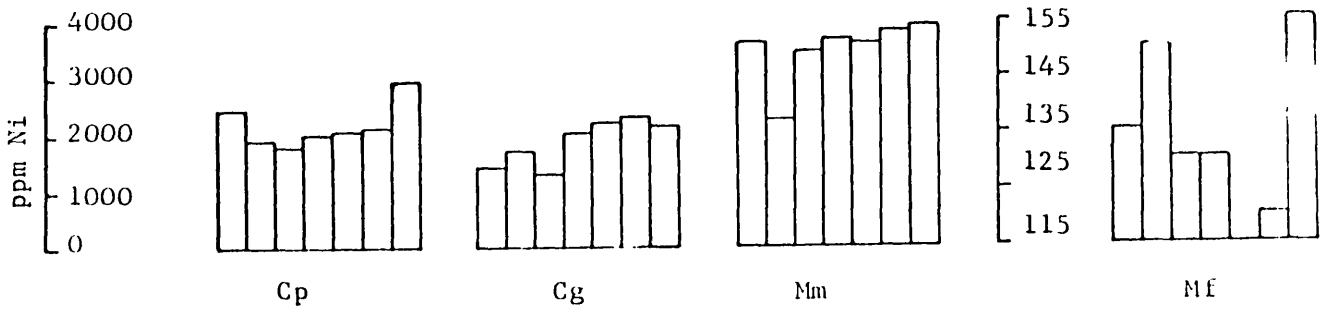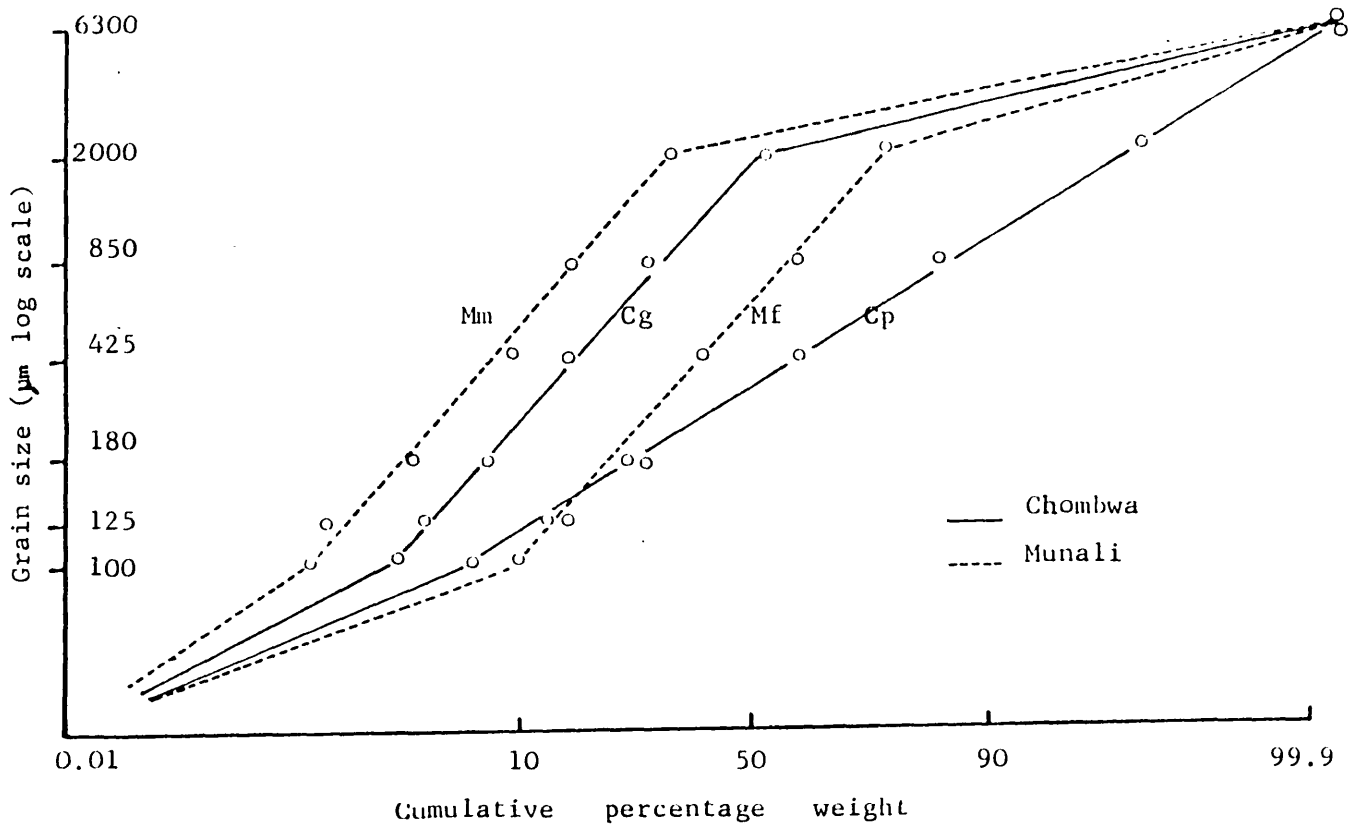
Ni content of size fractions (left to right = coarse to fine)

p = freely drained soil over peridotite

g = glei soil over meta-therzolite

m = freely drained soil over projected suboutcrop of mineralization

f = freely drained soil over gabbro

Figure 17: B horizon soil samples, cumulative frequency distribution by weight of grain size, and size fraction Ni content (ppm)

Ni content of size fractions (left to right = coarse to fine)
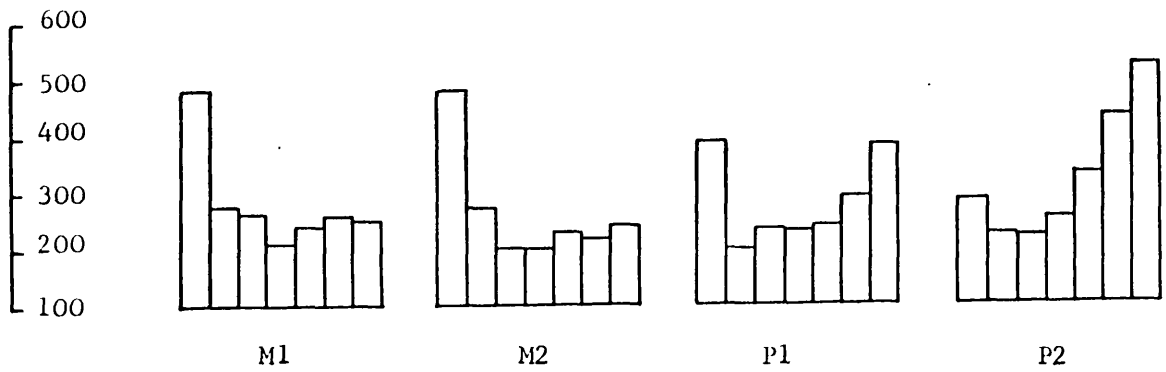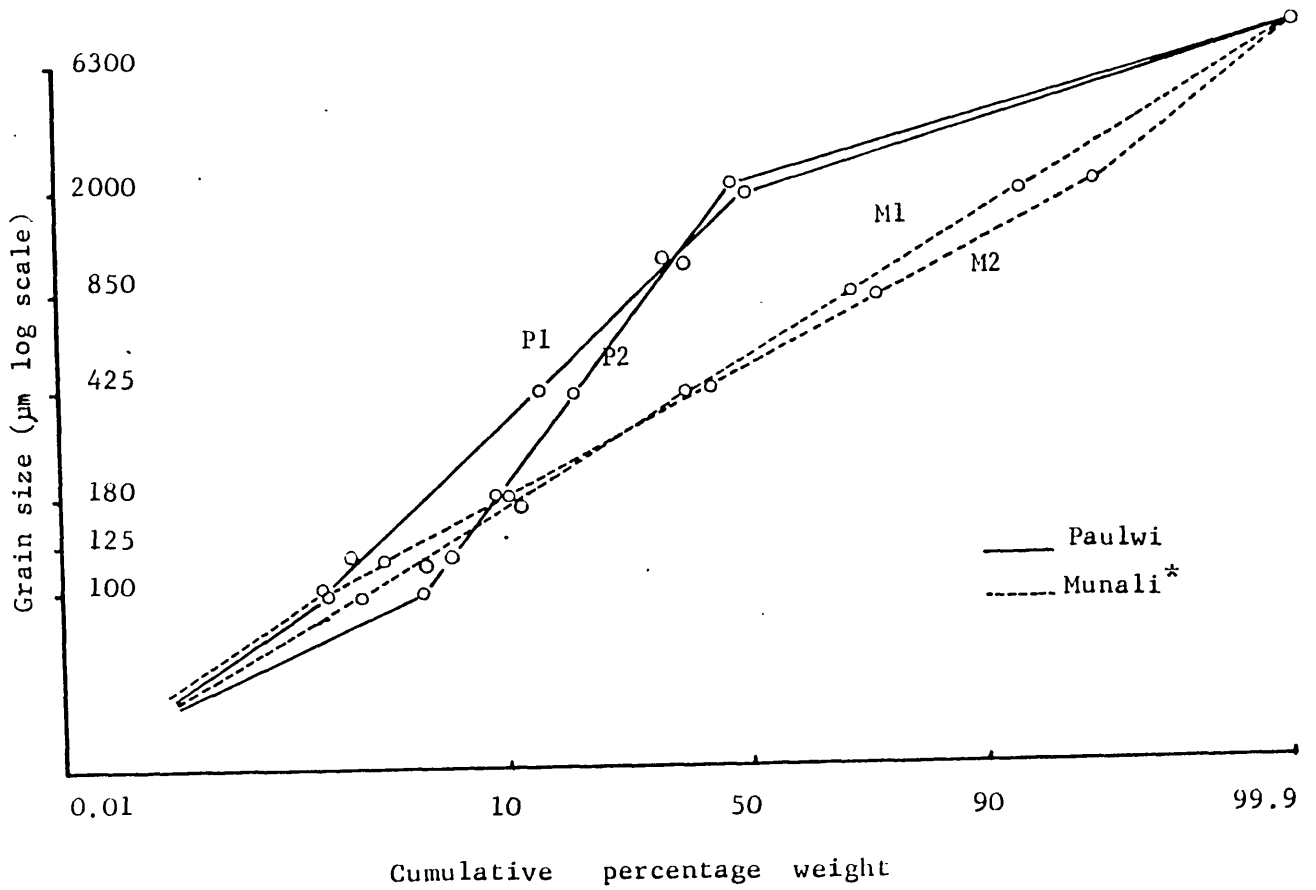
* Samples from stream draining mineralized locality

Figure 18:   Stream sediment samples,   cumulative frequency distribution
by weight of grain size, and size fraction Ni content (ppm)

3.1.1.   Sample grain-size distribution

Cumulative frequency distribution plots of grain-size distribution by weight among the seven arbitrary size fractions of pit profile, B horizon soil and stream sediment samples show that up to three grain-size populations can be present (figures 16 to 18). Where distinct, these three populations comprise the +2000 μm coarse fraction, the intermediate fractions in the size range -2000 + 100 μm, and the -100 μm fine fraction. Poorly-defined grain-size populations throughout the Chombwa pit profile and in the Chombwa freely-drained soil are attributed to the near-absence of laterite, whereas at Munali there are clear coarse, intermediate and fine grain-size populations and a lateritic soil. The origin of three grain-size populations in the Chombwa glei soil is different, because laterite is absent and the coarse fraction comprises residual quartz pebbles. There are poorly-defined grain-size populations in the Munali stream sediment, while there are distinct populations at Paulwi and the coarse fraction clearly comprises residual mineral grains.

The seven size fraction of the orientation samples were analysed for Ni using a HNO_3 - $HClO_4$ attack and atomic absorption spectrophotometric determination. In the vertical pit profiles at both Munali and Chombwa there are very high Ni values in all size fractions in the C horizon of the soil. Nickel is leached downwards from the A horizons and accumulates in the B horizons. Highest Ni concentrations usually occur in the fine fraction of samples, except in the B horizon at Munali, where the maximum Ni value is found in the coarse fraction. In the other B horizon soil samples, the highest Ni content occurs in the fine fractions, although there is some enrichment of Ni in the coarse fraction relative to intermediate fractions in Chombwa peridotite soil and Munali soil overlying mineralization. The particularly low Ni content of the coarse fraction of Chombwa glei soil is attributed to the non-ferruginous character of the quartz pebbles which comprise this fraction. In Munali stream sediments there is up to twice as much Ni in the coarse fraction of samples as in the intermediate and fine fractions. By contrast, at Paulwi there are similar concentrations of Ni in both coarse and fine fraction, or Ni enrichment in the fine fraction, and generally lower Ni values in the intermediate fractions. Thus Ni concentrations are

usually highest in the fine fraction of samples, but in some soil and stream sediment environments there is a tendency for Ni to become enriched in the coarse fraction.

Chemically-dispersed trace elements are usually enriched in the fine fraction of soil and stream sediment samples as a result of adsorption and absorption by clay minerals (Hawkes and Webb, 1962). The presence of Ni enrichment in the coarse fraction of samples is noted in the soil overlying the Kambalda nickel sulphide deposit in Australia, where secondary iron oxides are thought to play an important role in Ni fixation (Mazzucchelli, 1972). In the coarse fraction of stream sediments, a substantial enrichment of Ni and other trace elements is sometimes found in the Fe and Mn oxide coatings (Carpenter, Pope and Smith, 1975; Whitney, 1975). However, the significance in mineral exploration of Ni associated with secondary Fe and Mn has not been clearly established.

3.1.2. Sample mineralogy

The principal mineral constituents of the coarse and fine fractions of the orientation B horizon soils and stream sediments were compared by X-ray diffraction. The samples were pulverized to less than 90 μm, packed into cavity mounts, and analysed using Co Kα radiation and a scan speed of 1° per minute to produce a chart record from which sample mineralogy was interpreted (table 4). Secondary silicates, especially chlorite, talc and clay minerals, plus quartz, make up most of the bulk of all samples. Clay minerals are always enriched in the fine fraction. In both the Munali soil and stream sediment samples, which are from mineralized localities, there is a substantial amount of goethite almost exclusively in the coarse fraction, but goethite is not identified elsewhere, including the soil sample from a mineralized locality at Trojan (figure 19). There is no evidence for the presence of secondary Mn oxides, such as todorokite, in any samples. Both Fe and Mn oxides, however, are commonly amorphous in the secondary environment, and not readily identified by X-ray diffraction. The reddish colour of some soils and sediments belies their ferruginous character, but black coatings suggestive of Mn oxide were never observed.

	B horizon soils				Stream sediments			
	M*	T*	C	K	M*	T*	P	KE
Quartz	f	f	c	f	1	1	c	f
Chlorite	c	c	1	c	1	c	f	c
Talc	1	1	-	c	c	c	f	f
Enstatite	-	-	-	-	-	c	-	-
Anthophyllite	-	-	-	-	-	-	c	f
Serpentine	-	c	-	-	-	c	-	-
Plagioclase	-	-	-	-	c	-	-	-
Phlogopite	-	-	-	c	-	-	-	-
Clay minerals	f	f	f	f	f	f	f	f
Hematile	1	1	1	f	-	c	-	-
Magnetite	c	-	f	f	-	-	-	-
Goethite	c	-	-	-	c	-	-	-

C = Chombwa   * mineralized locality

K = Kingston   c mineral enriched in coarse fraction

KE = King Edward   f mineral enriched in fine fraction

M = Munali   1 similar content in both fractions

P = Paulwi   - mineral not identified in XRD

T = Trojan

Table 4:   Principal mineral constituents of orientation soil and
           stream sediment samples determined by X-ray diffraction.
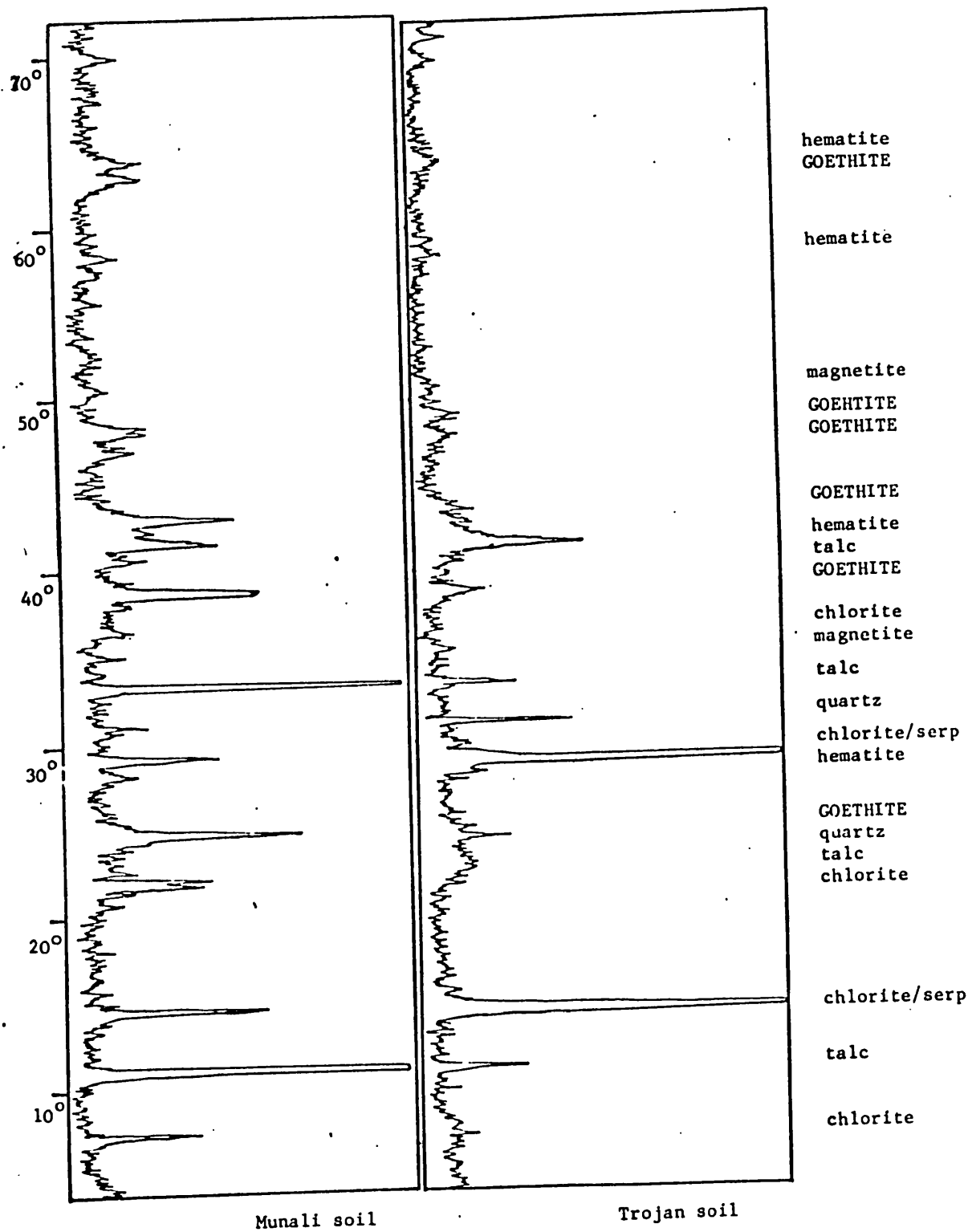
Figure 19: X-ray diffraction traces of the coarse fractions of Munali and Trojan soils, showing goethite enrichment at Munali.

Fe(OH)$_2^+$

FeOH^{2+}

MnO$_2$

Fe(OH)$_3$

FeO$_4^{2-}$

Mn^{2+}

Fe^{2+}

Mn$_2$O$_3$

Mn$_3$O$_4$

MnCO$_3$

FeS$_2$

FeCO$_3$

Eh
(volts)

+ 1.0

+ 0.8

+ 0.6

+ 0.4

+ 0.2

0

- 2.0

3   4   5   6   7   8   9   10

pH
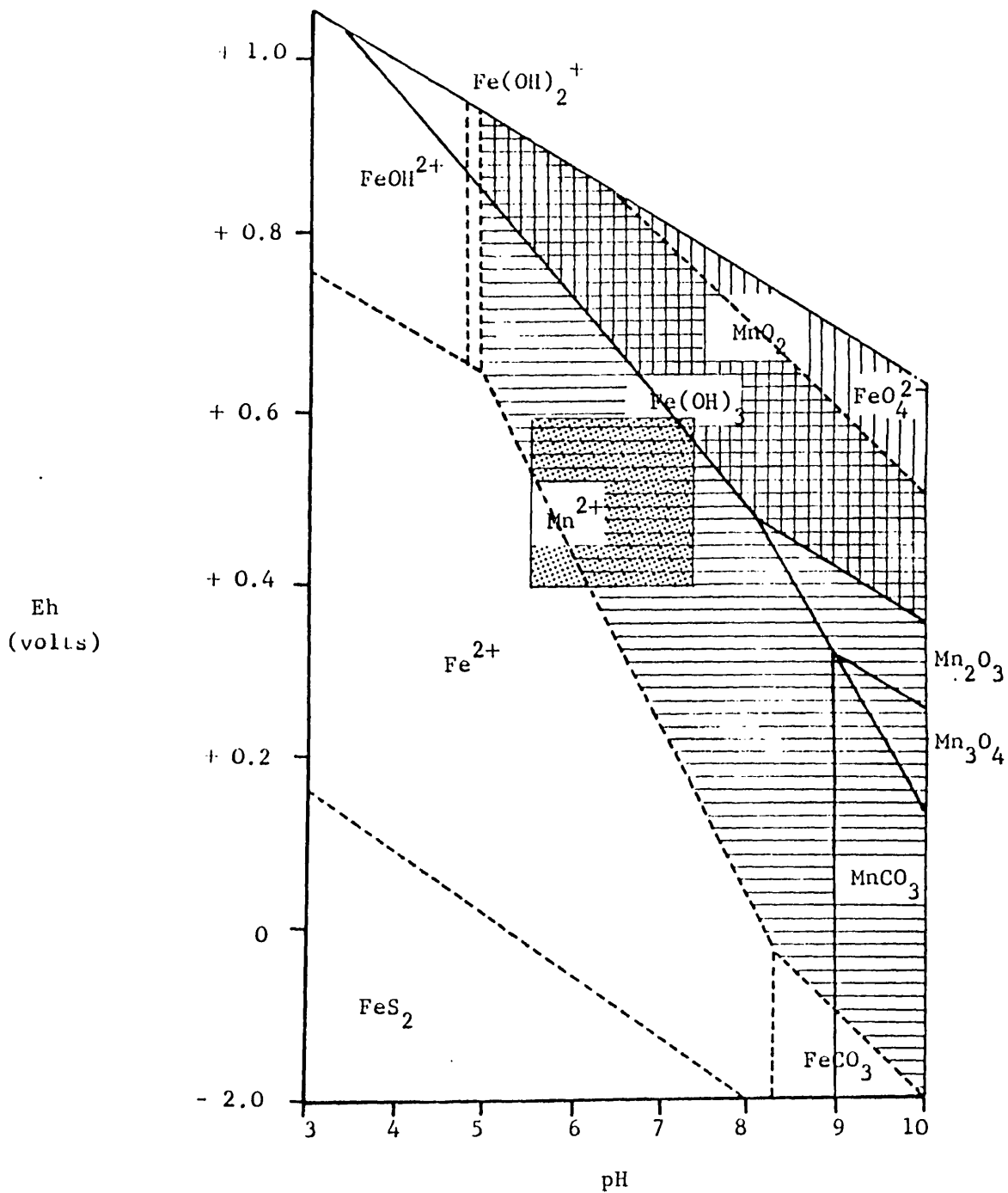
Boundaries of stability fields: ━ ━ ━ species of Fe;   ━━━ species of Mn

Activities at 25°C and one atmosphere pressure: 5.6 µg/l Fe;   10 µg/l Mn
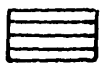
Fe (OH)$_3$ = goethite, etc   MnO$_2$ = todorokite, etc

Eh-pH of soil and stream environment of Central African field areas

Figure 20:   Stability fields for Fe and Mn species as a function
of Eh and pH at 25°C and one atmosphere pressure (Hem, 1970).

The formation of Fe and Mn oxides is dependent upon the concentrations of Fe^{2+} and Mn^{2+} in solution and the pH and Eh of the environment (figure 20; Hem, 1970). The pH of the four soils was determined and ranges from 5.5 at Munali to 6.3 at Trojan, while the pH of the four streams (based on stream sediment pH determination) ranges from 5.5 at Munali to 7.3 at King Edward. The Eh of the soils and streams was not measured, but they are clearly well-aerated, oxidizing environments and can be estimated to have an Eh between +0.4 and +0.6. The Fe^{2+} and Mn^{2+} activities illustrated in figure 20 are about average for natural soil and stream water, and the Fe^{2+} - $Fe(OH)_3$ and Mn^{2+} - MnO_2 interfaces shift to the left at higher activity levels.

Figure 20 shows that in the environments of the orientation samples, the formation of MnO_2 is unlikely. The only exception could be the King Edward stream, where the known high pH might be linked with a sufficiently high Eh to cause a little MnO_2 precipitation. The formation of $Fe(OH)_3$, which would dehydrate to goethite, is more readily favoured, although fairly high pH and Eh conditions would be necessary for significant quantities to form, except where high Fe^{2+} concentrations are present. Pyrrhotite, one of the principal minerals of nickel sulphide ores, has a high Fe content, and pyrite and other iron-bearing sulphides are usually associated with such ores. As figure 20 demonstrates, pyrite (and presumably other Fe sulphides) releases Fe^{2+} into solution in acid, mildly oxidizing environments, and such conditions are present in the upper zones of sulphide orebodies in contact with slightly aerated waters. Thus in mineralized areas, Fe^{2+} activity is likely to be exceptionally high and in soil and stream environments the Fe^{2+} - $Fe(OH)_3$ boundary is moved in favour of Fe oxide formation. This accounts for the X-ray diffraction identification of crystalline goethite in soils and stream sediments at Munali, where there is massive sulphide ore at depth. At Trojan, the other mineralized area, goethite was not noted in X-ray diffraction studies, and may be less conspicuous because Trojan ore is disseminated, while failure to identify goethite elsewhere is attributed to the absence of mineralization.

The orientation study results suggested that the more

consistent mineralogy of the fine fraction commended its
adoption for general analysis for total metal, while the
coarse fraction warranted further study on a limited scale.

3.2   Total metals by atomic absorption spectrophotometry

Atomic absorption analysis is a relatively high-
precision technique and was adopted for total metal determination
of all those trace elements characteristic of primary nickel
mineralization and the mafic-ultramafic suite amenable to the
technique. Total metals analysis was carried out by weighing
250 mg of sample into a test tube and adding about 5 ml of
4:1 HNO_3-$HClO_4$. The samples were taken to dryness in an air
bath by gentle heating over 36 to 48 hours, and then leached
in 2 ml of 6M HCl on a warm sand bath. The solutions were made
up to 12.5 ml with deionized water, and analysed for Ni, Cu, Co,
Zn, Cr, Fe, Mn and Ti by atomic absorption spectrophotometry using
a Perkin-Elmer 403 spectrophotometer with an air-acetylene flame
and Perkin Elmer hollow cathode lamps. The HNO_3-$HClO_4$ attack
takes into solution all the Ni, Cu, Co, Zn and Mn content of
biotite, limonite and olivine, and 40 to 80% of the total amounts
of each of these metals in amphiboles and pyroxenes (Foster, 1973).
Chromium, Fe and Ti results are not necessarily total metal,
because HNO_3-$HClO_4$ performs only a limited attack on any resistant
oxide minerals, such as chromite, ilmenite and magnetite, which
may be present in the sample. The samples analysed comprised the
fine fraction of all pit profile, soil and stream sediment samples,
and the coarse fraction of some of these samples, and DDH MH58
core. The samples were analysed in 10 batches, each containing
several blanks, three soil standards and about 10% duplicate samples.

Most blanks contained no trace elements, but small
quantities of Zn, exceptionally reaching the equivalent of 25 ppm,
were not uncommon and are attributed to either imperfectly deionized
water or the attack of metallic parts of acid dispensers. A few
traces of Cr, with a maximum equivalent of 65 ppm, are thought to
originate from the handling of asbestos sheets used to cover the
tops of partially empty air baths during sample preparation.

The results of 10 replicate analyses of each of three
soil standards show minimal variation (figures 21 and 22) with few
exceptions. There is one exceptionally high Ti result and one high
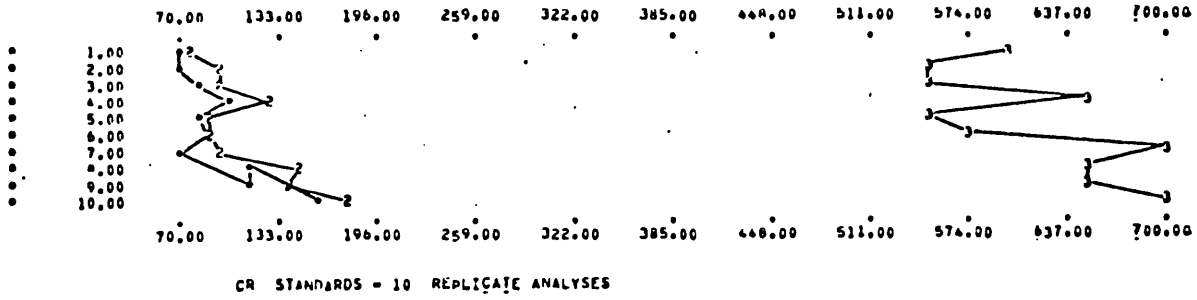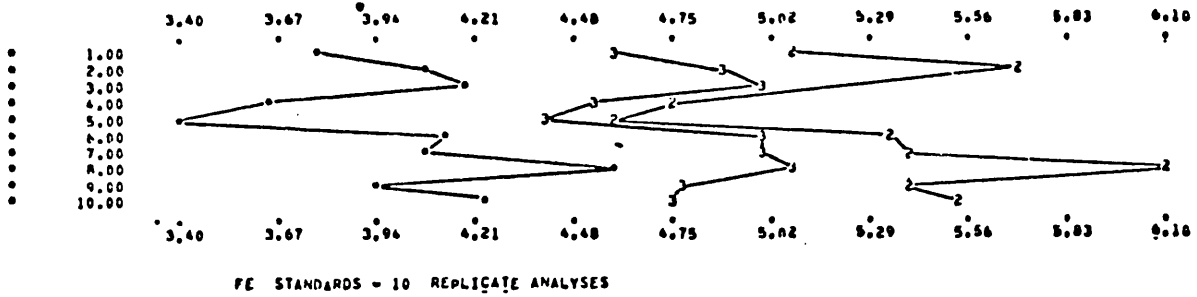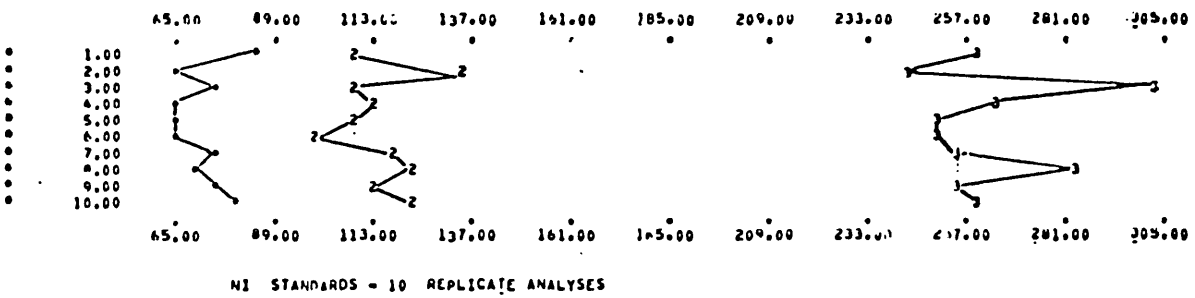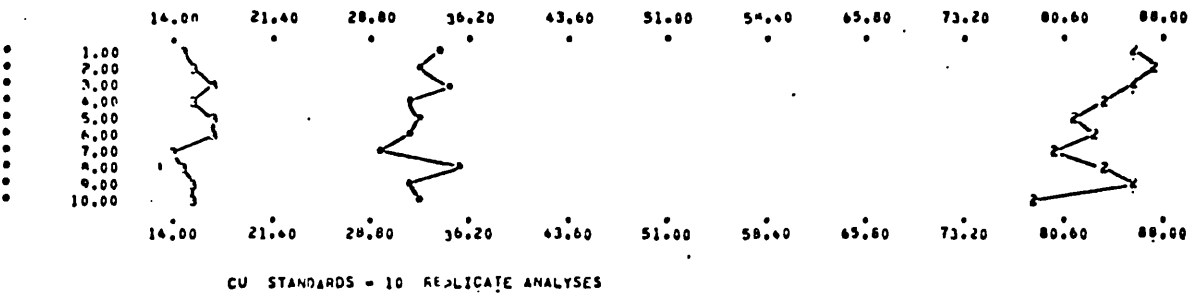
Figure 21: Atomic absorption analysis inter-batch variation of Cr, Fe, Ni and Cu standards (ppm, except Fe in %).

ANALYTICAL RESULTS CO

CO STANDARDS - 10 REPLICATE ANALYSES

ANALYTICAL RESULTS ZN

ZN STANDARDS - 10 REPLICATE ANALYSES

ANALYTICAL RESULTS TI

TI STANDARDS - 10 REPLICATE ANALYSES

ANALYTICAL RESULTS MN

MN STANDARDS - 10 REPLICATE ANALYSES
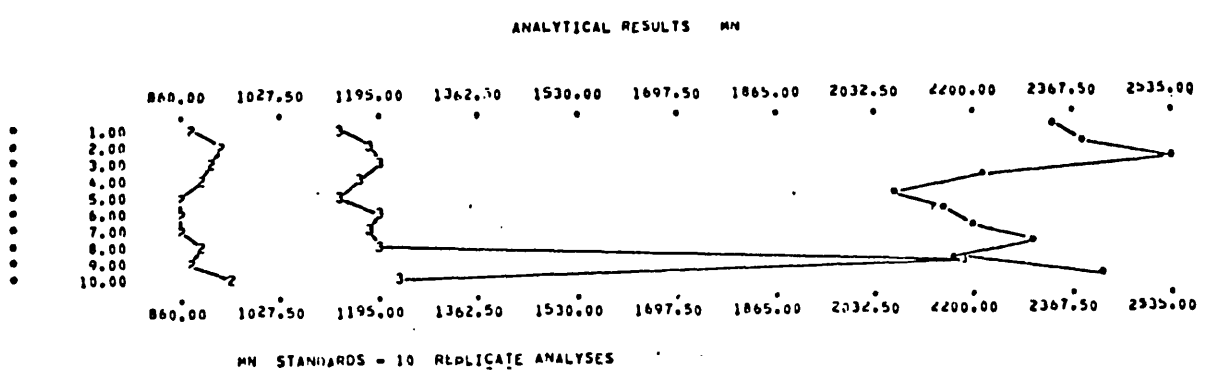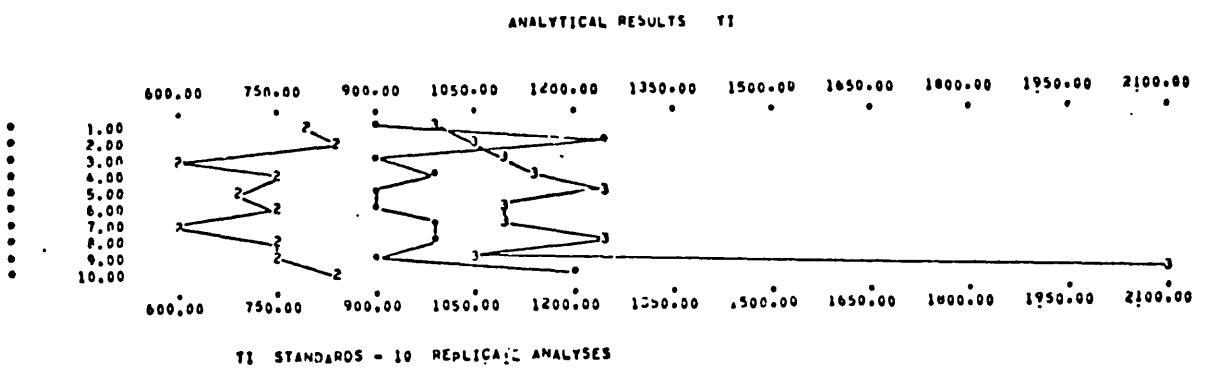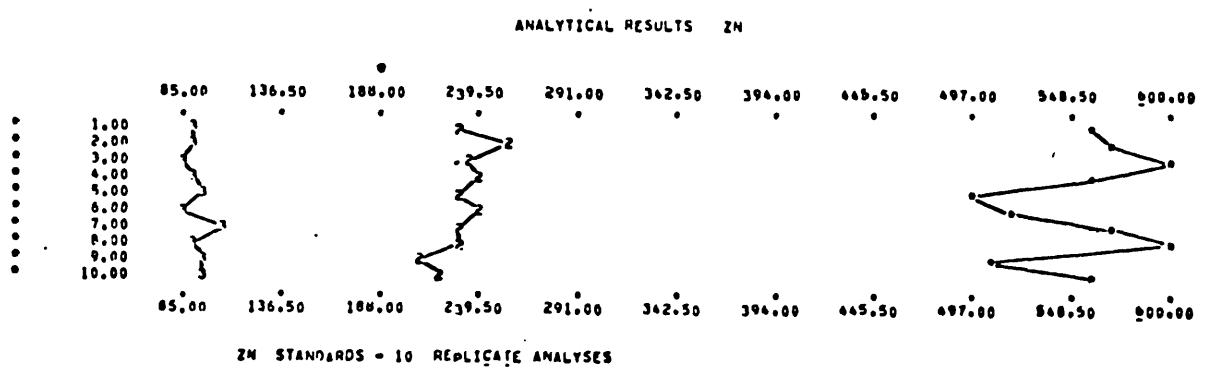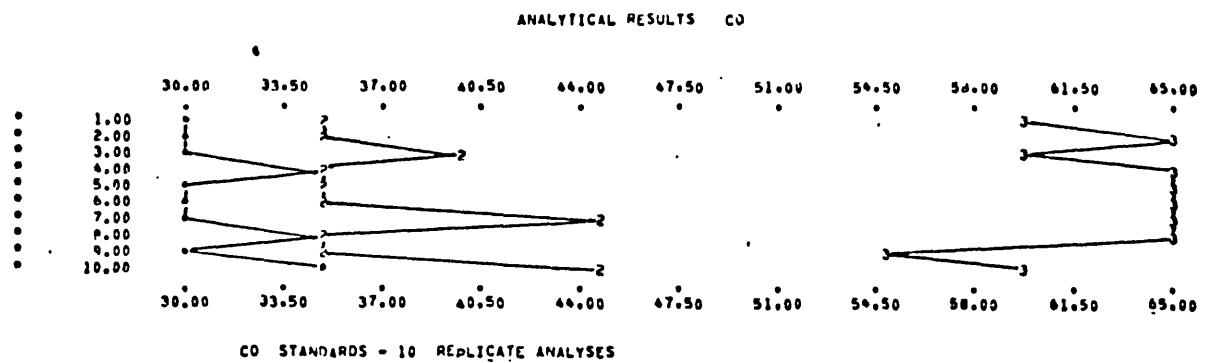
Figure 22: Atomic absorption analysis, inter-batch variation of Co, Zn,
Ti, and Mn standards (ppm)

Element	Coefficient	Intercept	Asymptotic Precision (%)	Limit of Detection(ppm)
Ni	0.046214	-4.431260	9.243	-4.4
Cu	0.021200	0.768869	4.240	0.8
Co	0.014784	3.459603	2.957	3.5
Zn	0.004997	2.981171	0.999	3.0
Cr	0.031960	17.057327	6.392	17.1
Fe	0.035895	0.011103	7.179	111.0
Ti	0.082632	23.950476	16.526	24.0
Mn	0.030675	4.062469	6.135	4.1

Table 5: Atomic absorption analysis, precision and limits of detection for elements determined

Mn result. Iron results are slightly erratic although variations are consistent in each of the three standards. This variability in Fe standards is attributed to the absorption of minor amounts of Fe onto hydrolysed colloidal silica. The silica hydrolysis itself is probably a function of the standing time of sample solutions prior to atomic absorption analysis. Colloidal Fe precipitation evidently did not cause co-precipitation of other metals.

For precision determination a total of 120 samples were analysed in duplicate. The means and differences of duplicates were used to evaluate precision employing a computer program PRESIN which incorporates a subroutine DUPAN2 (Thompson and Howarth, 1976). The program calculates the coefficient and intercept of the function of mean element concentration verus standard deviation (or difference) for duplicate pairs, and provides a matrix illustrating the distribution of concentrations and differences (appendix 3). From the coefficient an estimate of asymptotic precision (in percent) can be calculated, and the intercept is roughly equivalent to the limit of detection (table 5).

The analytical results of replicate standards and duplicate samples are considered to render the analytical results for this technique thoroughly satisfactory.

3.3.   Total metals by emission spectrography

Core and outcrop samples, fine fraction pit profile and soil samples, and regional drainage sample suites were analysed by an ARL direct-reading emission spectrometer for Fe, Mn, Cu, Pb, Zn, Cd, Ag, Mo, V, Co, Ni, Cr, Ga, Sn, Ti, Be, Mg, Ca, Sr, Ba, K, Li, Al, Sc and Si. The samples were analysed in four batches according to sample type. The sample order within each batch was randomized and each batch required several days for analysis.

The analytical technique is a standard AGRC procedure. In preparing samples for analysis each sample, except core and outcrop samples, was first ignited in a furnace at 450°C to drive off organic matter which would otherwise volatilize during analysis and cause interference by flooding the arc source with gases. Then 100 mg of

ignited sample was mixed with 150 mg of buffer comprising a 1:2 mixture of sodium fluoride and carbon powder. A portion of this was packed into the conical cavity of a carbon rod electrode to provide an estimated sample weight of 35 mg. The electrode sample holder was then fitted into the spectrometer DC arc unit to constitute the cathode, and a current of 8.0 amps was passed for 90 seconds, causing sample volatilization. The light from the arc was dispersed by a plane grating and the intensity of wavelengths of interest was recorded by photomultiplier cells. The initial output from the photocells was electronically converted to digital form and automatically punched onto cards.

Continuous calibration of the spectrograph was maintained by the analysis of three calibrators some 15 times each day. The calibrators comprised:

(a) baseline - specpure silica;

(b) trace   - 63 ppm or 630 ppm of each trace element in a silica matrix

(c) major   - 5%, 10% or 15% of major elements in a silica matrix

Ten rock standards were analysed in replicate to check on inter-batch consistency, while intra-batch precision was monitored by the duplicate analysis of about 10% of samples.

Raw output from the spectrometer was computer processed by day sub-batches, using a procedure which incorporated analytical control. The program, GENSYS, calibrated all channels from the calibrator results, corrected the results of standards and samples accordingly, provided the analytical results (in ppm and percent) for standards and samples, daily summaries of duplicates and precision information, standards results compared with 'grand mean' values and indications of those elements reading high or low on this basis. Each day sub-batch was considered satisfactory on the basis of this information.

AG STANDARDS - 17 REPLICATE ANALYSES

AL STANDARDS - 17 REPLICATE ANALYSES
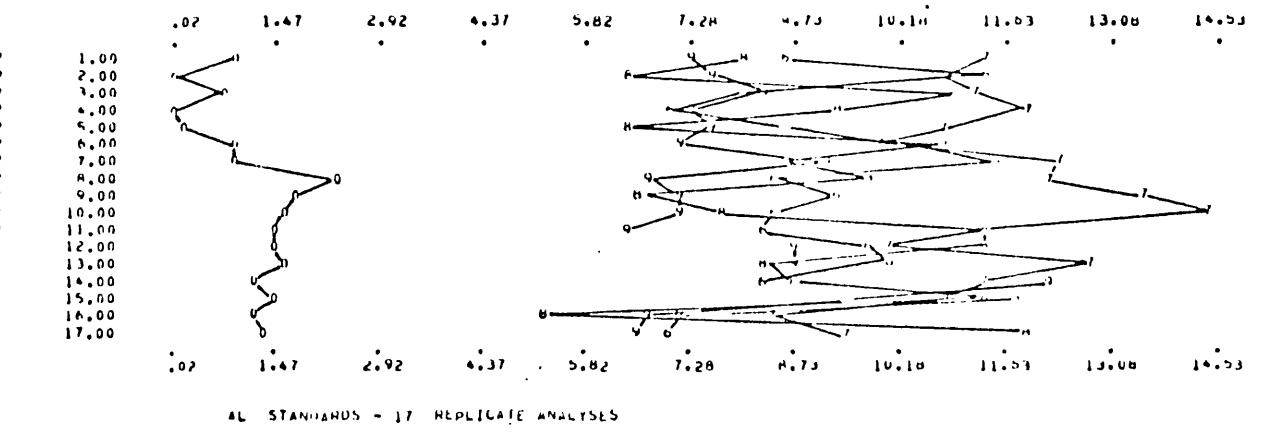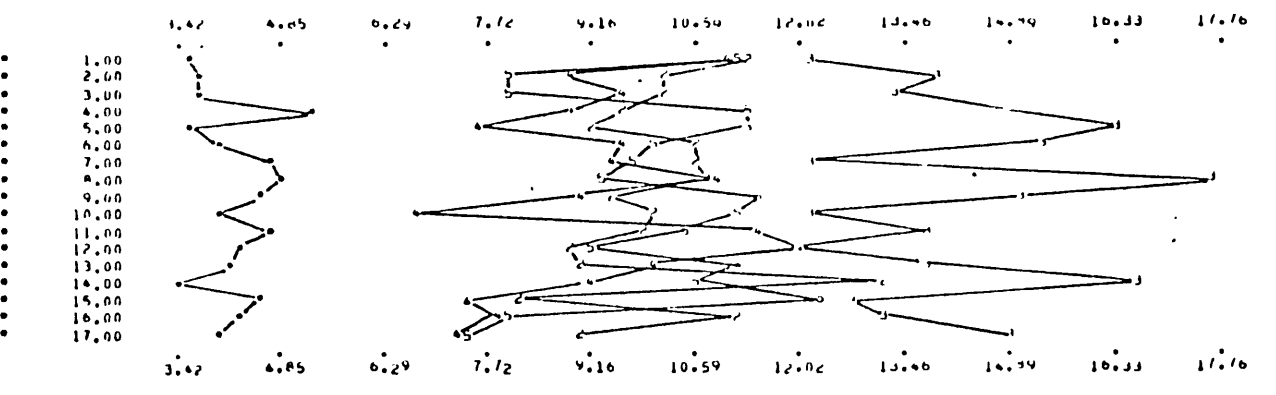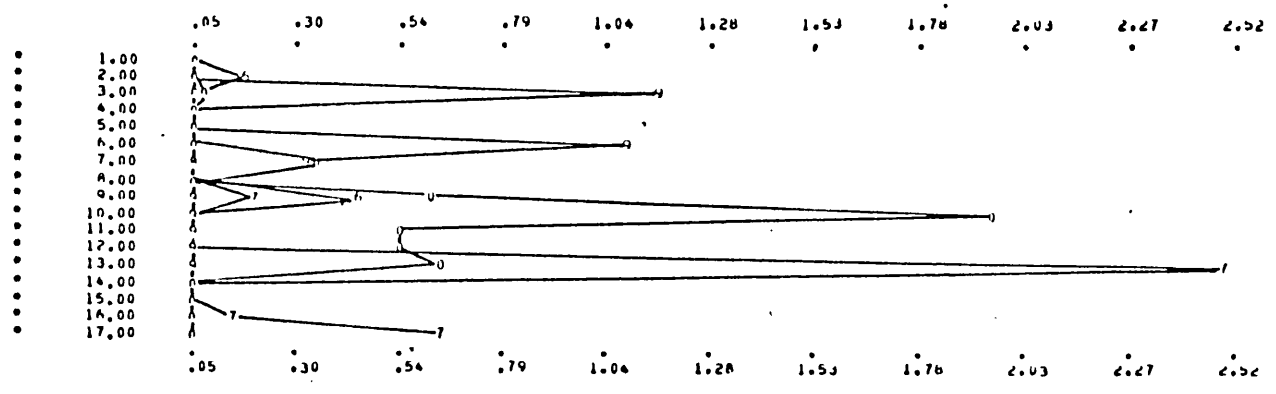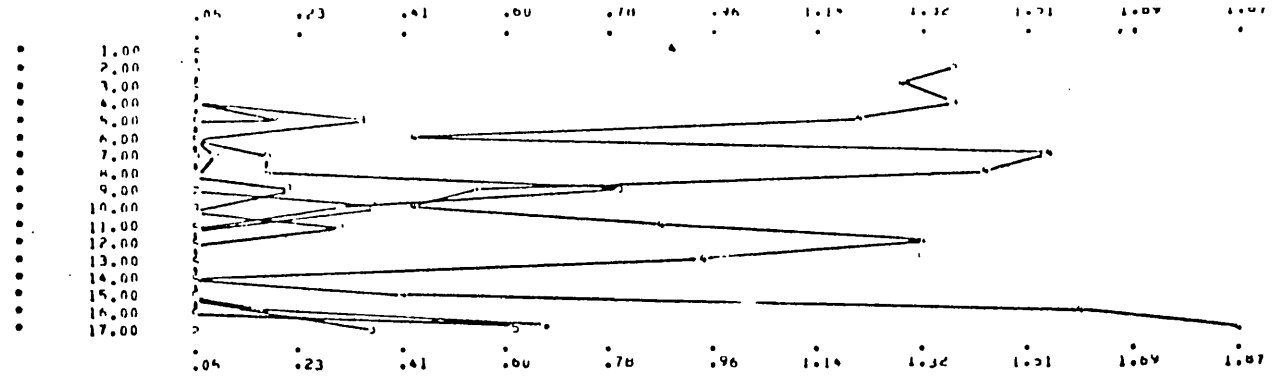
Figure 23:   Emission spectrography standards, Ag (ppm) and Al (%)
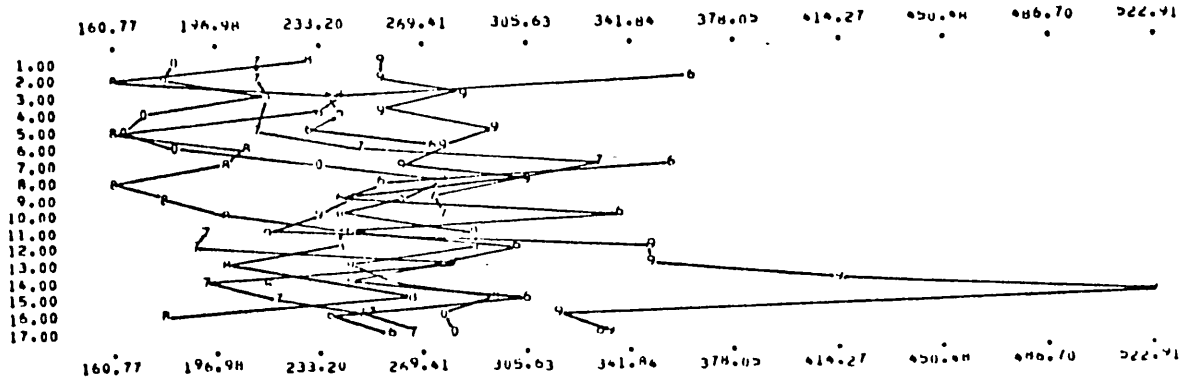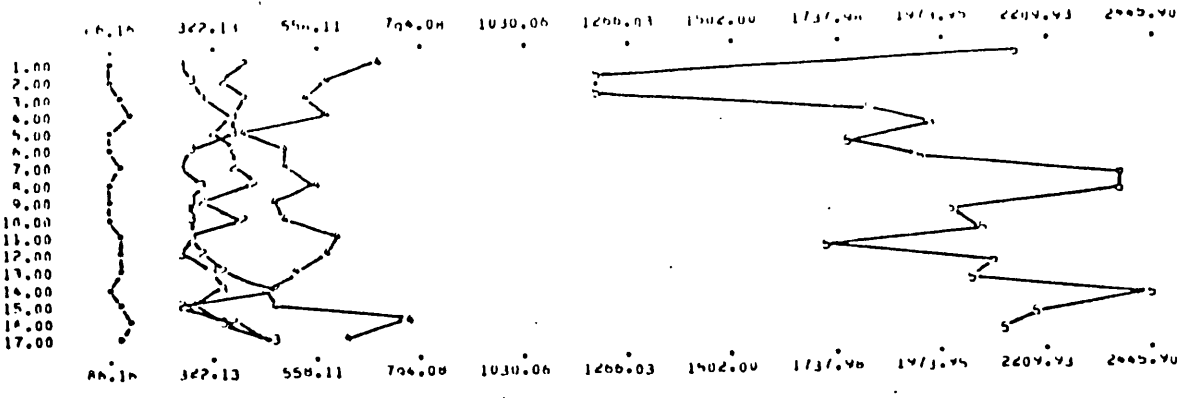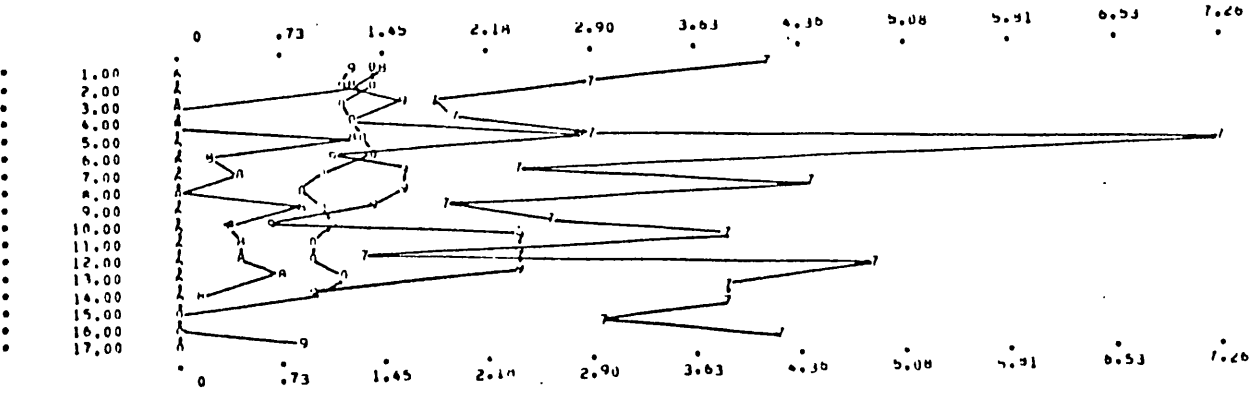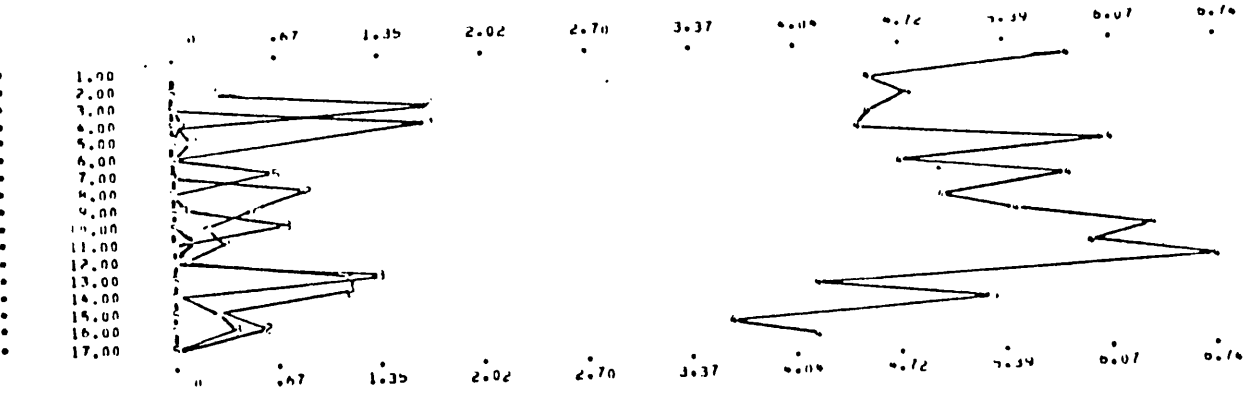
Figure 24: Emission spectrography standards, Ba (ppm) and Be (ppm)
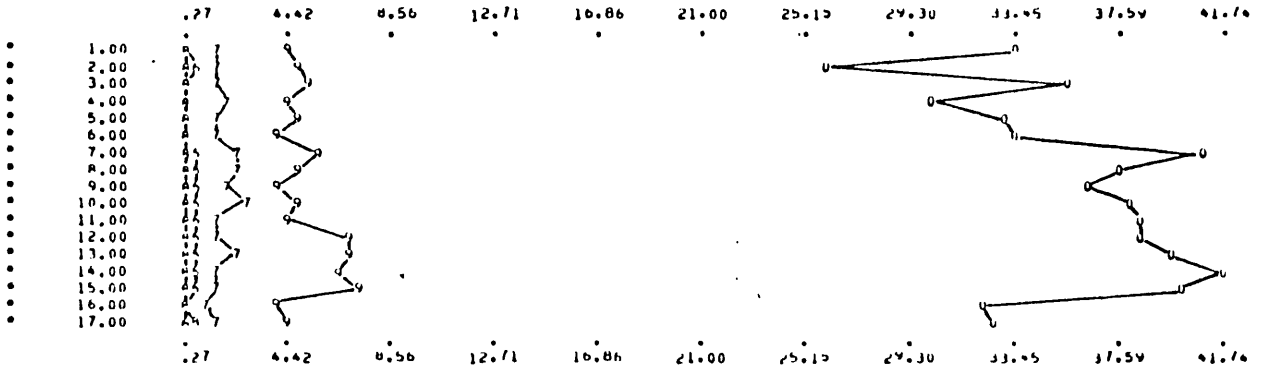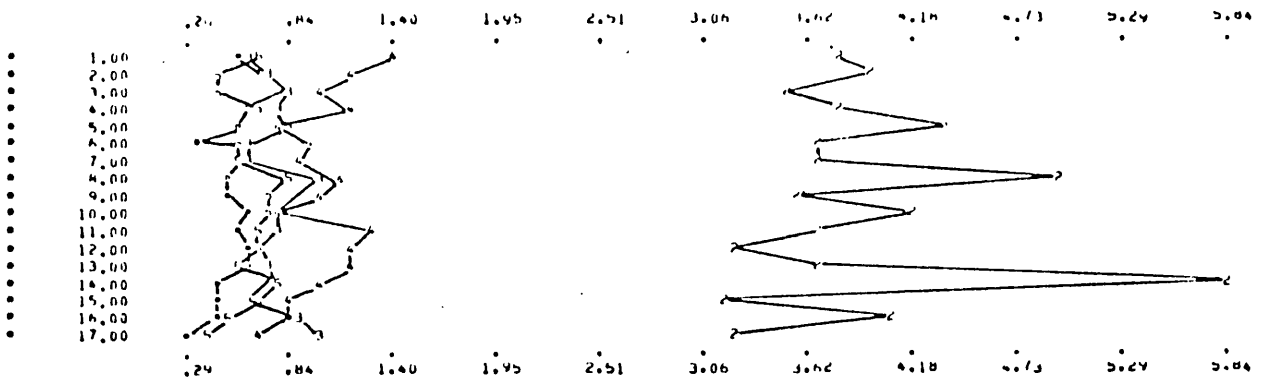
CA STANDARDS - 17 REPLICATE ANALYSES
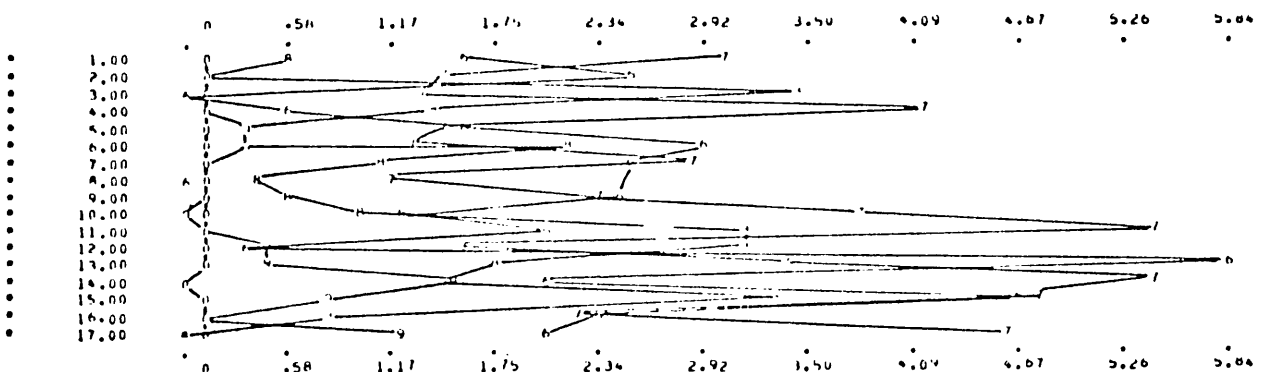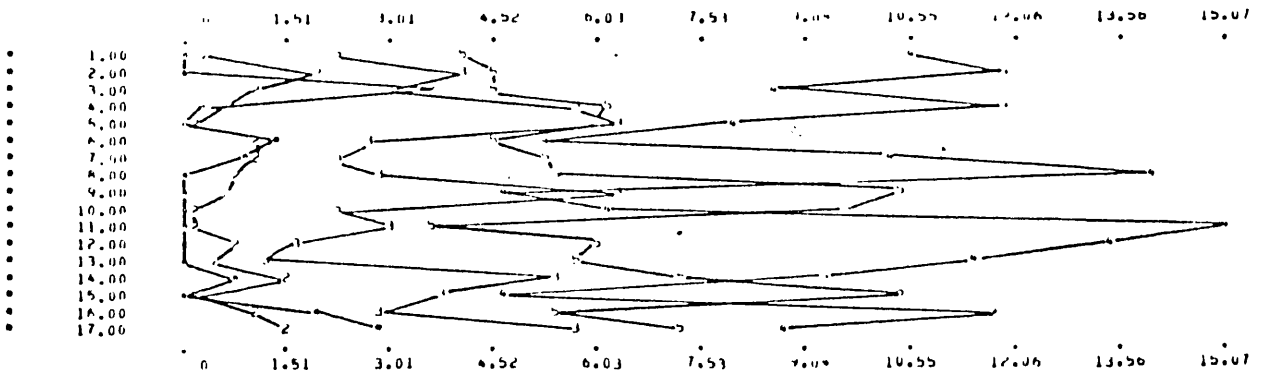
CD STANDARDS - 17 REPLICATE ANALYSES

Figure 25: Emission spectrography standards, Ca (%) and Cd (ppm)
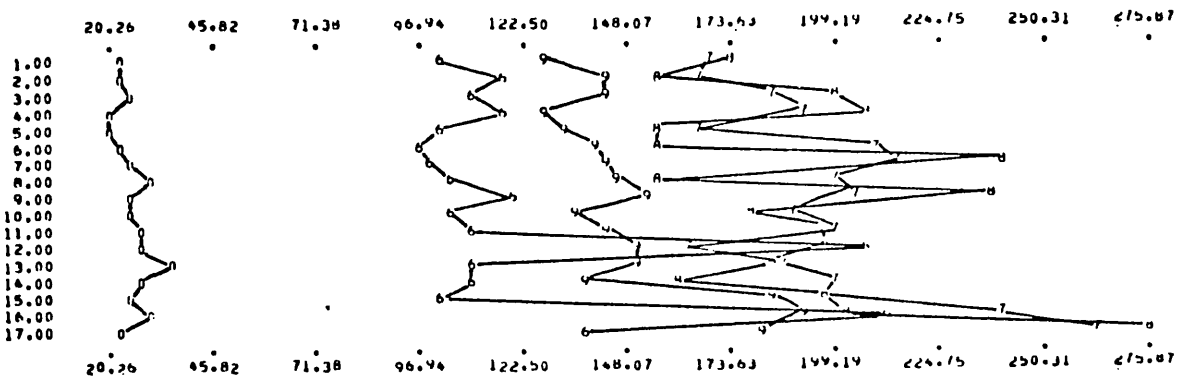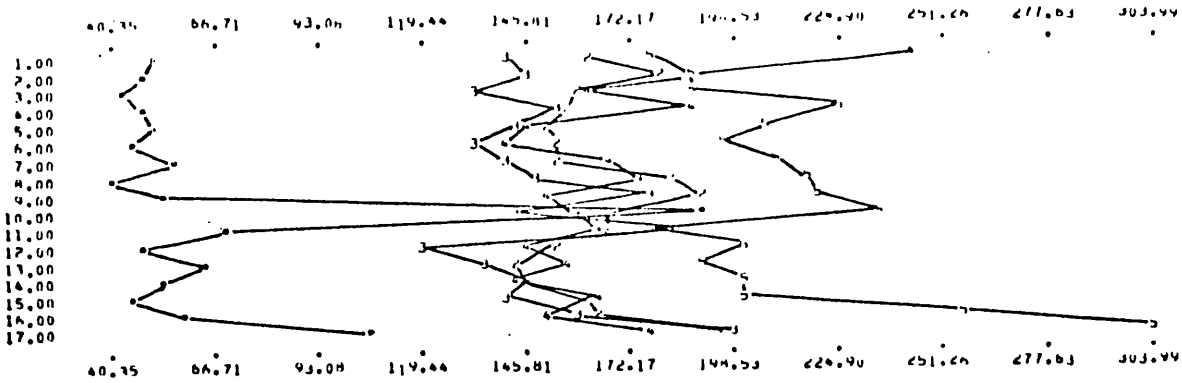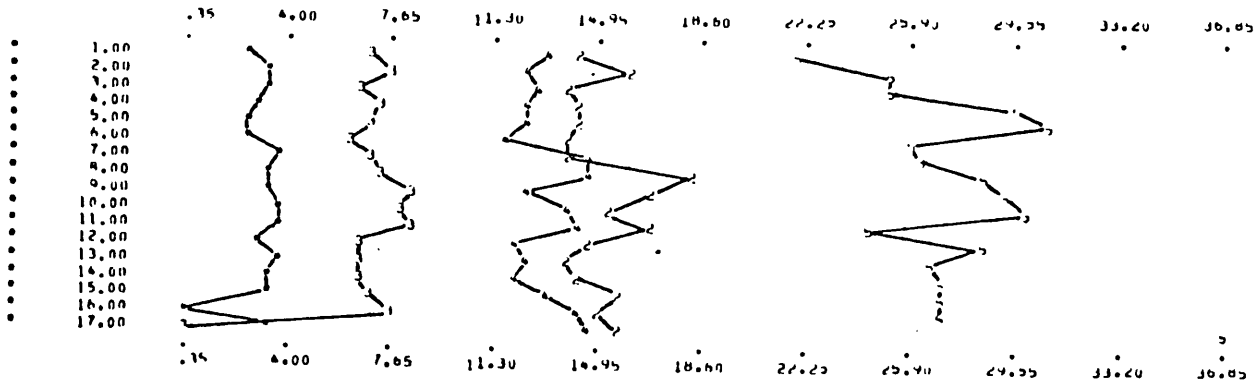
Figure 26: Emission spectrography standards, Cr (ppm) and Co (ppm)
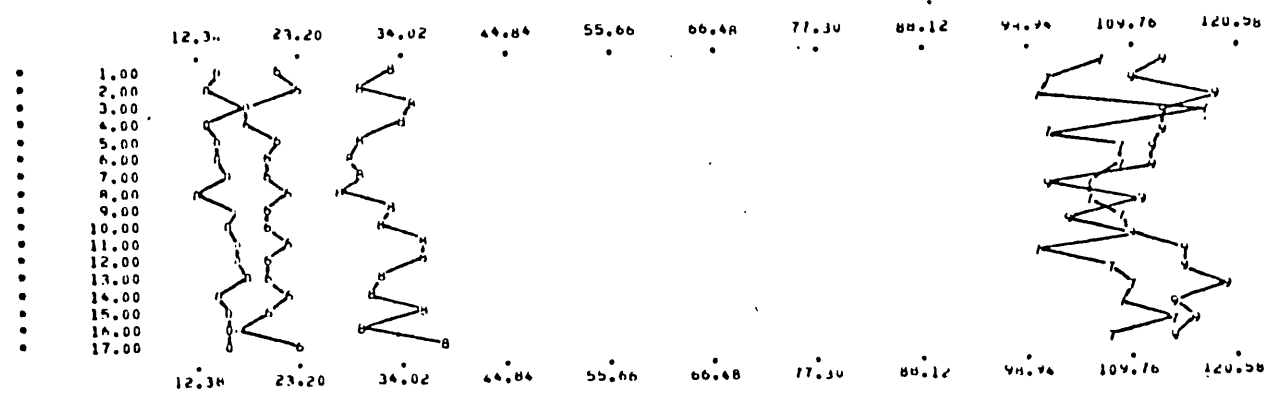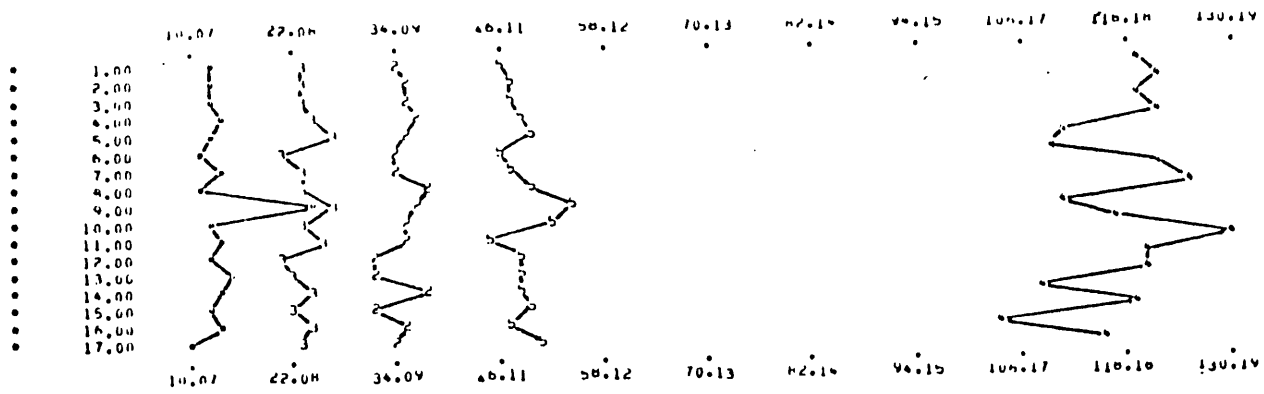
CU STANDARDS - 17 REPLICATE ANALYSES
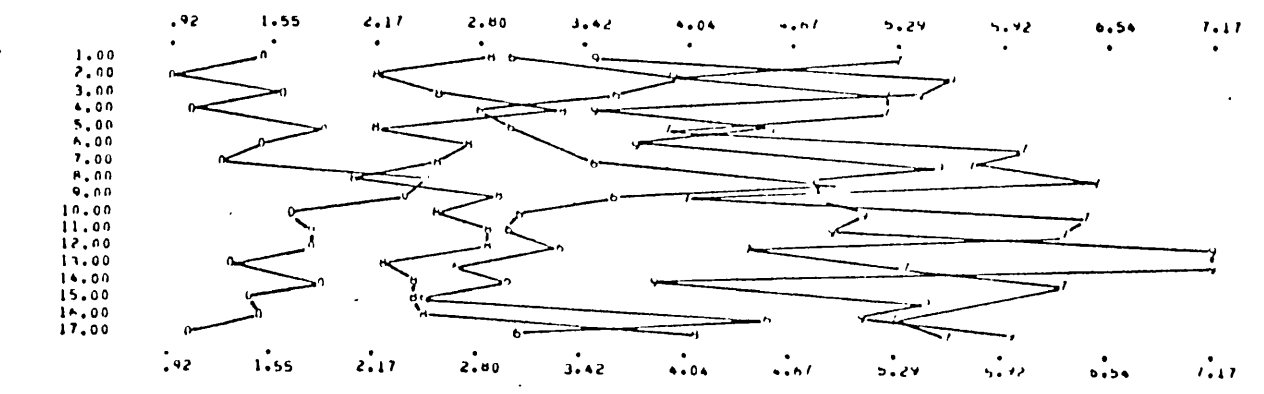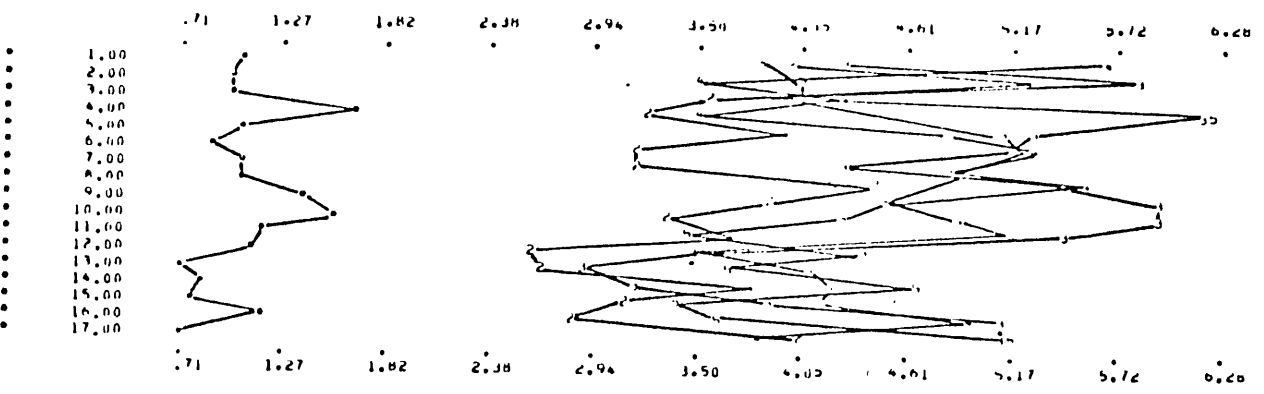
FE STANDARDS - 17 REPLICATE ANALYSIS

Figure 27: Emission spectrography standards, Cu (ppm) and Fe (%)

GA STANDARDS - 17 REPLICATE ANALYSES

K STANDARDS - 17 REPLICATE ANALYSES
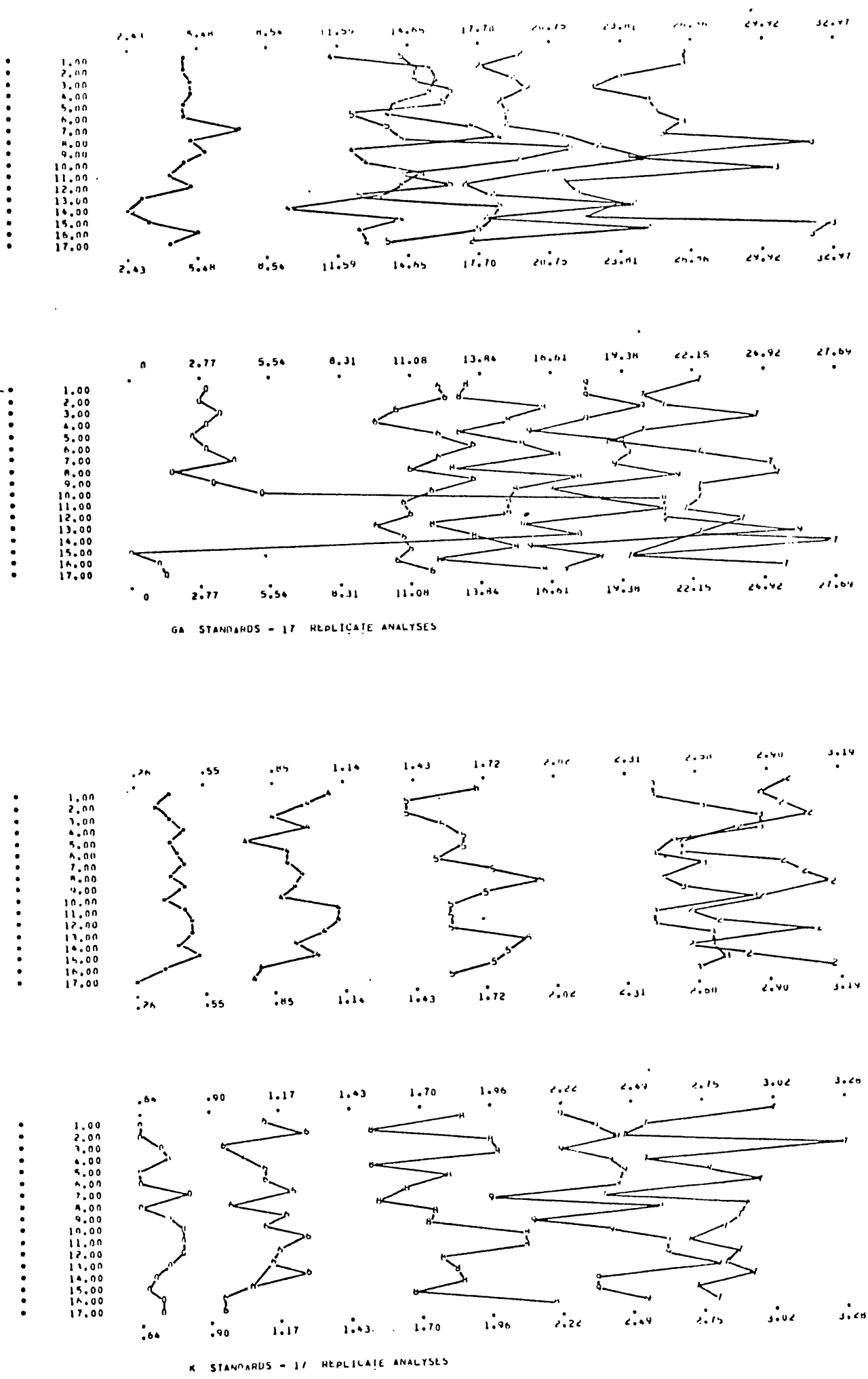
Figure 28: Emission spectrography standards, Ga (ppm) and K (%)
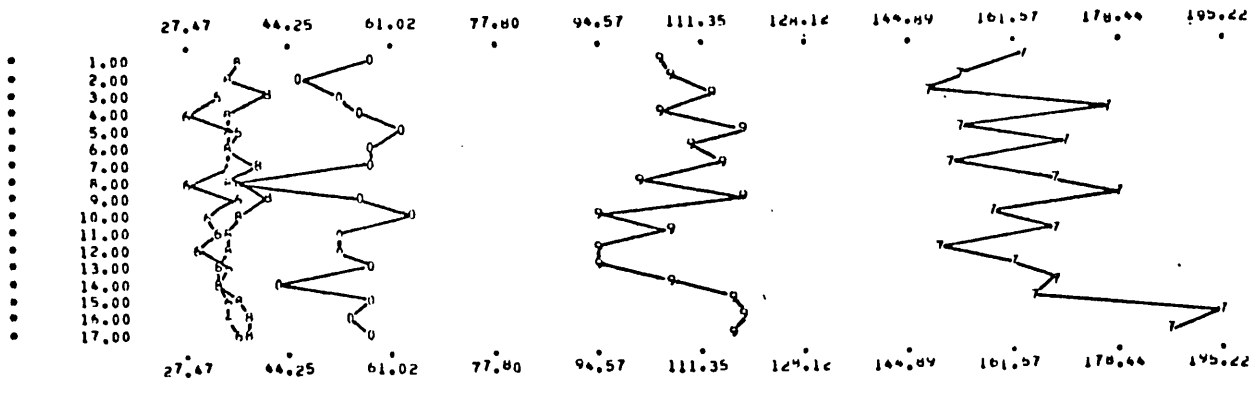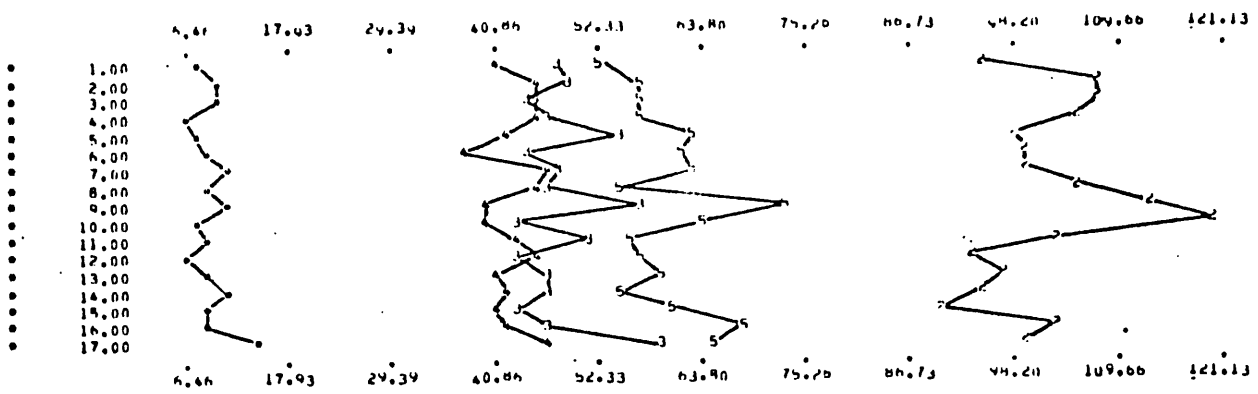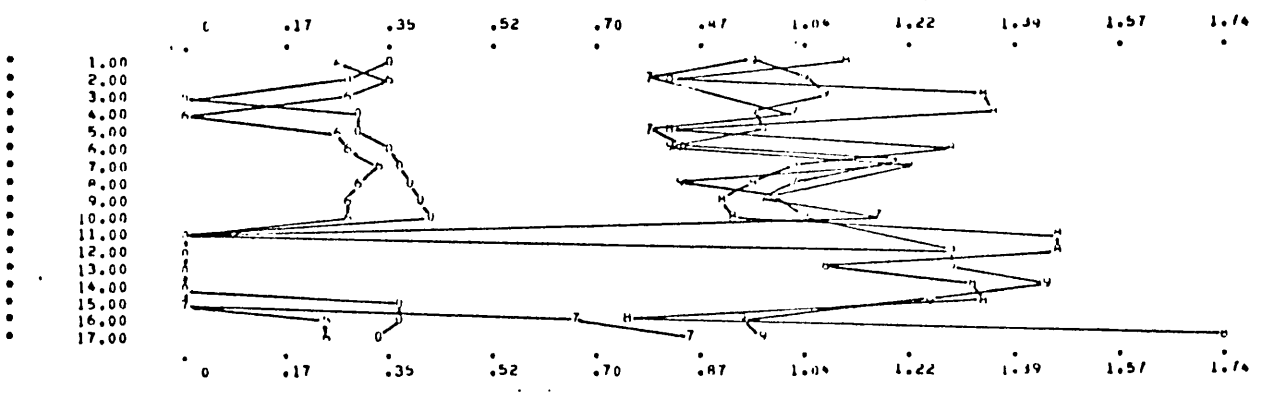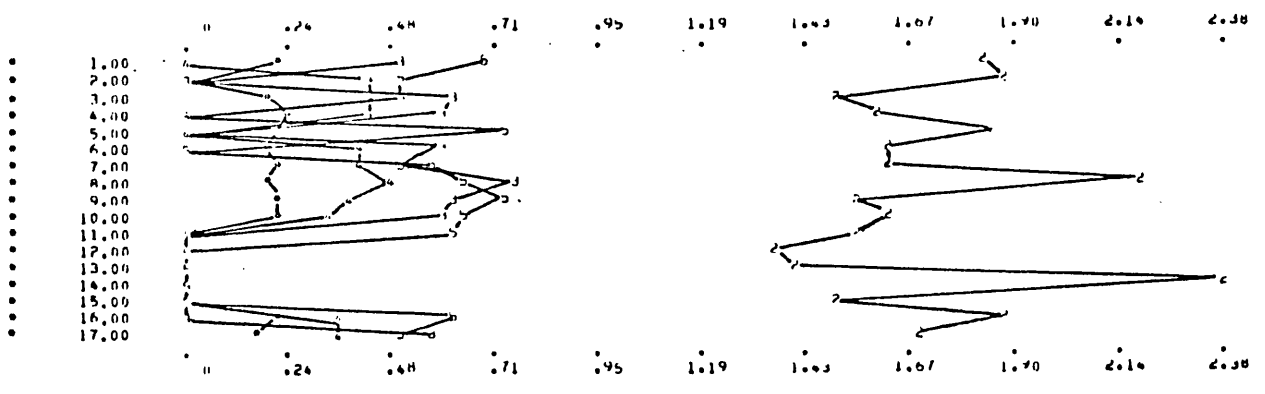
Figure 29: Emission spectrography standards, Li (ppm) and Mg (%)
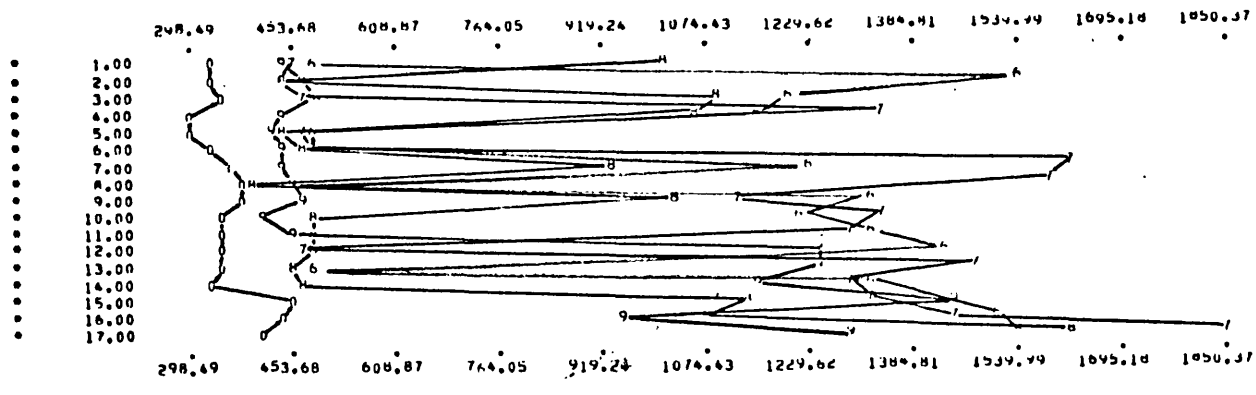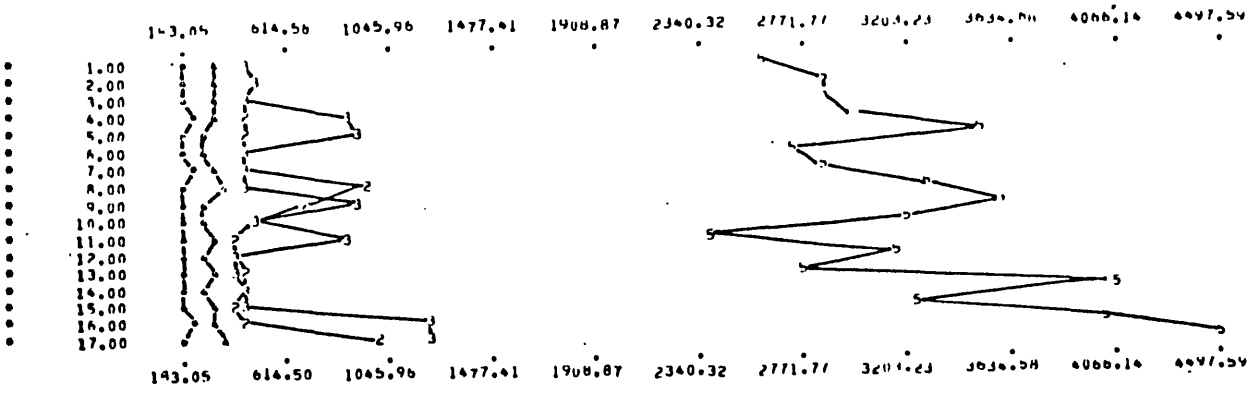
MN STANDARDS - 17 REPLICATE ANALYSES
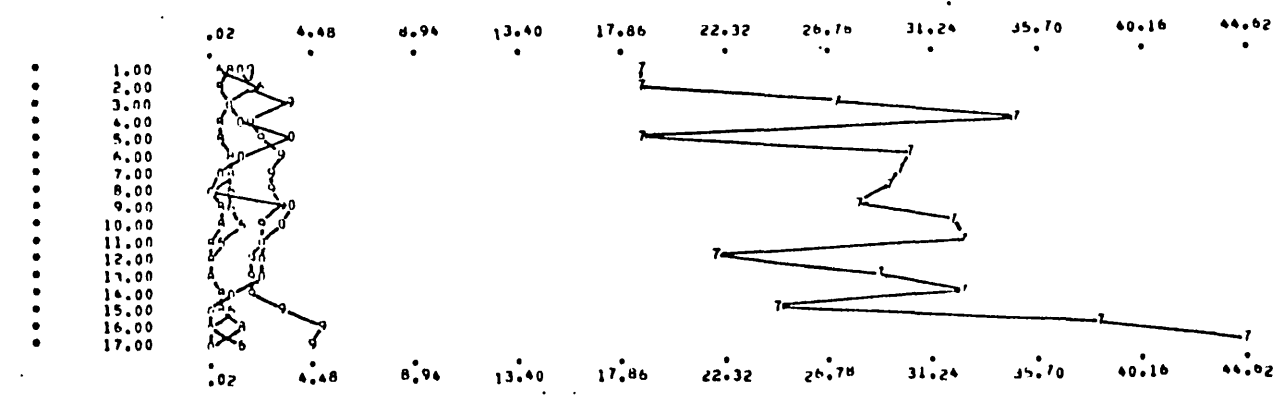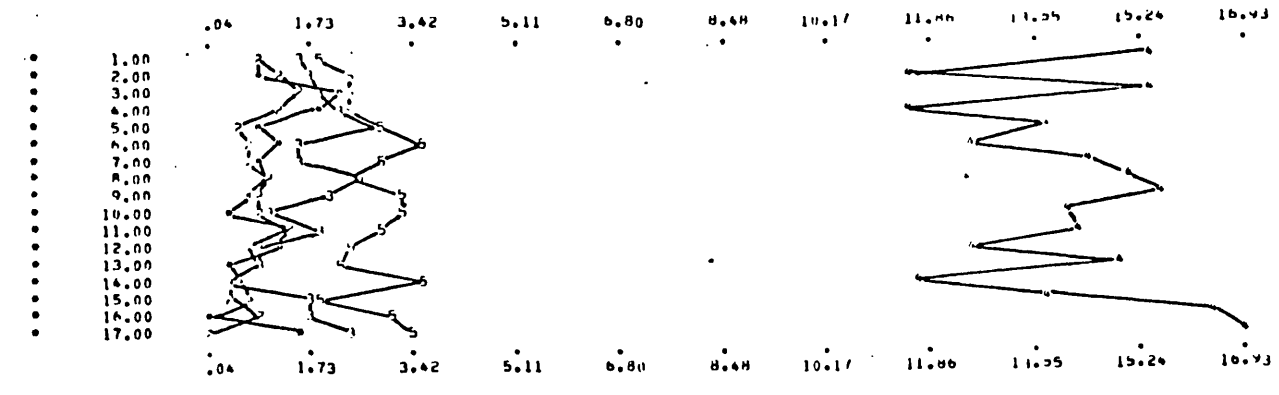
MO STANDARDS - 17 REPLICATE ANALYSES

Figure 30: Emission spectrography standards, Mn (ppm) and Mo (ppm)
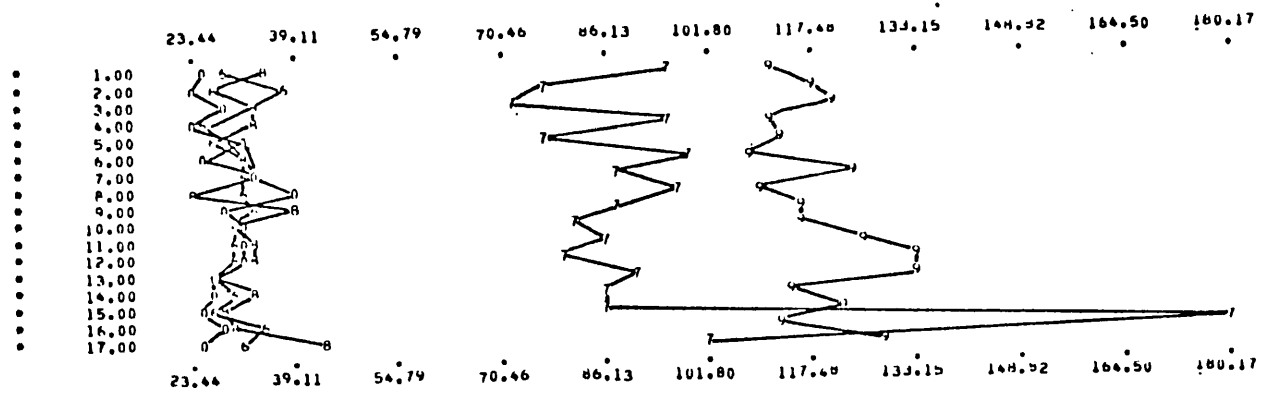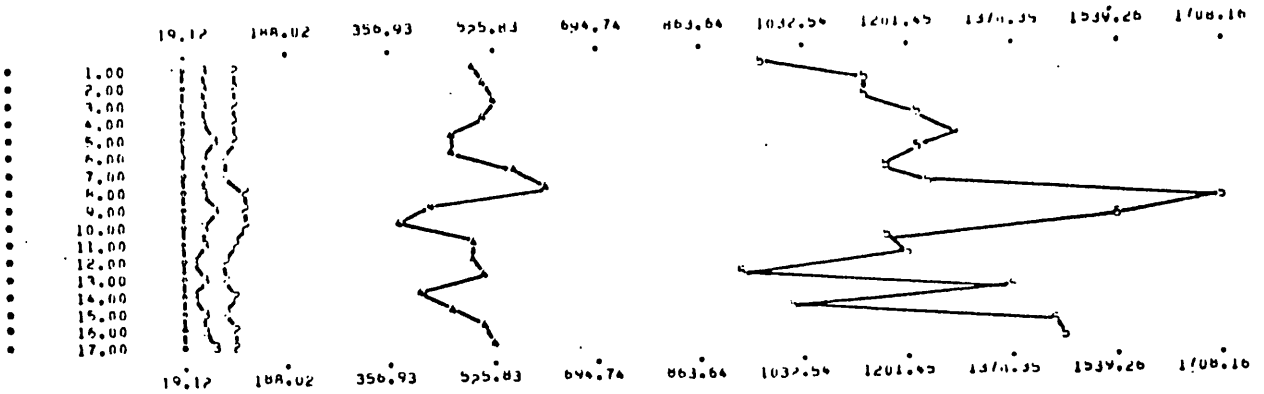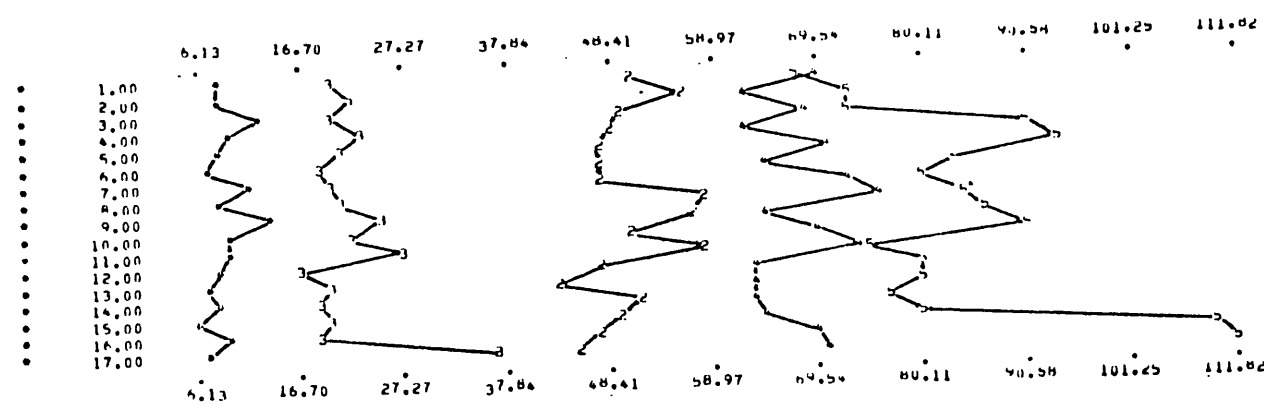
Figure 31: Emission spectrography standards, Pb (ppm) and Ni (ppm)
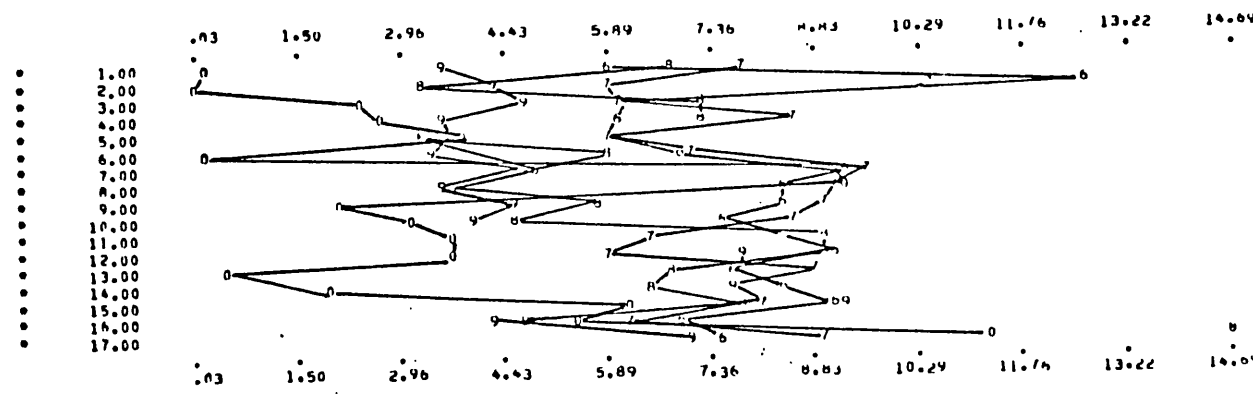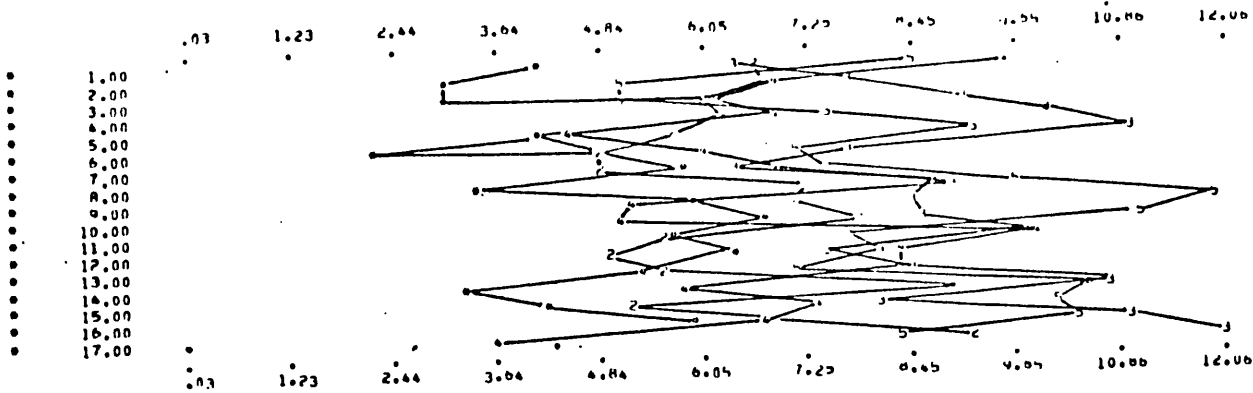
SC STANDARDS - 17 REPLICATE ANALYSES
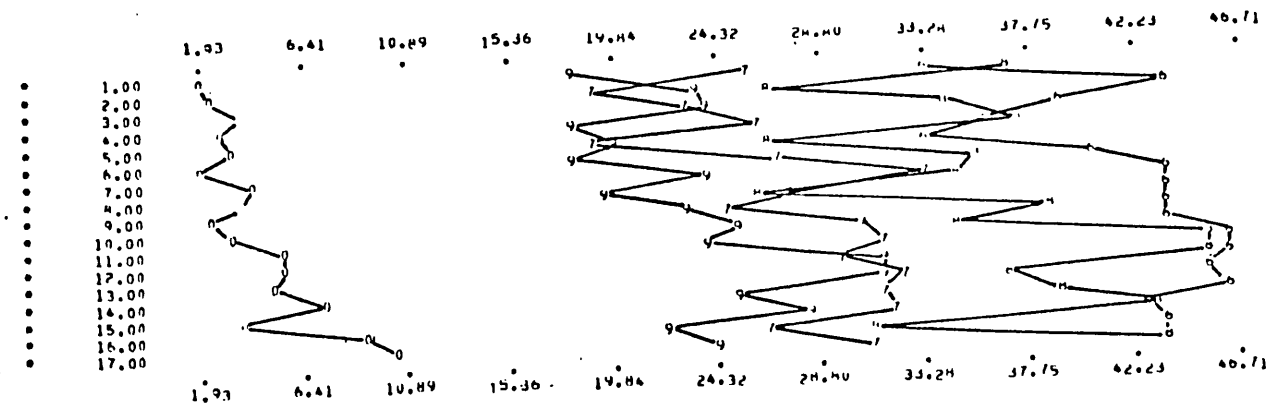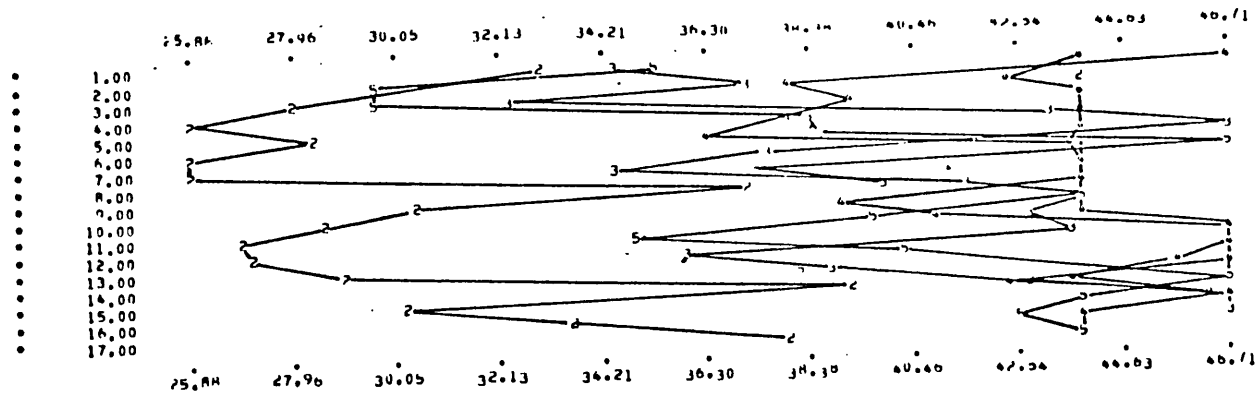
SI STANDARDS - 17 REPLICATE ANALYSES

Figure 32: Emission spectrography standards, Sc (ppm) and Si (%)
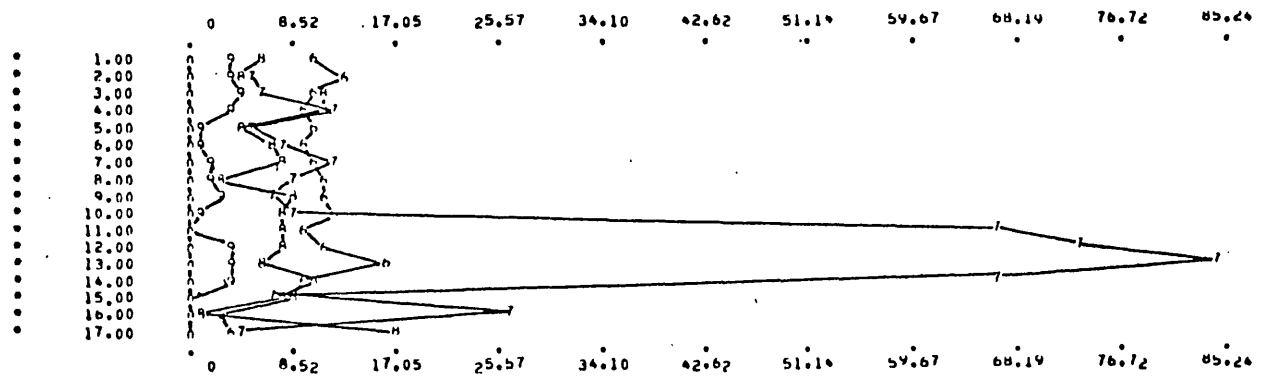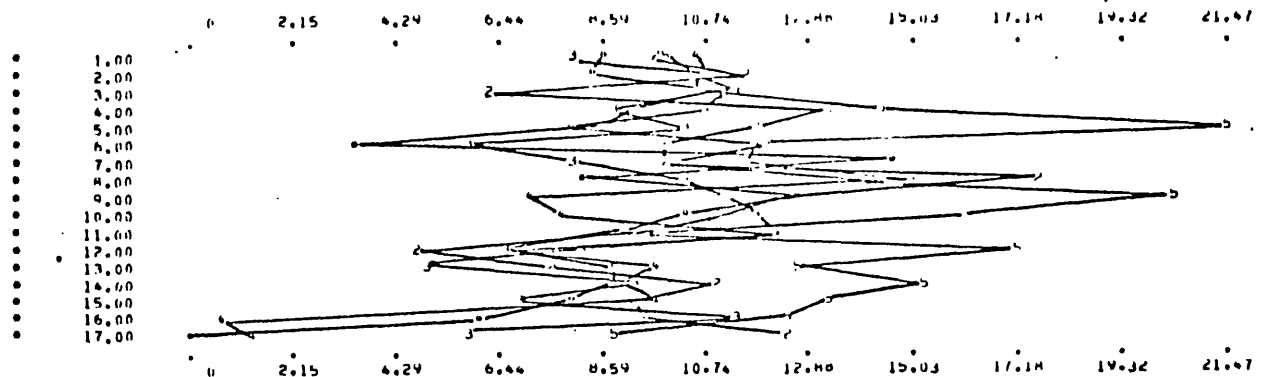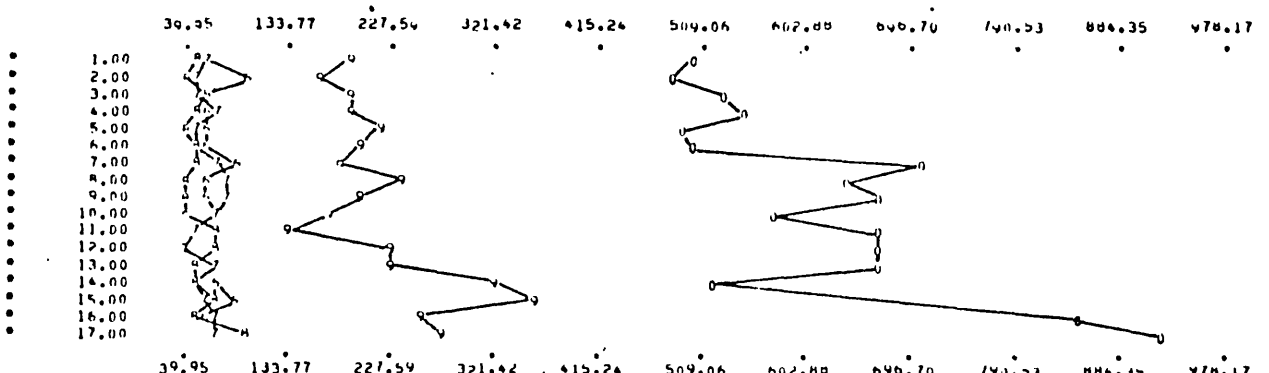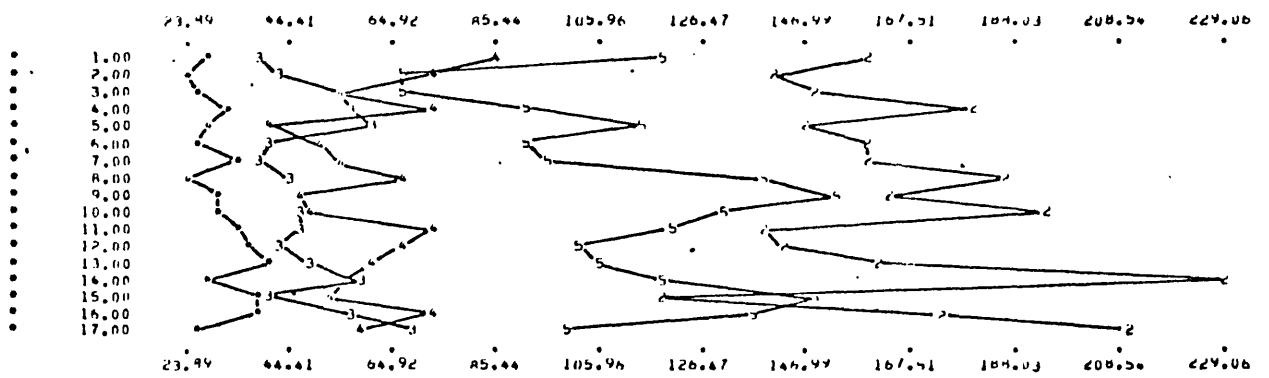
Figure 33: Emission spectrography standards, Sn (ppm) and Sr (ppm)
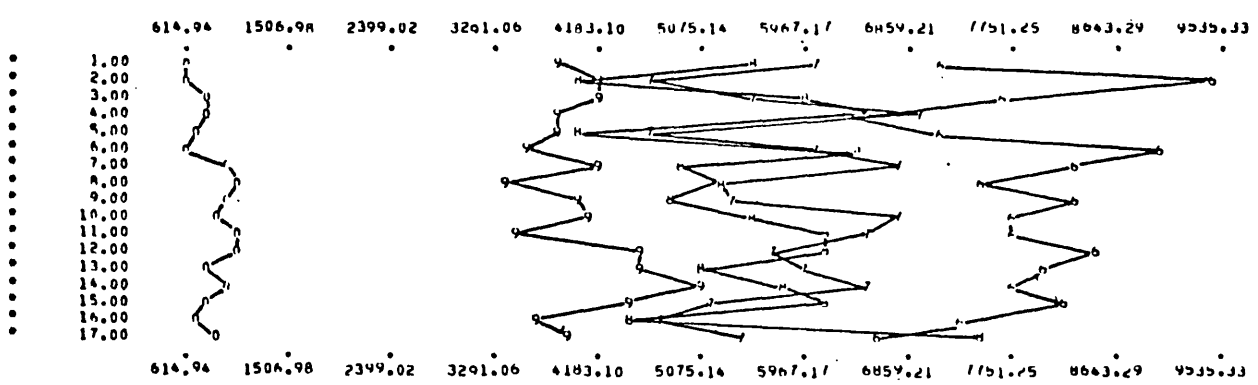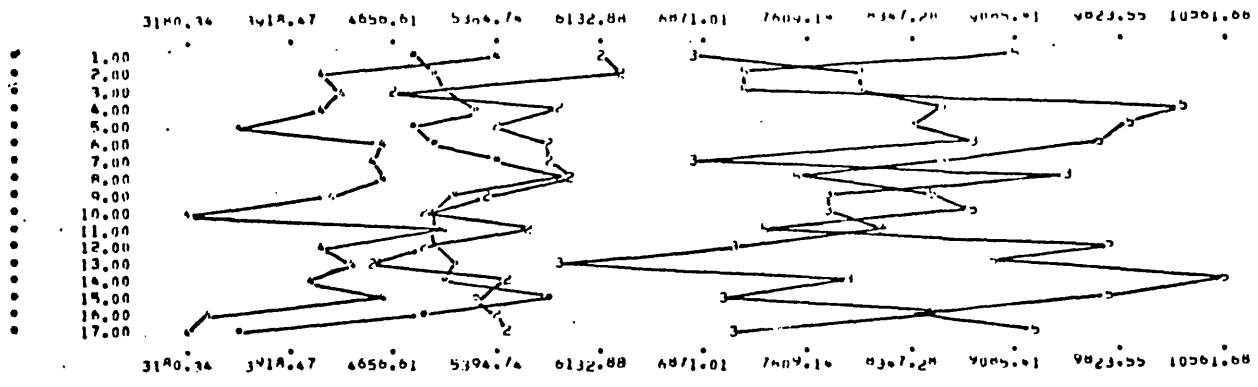
TI STANDARDS - 17 REPLICATE ANALYSES
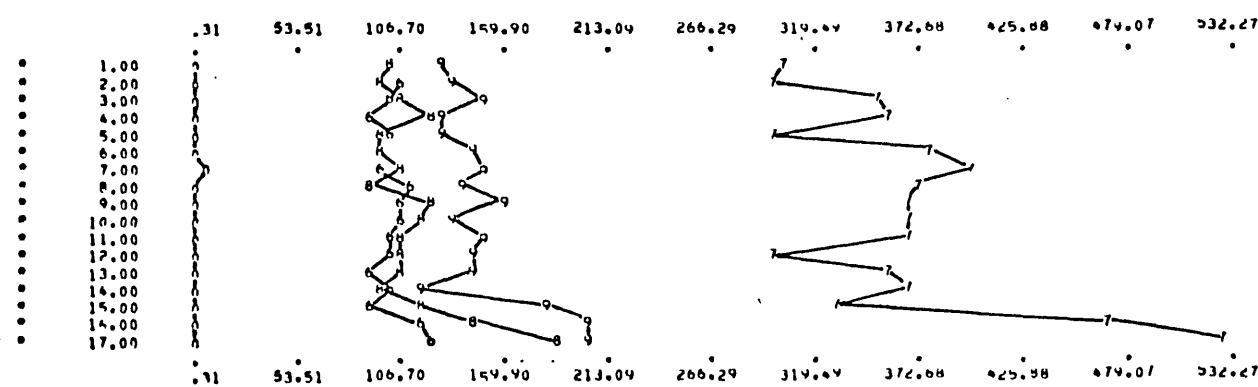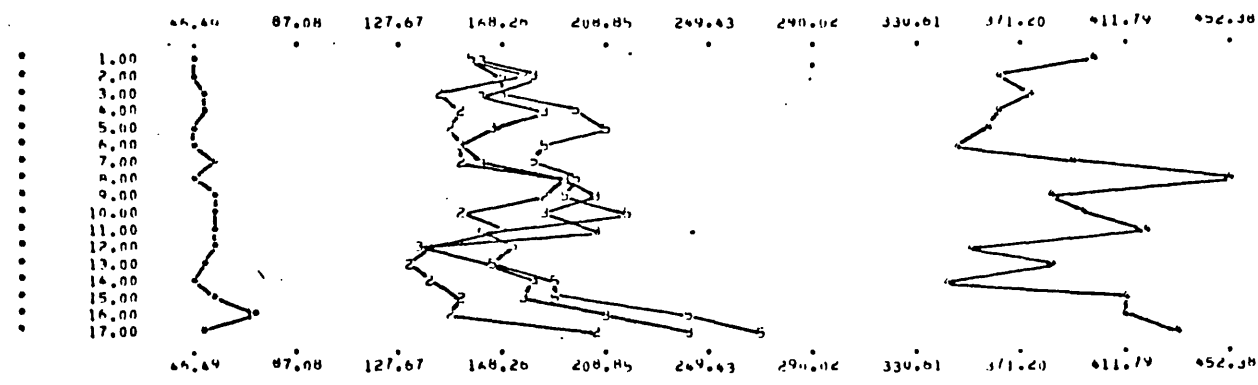
V STANDARDS - 17 REPLICATE ANALYSES

Figure 34: Emission spectrography standards, Ti (ppm) and V (ppm)
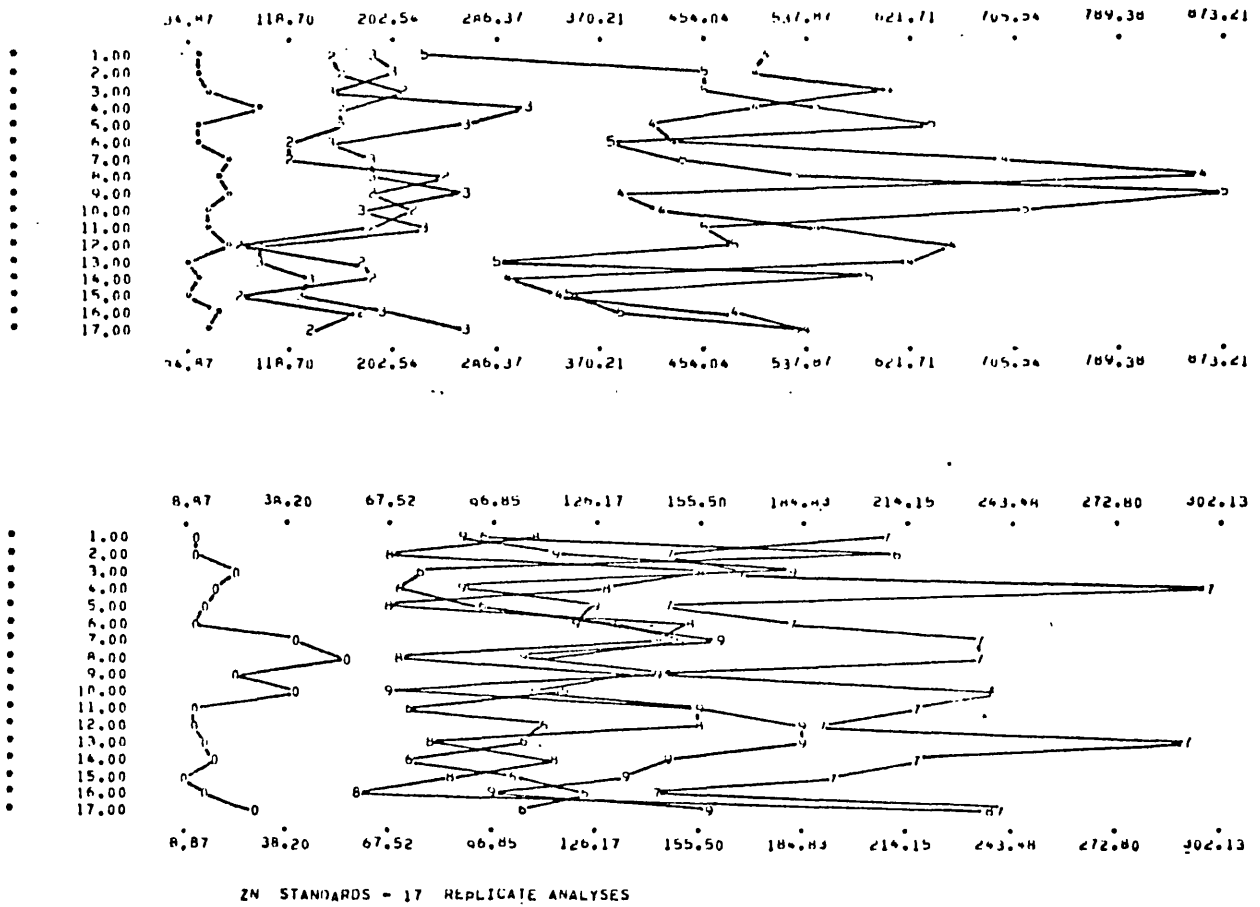
Figure 35: Emission spectrography standards, Zn (ppm)

During the period over which all samples were analysed there were 17 replicate analyses of each of 10 standards and duplicate analyses of 126 samples. The standards results are slightly erratic, but no more so than was to be expected with this technique (figures 23 to 35). The means and differences of duplicate pairs were processed using PRESIN, which produced matrices illustrating the distribution of concentrations and differences in duplicate pairs (appendix 3). This program also computed coefficients and intercepts from which the asymptotic precisions and limits of detection were calculated (table 6). The precision of Zn, Cd, and Ag analyses, of 90%, 153% and 96% respectively, is considered to be bad, and the standards results of these elements are highly erratic. Sample values for Zn, Cd and Ag are not used in the subsequent research. The precisions for Mo at 67%, Be 55% and Sn 44% are regarded as poor, and sample data for these elements are to be treated with caution. Other elements show precision of better than 40%, which is considered satisfactory within the limitations of the analytical technique. Good precision is noted for Ni at 9%, Cu 10%, Cr 12% and Li 12%.

3.4. Trace metals in sulphide minerals.

Two techniques for leaching metals from sulphide minerals were first tested on unweathered core specimens of mineralized Munali gabbro and non-mineralized Paulwi peridotite. One method employed bromine as an oxidizing agent (Czamanske and Ingamells, 1970; Hausen, Ahlrichs and Odekirk, 1973) and the other hydrogen peroxide (Lynch 1971). These tests were intended only to establish which of the two methods yielded the better results when using typical field area specimens, and did not involve detailed studies of the chemistry of the processes.

In the bromine method, the experimental procedure was to weigh 250 mg aliquots of pulverised sample into small beakers and add 12.5 ml of 0.07M HCl solution, followed by 0.5 ml of Br. The beakers were allowed to stand for periods ranging from 30 mins to 5½ hours with gentle agitation at frequent intervals. Then the Br was boiled off at about 65°C, the contents of the beakers were transferred to a test tubes, made up to 12.5 ml with the acid solution, and centrifuged. Finally the extractants were

Element	Coefficient	Intercept	Asymptotic Precision (%)	Limit of Detection (ppm)
Fe	0.211218	0.044519	42.244	445.2
Cu	0.051332	2.388362	10.266	2.4
Pb	0.127912	1.098176	25.582	1.1
Zn	0.451932	-10.900376	90.386	-10.9
Cd	0.766469	0.071764	153.294	0.07
Ag	0.480228	-0.012666	96.046	-0.01
Mo	0.335285	0.139454	67.057	0.1
V	0.100825	2.554173	20.165	2.6
Co	0.091881	0.221137	18.376	0.2
Ni	0.043402	22.080123	8.680	22.1
Cr	0.062151	16.213972	12.430	16.2
Ga	0.161095	-0.276978	32.219	-0.3
Sn	0.222681	1.573211	44.536	1.6
Ti	0.149106	201.465735	29.821	201.5
Be	0.272835	0.070930	54.567	0.07
Mg	0.200087	0.037777	40.017	377.8
Ca	0.161876	0.035928	32.375	359.3
Sr	0.189093	-1.058024	37.819	-1.1
Ba	0.185440	-3.192258	37.088	-3.2
K	0.100004	0.000934	20.001	9.3
Li	0.052868	1.210510	11.736	1.2
Al	0.141413	0.159519	28.283	159.5
Sc	0.098690	1.197299	19.738	1.2
Si	0.186253	-0.812457	37.251	8124.6
Mn	0.165375	79.277446	33.075	79.3

Table 6: Emission spectrographic analysis, precision and limits of detection for elements determined.
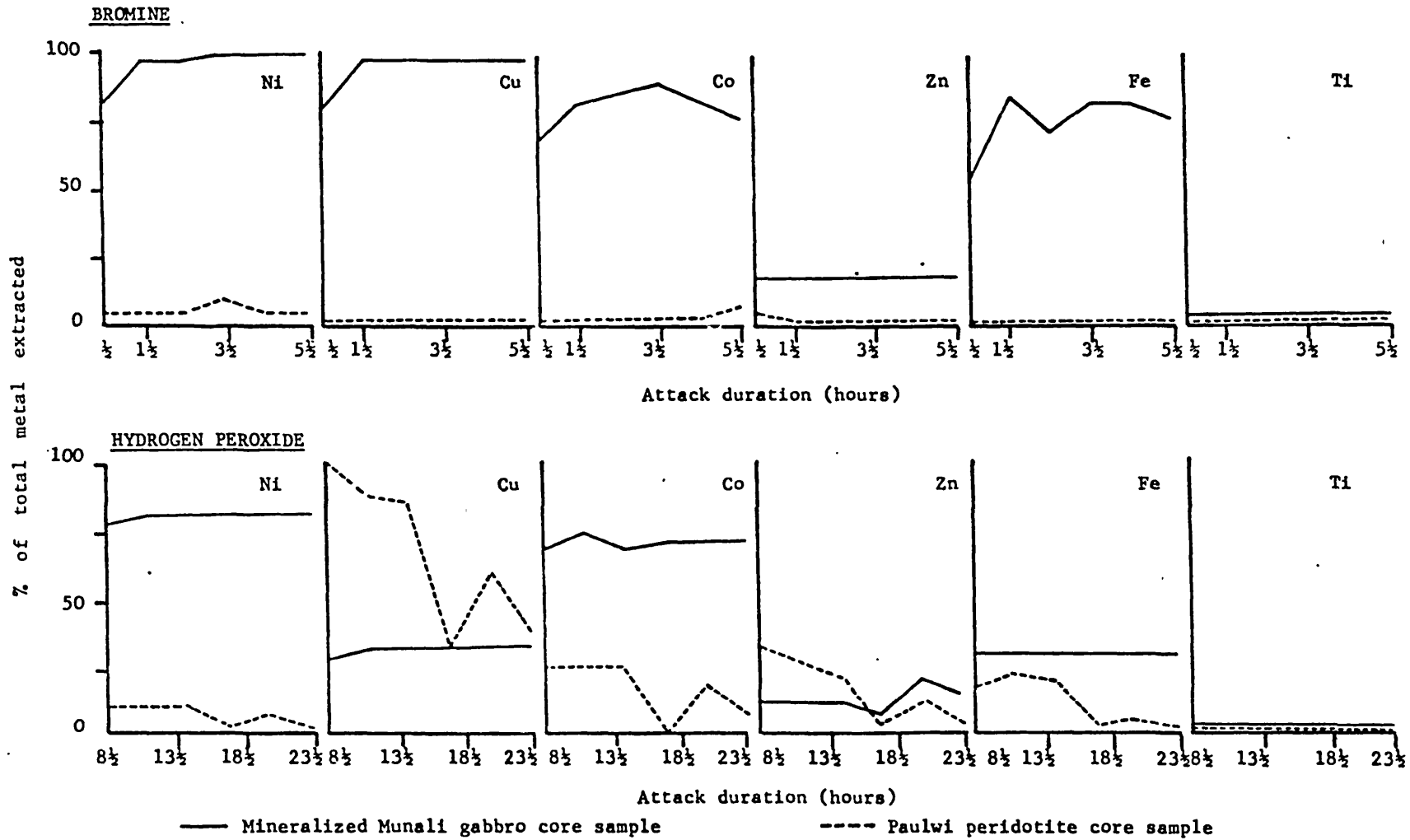
Figure 36:   Percentage of total metal extracted from Munali and Paulwi core samples by bromine and hydrogen peroxide attacks on sulphide minerals.

Munali mineralized gabbro

	Ni ppm	Ni %	Cu ppm	Cu %	Co ppm	Co %	Zn ppm	Zn %	Fe ppm	Fe %	Ti ppm	Ti %
HNO$_3$ - HClO$_4$	18500		1640		1350		48		375000		1600	
0.07M HCl	900	5	19	1	42	4	21	45	4980	2	0	0
Residue	17500	95	1510	99	1150	96	26	55	210000	98	2050	100
Sum	18400	100	1539	100	1192	100	47	100	214980	100	2050	100
0.07M HCl + Br	19500	97	1700	98	1200	90	25	52	318000	93	90	6
Residue	550	3	43	2	130	10	23	48	23100	7	1450	94
Sum	20100	100	1743	100	1330	100	48	100	341100	100	1540	100
0.03M HCl	540	3	4	0	27	2	10	21	47	0	0	0
0.008M HCl	570	3	3	0	24	2	6	13	23	0	0	0
0.008M HCl + Br	18000	97	1600	98	980	73	19	31	280000	74	60	10

Paulwi non-mineralized peridotite

	Ni ppm	Ni %	Cu ppm	Cu %	Co ppm	Co %	Zn ppm	Zn %	Fe ppm	Fe %	Ti ppm	Ti %
HNO$_3$ - HClO$_4$	2800		36		150		58		71500		100	
0.07M HCl	570	18	33	85	30	19	19	18	11500	26	0	0
Residue	2250	82	6	15	130	81	85	82	31800	74	150	100
Sum	3120	100	39	100	160	100	104	100	43200	100	150	100
0.07M HCl + Br	870	31	37	90	75	50	27	26	16800	34	0	0
Residue	1950	69	4	10	75	50	76	74	33000	66	350	100
Sum	2820	100	41	100	150	100	103	100	49800	100	350	100
0.03M HCl	84	3	6	17	6	4	10	17	19	0	0	0
0.008M HCl	30	1	7	19	3	2	7	12	15	0	0	0
0.008M HCl + Br	18	1	1	3	2	1	2	3	0	0	0	0

% refers to proporation of summed analyses where applicable; of HNO$_3$ - HClO$_4$ values elsewhere.

Table 7: Optimization of bromine attack for metals in sulphide minerals.

decanted and analysed by atomic absorption spectrophotometry for
the siderophile and chalcophile elements, Ni, Cu, Co, Zn and Fe,
and as a check on the extent to which silicates were attacked, for
a lithophile element, Ti. The use of Br requires special care and
the attacks were conducted throughout in a fume cupboard. The
dilute acid solution is needed to maintain a pH of less than 2.5
in order to prevent the hydrolysis of soluble ferrous and ferric ions
to ferric hydroxide, which colloidally precipitates and may co-precipitate
other metals from solution.

Using hydrogen peroxide, 250 mg pulverised sample
aliquots were weighed into 100 ml polythene flip-top bottles and
12.5 ml of 30% H_2O_2 in 1% ascorbic acid solution was added. The
bottles were shaken on a mechanical shaker for periods of 8½ to 23½
hours, then the contents were transferred into test tubes, centrifuged,
and the extractants decanted into other test tubes. The extractants
were analysed by atomic absorption spectrophotometry for Ni, Cu, Co,
Zn, Fe and Ti. Hydrogen peroxide is comparatively safe to handle.
Ascorbic acid is used to provide a solution of less than pH 2.5 and
prevent the hydrolysis of ferrous and ferric ions.

The two core samples were also analysed for total
metals by digestion in HNO_3-$HClO_4$ and atomic absorption spectrophotometric
metal determination. The results of the leaching experiments are
expressed as percentages of total metal extracted (figure 36).

The bromine attack leaches almost all Ni and Cu, most
Co and Fe, and some Zn from the mineralized Munali gabbro, but no more
than traces of these metals from the non-mineralized Paulwi peridotite.
The absence of Ti in the leachates shows that silicate minerals are
not extensively attacked by the acid medium. The hydrogen peroxide
leach tends to remove less metal than bromine from the mineralized
sample and more from the non-mineralized sample. Although contrast
between the two samples is fair for Ni and Co, it is poor for Zn
and Fe, and a higher percentage of Cu is extracted from the Paulwi
peridotite than the mineralized Munali gabbro. Thus, these preliminary
analyses indicate that hydrogen peroxide is less effective than
bromine in oxidizing sulphide minerals, while ascorbic acid attacks

silicate minerals more than hydrochloric acid. The sharp drop in
the recorded concentrations of metals from Paulwi samples leached
for 17½ hours and more is presumed to be due to the formation of
colloidal silica and co-precipitation with this of heavy metals.

The bromine attack is therefore the more successful,
and the maximum concentrations of most ore metals are leached by an
attack of 3½ hours duration or more. Further optimization of this
analytical procedure was attained by studying the leaching effect of
the hydrochloric acid medium on the two testwork samples over 3½ hours.
In these experiments the post-leaching residues were also analysed
for total metals, using a HNO_3-HClO_4 attack and atomic absorption
spectrophotometry.

The leaching effect of 0.07M HCl is generally minimal
for the Munali sample, which comprises mainly sulphide minerals and
pyroxenes, and only a few percent of total metal (except Zn) are
leached into solution by this acid alone (table 7). From the Paulwi
sample, however, which comprises mainly olivines and some serpentine,
the acid leaches 20% of most metals and 85% of the Cu. The experiment
was repeated using more dilute concentrations of hydrochloric acid.
With 0.008M HCl (pH 2.2) the amounts of metals leached from the Paulwi
sample fall to roughly the same few percent as was extracted from the
Munali sample, except that Cu extraction remains higher at 36%. The
concentration of Zn leached from the Munali sample falls to 13%.

Using a 0.008M   HCl   solution for a bromine attack,
high ore metal values and low Ti values, similar to earlier results
with a more concentrated HCl solution, are obtained for the Muanli
sample, while the Paulwi sample yields low values similar to those
obtained without bromine present. This demonstrates that a much more
dilute acid solution than had previously been employed can successfully
be used to prevent hydrolysis during the bromine attack, and so further
confine the attack to sulphide minerals. Core and outcrop samples of
visibly non-mineralized mafic and ultramafic intrusive rocks from
six field areas were analysed by the method developed. The samples were
analysed in three batches and within each batch sample numbers were
randomized. Each batch included the previously analysed Munali and
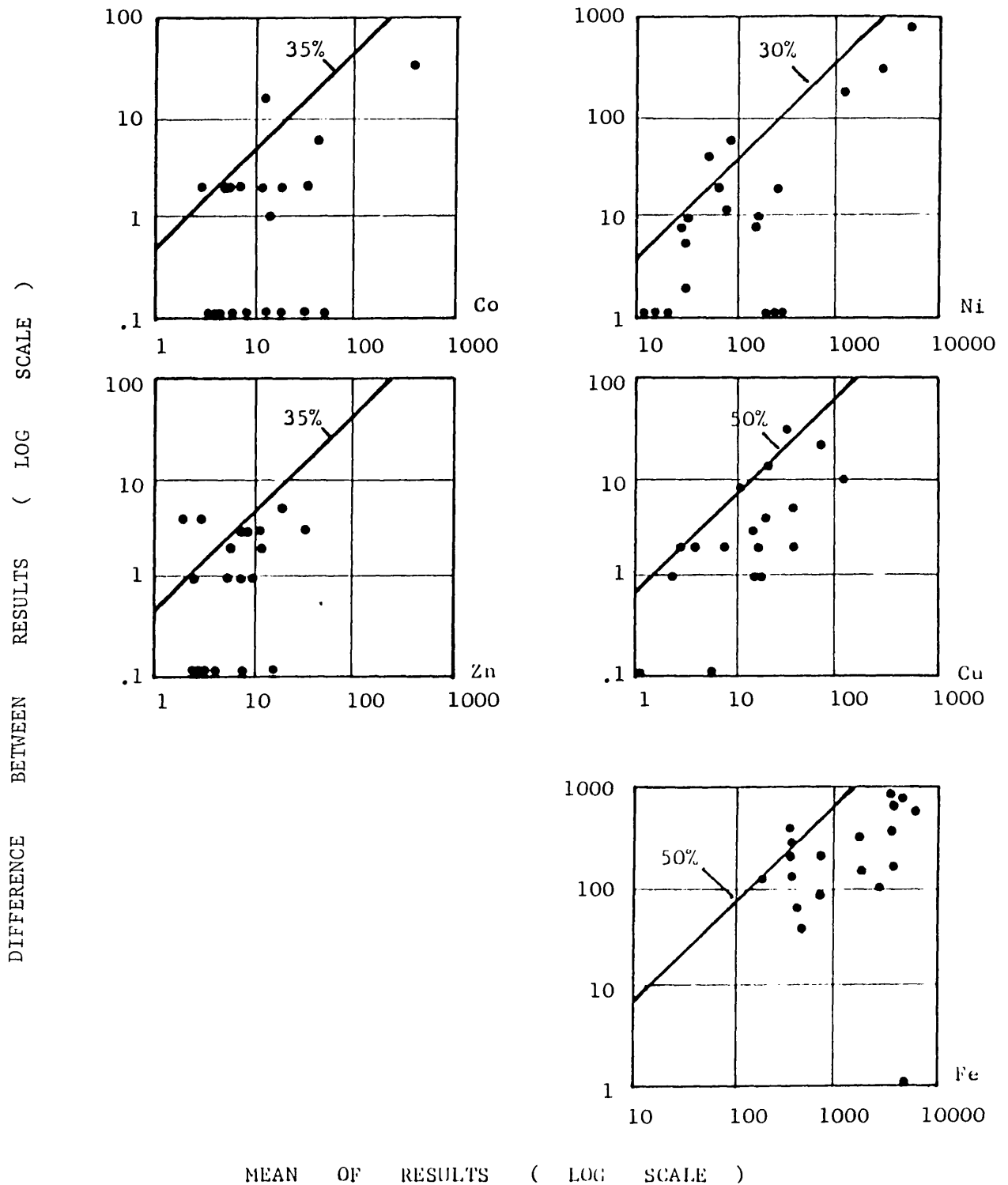
Figure 37: Duplicate determinations and precision estimates for metals in sulphide minerals (for details of chart construction see Thompson and Howarth, 1973; all trace element values in ppm).

Code(figures 38 to 43)	Outline method and reference
M_t	4:1 HNO_3 - $HClO_4$; evaporate to dryness in air bath, leach residue with 6M HCl, make up to volume with deionized water (section 3.2).
M_a	0.3M ammonium oxalate in oxalic acid at pH 3.4; warm gently and shake at intervals for 2 hours, centrifuge,decant leachate, make up to volume with reagent (Le Riche and Weir, 1963). Leaches Fe oxides and associated trace elements.
M_b	0.5M HCl (pH 2.3); warm gently and shake at intervals for 2 hours, centrifuge, decant leachate, make up to volume with reagent (Clews, 1962; Ellis, Tooms, Webb and Bicknell, 1967). Leaches secondary oxides and associated trace elements.
M_c	0.1M EDTA adjusted to pH 4.5 with NH_4Cl; maintain at room temperature and shake at intervals for 3 hours, centrifuge, decant leachate (Evans, 1971). Complexes absorbed and adsorbed trace elements.
M_d	0.3M sodium citrate in citric acid at pH 7.3; heat in water bath at $90^\circ C$, add dithionite reagent and shake at intervals for 20 mins, add saturated NaCl solution, shake, centrifuge, decant leachate and make up to volume with citrate reagent (Aguilera and Jackson, 1953). Leaches secondary oxides and associated trace elements.
M_e	4.2M CH_3COOH (pH2.0); heat in water bath at $90^\circ C$ and shake at intervals for 2 hours, centrifuge, decant leachate, make up to volume with reagent (Chester and Hughes, 1967). Leaches Fe oxides and associated trace elements.
M_f	0.02M hydroxylamine hydrochloride (pH 2.8); maintain at room temperature and shake at intervals for 4 hours, centrifuge, decant leachate (Chester and Hughes, 1967). Leaches Mn oxides and associated trace elements.

Table 8: Outline analytical methods for extraction of trace elements associated with secondary iron and manganese oxides.

		M_t	M_a	M_b	M_c	M_d	M_e	M_f
Chombwa								
C	Ni	1,950	800	640	280	128	320	80
I	Ni	750	600	360	96	68	120	60
F	Ni	2,300	440	480	112	68	146	64
C	Fe	140,000	13,360	28,400	11,600	2,600	2,600	950
I	Fe	39,500	5,920	20,200	860	890	230	160
F	Fe	160,000	4,000	25,400	800	1,000	300	180
C	Mn	1,550	120	800	670	390	660	490
I	Mn	460	100	665	520	390	270	470
F	Mn	1,580	70	680	460	350	320	400
King Edward								
C	Ni	3,150	1,680	1,800	800	640	520	280
I	Ni	2,750	1,000	1,200	440	300	240	176
F	Ni	2,850	840	1,280	340	380	260	144
C	Fe	225,000	4,400	37,200	3,200	8,600	4,500	590
I	Fe	245,000	7,360	34,800	1,660	3,500	1,120	320
F	Fe	230,000	4,400	39,400	1,540	3,800	130	270
C	Mn	2,400	170	1,950	1,240	1,190	690	890
I	Mn	2,500	160	1,300	1,040	890	260	740
F	Mn	2,050	110	1,100	800	680	310	500
Munali *								
C	Ni	750	280	120	36	20	32	12
I	Ni	1,350	400	520	48	36	44	16
F	Ni	1,200	400	520	56	40	52	16
C	Fe	530,000	10,800	28,600	22,800	4,000	7,200	1,900
I	Fe	285,000	6,840	16,600	1,440	1,500	280	170
F	Fe	229,000	5,560	17,200	2,180	1,300	400	180
C	Mn	750	20	150	140	70	130	90
I	Mn	850	30	290	230	140	129	120
F	Mn	690	30	290	210	135	160	100
Trojan*								
C	Ni	10,500	3,440	3,000	960	620	800	480
I	Ni	12,500	3,520	3,200	1,000	720	720	440
F	Ni	10,000	2,720	3,200	1,120	800	920	400
C	Fe	180,000	6,000	26,000	1,380	2,200	670	350
I	Fe	200,000	6,840	29,200	1,300	1,900	360	200
F	Fe	190,000	4,800	24,600	1,000	2,000	360	210
C	Mn	2,300	140	1,250	950	730	530	720
I	Mn	2,400	160	1,550	1,200	900	390	760
F	Mn	2,200	190	1,900	1,150	920	580	760

C = coarse fraction   I = intermediate fraction   F = fine fraction

* mineralized locality

Table 9:   Extractable trace metal content (ppm) of soil orientation samples.

		M_t	M_a	M_b	M_c	M_d	M_e	M_f
King Edward								
C	Ni	2,150	1,600	1,440	960	760	440	140
I	Ni	1,450	560	600	124	100	140	12
F	Ni	1,650	800	840	200	124	196	12
C	Fe	150,000	4,640	35,800	1,800	2,600	4,400	10
I	Fe	130,000	4,160	24,200	1,480	670	1,500	30
F	Fe	160,000	6,200	33,000	1,960	690	2,000	10
C	Mn	6,500	530	5,300	4,400	3,700	1,600	2,900
I	Mn	1,500	80	840	530	460	420	220
F	Mn	2,080	110	1,200	770	600	760	280
Munali*								
C	Ni	500	200	80	25	12	16	12
I	Ni	269	80	48	4	8	1	4
F	Ni	240	80	88	12	12	8	8
C	Fe	190,000	5,320	11,000	9,200	2,600	2,500	1,200
I	Fe	370,000	4,800	9,200	260	1,000	240	150
F	Fe	150,000	3,080	14,600	620	1,000	280	210
C	Mn	430	20	150	140	85	110	90
I	Mn	570	20	140	110	110	70	100
F	Mn	450	20	240	190	145	160	130
Paulwi								
C	Ni	155	120	80	44	28	32	20
I	Ni	185	80	76	12	20	16	8
F	Ni	300	160	128	44	26	32	16
C	Fe	29,000	2,000	13,000	9,600	3,100	4,000	1,800
I	Fe	40,000	1,240	10,000	480	660	380	160
F	Fe	63,000	1,840	12,800	1,500	720	680	280
C	Mn	570	50	330	360	260	260	210
I	Mn	490	30	240	180	150	120	120
F	Mn	900	50	440	390	260	280	230
Trojan*								
C	Ni	1,250	800	600	360	280	320	80
I	Ni	1,650	1,200	1,120	960	560	560	96
F	Ni	2,900	1,680	1,840	960	1,320	880	144
C	Fe	160,000	5,240	20,400	3,040	2,400	2,000	230
I	Fe	82,000	4,480	18,200	1,640	2,200	560	140
F	Fe	76,000	5,480	24,000	3,300	3,600	1,800	220
C	Mn	2,000	110	1,150	370	600	800	470
I	Mn	2,250	160	1,500	1,160	1,100	1,100	600
F	Mn	2,200	160	1,650	1,220	1,100	1,200	710

C = coarse fraction   I = intermediate fraction   F = fine fraction
  * mineralized locality

Table 10:   Extractable trace metal content (ppm) of stream sediment
            orientation samples.
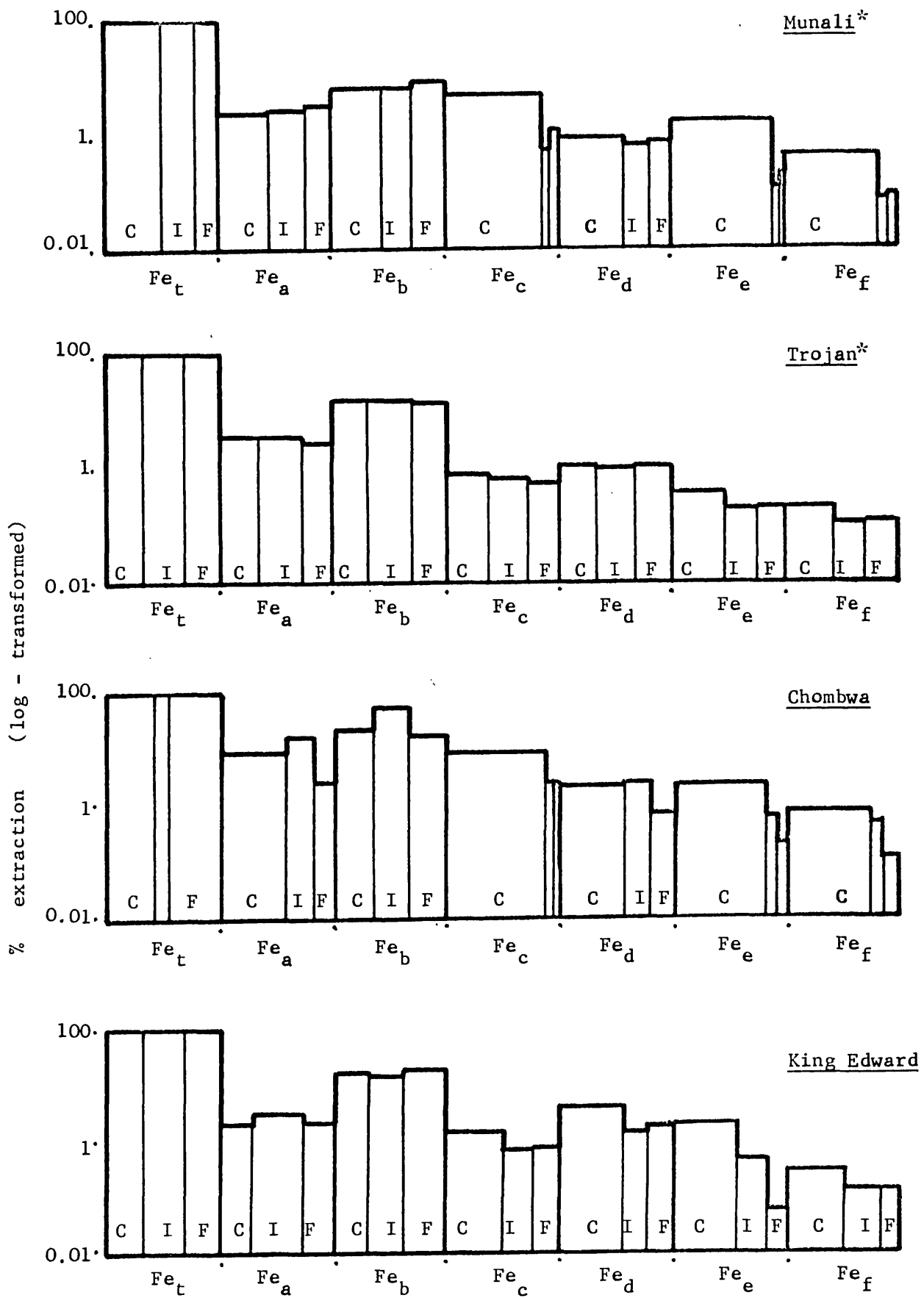
C = coarse fraction   I = intermediate fraction   F = fine fraction

* mineralized locality

Figure 38:   Extractable Fe content of soil orientation samples (see table 8 for codes).

Paulwi core specimens as standards, a blank and about seven
duplicates for precision evaluation.

The blanks analysed contained no trace elements and
the standards returned consistent results. Too few duplicate
analyses were made to permit computerized precision evaluation using
PRESIN. As an alternative, asymptpotic precision is estimated
graphically by plotting on log-log co-ordinates the mean trace
element concentrations and differences (approximating to standard
deviations) of duplicate pairs of analyses. The precision is
estimated from the diagonal above which 10% of the points plot
(Thompson and Howarth, 1973). Relatively poor precision was anticipated
for this analytical technique, and graphical estimates confirm
this (figure 37). Precision for Ni is about 30%, Co and Zn 35% and
Cu and Fe 50%. Titanium precision was not estimated because most
titanium values were zero.

3.5. Trace elements associated with iron and manganese oxides

The prospecting significance of Ni co-precipitated
with secondary Fe oxides and any Mn oxides in soils and stream
sediments was assessed by a comparison of analytical results from
different sample attacks. These attacks included total trace
element dissolution using HNO_3-$HClO_4$ and a series of leaches
considered to be somewhat selective in dissolving Fe and Mn oxides
and their associated trace elements (table 8). The study was
confined to a simple comparison of the analytical results obtained
using these attacks on soils and stream sediments from the Central
African field areas, and was not intended to be an exhaustive evaluation
of the chemistry of the different leaching processes.

The coarse, intermediate (-425 + 180μm) and fine
fractions of Munali, Trojan, Chombwa and King Edward soil orientation
samples and Munali, Trojan, Paulwi and King Edward stream sediment
orientation samples were analysed by these methods, suitably modified
for 250 mg samples in test tubes. The amounts of Fe, Mn and Ni
extracted were determined by atomic absorption spectrophotometry, using
multi-element standards made up in each of the same reagents (tables 9
and 10). Figures 38 to 43 show these results as sets of seven histograms.
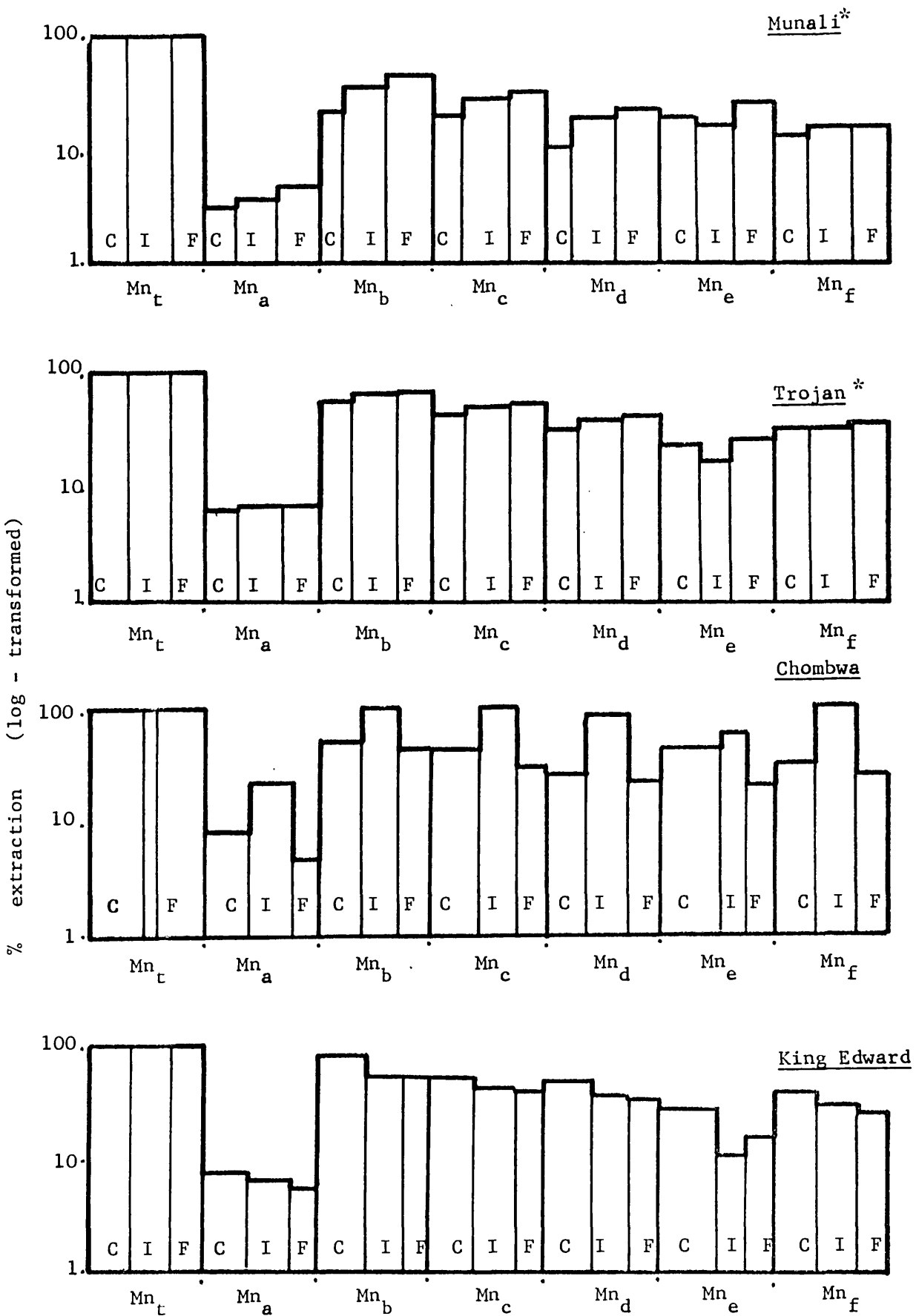
C = coarse fraction   I = intermediate fraction   F = fine fraction

*mineralized locality

Figure 39:   Extractable Mn content of soil orientation samples (see table
             8 for codes)

Munali *

Trojan *

Chombwa

King Edward

y-axis label: % extraction (log - transformed)
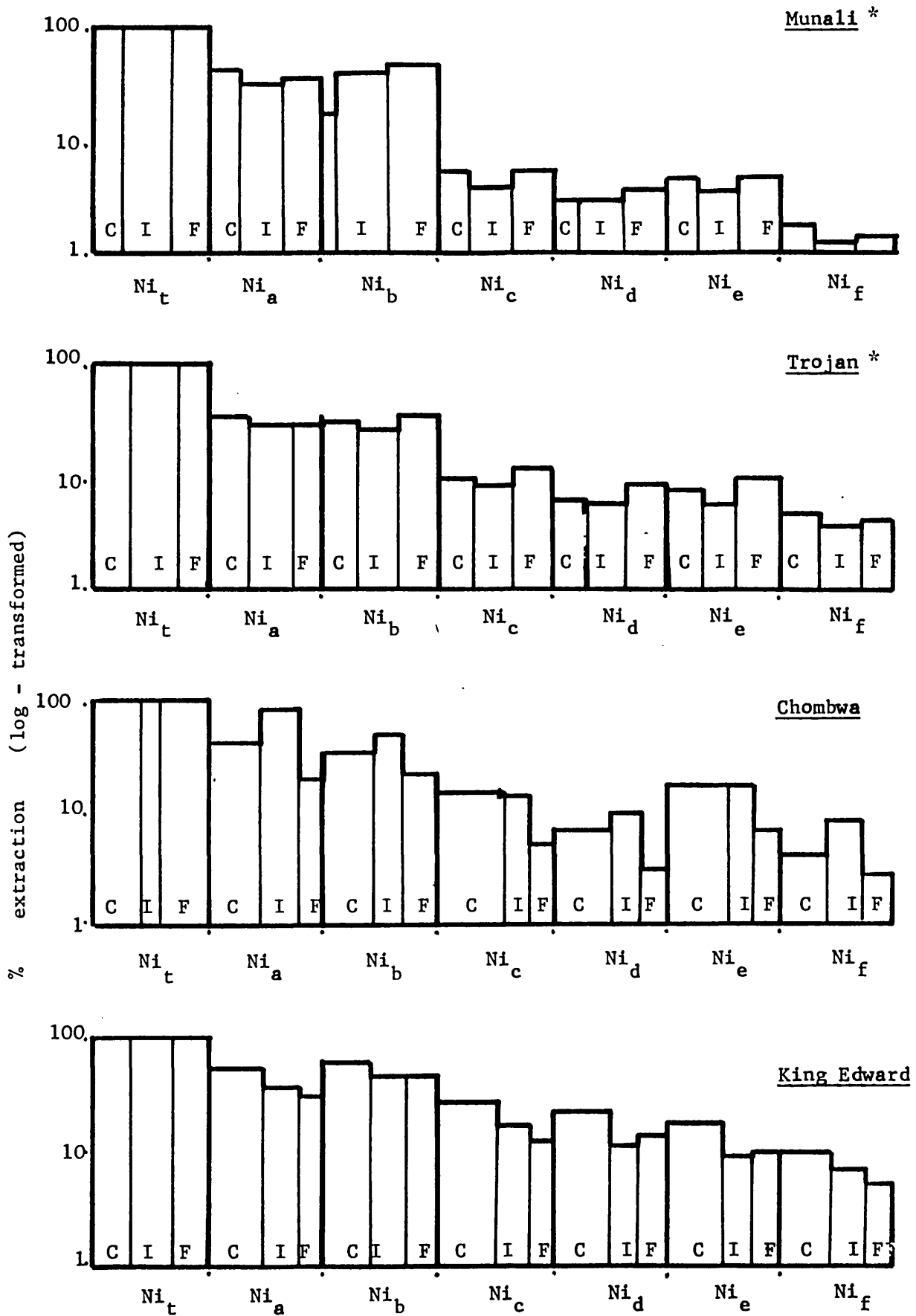
C = coarse fraction I = intermediate fraction F = fine fraction
  * mineralized locality

Figure 40: Extractable Ni content of soil orientation samples (see
            table 8 for codes)
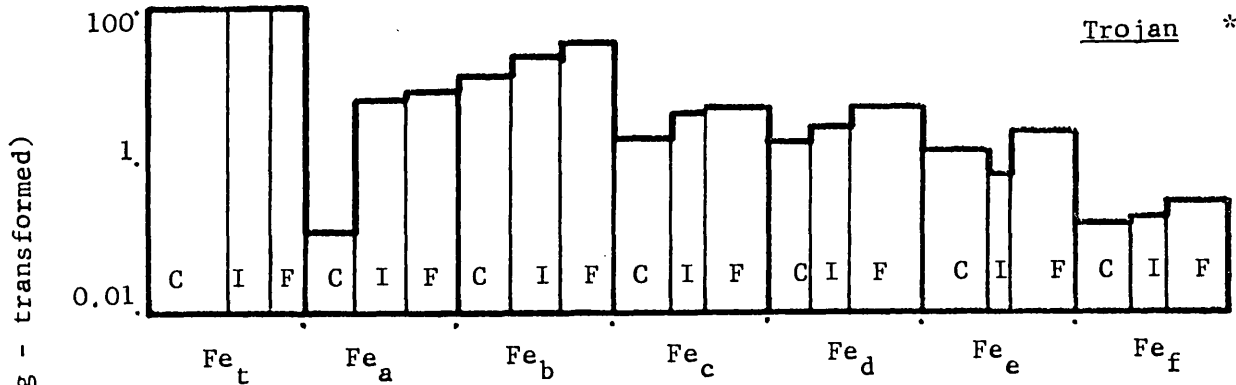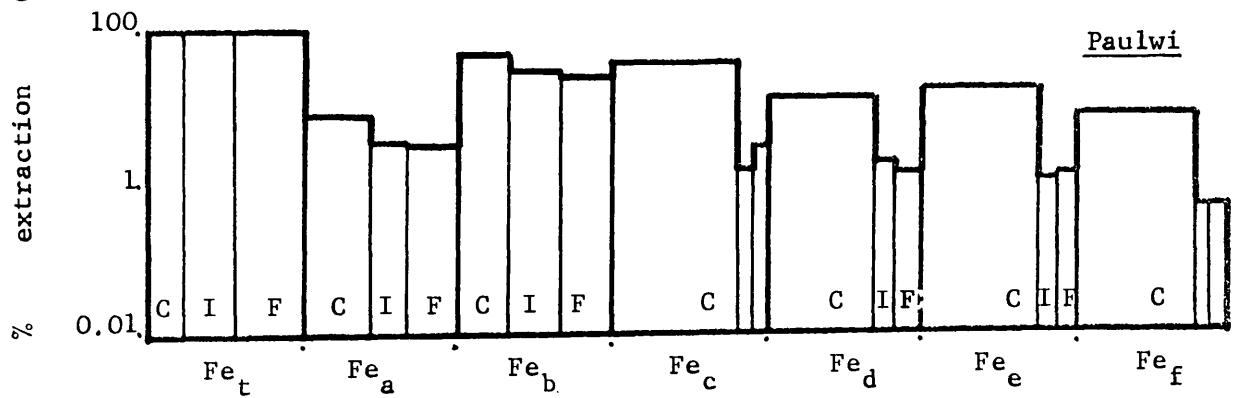
C = coarse fraction   I = intermediate fraction   F = fine fraction
*   mineralized locality

Figure 41:   Extractable Fe content of stream sediment orientation
samples (see table 8 for codes)
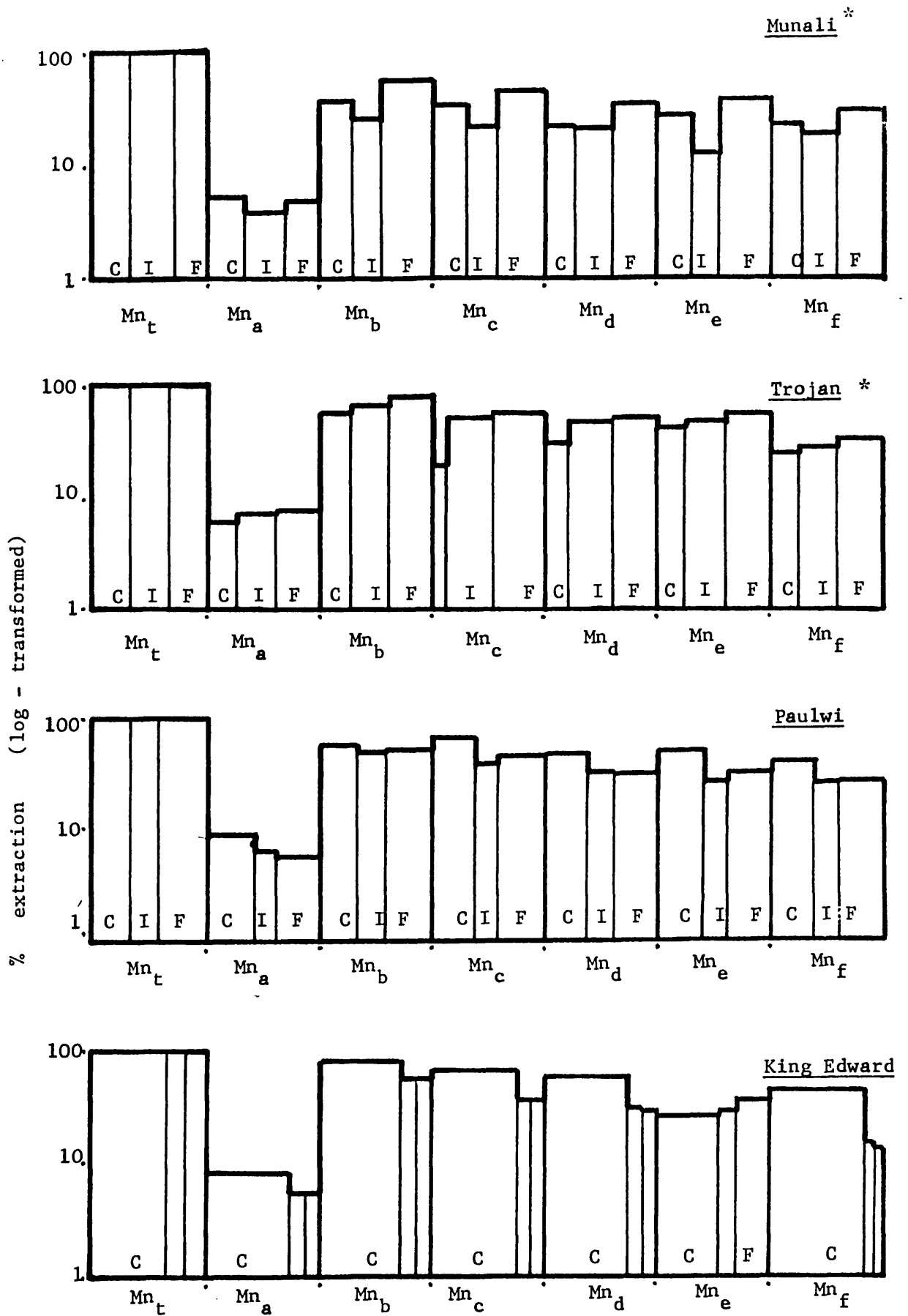
C = coarse fraction   I = intermediate fraction   F = fine fraction

*mineralized locality

Figure 42:   Extractable Mn content of stream sediment orientation
              samples (see table 8 for codes)

Munali *

Trojan *

Paulwi

King Edward

extraction (log – transformed)

%
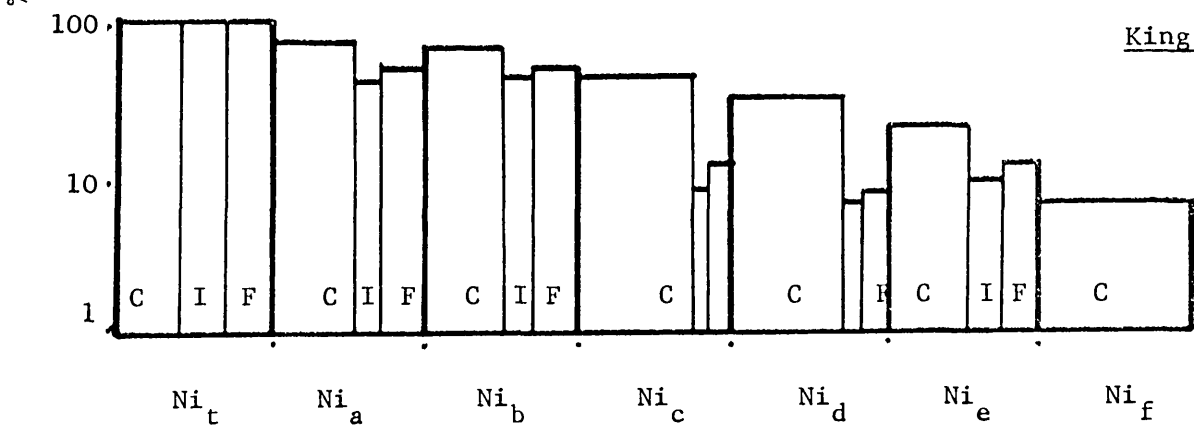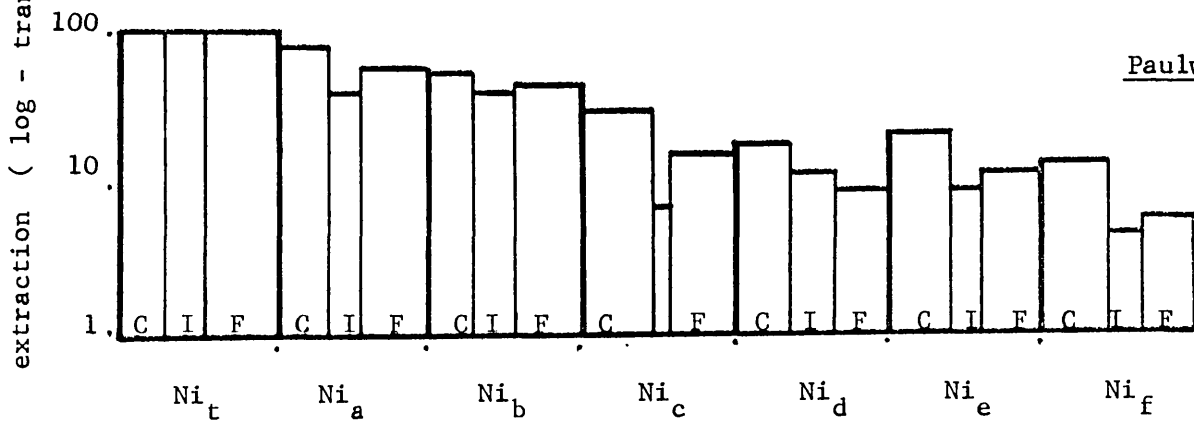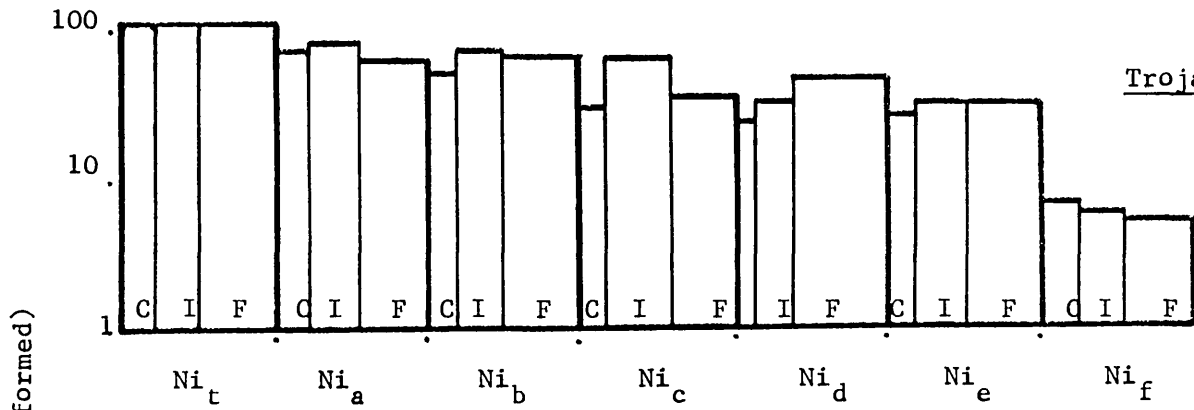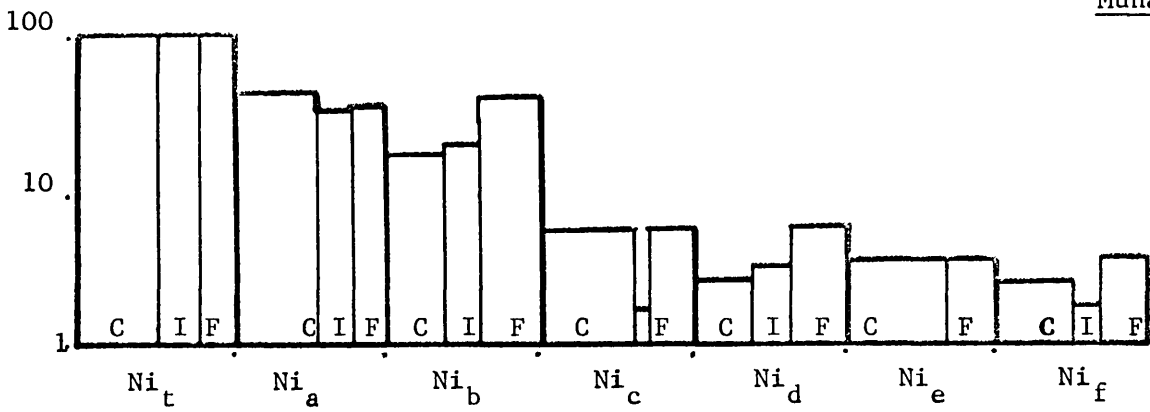
C = coarse fraction   I = intermediate fraction   F = fine fraction
*mineralized locality

Figure 43:   Extractable Ni content of stream sediment orientation
             samples (see table 8 for codes)

Each histogram illustrates the analytical results for one sample
and one reagent, with three vertical bars to represent, from left
to right, the results for the coarse, intermediate and fine
fractions. The height of the bars expresses the log-transformed
percentage extraction of metal by each of the reagents relative
to total metal content (M_t), and therefore M_t values are set at
100%. The width of the bars shows the relative amounts of
extractable metal in each of the three sample size fractions.

In general terms, the hydrochloric acid leach extracts
the highest percentage of total Fe from samples, while a high percentage
of total Mn is removed by all leaches except ammonium oxalate. The
maximum percentages of total Ni are extracted by ammonium oxalate and
by hydrochloric acid, suggesting an association of Ni with Fe rather
than Mn.

In most cases, Fe is somewhat enriched in the coarse
fraction of samples, and the less vigorous leaches, such as EDTA,
sodium citrate, acetic acid and hydroxylamine hydrochloride, often extract
very much more Fe from the coarse fractions than from the intermediate
and fine fractions. Manganese is more evenly distributed among the
sample size fractions, except in the King Edward stream sediment, where
there is a conspicuous total and extractable Mn enrichment in the
coarse fraction. Nickel also exhibits a fairly even distribution among
the size fractions of most samples. However, there is a clear Ni
enrichment in the coarse fraction of the Munali stream sediment and
Chombwa and King Edward soils, presumably in conjunction with the
observed Fe enrichment. Nickel enrichment in the coarse fraction of
the King Edward stream sediment is correlated with Mn.

None of the selective leaches consistently extract
a higher percentage of Ni from sample fractions from mineralized
localities compared with those from non-mineralized localities.
Therefore the extraction experiments confirmed the enrichment of
secondary Fe, Mn and associated Ni in the coarse fraction of samples
from some places, but indicated that such enrichment was not necessarily
related to the presence or absence of mineralization. Furthermore,

none of the leaches yielded Ni results that improve total Ni contrast between mineralized and non-mineralized localities.

3.6.   Sulphur

The determination of sulphur in rocks and soils was considered to be a particularly important aspect of the research. However, it was essential to adopt or devise an analytical method that would have a realistic commercial throughput rate of, say, 10 or more S determinations per hour.

3.6.1.   Argon plasma emission spectrography

A relatively new innovation for the analysis of geochemical samples for S is fractional thermal decomposition of sample material accompanied by the flushing of volatile components in an argon stream, into a microwave-induced plasma, and S determination by emission spectrography (Meyer, 1973). The appropriate equipment was assembled to perform S analysis by argon plasma emission spectrography, but the method proved unsatisfactory due to carbon interference. A full appraisal of the work involved is given in appendix 1.

3.6.2.   Combustion technique

The basis of an alternative rapid S analysis method was combustion. A simple combustion technique was tested whereby the sample was heated in a stream of air or oxygen to more than $900^{o}C$ in a LECO furnace or a muffle furnace, and the evolved SO_2 was absorbed in a potassium tetrachloromercurate solution (TCM) and subsequently determined colorimetrically (West and Gaeke, 1956).

In preliminary experiments the results from rock samples were not reproducible, a problem ascribed to probable partial oxidation of the evolved SO_2 to SO_3.
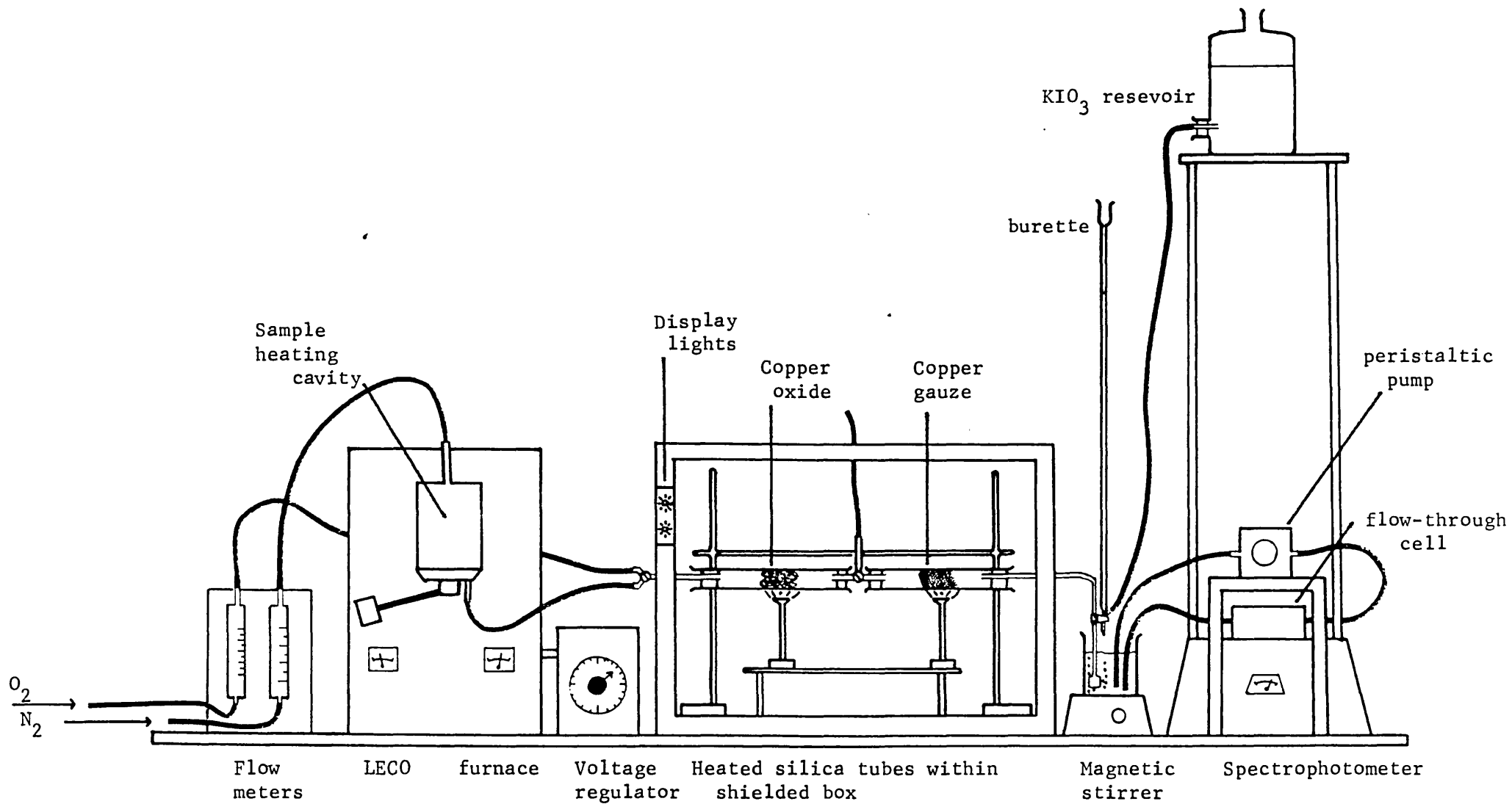
Figure 44: Diagram of apparatus for S analysis using a modified combustion technique

In the analysis of soils, the same lack of
reproducibility was encountered, and in some cases a white
precipitate of $HgCl_2$ was formed in the TCM solution. The soil
samples were re-analysed using alternative SO_2 absorbants. A
dilute solution of NaOH with universal indicator was employed,
and was expected to become visibly more acidic on absorbing SO_2
(and SO_3), but the gases evolved on sample heating caused the
solution to become more strongly alkaline. In re-analysis with
an I_2-KI absorbing solution coloured pale blue by starch indicator,
the expected reducing effect of SO_2 turning the solution colourless
was negated by an oxidizing gas turning the solution black due to
the liberation of further free I_2. Thus the simple combustion
method of determining S in soils as SO_2 was subject to a subtractive
interference due to the simultaneous evolution from the sample
of an alkaline oxidizing gas, possibly ammonia. This was presumed to
be derived from the destructive distillation of organic matter.

In order to eliminate these problems a series of
apparatus and technique modifications were made to the simple
combustion method which produced a satisfactory rapid S analysis
system for rock, soil and stream sediment samples (figure 44).
Using this system a sample weight of 250 mg was mixed with about
125 mg of V_2O_5 and placed in a small platinum crucible in a LECO
induction furnace. A stream of N_2 was passed over the sample and
95% of maximum voltage to the furnace grid was applied, raising the
temperature of the crucible to more than $900^{o}C$. As this temperature
the sample fused with the oxidizing V_2O_5 flux and the gases evolved,
including any SO_2, were carried in the N_2 stream into the first of
two horizontal silica tubes, each about 50 cm long and 1.5 cm wide.
The first tube contained a plug of copper oxide heated to about $800^{o}C$
from below by a Mekker burner, and here any alkaline oxidizing organic
vapours evolved from the sample were oxidized to CO_2 and NO_2;some $SO_2$was
converted to SO_3. The gas stream then passed into a second silica
tube containing a plug of copper gauze, also heated to about $800^{o}C$
from below by Mekker burner, where any SO_3 previously formed was
reduced to SO_2. The heated silica tubes were surrounded by an
open-topped framework of aluminium foil heat-shielding. Finally the
gas stream was bubbled through a magnetically stirred solution of
acidified KI containing a little free I_2 in a 400 ml beaker. This
solution was prepared by adding to about 200 ml of approximately

0.1M HCl a few crystals of KI, a little KIO_3 solution, and a few drops of starch solution to provide a light blue colour, as an indicator of free I_2 concentration:

$$5KI + KIO_3 + 6HCl \longrightarrow 3I_2 + 6KCl + 3H_2O$$
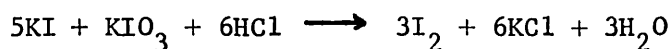
Any SO_2 in the gas stream reduced the free I_2 in solution with the loss of pale blue colouration:

$$2H_2O + I_2 + SO_2 + 2KCl \longrightarrow 2KI + H_2SO_4 + 2HCl$$
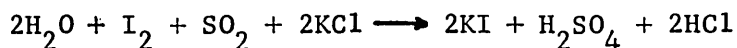
As the colour was lost additional KIO_3 solution of known concentration was run in to the flask from a burette to restore the original pale blue colour.

The blue colour of the solution in the beaker was monitored using a flow-through cell in a SP600 spectrophotometer. The most sensitive absorption wavelength for the blue solution was found to be 512 nm, and the spectrophotometer was zeroed on a freshly-prepared solution at this wavelength. During sample heating the absorbing solution in the beaker was continuously monitored via a feed capilliary to the flow-through cell and a similar return capilliary to maintain constant volume of iodide and I_2 in the beaker. The flow was powered by a peristaltic pump on the return capilliary. Iodate solution from the burette was added to the beaker in sufficient quantity to maintain the spectrophotometer needle in the zero position throughout analysis of the sample.

The quantity of KIO_3 solution required to maintain the initial blue colour throughout sample analysis was noted from the burette, and the concentration of S in the sample was calculated from this. A KIO_3 solution containing 0.111 g KIO_3 per litre was used, so that with a 250 mg sample, S concentration was given by the simple formula:

$$ppm\ S = ml\ KIO_3 \times 200$$

A self-filling 10 ml burette with 0.2 ml graduations was used to

combine reading accuracy with the ability to cope with sulphur-rich samples.

On completion of analysis of each sample the voltage to the furnace grid was cut, the sample-holding cavity was opened and the crucible was removed. A pair of three-way glass stopcocks were operated on the inlet of the first silica tube and the tee-piece joining the first and second silica tubes. The N_2 stream was automatically cut when the furnace sample holder was in the open position and the stopcock switches permitted a stream of O_2 to flow over the hot copper oxide, thereby facilitating any necessary oxidation, but not over the hot copper gauze.

The stopcocks were fitted with copper contacts coupled to a 12V circuit with red and green display lights which ensured both stopcocks were correctly positioned for each mode of operation.

The time required for each sample analysis varied with the S content of the sample, for heating was continued until the blue colour of the absorbing solution was stable without the addition of further KIO_3 solution. On average the throughput rate was about eight samples per hour. In the absorbing solution the same blue colour was restored continuously and the same solution was used in numerous successive analyses, up to a limiting factor of about 50% dilution; a new solution was prepared only once or twice each day, as necessary. At the beginning of each day the copper gauze was removed from the silica tube and re-activated by heating to red heat and plunging into methyl alcohol vapour.

The use of a LECO induction furnace as a heating source was optional insofar as a fused silica boat containing the sample and heated within the first horizontal silica tube by a Mekker burner would suffice. The LECO furnace, however, facilitated faster sample changeover and greater temperature control. Spectrophotometric end-point monitoring was also optional, but eliminated tedious observation of the shade of colour of the absorbing solution and increased sensitivity near the limit of detection. Continuous, slight background drift in the blue colour was more readily controlled by spectrophotometric

Depth (cm)	Soil horizon	Chombwa		Munali *	
		Coarse	Fine	Coarse	Fine
7	A	115	195	390	155
50	B	120	140	335	210
400	C	75	120	160	220

*Mineralized locality

Table 11: S content of coarse and fine fractions of principal soil horizons at Chombwa and Munali (ppm).

Depth (cm)	Soil horizon	Chombwa		Munali *	
		Coarse	Fine	Coarse	Fine
7	A	360	475	245	266
50	B	380	285	190	247
400	C	133	133	285	400

*Mineralized locality

Table 12: F content of coarse and fine fractions of principal soil horizons at Chombwa and Munali (ppm).

monitoring; the instrument needle moved slowly and irregularly away from centre under drift, and more sharply and permanently in response to SO_2 reduction of free I_2. Thus distinction between the two colour changes was aided, and it was found that S concentrations down to 10 ppm could be measured.

As a preliminary guide to the suitability of the combustion technique developed, two USGS standards of known preferred S content were analysed several times, and one rock and one soil sample from Central Africa were analysed in replicate with satisfactory results. However, there is the possibility of less satisfactory results from rock samples with a high carbonate content: SO_2 may react with CaO derived from $CaCO_3$ to form thermally-stable $CaSO_4$, thereby reducing the amount of gaseous SO_2 liberated and determined.

All pulverised core and outcrop samples were analysed for S. In order to conduct general S analysis of pit profile, soil and stream sediment samples using the size fraction in which contrast between mineralized and non-mineralized locations was greatest, the coarse and fine fractions of samples from the principal soil horizons in two vertical pit profiles were first analysed. In a profile over non-mineralized peridotite at Chombwa, the S concentrations are similar in each soil horizon, with slightly higher S values in the fine fractions. At Munali, in a profile over mineralized gabbro the S content of the two size fractions is similar in the C horizon, but some enrichment of S in the coarse fractions is conspicuous in the A and B horizons (table 11). This distribution is attributed to an association of S with secondary goethite, in which sulphate ions may have substituted for hydroxyl ion bridges during the polymerization of colloidal iron hydroxides (Stumm and Morgan, 1962). The coarse fraction of samples was therefore selected for general S analysis.

The coarse fraction of pit profile and soil traverse samples from six field areas were analysed for S. In some cases, where high S values were encountered, both the coarse and fine fractions of the sample were analysed, and in most cases the fine fraction

173.°0   191.70   193.47   199.10   2.7.9u   216.50   225.20   233.90   242.60   251.30   263.00

SOIL STANDARDS -   S (PPM) IN 8 BATCHES
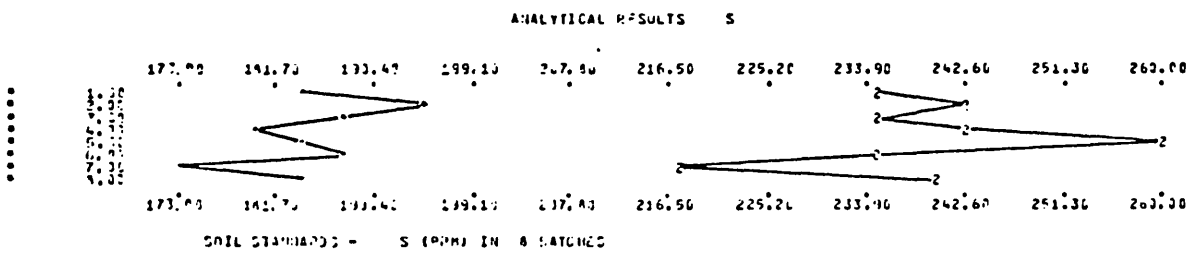
Figure 45: Sulphur analysis, variability of standards

352.°u   357.70   193.49   369.10   374.80   390.50   385.20   391.90   397.60   403.30   409.00

SOIL STANDARDS -   F (F PM) IN 4 BATCHES
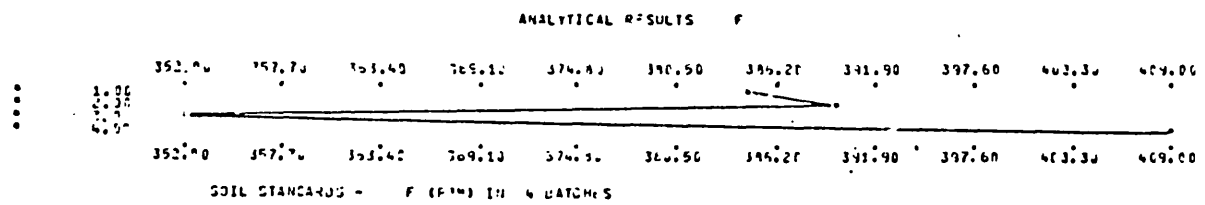
Figure 46: Fluorine analysis, variability of standards

was found to contain less S than the corresponding coarse fraction. The analysis of stream sediments for S was not pursued, because the uni-element analysis samples in regional drainage reconnaissance was thought likely to be uneconomic on a commercial scale. The pit profile and soil samples were analysed as a single batch, with 40 randomly selected duplicates and one rock and one soil sample analysed in replicate as standards. The rock and soil sample standards were each analysed eight times and show little variation over the period of S analysis (figure 45). The means and differences of duplicate samples were processed by PRESIN, which computed a coefficient of 0.067538 and intercept of -6,867720, and provided a matrix of the distribution of concentration and differences (appendix 3). From these figures the asymptotic precision of S analysis is calculated as 13.508% and the limit of detection -6.9 ppm.

3.7. Fluorine

Fluorine analyses were performed by Charter Consolidated Limited. The method of determing the total F content of samples was to mix 200 mg of sample, 2.5 ml of 25M NaOH solution and a few drops of ethyl alcohol (to break down particle surface tension) in a nickel crucible, and dry the mixture for several hours in an oven at $150^{\circ}C$. Then the crucible was covered with a lid, transferred to a muffle furnace and fused for 20 minutes at $425^{\circ}C$. After cooling the crucible was placed in a polypropylene beaker containing 100 ml of sodium citrate buffer solution. This buffer was prepared by dissolving 1875 g of sodium citrate and 300 g NaCl in 15 litres of deionized water, and adjusting to pH 5 with acetic acid. The fused melt dissolved in the solution within two hours, and then the crucible was cleaned and removed. The solution in the beaker was magnetically stirred, its pH was adjusted into the range 7.0 to 7.5 using a 1:1 mixture of $NaOH/CH_3COOH$, and then the conductivity of the solution was measured with a fluoride ion electrode. Calibration was achieved by measuring the conductivity of eight fluoride solutions containing 0.019 to 1900 ppm F, made by repeated dilutions of a master solution of 1.0498 g NaF in 250 ml of deionized water. Using the calibration curve obtained the conductivity of the sample solution was converted to F concentration.

In preliminary experiments the coarse and fine fractions of six samples representing the three major soil horizons in vertical pit profiles overlying mineralized gabbro at Munali and non-mineralized peridotite at Chombwa were analysed for F (table 12). In the A and B soil horizons results are mainly in the range 190 to 475 ppm F, and are higher at Chombwa than Munali. At Chombwa, F values fall in the C horizon to 133 ppm while at Munali they rise to 400 ppm. In general higher F results are obtained from the fine fraction of samples and in the C horizon this fraction provides better contrast between mineralized and non-mineralized localities. This F distribution is attributed to minor hydrothermal serpentinization in association with the emplacement of the sulphide mineralization at Munali, whereas there is no suggestion of hydrothermal activity at Chombwa. Volatiles including F occur in hydrothermal fluids, and F substitutes for hydroxyl groups in serpentine in the primary environment and hydroxyl groups in clay minerals in the soil (Boyle, 1976). The fine fraction of samples was therefore adopted for general F analysis.

About 40 samples were analysed in duplicate and a USGS rock standard with a preferred value of 400 ppm F was analysed four times for analytical control. Because F analysis was performed on a commercial basis, only a limited number of samples could be analysed, and pit profile samples from five field areas and four soil traverse lines were selected.

The four replicate analyses of the USGS rock standard gave results in the range 352 to 409 ppm F (figure 46). The means and differences of duplicates were processed by PRESIN, which computed values for the coefficient of 0.119238 and for the intercept of 23.196649, and provided a matrix of concentration and difference distribution (appendix 3). The asymptotic precision is calculated from this data to be 23.848% and the limit of detection 23.2 ppm F.

Soil sample	Size Fraction	pH after 30 mins	pH after 60 mins
Munali*	C	5.95	5.85
	I	5.85	5.90
	F	5.75	5.80
Munali*	C	6.45	6.45
	I	5.75	5.60
	F	5.90	5.90
Chombwa	C	5.10	5.10
	I	5.05	5.05
	F	5.05	5.00
King Edward	C	6.70	6.65
	I	6.10	6.05
	F	6.30	6.15

C = coarse fraction   I = intermediate fraction   F = fine fraction
   *mineralized locality

Table 13:   pH determinations; comparative pH obtained by performing
           determinations on different soil sample size fractions.

3.8.   pH determination

A preliminary study of pH determination was
made by taking 5 g of the coarse, intermediate ($-425 + 180$ μm)
and fine fractions of four soil samples, mixing each sample
fraction with 25 ml of 0.01M $CaCl_2$ buffer solution, and measuring
the pH after 30 and 60 minutes (table 13). For each sample
the highest pH is recorded from the coarse fraction, with
lower (and similar) values from the intermediate and fine
fractions, reflecting their slightly more organic and therefore
more acidic character. The pH differences between fractions
of the same sample range from zero to 0.85, with a mean
difference of 0.38 between coarse and intermediate fractions,
and 0.13 between intermediate and fine fractions. Generally
slightly lower pH readings are returned after 60 minutes
compared with 30 minutes, but the maximum difference is 0.15.
Further experimentation indicated that estimated 5 g sample
aliquots gave satisfactory pH results.

The intermediate size fraction was selected
for general pH determination in order to conserve coarse and
fine fractions for trace element analysis. The method of pH
determination adopted was to place a scoopful of sample, approximately
5 g, in a 50 ml beaker and add 25 ml of 0.01M $CaCl_2$ buffer solution,
stir, and allow sample and solution to equilibriate for 30 minutes
with occasional stirring. The pH of the solution was then
determined using a pH electrode and Pye laboratory pH meter. The
pH of pit profile,soil and stream sediment samples was determined,
and a few duplicate determinations showed near-perfect
reproducibility.

3.9.   Leaf ashing and analysis

Biogeochemical leaf samples were analysed as
ash. A preliminary laboratory study was undertaken to determine
the most effective ashing technique, using sub-samples of
Diplorynchus condylocarpon and Combretum ghasalense orientation
samples taken in July 1973 from two trees standing in soil
overlying gabbro at King Edward. In a series of experiments,
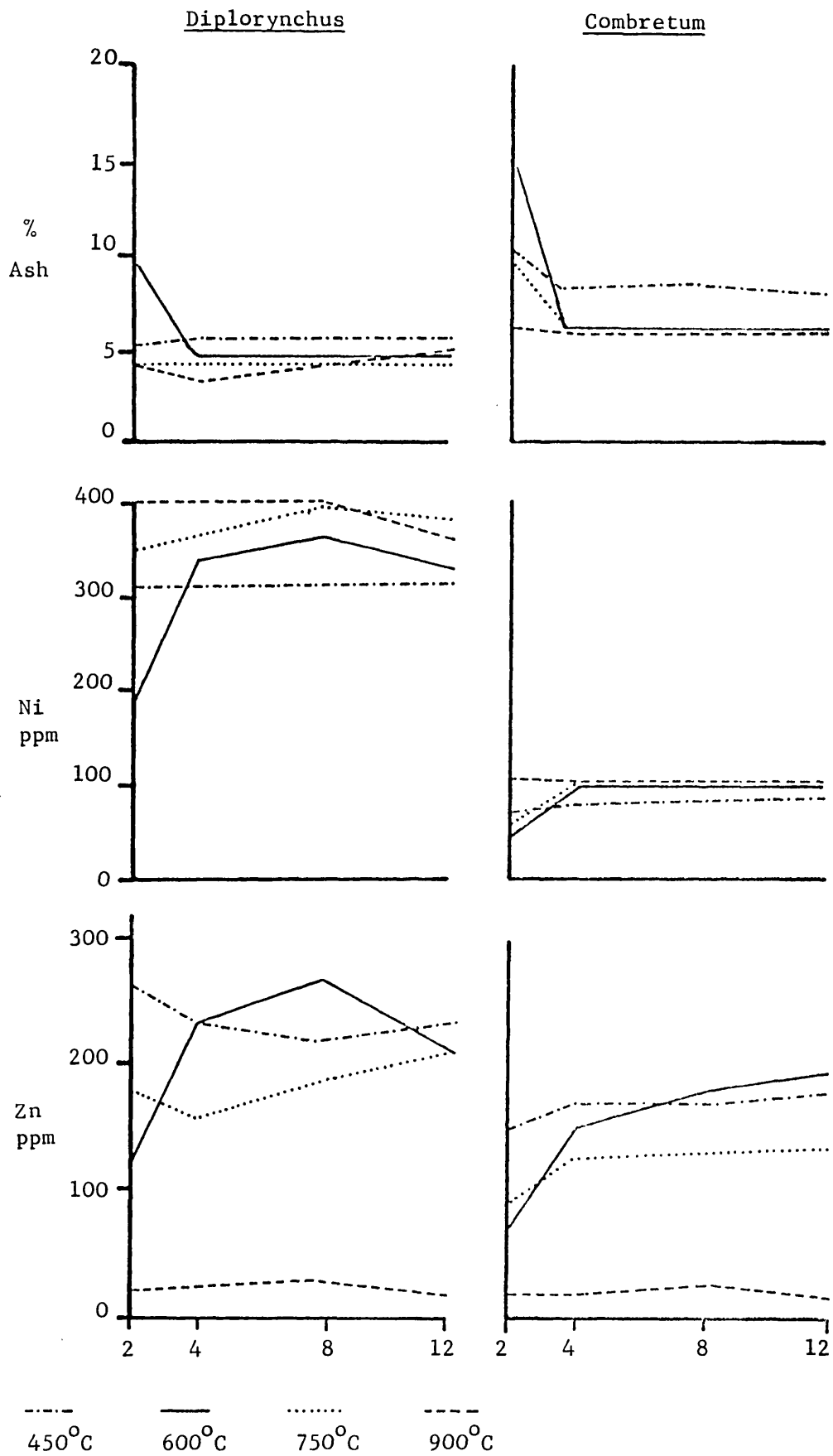
Figure 47: Preliminary leaf ashing and analysis experiments, % ash,
Ni and Zn concentrations obtained using different ashing
times and temperatures.

approximately 10 g of dried, crushed Diplorynchus leaf and
10 g of dried, crushed Combretum leaf were accurately
weighed into porcelain crucibles of known tare weight, and
these were placed in a muffle furnace at a fixed temperature
and for a measured time period. Then the crucibles were
removed from the furnace, allowed to cool and reweighed to
determine the weight of leaf ash, and the percentage ash
obtained from each sample was calculated. Sixteen such
experiments were performed using ashing times of 2, 4, 8 and
12 hours at furnace temperature settings of $450^{\circ}C$, $600^{\circ}C$,
$750^{\circ}C$ and $900^{\circ}C$. A number of duplicate ashings were carried
out as a rough control on ashing precision.

The percentage ash of both Diplorynchus and
Combretum samples ashed at most temperatures tends to fall
between the ashing times of 2 and 4 hours, but over longer
ashing times remains constant (figure 47). The percentage ash
of samples ashed at $600^{\circ}C$, $750^{\circ}C$ and $900^{\circ}C$ is very similar for ash-
ing times over 4 hours, but at $450^{\circ}C$ the percentage ash is
significantly higher. These features may be at least partly
a function of the type of crucibles and furnace employed, but
using this equipment the most effective ashing is achieved
over a period of 4 hours or more at a temperature of $600^{\circ}C$.

The ashed samples were finely ground in an
agate pestle and mortar, digested in 6M HCl, and analysed for
Ni and Zn by atomic absorption spectrophotometry. The samples
ashed for 2 hours or at $450^{\circ}C$ usually exhibit the lowest Ni values
because these samples are least efficiently ashed, and therefore
the trace elements are diluted by organic material. In the
longer duration and higher temperature ashings, comparatively
higher and fairly uniform Ni values are obtained. Zinc was
determined to assess the effect of ashing temperature on the
more volatile elements, and Zn values are highest at $450^{\circ}C$
and $600^{\circ}C$, slightly lower at $750^{\circ}C$, and fall sharply at $900^{\circ}C$
due to volatilization of Zn.
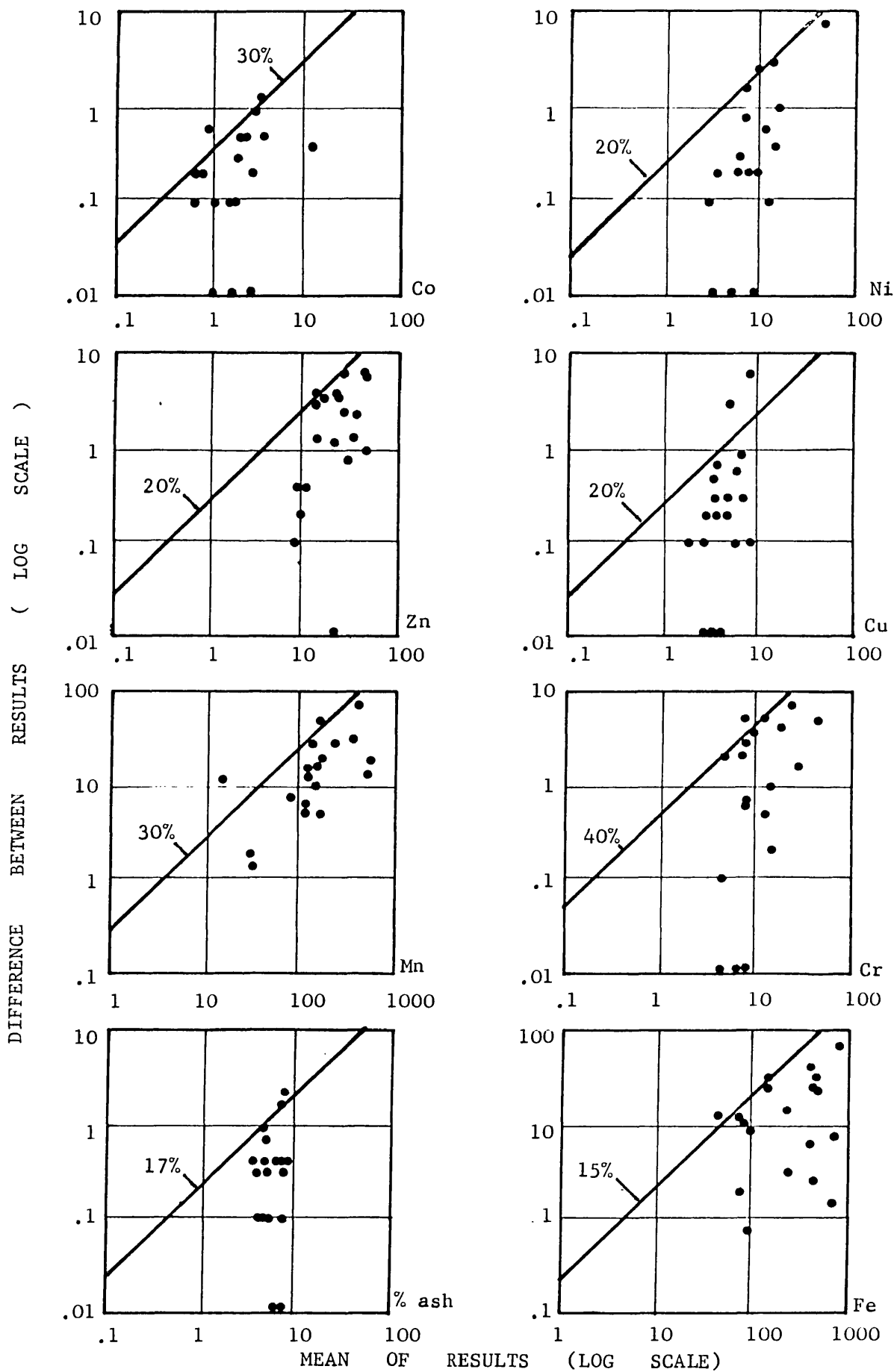
Figure 48: Duplicate determinations and precision estimates for leaf sample ashing and analyses (for details of chart construction see Thompson and Howarth, 1973; all trace element val in ppm).

From the percentage ash and analytical results
it appears that the most valid leaf ash trace element
data are obtained by ashing for 4 hours or more at a furnace
temperature setting of $600^\circ C$, although a temperature of
about $450^\circ C$ is conventially used in ashing biogeochemical
samples (Brooks, 1972). The higher temperature setting required
for effective ashing is attributed to poor calibration and
heat distribution of the muffle furnace employed. All
Diplorynchus and Combretum leaves were therefore ashed for 4
to 5 hours at a furnace temperature setting of $600^\circ C$, and the
ash was analysed for Ni, Cu, Co, Zn, Cr, Fe and Mn by atomic
absorption spectrophotometry. The percentage ash figures and
analytical results were processed by a computer program PRASH,
which calculated the trace element content of the original
dried leaf material.

No biogeochemical standards were available for
analysis. A total of 19 leaf specimens were ashed and analysed
in duplicate, and a graphical estimate of asymptotic precision
was made from the duplicate data (figure 48). The precision
of duplicate ashing weights of 17% is considered fair. Overall
biogeochemical trace element precision, incorporating ashing
and analytical precision, was estimated by graphically plotting
the computed trace element content of the original leaf
material, and was found to be approximately 15% for Fe, 20% for
Ni, Cu, Zn and Mn, 30% for Co and 40% for Cr. A poor hollow
cathode lamp was employed in Cr analysis, and these results
are to be interpreted with reservation.

3.10. Data manipulation

All data generated in the general analysis
programme were coded and punched onto cards for computer
manipulation prior to statistical evaluation. Initially five
master files were created on disk, comprising: (i) total
metals by atomic absorption spectrophotometry; (ii) total
metals by emission spectrography; (iii) metals in sulphide
minerals; (iv) S-F-pH and (v) metals in leaves. These
master files were rationalized by processing with a succession

of specially-written programs.

The total metals by emission spectrography master
file was processed by MANGAN to select the appropriate Mn
value from the two provided by separate channels of the
spectrometer covering different Mn concentration ranges. Then
DUPROC took each master file in turn, sorted the data from
random in ascending sample number order, replaced duplicate
analyses by mean values and created new files of means and
differences (which were used as input to PRESIN). The five
sorted master files were divided into subsidiary field area files
and, where appropriate, sample type files, by SPLITUP. Then
MERGEF performed amalgamation of the total metals by atomic
absorption spectrophotometry (or metals in sulphide minerals),
emission spectrography and S-F-pH files for each field area
and sample type. The numerous field area and sample type
files now created were written onto duplicate magnetic tapes
as UPDATE libraries for permanent storage. Two further programs,
SOURCER and UPNAM were prepared for conveniently extracting
individual files from the library for statistical processing,
and for submitting newly processed information into the library
for storage.

4. **PRIMARY DISPERSION PATTERNS**

Core and outcrop samples were analysed for total metals by emission spectrography, for metals in sulphide minerals, and for S. The core samples from diamond drillhole MH58 were used in an initial appraisal of the elements indicating mineralization, and were additionally analysed by atomic absorption spectrophotometry, with these results substituted for corresponding emission spectrography data. Analytical results are given in detail in appendix 2.

4.1. **Diamond drillhole MH58**

Diamond drillhole (DDH) MH58, at Munali, was drilled to intersect at depth shear zones within the gabbro and near to the gabbro contact along the northeastern contact of the intrusive. The drillhole was collared in gabbro and passes through 303 m of gabbro, including calcareous gabbro and shear zones, and then passes into schistose calcareous quartzite, and was stopped at 320 m. Specks of sulphides were noted throughout the core during logging, and blebs and veinlets were recorded between 135 and 155 m from surface, and 260 and 290 m. The sulphides present are mainly pyrite, and this is accompanied by pyrrhotite in the bands of blebs and veinlets and a little chalcopyrite around 78 m and 194 m.

The core of DDH MH58 was specially chosen for its zones of weak mineralization, in order to provide analytical results within the usual working range of the techniques used. The core was sampled at 5 m intervals to furnish 63 samples (a sample from 250 m was lost) representative of the drilled profile.

The sulphides in the core, recorded as pyrite, pyrrhotite and chalcopyrite, contain much, but not all, of the Ni, Cu, Co, Zn and to a lesser extent Fe. The results of bromine attacks show that of a mean of 87 ppm Ni, 53% occurs as Ni_s (i.e. in sulphide minerals; table 14). The mean Cu content of the core is 55 ppm, of which 67% is in the form of Cu_s. About 48% of the 46 ppm Co present is Co_s, while 38% of the 24 ppm Zn is Zn_s.
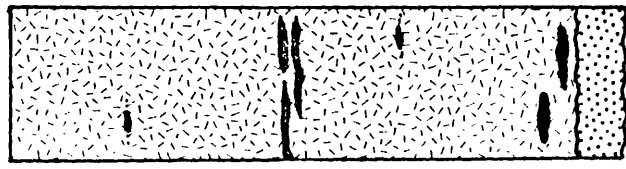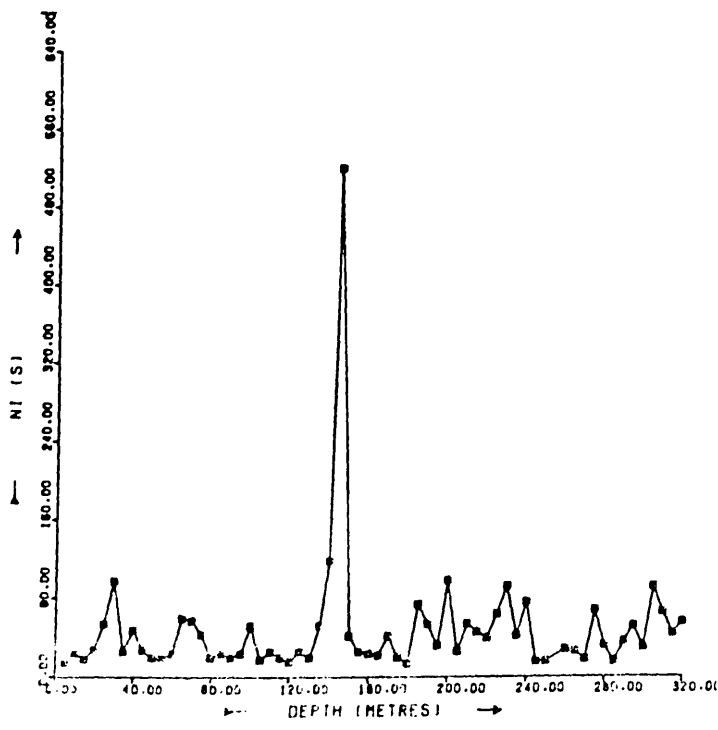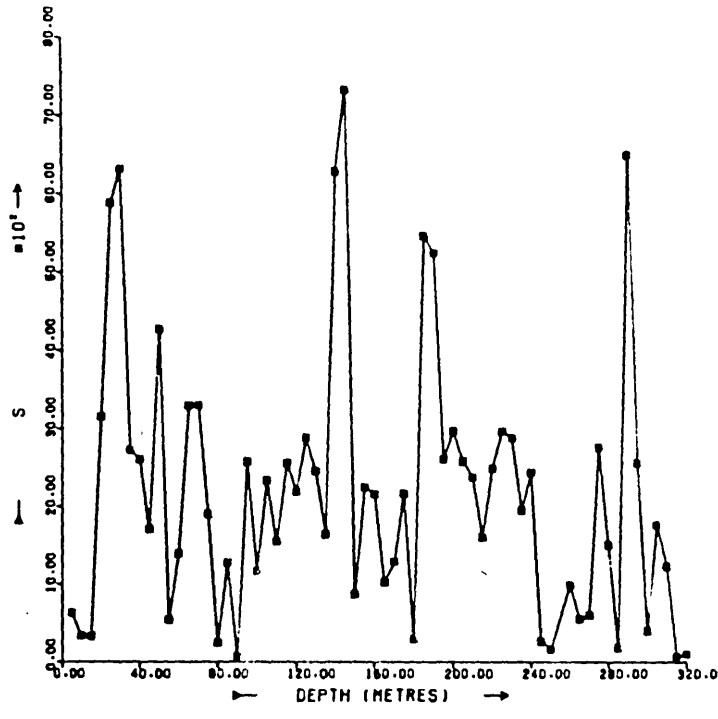
Figure 49: DDH MH58, distribution of Ni$_s$ (ppm) and S (ppm)
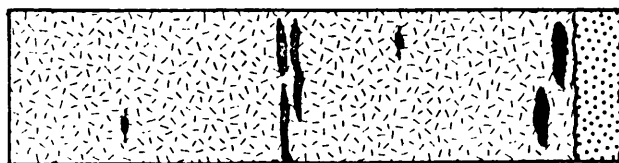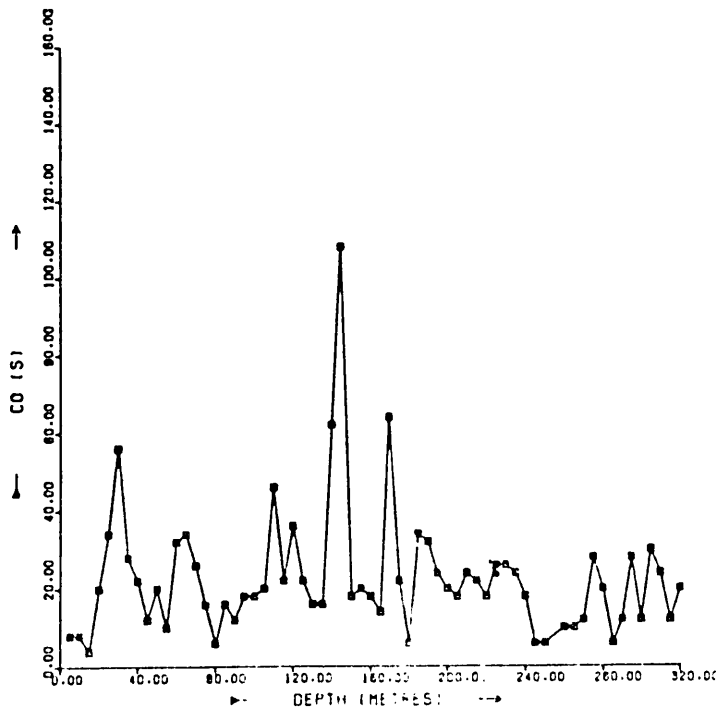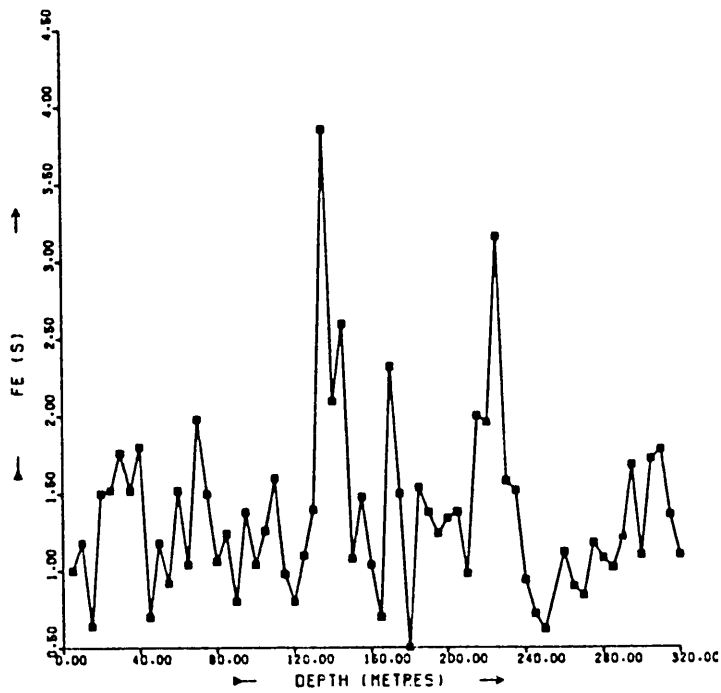
Figure 50: DDH MH58, distribution of Co_s (ppm) and Fe_s (%)
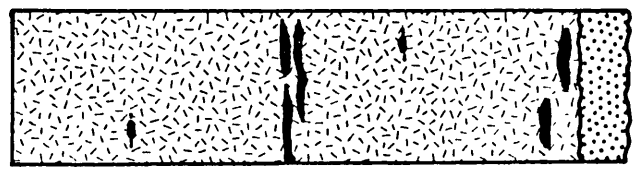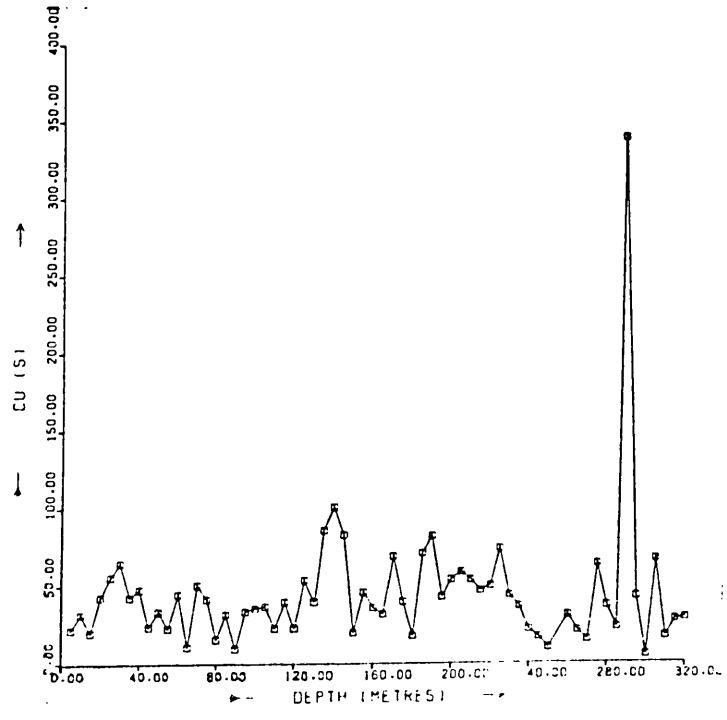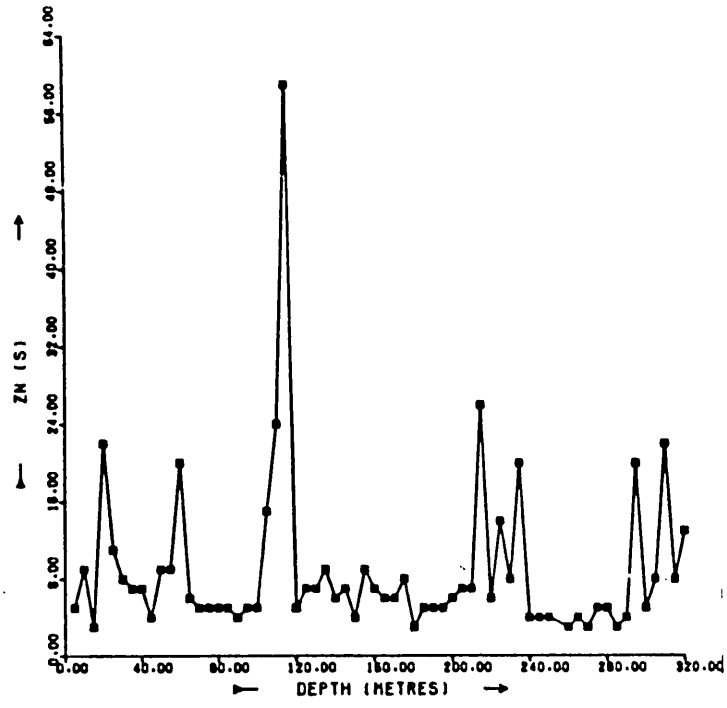
Figure 51: DDH MH58, distribution of Cu_s (ppm) and Zn_s (ppm)

The core contains 10.7% Fe, but only 12% of this amount is present as Fe_s. The non-sulphide Fe is distributed among ferro-magnesian silicates, mainly augite, and the magnetite and ilmenite clearly visible in the rock. There is 2380 ppm S in the core, fully ascribed to sulphides. As a guide to the success of the bromine attack in extracting metals from sulphide minerals only, Ti_x (the amount of Ti extracted during the bromine attack) was determined, and averages 55 ppm. This Ti_x level represents less than 2% of the mean of 4840 ppm Ti in silicates (extracted by HNO_3-HClO_4)and less than 0.4% of 15,300 ppm total Ti (determined by emission spectroscopy), believed to be mainly in magnetite and ilmenite.

The correlations between S and metals in the sulphide phase are obscured by the diversity of the sulphide minerals present and their varying chemical composition. There are correlations between S and the chalcophile and siderophile elements of + 0.72 with Co_s, + 0.47 with Cu_s, + 0.47 with Ni_s, + 0.39 with Fe_s and +0.22 with Zn_s. There is a correlation of + 0.78 between Ni_s and Co_s, reflecting the substitution of Co for Ni in nickeliferous pyrrhotite and any exsolved pentlandite within the pyrrhotite.

Some samples (but not all) from the weakly mineralized zone between 135 and 155 m have very high concentrations (in excess of the mean plus three standard deviations) of 520 ppm Ni_s, 108 ppm Co_s, 3.9% Fe_s, 3.3 ppm Mo, and high concentrations (mean plus two standard deviations) of 16.2% Ca, 7.4% Mg and 7340 ppm S (figures 49 and 50). The mineralized zone between 260 and 290 m includes samples with very high values of 340 ppm Cu_s and 6530 ppm S, presumably attributable to unobserved chalcopyrite, while the maximum Zn_s concentration of 59 ppm is found at 115 m and may be due to a trace of sphalerite, or more than average zinc in other sulphides (figure 51).
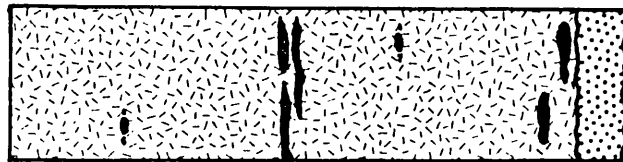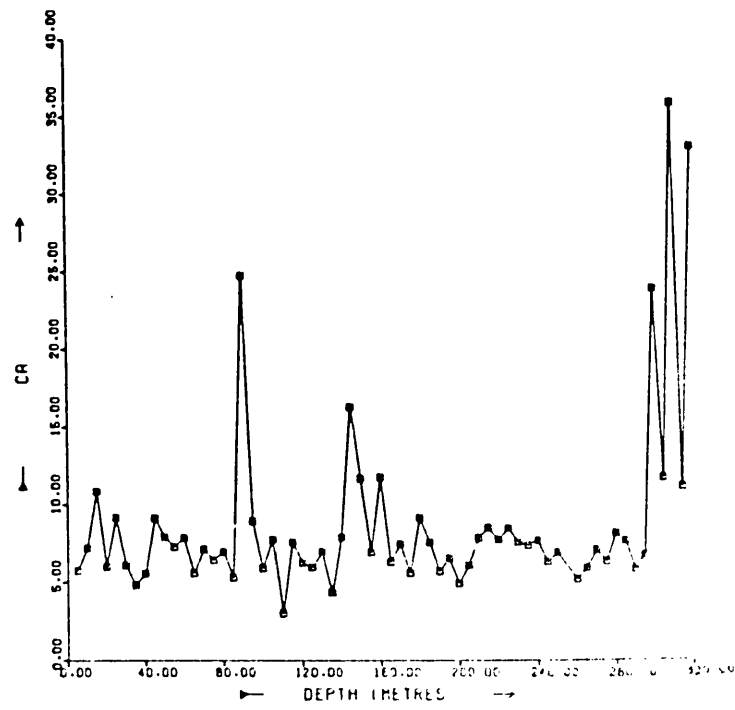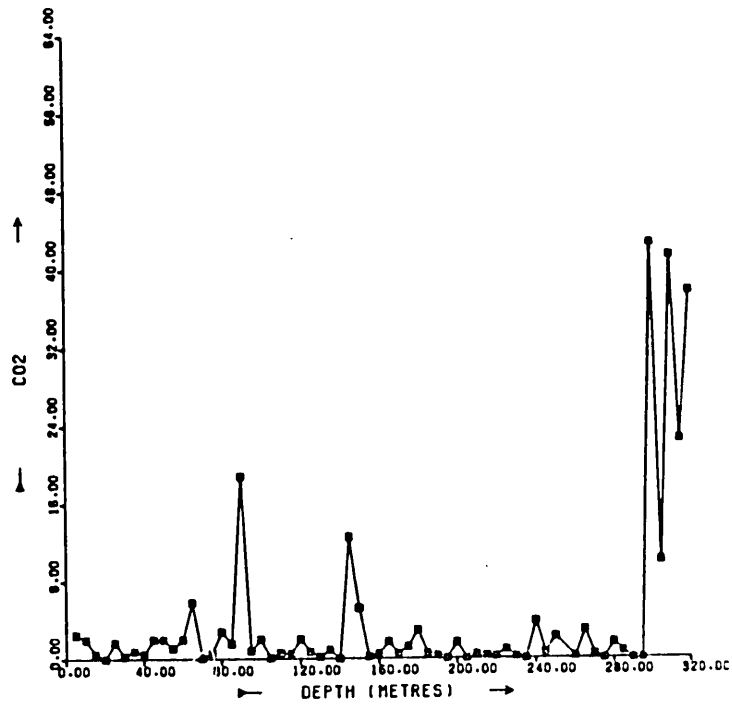
Figure 52: DDH MH58, distribution of Ca(%) and CO_2(%)
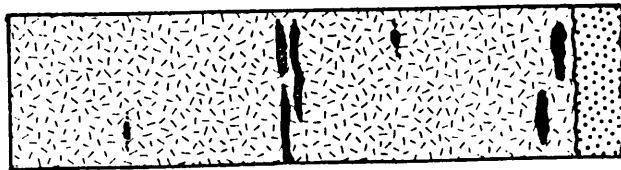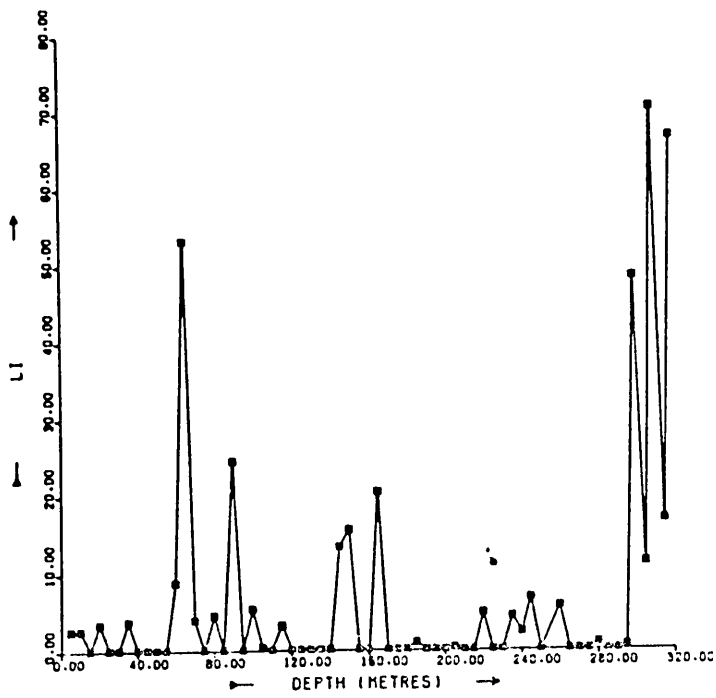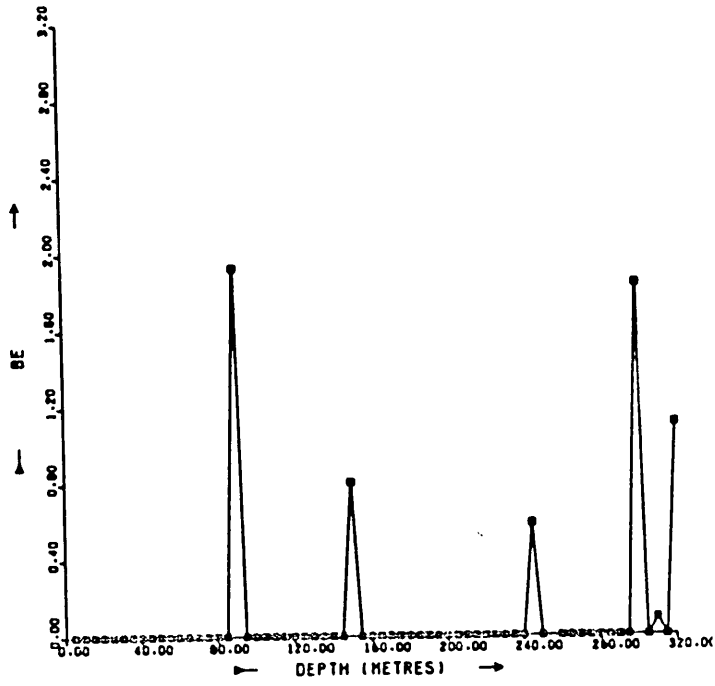
Figure 53: DDH MH58, distribution of Li (ppm) and Be (ppm)
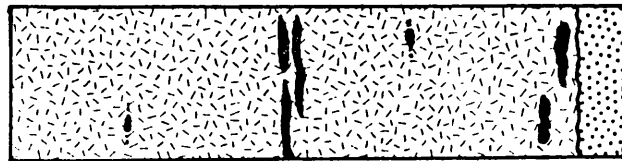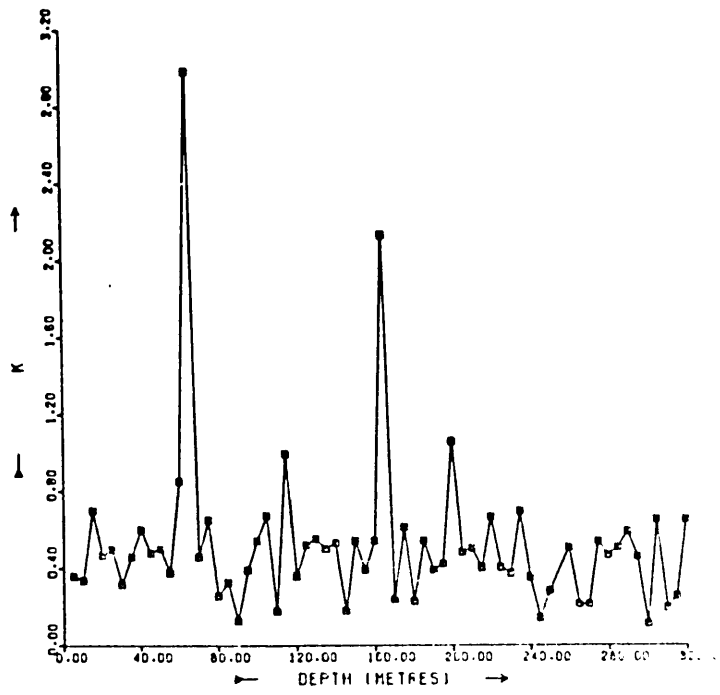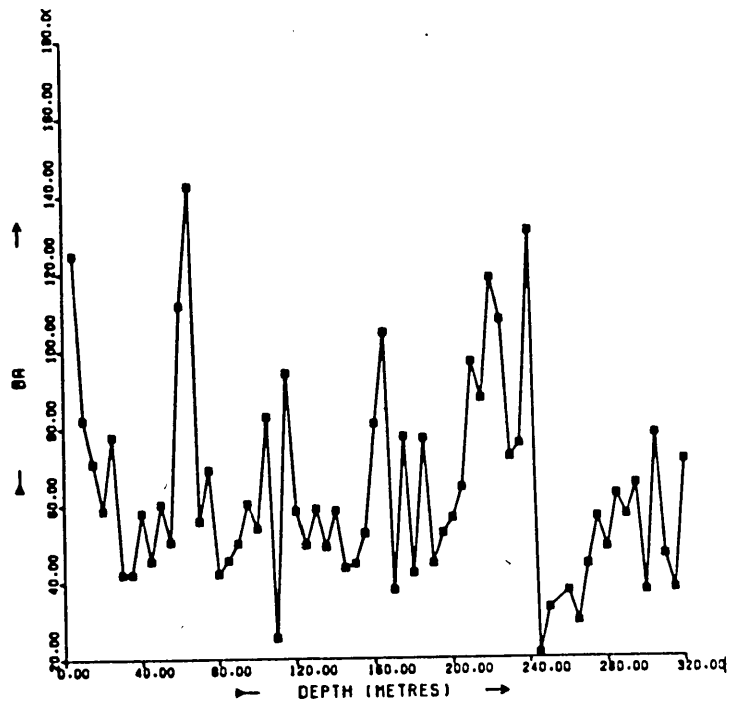
Figure 54: DDH MH58, distribution of K (%) and Ba (ppm)

The Ca content of the core occurs predominantly in calcite in the schistose calcareous quartzite and calcareous gabbro shear zones, and consequently Ca does not exhibit a strong correlation with other elements in silicate minerals, which contain comparatively little Ca. The mean Ca content of the core is 8.6%, and its strong association with carbonate minerals is shown by a correlation of + 0.91 with CO_2 (figure 52). The core contains 212 ppm Sr and 7 ppm Li, and there appears to be substitution of Ca by Sr, since Ca and Sr are related by a correlation coefficient of + 0.81. Li is commonly closely associated with carbonate minerals, and Ca and Li exhibit a correlation of + 0.81, while Be, only present in a few samples, has a correlation of + 0.65 with Ca. There is some association of Mn and Zn with carbonates, but these elements exhibit non-significant correlations with Ca. The mean Mg content is 4.1%, but Mg is only moderately correlated at + 0.59 with Ca, and slightly elevated Mg values reflect the presence of talc and chlorite in shear zones. In the calcareous quartzite between 303 and 320 m there are exceptionally high concentrations of up to 35.7% Ca, 1240 ppm Sr, 71 ppm Li, 1.8 ppm Be, and fairly high levels of 8.2% Mg and 1280 ppm Mn. These same elements are enriched in shear zones within the gabbro. Around 90 m there is 24.7% Ca, 1.9 ppm Be, 8.0% Mg and 1180 ppm Mn; and in the mineralized shear zone between 135 and 155 m there are values of 16.2% Ca, 7.4% Mg, 16 ppm Li, and 0.8 ppm Be (figure 53). These associations suggest that the calcareous quartzite contact rock and the shear zones within the gabbro are zones which have been subjected to hydrothermal alteration, and in places, sulphide mineralization appears to be associated with the hydrothermal alteration.

Augite contains much of the Al, Sc, Si, Ti, V, and Ga present in the core. The mean Al content of the core is 9.0% and the Sc level is 21 ppm, and a + 0.83 correlation indicates some substitution for Al by Sc. The Si mean is a 23.9% and Si shows a + 0.68 correlation with Al. The Ti level of 4840 ppm is higher than usual for common augite, but not sufficiently high to warrant titanaugite nomenaclature. There is a + 0.81 correlation between Ti and Al and + 0.61 between Ti and Si. Ga and V, averaging 39 and 304 ppm respectively, probably substitute for Ti in the augite lattice. The augites can also be expected to contain some Fe, Ca, Mg and traces of

Ni, Cu, Co, Zn, Cr and Mn.

A significant proportion of the Al, Sc and Si content of the core is contained in plagioclase. This also contains the 0.5% K and 64 ppm Ba which are present, probably in orthoclase molecules within the plagioclase. Ba substitutes for K, and the two are related by a correlation coefficient of + 0.52. The plagioclase contains some of the Ca present in the core and possibly a little of the Fe, but probably no significant amount of heavy metals. At 65 m there appears to be a somewhat feldspathic, poorly mineralized shear zone with high concentrations of 3.0% K, 142 ppm Ba, 53 ppm Li, and elevated values of 60 ppm Ni_s, 34 ppm Co_s and 20 ppm Zn_s (figure 54).

The elements providing the best guide to the zones of mineralization in DDH MH58 are Ni_s, Cu_s, Co_s, Fe_s, Zn_s, and S, while what are regarded as consistently high Fe_s values suggest a high level of S activity in the Munali gabbro. High concentrations of Ca, Be and Li in particular delineate hydrothermally-altered shear zones which are favourable environments for the best grades of mineralization. Although Mg values are higher in shear zones there is little contrast with background. Other elements showing some apparent association with mineralization and shear zones are K, Ba, Sr, Mn and Mo.

4.2. Random core samples

Randomly selected samples of visibly non-mineralized mafic and ultramafic rocks were taken from drill cores at the mineralized Munali and Trojan areas and the non-mineralized Chombwa and Paulwi areas. Between 12 and 25 core samples were taken in each area, according to the drilling meterage and distribution. Since the Trojan and Kingston intrusives are believed to derive from the same parent body, the core (and outcrop) samples from both of these areas are considered as a single group termed Trojan.

```
      .600      1.535      2.470      3.405      4.340      5.275      6.210      7.145      8.080      9.015      9.950
      +----------+----------+----------+----------+----------+----------+----------+----------+----------+----------+
      I                                                                                              ?       I
      +-M+                                                                                                   I
      I                                                                                                      I
      I    +--B---+                                                                                          I
      I                                                                                                      I
      I           +---P----+                                                                                 I
      I                                                                                                      I
      I                                                     +--------------------T----------------------+    I
      I                                                                                                      I
      I                                                                                                      I
      +----------+----------+----------+----------+----------+----------+----------+----------+----------+----------+
      .600      1.535      2.470      3.405      4.340      5.275      6.210      7.145      8.080      9.015      9.950



      .100       .320       .540       .760       .980      1.200      1.420      1.640      1.860      2.080      2.300
      +----------+----------+----------+----------+----------+----------+----------+----------+----------+----------+
      I                                                             /                                        I
      I  +-M+                                                                                                I
      I                                                                                                      I
      I            +----------B---------+                                                                    I
      I                                                                                                      I
      I                               +--------P---------+                                                   I
      I                                                                                                      I
      I                                             +-----T------+                                           I
      I                                                                                                      I
      +----------+----------+----------+----------+----------+----------+----------+----------+----------+----------+
      .100       .320       .540       .760       .980      1.200      1.420      1.640      1.860      2.080      2.300
```
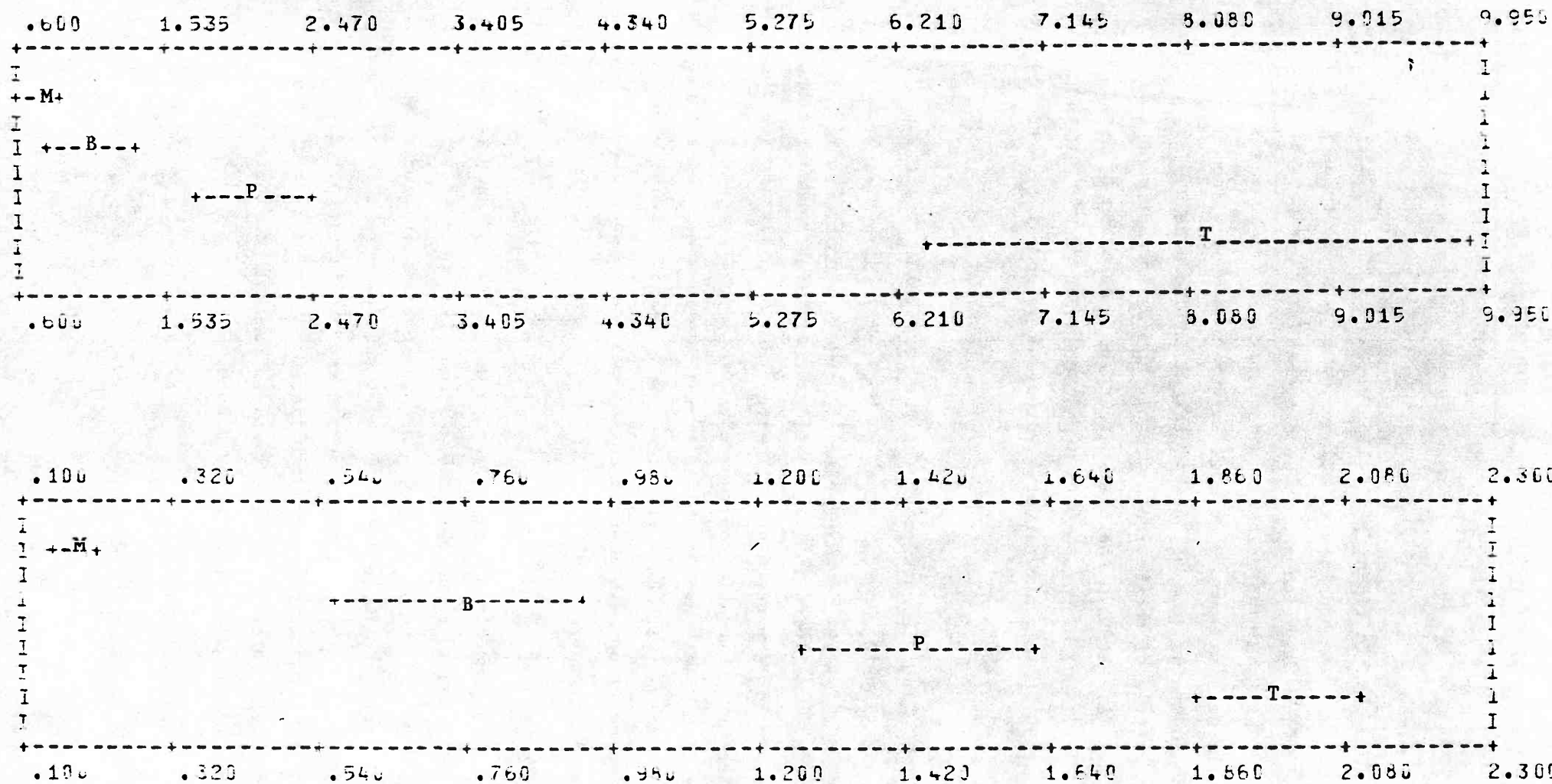
Figure 55:   Plot of mean and standard error range of variables determined in random core samples; top Ni_s (ppm, scaling factor 100); bottom Ni (ppm, scaling factor 1000)

	DDH MH58	Random core samples				Random outcrop samples						
		M	B	P	T	M	B	P	K	A	C	T
Ni	48	79	114	214	819	22	118	68	145	39	29	390
Cu^S	37	33	19	42	52	17	60	11	1	58	46	121
Co^S	23	20	16	15	35	5	15	4	6	6	8	16
Zn^S	9	15	5	10	30	5	13	6	4	6	8	5
$Fe^S\%$	1.4	0.7	0.7	0.3	0.7	0.2	0.8	0.3	0	0.5	0.6	0.1
Ti^S	55	13	13	8	11	1	0	0	0	3	4	0
$Fe^X\%$	10.7	6.7	4.6	5.9	5.0	12.0	4.6	5.6	6.0	4.8	3.9	5.5
Cu	55	60	35	55	99	148	77	32	23	64	76	96
Pb	11	11	13	15	17	11	11	18	14	21	12	13
Mo	0.4	0.2	0.3	0.4	0.3	0.6	0.3	0.3	0.2	0.6	0.3	0.6
V	304	694	163	102	63	572	198	119	63	161	256	57
Co	46	33	63	101	104	61	57	95	108	71	45	113
Ni	87	189	768	1460	1990	748	518	1450	1770	775	262	2590
Cr	58	235	1130	2190	1420	303	1200	2100	1060	1210	365	1450
Ga	39	23	9	7	4	20	11	6	6	10	16	4
Sn	14	8	12	18	19	6	8	17	12	6	3	12
Ti	1.5%	1.3%	3430	1530	388	1.3%	4080	1200	1400	2250	3770	544
Be	0.1	0	0	0.1	0.1	0.2	0	0.1	0	0.3	0	0.2
Mg %	4.1	4.3	7.1	8.2	9.8	3.5	6.3	8.1	8.3	6.5	3.2	8.7
Ca %	8.6	5.2	3.7	1.7	1.4	3.8	5.3	2.6	1.3	3.0	4.8	0.4
Sr	212	202	129	69	19	127	236	49	35	95	274	15
Ba	64	69	107	105	43	113	136	81	63	200	349	44
K %	0.5	0.7	0.5	0.6	0.1	0.3	0.4	0.2	0.1	0.2	1.1	0.1
Li	6.6	4	13	12	3	1	7	4	0	7	12	0
Al %	9.0	6.7	5.6	2.3	1.4	5.6	7.1	2.0	1.2	4.5	8.0	0.8
Sc	21	26	12	8	4	28	15	9	4	12	15	2
Si %	23.9	17.6	13.0	12.8	10.3	16.1	16.1	12.4	7.3	15.6	21.4	11.9
Mn	393	1170	1360	1250	810	872	1770	1240	904	1620	1380	714
S	2380	1540	1070	386	2430	460	598	170	193	237	578	528
Zn	24											

C = Chinkozia   B = Chombwa   K = King Edward   M = Munali

A = Musangashi   P = Paulwi   T = Trojan (incl. Kingston)

*By atomic absorption = 4840 ppm Ti

Table 14: Mean trace and major element content of core and outcrops samples (ppm, except as stated).
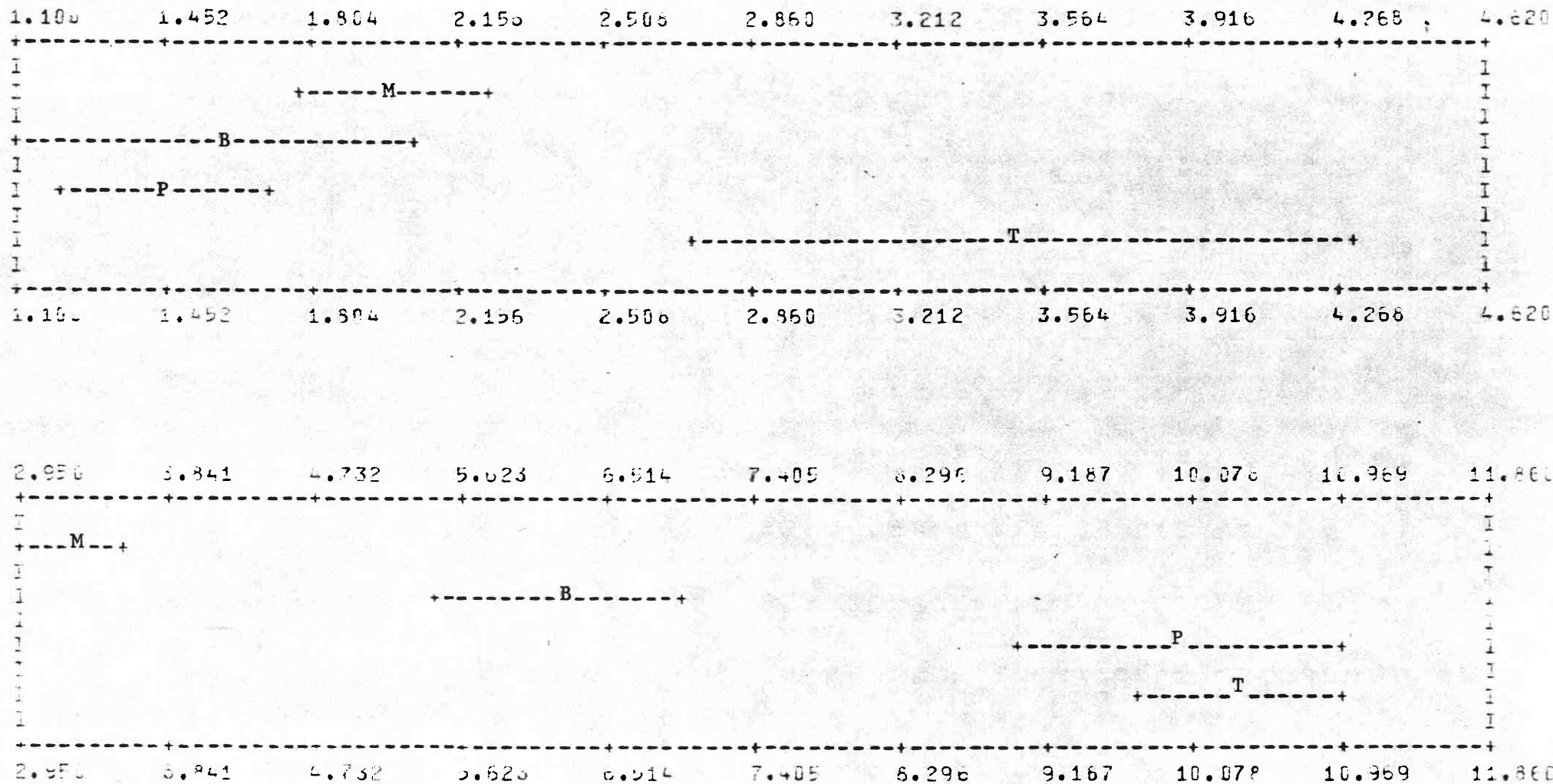
Figure 56: Plot of mean and standard error range of variables determined in random core samples ; top Co_s (ppm, scaling factor 10) ; bottom Co (ppm, scaling factor 10).

These core samples were used as a training set for the identification of the most suitable variables to distinguish between the mineralized class and the non-mineralized class of intrusives. The elements found to occur in high concentrations in the mineralized zones of DDH MH58, plus other selected variables, were computer processed by a program MARPLOT, which compiled comparative plots of the mean and standard error of each variable for each field area (figures 55 to 61). The nemorics used to indicate variable means in these figures also define field areas according to the legend in table 14.

The plots of Ni and Ni_s show that Ni is highest in the older serpentinized ultramafic intrusives at Paulwi and Trojan, and lowest in the post-Katanga gabbroic intrusives at Chombwa and Munali (figure 55). The Ni_s variable is successful in identifying the Trojan area as mineralized by token of its clearly higher mean of 819 ppm Ni_s, but Munali, with the lowest Ni content of the four areas, also exhibits the lowest mean Ni_s value of 79 ppm (table 14). This reflects the modes of occurrence of the mineralization which is disseminated ore at Trojan but massive and localized concentrations at Munali.

By contrast, although Co shows a similar distribution to Ni and reflects the mafic and ultramafic nature of the different rock types, Co_s is better than Ni_s in identifying mineralized areas (figure 56). The Trojan area, again, has clearly the highest Co_s content. At Munali the 20 ppm Co_s mean is higher than 16 ppm at Chombwa and 15 ppm at Paulwi, although there is some overlap in the standard error ranges at Munali and Chombwa.

The Cu_s and Fe_s variables are each only partly successful in selecting the mineralized areas (figure 57). The Cu_s level is highest at Trojan, followed by Paulwi then Munali. There is extensive overlap in the Fe_s standard error ranges, but Chombwa exhibits the highest mean, followed by Munali and Trojan.

Figure 57: Plot of mean and standard error range of variables determined in random core samples; top Cu_s (ppm, scaling factor 10); bottom Fe_s (%, scaling factor 10)

```
     .350        .724       1.098       1.472       1.846       2.220       2.594       2.968       3.342       3.716       4.090
   +-------------+-----------+-----------+-----------+-----------+-----------+-----------+-----------+-----------+-----------+
   I                                                                                                                        I
   I                                    +------M------+                                                                     I
   -                                                                                                                        -
 I +-B-+                                                                                                                    I
   I                                                                                                                        I
   I                        +----P-----+                                                                                    I
   I                                                                                                                        I
   -                                              +-----------------------T------------------------+                        -
   I                                                                                                                        I
   +-------------+-----------+-----------+-----------+-----------+-----------+-----------+-----------+-----------+-----------+
     .350        .724       1.098       1.472       1.846       2.220       2.594       2.968       3.342       3.716       4.090


     .250        .597        .943       1.290       1.636       1.983       2.329       2.675       3.022       3.369       3.715
   +-------------+-----------+-----------+-----------+-----------+-----------+-----------+-----------+-----------+-----------+
   -                                                                                                                        -
   I                                    +--------M------+                                                                   I
   I                                                                                                                        I
   I      +---------------B-----------------+                                                                               I
   I                                                                                                                        I
 I +--P---+                                                                                                                 I
   I                                                                                                                        I
   I                                              +-------------------T----------------------+                             I
   I                                                                                                                        I
   +-------------+-----------+-----------+-----------+-----------+-----------+-----------+-----------+-----------+-----------+
     .250        .597        .943       1.290       1.636       1.983       2.329       2.675       3.022       3.369       3.715
```
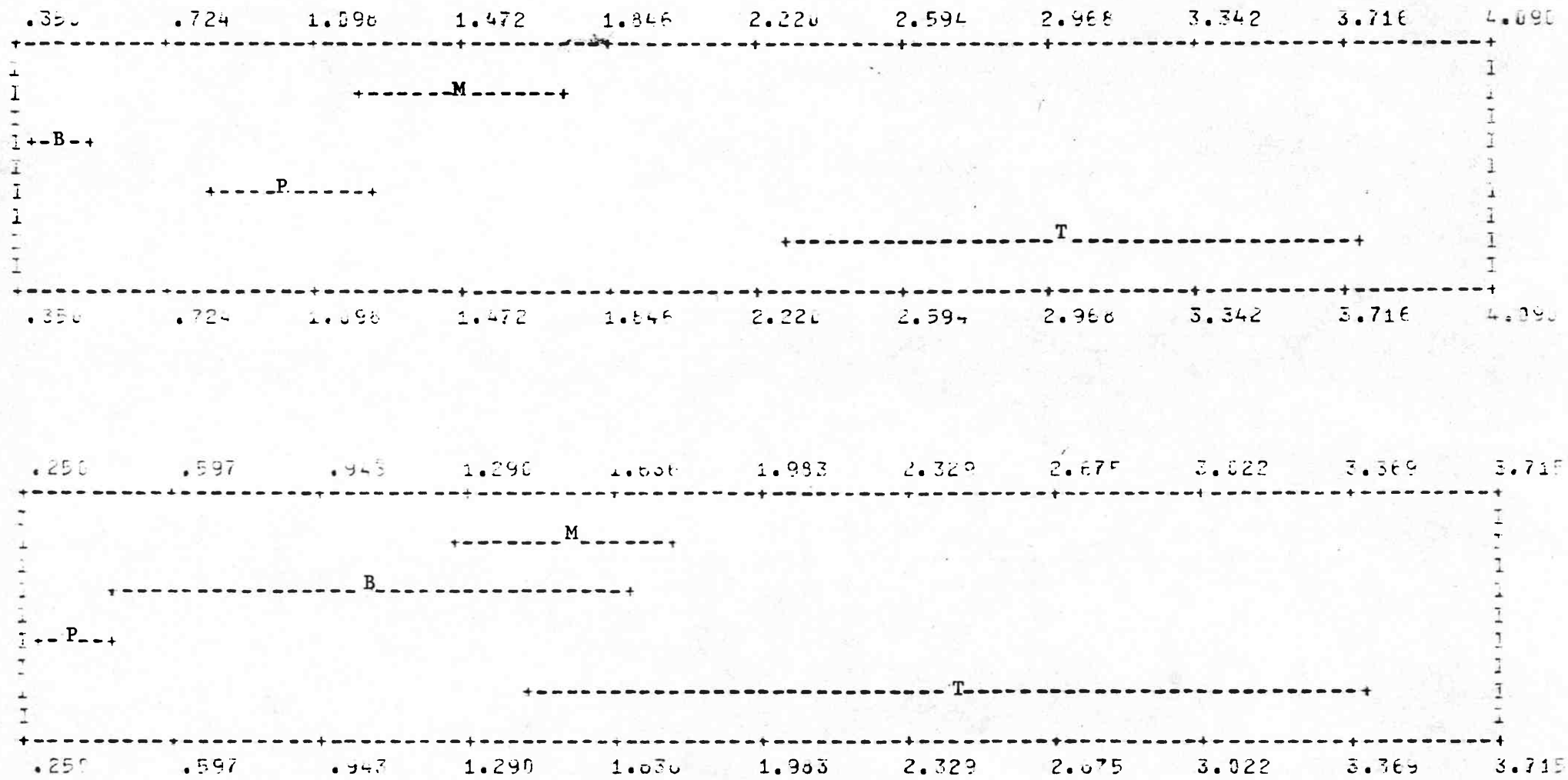
Figure 58: Plot of mean and standard error range of variables determined in random core samples; top Zn_s (ppm, scaling factor 10); bottom S (ppm, scaling factor 1000).
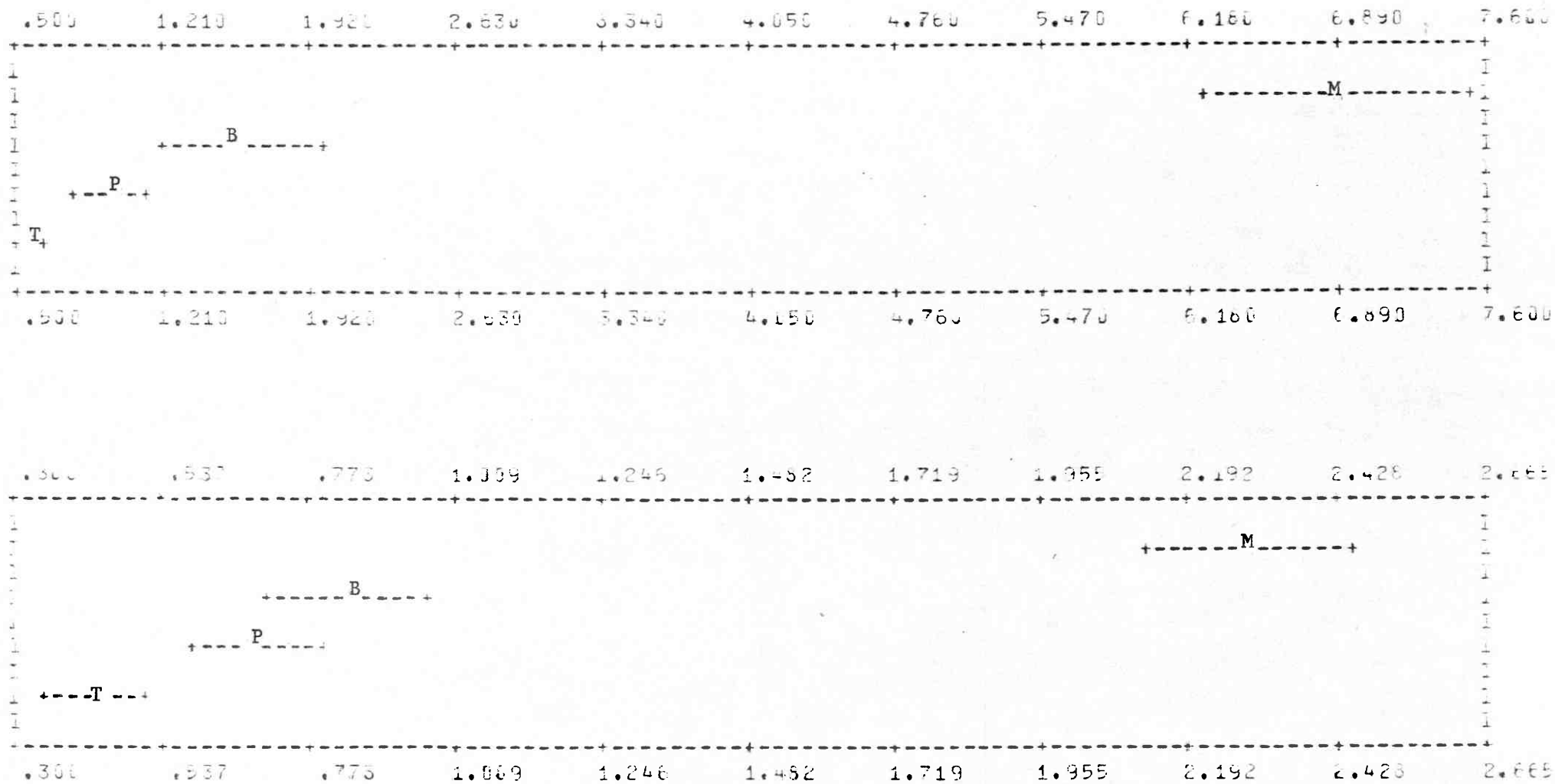
Figure 59:   Plot of mean and standard error range of variables determined in random core samples; top V (ppm, scaling factor 100); bottom Ga (ppm, scaling factor 10).

The Zn_s variable appears to be a useful identifier
of mineralization, with high mean concentrations of 30 ppm at Trojan
and 15 ppm at Munali, and low levels of 10 ppm at Paulwi and 5 ppm
at Chombwa (figure 58). There is little overlap of the standard
error ranges for the different field areas. This surprising
distribution of Zn_s does not correlate significantly with other
metals in sulphide minerals, and therefore seems likely to be
attributable to fine grains of disseminated sphalerite.

Similar good contrast between the mineralized and
non-mineralized classes is furnished by S (figure 58). At Trojan
there is a high mean of 2430 ppm S and at Munali 1540 ppm, while
at Chombwa there is 1070 ppm and at Paulwi 386 ppm. This
similarity between the Zn_s and S patterns is not taken to imply
a close sample-for-sample relationship between the two variables,
because their correlation coefficient is only + 0.28.

The Ti and Ti_x data confirm the general success
of bromine in attacking only sulphide minerals. The mean Ti
content of the rocks of the different areas varies from 1.3% at
Munali to 388 ppm at Trojan. The amount extracted during bromine
attacks varies from a mean of 8 ppm Ti_x at Paulwi to 13 ppm at
Chombwa indicating that a small and constant amount of Ti_x is
obtained irrespective of the quantity of total Ti in silicates and
any ilmenite in the rock.

The Ga and V contents of the rocks in each area
correlate closely with one another and with Ti. By far the highest
values occur at Munali, and are mutually related by correlation
coefficients ranging from + 0.57 to + 0.88 (figure 59). These high
levels of Ti, V and Ga are attributed to titanium-rich augite, with
substitution of V and Ga for Ti in the crystal lattice. At Chombwa
fairly high levels of Ti, V and Ga probably occur in hornblende,
and are mutually correlated by coefficients in the range + 0.69 to
+ 0.95.
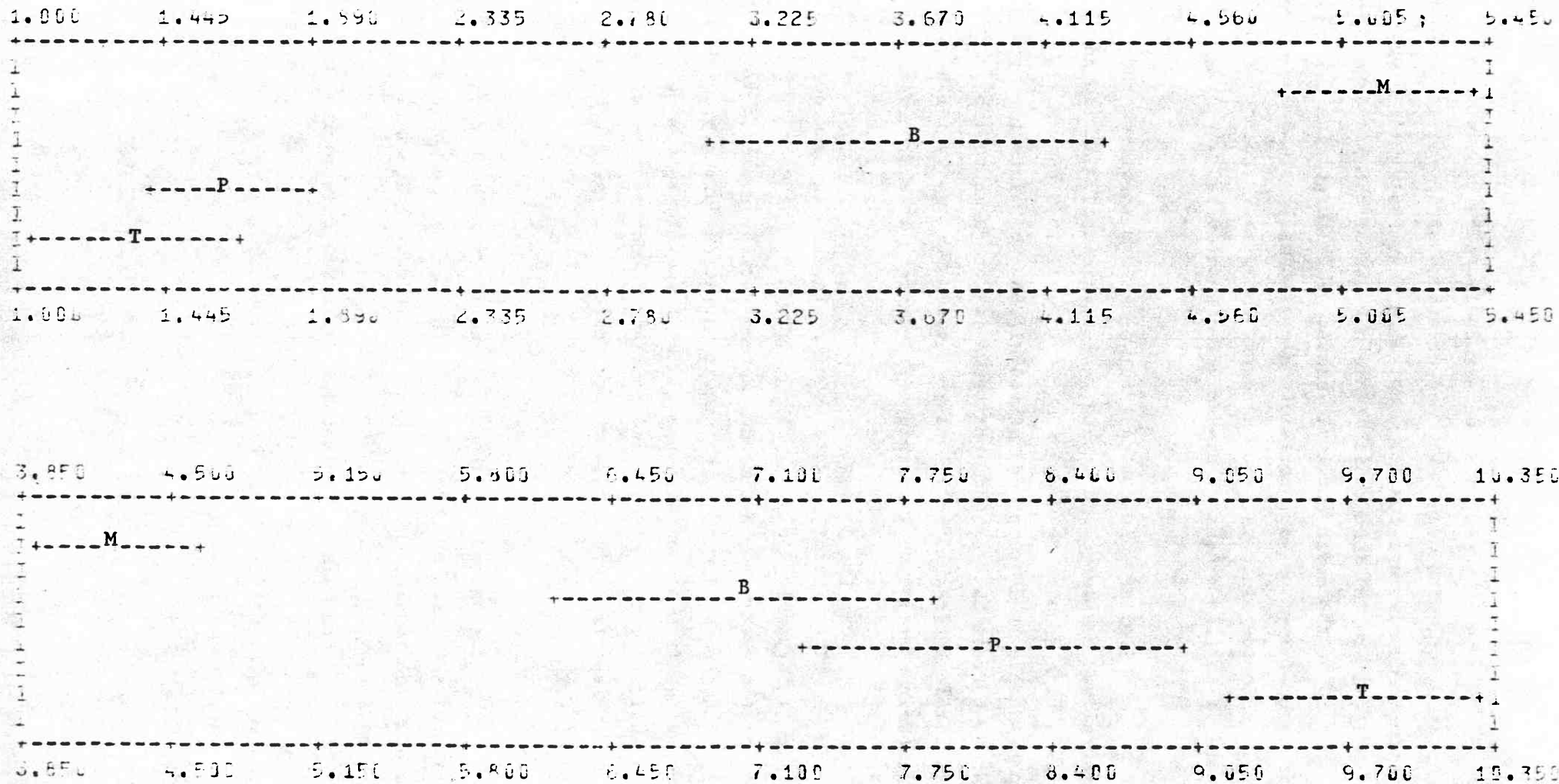
Figure 60: Plot of mean and standard error range of variables determined in random core samples; top Ca (%, scaling factor 1); bottom Mg (%, scaling factor 1)

The values of these elements in the low pyroxene and amphibole
ultramafic rocks is much lower. The olivine-rich and serpentine-
rich rocks of the Trojan-Kingston complex contain only 388 ppm Ti,
63 ppm V and 4 ppm Ga, with correlations of between + 0.85 and
+ 0.91. At Paulwi the mean Ti, V and Ga levels are slightly
elevated due to a single sample of pyroxenite core containing
1.4% Ti, 293 ppm V and 19 ppm Ga. Nevertheless the elements have
mutual correlation coefficients ranging from + 0.86 to + 0.95.

Localized enrichments of Ca, Mg, Li and Be in
hydrothermal minerals in shear zones such as those noted in DDH
MH58, are not observed in random core sampling. High levels of
Ca at Munali, where the mean is 5.2%, may be ascribed to the high
calcite content of the rocks, especially as Ca is not strongly
correlated with other elements, but this is probably derived by
assimilation of the limestone host rock during intrusion (figure 60).
At Chombwa a mean of 3.7% Ca is clearly correlated with Al, Si, Ti,
V, and Ga by coefficients in the range + 0.73 to + 0.96, suggesting
that here most Ca occurs in hornblende and plagioclase. Lower
concentrations of 1.7% Ca at Paulwi and 1.4% Ca at Trojan are typical
of ultramafic rocks. The distribution of Sr follows the same pattern
as Ca, and the elements are linked by correlation coefficients ranging
from + 0.41 at Chombwa to + 0.82 at Paulwi.

In contrast to Ca, the highest Mg is found in ultramafic
rocks (figure 60). The highest mean Mg values are 9.8% Mg at Trojan
and 8.2% Mg at Paulwi, where Mg correlates by coefficients of up to
+ 0.89 with Ni, Co and Cr, and occurs mainly in olivine and serpentine.
Fairly high Mg correlated with Ni, Co and Cr at Chombwa is ascribed to
lenses of olivine-bearing rock within the gabbro. By comparison, Mg
values at Munali are low, and Mg is not strongly correlated with other
elements.
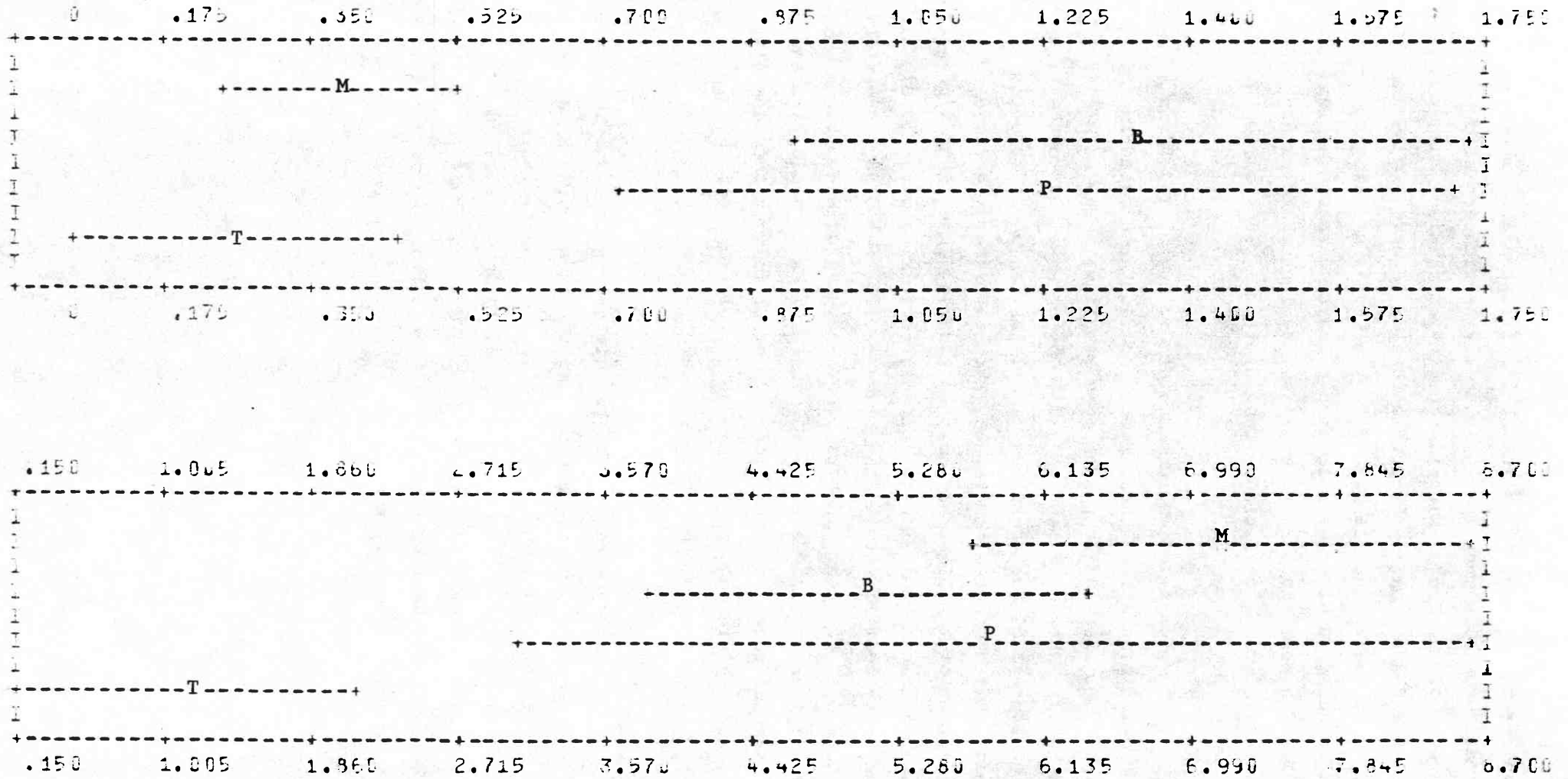
Figure 61: Plot of mean and standard error range of variables determined in random core samples; top Li (ppm, scaling factor 10); bottom K (%, scaling factor 0.1)

The Chombwa and Paulwi rocks are significantly enriched in Li, with mean concentrations of 13 ppm Li at Chombwa and 12 ppm at Paulwi (figure 61). Li is correlated by coefficients of + 0.63 to + 0.89 with Ca, Al, Si, Ti, V and Ga at Chombwa, and therefore probably occurs in hornblende and feldspar. At Paulwi, Li exhibits lower correlations in the range + 0.36 to + 0.59 with the same suite of elements, and can be traced to samples of pyroxenite, where these elements probably occur in augite and enstatite. In contrast there are low Li values of 4 ppm at Munali and 3 ppm at Trojan, and these appear attributable to the near absence of calcium-bearing alumino-silicate minerals.

The presence of any feldspathic shear zones is also not revealed by the random core specimens. At Chombwa, Munali and Paulwi there are mean concentrations of around 0.6% K and 100 ppm Ba, thought to occur mainly in feldspars. At Trojan, where there are no feldspathic rocks, there is 0.1% K and 43 ppm Ba (figure 61).

Concentrations of Mo in the core range 0 to 2 ppm in all areas, and Be is detected in only a few samples, mainly from Paulwi and Trojan.

Thus the variables seen as most likely to furnish a guide to the mineralization potential of an intrusive on the basis of random core sampling are S, Co_s and Zn_s, with a lesser but useful contribution made by Cu_s, Fe_s, and Ni_s data. The heavy metals extracted from sulphide minerals by bromine attack provide a better guide than the same total metals, but S is the most diagnostic variable. In general this is inkeeping with conclusions based on other intrusives (Cameron, Siddeley and Durham, 1971). However, the Zn_s variable has not previously been studied in this context, and its apparent discrimination potential may eventually prove to be a chance localized phenomenon.

Supplementary information from elements indicative of hydrothermal activity, such as Ca, Mg, Li and Be, is not a viable guide to mineralization because other modes of occurrence of these elements in the rock produce a camouflage effect.

The six apparently most useful variables were used as a training set in a computerized backwards regression performed by a program BAKWRD (Howarth, 1973). The data set was split into a mineralized class of 47 samples (Munali and Trojan) and a non-mineralized class of 27 samples (Chombwa and Paulwi) and sequential backwards regressions, using smoothing factors in arithmetic mode of 5, 10 and 15, and in log-transformed mode of 0.08, were applied to identify the optimum combination of the six variables for discriminating between the two classes.

The best combination of variables was obtained using an arithmetic mode regression with a smoothing factor of 10 or 15. The optimum combination is S and Zn_s, which provides a level of discrimination of 73.2%, followed by S, Zn_s and Fe_s. High values of these variables identify the mineralized areas compared with low values for the non-mineralized areas.

The Ni_s variable makes the least contribution towards the discrimination, and this is attributed to the great variation in silicate Ni content of the different rock types from different areas; some of this Ni is inevitably leached into solution during a bromine attack, and relatively small percentages of high silicate Ni can substantially effect the amount of Ni in solution, which is metal theoretically ascribed to sulphide minerals.

		S:Ni	S:Co	S:Cu
Random core samples	Munali	16.00	49.36	30.50
	Chombwa	14.94	28.29	22.12
	Paulwi	0.82	4.70	11.47
	Trojan	1.47	27.90	30.89
Random outcrop samples	Munali	1.44	9.00	4.88
	Chombwa	6.73	13.28	9.01
	Paulwi	0.25	2.13	8.86
	King Edward	0.12	1.77	11.59
	Musangashi	1.13	5.36	6.01
	Chinkozia	13.38	19.73	9.29
	Trojan	0.30	4.16	7.93

Table 15: Mean sulphur-to-metal ratios for core and outcrop samples.

The S:Ni ratio of serpentinites is considered to favour the presence of mineralization when greater than unity, and indicate the absence of mineralization if less than unity (Hausen, Ahlrichs and Odekirk, 1973). Comparing the two serpentinized ultramafics at Paulwi and Trojan, the S:Ni ratio is found to average 0.82 at Paulwi and 1.47 at Trojan (table 15). This criterion therefore clearly distinguishes the presence of mineralization, and seems particularly useful in view of the limitations of Ni_s analyses. Much higher ratios are to be expected in gabbroic intrusives, and the average S:Ni ratio of 16.00 at Munali is only marginally higher than 14.94 at Chombwa. Extending the sulphur-to-metal ratio concept to other ore metals, it is found that the Trojan ultramafic intrusive has a much higher S:Co ratio than Paulwi, and the gabbroic Munali intrusive has a higher S:Co ratio than Chombwa. In the case of S:Cu ratios, both types of intrusive can be compared simultaneously, with the mineralized areas exhibiting ratios around 30 compared with 11 and 22 for the non-mineralized areas.

4.3.   Random outcrop samples

The variables found to distinguish between the mineralized and non-mineralized classes of intrusive rocks in the training set of core samples were examined in outcrop samples collected in the mineralized Munali and Trojan field areas and the non-mineralized Chinkozia, Chombwa, King Edward, Musangashi and Paulwi areas (table 14). For the most part outcrops are not abundant in these field areas, and samples were collected from those observed exposures of solid rock scattered over the whole surface area of the intrusive. Thus the pattern of sampling was random within the limitations of outcrop density, and between nine and 30 samples were obtained in each area. At outcrop sites, some effort was made to obtain specimens of rock exhibiting minimum weathering. However, the general degree of weathering clearly varies between field areas, and simple observation established that weathering of outcrops was most advanced at Munali and Musangashi, and least conspicuous at Chinkozia and Chombwa. As anticipated, rocks were severely oxidized where gossan was developed over sulphide mineralization.
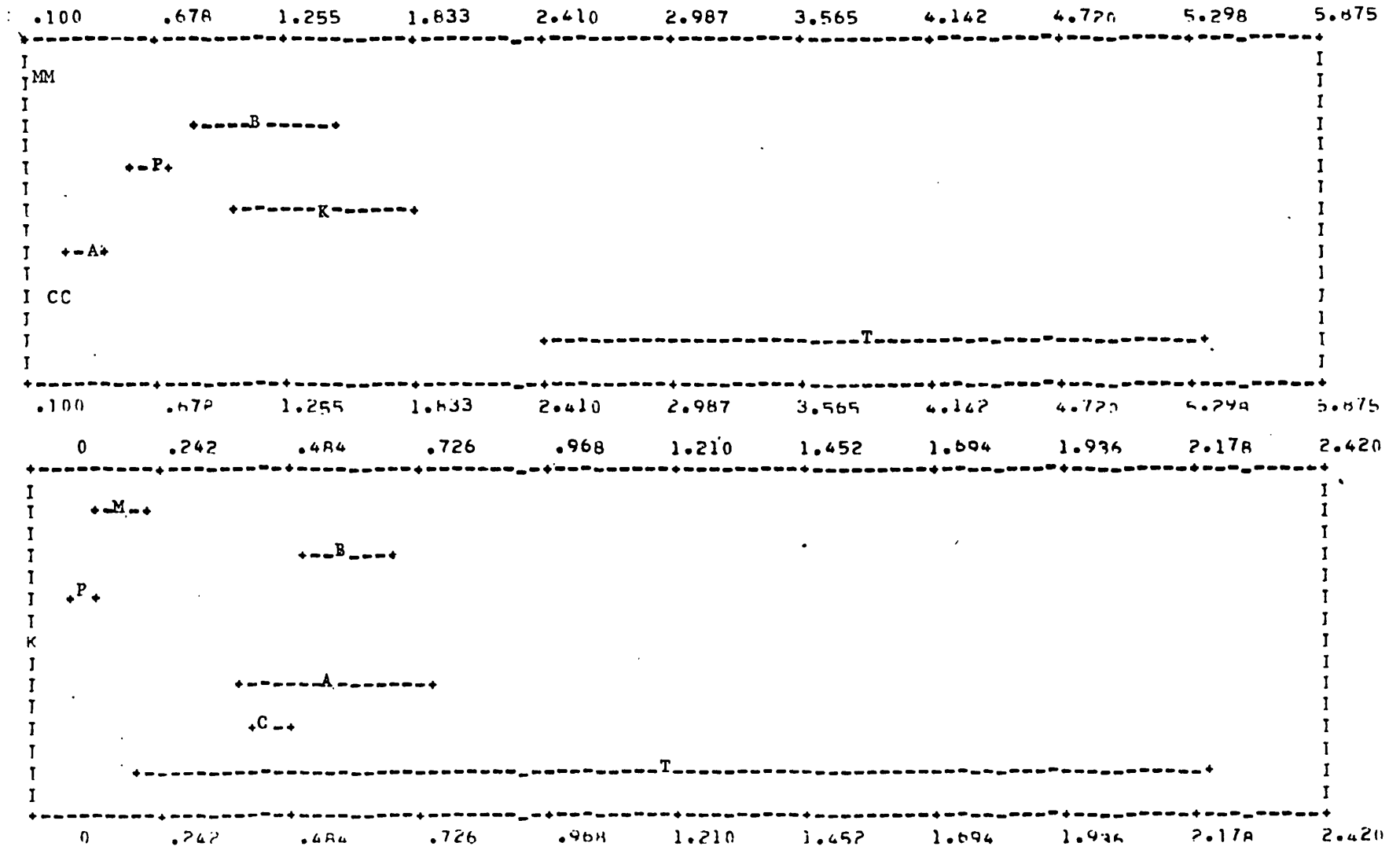
Figure 62: Plot of mean and standard error range of variables determined in random outcrop samples; top: Ni_s (ppm, scaling factor 100,); bottom Cu_s (ppm, scaling factor 100)

The highest Ni_s mean of 390 ppm is found at
Trojan, and is more than twice as high as the next highest
levels of 145 ppm at King Edward and 118 ppm at Chombwa. The
remaining areas have low Ni_s and among them the lowest is 22 ppm
at Munali (figure 62). The Co_s distribution is somewhat similar,
with high values of 16 ppm at Trojan followed by 15 ppm at Chombwa,
and lower Co_s levels elsewhere, including 5 ppm at Munali. The
highest Cu_s mean of 121 ppm,accompanied by a broad standard error
range, occurs at Trojan. Munali is among the areas with low Cu_s at
17 ppm (figure 62). Only Chombwa exhibits high Zn_s at 13 ppm, and
both Munali and Trojan outcrops contain 5 ppm, a level similar to
the other areas. Also, Chombwa exhibits the highest Fe_s content,
with a mean of 0.8%. There is an intermediate group comprising
Chinkozia at 0.6% and Musangashi with 0.5%, and a low group
including Munali with 0.2% and Trojan at 0.1% (figure 63). Most
Ti_x values are zero, and the mean concentration of Ti_x for each
area is less than 5 ppm.

There are two distinct groups of S concentrations
(figure 63). The high group comprises the Chinkozia, Chombwa,
Munali and Trojan areas, with S means between 460 and 598 ppm.
In contrast, the low group of King Edward, Musangashi, and Paulwi
has S means of 170 to 237 ppm. Clearly S alone gives a considerable
but inconclusive measure of discrimination between mineralized
and non-mineralized areas.

Sequential backwards regression using BAKWRD
in arithmetic mode with a smoothing factor of 10 was applied to
other analytical data for the samples from the four areas with
high S means. A total of 53 samples comprised the mineralized
class (Munali and Trojan) and 41 samples the non-mineralized
class (Chinkozia and Chombwa). The variables tested were
Ni_s, Cu_s, Co_s, Zn_s, and Fe_s, and in multi-variate combination
these contribute a high order or discrimination of 87.1% between
the two classes, but no single variable or simple combination
yields better discrimination.
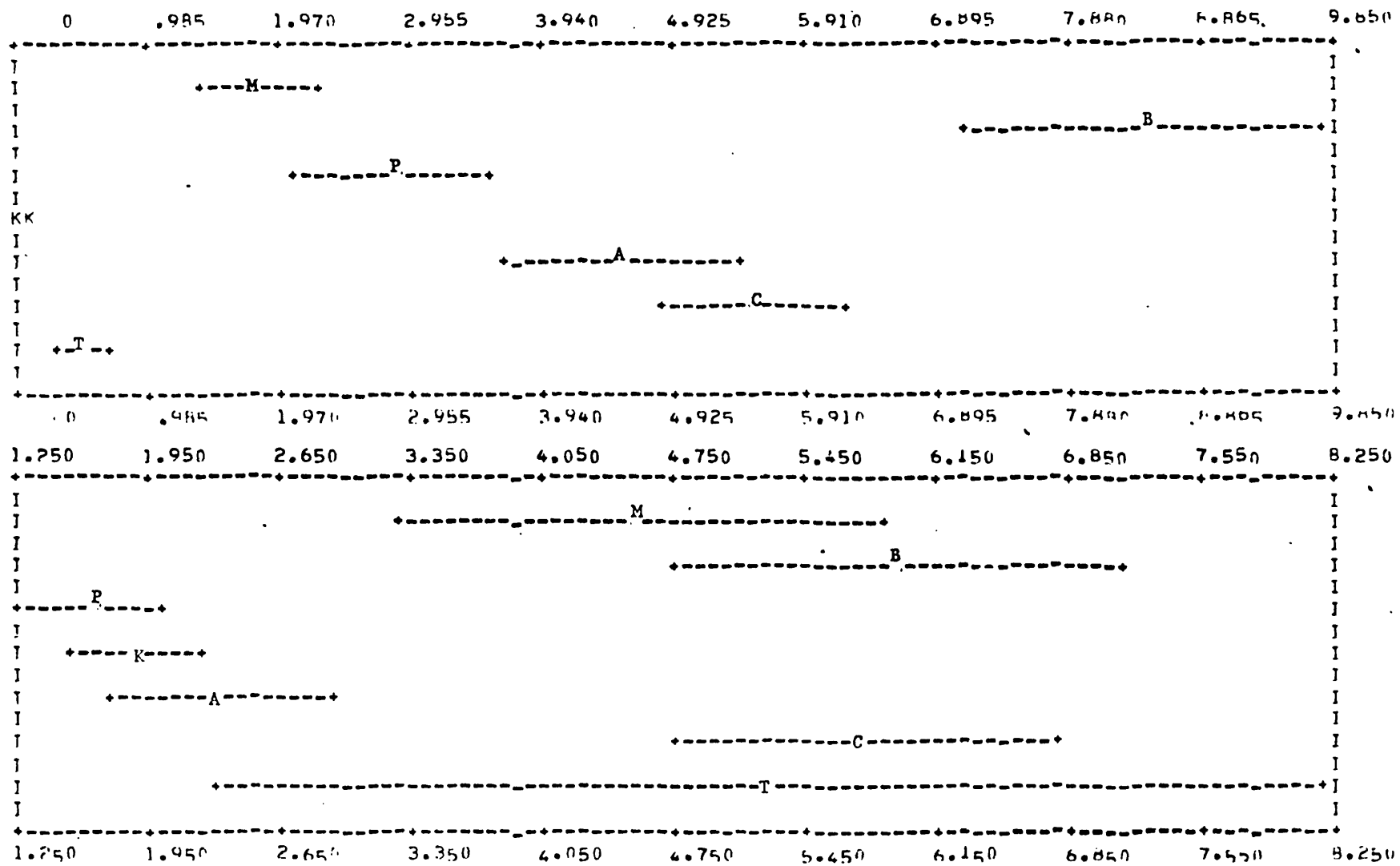
Figure 63:   Plot of mean and standard error range of variables determined in random outcrop samples ; top Fe_s (%, scaling factor 0.1); bottom S (ppm, scaling factor 100).

It may be significant that among the areas with high S in outcrops, S is most closely correlated with Fe_s at Chinkozia, by a coefficient of + 0.88, and at Chombwa, by + 0.54, which suggests that pyrite is probably the source of both elements. On the other hand, S is best correlated with Ni_s, Cu_s and Co_s at Trojan, by coefficients of + 0.96 to + 0.99, indicating an association with pyrrhotite, pentlandile and chalcopyrite. At Munali the highest S correlation is + 0.46 with Ni_s, also implying the presence of nickel sulphides.

The S:Ni ratios for outcrops do not provide any criterion for discriminating mineralization (table 15). The Paulwi and Trojan serpentinites, which produce archetypal S:Ni ratios for random core samples, both exhibit low ratios around 0.3 for outcrops. Not surprisingly, the highest S:Ni ratios are obtained for areas where outcrop weathering is known to be minimal, such as Chinkozia and Chombwa, and this is also clearly seen in S:Co ratios. Although this pattern is less evident for S:Cu ratios, these too fail to offer any means of discrimination.

4.4.   Discussion

In order to discuss the analytical results obtained from unweathered rock specimens, it is necessary to invoke various models of magma crystallization and ore genesis for the mafic and ultramafic intrusives under consideration. Strictly speaking, this is beyond the scope of the present research, and it is not suggested that the research data are the source of these geological history hypotheses. Rather that the research findings are generally consistent with such geological histories.

The central problem in the interpretation of primary
nickel dispersion patterns is the dichotomous behaviour of the
nickel ion during the crystallization history of the parent
magma. Nickel can behave in a lithophile manner, as evidenced
by the almost ubiquitous substitution of Ni for Mg in the
forsterite lattice such that forsterite olivines usually contain
around 2000 ppm Ni. On the other hand, Ni can exhibit
siderophile and chalcophile tendencies by virtue of its
incorporation into pyrrhotite and pentlandite. These two
processes can apparently both occur early in the crystallization
history of a magma, and it is not clear which chemical or
physical constraints control the partition of Ni.

Since a magma is primarly a silicate melt, olivine
will most certainly crystallize from melt of suitable chemical
composition under the appropriate cooling conditions. The
factors governing the possible formation of pyrrhotite and
pentlandite are more complex. A small quantity of S can
remain in solution in a magmatic liquid, but an immiscible
sulphide liquid separates from the silicate liquid if the S
saturation point is exceeded. In the event of the S
solubility product being exceeded when the intrusive mass is
predominantly liquid, the immiscible sulphide phase tends
to settle by gravitation at the base of the structure. The
remaining magmatic liquid will still contain S in solution in
quantities not exceeding the solubility product. As the
magma cools and silicates crystallize, this residual S forms
a separate phase which is trapped in the interstices of the
silicate crystal mesh, and finally crystallizes as finely
disseminated sulphide minerals. In a sulphur-bearing but
undersaturated magma, the same process will occur without
the early separation of an immiscible sulphide phase, while
other magmas may contain no S.

The sulphide phase is composed of mainly S and Fe. The results of experiments by Clark and Naldrett (1972) show that where silicate and sulphide phases separate from a peridotite melt, Ni is partitioned between the two phases in the same proportion as Fe, in that the partitioning ratio is constant for any concentration of Ni and Fe in a melt. The equilibrium between Fe in the silicate and sulphide phases is a significant control over the capacity of the melt to dissolve S. Haughton, Roeder and Skinner (1969) demonstrated experimentally that the S saturation level rises with increasing FeO content, and subsequent analyses of basic rocks from the Bushveld Complex by Buchanan (1975) supports this. However FeO activity in the melt is in turn influenced by oxygen fugacity, since FeO and O_2 will react to form magnetite, thereby decreasing FeO activity in the liquid phase and hence lowering the S solubility product. The Munali gabbro is rich in magnetite, and the sequence of reactions described above may well account for the separation and accumulation of nickeliferous sulphides associated with the Munali gabbro. At King Edward, where magnetite is also present in the rock, there is no mineralization. Although the formation of magnetite may favour the separation of a sulphide phase, the melt must nevertheless contain a certain minimal concentration of S before this can occur. It seems that this level of S was exceeded at Munali, but not at King Edward.

Nor is magnetite crystallization the sole mechanism which can initiate a chain of reactions inducing the separation of a sulphide phase. The solubility of S in a silicate melt is highly temperature dependent. According to Haughton and co-workers, the solubility of S in a cooling magma would decline by a factor of ten between $1200^{o}C$ and $1040^{o}C$, if all other variables remained constant, and this relationship can be extrapolated with reservation over much of the cooling range of magmas in the crust. Other features of bulk composition influence S solubility in a magma. The effect of Ti correlates strongly with that of Fe, and titano-magnetite or ilmenite, has crystallized from the Munali gabbro melt, thereby contributing to the separation of the

sulphide phase. Conversely increasing SiO_2 and Al_2O_3 in
the melt decreases the S capacity (Haughton, Roeder and
Skinner, 1969).

Where a magma is initially undersaturated with
S, an immiscible sulphide phase will not separate at an
early stage of crystallization, and nickeliferous olivines
and sulphide liquids will not form in equilibrium. Continuing
crystallization of the silicate phase produces minerals such
as pyroxenes and amphiboles which usually contain much less
Ni than olivines. As the pre-existing olivines react with the
surrounding liquid to form new silicates some Ni may be
liberated. At the same time, falling temperature, falling FeO
activity and rising SiO_2 and Al_2O_3 concentrations in the liquid
phase will eventually cause the separation of an immiscible
sulphide phase, and liberated Ni may be incorporated into this.
By virtue of the late stage of segregation, the sulphide phase
is likely to be trapped in the silicate crystal mesh, and
ultimately crystallize as finely disseminated pyrite and
pyrrhotite, which may be slightly nickeliferous. Mineralization
of this origin is unlikely to be economic, but may have a broad
geometric distribution within the intrusive body which would
yield a favourable response to random sampling. High
concentrations of Fe_s and S at Chombwa suggest that this
intrusive may have experienced such a crystallization history,
but the sulphide minerals are not highly nickeliferous.

Even a melt initially containing little or no S
may undergo sulphurization, in which S from an external
source reacts with the partially-consolidated intrusive body
(Naldrett,1966). Warm intrusion of olivine-rich differentiates
into sulphur-bearing sediments, perhaps accompanied by regional
metamorphism, will provide conditions under which the S can
react with Ni in the olivines. Naldrett (1966) suggests that the
Alexo orebody, eastern Canada, was formed by the injection
of a hot mush of olivine crystals lubricated by a pyroxene
fluid into pyrite-bearing volcanic rocks. Pyrite broke
down to pyrrhotite and migrated into the intrusive and
reacted to form Fe-Ni sulphides. As the intrusive cooled,

shearing occurred, and the sulphides migrated into shear
zones to form economic concentrations. Chamberlain (1967)
invokes the action of hydrogen-rich fluids introduced during
serpentinization for the redistribution of sulphides and S
in the Muskox intrusive, northern Canada. Among the older,
regionally metamorphosed intrusives studied in Central
Africa, Chinkozia, Chitina and Musangashi are not mainly ultra-
mafic in compostion, and are thus not well disposed to the
development of economic mineralization by sulphurization. The
Paulwi and Trojan/Kingston intrusives, however, comprise mainly
peridotite in varying degrees of serpentinization, and the
origin of the mineralization at Trojan/Kingston may be
attributable to sulphurization. The source of S may have
been the pyritic shale formation adjacent to the mineralized
Trojan intrusive, or sulphurous fluids from an extraneous
source may have permeated and reacted with both the ultramafic
rock and shale, forming sulphide minerals. The association
of the better grade of mineralization with the serpentinized
Trojan intrusive compared with weak mineralization in the
unaltered Kingston peridotite suggests that the fluids
effecting serpentinization influenced the distribution of
the mineralization in some way, as proposed by Chamberlain (1967)
for the Muskox intrusive. Sulphurization produces
disseminated mineralization and the wide distribution of
sulphide minerals that this implies can be expected to
produce the best response in random sampling methods. This
is indeed the case, with Trojan/Kingston core samples
exhibiting the highest concentrations of S and several metals
in sulphide minerals, and therefore the best mineralization
potential. The Paulwi intrusive, although strongly serpentinized,
has not undergone sulphurization, and there are no sulphide-
bearing meta-sedimentary rocks in the vicinity.

The efficiency of Br in oxidizing sulphide minerals has been well known for some time and was thoroughly tested on a wide range of base metal sulphides with satisfactory results by Czamanske and Ingamells (1970). However, Hausen, Ahlrichs and Odekirk (1973) examined the residues of rock samples after Br attacks, and express concern over their microscopic identification of varying degrees of attack on silicate minerals. The attack of silicates is attributed to the dilute acid medium in which the Br oxidation must be conducted in order to avoid the hydrolysis of ferrous ions to ferric ions. Part of the present research strove to minimize this problem, with promising results on trial samples. However, the principal problem lies in the variability of attack on different rock types and even different specimens of the same type.

In terms of trace metals taken into solution, the deleterious effects of the silicate attack problem are most acute for those elements which are both more readily removed from the silicate crystal lattice and occur in relatively high concentrations in silicate minerals in the rock in question; for example, higher concentrations of Ni (attributed to Ni_s) are leached from samples of serpentinized peridotites from Paulwi and Trojan/ Kingston by Br in acid solution than from the Munali and Chombwa specimens which are mainly gabbroic. Because of the high concentration of Ni available from the silicate minerals compared with the minute amounts of Ni in sulphides which may occur in some samples, any discrimination of mineralization potential on the basis of Ni in the leachate (Ni_s) tends to be masked. However, closer inspection of the data reveals that the percentage of total Ni taken into solution by the Br attack may afford some discrimination: more than 41% of total Ni was taken into solution from Munali and Trojan/Kingston samples by the Br attack, and less than 15% from Chombwa and Paulwi samples.

The amount of Fe leached from the rocks may suffer the same problem as Ni, but even accurate Fe_s data might not suggest nickel mineralization. This is borne out by the core specimen results, which show that the Chombwa area, with visible pyrite in the core but no nickeliferous sulphides, is grouped with the mineralized Munali and Trojan/Kingston intrusives, but Paulwi has distinctly lower Fe_s.

The Cu_s yielded inadequate discrimination between mineralized and non-mineralized intrusives. In contrast, Cameron, Siddeley and Durham (1971) found Cu_s a most useful parameter for classifying the mineralization potential by ultramafics of the Canadian Shield. The poor response obtained in Central Africa may be explained by different ore genesis models for the Munali and Trojan/ Kingston mineralization. The Munali intrusive is predominantly gabbro of Katanga age and the associated mineralization is almost certainly a sulphide segregation from a sulphur-rich parent magma. The sulphides remained liquid until a late stage of cooling and were finally injected along with hydrothermal fluids into a contact zone. The Chombwa intrusive is more or less the non-mineralized counterpart of Munali. The Trojan/Kingston and Paulwi intrusives were peridotite differentiates intruded into their surrounding sediments during a period of regional hectonism (Tyndale-Biscoe, 1933; Barr, in print). The degree of serpentinization now observed occurred either contemp- oraneously with intrusion or immediately afterward in the same tectonic events. The origin of the aqueous fluids causing serpentinization is unclear, but Keep (1929) concluded that elsewhere in Rhodesia magmatic water associated with granite emplacement had caused serpentinization of ultramafic rocks. Where such fluids were sulphurous, the simultaneous sulphurization and serpentinization of the peridotite might be expected to occur. This genesis model

has been considered for Trojan/Kingston by Le Roex (1964),
who also points out that the nickel-free sulphides in the
adjacent graphite argillile could have formed in the same
event. This hypothesis is consistent with the occurrence
of higher grade mineralization in the serpentinized Trojan
area than in the Kingston peridotite. In the case of the
Paulwi intrusive the aqueous fluids which caused
serpentinization were not sulphurous, and hence the intrusive
is not mineralized.

Magmatic segregation ores of the Munali type
are typified by a relatively high Cu_s content. However, Le
Roex (1964), quoting Michener (1957), points out that "copper
is practically absent" in deposits formed by sulphurization,
and that the Ni:Cu ratio in concentrates of ore from the
Trojan mine is 20 or higher. Consequently, the mean and
standard error range of Cu_s values from the mineralized
Munali gabbro is clearly higher than the mean and standard
error range of Cu_s from the non-mineralized Chombwa intrusive.
But this distinction is not maintained when Paulwi and Trojan/
Kingston are considered. The mineralized Trojan/Kingston
serpentinite-peridotite complex has only a slightly higher
Cu_s mean than its non-mineralized equivalent at Paulwi, and
the standard error ranges of both data sets are large with
extensive overlap.

The other chalcophile elements extracted from
sulphide minerals produce better discrimination than Cu_s,
with the mineralized Munali and Trojan/Kingston intrusives
exhibiting the highest Co_s and Zn_s contents. The discrimination
between mineralized and non-mineralized mafic and ultramafic
intrusives provided by Zn_s in unweathered rock specimens must
be regarded as inconclusive without supporting evidence from
other workers or further research. The occurrence and
significance of zinc-bearing sulphide minerals in mafic and
ultramafic bodies has so far received little attention. Zinc
enjoys a high degree of mobility in the primary environment,

and this seems likely to be a vital consideration when
evaluating the merits of a random sampling scheme for
indicating mineralization potential. It is interesting
to note that Davenport and Nichol (1973), investigating
the massive base metal mineralization potential of different
cycles of volcanic rocks in the Birch-Uchi Lakes area of
Canada, found that the primary dispersion of Zn provided
the best discrimination of mineralized and non-mineralized
cycles.

Good mineralization discrimination was provided
by S in Central Africa, a result consistent with the findings
of Cameron, Siddeley and Durham (1971) studying the mineralization
potential of ultramafics of the Canadian Shield, and Hausen,
Ahlrichs and Odekirk (1973), in a comparison of the mineralization
potential of ultramafic intrusives in Canada and Australia.
Munali rock specimens contain around 1500 ppm S compared with
1100 ppm at Chombwa and 400 ppm at Paulwi. The higher S load
in the Munali magma would favour the early separation of an
immiscible sulphide phase, which would be nickeliferous by
virtue of the proportional partition of Ni between silicate
and sulphide phases proposed by Clark and Naldrett (1972).
Early phase separation also favours the localization of the
sulphide liquid into a potentially economic concentration.
The lower S content of the Chombwa magma may have resulted
in the separation of a sulphide phase at a later stage of
cooling, producing two effects which contrast with Munali.
At this later stage, most of the Ni originally in the melt
was incorporated into olivines, and therefore a predominantly
non-nickeliferous sulphide phase was formed. Secondly the
sulphide phase was trapped in a semi-crystalline mesh, and
therefore remained distributed throughout the intrusive body
as it continued to cool. At Paulwi, insufficient S was

present within the peridotite body at the time of intrusion
to form economic mineralization, apparently a characteristic
of most intrusives of the alpine type. Quite probably the
Trojan/Kingston body was initially comparable with Paulwi
in this respect, but S was subsequently introduced in a
sulphurization process, and unweathered rock specimens now
exhibit the highest S content of the intrusives studied,
with a mean of 2400 ppm.

Thus S is probably the most reliable
discriminator of mineralization potential, especially
since the concentrations observed are apparently independent
of the mafic or ultramafic silicate lost rock type and the
mode of ore genesis. In addition, S determination does not
suffer from the same analytical complications as does the
selective extraction of metals from sulphide minerals in a
silicate matrix; and the modified combustion method facilitates
the analysis of more than 60 samples per day for S, compared
with 18 samples per day achieved by Cameron, Siddeley and
Durham (1971).

Although Cameron, Siddeley and Durham (1971)
included both outcrop and subsurface samples in their study
of the mineralization potential of ultramafics of the Canadian
Shield, outcrops from the Central African intrusives yielded,
upon analysis, significantly different data from the
corresponding core. In Central Africa weathering tends to
be intense, though somewhat variable according to rock
mineralogy, and sulphide minerals in particular are readily
oxidized. By and large, the trace elements extracted using
Br in acid solution are probably leached from the lattices

of minerals weakened, rather than destroyed, by the
weathering process, and from secondary minerals formed in
situ. The data suggest that none but an empirical
interpretation is applicable, and the most promising result
is again achieved with S. Two groups of S values are clearly
present, of which the lower group, less than 300 ppm S,
includes the non-mineralized King Edward, Musangashi and
Paulwi intrusives. The group with over 300 ppm includes
the mineralized Munali and Trojan/Kingston intrusives and
also the non-mineralized Chombwa and Chinkozia intrusives.
Chombwa was recognized from core samples for its high iron
sulphide content, and Chombwa outcrops exhibit a high Fe_s
level. This latter characteristic is also seen at Chinkozia.
By contrast, Ni_s and S show a fair correlation in Munali
and Trojan/Kingston outcrops.

Hausen, Ahlrichs and Odekirk (1973) favoured
the use of S and total Ni for evaluating the mineralization
potential of mafic and ultramafic rocks in Australia and
Canada, stating reservations about the efficiency of various
selective leaches for sulphide minerals. Their approach in-
volved comparison of S:Ni ratios of mafic and ultramafic rocks
of the same or similar silicate mineralogy. This proved
successful in their Australian/Canadian study and in the
present Central African research, with high ratios in
unweathered rock samples illustrating the presence of
mineralization. The S:Co and S:Cu ratios, not investigated
by Hausen and co-workers were clearly higher for both
mineralized gabbros and serpentinites compared with their
non-mineralized counterparts in Central Africa. This is in
keeping with the chalcophile nature of these metals and
the contrast obtained with Co_s and Cu_s.

Sulphur-to-metal ratios were much lower in outcrop samples compared with the corresponding core, and failed to distinguish the presence of mineralization. This is attributed to the disproportionate loss of S through the ready oxidation of sulphide minerals in comparison with a more limited loss of trace metals from incompletely weathered silicate minerals.

In view of the range of variables influencing the occurrence of mineralization with a mafic or ultramafic intrusive, and the difficulties of determining and interpreting all of these variables, the investigation of prospecting techniques for the direct identification of primary nickel mineralization were considered more remunerative than the assessment of mineralization potential of an intrusive body, and the subsequent research was planned accordingly.

5. THE VERTICAL DISTRIBUTION OF ELEMENTS IN SOIL PROFILES

Pits up to 5 m deep were dug to reach the C soil horizon at locations of Ni soil anomalies defined during prospecting in the Chitina, Chombwa, King Edward, Munali, Musangashi, Kingston and Trojan field areas. The pits at Munali and Trojan were sited on the projected suboutcrop of mineralization. Horizontal channel samples were taken from the pit walls at approximately 7, 20, 35 and 50 cm, at one m and then at one m intervals from surface, in order to ensure sampling of each major soil horizon. The fine fractions were analysed for total metals by atomic absorption spectroscopy and emission spectrography, while the intermediate and coarse fractions were used for pH and S determinations respectively. Most samples were analysed for F, and total metals in the coarse fraction were also determined in a few profiles. The analytical results, detailed in appendix 2, are reviewed in order to trace the dispersion of elements during the weathering of mafic and ultramafic rock and soil formation, and with particular reference to changing Ni values through the soil profile as a guide to mineralization (Wilding, 1965).

Many primary minerals in the parent rock break down when exposed to aerated water and air to form a soil cover. Of the principal consituents of mafic and ultramafic rocks, olivine weathers rapidly, because Fe and Mg ions which bond the silica tetrahedra readily pass into solution and individual tetrahedra fall away to expose fresh surfaces. Pyroxenes possess a more stable silicate chain structure, but the bonding Mg, Fe and Al ions are relatively susceptible to dissolution, releasing chain units. The silicate units readily polymerize to form secondary minerals, mainly smectites and chlorite (Loughlan, 1969).

Iron and Al form colloids which ultimately precipitate in the B horizon as secondary oxides and hydroxides, such as goethite and gibbsite. There is often a substantial concentration of these minerals in the B horizon, where a lateritic zone may be formed. For the most part Mg is not incorporated into these secondary minerals and is leached from the soil. The behaviour of other major and trace elements is mainly controlled by this process of primary mineral weathering and secondary mineral

formation.

Many elements, including Ni, Cu, Co, Cr, Ti, Mn, Mo, V, Ga, Li, Sc and S pass into solution during mineral breakdown and then precipitate as secondary minerals or are absorbed or adsorbed by secondary minerals. By these processes, concentrations of elements in excess of their primary levels commonly occurs. Secondary enrichment of trace elements is mostly achieved by adsorption and co-precipitation with goethite, gibbsite and other clay minerals. Where organic matter is present, usually only in the A and uppermost B horizons of tropical soils, some soluble metals are fixed as organo-metallic complexes.

Other elements, notably, Mg, Ca, Sr, K and Ba pass into solution and are not readily locally precipitated, but are often leached away in solution. Such leaching leads to a relative enrichment, involving little or no physical re-distribution of elements, of Si in residual silicate minerals, Cr in chromite, Ti in ilmenite and other elements in resistant minerals.

5.1.   Chitina

At Chitina a pit 3.2 m deep was dug in a locality where prospecting operations had defined a 1500 ppm Ni anomaly (sample nos. 455-33 to 455-39; figure 6). The pit exposed a light brown, friable sandy A soil horizon to a depth of about 20 cm, followed by an orange-brown B horizon with coarse quartz rubble to about 80 cm. This grades downward into a C horizon of soft, green, weathered rock with talcose partings and finally more compact green to black rock, probably peridotite.

Among the major elements, the lowermost exposed C horizon is relatively rich in Fe and Mg and low in Al, supporting the observation of an ultramafic parent rock (table 16). Iron is clearly leached from the A horizon but retained in the B horizon, although concentrations do not exceed that in the lower C horizon.

	Fe%	Al%	Si%	Mg%	pH	Ni	Cr	Cu	Ti	V	S	F	Mn
A	5.8	8.2	41.1	4.8	5.2	650	700	51	1350	119	10	143	630
	7.5	9.9	34.5	5.5	5.3	950	1450	62	1250	128	40	117	770
	9.9	8.8	22.4	4.3	5.3	1200	1400	70	1000	127	140	95	660
	11.5	10.8	28.4	5.2	5.5	1800	2000	73	1200	123	240	95	1020
B													
	8.0	9.4	33.7	4.4	5.7	1100	850	68	1150	138	10	95	1700
	8.3	7.3	26.7	5.8	6.0	1200	1150	70	1050	117	40	83	1330
C													
	14.0	1.8	15.3	6.5	6.2	6000	1950	83	300	68	10	38	4000
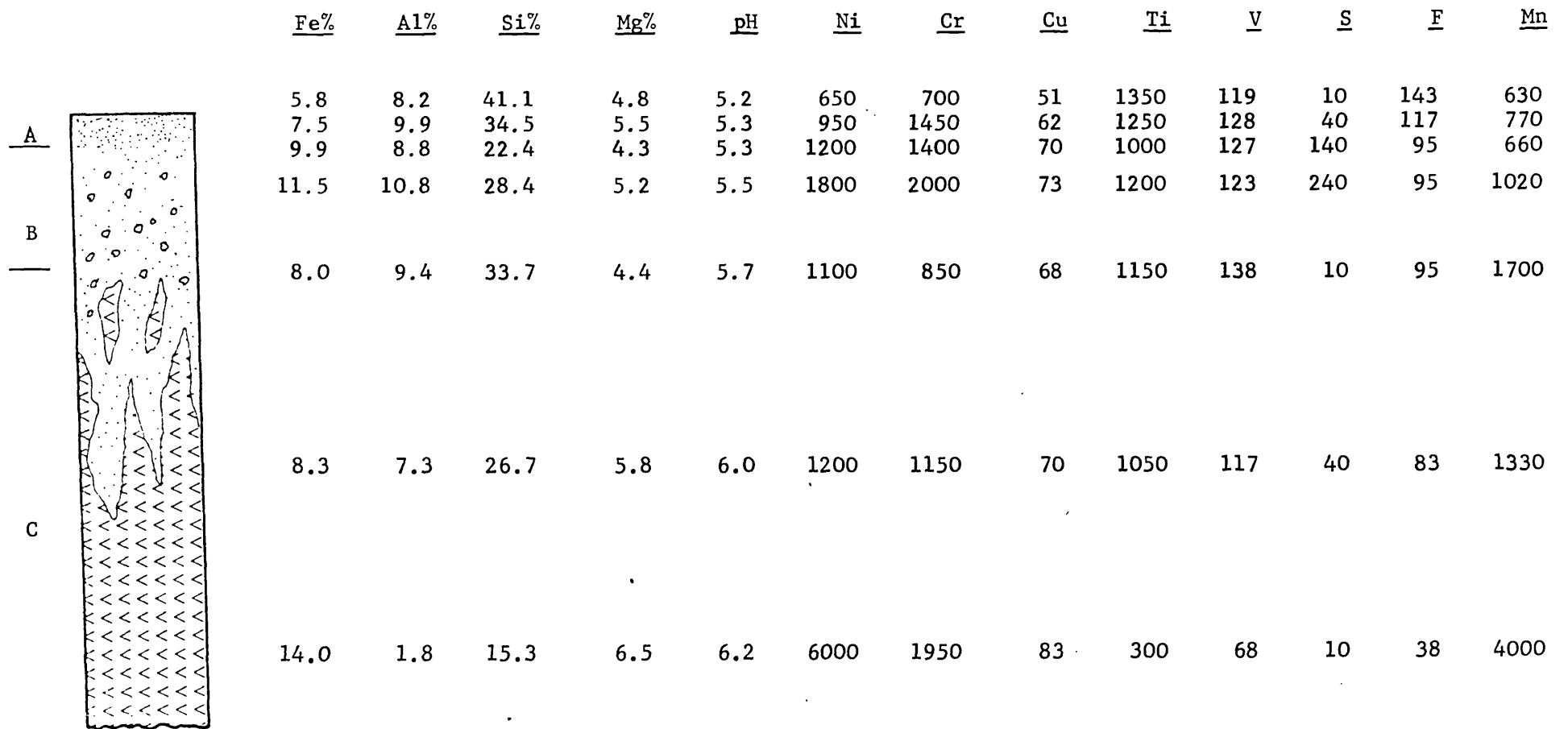
Table 16: Chitina, distribution of major and trace elements in the vertical soil profile (ppm, except as stated; approximate vertical scale 1:30; for geological legend see figure 6)

Aluminium exhibits a similar distribution, although values are higher throughout the A, B and upper C horizons than in the lower C horizon. Magnesium shows no such B horizon enrichment, and all Mg values in the A and B horizons are lower than in the C horizon as a result of leaching. By contrast, there is a substantial relative enrichment of Si in the B horizon and especially the A horizon as a result of the immobility of silica. The pH rises with depth, as the organic content of the soil decreases and the alkaline characteristics of the ultramafic rock become prominent.

Nickel and Cr are substantially leached from the A horizon and adsorbed by Fe in the B horizon, reaching 1800 ppm Ni and 2000 ppm Cr. Lower concentrations of these metals are again encountered in the upper C horizon, but values of 6000 ppm Ni and 1950 ppm Cr in the lower C horizon indicate a parent rock relatively rich in these two metals. A little Cu is leached from the A horizon, but there is about 70 ppm Cu throughout the B and C horizons. The A and B horizons both show some enrichment of Ti, V, Ga and Li, with up to 1350 ppm Ti, 138 ppm V, 18 ppm Ga and 38 ppm Li compared with 300 ppm Ti, 68 ppm V, 1 ppm Ga and 2 ppm Li in the lower C horizon. The distribution of these elements is loosely correlated with Al. There is much less Mn in the A and B horizons than in the lower C horizon, and secondary Mn oxides would not seem to be significant in the co-precipitation of other trace metals.

Low S levels of 10 to 40 ppm characterize the A and C horizons, but enrichment of S in association with Fe in the B horizon is quite clear, with up to 240 ppm S. Fluorine falls steadily with depth from 143 ppm in the A horizon to a low level of 38 ppm in the lower C horizon, suggesting ultramafic rock.

It is interesting to note that although the general trend of Ni values is to increase with depth, most lower C horizon geochemical criteria, such as high Fe, Mg and Cr, low F, indicate the presence of ultramafic rock, which is likely to contain nickel-rich silicates. Of course, this does not preclude the possibility of mineralization, but fairly low Cu and especially low S provide a most unfavourable indication. In seeking to evolve a near-surface traverse or grid prospecting method, the strong B horizon enrichment of S must be considered as presenting a potential data interpretation problem if encountered on the same scale in other pits.

5.2.   Chombwa

At Chombwa a 5.1 m pit was dug within a Ni soil anomaly of 2500 ppm defined during prospecting (sample nos. 255-13 to 255-21; figure 7). The underlying rock intersected in a diamond drillhole is peridotite. The pit exposed an A horizon of red-brown, friable, sandy soil to 20 cm, followed by a thick B horizon of red-brown to orange-brown sandy soil with a few small scattered quartz pebbles. Below 3.3 m is the C horizon of soft yellow-green weathered rock, probably peridotite, with a few soil partings.

As at Chitina, the major element composition of the lowermost exposed C horizon is high Fe and Mg and low Al, affirming the observation of ultramafic rock (table 17). There is marked enrichment of Al in the B horizon, and a more moderate enrichment of Fe, with up to 23.3% Al and 19.5% Fe. However, Mg is completely leached out of the A and B horizons. Silicon again exhibits strong relative enrichment near the top of the profile with around 30% Si in the A and upper B horizons. The pH rises with depth, from 4.8 near the surface, where some organic acids are likely to be present, to 6.2 in the C horizon.

	Fe%	Al%	Si%	Mg%	pH	Ni	Cr	Cu	Ti	V	S	F	Mn
A	15.0	19.4	31.1	0	4.9	2550	3200	64	2250	232	115	475	1350
	16.5	16.3	27.0	0	4.8	2500	3300	64	2250	215	120	247	1120
	16.0	17.5	23.2	0	4.8	2650	2400	68	2200	231	115	447	1090
	17.5	23.3	31.4	0	4.8	2650	3300	68	2000	273	120	285	1110
	17.0	16.4	24.2	0	4.9	2690	2650	67	2100	227	95	459	1050
B	18.0	12.5	15.5	0	5.0	2900	2800	66	2150	199	120	366	1250
	19.5	20.9	30.6	0	5.2	3750	3150	73	2250	236	105	285	2000
C	10.3	1.4	12.5	7.1	6.2	15000	4500	17	400	66	75	133	3400
	13.0	1.4	14.2	6.0	6.2	8000	10500	11	350	71	80	109	4200

Table 17: Chombwa, distribution of major and trace elements in the vertical soil profile
(ppm, except as stated; approximate vertical scale 1:40; for geological legend see figure 7).

Nickel is leached from the A horizon and accumulates, probably through adsorption by Fe, in the lower B horizon. The very high value of 15,000 ppm Ni at the top of the C horizon may also be partly attributable to this type of accumulation, although the value of 8000 ppm in the lower C horizon indicates that the parent rock is nickel-rich. There is no Cr enrichment in the B horizon, and levels around 3000 ppm throughout the A and B horizons suggest significant leaching of Cr, when compared with 10,500 ppm in the lower C horizon.

There is about 70 ppm Cu in the A and B horizons, and this represents a considerable enrichment since there is only 11 ppm in the lower C horizon. Although 70 ppm Cu in the soil is not sufficiently high to constitute an indication of mineralization, the principal of seven-fold Cu enrichment points to the need for care in interpreting Cu data in soil surveys. In common with Chitina, there are much higher concentrations of Ti, V, Ga and Li in the B horizon than in the C horizon. There is up to 2250 ppm Ti and 273 ppm V in the B horizon compared with 350 ppm Ti and 71 ppm V in the C horizon, and this distribution of these elements appears to correlate with Fe. Maximum values of 39 ppm Ga and 40 ppm Li occur in the B horizon, whereas there is only 4 ppm Ga and 1 ppm Li in the C horizon, and Ga and Li are most closely correlated with Al. The Mn content of the soil again rises steadily with depth, and there is no obvious Mn enrichment or evidence of co-precipitation of other metals by secondary Mn oxides.

Sulphur reaches 120 ppm in the A and B horizons but about 80 ppm is found in the C horizon, and thus enrichment in the upper part of the profile is not as marked as at Chitina. Fairly high F, over 400 ppm, characterizes the A and upper B horizons, but F values fall to 109 ppm in the lower C horizon, exhibiting a similar pattern to that at Chitina.

	Fe%	Al%	Si%	Mg%	pH	Ni	Cr	Cu	Ti	V	S	F	Mn
A	16.0	6.0	17.6	3.8	6.2	2000	3500	340	2900	132	150	190	1400
	18.0	5.8	18.4	4.1	6.3	2100	3750	350	3500	182	120	117	1440
	19.0	6.7	12.1	3.9	6.4	2650	4000	330	3600	118	95	68	1440
B	18.5	6.1	13.1	5.9	6.6	2750	2500	235	2700	94	50	60	1470
	12.0	3.9	12.7	6.4	6.8	2000	990	116	2290	65	20	60	1400
C	8.9	3.9	11.5	9.6	7.0	1900	400	101	1300	56	10	60	1350
	9.8	3.7	10.0	9.6	7.2	1400	550	70	1200	59	30	95	1270

Table 18: King Edward, distribution of major and trace elements in the vertical soil profile (ppm, except as stated; approximate vertical scale 1:30; for geological legend see figure 8).

There is much more Ni in the C horizon than the A and B horizons, and Ni values must be regarded as increasing with depth. However, they are accompanied in the C horizon by high Mg and Cr, and low Al and F, suggesting an ultramafic rock, and low S and Cu pointing to the absence of mineralization. Furthermore these geochemical guides are confirmed by the intersection of non-mineralized peridotite in a diamond drillhole passing beneath the pit.

5.3. King Edward

The pit at King Edward, though outside the area of the main Ni soil anomaly defined during prospecting, was sited at a point where Ni values of over 2000 ppm are linked with the highest Cu seen in the King Edward soil (sample nos. 555-13 to 555-19; figure 8). This particular site was not drilled (since the small amount of drilling carried out at King Edward was largely based on geophysical survey data, and met with no success), but from surface mapping is thought to be underlain by peridotite. The pit exposed an A horizon of yellow-brown sandy soil to 10 cm, then a red-brown sandy B horizon with scattered quartz pebbles to 80 cm, and then a C horizon of dark green to black fairly compact but fractured and weathered rock to the base of the pit at 3.1 m.

The major element distribution in the C horizon again supports an ultramafic parent rock (table 18). There is fairly high Fe at about 9%, under 4% Al and very high Mg at 9.6% in the C horizon. Iron and Al are enriched in the B horizon as a result of secondary oxide precipitation, but lower Mg values are encountered due to leaching. Silicon undergoes relative enrichment in the A and upper B horizons, with almost twice as much Si here than in the C horizon. There is an unusually high pH throughout the profile, rising from 6.2 at surface to 7.2 in the C horizon.

Nickel and Cr concentrations increase from the
A horizon into the B horizon, and over this part of the profile
soluble Ni and Cr are probably adsorbed by Fe. In the C horizon,
Ni and Cr fall to much lower levels, but still indicate ultramafic
rock. Titanium and V show a similar pattern of B horizon enrichment.
The high Cu noted in the soil during prospecting reaches 350 ppm
in the B horizon in the pit, but falls dramatically to 70 ppm in
the C horizon. This exceptional five-fold enrichment of Cu in
the B horizon seems most likely to be attributable to the
unusually high pH, inhibiting the mobility of metals such as Cu,
which are normally fairly mobile in slightly more acid conditions.
Manganese, at around 1400 ppm ,changes little over the profile,
and there is no evidence of secondary Mn oxide precipitation in
the B horizon.

Sulphur values are moderately high in the A and
upper B horizon, with a maximum of 150 ppm. In the C horizon,
however, there is about 20 ppm S. There is a similar distribution
of F, with 190 ppm in the A horizon, falling through the B horizon
to 60 ppm and 95 ppm in the C horizon.

The major and trace element composition of the lower
C horizon indicates non-mineralized ultramafic rock. Many metals,
including Ni, are moderately enriched in the B horizon, and this
produces the accepted pattern of falling Ni values with depth through
the profile over non-mineralized rock. The high Cu seen in the B
horizon, however, is very deceptive; it occurs in soil over parent
rock no richer in Cu than that at Chitina, where there is no Cu
soil anomaly. This emphasizes the relevance of pH in interpreting
soil data.

Fe%	Al%	Si%	Mg%	pH	Ni	Cr	Cu	Ti	V	S	F	Mn
27.0	10.5	17.3	3.3	5.5	2900	280	400	2400	620	390	266	555
31.5	7.9	15.5	1.7	5.1	3000	395	500	1750	734	465	447	390
32.0	10.9	11.8	2.5	5.3	3550	300	560	2400	409	525	352	410
25.0	7.9	11.8	3.7	5.6	9500	405	800	1900	445	335	247	540
36.0	4.1	12.2	4.3	5.5	4600	300	1050	1650	361	390	323	370
18.0	7.2	16.8	6.9	5.8	9500	65	1510	3450	337	310	2280	350
20.0	7.1	15.6	3.3	6.1	18000	105	720	1950	382	240	974	535
19.0	10.4	16.2	6.3	7.5	7500	350	540	2500	505	160	400	700

Table 19: Munali, distribution of major and trace elements in the vertical soil profile
(ppm, except as stated; approximate vertical scale 1:40, for geological legend
see figure 9).

5.4.   Munali

                At Munali a pit was sited within a 3000 ppm Ni
soil anomaly at the projection to surface of a mineralized
zone intersected at depth in a diamond drillhole (samples nos.
155-16 to 155-23; figure 9). The pit reached 4.5 m, exposing
a grey-brown friable A horizon to 20 cm followed by a distinctly
lateritic B horizon. The top of the B horizon is characterized
by a fairly compact red-brown and orange-yellow ferruginous
nodular layer, with a more sandy red-brown layer with scattered
quartz pebbles beneath. The C horizon starts at about 1.6 m
with red to green, soft, weathered gabbro with ferruginous soil
partings, grading into more compact green rock near the base
of the pit.

                The profile is conspicuous by its high Fe content,
with up to 36.0% Fe in the B horizon (table 19). Relative
enrichment of Si near the top of the profile is slight in comparison
with other areas, but reaches 17.3% in the A horizon. There is
up to 10.4% Al in the C horizon, and this is accompanied by 2500 ppm
silicate Ti and 505 ppm V. These high concentrations of Al, Ti
and V indicate a mafic parent rock containing alumino-silicate
minerals such as pyroxenes and amphiboles, and confirm the
observation of gabbro in the base of the pit. However there is little
or no enrichment of Al (or Ti and V) in secondary minerals in the
A and B horizons, with the result that Al in the B horizon is
present in much the same concentration over gabbro at Munali as
over peridotite at Chitina and Chombwa, and would make little
contribution to deducing the underlying rock type from soil
traverse or grid data.

                High Mg accompanied by low Cr is attributed to
chlorite, talc and shear zone minerals in view of the deduction
that the parent rock is not ultramafic. Evidence of shearing
and hydrothermal activity is supported by higher Ca than usual,
with up to 2.9% in the C horizon. Both Mg and Ca are partly
leached from the A and B horizons. The pH increases down the
profile from 5.1 near surface to 7.5 at the base of the pit.

Nickel values increase down the profile from
around 3000 ppm in the A and upper B horizons to 9500 ppm in
the lateritic zone and reach 18,000 ppm over part of the C
horizon, presumably the weathered vestige of the mineralized
zone. A similar pattern is exhibited by Cu, with high values
around 500 ppm in the A and upper B horizon rising to 1050 ppm
at the base of the lateritic zone and 1510 ppm in the C horizon.
These exceptionally high Ni and Cu concentrations are almost
certainly due to enrichment in the B horizon and the upper part
of the C horizon through adsorption by scavenging secondary
oxides, especially Fe oxides since Mn concentrations are low
throughout the profile. However, persistently high Ni and Cu
in weathered mafic rock in the lowermost exposed C horizon of
7500 ppm Ni and 540 ppm Cu are clear indications of mineralization.
Further evidence of the presence of sulphides at depth is given
by high S, which ranges from 160 to 310 ppm in the C horizon and,
as is typical elsewhere, is enriched to still higher concentrations
in the B horizon and reaches 525 ppm. The hydrothermal origin
of the mineralization is emphasized by exceedingly high F in the
C horizon, with a maximum of 2280 ppm, but any real indication of
this is lost in the A and B horizons, where F values around 300 ppm
are comparable with Chombwa.

A second pit 3.1 m deep was dug over non-mineralized
gabbro at Munali to expose the C horizon below 1.7 m (sample nos. 155-09 to
155-·15; figure 9). The C horizon at 3 m contains comparatively
low concentrations of 200 ppm Ni, 36 ppm Cu, and 6.0% Fe, confirming
that these elements indicate mineralization at the other pit. There
is 8.0% Al, 3000 ppm Ti and 400 ppm V in the C horizon of the
second pit, and these amounts are similar to those in the first,
showing that these metals reflect the composition of the silicate
minerals and parent rock type. Sulphur and F were not determined,
but by comparison with other areas are clearly sound indication
of mineralization and hydrothermal activity respectively; the
latter is often accompanies the injection of mineralizing fluids,
as at Munali.

Fe%	Al%	Si%	Mg%	Ni	Cr	Cu	Ti	V	S	F	Mn
10.8	14.9	30.0	2.7	900	1750	63	2250	207	240	119	945
13.0	11.4	26.5	2.0	1000	2500	67	2250	164	140	109	930
14.0	13.2	21.3	1.7	1100	1800	72	2250	159	40	109	1070
11.0	11.0	20.3	1.4	1150	950	120	1700	179	80	95	700
13.0	14.1	27.3	4.9	1500	1750	60	2050	123	120	95	3050
10.6	7.9	23.1	3.8	1300	1050	52	1750	101	100	60	2100
7.5	6.8	23.5	3.5	1000	550	79	1350	85	60	76	1260
7.3	8.1	19.8	4.0	900	600	84	1100	67	160	60	860

Table 20: Musangashi, distribution of major and trace elements in the vertical soil profile (ppm, except as stated; approximate vertical scale 1:40; for geological legend see figure 10).

5.5.   Musangashi

Within the 800 ppm Ni soil anomaly outlined
during prospecting, a 4.2 m pit was dug (sample nos. 655-01
to 655-08; figure 10). The pit exposed a grey-brown friable,
sandy A horizon over the first 10 cm, followed by a yellow-brown
sandy B horizon with a zone of black specks and partings and
some quartz pebbles. The transition to C horizon is gradational
between 2 and 3 m, and the C horizon material is soft, pale green
to grey-white, fairly schistose in places and with greasy
partings. The parent rock is inferred as gabbro or norite
altered to talc-chlorite-actinolite schist.

A parent rock of gabbroic character is suggested
by low Fe and Mg, and high Al in the C horizon (table 20). Iron and Al are
enriched in the A and B horizons but Mg is leached. There is also
relative enrichment of Si, especially in the A horizon. Nickel
values initially increase with depth from 900 ppm in the A horizon
to a maximum of 1500 ppm in the zone of black specks and partings
in the B horizon, and then fall back to 900 ppm in the lowermost
exposed C horizon. An analogous distribution is shown by Mn,
increasing from 945 ppm in the A horizon to 3050 ppm one m from
surface, then falling to 860 ppm at the base of the pit. It
therefore seems probable that the black mineral seen in the B
horizon is a secondary Mn oxide. The enrichment of Ni in the
zone where this mineral has formed can thus at least be partly
attributed to adsorption of Ni by secondary Mn oxide, although
fixation of some Ni by Fe is also likely. The Musangashi area
is unique among those studied in exhibiting a B horizon Ni anomaly
caused by the accumulation of Ni fixed by secondary Mn.

There are fairly low concentrations of Cr, Cu,
Ti and V in the C horizon, and each of these show some enrichment
in the B horizon, though without an obvious correlation with Mn.

Fe%	Al%	Si%	Mg%	pH	Ni	Cr	Cu	Ti	V	S	F	Mn
17.0	5.2	24.8	4.5	6.1	8500	2450	340	1000	69	10	53	1800
16.0	7.2	26.3	5.4	6.0	8000	2600	360	700	80	80	78	1600
17.0	6.4	23.0	5.5	5.9	9000	2100	400	1000	89	80	90	1370
15.0	4.7	14.5	5.5	5.9	8500	2650	420	600	46	180	109	920
13.0	2.0	13.5	7.1	5.9	9000	950	270	350	43	280	119	840

AB / C

Table 21:   Trojan, distribution of major and trace elements in the vertical soil profile

(ppm except as stated; approximate vertical scale 1:40; for geological legend see figure 12).
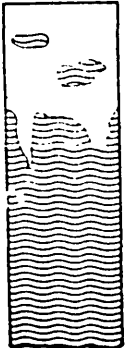
Fe%	Al%	Si%	Mg%	pH	Ni	Cr	Cu	Ti	V	S	F	Mn
13.0	1.9	34.7	7.3	6.2	6500	1650	81	550	48	10	15	1750
13.5	2.7	33.5	5.6	6.1	6500	2000	81	600	49	20	15	1360
14.0	1.7	32.4	5.4	6.1	7500	1500	86	750	56	10	43	1240
12.5	0.6	28.5	4.8	6.3	9000	1000	84	200	26	20	30	1330
9.4	0.6	33.0	5.0	6.4	11500	350	52	100	20	40	30	1900
8.8	0.2	33.4	7.0	6.5	9500	300	85	300	24	120	32	1510

AB / C

Table 22:   Kingston, distribution of major and trace elements in the vertical soil profile

(ppm, except as stated; approximate vertical scale 1:40; for geological legend see figure 13).

The highest S value of 240 ppm occurs in the A horizon, and around 100 ppm characterizes the B and C horizons. Lack of significant S enrichment in the B horizon, seen in most other areas, is attributed to the relatively low order of secondary Fe oxide formation. Fluorine levels are low throughout the profile, and fall from 119 ppm in the A horizon to 60 ppm in the lower C horizon.

In a B horizon soil traverse or grid a Ni anomaly due to adsorption of Ni with secondary Mn might prove difficult to identify. Clearly, high Mn promotes caution in data interpretation, but in this case low Cu and S point to the absence of mineralization. Copper enrichment in the B horizon such as that at King Edward, or even Cu adsorbed by secondary Mn oxides, might confuse interpretation in other cases.

5.6.   Trojan

At Trojan there are immature skeletal lithosols, and a pit within a 6000 ppm Ni anomaly and sited over the Trojan Hill orebody reached only 1.2 m (samples nos. 855-01 to 855-05; figure 12). A brown to red-brown sandy AB horizon grades at about 50 cm below surface into white to pale green weathered serpentinite. High Fe and Mg, along with low Al in the C horizon confirm an ultramafic parent rock (table 21). There is slight Fe, Al and Si enrichment in the AB horizon, but Mg is only moderately leached, and the pH remains at about 6.0 over the whole of the exposed profile.

Nickel values are extremely high at around 8500 ppm, change little over the profile, and are bound to be considered much higher than the Ni content of an ultramafic parent rock. They are accompanied by high Cu, with about 350 ppm in the AB horizon falling to 270 ppm in the C horizon. This combination of high Ni and Cu is a good indication of mineralization, but it is interesting to note that the Cu values in the AB horizon are in fact similar to those found in the non-mineralized King Edward area.

Fairly high Cr and low Ti and V in the C horizon support an ultramafic parent rock, and these metals exhibit a two to three times enrichment in the AB horizon. Manganese, too, shows this order of AB horizon enrichment, but there is no visible evidence of black secondary Mn oxide minerals in the pit, and Ni certainly does not correlate with Mn distribution in the profile.

There are low concentrations of S at the top of the AB horizon, but values increase with depth to a fairly high level of 280 ppm in the C horizon. Unusually, F increases with depth, but the maximum of 119 ppm in the C horizon is still low and reflects ultramafic parent rock, with no suggestion of hydrothermal activity. Hence, the best guide to mineralization at Trojan is high Ni and Cu, with a supporting indication from high S provided the C horizon is investigated.

A second pit at Trojan was dug over the graphitic argillite formation and reached 1.0 m (sample nos. 855-23 to 855-27; figure 12). The C horizon is slightly weathered, black, poorly laminated argillite with abundant yellow-orange, iron-stained partings and surfaces after oxidized pyrite. The sample from the base of the pit contains 28.0% Fe and 1480 ppm S, even in the absence of visible pyrite. There is also 460 ppm Ni, 420 ppm Cu and, though not readily explained, a high value of 493 ppm F. Clearly the argillite, a host rock of the ultramafic intrusive, is likely to have been the source of S which facilitated the formation of disseminated pyrrhotite and associated sulphides within the serpentinite.

5.7.   Kingston

A pit at Kingston was sited within a 6000 ppm Ni soil anomaly where diamond drilling had established that only exceedingly weak and uneconomic mineralization was present (sample nos. 855-17 to 855-22; figure 13). As at Trojan, the soil is thin and immature, with a brown to red-brown friable, sandy to rubbly AB horizon down to 60 cm, and below a pale green to yellow, soft, weathered peridotite becoming more compact towards the base of the pit at 2.0 m.

In the C horizon, high Fe and Mg with low Al affirm an ultramafic parent rock (table 22). There is only slight Fe and Al enrichment in the AB horizon, and Mg is not conspicuously leached. High Si, around 30%, prevails throughout the profile, and the pH changes little from 6.1 in the AB horizon to 6.5 in the C horizon.

Nickel values increase with depth from 6500 ppm in the upper AB horizon to 9500 and 11,500 ppm in the C horizon. This modest but clear increase contrasts unfavourably with Trojan, where there is no increase in Ni with depth in the soil profile over economic ore. However, Cu concentrations are much lower at around 85 ppm at Kingston, and change little through the profile. In the C horizon there is fairly low Cr, Ti and V, but there is some enrichment of these metals, especially Cr, in the AB horizon. Enrichment of mobile elements in the AB horizon is probably a result of their adsorption by secondary Fe oxides, since Mn, though quite high at around 1500 ppm, has not accumulated in the AB horizon.

Both S and F are conspicuously low, with maxima of 120 ppm S indicating the near-absence of mineralization and 43 ppm F reflecting ultramafic parent rock and lack of hydrothermal activity. Thus extremely high Ni in conjunction with low Cr falsely suggests mineralization, while low Cu, S and perhaps F point to a non-mineralized parent rock.

5.8.   The general behaviour of other elements

Some elements show the same consistent correlations
throughout the soil profile as they exhibit in the primary
environment. The concentration of Co is clearly always related to
Ni, irrespective of the origins of these metals in silicate or
sulphide primary minerals, and Co values vary from 60 ppm at
Chitina to 900 ppm at Munali. Nickel levels tend to be from 3
to 13 times Co concentrations. There is invariably a high
correlation between Al and Sc, including enrichment in the B
horizon, and Sc values range from 4 to 35 ppm. Also linked to Al
distribution are Ga and Li. Thus over ultramafic rocks, there are
very low concentrations of a few ppm Ga and Li in the C horizon,
but values rise more than tenfold in the B horizon, with maxima
of 33 ppm Ga and 40 ppm Li at Chombwa. There is little Ga and no
Li in the immature profiles over the Trojan-Kingston intrusive.
Along with Al, there is generally more Ga and Li than elsewhere in
the C horizon over mafic rocks, and at Munali the levels of these
elements are lower in the B horizon.

Strontium follows Ca, though there are widely
varying concentrations of these elements in the C horizon, ranging
from 0.4% Ca and 9 ppm Sr at Kingston to 2.9% Ca and 119 ppm Sr
at Munali. These elements are usually leached from the A and B
horizons, however, and concentrations of less than 1.0% Ca and
50 ppm Sr are typical. Low levels of K and Ba are usual in the
C horizon because of the general lack of feldspars in the parent
rock, and range from 0.1% K and 24 ppm Ba at Kingston to 1.2% K
and 405 ppm Ba at Musangashi. The close correlation between K and
Ba is preserved throughout the profile, and any slight enrichment of
K in the A and B horizons is attributed to clay mineral formation.

The amounts of Pb and Zn change little over the
vertical profile, and most samples contain between 8 ppm Pb and
21 ppm Zn, as at Munali, and 36 ppm Pb and 220 ppm Zn seen at
Trojan. The Chitina area is an exception, however, with high values
throughout the profile, reaching 141 ppm Pb and 520 ppm Zn. Both
Be and Sn usually exhibit a fairly erratic vertical distribution,

and possibly occur in grains of resistant minerals such as corundum
and cassiterite and so undergo little chemical dispersion. In the
different field areas there is from less than   1 ppm to 8 ppm Be
and from less than 2 ppm to 22 ppm Sn.

5.9.   <u>The significance of multi-element behaviour</u>

The widely differing geochemical characteristics
of the pit profiles studied emphasizes the problem of Ni soil
anomaly interpretation. Exceptionally high Ni values at Trojan
indicate mineralization, but comparable Ni levels occur at Kingston,
which can be regarded as non-mineralized by comparison. Equally high
Ni occurs in the lateritic horizon at Munali, but might be missed
in convential soil sampling, producing values similar to those in
other non-mineralized areas.

Even when other elements are taken into account
there remains the possibility of ambiguity in anomaly interpretation.
High Cu in the B horizon indicates mineralization at Munali and
Trojan, and can be traced into the C horizon, but high Cu in the B
horizon at King Edward is a misleading surface enrichment. Thus
although in B horizon samples a combination of high Ni and Cu may
indicate mineralization (Coope, 1958), there are cases when this is
a false guide. By contrast, a combination of high Ni and Cr reflects
an olivine-bearing ultramafic parent rock, and where present, can be
seen in both the C and B horizons. Nickel values in excess of Cr
indicate mineralization at Trojan and Munali, although this feature
is also observed at Kingston. At King Edward, however, the criterion
of higher Cr than Ni in the soil could be set against the high Ni
and Cu values in anomaly interpretation.

High concentrations of Al, Ti, V, Ga and Li indicate
a parent rock containing alumino-silicate minerals such as pyroxenes
and amphiboles, and low concentrations of these elements indicate
ultramafic parent rock. However, these guides to bedrock are usually
valid only in the C horizon because low concentrations of these elements
in ultramafic rocks tend to become relatively enriched in the B horizon
as a result of the leaching and depletion of more soluble elements. Of
this alumino-silicate group of elements, only high concentrations of V in
the Munali B horizon differ from the levels of these elements in the B
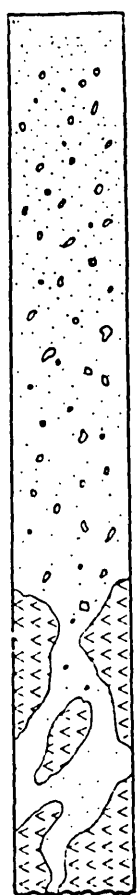
Coarse fraction content				Coarse-to-fine fraction ratios			
Ni	Cu	Fe %	Mn	Ni	Cu	Fe	Mn
1950	48	13.0	1190	0.76	0.75	0.87	0.88
2150	55	14.5	1210	0.86	0.86	0.88	1.08
2150	52	13.5	1320	0.81	0.76	0.84	1.21
2400	56	14.0	1310	0.90	0.82	0.80	1.18
1900	52	12.5	1300	0.72	0.78	0.74	1.23
2700	61	14.5	1500	0.93	0.92	0.81	1.20
3250	66	16.5	1840	0.37	0.90	0.85	0.92
13000	18	10.0	980	0.87	1.06	0.97	0.29
8000	12	9.6	1000	1.00	0.92	0.74	0.24

Table 23: Chombwa, metal content of coarse fraction of soil profile samples, (ppm except as stated) and coarse-to-fine fraction ratios; (approximate vertical scale 1:40; for geological legend see figure 7).

horizon elsewhere, and reflect high concentrations of V in the C
horizon and parent gabbro. Hence high Ni and V in the soil
may prove a useful indicator of a gabbroic parent rock
accompanied by unusual Ni concentrations, perhaps in the
form of sulphides.

In the C horizon, S provides a diagnostic guide to
mineralization, with up to 310 ppm at Munali, and 280 ppm at
Trojan. There is less than 80 ppm S in all other areas except
Kingston where, as might be expected, there is a slightly elevated
value of 120 ppm. In the B horizon S shows an affinity for
secondary Fe oxides and is often enriched in mature profiles.
As a result, by far the highest S in the B horizon is found at
Munali, where there is up to 525 ppm reflecting mineralization
at depth. Among the non-mineralized areas the maximum value is
240 ppm, found at both Chitina and Musangashi. At Trojan and
Kingston, however, there are low S levels of less than 80 ppm
in the AB horizon, presumably due to the ease with which S is
lost from an immature soil with limited secondary Fe oxide
precipitation. The contribution made by S to Ni anomaly
interpreation is perhaps limited to areas of mature soil formation,
but where skeletal lithosols are developed it is often practical
to obtain C horizon samples along a prospecting traverse or grid,
and these would yield particularly useful S data.

Fluorine, though conspicuously enriched in the A
horizon of soils, is usually below 100 ppm in the B horizon, and
around 300 ppm at Munali and Chombwa appears to be anomalous.
High F can be traced into the C horizon, reaching 2280 ppm at
Munali, and is attributed to minerals of hydrothermal origin.
However, the C horizon at Chombwa contains only 133 ppm F, and
the strong B horizon enrichment is not readily explained. At
Trojan F values are low, although the highest value of 119 ppm F
in the C horizon is much higher than the F content of the C
horizon over peridotite, and may be related to the Trojan
mineralization of serpentinization. It is possible that the
high F content of the pyritic graphitic argillite
is related to the same source. Thus F in soils may prove a
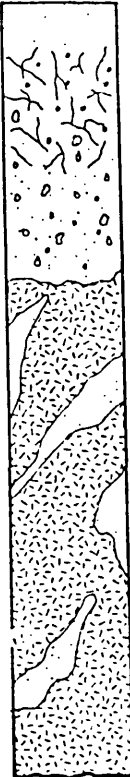
Coarse fraction content				Coarse-to-fine fraction ratios			
Ni	Cu	Fe %	Mn	Ni	Cu	Fe	Mn
2500	550	50.5	360	0.86	1.38	1.87	0.65
2650	670	50.3	290	0.88	1.34	1.60	0.74
32??	610	50.0	280	0.90	1.09	1.56	0.68
10000	1080	33.0	440	1.05	1.35	1.32	0.81
4600	1000	40.0	350	1.00	0.95	1.11	0.95
9000	1410	19.0	310	0.95	0.93	1.06	0.89
7000	470	18.0	720	0.59	0.65	0.90	1.35
3000	121	11.5	640	0.40	0.22	0.61	0.91

Table 24: Munali, metal content of coarse fraction of soil profile samples
(ppm, except as stated) and coarse to fine fraction ratios (approximate
vertical scale 1:40; for geological legend see figure 9).

useful supplementary guide to primary mineralization, although the maximum number of other variables must be taken into account, since F anomalies are not always derived from mineralization.

5.10.   The distribution of ore metals in the coarse fraction

As part of a limited study comparing the distribution of ore metals in the coarse and fine fractions, the coarse fraction of samples from the Chombwa profile overlying non-mineralized peridotite and the Munali profile over mineralized gabbro were analysed for Ni, Cu, Fe and Mn by atomic absorption spectrophotometry.

At Chombwa the Ni and Cu concentrations in the coarse fraction are generally slightly lower than the amount in the corresponding fine fraction, resulting in coarse-to-fine fraction ratios of less than unity (table 23). While Fe distribution is similar to Ni and Cu, with ratios of less than unity, Mn concentrations are rather higher in the coarse fraction in the B horizon but are much higher in the fine fraction in the C horizon. Thus precipitation of Fe as secondary oxides in the B horizon seems to regulate Ni and Cu adsorption, but in the absence of a nodular lateritic layer there is no enrichment of Fe in the coarse fraction.

At Munali, however, Ni and Cu are enriched in the coarse fraction in the B horizon, and coarse-to-fine fraction ratios are close to or greater than unity (table 24). Very high Fe values characterize the coarse fraction in the B horizon, where a nodular laterite zone is developed, and ratios are greatly in excess of unity. All three metals occur predominantly in the fine fraction in the C horizon, and this is attributed to the ease with which trace elements have been leached from the rock and sorbed by fine secondary minerals, while the more resistant silica minerals form the coarse, weathered rock fraction. In the B horizon, Ni and Cu adsorption is clearly controlled by secondary Fe minerals, while Mn, which occurs in higher concentrations in the fine fraction, increases with depth in both fractions and shows no B horizon enrichment.

On the basis of the two soil profiles examined,
Ni and Cu accumulation in the B horizon appears to be largely
controlled by Fe. For the most part, Ni and Cu concentrations
are not markedly different in the two fractions, but where a
lateritic zone is present Fe, and hence Ni and Cu, tends to be
enriched in the coarse fraction because the secondary Fe oxides
form small nodules. The development of a lateritic zone in the
B horizon is probably favoured where the parent rock is rich in
Fe, as is the case with mineralized localities. Thus in a soil
traverse or grid, analysis of the coarse fraction of samples
for Ni and Cu might be adopted with a view to increasing anomaly
contrast over mineralization. However, any Fe accumulation in
the soil from sources other than mineralization could also be
expected to be enriched in the coarse fraction and to enhance
Ni and Cu.

5.11   Discussion

In recent years, several researchers working in
Australia have addressed themselves to the problems of
nickel exploration geochemistry, and especially distinguishing
Ni gossans from nickeliferous and ferruginous outcrops of no
economic significance. As in this research, their methods of
evaluating Ni anomalies have usually involved multi-element
analysis and interpretation, and their findings can usefully
be incorporated into a discussion of the early stages of
secondary dispersion of Ni and associated elements.

In the Pioneer area, Western Australia, Cox (1975)
found that Ni and Cu concentrations in the vertical soil
profile overlying mineralization increased with depth, and
that maximum levels of 10,000 ppm Ni and 1050 ppm Cu were
encountered in a visibly iron-rich zone, termed gossan, about
one metre below surface. This situation is comparable with

distribution of Ni and Cu in the profile over mineralization
at Munali. Nickel values increase with depth less dramatically
over non-mineralized ultramafic rock at Pioneer, reaching
about 2000 ppm at one metre, while Cu concentrations are
consistently around 100 ppm. This is similar to the Ni and Cu
distribution in the profiles over non-mineralized ultramafic
rock at Chitina and Musangashi. Cox (1975) also comments up-
on the relationship between Ni and Cr in the soil profile,
and shows that the Ni:Cr ratio in weathered bedrock overlying
mineralization at Pioneer is as high as 31.25, compared with
1.14 over non-mineralized ultramafic rock. This contrast is
diminished but not lost near the top of the soil profiles at
Pioneer, with Ni:Cr ratios of 3.83 over mineralization and
1.77 over non-mineralized ultramafic rock. In Central Africa,
Cr values are similar to or exceed Ni values at most points
in profiles overlying non-mineralized ultramafic rock, and
hence Ni:Cr ratios are low. High Ni:Cr ratios occur in the
profiles over mineralization at Munali and Trojan and weak
mineralization at Kingston, with a maximum of 171.43 in
weathered bedrock at Munali. Moeskops (1976) has tentatively
suggested that the Cr leached into solution by a HNO_3-HClO_4
attack occurs in the bedrock and soil in ferrochromite. The
Cr is readily leached from ferrochromite by dilute acids, and
this process may occur in low pH natural environments, as in
the vicinity of oxidizing sulphide mineralization. In this
way, low Cr and high Ni:Cr ratios would tend to characterize
mineralization and the overlying soil.

Wilmshurst (1975) examined the geochemistry of
oxidized and leached outcrops and trench exposures of
weathered and ferruginized mineralized and non-mineralized
ultramafic rocks at Spargoville and other localities in
Western Australia. Over non-mineralized ultramafic rock, both
weathered rock and lateritic material have high Ni contents

and low Cu contents, and hence a high Ni:Cu ratio. The
same features are evident in the C and B horizons of the
soil profiles over non-mineralized ultramafic rocks at
Chitina, Chombwa, Musangashi and Kingston. Wilmshurst (1975)
suggests a Ni:Cu ratio greater than 15 in weathered and
ferruginized ultramafic rocks indicates the absence of
mineralization at depth, and in the aforementioned Central
African areas this ratio ranges from 11 to 882. Wilmshurst
(1975) states that lower ratios can occur in ferruginized rocks
over non-mineralized parent material where Cu is derived
from an exotic source; this may be the case in the King
Edward soil profile, where there is up to 350 ppm Cu in the B
horizon and Ni:Cu ratios range from 6 to 17. In the
Spargoville area, weathered massive sulphides form a boxwork
gossan, but ferruginized massive sulphides have a less
characteristic appearance. Both Ni and Cu concentrations
are high in the gossans and laterites derived from mineralization,
and Ni:Cu ratios are usually lower than 15. Research by
Moeskops (1976) on other Australian ultramafics indicates that
Ni:Cu ratios in the range two to six characterize weathered
outcrops derived from mineralization. In Central Africa, there
is up to 18,000 ppm Ni and 1510 ppm Cu in the C and B horizons
over mineralization at Munali, and Ni:Cu ratios are mainly at
the lower end of the range 4 to 25. Trojan is not strictly
comparable, since the mineralization is disseminated rather
than massive, and since the inferred mode of ore genesis by
sulphurization produces less cupriferous mineralization; there
are maxima of 9000 ppm Ni and 420 ppm Cu, with Ni:Cu ratios in
the range 22 to 33. Butt and Sheppy (1975), examining primary
and secondary dispersion in the mineralized Mt Keith ultramafic
intrusive, Western Australia, note that the mineralization is
disseminated and primary Cu concentrations are low compared with
massive sulphides. Consequently Ni:Cu ratios are high at about
60 compared with 11 for massive sulphides at Kambalda. Low Cu

levels and high Ni:Cu ratios associated with primary
mineralization at Mt Keith are reflected in lateritic soil
horizons, where Cu concentrations over 300 ppm pick out
only the richer mineralized zones, and the lower grade
mineralization is not indicated by Cu anomalies.

Another problem associated with the use of Ni:Cu
ratios in soils for distinguishing mineralization is that Ni
and Cu tend to precipitate in different parts of the profile.
Nickel accumulates near the top of the C horizon and Cu
accumulates slightly higher in the profile in the lower B
horizon. This phenomenon is especially obvious in the Chombwa
and Munali soil profiles, and has been noted in Western
Australia by Butt and Sheppy (1975) and Smith (1976), and in
Rhodesia by Wilding (1965). This redistribution of Ni and Cu
is attributed to the varying mobilities of the two metals in
the oxidizing environment. Over mafic and ultramafic rocks
the pH usually increases with depth and metals leached into
solution in the A horizon percolate downwards and precipitate
as their pH of hydrolysis is exceeded. Copper precipitates
earlier than Ni, that is, higher in the profile, because the pH
of hydrolysis for Cu is lower than for Ni. However,
coprecipitation with and adsorption by secondary Fe oxides also
contributes to Ni and Cu distribution in the soil profile.

Thus, although a useful range of Ni:Cu ratios can
be evaluated when the vertical soil profile is studied in full,
a single Ni:Cu ratio from one point in the profile is likely to
be less meaningful. Therefore Ni:Cu ratios are not usually
considered in subsequent sections which deal with soil
geochemistry based on samples taken along traverse lines from a
single point in the B horizon. This problem of Ni and Cu

redistribution in the soil profile is probably the reason
why Clema and Stevens-Hoare (1973) found that Ni:Cu ratios
for outcrop specimens of true gossans, ironstones, laterites
and wads from the Yilgarn Block, Western Australia, were not
successful in distinguishing the true gossans.

In places where an unusually high pH prevails
in the upper part of the soil profile a considerable enrichment
of Cu can occur. This is the case at King Edward, where there
is fivefold enrichment of Cu in the B horizon compared with the
lowermost exposed C horizon in the soil profile. As a result,
Cu concentrations in the B horizon of soil overlying non-
mineralized ultramafic rock at King Edward are similar to those
in soil overlying disseminated mineralization at Trojan. Thus
high Cu levels in the C horizon are a more promising guide to
mineralization than B horizon data, and where geochemical soil
surveys are carried out by sampling the B horizon material, pH
determination will aid Cu anomaly interpretation.

High concentrations in the C horizon of the soil
profile of Al, Ti, V, Ga and Li indicate a mafic rather than
ultramafic parent rock, because these elements are contained in
or derived from alumino-silicates such as pyroxenes and
amphiboles. The C horizon of soils overlying ultramafic rock
are characterized by high Mg, Ni and Cr. During soil formation,
Al and its associated elements tend to become incorporated into
the lattice of secondary clay minerals, whereas Mg is readily
leached from the soil. In this way, Al, Ti, V, Ga and Li are
largely retained in the A and B horizons of soils over mafic
rocks, while they undergo considerable relative enrichment, due
to loss of Mg, in the A and B horizons of soils over ultramafic
rock ; for example, at Munali, Al, Ti and V concentrations change

little throughout the vertical soil profile and concentrations
of these elements are comparatively high in the C horizon.
In all other areas the levels of these three metals fall with
increasing depth in the soil profile, while Mg concentrations
increase. Therefore, in the C horizon, high Ni coupled with
high Al, Ti and V is anomalous in the sense that this pattern
does not solely reflect the parent silicates, and may be
indicative of mineralization in a mafic lost rock, as at Munali.
However, this pattern becomes masked in the A and B soil horizons.
On purely empirical grounds, high V in the A and B horizons of
the Munali soil contrasts with lower V in the same soil horizons
elsewhere, and is the best indicator of a mafic parent rock.
Thus, a Ni soil anomaly associated with high V might be a more
promising exploration target than coincident high Ni and low V.

An enrichment of Ni over and above the levels
typical of the non-mineralized parent rock, as suggested by
analyses of core and outcrop samples, occurs near the top of
the C horizon in the Chitina, Chombwa, Munali and Kingston soil
profiles. The same phenomenon was noted in the soil profile over
some Rhodesian ultramafics by Wilding (1965). The most marked
rise in Ni concentration appears to occur as the pH increases
down the profile to more than 6. Such enrichment is not always
present, for example at King Edward, where a high pH persists
throughout the profile and probably inhibits any redistribution
of Ni. At Trojan also, there is no Ni enrichment at the top of
the C horizon, perhaps because the pH is less than 6. Indeed,
the presence of oxidizing mineralization may in some places be
instrumental in lowering the pH and diminishing the Ni enrichment.
At Munali, however, a high pH pertains in the upper part of the
C horizon and Ni values reach 18,000 ppm.

Wilding (1965) suggests that increasing Ni content
with depth in the C horizon indicates the presence of underlying
sulphide mineralization, but the limited opportunities to test
this hypothesis in the present research have not substantiated this.
In the C horizon over non-mineralized peridotite at Chombwa, Ni
is initially enriched at 4 m from surface where there is 15,000
ppm Ni, and this falls to 8000 ppm at 5 m. Over mineralization
at Munali, uppermost C horizon Ni enrichment occurs at 3 m from
surface where there is 18,000 ppm Ni, but this too falls sharply
with increasing depth, to 7500 ppm at 4 m. When contrasting
the Chombwa and Munali profiles it is evident that Ni accumulation
in the ferruginous B horizon at Munali is far greater with a
maximum sample value of 9500 ppm Ni, whereas at Chombwa the
highest Ni concentration in the B horizon is 3750 ppm. The B
horizon of mature soil profiles of other non-mineralized areas
exhibit still lower Ni levels. Thus, this horizon presents
the sampling medium likely to yield the best anomaly contrast
in geochemical soil surveys.

Iron accumulates high in the soil profile because
its low pH of hydrolysis inhibits mobility. Where Fe is
abundant, as in the environment of weathering sulphides, secondary
Fe minerals tend to accrete and form coarse nodules. Hence Fe and
secondary Fe minerals such as goethite are found to be enriched
in the coarse fraction of soils overlying mineralization. Where
Fe in the primary environment is less abundant, Fe and goethite
enrichment in the coarse fraction is less conspicuous or absent.
In the presence of nodular Fe enrichment, as at Munali, Ni and Cu
appear to be coprecipitated and adsorbed by these secondary Fe
oxides high in the soil profile, so that coarse-to-fine-fraction
ratios for these metals are higher than the corresponding ratios
over non-mineralized ultramafic rock, as at Chombwa. The partition
of Ni and Cu between coarse and fine fractions near the top of
the Munali profile seems to be influenced by the relative mobilities
of the two metals: the nodular secondary Fe oxides first scavenge
a higher proportion of less mobile Cu, producing maximum
coarse-to-fine-fraction Cu ratios from surface to 50 cm; then

relative enrichment of more mobile Ni in the coarse fraction
and maximum coarse-to-fine-fraction Ni ratios occur between
50 cm and one metre.

At Kambalda, Western Australia, Mazzucchelli
(1972) noted an even more marked enrichment of Ni and Cu in the
coarse fraction compared with finer fractions in the soil profile
from 3 to 16 inches overlying mineralization. The Ni enrichment
in the coarse fraction is attributed to fragments of chrysoprase,
and Ni in the fine fractions is associated with quartz thought
to be derived from the weathering of primary silicates. The
Kambalda soils are not lateritic and contain only a few percent
Fe, so that fixation of Ni and Cu by Fe is unlikely to assume
the same importance as at Munali. Whether or not the enrichment
of Ni and Cu in the coarse fraction of the soils at Kambalda
has any prospecting significance comparable with that indicated
in Central Africa is unclear, because soil profiles over non-
mineralized ultramafic rock were not investigated.

Surprisingly poor contrast between soils overlying
mineralized and non-mineralized ultramafic rock was furnished by
S considering the unique association of the element with sulphide
minerals in the primary environment. The oxidation of sulphide
minerals yields, among other products, the sulphate anion, which
is highly soluble and mobile in most surface environments, and a
large proportion of sulphate is lost from the immediate vicinity
of mineralization. The ubiquity of low concentrations of S in
almost all soils is attributed to the ease with which the soluble
sulphate anion travels in circulating groundwater and from which
plants acquire S essential to their metabolism. Sulphur is
returned to the surface of the soil by rotting vegetation, and
that S which is not then leached is largely retained in organic
forms such as humic acids and anion acids (Peters, 1974).

During the oxidation of sulphide minerals such as
pyrrhotite, ferric hydroxide is one of the principal products.
Sulphate anions are clearly also abundant in the environment of
oxidizing sulphides and, according to Stumm and Morgan (1962)
can substitute for hydroxyl groups during the polymerization of
ferric hydroxide molecules. This ferric hydroxide is relatively
immobile and tends to precipitate near to source as goethite and
other secondary Fe oxides, which may form a ferruginous zone
within the soils or a gossan. By this process, anomalous
concentrations of S can occur in ferruginous soils overlying
mineralization. The correlation of S with Fe and enrichment of
both elements in the coarse fraction of soils overlying the
Munali ore suggests that such a process is indeed operative.
Clearly, a method determining only this S species associated
with secondary Fe oxides, and not S related to organic matter
in the soil, should further improve anomaly contrast.

Fluorine concentrations in the weathered bedrock
from all pits, except at Munali, are less than 133 ppm, which is
consistent with the F levels expected in ultramafic rocks. Low
F at Trojan suggests that relatively little F was introduced
during serpentinization. In the upper horizons of mature soils
developed over ultramafic rocks, some F enrichment occurs, mainly
in the A horizon. This enrichment is thought to result from the
substitution of F^- anions for OH^- anions in the clay minerals which
form during weathering. There is no field evidence to suggest
that F is correlated with secondary Fe oxides, and according to
Boyle (1976), F shows only a weak association with Fe and Mn in
the secondary environment. In lateritic profiles, the clay
minerals tend to be more abundant in the A horizon than the
ferruginous B horizon. Boyle and Dass (1967) and Lalonde (1974)
found that the F content of the A horizon of soils over other
types of mineral deposits in Canada gave the best anomaly contrast.

In gabbroic rocks at Munali, much higher F levels, reaching
2280 ppm F in the C horizon, may be directly associated with
the mineralization. The Munali sulphides are believed to have
accumulated in late stage fluids which were injected into a weak
contact zone. These late stage fluids would possibly have some
enrichment in volatiles such as F. However, F concentrations
in the A and B horizons of the Munali profile are much the same
as at Chombwa. The A and B horizons of the soil overlying
mineralization at Munali are highly ferruginous. This lowers
the clay mineral content of the soil and hence the F holding
capacity of the soil. Fluorine is relatively mobile and is no
doubt readily leached from such soils.

	Chitina Mean	Chitina Range	Musangashi Mean	Musangashi Range	Paulwi Mean	Paulwi Range	Kingston Mean	Kingston Range	Trojan* Mean	Trojan* Range
Ni	401	20 - 1250	581	25 - 1500	6030	4000 - 8250	5790	420 - 12500	4050	1000 - 8000
Cu	79	22 - 160	59	6 - 120	22	8 - 60	280	34 - 1020	288	79 - 520
Co	56	5 - 100	84	15 - 450	370	225 - 430	242	70 - 400	220	65 - 400
Zn	177	37 - 360	55	24 - 91	153	84 - 240	98	50 - 320	437	81 - 1900
Cr	447	25 - 1550	1360	30 - 4930	10900	4880 - 19500	2700	950 - 5200	1970	900 - 2550
Ti	1230	700 - 1700	1640	1350 - 2200	851	400 - 2950	962	350 - 2500	904	700 - 1750
V	209	48 - 500	175	63 - 626	89	33 - 361	161	44 - 500	103	31 - 146
Fe %	6.5	0.9 - 10.5	8.1	0.9 - 13.5	18.4	13.5 - 21.5	14.8	8.0 - 21.0	10.9	6.7 - 15.5
Al %	14.3	6.2 - 22.6	10.2	3.7 - 17.7	3.5	0.3 - 11.4	5.2	0.3 - 15.7	6.7	4.2 - 10.1
Mg %	1.8	0.3 - 28.6	3.1	0.3 - 12.9	6.4	1.7 - 16.3	4.5	1.3 - 7.3	5.1	1.6 - 7.4
Mn	650	190 - 1500	978	95 - 6100	2230	1640 - 2900	1500	1100 - 1980	1390	390 - 2000
S	98	30 - 185	51	20 - 100	-	-	46	15 - 75	90	20 - 185
F	-	-	-	-	-	-	72	15 - 570	69	15 - 178
pH	5.1	4.6 - 5.8	5.1	4.3 - 6.1	-	-	6.0	5.7 - 6.4	6.2	5.4 - 6.9

*Excludes samples over pyritic graphitic argillite

Table 25: Mean and range of major and trace element concentrations along soil traverses across intrusives of Basement age (ppm, except as stated).

6. THE DISTRIBUTION OF ELEMENTS ALONG SOIL TRAVERSE LINES

Soil samples were taken along traverse lines across
the intrusives at Chitina, Chombwa, King Edward, Munali, Musangashi,
Paulwi, Kingston and Trojan. The normal sampling interval was 50 m,
closing to 10 m over Ni soil anomalies defined during prospecting.
The full width of the intrusive was traversed where practical. The
B soil horizon was sampled, usually at a depth of about 30 cm, but in
areas of immature soil development, such as Paulwi and Trojan, the
AB horizon is not always this thickness, and some samples were taken
at shallower depths. The fine fraction of samples were analysed for
total metals by atomic absorption spectroscopy and emission
spectrography, while the intermediate and coarse fractions were used
for pH and S determinations respectively. Fluorine was determined
along some traverses, with the expense of commercial analyses proving
the limiting factor, and total metals in the coarse fraction were
determined at Munali and Chombwa. The analytical results, given in
detail in appendix 2, are reviewed in conjunction with the observed
dispersion of elements in the vertical soil profile with a view to
distinguishing the geochemical characteristics of primary
mineralization, and with particular reference to multi-element behaviour
as a useful guide.

6.1. Chitina

At Chitina a traverse of 1600 m was made across the
full width of the mafic-ultramafic intrusive including a Ni soil
anomaly defined during prospecting (samples nos. 435-01 to 439-49;
figure 6). In the traverse the Ni anomaly is reflected by Ni values
reaching 1250 ppm, while the mean Ni concentration for the traverse
is 401 ppm (table 25).

About 10% Fe accompanies the Ni anomaly in the traverse,
compared with a mean of 6.5% Fe, and there is a +0.71 correlation
between Ni and Fe. Aluminium values range from 6.2% to 22.6%, but
Ni shows no significant correlation with Al. There is a close
relationship between Ni and Cu distribution reflected by a correlation
of +0.83. Although Cu values are not especially high, averaging 79 ppm,
they increase over the Ni anomaly to 160 ppm to produce coincident
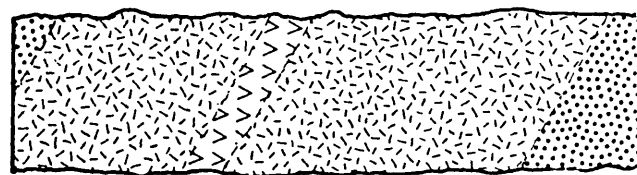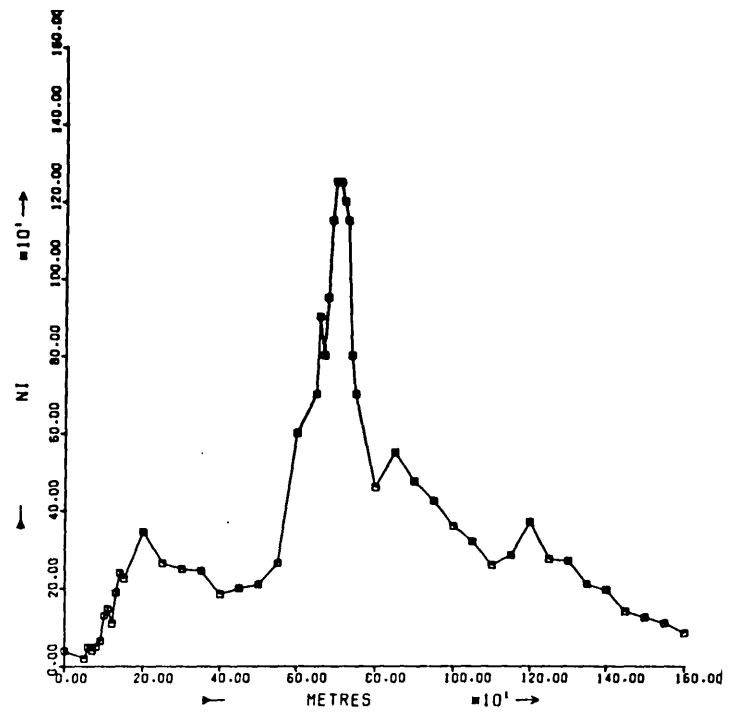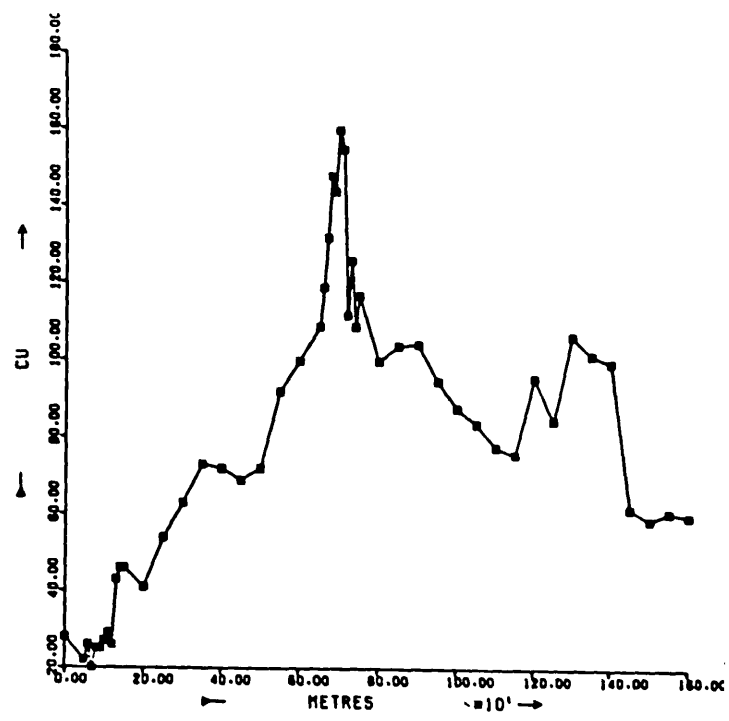
Figure 64:   Chitina, distribution of Ni (ppm) and Cu (ppm) along
             soil traverse line (for geological legend see figure 6).
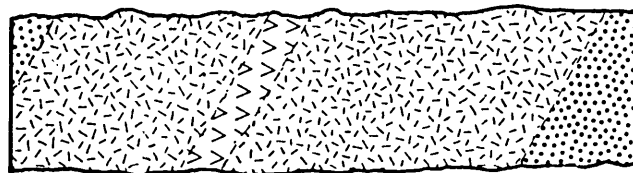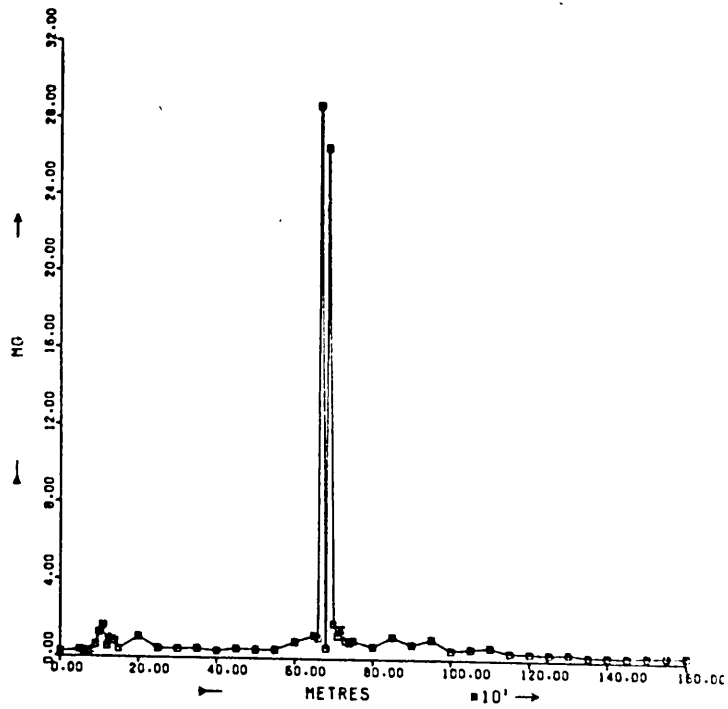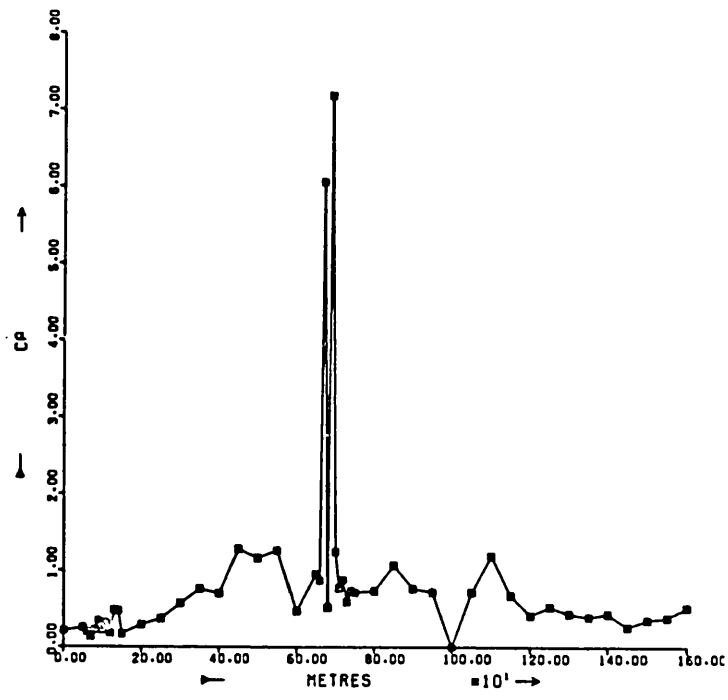
Figure 65: Chitina, distribution of Mg (%) and Ca (%) along
soil traverse line (for geological legend see figure 6).
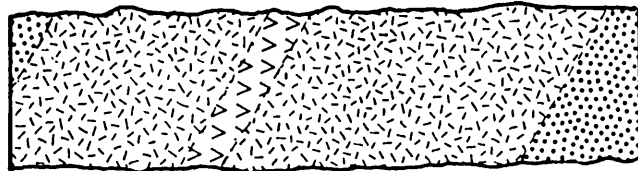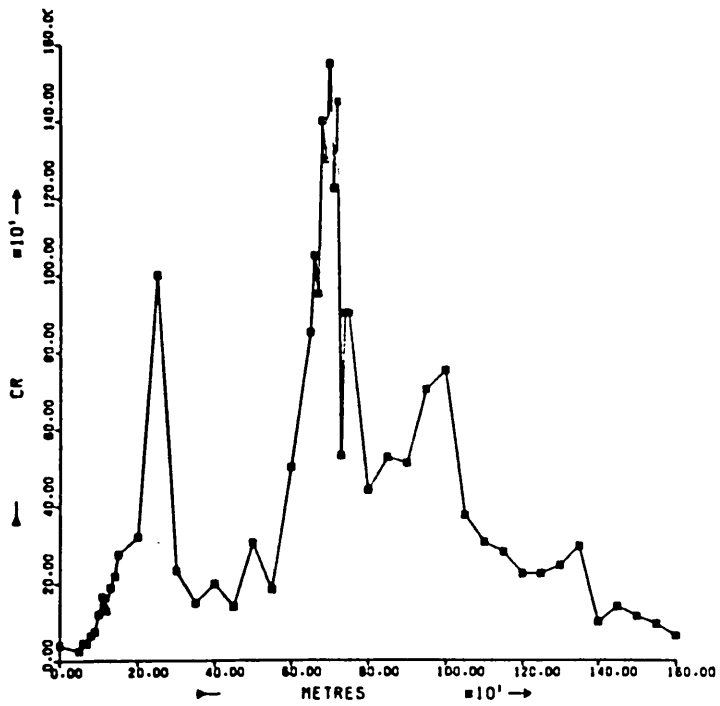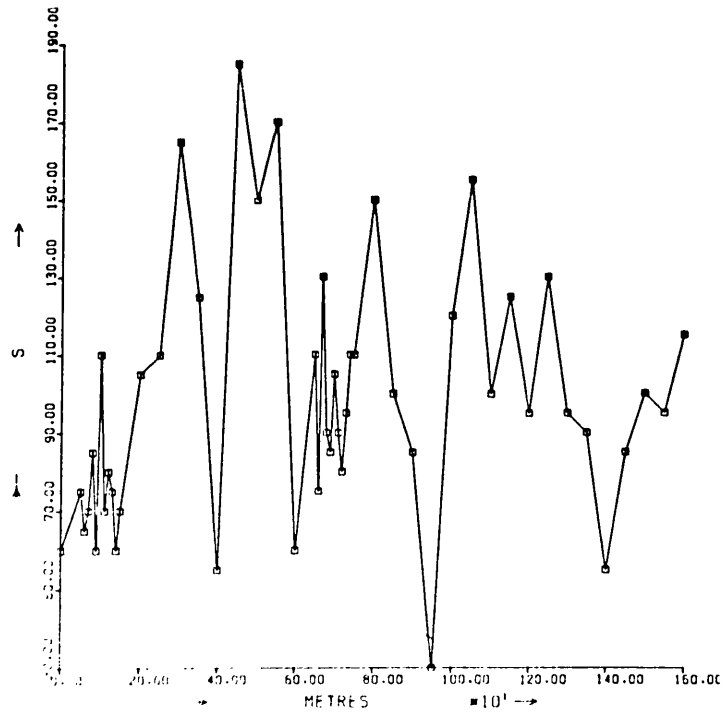
Figure 66: Chitina, distribution of Cr (ppm) and S (ppm) along
soil traverse line (for geological legend see figure 6).

Ni and Cu peaks suggestive of mineralization (figure 64).

This zone is also characterized by some exceptionally high Mg, Ca and Li concentrations. These elements tend to be substantially leached from the Chitina soils, and background levels are less than 1% Mg , 1% Ca and 40 ppm Li. However, in conjunction with the Ni anomaly there is up to 28.6% Mg, 7.2% Ca and 3680 ppm Li (figure 65). This anomaly combination is taken to indicate a zone of alteration, and presents a potentially good environment for mineralization. Fluorine, which might have contributed to this argument, was not determined at Chitina. However, Cr is strongly correlated with Ni at +0.65, and Cr values increase beyond the mean of 447 ppm to reach 1550 ppm in conjunction with the highest Ni. Chromium is thus generally present in higher concentrations than Ni, which indicates that both metals are derived from silicate minerals. The absence of mineralization is further supported by fairly low and erratic S distribution, ranging from 30 to 185 ppm, and with S values around the mean of 98 ppm in the zone of high Ni, Cu and Cr (figure 66).

There are relatively high Zn levels along the Chitina traverse compared with other areas, but the highest values, reaching 360 ppm, are not related to the Ni anomaly. Rather Zn distribution in the soil may be controlled by secondary Mn oxides, although the mean Mn concentration is low at 650 ppm. The maximum Zn values occur in conjunction with high Mn, reaching 1500 ppm, and there is a correlation of +0.62 between Zn and Mn (figure 67). Cobalt, however, which is known to accumulate with secondary Mn oxides, does not exhibit this phenomenon, and is closely correlated with Ni.

Fairly high means of 1230 ppm Ti and 209 ppm V confirm the   inference made during prospecting of a predominantly mafic intrusive, and the Ni anomaly appears to be related to a lens of altered ultramafic rock with nickel-rich silicate minerals.
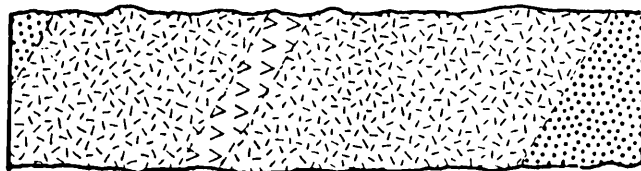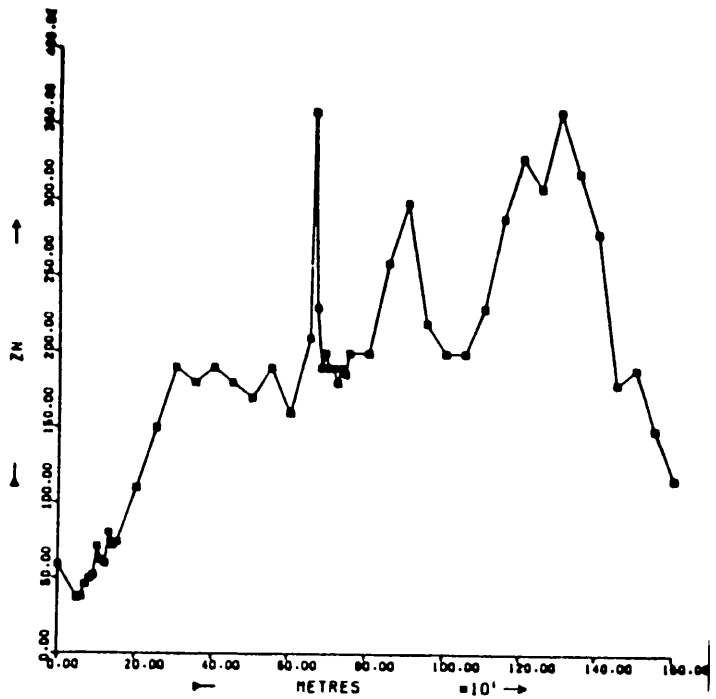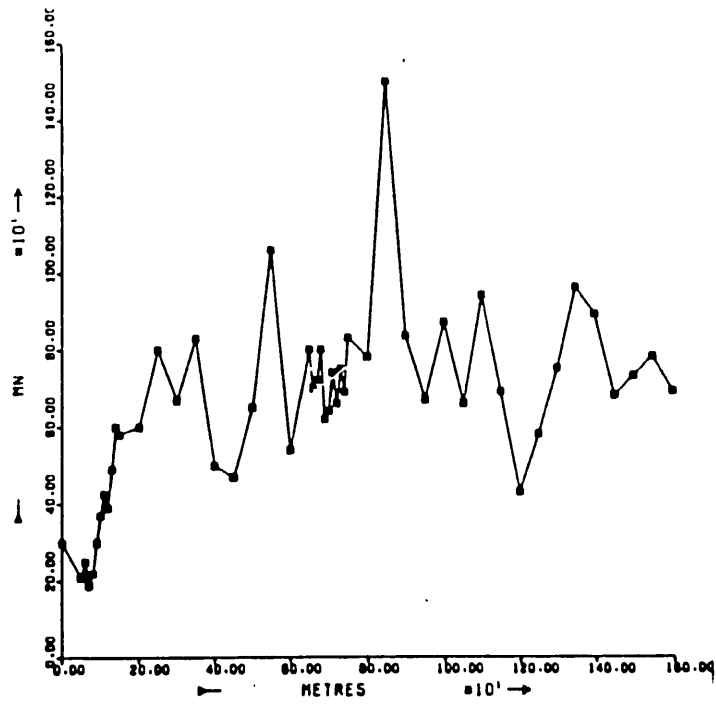
Figure 67: Chitina, distribution of Zn (ppm) and Mn (ppm) along
soil traverse line (for geological legend see figure 6).

6.2.   Chombwa

          The Chombwa traverse does not cover the full diameter
of the large Chombwa intrusive, but over 600 m crosses a lens of
peridotite within the gabbro (sample nos. 245-01 to 245-25; figure
7). The ultramafic rock was outlined by a Ni soil anomaly during
prospecting, and this anomaly reaches 3000 ppm along the traverse
line. The high mean Ni level of 1870 ppm recorded for the traverse
reflects the large proportion of samples overlying the ultramafic
lens, while the background over the surrounding gabbro is a few
hundred ppm (table 26).

          The distribution of Ni follows that of Fe, which ranges
from 5.6% to 16.5%, and the two elements are mutually correlated by
a coefficient of +0.92. There is no evidence that Ni or other trace
elements are linked to Al distribution. Chromium and Ni also have
a +0.92 correlation, and since Cr is consistently higher than Ni in the
anomalous zone, olivines are thought to be the principal source of
both metals (figure 68). Although Cu distribution is similar, and
there is a +0.83 correlation between Ni and Cu, the soil concentrations
of Cu are relatively low throughout the traverse, and only fluctuate
in the range 32 to 78 ppm.

          The Chombwa soil is readily leached of the more
soluble elements, and Mg and Ca values are usually below 1%, with less
than 40 ppm Li. Two samples at different points along the traverse
exhibit much higher values, reaching 36.9% Mg, 6.8% Ca and 7860 ppm Li.
However, neither position is coincident with the Ni anomaly, and
these high values must be attributed to possible zones of alteration
without mineralization. Manganese fluctuates from 570 to 1230 ppm
along the traverse, with no sign that secondary Mn oxides are
responsible for the fixation of anomalous concentrations of other
trace elements. Zinc, Ti and V levels are relatively low, although
higher V, over 300 ppm, tends to pick out mafic rock at the northern
end of the traverse.

Figure 67: Chitina, distribution of Zn (ppm) and Mn (ppm) along
soil traverse line (for geological legend see figure 6).
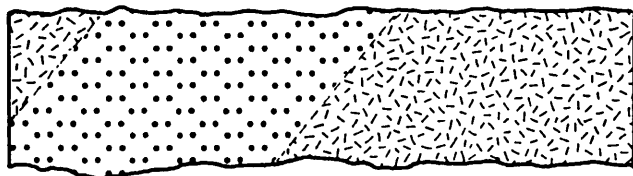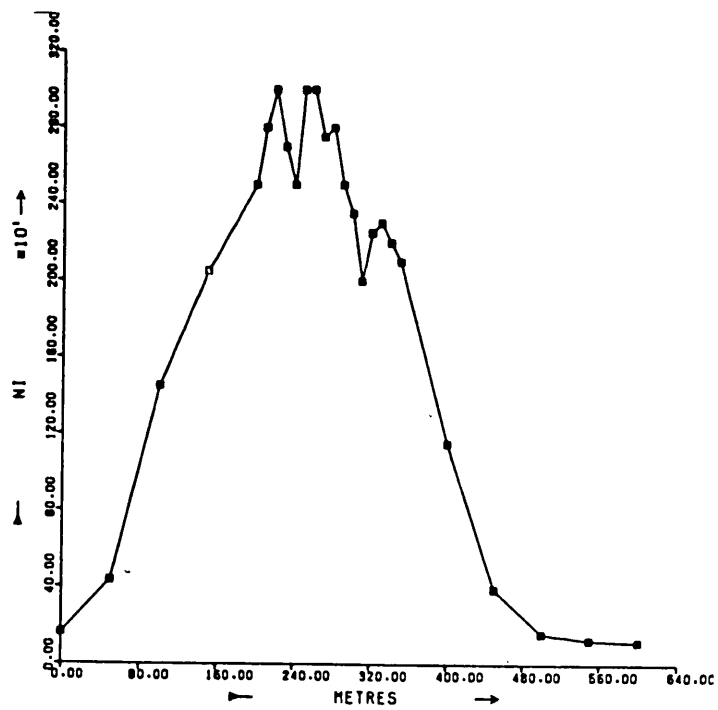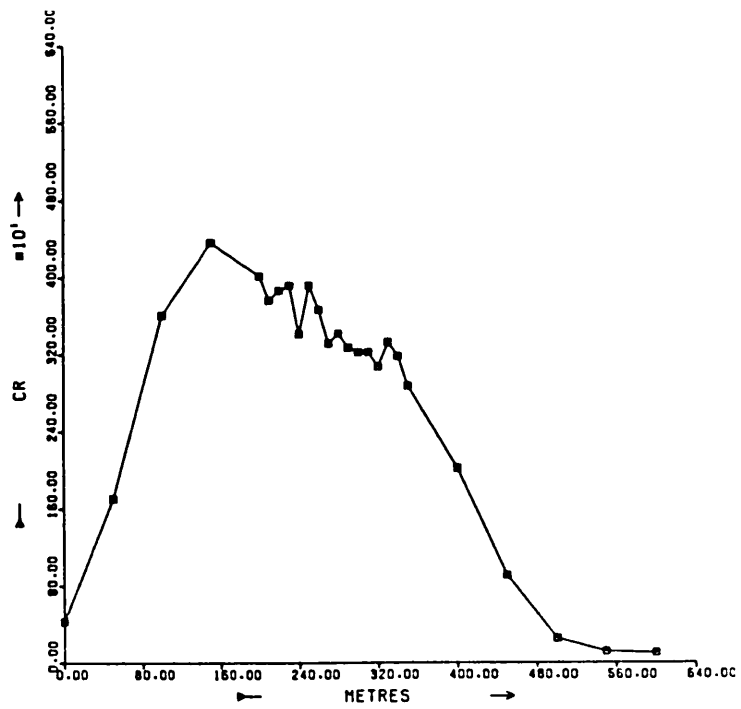
Figure 68: Chombwa, distribution of Ni (ppm) and Cr (ppm) along
soil traverse line (for geological legend see figure 7)

	Chombwa		King Edward		Munali[*]	
	Mean	Range	Mean	Range	Mean	Range
Ni	1870	115 - 3000	1350	100 - 3050	1340	58 - 6500
Cu	61	32 - 78	161	57 - 450	205	8 - 940
Co	129	45 - 170	109	30 - 200	117	23 - 450
Zn	70	8 - 110	81	20 - 220	16	2 - 40
Cr	2740	100 - 4350	2020	115 - 6500	130	33 - 500
Ti	1830	1350 - 2180	1710	750 - 3400	2160	700 - 4800
V	270	132 - 636	210	76 - 570	411	124 - 818
Fe %	12.8	5.6 - 16.5	13.9	1.4 - 24.0	10.2	3.8 - 25.5
Al %	15.1	5.8 - 22.5	7.2	0 - 16.6	9.5	3.1 - 17.5
Mg %	2.9	0.4 - 36.9	5.1	1.0 - 27.7	2.8	0.5 - 5.5
Mn	1020	570 - 1230	946	430 - 1640	354	130 - 895
S	216	130 - 430	107	55 - 440	131	30 - 535
F	257	119 - 447	-	-	298	64 - 998
pH	4.8	4.2 - 5.5	6.0	5.4 - 6.4	5.1	4.5 - 6.0

* Excludes samples over schist.

Table 26: Mean and range of major and trace element concentrations along soil traverses across intrusives of post-Katanga age (ppm, except as stated)

6.2.   Chombwa

The Chombwa traverse does not cover the full diameter
of the large Chombwa intrusive, but over 600 m crosses a lens of
peridotite within the gabbro (sample nos. 245-01 to 245-25; figure
7). The ultramafic rock was outlined by a Ni soil anomaly during
prospecting, and this anomaly reaches 3000 ppm along the traverse
line. The high mean Ni level of 1870 ppm recorded for the traverse
reflects the large proportion of samples overlying the ultramafic
lens, while the background over the surrounding gabbro is a few
hundred ppm (table 26).

The distribution of Ni follows that of Fe, which ranges
from 5.6% to 16.5%, and the two elements are mutually correlated by
a coefficient of +0.92. There is no evidence that Ni or other trace
elements are linked to Al distribution. Chromium and Ni also have
a +0.92 correlation, and since Cr is consistently higher than Ni in the
anomalous zone, olivines are thought to be the principal source of
both metals (figure 68). Although Cu distribution is similar, and
there is a +0.83 correlation between Ni and Cu, the soil concentrations
of Cu are relatively low throughout the traverse, and only fluctuate
in the range 32 to 78 ppm.

The Chombwa soil is readily leached of the more
soluble elements, and Mg and Ca values are usually below 1%, with less
than 40 ppm Li. Two samples at different points along the traverse
exhibit much higher values, reaching 36.9% Mg, 6.8% Ca and 7860 ppm Li.
However, neither position is coincident with the Ni anomaly, and
these high values must be attributed to possible zones of alteration
without mineralization. Manganese fluctuates from 570 to 1230 ppm
along the traverse, with no sign that secondary Mn oxides are
responsible for the fixation of anomalous concentrations of other
trace elements. Zinc, Ti and V levels are relatively low, although
higher V, over 300 ppm, tends to pick out mafic rock at the northern
end of the traverse.

Figure 69: Chombwa, distribution of S (ppm) and F (ppm) along
            soil traverse line (for geological legend see figure 7).

The S content of the Chombwa soil is high, with a mean of 216 ppm, and this may reflect the pyritic nature of the parent rock noted in core and outcrop samples. Furthermore, the maximum S concentrations of 360 and 430 ppm occur in conjunction with the peak of the Ni anomaly, and may be interpreted as an indication of mineralization. Fluorine distribution, however, shows the reverse pattern, with generally high F up to 447 ppm over the mafic rock, and a negative anomaly down to 119 ppm in conjunction with the Ni and S peaks (figure 69).

The Chombwa traverse presents a particularly confusing picture for interpretation, with Cr values exceeding Ni and low F indicating the presence of ultramafic rock under the anomalous zone, but high Fe and S reflecting the pyritic nature of this rock. Low Cu makes a most important contribution by indicating the absence of Ni mineralization.

6.3.   King Edward

A traverse of 900 m was made across the full width of the King Edward intrusive including the Ni soil anomaly established in prospecting (sample nos. 535-01 to 535-39; figure 8). The mean Ni content of the traverse line samples is 1350 ppm, with the anomaly peak along the southern contact zone of the intrusive expressed by concentrations reaching 3050 ppm (table 26).

There is a mean Fe level of 13.9% and, like Ni, Fe is generally higher over the intrusive than the surrounding limestone, and reaches 24.0%. Although the Ni and Fe peaks are not coincident there is a +0.76 correlation between the two metals. Aluminium values average 7.2% and show no sympathy with Ni distribution. While Ni and Cr have a correlation of +0.68 and Cr, reaching 6500 ppm, is generally higher than Ni, lower Cr occurs over the southern contact zone. Thus, here, Ni values exceed Cr and may suggest the presence of mineralization at depth (figure 70).
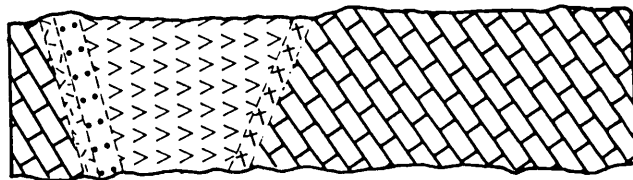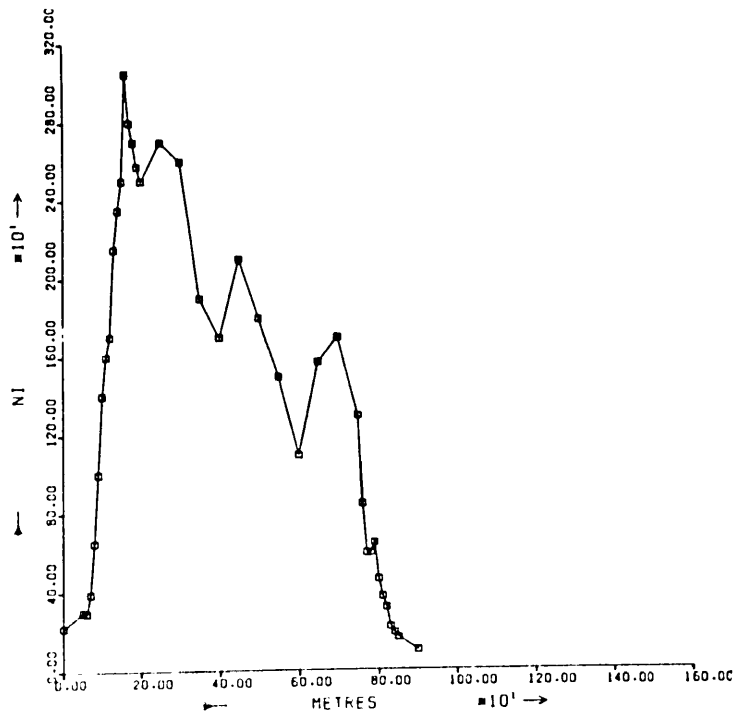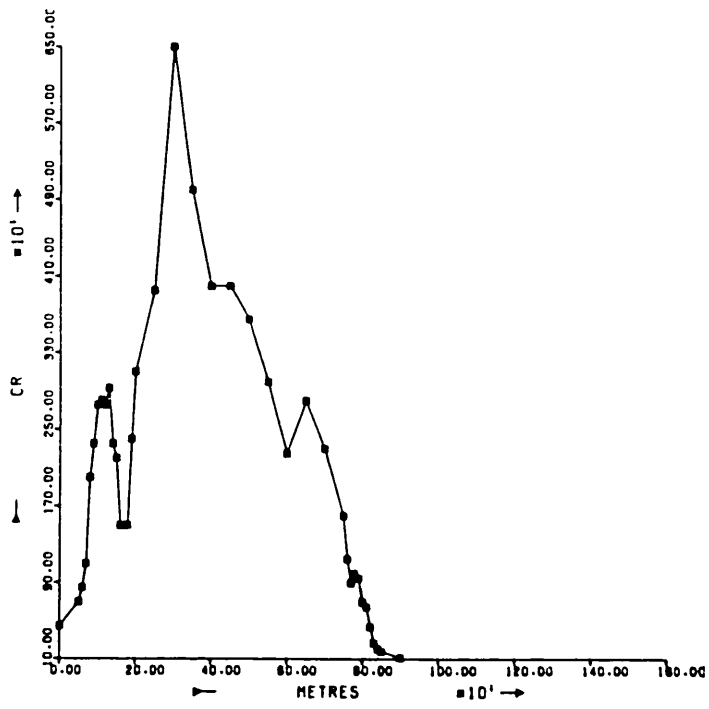
Figure 70: King Edward, distribution of Ni (ppm) and Cr (ppm) along soil traverse line (for geological legend see figure 8).
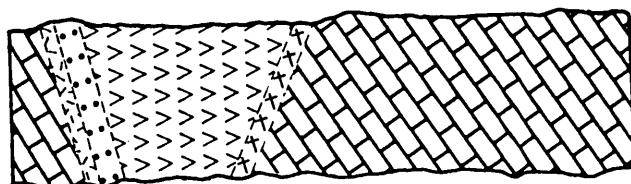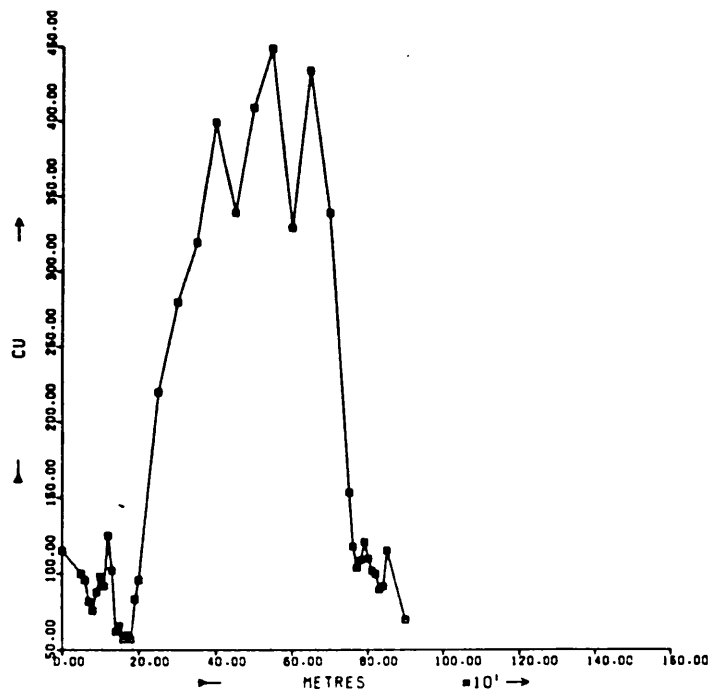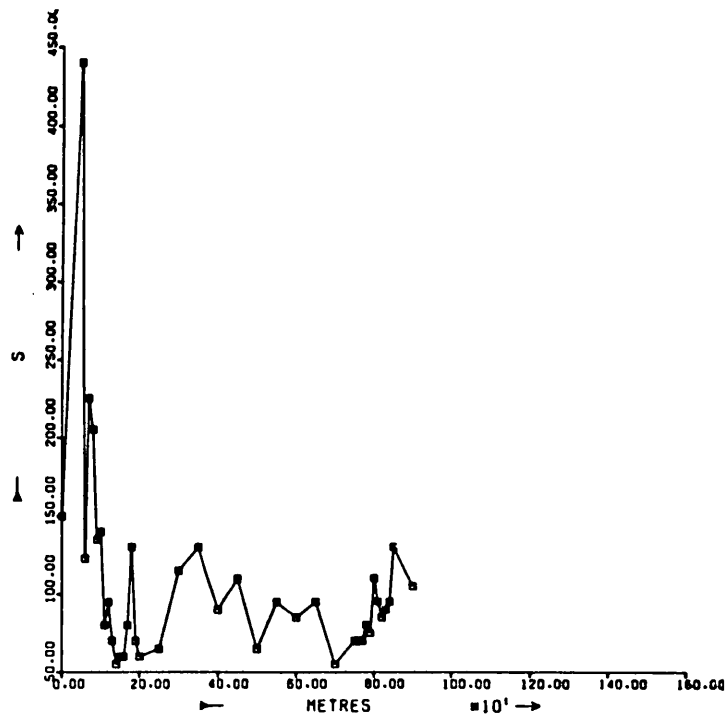
Figure 71: King Edward, distribution of Cu (ppm) and S (ppm) along
soil traverse line (for geological legend see figure 8).
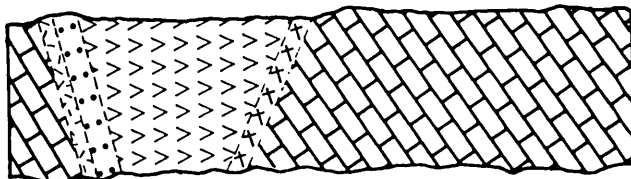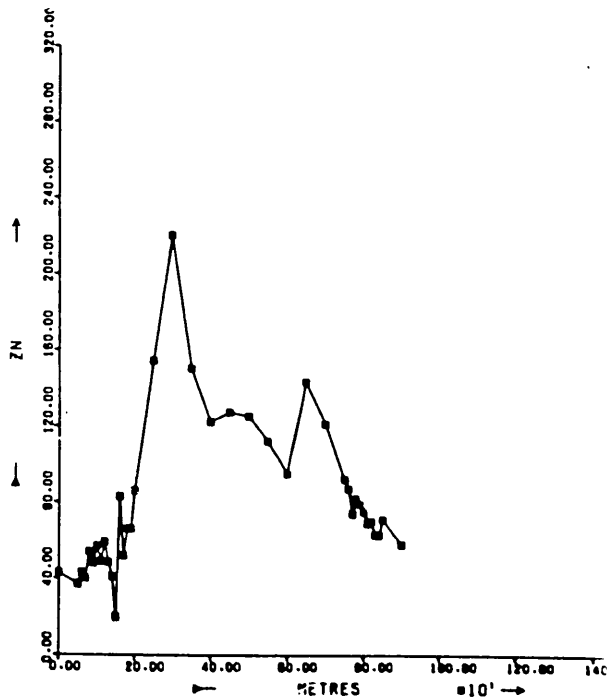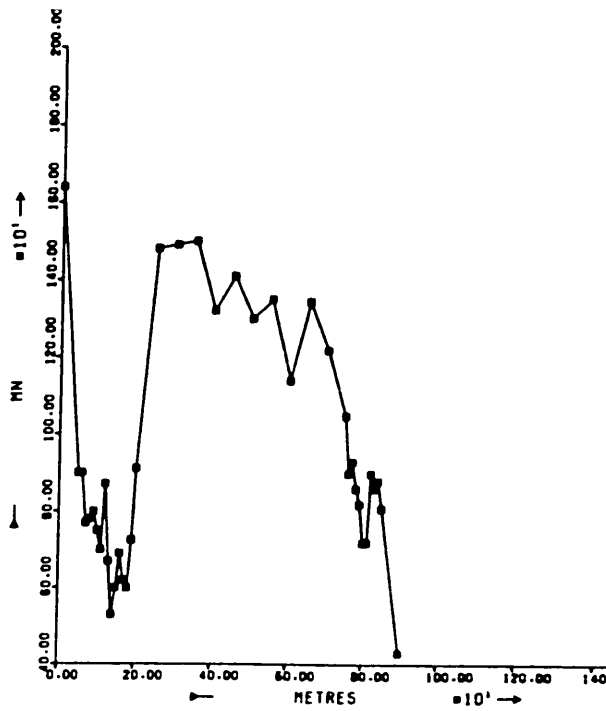
Figure 72: King Edward, distribution of Zn (ppm) and Mn (ppm) along
soil traverse line (for geological legend see figure 8).

However, low Cu concentrations, under 100 ppm, characterize the
southern contact and do not support a mineralized zone. Further
along the traverse, very high Cu is linked with moderately high
Ni, but here Cr values exceed Ni. Hence mineralization is not to
be suspected at King Edward because the three metals Ni, Cu and
Cr do not occur in a favourable combination. This deduction is
clearly confirmed by the distribution of S. The highest S
concentration occurs over the limestone to the south of the
intrusive, and values below 100 ppm are typical across the full
width of the Ni anomaly and the intrusive (figure 71).

The King Edward Cu anomaly may be at least partly
caused by adsorption of Cu by secondary Mn oxides. Along the
traverse, Mn concentrations range from 430 to 1640 ppm, with the
highest values occuring over the same part of the traverse as the
maximum Cu. In addition there is a +0.79 correlation between Cu
and Mn. A similar distribution is noted for Zn, with a +0.74
correlation between Zn and Mn (figure 72).

There is a high mean Ca level of 1.9% reflecting
the samples taken over limestone and the calcareous nature of parts
of the intrusive. Compared with other areas, Mg is not strongly
leached from the soil, which contains a mean of 5.1% Mg, indicative
of the ultramafic character of much of the intrusive. High Mg
values, reaching 27.7%, occur in conjunction with high Ca and Li
near the northern contact. Titanium and V cover wide ranges
of 750 to 3400 ppm and 76 to 570 ppm respectively, probably reflecting
the variation from mafic to ultramafic rock within the intrusive.

6.4.   Munali

At Munali, a traverse of 850 m crosses the full width
of the intrusive including the Ni anomaly overlying mineralization
(sample nos. 135-01 to 135-34; figure 9). Along the traverse there
is sharp contrast between the background of about 100 ppm Ni and
up to 6500 ppm over the mineralized zone (table 26).
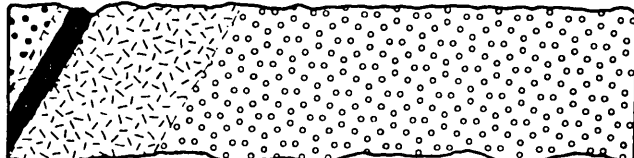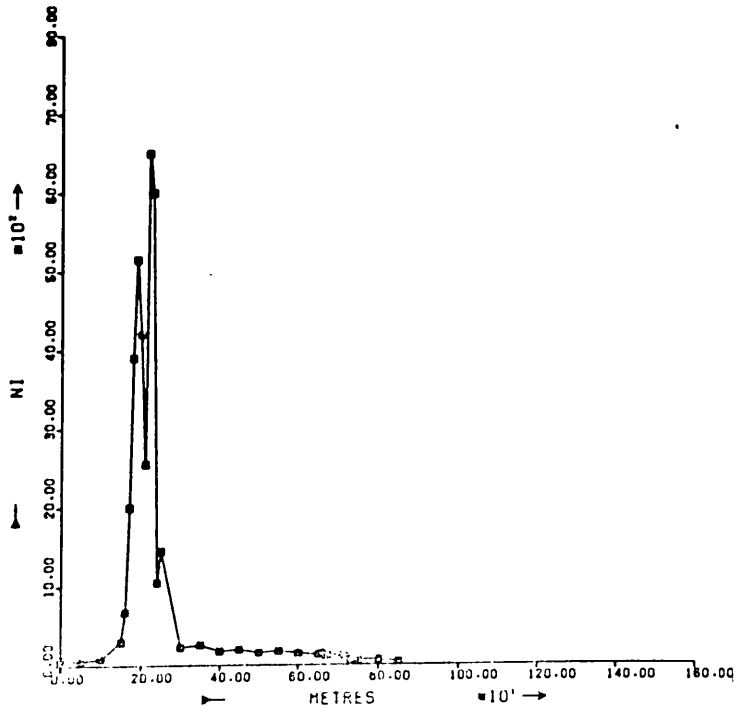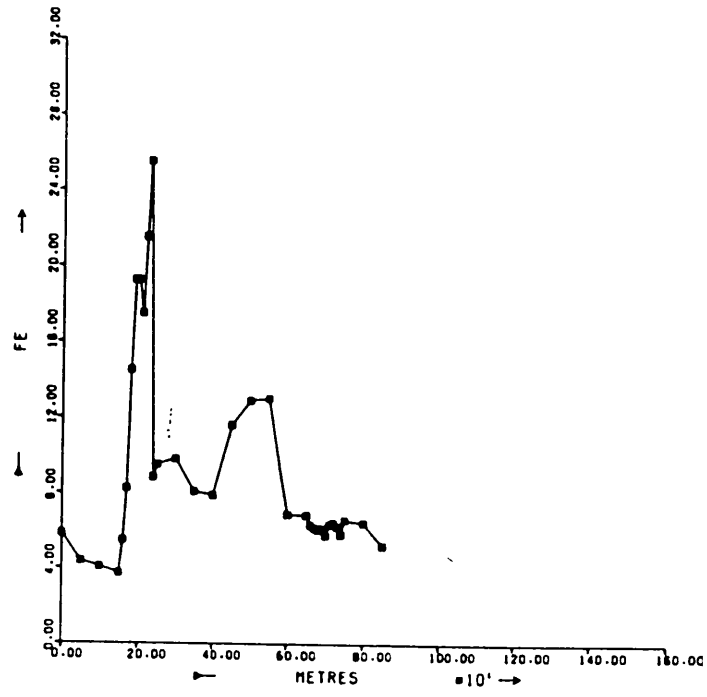
Figure 73: Munali, distribution of Ni (ppm) and Fe (%) along
soil traverse line (for geological legend see figure 9).
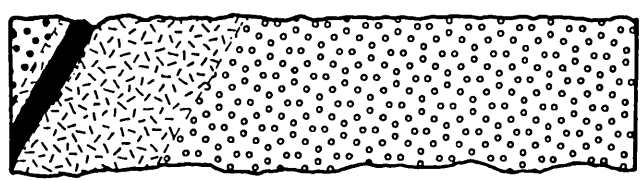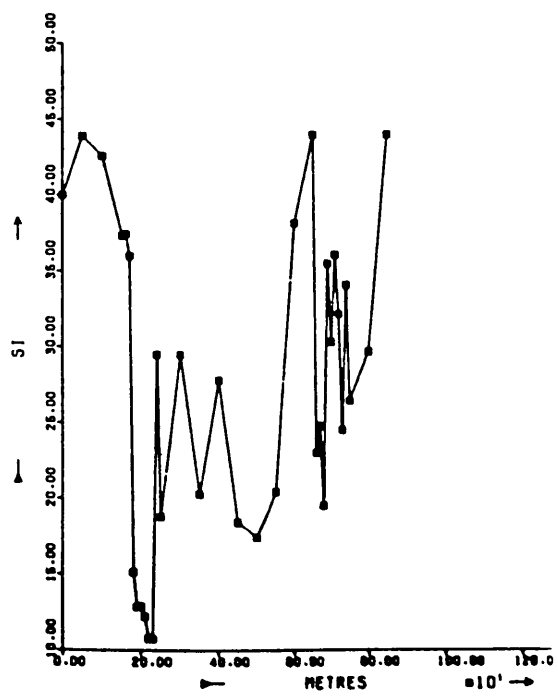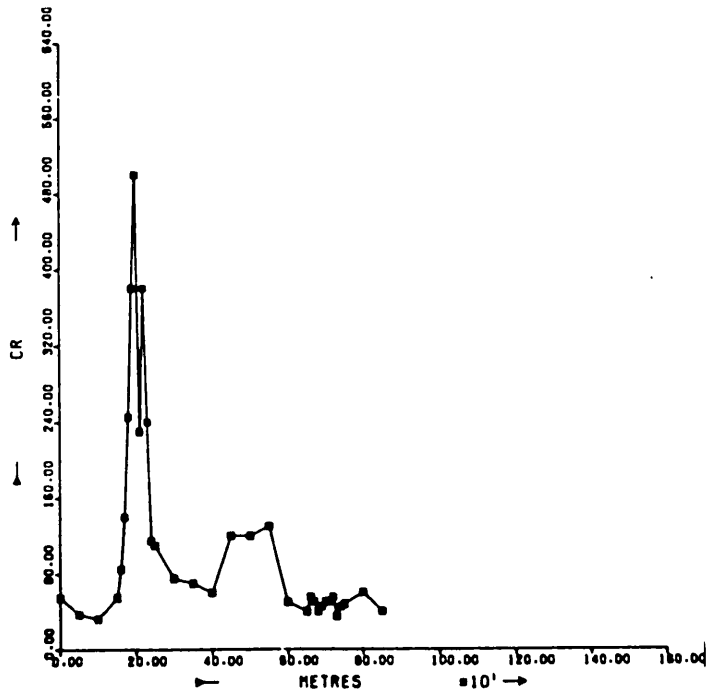
Figure 74: Munali, distribution of Si (%) and Cr (ppm) along
soil traverse line (for geological legend see figure 9).
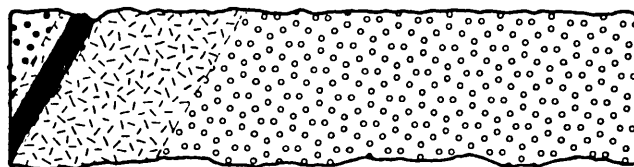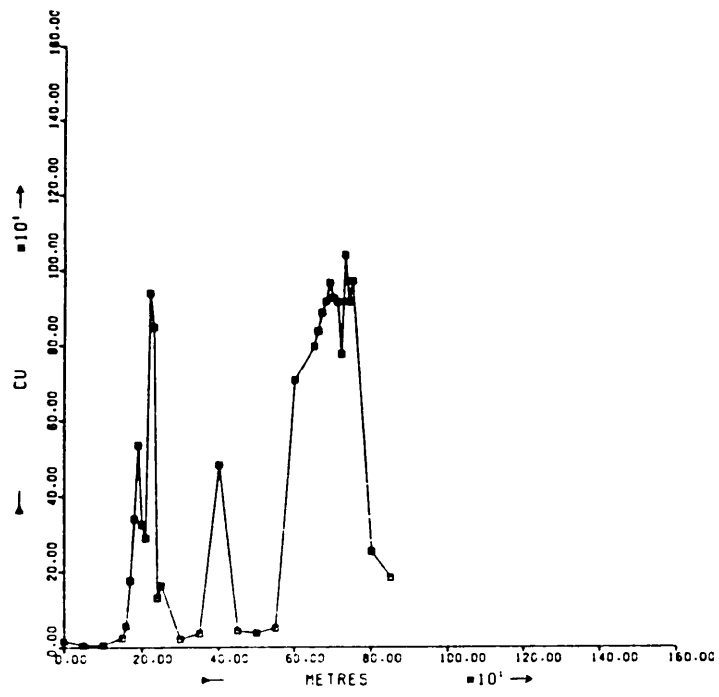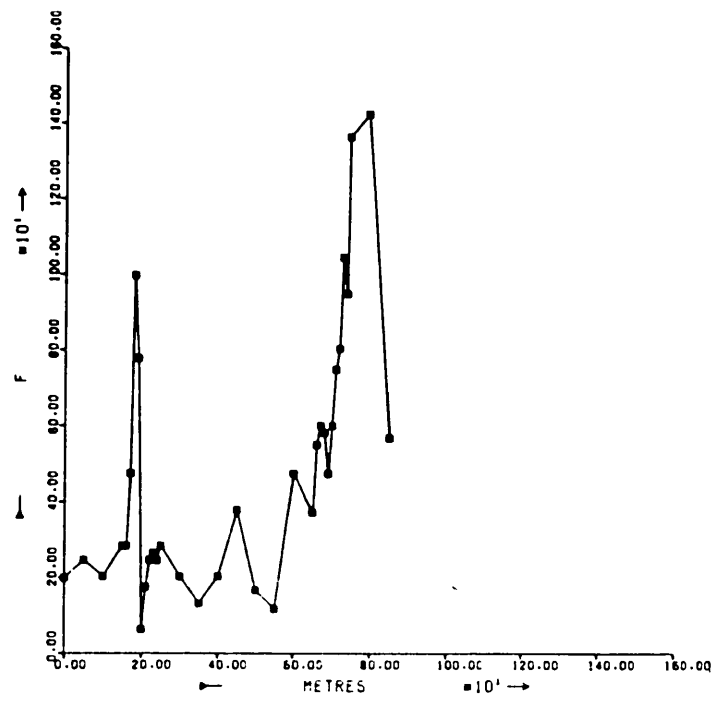
Figure 75: Munali, distribution of Cu (ppm) and F (ppm) along
soil traverse line (for geological legend see figure 9).

There is strong Fe enrichment in the mineralized
zone, evident in the ferruginous appearance of the soils as well
as values of up to 25.5% Fe, and there is a +0.89 correlation
between Ni and Fe (figure 73). Because of the high Fe content
of both parent mineralization and the soil of the anomalous zone,
other major elements are relatively impoverished at this point.
Thus Al values tend to be below the mean of 9.5% and Si levels
are much below the mean of 26.2%, falling to 10.8% in conjunction
with the highest Ni. Silicon and Ni show a clear negative correlation
of -0.65 (figure 74).

Chromium concentrations, though relatively low
throughout the traverse with a mean of 130 ppm, rise significantly
to a peak of 500 ppm in the mineralized zone, but since Ni values
are consistently greatly in excess of Cr, a lens of ultramafic
rock with nickel-rich silicates is not to be entertained as the
anomaly source (figure 74). Furthermore, the Ni anomaly should
be interpreted in the light of V concentrations across the mineralized
zone at least as high as the mean of 411 ppm for the traverse, thereby
indicating continuity of essentially gabbroic bedrock.

Over the intrusive there are mean Cu and F concentrations
of 205 ppm and 298 ppm respectively. Both elements exhibit strong
anomalies reaching 940 ppm Cu and 998 ppm F over mineralization
(figure 75). In conjunction with high Ni, this clearly indicates
the presence of sulphide ore of probable hydrothermal origin. However,
care must be exercised in Cu and F interpretation, since the soil
overlying schist to the northeast of the gabbro contains very high
concentrations of these two elements, but Ni values are very low.
An additional indication of hydrothermal activity associated with
the mineralized zone is given by elevated Ca, but even higher Ca occurs
elsewhere over the gabbro, probably because the intrusive was
emplaced into and largely assimilated a limestone formation. The
most important indication of mineralization is furnished by S data,
with excellent contrast between as much as 535 ppm S in the
mineralized zone compared with a background of less than 100 ppm
for the traverse (figure 76). There is a correlation of +0.81
between Ni and S.
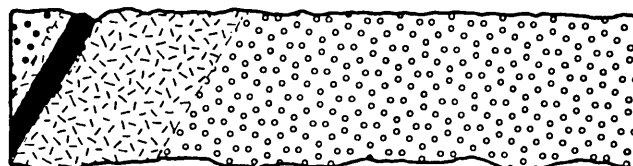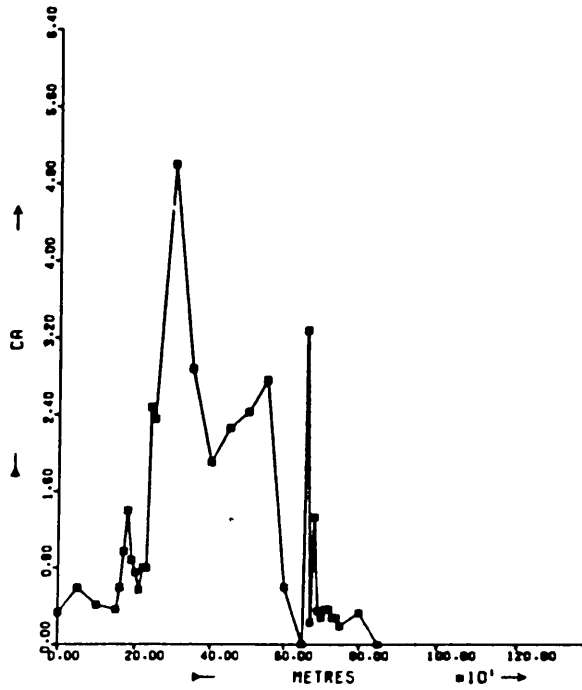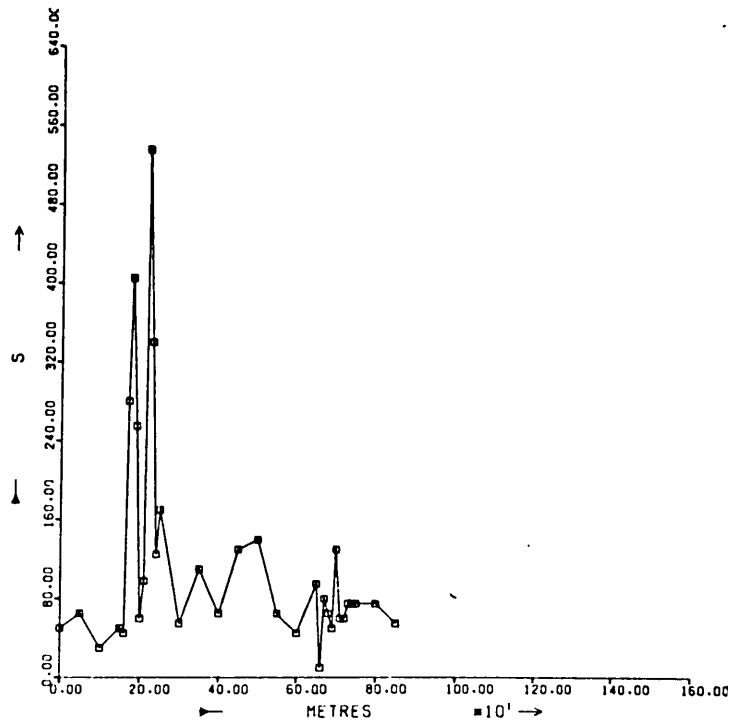
Figure 76: Munali, distribution of Ca (ppm) and S (ppm) along
soil traverse line (for geological legend see figure 9).
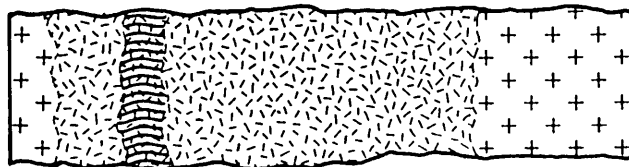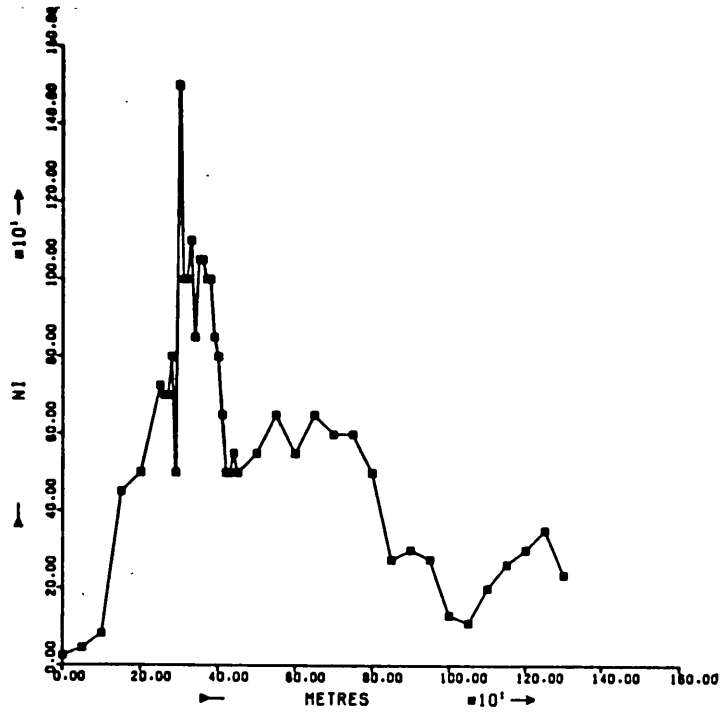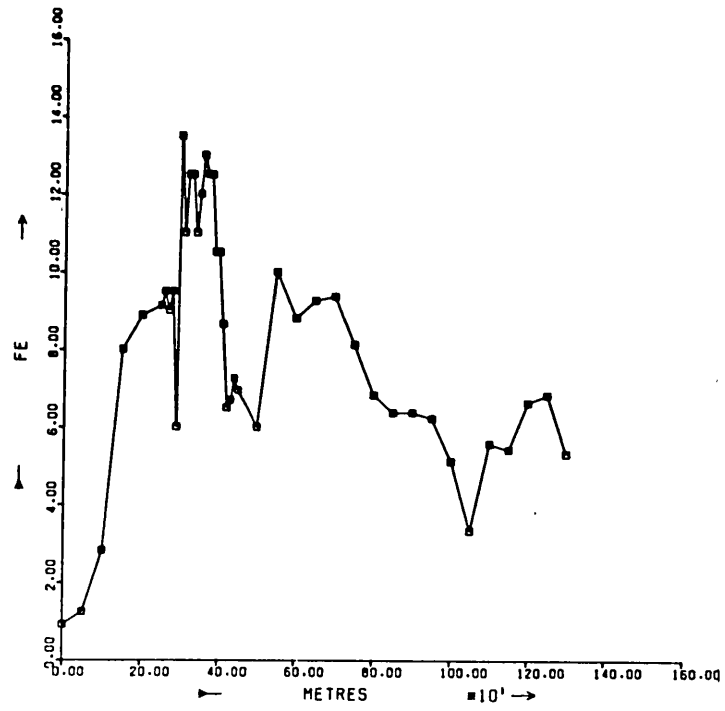
Figure 77: Musangashi, distribution of Ni (ppm) and Fe (%) along soil traverse line (for geological legend see figure 10).
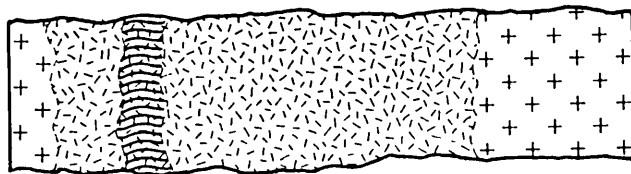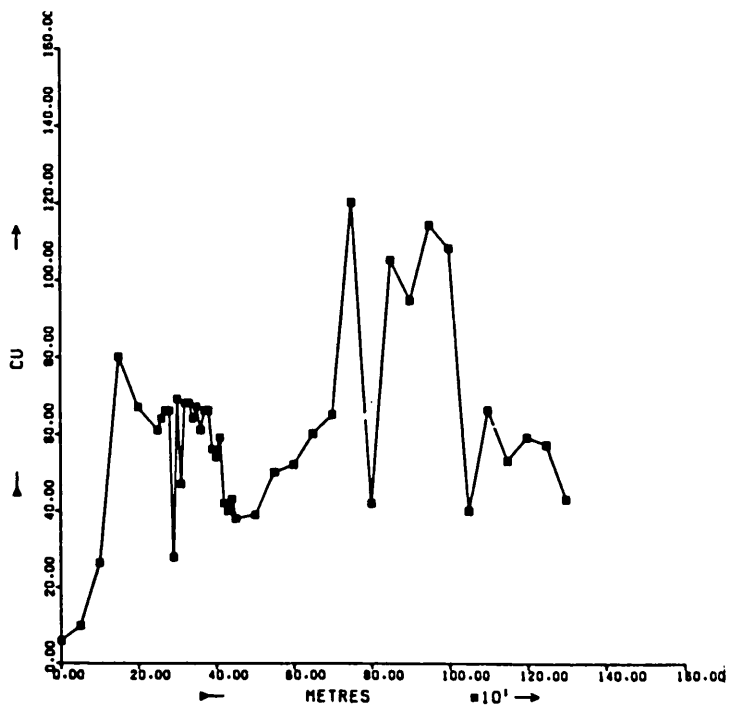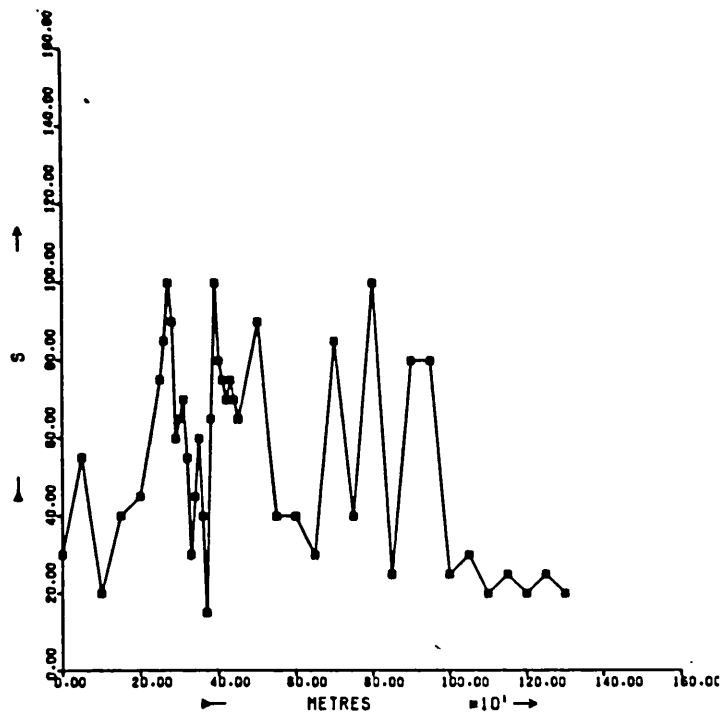
Figure 78: Musangashi, distribution of Cu (ppm) and S (ppm) along
soil traverse line (for geological legend see figure 10).

There are minor Zn and Mn anomalies reaching 40 ppm
Zn and 895 ppm Mn in the mineralized zone, but it seems unlikely
that secondary Mn oxides control trace element distribution in
any significant manner. Low Mg, averaging 2.8%, indicates
only mafic rock at depth, and a few higher Mg values correlate
with some elevated Ca and Li concentrations.

6.5.   Musangashi

The Musangashi traverse of 1300 m spans the full
width of the gabbroic intrusive, including the Ni soil anomaly
outlined during prospecting (sample nos. 635-01 to 635-43; figure 10).
For the traverse there is a mean of 581 ppm Ni and samples from
the anomalous zone contain up to 1500 ppm Ni (table 25).

The Fe content of the soil is relatively low,
averaging 8.1% and reaching a maximum of 13.5% in conjunction with
the highest Ni (figure 77). Iron and Ni are mutually correlated
by +0.95. Variation in Al concentration is apparently erratic in
the range 3.7% to 17.7%. Calcium, Mg and Li are generally strongly
leached from the soil, but in the vicinity of the Ni anomaly there
are some high values reaching 5.6% Ca, 12.9% Mg and 5210 ppm Li,
suggesting zones of alteration in the parent rock.

Those elements most relevant to anomaly interpretation
indicate the absence of mineralisation. There is a +0.63 correlation between
Ni and Cr, and Cr values are always substantially higher than Ni.
The mean Cu content of the soils along the traverse is 59 ppm, and
values close to the mean pertain in the anomalous zone, while up to
120 ppm Cu is found elsewhere. Similarly, S concentrations are low,
averaging 51 ppm and with erratic variation in the range 20 to 100 ppm
along the traverse (figure 78). There is no correlation between
Ni and Cu nor Ni and S.
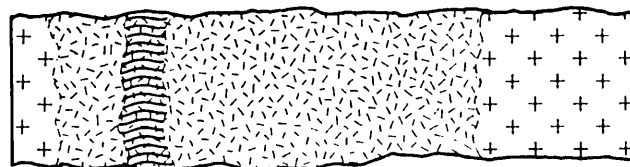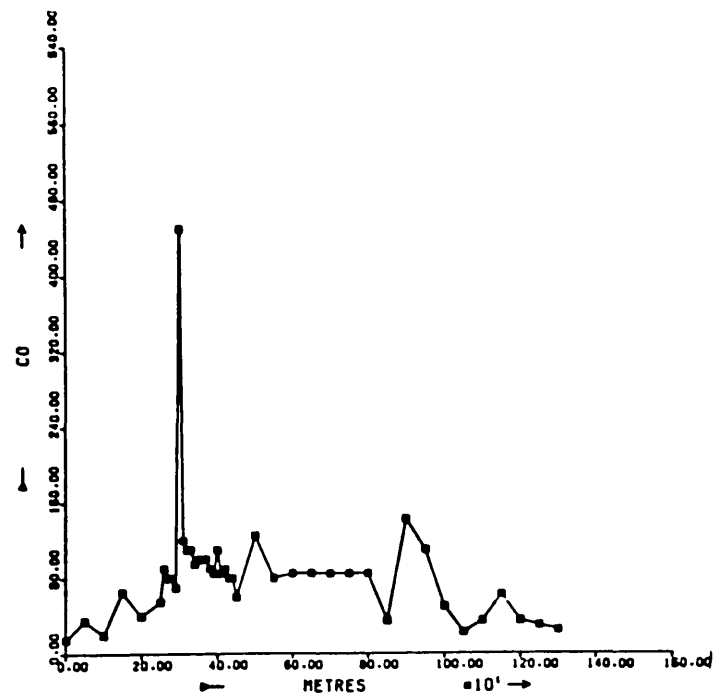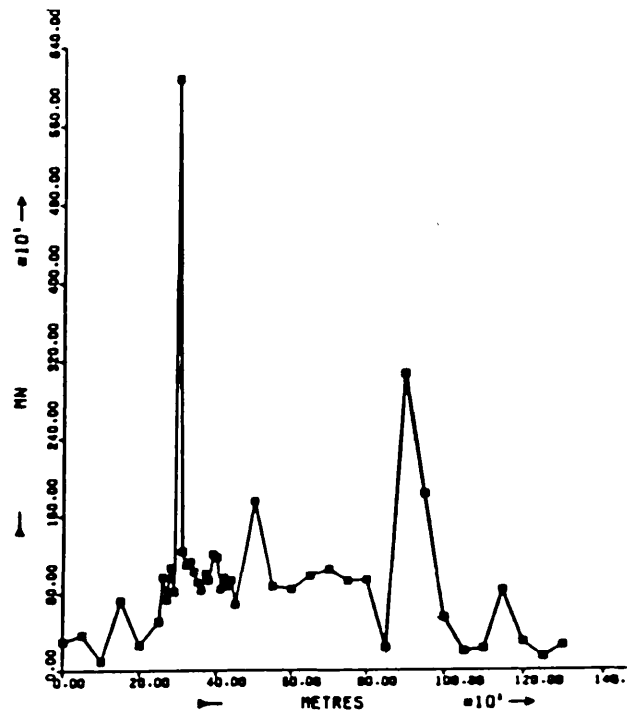
Figure 79: Musangashi, distribution of Co (ppm) and Mn (ppm) along
soil traverse line (for geological legend see figure 10).

Although Mn concentrations are not especially high
in Musangashi soils with a mean of 978 ppm, black coatings
presumed to be secondary Mn oxides were seen in the Musangashi
pit, and a value of 6100 ppm Mn occurs in conjunction with the
highest Ni result. There is little evidence that Ni distribution
is controlled by Mn, since the order of correlation between the
two elements is only +0.52, but Co appears to be closely associated
with Mn in the soil. Concentrations of Co range from 15 to 450 ppm
and there is a +0.96 correlation between Mn and Co (figure 79).
Zinc distribution, apparently related to Mn in other areas, is
independent at Musangashi.

6.6.   Paulwi

Paulwi soil samples were obtained from the AB
horizon of skeletal lithosols along a 600 m traverse within the
serpentinized peridotite including the zone of highest Ni
established by prospecting (sample nos. 345-01 to 345-41; figure
11). The traverse samples contain extremely high Ni concentrations
with a mean of 6030 ppm and a maximum of 8250 ppm (table 25).

The traverse is also characterized by extremely
high Fe in the range 13.5% to 21.5% and there is a clear correlation
of +0.70 between Ni and Fe (figure 80). This combination of
geological environment and closely correlated Ni and Fe distribution
suggests that Paulwi is showing the characteristics of nickel
laterite development. Among the other major elements, consistently
low Al averaging 3.5% and high Mg at 6.4% indicate an ultramafic
parent rock. The near-absence of alumino-silicate minerals in the
parent rock is further demonstrated by low mean Ti and V concentrations
of 851 ppm and 89 ppm respectively, while an abundance of olivine
and serpentinite is confirmed by a high Cr mean of 10,900 ppm.
Chromium values vastly in excess of Ni point to the absence of sulphide
mineralization, although additional information is required when
making interpretation in the face of such marked surface enrichment
of Ni and Cr. This is provided by Cu data, since concentrations
of Cu are exceptionally low compared with other areas, exhibiting a
mean of 22 ppm and a peak of only 60 ppm unrelated to the highest Ni.
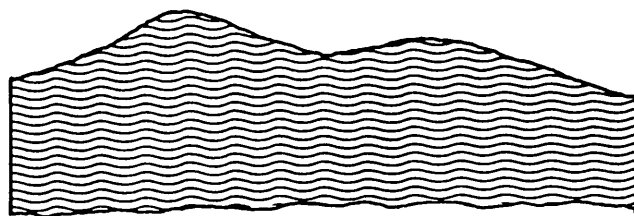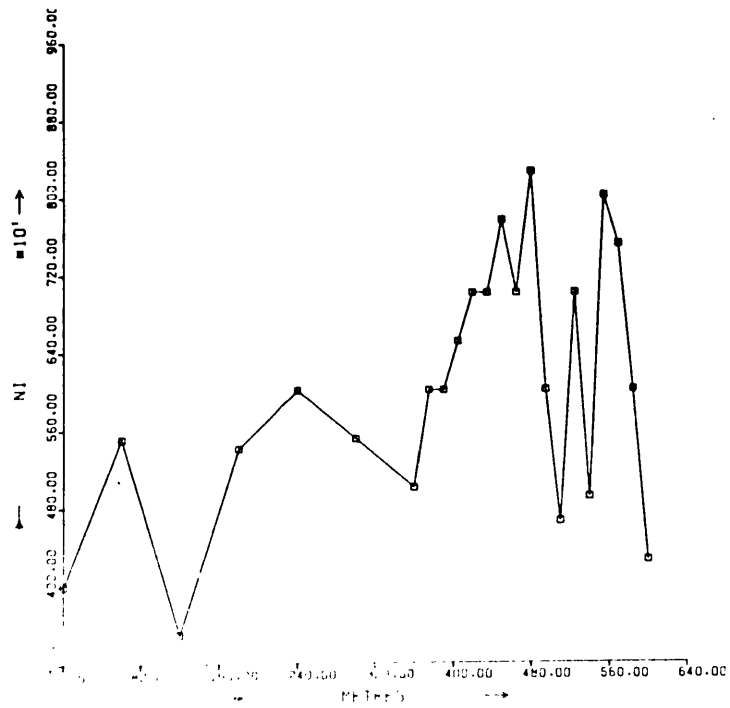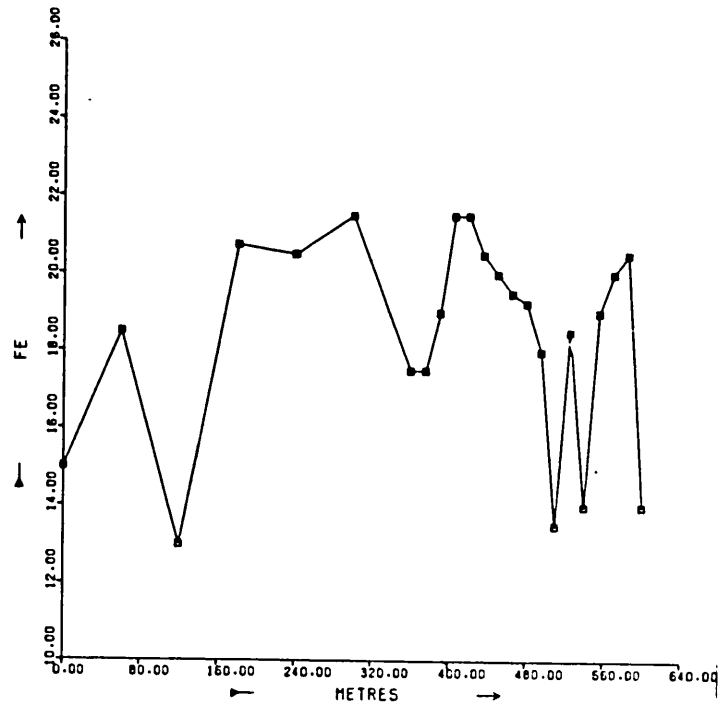
Figure 80: Paulwi, distribution of Ni (ppm) and Fe (%) along
soil traverse line (for geological legend see figure
11).
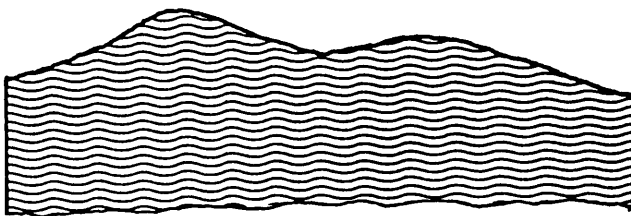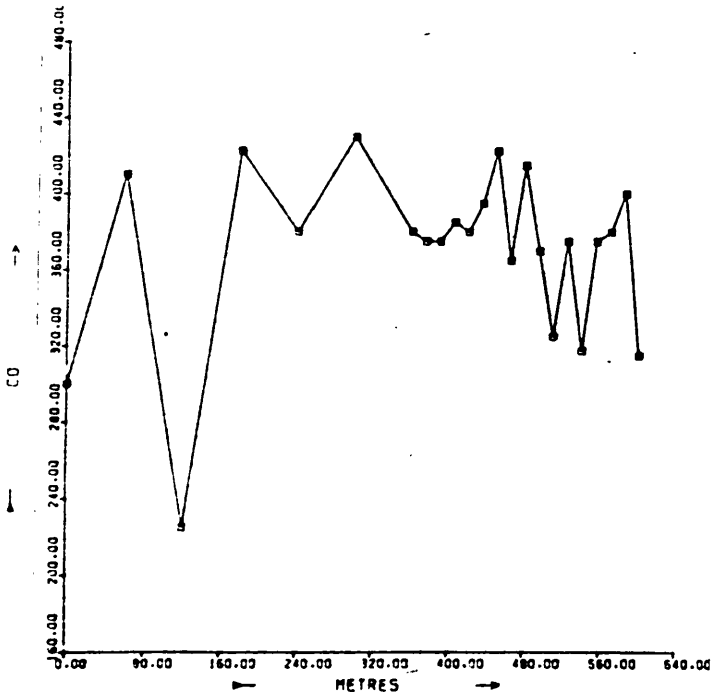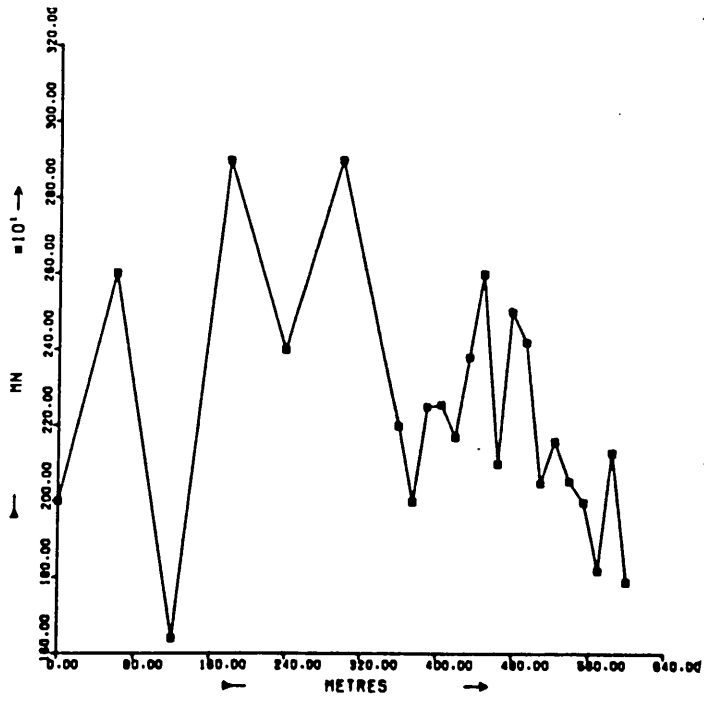
Figure 81: Paulwi, distribution of Co (ppm) and Mn (ppm) along
soil traverse line (for geological legend see figure
11).
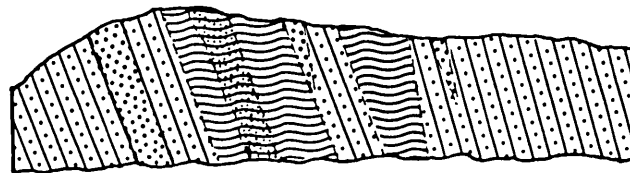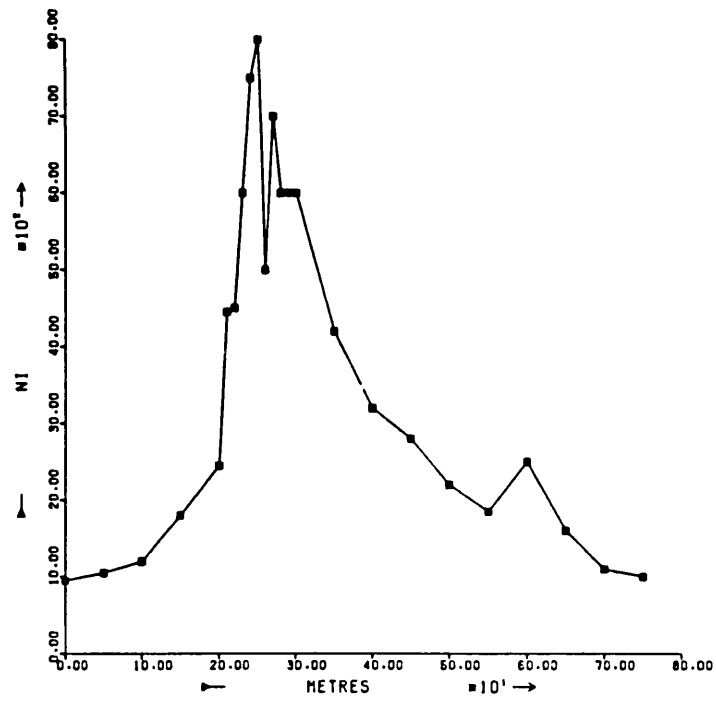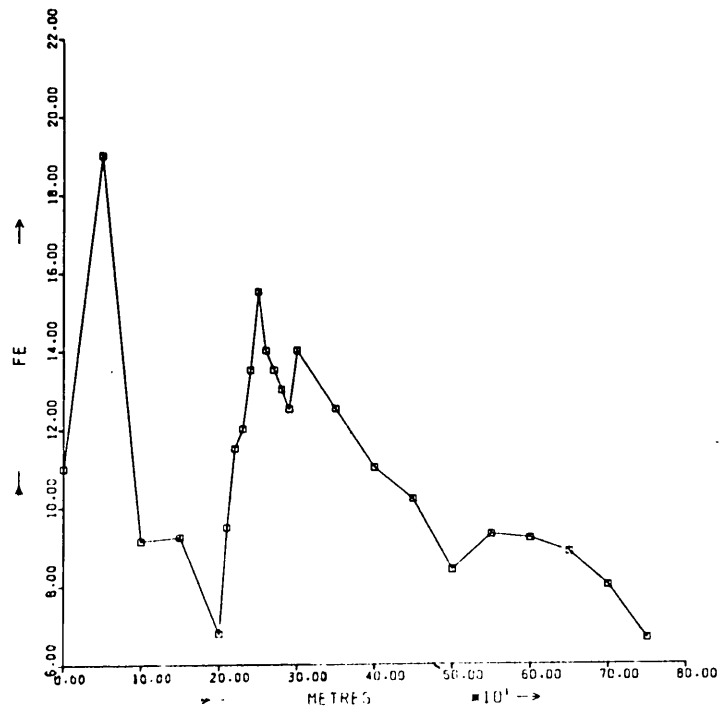
Figure 82: Trojan, distribution of Ni (ppm) and Fe (%) along
soil traverse line (for geological legend see figure
12).

The Paulwi traverse has unusually high Mn, with a
mean of 2230 ppm. The only trace element strongly correlated
with Mn is Co, by a coefficient of +0.78, and this is attributed
to the affinity of Co for secondary Mn oxides (figure 81). The
highest Co values, up to 430 ppm, are not associated with the
highest Ni. Thus it is evident from areas where there is very consid-
erable surface enrichment of metals in the soil that Ni and Co
become separated during secondary dispersion, and Ni tends to be
adsorbed by secondary Fe oxides while Co is adsorbed by secondary
Mn oxides. In view of this, Co cannot be regarded as a
convenient pathfinder element for primary mineralization.

6.7.   Trojan

Trojan is virtually the mineralized counterpart of
Paulwi. A traverse of 750 m was made across the full width of
the intrusive and mineralized zone at Trojan Hill, taking soil
samples in the AB horizon (sample nos. 835-01 to 835-24; figure 12).
Again Ni values in the traverse are very high, with a mean of 4050 ppm
and a maximum of 8000 ppm (table 25).

The soil over the intrusive contains a mean of 10.9% Fe,
and there is a correlation of +0.90 between Fe and Ni, with Fe values
reaching 15.5% in the mineralized zone (figure 82). Still higher
Fe concentrations of up to 19.0% occur over the pyritic argillite to
the north of the intrusive. The mean Al content of the soil is
fairly low at 6.7% while the Mg level is high at 5.1%. The relative
concentrations of these two elements reflects the general composition
of the underlying ultramafic rock. Low Ca, averaging 1.3%, and low Li,
19 ppm, are persistent throughout the traverse, and some unusually
low Mg results, accompanied by lower than typical Ca and Li, occur
in the mineralized zone (figure 83). High Cr, with a mean of 1970 ppm
over the intrusive and low Ti and V, with means of 904 ppm and 103 ppm
respectively, further reflect the ultramafic parent rock. There is
no significant increase of Cr over the Ni anomaly, and, in contrast
to Paulwi, Ni values are greatly in excess of Cr, thereby suggesting
the presence of mineralization (figure 84).
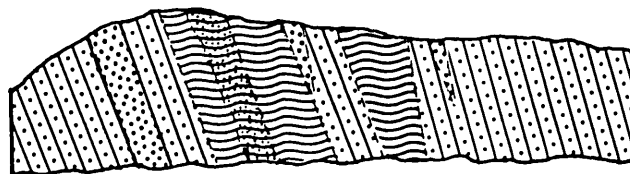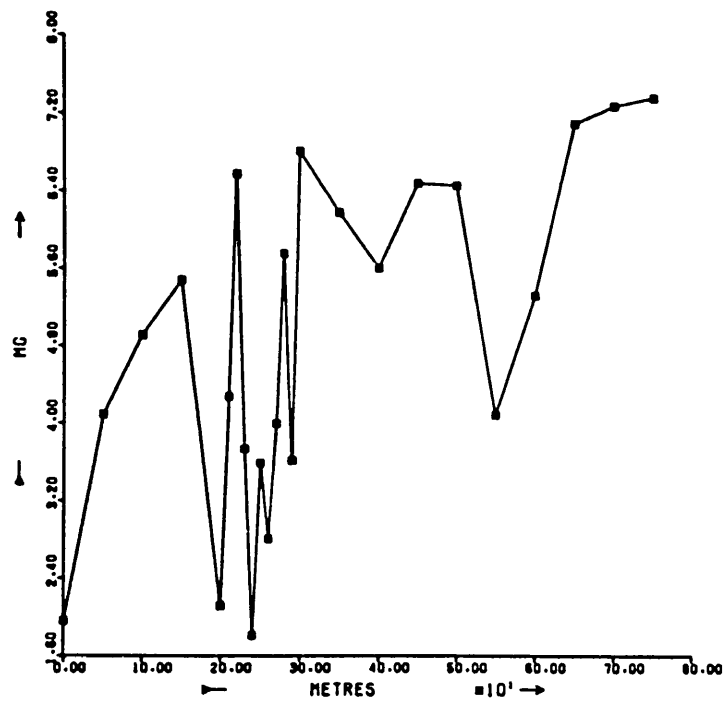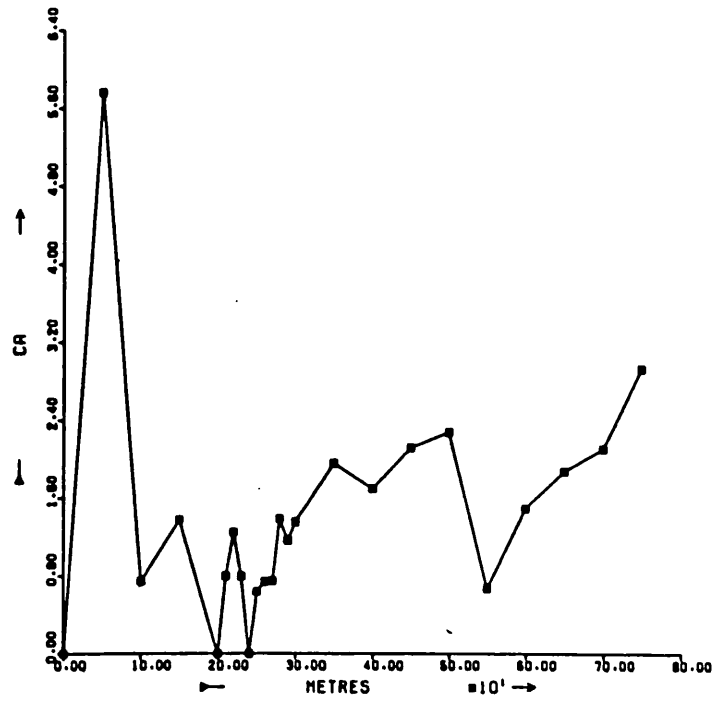
Figure 83: Trojan, distribution of Mg (%) and Ca (%) along
soil traverse line (for geological legend see
figure 12).
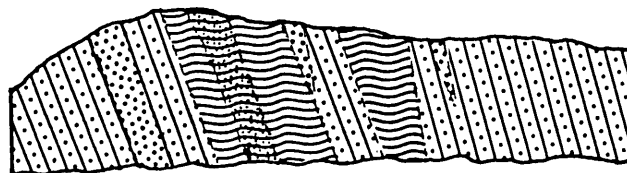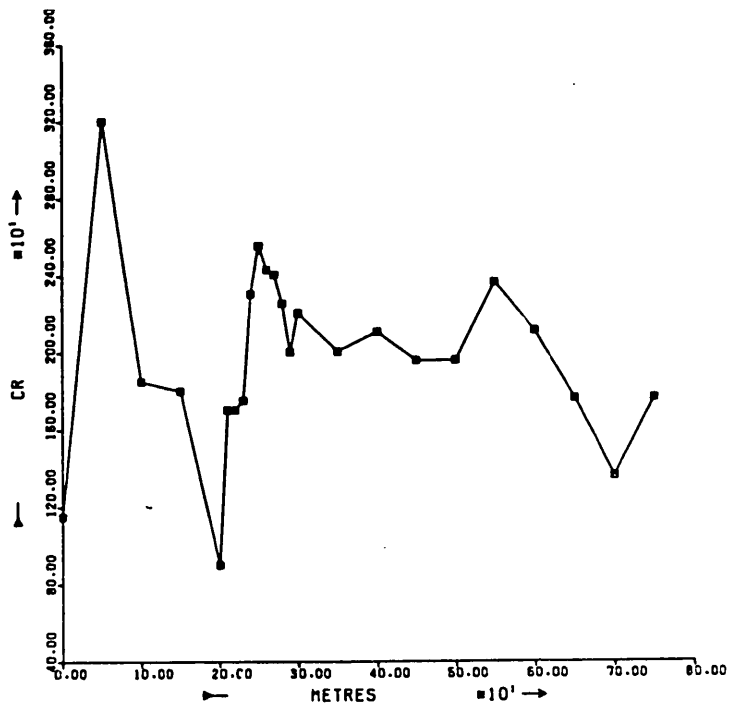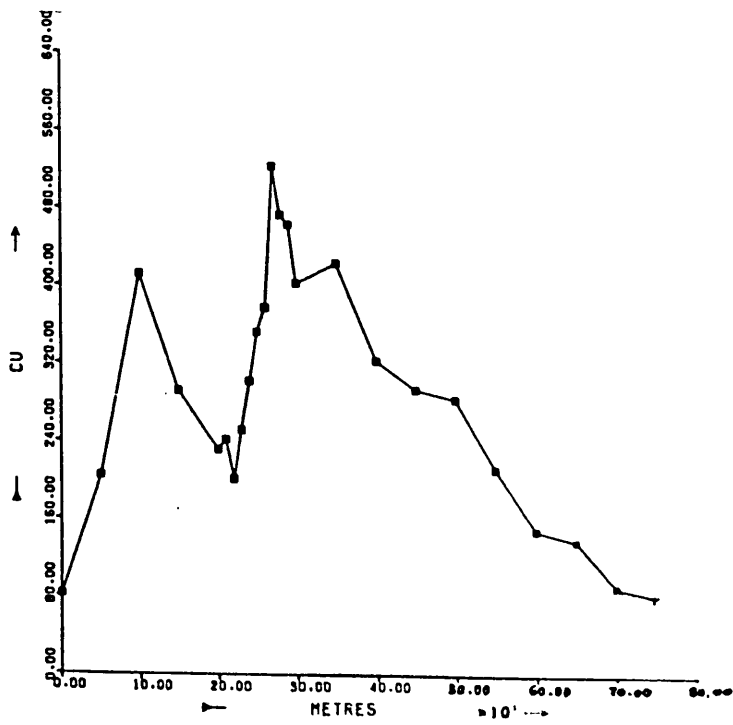
Figure 84: Trojan, distribution of Cr (ppm) and Cu (ppm) along soil traverse line (for geological legend see figure 12).
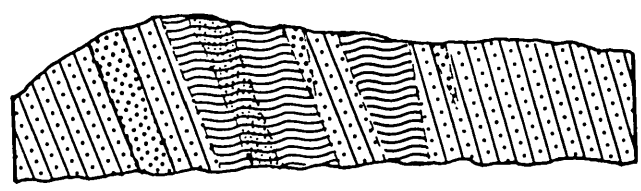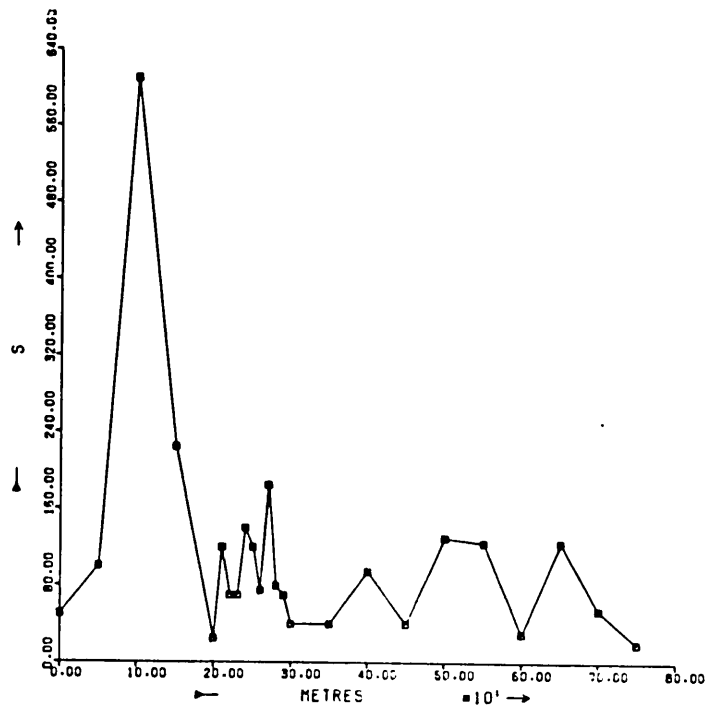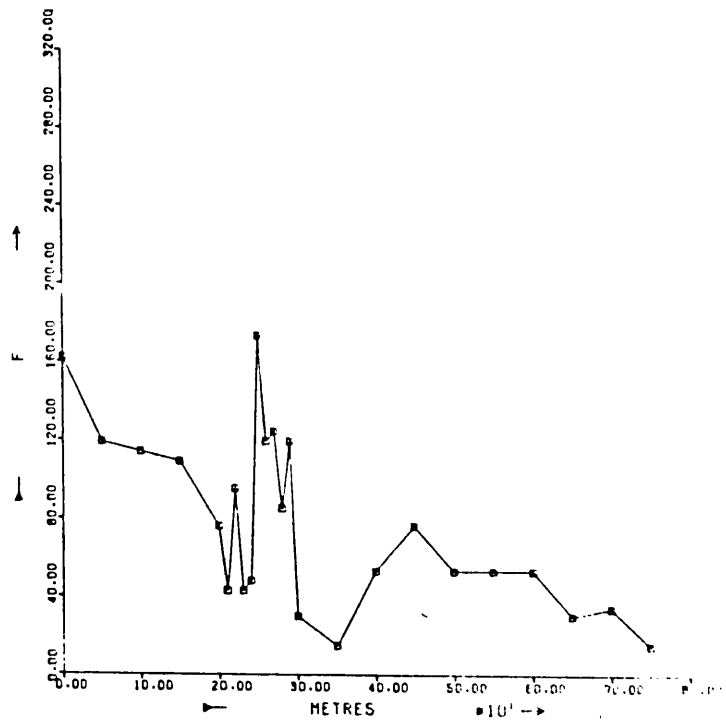
Figure 85: Trojan, distribution of S (ppm) and F (ppm) along
soil traverse line (for geological legend see figure
12).

A further guide to mineralization in the soil is a Cu anomaly in conjunction with the highest Ni. The maximum Cu value is 520 ppm, and there is a +0.72 correlation between Ni and Cu (figure 84). The mean S content of the soils overlying the intrusive is 90 ppm, and only slightly anomalous S values of up to 185 ppm occur in the mineralized zone. This is attributed to the relatively low Fe content of the soil (compared, for example, with the mineralized zone at Munali) which is probably due to the rugged terrain and absence of a true B horizon. The soil has a low F mean of 69 ppm, and generally higher F concentrations, up to 173 ppm, are found in the mineralized zone (figure 85). Since the Trojan ore is disseminated, this is not taken as an indication of hydrothermal activity, but the F may be traced to the graphitic argillite host rock, found to contain 493 ppm F, and a probable source of S for the intrusive. The soil over the graphitic argillite to the north of the intrusive contains up to 610 ppm S and 162 ppm F.

Manganese concentrations vary from 390 to 2000 ppm, and Fe and Mn are correlated by a coefficient of +0.76. Thus there is little evidence to indicate accumulation of any trace elements to be controlled by secondary Mn rather than secondary Fe oxides. The best guides to mineralization in the Trojan soils are therefore very high Ni values in conjunction with lower Cr and high Cu, while low order S and F anomalies can be regarded as positive supporting criteria. In areas such as Trojan,where leaching is not pronounced in the lower AB horizon, Mg may also constitute a useful variable, since a negative Mg anomaly suggests some replacement of ultramafic bedrock, in this case by mineralization.

6.8.   Kingston

At Kingston, the soil traverse spans the full width of the peridotite including the Ni anomaly defined during prospecting (sample nos. 845-01 to 845-25; figure 13). Along the traverse, the highest Ni concentrations encountered in any of the field areas are found, reaching 12,500 ppm (table 25).
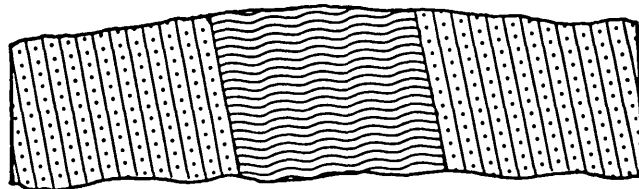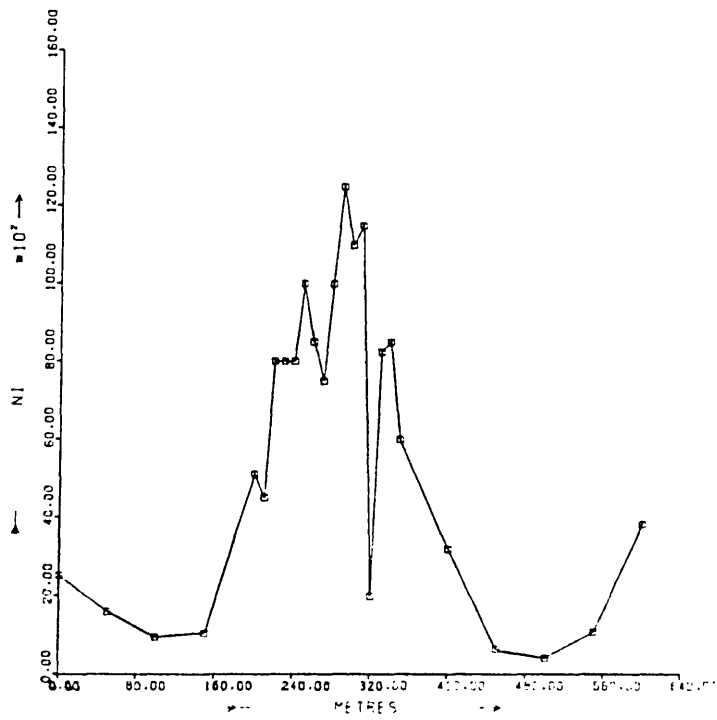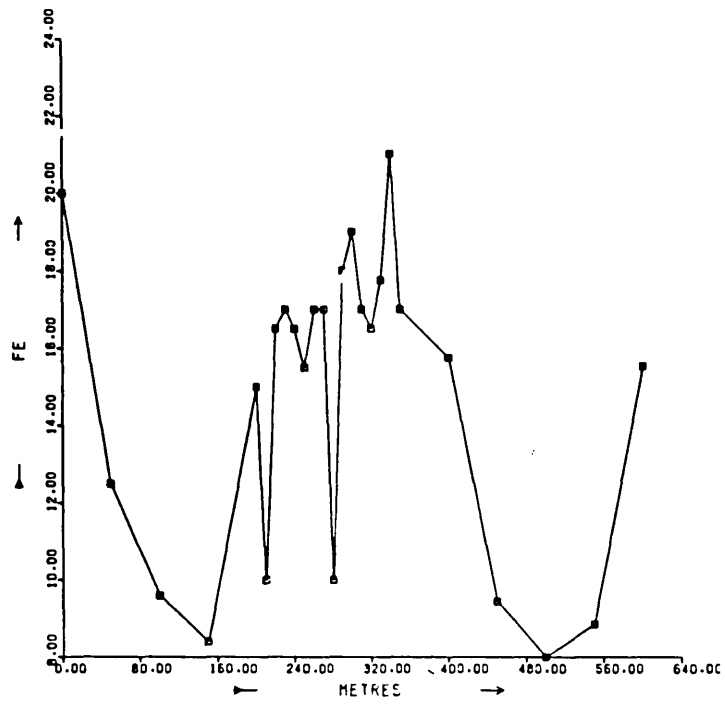
Figure 86: Kingston, distribution of Ni (ppm) and Fe (%) along
soil traverse line (for geological legend see figure
13).

High Fe in the Kingston soil, comparable with that seen at Paulwi, is probably responsible for the fixation of Ni. There is a mean Fe concentration of 14.8% and a peak value of 21.0% in conjunction with the Ni anomaly (figure 86). The correlation between Ni and Fe is +0.61. Although the Al mean for the traverse is 5.2%, higher values up to 15.7% occur over the amphibolite beyond the margins of the intrusive, and low Al, around 2%, characterizes the ultramafic intrusive. Titanium and V levels are also low, and there is a +0.86 correlation between Al and Ti. Magnesium exhibits an antipathetic distribution against Al, with up to 7.3% Mg retained in the lower AB horizon of the immature soil over the anomalous zone, and less than 4% Mg over amphibolite. Thus Al and Mg have a -0.57 correlation. Chromium distribution is similar to Mg, and the two are linked by a +0.59 correlation. However, Ni concentrations are greatly in excess of Cr, in spite of a Cr anomaly reaching 5200 ppm in conjunction with the Ni anomaly, and this indicates mineralization at depth. The guide provided by Cu also affirms the presence of mineralization, with a maximum of 1020 ppm Cu accompanying the Ni anomaly (figure 87).

However, there is no S anomaly, and S concentrations in the soil are relatively low, in the range of 15 to 75 ppm. Although one high S value occurs in the Ni anomaly zone, most samples there contain close to the mean of 46 ppm S. There is a low F mean of 72 ppm for the traverse, and since one unusually high result of 570 ppm occurs over the amphibolite, the F level over the ultramafic rock is generally below this mean (figure 88). The absence of both S and F anomalies is taken to show the absence of mineralization and hydrothermal alteration at Kingston.

Most Mn values are around the mean of 1500 ppm, and there is no evidence that Mn distribution controls other trace elements.

Perhaps not unexpectedly, the Kingston data proves the most ambiguous to interpret, because diamond drilling there has established weakly disseminated mineralization of no economic worth.
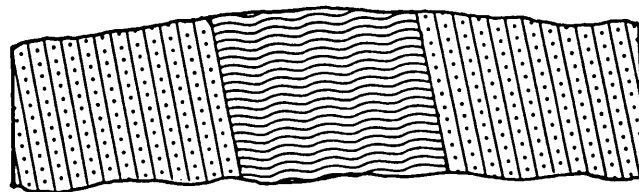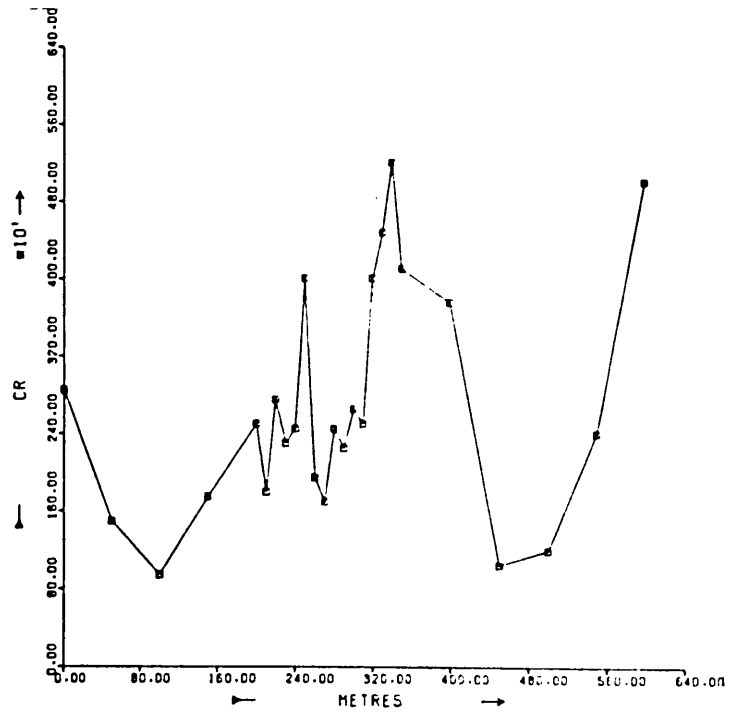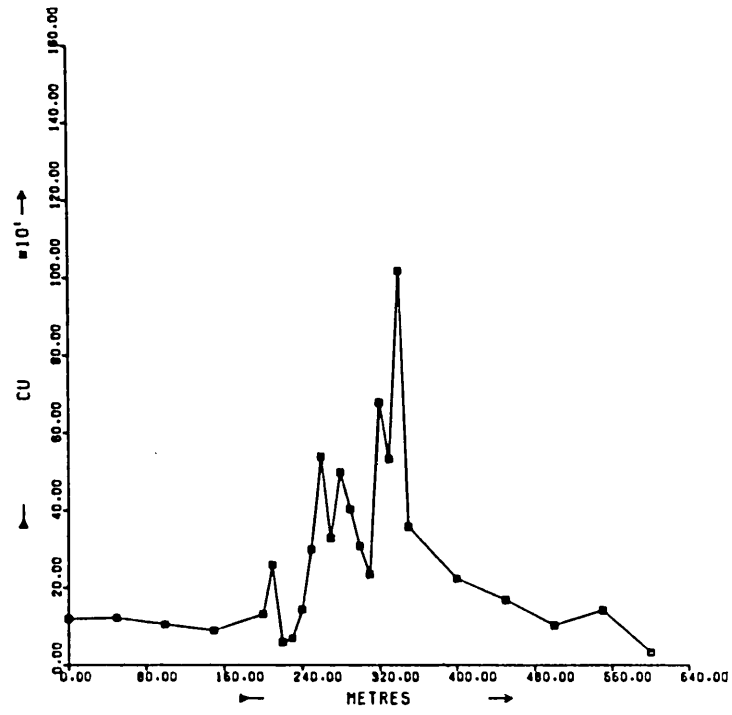
Figure 87: Kingston, distribution of Cr (ppm) and Cu (ppm) along
soil traverse line (for geological legend see figure
13).

The presence of mineralization is reflected by coincident Ni
and Cu anomalies and Ni levels in excess of Cr. Probably the
absence of a S anomaly, especially in the light of high Fe
which would be expected to adsorb S, is a sound guide to the
low grade of any sulphides. Persistent low F suggests
ultramafic bedrock over the full width of the intrusive,
while high Mg and Cr in the anomalous zone may reflect a zone
of shearing or alteration.

6.9.   The general behaviour of other elements

Other elements determined and examined along
soil traverses prove to be of little relevance in deducing
the mineralization potential of Ni anomalies. For the most
part Ca, Sr, Li and to a lesser extent Be are leached from the
soils, and such high values as do occur tend to correlate with
high Mg. Potassium and Ba are found in relatively low concentrations
in the predominantly non-feldspathic parent rocks, and also in the
overlying soil. Thus there are low mean concentrations of these
elements in the soils ranging from 0.8% Ca at Chitina to 1.9% Ca
at King Edward, 35 ppm Sr at Trojan to 217 ppm Sr at Kingston,
0.9% K at Chitina and Trojan to 1.3% K at King Edward, Munali and
Paulwi, 120 ppm Ba at Chombwa to 233 ppm Ba at Munali, 19 ppm Li
at Trojan to 598 ppm Li at Munali and Be concentrations usually
range from less than 1 ppm to 3ppm. Scandium and Ga are both closely
correlated with Al, Ti and V, and mean concentrations of these
elements along traverses vary from 11 ppm Sc at King Edward, Paulwi
and Trojan to 21 ppm Sc at Chombwa, and 9 ppm Ga at Paulwi to 26 ppm
Ga at Chombwa. Concentrations of around 10 ppm Pb and 10 ppm Sn are
typical of most samples. The pH of the soils ranges from 4.2 to 6.9.
The lower pH values are found in glei soil as at Musangashi, and
the higher pH levels occur in immature soils at Trojan and Kingston.
However, the range of pH encountered in soils has apparently little
bearing on the major or trace element content, except that the less
leached, immature soils with a higher Ca and Mg content have a more
alkaline pH.
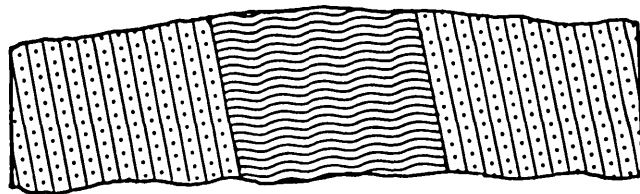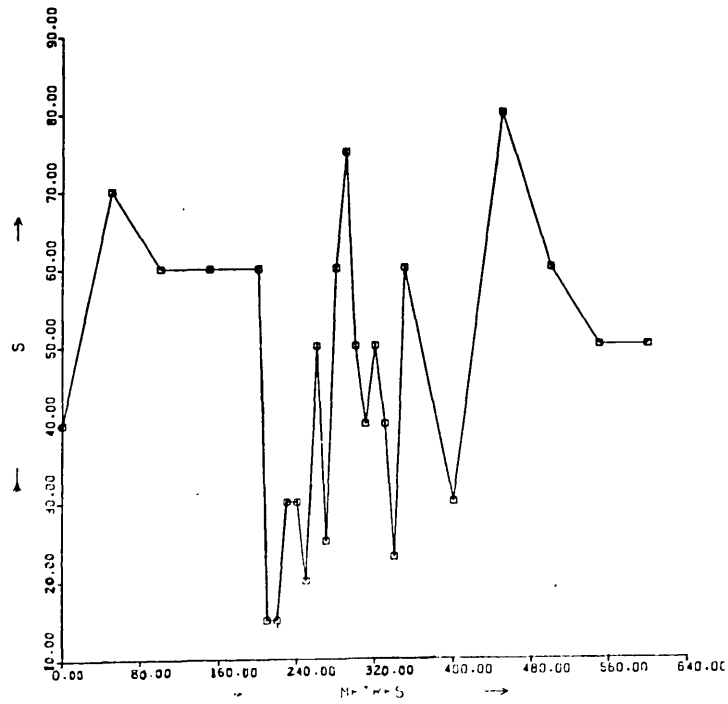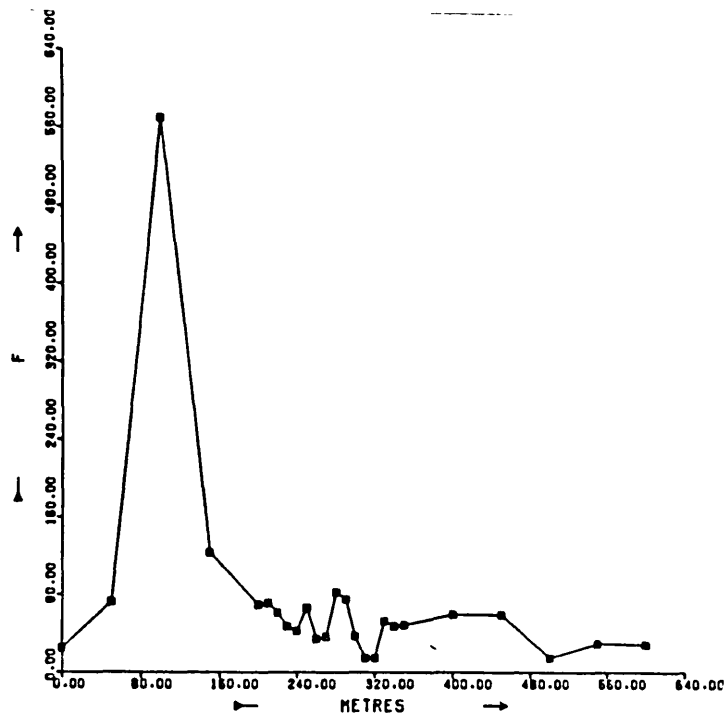
Figure 88: Kingston, distribution of S (ppm) and F (ppm) along
            soil traverse line (for geological legend see figure
            13).

6.10.   The significance of multi-element behaviour

As noted from vertical pit profiles, B soil horizon
Ni concentrations usually provide a fair reflection of the Ni
content of the underlying parent material. The soil content of
some other elements can contribute to identifying the nature of
the parent material, and thus an anomalous Ni zone in a soil
traverse may be accompanied by positively or negatively anomalous
levels of other elements according to the origin of the Ni anomaly.

The primary relationship between Ni and Fe is
largely preserved during chemical dispersion. In the secondary
environment, as in the primary environment, Ni behaves in a
siderophile manner, and secondary Fe oxides in the soil, such as
goethite, are mainly responsible for the fixation of Ni. The level
of Fe in the soil is largely controlled by the amount of Fe in the
underlying parent material. High Fe concentration in the soil (and
rock) sometimes results in a relative impoverishment of Si, which
may be expressed as a negative Si anomaly.

Secondary Mn oxides, on the other hand, appear to
play no part in the fixation of Ni in the soil. In some areas
where rather higher than usual Mn concentrations occur in the soil,
Co, Cu and Zn values are also elevated, and this correlation
between Mn and these trace elements is believed to demonstrate
selective trace element adsorption by secondary Mn oxides. Along
most traverses, however, Co is closely related to Ni while Zn and
Cu exhibit an independent distribution. In the primary environment
Cu is strongly chalcophile and accumulates in sulphide minerals,
and therefore Cu soil anomalies over mafic and ultramafic rocks can
usually be attribed to mineralization. There are strong Cu anomalies
in soils of the mineralized zones at Munali and Trojan, and the
great affinity of Cu for sulphides produces a Cu anomaly even over
weakly disseminated mineralization at Kingston. Conversely, Cr,
which is predominantly lithophile in the primary environment, attains
anomalous concentrations in the soil over ultramafic rocks, which
can contain both high Ni and Cr. These characteristics of Ni, Cu,
Cr and Mn have been used to distinguish mineralized gossans from
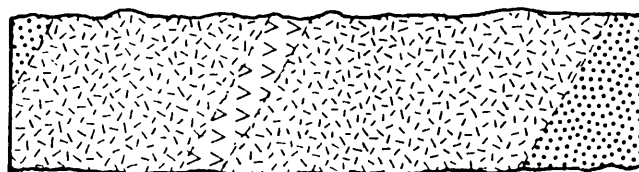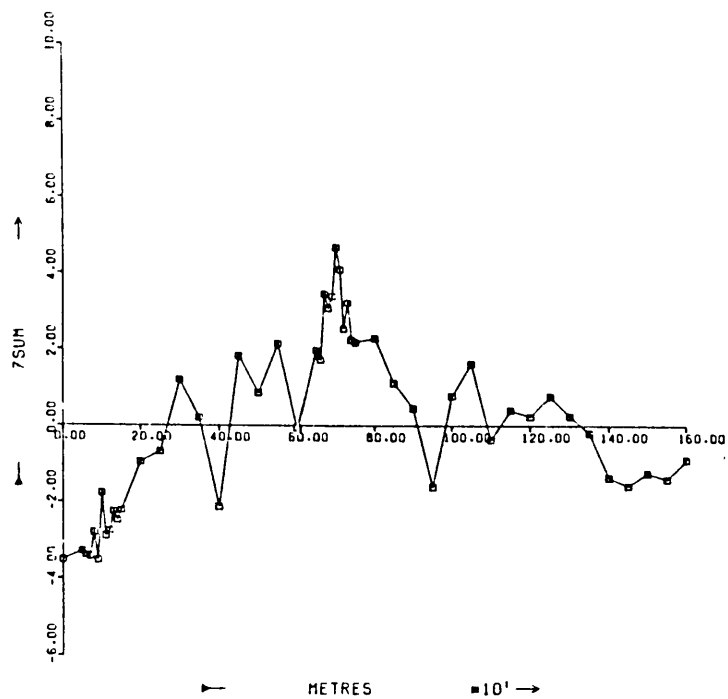
Figure 89: Chitina, Zsums along soil traverse line (for geological legend see figure 6).

laterite, chert and other ironstone outcrops in Australia, by
token of the relatively high Ni and Cu, low Cr and Mn in the
gossans (Clema and Stevens-Hoare, 1973).

The most chalcophile element is S, and the S
content of the soil adequately reflects that of the parent rock,
although S retention in the soil is probably controlled by
secondary Fe oxides, and therefore S concentrations may be in
part related to soil Fe content (Stumm and Morgan, 1962). Sulphur
anomalies in conjunction with Ni (and Fe) anomalies are found
at Munali and Trojan reflecting massive and disseminated
mineralization at depth, but high S in the Chombwa soil and
coincident Ni and S anomalies occur over non-mineralized peridotite.

The mean F content of the soil is comparatively
high over predominantly mafic rocks, for example 257 ppm at Chombwa
and 298 ppm at Munali, and low over ultramafic rocks such as 69 ppm
at Trojan and 72 ppm at Kingston. Thus a negative F anomaly is to
be expected over lenses of more ultramafic rock within a mafic
intrusive and this feature is seen in conjunction with the Ni soil
anomaly at Chombwa. Over hydrothermal mineralization, on the other
hand, F concentrations increase to produce a positive F anomaly,
with maximum of 998 ppm at Munali.

Of other elements potentially useful in distinguishing
lenses of ultramafic rock, low primary levels of Al and Ti are
masked by a general enrichment of these elements, especially Al,
in the soil, but low V is a fairly persistent criterion. Although
Mg is often readily leached from the soil, where retained it can
produce a positive anomaly in conjunction with high Ni over an
ultramafic unit, as at Kingston.
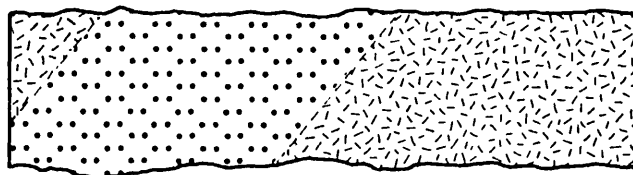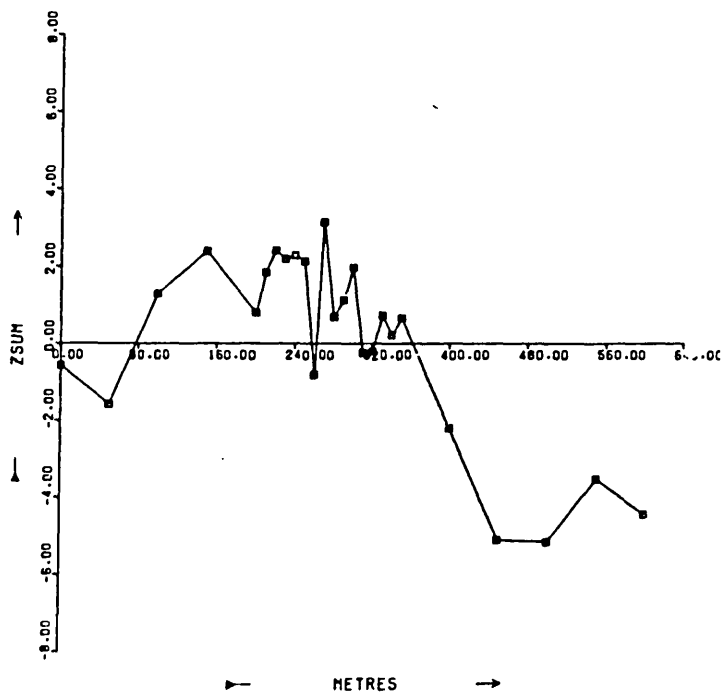
Figure 90: Chombwa, Zsums along soil traverse line (for geological legend see figure 7).

Thus Ni soil anomalies can best be intrepreted by considering not one supplementary variable, such as Cu, but by scrutinizing four or even five relevant variables, namely Cu, S, F, Cr and possibly Mg, and their behaviour in conjunction with Ni in soils. The relative merits of these variables were assessed by sequential backwards regression using the program BAKWRD. Two training sets, comprising soils from mineralized zones and soils from anomalous Ni zones not overlying mineralization, were compiled. The mineralized set was made up of 9 samples from the mineralized zone of the Munali traverse (sample nos. 135-06 to 135-14) and 11 samples from the mineralized zone of the Trojan traverse (sample nos. 835-06 to 835-16) plus a further 11 samples collected over other parts of the suboutcrop of the Trojan Hill orebody (sample nos. 835-85 to 835-95), a total of 31 samples. The non-mineralized set comprised 17 samples from the anomalous zone at Chombwa (sample nos. 245-04 to 245-20) and 16 samples from the anomalous zone at Kingston (sample nos. 845-05 to 845-20), a total of 33 samples. In the sequential backwards regression the variables Ni, Cu, Cr, S and F were used, and Mg was excluded because any discrimination rendered by this variable was confined to areas of limited soil leaching. In fact the training sets incorporated the most exceptional features of distribution of the five elements, including high S values in the non-mineralized Chombwa samples, high Cu in the weakly or non-mineralized Kingston samples, low S in the mineralized Trojan samples, and mainly low F at Kingston and Trojan compared with Chombwa and Munali. The data were tested in arithmetic mode with smoothing factors of 5, 10 and 15 and in log-transformed mode with a smoothing factor of 0.08.

The most conspicuous feature of the sequential backwards regression results is that the combination of all five variables initially tested gives a high level of discrimination between the two groups, ranging from 85.9% for log-transformed data to 92.3% for arithmetic data with a smoothing factor of 5.
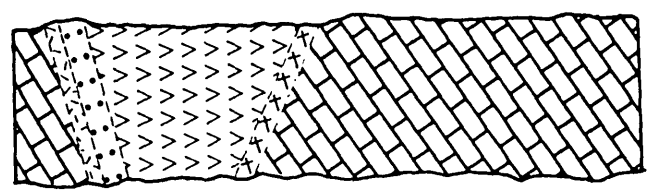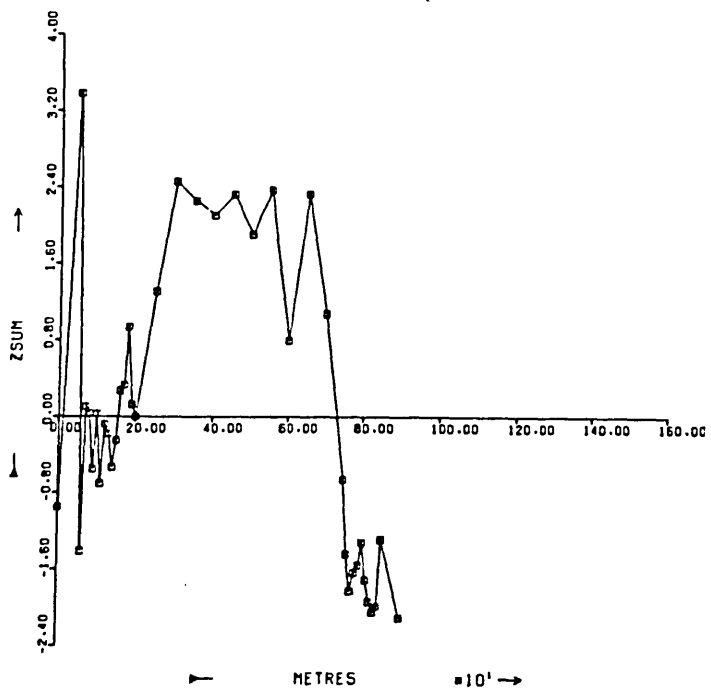
Figure 91:   King Edward, Zsums along soil traverse line (for
             geological legend see figure 8).

Subsequent regressions reveal that the highest level of
discrimination is 92.2% for log-transformed data using the
Ni, Cu and S variables, or 94.1% using arithmetic data with
a smoothing factor of 5, when the optimum combination is
Ni, Cu, Cr and F. Therefore the evaluation of all five
variables, plus Mg, seems the most desirable for distinguishing
between Ni soil anomalies reflecting mineralization and those
of other origins.

6.11. Summed standard normal deviates

A technique was devised for the appraisal of
multi-variate anomalies whereby the standard normal deviates
of elements of interest in each sample of a traverse are
totalled, and the summed standard normal deviates thereby
furnish a univariate guide to multi-variate behaviour.

6.11.1. Traverse line patterns

Standard normal deviates of elements were computed
for each traverse using a program GESTAT (Garrett, 1967).
These were then processed by a program SUMSND, in which options
could be excercised to add, take no action on, or subtract each
one of up to 14 standard normal deviates for each sample in the
traverse. Since the mean standard deviation for each element
in a traverse is zero, the mean of the summed standard normal
deviates is also zero. However, in the samples of a mineralized
zone the enriched elements (such as Cu, S, F) have positive
standard normal deviates and these, when added, produce high
summed standard normal deviates. Conversely, when the same
elements are not enriched or are depleted in an anomalous
zone not related to mineralization they have zero or negative
standard normal deviates and these, when added, do not produce
high summed standard normal deviates. By the same token, elements
which are enriched in anomalous zones (such as Mg at Kingston)
have positive standard normal deviates which can be subtracted
to reduce the summed standard normal deviate. When the same
elements are not enriched or are depleted in a mineralized zone
(as at Trojan) they have zero or negative standard normal
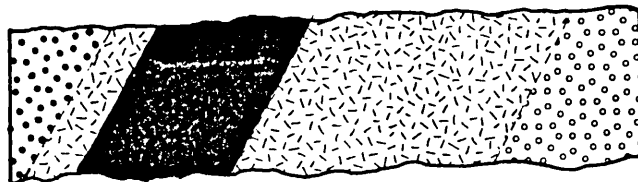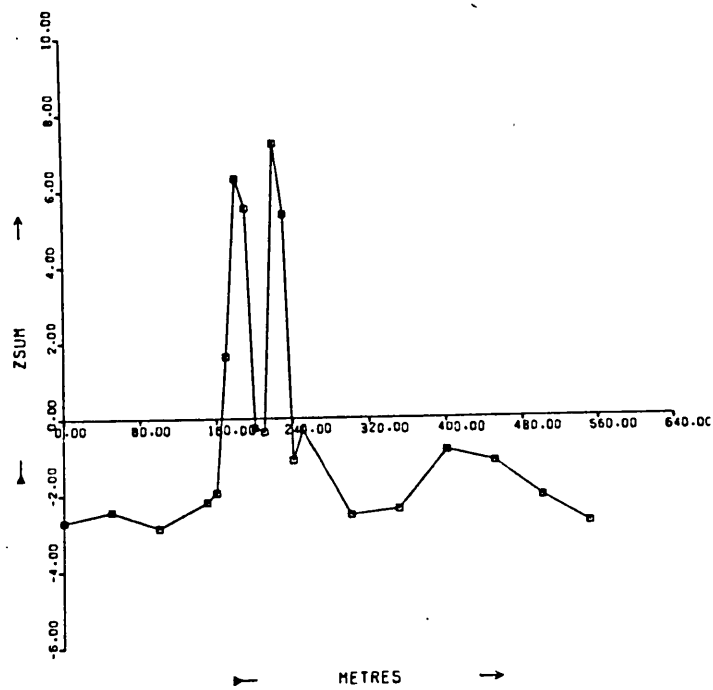
Figure 92: Munali, Zsums along soil traverse line (for geological legend see figure 9).

deviates which on subtraction may increase the value of summed standard normal deviates.

This technique of generating a uni-variate discriminant was used for each soil traverse, exercising the SUMSND add and subtract options according to the elements determined in each traverse. The Ni variable was always added, and since the Ni standard normal deviates (NiZ) are positive in both mineralized zones and non-mineralized anomalous zones, this invariably produces at least one positive component in the summed standard normal deviates (Zsums) of samples containing high Ni values. Thus it is the size of a positive Zsum rather than the simple presence or absence thereof, which determines its significance, and at least slightly elevated Zsums can be expected to delineate zones of high Ni values.

For the Chitina soil traverse Zsums were generated by adding the NiZ, CuZ and SZ factors. The anomalous zone is delineated by NiZ factors slightly in excess of +2.00 (sample nos. 435-26 to 435-30). In fact, the Zsums of the anomalous zone are still higher, due mainly to the association of a modest Cu soil anomaly with the Ni anomaly and the maximum Zsum is +4.69 (figure 89). Lower Zsums prevail elsewhere along the traverse, with a minimum of -3.52.

The Chombwa traverse is a little unwieldy for the Zsums exercise because the proportion of background to anomalous zone samples is low. The peak of the Ni soil anomaly has NiZ factors of +1.09 (sample nos. 245-07 to 245-11), but background Ni values have NiZ factors as low as -1.69. The NiZ, CuZ, SZ and FZ factors were added, and the higher Zsums reach +3.15 in the anomalous zone, while the minimum Zsum over background gabbro is -5.18 (figure 90).
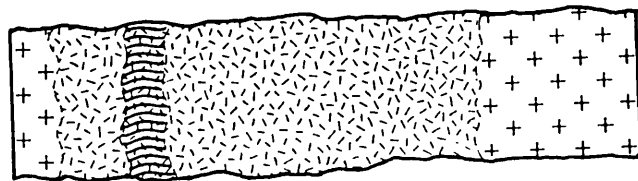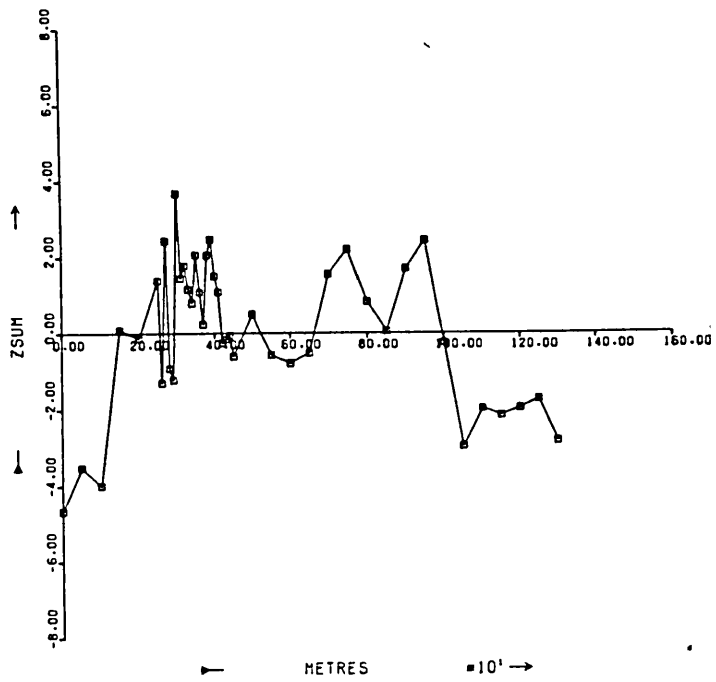
Figure 93: Musangashi, Zsums along soil traverse line (for geological legend see figure 10).

In the King Edward traverse the maximum NiZ factor is +1.83 in the Ni soil anomaly zone (sample no. 555-13). The NiZ, CuZ and SZ factors for the traverse were added to generate Zsums, and the Zsums pattern excellently illustrates the absence of mineralization beneath the Ni soil anomaly (figure 91). The full range of Zsums for the traverse is confined to the range -2.11 to +3.38. Over the southern contact Ni anomaly, Zsums are very close to zero, and further along the traverse where high Cu is found, Zsums slightly exceed +2.00. However the highest Zsum of +3.38 is found over limestone to the south of the intrusive.

At Munali, standard normal deviates were calculated for only that part of the traverse over the intrusive, because complications of interpretation of Zsums were anticipated if the high Cu and F values over the schist were unnecessarily included. Two samples in the mineralized zone have NiZ factors in excess of +2.00 (sample nos. 135-11 and 135-12). The NiZ, CuZ, SZ and FZ factors were added in generating Zsums, and these demonstrate remarkable contrast between the mineralized zone and background compared with the limited difference between non-mineralized anomalies and background in other areas (figure 92). The highest Zsums reaching +7.35 clearly delineate the mineralized zone, while over background gabbro Zsums are consistently below zero.

The anomalous zone at Musangashi includes one sample with a NiZ factor greater than +2.00 (sample no. 635-11). The Zsums for the traverse were obtained by adding the NiZ, CuZ and SZ factors, and range from -4.66 over country rock to +3.69 (figure 93). This maximum is coincident with the highest Ni value in the traverse, but is in fact little higher than most other Zsums over the intrusive, and the overall Zsum pattern does not suggest mineralization.
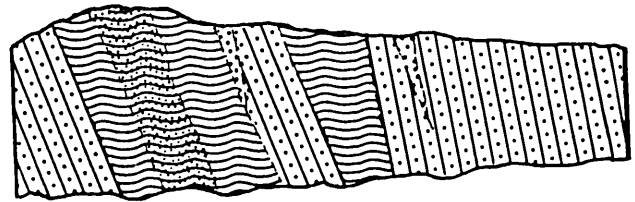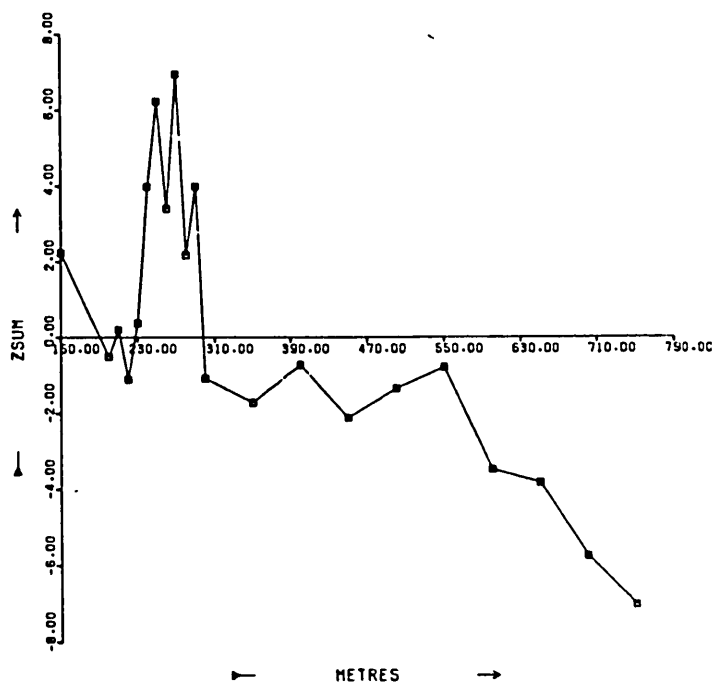
Figure 94: Trojan, Zsums along soil traverse line (for geological legend see figure 12).

Owing to the high Ni means at Trojan and Kingston, even those samples with the highest Ni values have relatively modest NiZ factors. At Trojan the maximum NiZ factor is +1.79 (sample no. 835-10). The Zsums for the Trojan traverse were generated by adding the NiZ, CuZ, SZ and FZ factors and, in view of the limited leaching from the soil, subtracting the MgZ factor. As at Munali, sharply higher Zsums reflect the mineralized zone, with a maximum of +6.93, while over background serpentinized peridotite and amphibolite, Zsums are generally below zero (figure 94). Unfortunately it was not possible to compare Zsums at Trojan and Paulwi because S and F data were not available for Paulwi.

In the Kingston traverse the maximum NiZ factor is +1.74 in the anomalous zone (sample no. 845-14). Again, Zsums were compiled by adding the NiZ, CuZ, SZ and FZ factors and subtracting the MgZ factor. The Zsum pattern is roughly in keeping with that for a non-mineralized area, with the Ni anomaly reflected by Zsums of up to +3.49 (figure 95). The highest Zsum along the traverse is +3.81, and it occurs beyond the anomalous zone.

Thus, high Zsums, up to +6.93 at Trojan and +7.35 at Munali, and good contrast with background, characterize mineralization. Nickel anomalies attributable to origins other than mineralization have Zsums of less than +4.70, and Zsums are particularly efficient in placing the Kingston anomaly in this group. However, the use of single traverse lines to exemplify the potential of Zsums is limited because of the restricted number of background samples.

6.11.2. Simulated grid pattern.

In a grid of soil samples over a mafic or ultramafic intrusive, the vast majority of standard normal deviates would be close to zero. Some combination of distinctly positive and negative NiZ, CuZ, SZ and FZ (and possibly MgZ) factors would be expected to occur in conjunction with Ni soil anomalies, and very high Zsums generated from these variables would clearly define those Ni anomalies derived from mineralization.
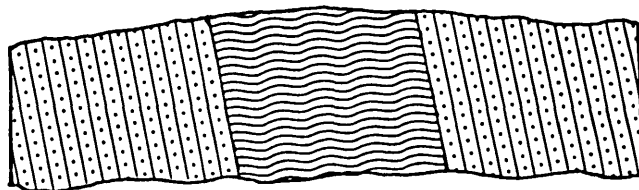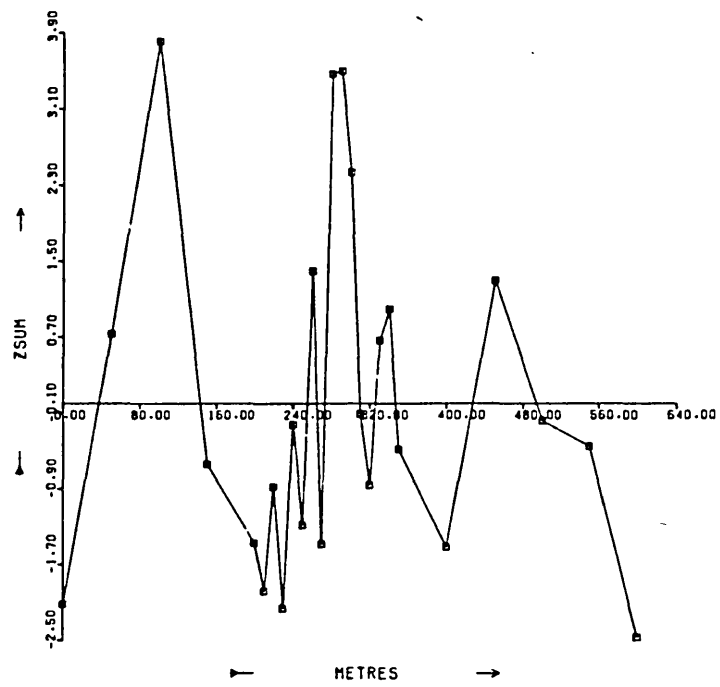
Figure 95: Kingston, Zsums along soil traverse line (for geological legend see figure 13).

To test this hypothesis, a soil sampling grid
over a mafic-ultramafic complex and adjacent country rock
was crudely simulated by taking the Chitina, Chombwa, King Edward,
Munali, Musangashi, Trojan and Kingston traverses together to
give a total of 229 samples. The mean Ni concentration of the
artificial grid these samples create is 1790 ppm, the Cu mean
is 165 ppm and the S mean 102 ppm. Because not all samples
were analysed for F it was not possible to include this variable
in this exercise. The NiZ, CuZ, and SZ factors for the grid
were computed and added to give Zsums.

The Zsum background for the grid can be regarded
as about -1.00, with 95% of Zsums in the range -2.46 to +3.56
(table 27). Higher Zsums are associated with the remaining 5%
of samples and these occur in four groups which would constitute
possible follow-up targets. The group of highest Zsums is associated
with the Munali mineralization and comprises four samples with Zsums
between +5.22 and +11.42. The Trojan mineralization is picked out
by a group of three samples with Zsums of +3.56 to +5.03, while the
Kingston anomaly is reflected by seven samples with Zsums in the
range +3.62 to +6.08.

The fact that high Zsums attach to the Kingston
anomaly is not surprising in view of the weakly disseminated
mineralization known to be present, and in the light of the
omission of the F and Mg factors in this exercise. Finally a
single sample from the Chombwa anomalous zone has a Zsum of +4.11,
and this isolated result is unlikely to command the same follow-
up attention as the other three multi-sample groups of high Zsums.
The other Ni anomalies within the grid, represented by the Chitina,
King Edward and Musangashi anomalies, have inconspicuous
Zsums around, and commonly below, zero.

ID	Zsum		ID	Zsum	ID	Zsum	ID	Zsum	
13501	-2.11		43511	-1.79	53524	1.22	84504	-1.23	
13502	-1.99		43512	-1.66	53525	.33	84505	.67	
13503	-2.43		43513	-1.18	53526	1.17	84506	.49	
13504	-1.98		43514	-1.09	53527	.24	84507	.95	
13505	-1.74		43515	-.34	53528	-.67	84508	1.19	
13506	2.44		43516	-.81	53529	-1.04	84509	1.55	
13507	6.66	*	43517	-1.74	53530	-1.22	84510	3.06	
13508	5.22	*	43518	-.57	53531	-1.06	84511	4.02	*
13509	1.27		43519	-.81	53532	-1.04	84512	2.24	
13510	.69		43520	-.13	53533	-.72	84513	4.57	*
13511	11.42	*	43521	-1.37	53534	-1.00	84514	5.34	
13512	8.25	*	43522	-.63	53535	-1.15	84515	4.92	*
13513	-.18		43523	-.44	53536	-1.19	84516	3.62	*
13514	.73		43524	-.22	53537	-1.13	84517	2.01	
13515	-1.97		43525	-.59	53538	-.57	84518	3.76	*
13516	-1.17		43526	-.69	53539	-1.15	84519	6.08	*
13517	-.46		43527	-.22	63501	-2.46	84520	2.20	
13518	-.91		43528	-.43	63502	-2.11	84521	-.03	
13519	-.83		43529	-.60	63503	-2.46	84522	-.74	
13520	-1.71		43530	-.46	63504	-1.78	84523	-1.42	
13521	1.32		43531	-.48	63505	-1.76	84524	-1.06	
13522	2.40		43532	-.69	63506	-1.31	84525	-.46	
13523	1.51		43533	-.27	63507	-1.18	83504	2.20	
13524	2.65		43534	-.05	63508	-.98	83505	-.36	
13525	2.61		43535	-1.07	63509	-1.66	83506	1.72	
13526	2.67		43536	-1.84	63510	-1.77	83507	.49	
13527	3.48		43537	-.75	63511	-1.07	83508	1.77	
24501	-.78		43538	-.33	63512	-1.33	83509	3.56	*
24502	-.44		43539	-1.10	63513	-1.42	83510	3.76	*
24503	.77		43540	-.76	63514	-1.70	83511	2.05	
24504	1.81		43541	-1.03	63515	-1.63	83512	5.03	*
24505	.87		43542	-.67	63516	-1.34	83513	3.01	
24506	.86		43543	-1.02	63517	-1.62	83514	2.43	
24507	1.81		43544	-1.13	63518	-1.94	83515	2.15	
24508	1.69		43545	-1.60	63519	-1.30	83516	1.50	
24509	2.81		43546	-1.42	63520	-.96	83517	1.28	
24510	3.36		43547	-1.25	63521	-1.25	83518	.25	
24511	.40		43548	-1.31	63522	-1.35	83519	1.10	
24512	4.11	*	43549	-1.07	63523	-1.57	83520	.54	
24513	1.50		53501	-.29	63524	-1.61	83521	-.71	
24514	1.61		53502	1.40	63525	-1.54	83522	.07	
24515	1.30		53503	-.70	63526	-1.65	83523	-1.27	
24516	.20		53504	.57	63527	-1.30	83524	-1.41	
24517	.40		53505	.40	63528	-1.45			
24518	1.48		53506	-.29	63529	-1.48			
24519	.75		53507	-.91	63530	-1.43			
24520	.38		53508	-.73	63531	-1.21			
24521	-.04		53509	-.33	63532	-1.52			
24522	-.35		53510	-.58	63533	-1.18			
24523	.44		53511	-.09	63534	-1.91			
24524	-.36		53512	-.74	63535	-1.26			
24525	-.34		53513	-.55	63536	-1.17			
43501	-1.96		53514	-.39	63537	-1.96			
43502	-1.60		53515	.20	63538	-2.25			
43503	-1.90		53516	-.49	63539	-2.21			
43504	-1.47		53517	-.59	63540	-2.18			
43505	-1.64		53518	.18	63541	-2.20			
43506	-1.96		53519	1.08	63542	-2.17			
43507	-1.27		53520	1.19	63543	-2.31			
43508	-1.78		53521	.99	84501	-.72			
43509	-1.68		53522	.12	84502	-.70			
43510	-1.62		53523	.76	84503	-1.19			

* Anomaly selection –
5% of samples with
highest Zsums

Table 27: Zsums for simulated soil sampling grid.

Thus very high Zsums clearly delineate the Munali
mineralized zone as a most promising target, while both the
Kingston anomaly and the Trojan mineralized zone appear to have
good potential, and would be further distinguished by consideration
of other features such as F and Mg concentrations and incorporation
of FZ and MgZ factors into the Zsums for the grid.

6.12.   The distribution of ore metals in the coarse fraction.

Continuing the limited evaluation of the prospecting
use of the coarse fraction of samples, the coarse fraction of the
soils along the Munali and Chombwa traverses were analysed for Ni,
Cu, Fe and Mn by atomic absorption spectrophotometry. The analytical
results are given in appendix 2.

In the Chombwa soils, the concentrations of
Ni and Cu in the coarse fraction are similar to and generally
slightly less than corresponding sample values for the fine
fraction. The maximum Ni value in the coarse fraction is 2750 ppm
in the anomalous zone, compared with a maximum of 3000 ppm Ni in
the fine fraction. Similarly the highest Cu levels are 73 ppm in
the coarse fraction and 78 ppm in the fine fraction. As observed
in the pit profile, the distribution among the size fractions of Ni
and Cu is largely controlled by Fe concentration. The maximum
Fe values are 13.0% in the coarse fraction and 16.5% in the fine
fraction, and so there is no enrichment of Fe, and therefore neither
of Ni and Cu, in the coarse fraction. The coarse-to-fine fraction
ratios are generally around 0.80 for all three elements, with
ratios in excess of unity in very few samples and coincident highs of
1.00 for Ni, 1.19 for Cu and 1.14 for Fe at the northern end
of the traverse (figure 96). Although there is more Mn in the fine
fraction over much of the traverse, across part of the Ni anomaly
there is strong Mn enrichment in the coarse fraction, with up to
3400 ppm Mn compared with a maximum of 1230 ppm Mn in the fine fraction.
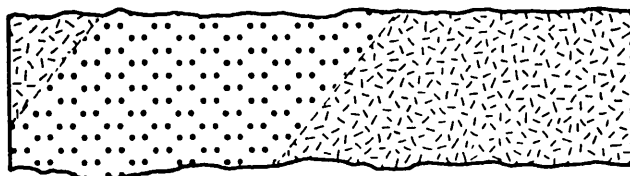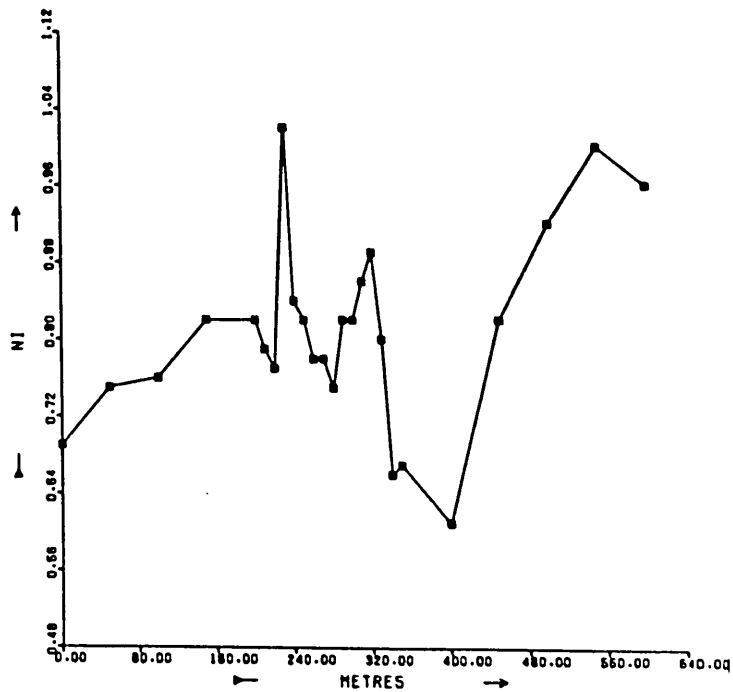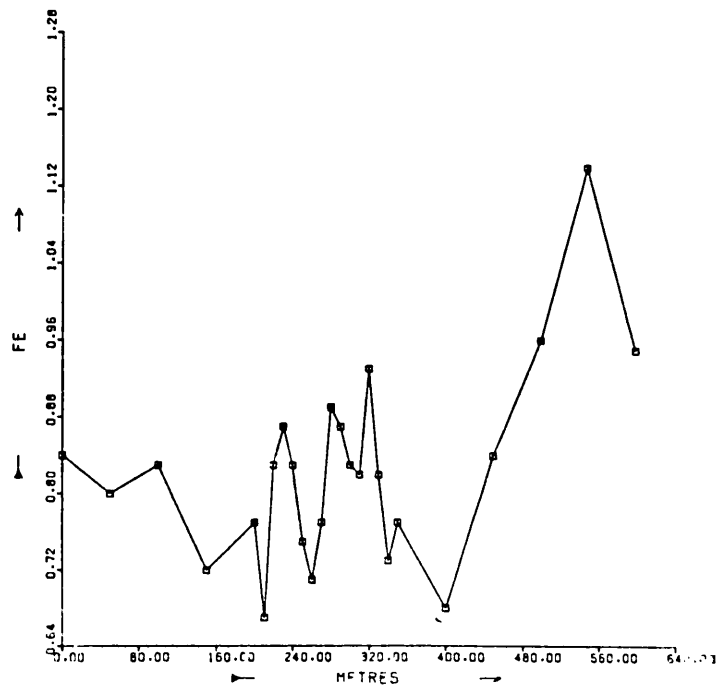
Figure 96: Chombwa, coarse-to-fine fraction ratios for Ni and Fe along soil traverse line (for geological legend see figure 7).

This produces coarse-to-fine fraction ratios reaching 3.21.
Because of the evident association of Ni and Cu with secondary
Fe, it is commonly difficult to identify any relationship with
Mn, but here there are sharp Ni and Cu coarse-to-fine fraction
ratio peaks in conjunction with the Mn peak (figure 97).

        Although Co and Zn distribution in soils is often
partly controlled by secondary Mn oxides, and Cu distribution is
closely correlated with Mn at King Edward, the coarse fraction of
the Chombwa soil provides the only case of both Ni and Cu linked
to Mn.

        At Munali high Fe characterizes the mineralized
zone, and the concentration of Fe is often higher in the coarse
fraction than the fine fraction. There is up to 38.5% Fe in
the coarse fraction compared with 25.5% in the fine fraction in the
mineralized zone. Enrichment of Fe in the coarse fraction occurs
elsewhere along the traverse, but is less marked, so that coarse-to-
fine fraction ratios reach a maximum of 2.77 in the mineralized zone.
Similarly, Ni values tend to be a little higher in the coarse
fraction of many samples,and highest Ni concentrations and size
fraction contrast occurs in the mineralized zone, with up to 8000 ppm
Ni in the coarse fraction compared with 6500 ppm Ni in the fine
fraction. This produces a maximum coarse-to-fine fraction ratio
for Ni of 1.76 in the mineralized zone (figure 98). Still better
contrast is exhibited by Cu, because outside the mineralized zone
Cu values are almost always lower in the coarse fraction than the
fine fraction, but in the mineralized zone the highest Cu is
1580 ppm in the coarse fraction and 940 ppm in the fine fraction.
Thus the coarse-to-fine fraction ratios for Cu are usually below
unity except in the mineralized zone, where the ratios are
significantly above unity and reach 1.93 when in company with the
highest Fe and Ni ratios. Manganese values in the coarse fraction
are generally low and comparable with those in the fine fraction.
There is no link between Mn and Ni or Cu distribution (figure 99).
An unusual Mn enrichment in the coarse fraction of a single sample
over schist produces a maximum coarse-to-fine fraction ratio for Mn
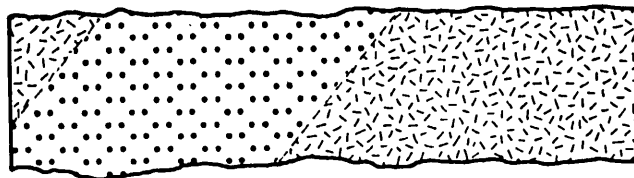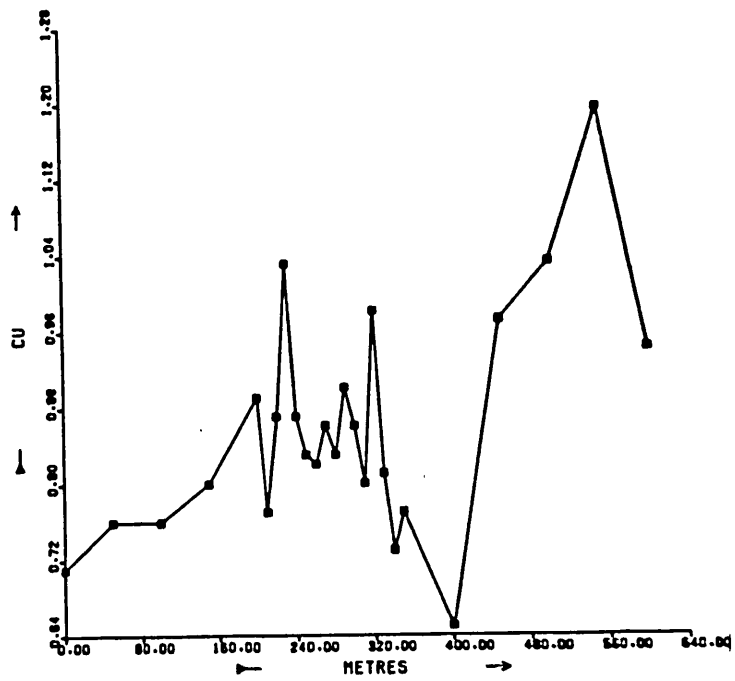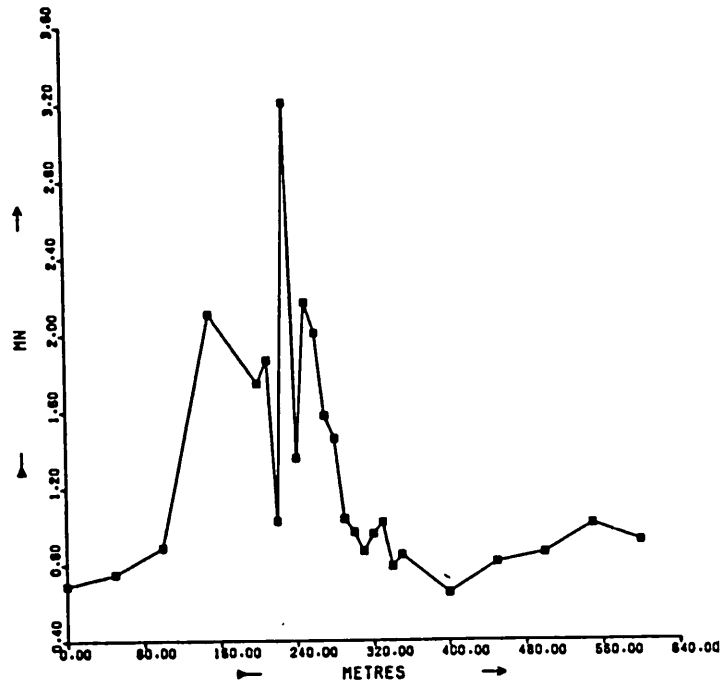
Figure 97: Chombwa, coarse-to-fine fraction ratios for Cu and Mn along soil traverse line (for geological legend see figure 7).

of 4.81, but is unaccompanied by Ni or Cu enrichment.

Cu and Fe accumulate in the coarse fraction of
soils over mineralization and this fraction therefore exhibits
the maximum contrast with background. Soils overlying
mineralization have coarse-to-fine-fraction ratios for Ni, Cu
and Fe considerably in excess of unity, whereas in soils over
non-mineralized ultramafic rock these ratios are less than
unity.

6.13   Discussion

The geochemical soil traverses across mafic and
ultramafic intrusives generally confirm the dispersion features
noted during studies of the vertical soil profiles. Nickel
mainly behaves in a siderophile manner during weathering and
soil formation, with the result that there is always a close
correlation between Fe and Ni in the soil traverses. Some Ni
anomalies are associated with Fe enrichments not related to
primary mineralization, for example, the Chitina Ni anomaly.
Strong and coincident Ni and S soil anomalies occur where the
Fe, Ni and S are intimately associated in the primary environment,
probably because only limited redistribution of Fe, Ni and to
some extent S is allowed during weathering. Only massive nickel
sulphide mineralization furnishes this close association of Fe,
Ni and S, and so strong and coincident Ni and S soil anomalies
are clearly good indicators of such mineralization, as at Munali.
Disseminated mineralization, as at Trojan, produces a more modest
Ni and S anomaly in a less ferruginous soil.

Copper and Co are not consistently siderophile
during the weathering cycle. Where present in sulphide minerals,
as at Munali and Trojan, Cu tends to maintain a close relationship
with Fe in the soil, yielding coincident Ni, Cu and S soil anomalies.
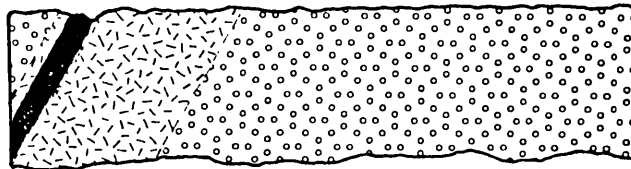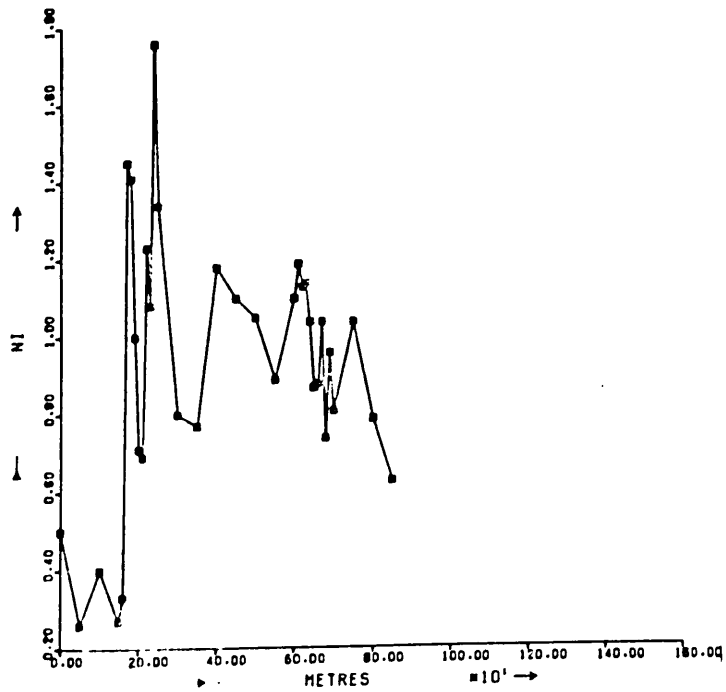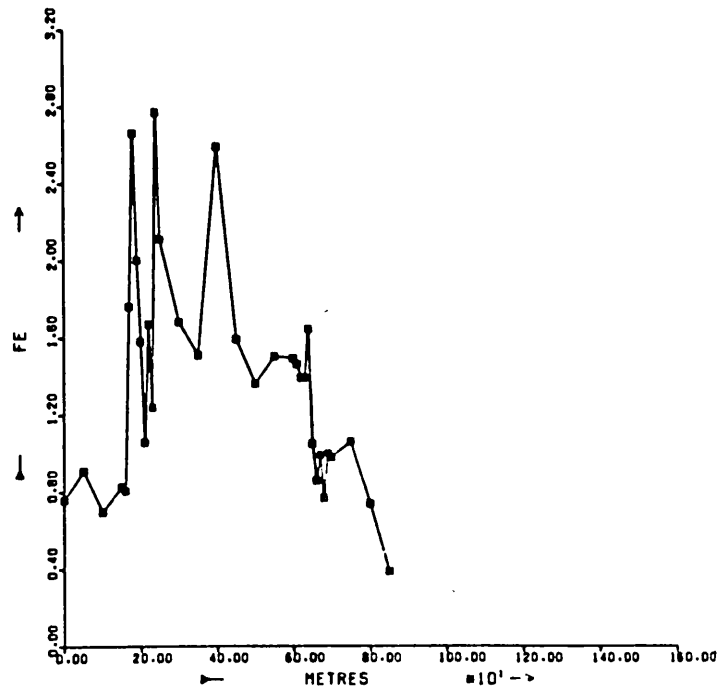
Figure 98: Munali, coarse-to-fine fraction ratios for Ni and Fe along soil traverse line (for geological legend see figure 9).

Copper and Co derived from silicate minerals may be preferentially coprecipitated and adsorbed by secondary Mn oxides in the soil, and this appears to be the case with Co at Paulwi and Cu at King Edward (and the high soil pH probably contributes to immobilizing Cu in the latter case). Substantial and misleading enrichment of these metals can occur as a result of Mn scavenging and pH fluctuations;for example, the King Edward Cu anomaly seemingly caused by these mechanisms is coincident with relatively high Ni concentrations in the soil, although neither metal is derived from sulphide mineralization.

The underlying parent rock type can be monitored from B horizon soil samples with reasonable success using Cr, and perhaps V, data. Nickel soil amomalies derived from lenses of non-mineralized ultramafic rock are accompanied by Cr levels which exceed Ni. Over mineralization the soil Ni content rises dramatically to levels in excess of Cr, and hence the Ni:Cr ratio increases. However, there is no evidence for increased leaching of Cr, with a resultant decline in Cr concentrations contributing to the higher Ni:Cr ratios over mineralization, as suggested by Moeskops (1976). Ultramafic rock at depth is also indicated by high Mg in soils which are not strongly leached.

Pit profile studies suggested that the B soil horizon V content might be a useful indicator of parent rock type and thereby aid Ni anomaly interpretation in some cases. Along the Chombwa traverse, low V levels around 200 ppm accompany the high Ni concentrations over peridotite, and high V, around 400 ppm, occurs with lower Ni over gabbro. At Munali the V mean is 411 ppm and V concentrations of this order persist in conjunction with high Ni values which reflect mineralization. Coincident high Ni and low V at Chombwa directly reflects ultramafic parent rock, whereas Ni enrichment without V depletion at Munali is an anomalous combination, indicative of mineralization. In other areas, V distribution along soil traverses is more erratic, and no systematic correlation with Ni is evident. No significant difference in V concentrations is to be expected in soils overlying mineralized and non-mineralized ultramafic rock.
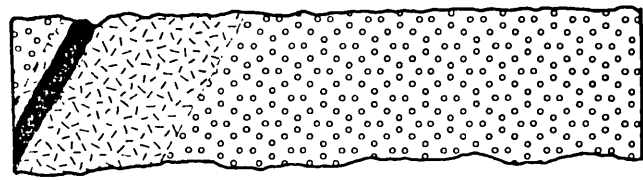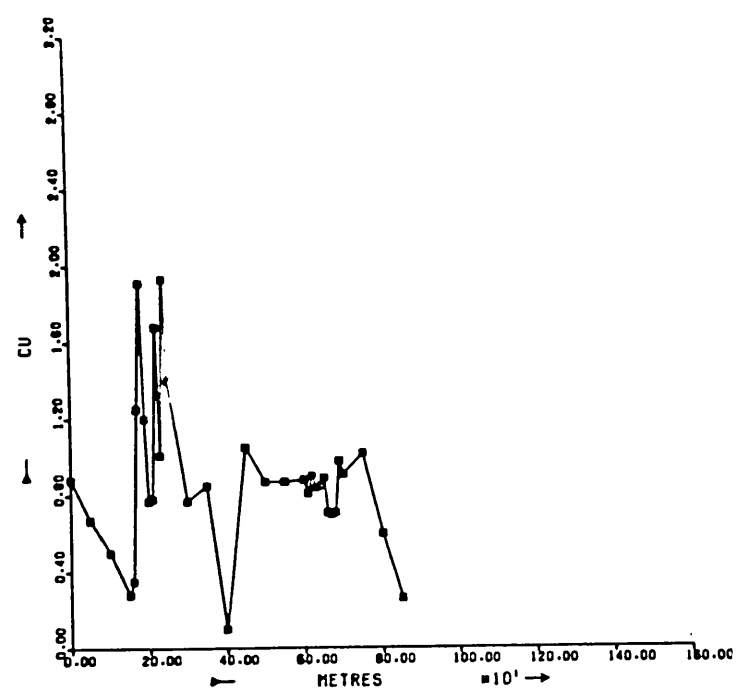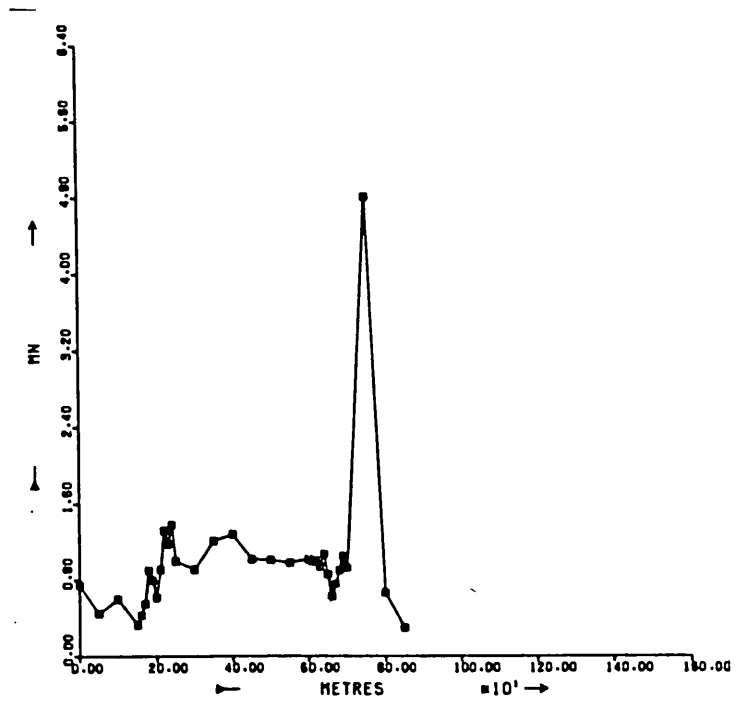
Figure 99: Munali, coarse-to-fine fraction ratios for Cu and Mn
along soil traverse line (for geological legend see
figure 9).

The tenet on which the F investigation was based is that the F⁻ anion substitutes for the OH⁻ anion in primary silicates and is therefore more abundant in mafic minerals formed late in the reaction series, such as amphiboles, and to a lesser extent augite (Boyle, 1976). Silicates such as olivines which crystallize early in the cooling sequence of a basaltic melt and most pyroxenes, cannot accomodate F. Thus, predominantly ultramafic rocks such as dunites, peridotites and many pyroxenites contain lower concentrations of F, a mean of 130 ppm according to Boyle, while gabbroic rocks have higher F levels, with a mean of 430 ppm F. Serpentinites can contain up to 2000 ppm F, depending upon the quantity of F introduced by the fluids effecting serpentinization. If the F content of the soil adequately distinguishes the underlying rock type, then Ni soil anomalies derived from lenses of ultramafic rock within mafic intrusives could readily be distinguished from Ni soil anomalies derived from mineralization on the basis of the associated F level.

The F data obtained in the study of soil profiles suggested that the primary F distribution was substantially modified during weathering, and secondary dispersion patterns would not necessarily closely reflect the underlying primary distribution. This is clearly the case in soil traverses, although it should also be emphasized that B horizon samples were analysed, and these are sub-optimal material for F dispersion studies. In traverses over the predominantly mafic intrusives, a weak F trough over a non-mineralized peridotite lens at Chombwa contrasts with a sharp F anomaly over mineralization at Munali. There is no obvious contrast between amphibolite and serpentinite at Trojan or amphibolite and peridotite at Kingston, although a weak F anomaly overlies the mineralized zone at Trojan. The F contrast between mafic and ultramafic rocks must be considered somewhat disappointing, and might be improved by use of A horizon soil samples. The presence of a F anomaly over mineralization may be

fortuitous in the cases investigated here, or may have
reasonably general applicability to mobile elements which tend
to accumulate in the fluid phase in both the primary and
secondary environments. In the magmatic environment, such
fluids may be differentiates of mafic or ultramafic rocks,
and are often injected into zones of weakness within the
parent rock to form massive sulphides, as at Munali. In
other cases, extraneous fluids, either juvenile or meteoric,
may permeate cooling mafic and ultramafic rocks and cause
sulphurization and serpentinization, which is the probable
mode of ore genesis at Trojan. However, whether or not F
is associated with the mineralization depends upon the F
content of the mineralizing fluids. At Trojan there is a
low order F soil anomaly over the mineralization, indicating
that the mineralizing fluids were slightly fluoriferous,
although the F background in the Trojan/Kingston soil is
generally low, which suggests that relatively little F was
introduced during serpentinization. Thus it seems that F is
a fair indicator of primary Ni mineralization, although F
anomaly magnitude is likely to be highly variable according
to the F content of the fluids with which the mineralization
was associated during ore genesis or emplacement. Identification
of useful F anomalies in soils to aid Ni anomaly interpretation
depends upon further research to optimize soil sampling and
perhaps analytical techniques. The F content of many acidic
and alkalic rock types is also high compared with mafic and
ultramafic rocks, and the possibility that a F soil anomaly may
reflect such a rock type should always be considered.

In soils developed over iron-rich parent material
such as oxidizing sulphide mineralization, a coarse, nodular,
highly ferruginous B horizon tends to form. Analysis of the
coarse fractions of Chombwa and Munali soils shows that Ni and
Cu are relatively enriched in this fraction in soils over
mineralization and so high coarse-to-fine-fraction ratios for Ni
and Cu suggest mineralization at depth. In the absence of

oxidizing mineralization the B horizon is less ferruginous and not necessarily nodular, and hence the coarse material is a less efficient collector of heavy metals.

Secondary Mn oxides tend to coat suitable rock and mineral fragments, and once begun Mn oxide deposition is autocatalytic (Stumm and Morgan, 1970). Considerable enrichment of Mn in the coarse fraction of soils can occur in this way, ultimately forming wad. Some correlation of Ni with Mn is noted in the coarse fraction of soils overlying non-mineralized ultramafic rock at Chombwa, and Carpenter, Pope and Smith (1975) found Ni concentrated in the Mn coatings of the sediments of streams draining a non-mineralized locality in the southeast USA. It seems possible that even Ni, which is normally siderophile in a ferruginous secondary environment, may coprecipitate with and be absorbed by secondary Mn oxides in some places when large concentrations of Fe are not present. Copper is still more prone to scavenging by Mn, and although very high concentrations of Mn in soil were not encountered in these research studies, such enrichments could substantially influence both Ni and Cu distribution, possibly producing non-significant coarse fraction and coarse-to-fine-fraction ratio anomalies. Therefore not only the coarse fraction enrichment of Ni and Cu, but also their correlation with Fe or Mn is important for distinguishing soils underlain by mineralization.

The number of elements contributing to the identification of significant Ni soil anomalies prompted the use of multi-variate interpretive techniques. Researchers in Australia have adopted similar approaches. The generation of Zsums facilitates the simultaneous evaluation of the significance of the more quantifiable variables that together may indicate the presence of mineralization, such as Ni, Cu, S, F and Mg. Other useful elements, such as Cr and V, are best considered on a qualitative basis. The Zsums technique of anomaly

interpretation essentially involves normalization of
individual elements in a sample suite, followed by
summation of the standard normal deviates of these
elements for each sample according to an empirical
formula. One can then talk of Zsum anomalies in terms
more or less equivalent to accepted geochemical prospecting
jargon. Thus just as an element concentration in excess of
mean plus two standard deviations is considered anomalous
an idealized Zsum anomaly might reasonably be expected to
exceed a minimum value of two standard normal deviations
times the number of variables incorporated into the formula.
In fact, Zsums of this magnitude were never obtained in the
geochemical traverse data for the very reason that multi-
variate data interpreation was invoked, i.e. elements in
the soil that are possible indicators of mineralization
are not necessarily all clearly anomalous for each occurence
of mineralization. On the other hand, chance elevated
concentrations of all of the indicator elements in soils over
non-mineralized rock is especially unlikely, and therefore
lower Zsums pertain than over mineralization.

The Zsums technique incorporates all useful
variables simultaneously into a uni-variate expression and is
thought to compare favourably with an empirical method of
distinguishing true nickel gossans from cherts, laterites
and wads in Western Australia, devised by Clema and Stevens-
Hoare (1973). In their method the Ni + Cu content of samples
is expressed as a percentage of Cu + Ni + Zn + Pb + Mn + Cr
(= M), and high percentages coupled with high absolute values
for M indicate true gossans. Similarly low percentages of

Mn + Cr coupled with high values for M indicate mineralization.
All metals are determined in the same leachate by atomic
absorption spectroscopy, and absolute metal concentrations
are used in the data processing. The metal distribution
underlying the merit of this data processing method appears
to be much the same in Central Africa, where high Cu with
especially high Ni indicates mineralization, low Cr compared
with Ni indicates mineralization, and high Mn can cause
spurious enrichment of other indicator metals.

The work by Clema and Stevens-Hoare (1973) and other
Australian research into geochemical prospecting for primary
nickel ore is characterized by interpretive work on multi-
element data acquired by a series of atomic absorption
spectroscopic determinations using a single leachate per
sample. It seems reasonable to speculate that an investigation
of the S content of samples might have been apposite in the
Australian problems, but it was probably neglected owing to
less economical analytical methods compared with atomic
absorption spectroscopy. At this stage it seems that this
type of prejudice against more expensive raw data is likely
to persist in many cases, in spite of the fact that the more
expensive data may well be of higher quality in terms of
mineral exploration objectives.

No. samples	Chitina 25		King Edward 19		Munali 31		Musangashi 31		Kingston 20	
	Mean	Range	Mean	Range	Mean	Range	Mean	Range	Mean	Range
% ash	4.6	3.6 - 5.6	6.2	4.1 - 8.8	4.5	3.2 - 8.3	4.6	3.2 - 5.9	5.5	3.9 - 9.2
Ni	8	3 - 19	15	4 - 29	11	4 - 20	11	5 - 35	58	18 - 154
Cu	5	3 - 7	4	2 - 7	5	3 - 10	4	2 - 6	9	5 - 14
Co	1	1 - 2	1	1 - 2	1	1 - 3	1	1 - 2	2	1 - 4
Zn	13	9 - 19	15	7 - 20	11	6 - 20	13	7 - 22	8	5 - 16
Cr	8	4 - 14	9	5 - 14	6	4 - 10	7	4 - 31	3	0 - 9
Fe	147	21 - 501	216	139 - 298	176	66 - 747	110	56 - 662	269	134 - 1040
Mn	806	147 - 1720	310	134 - 674	323	105 - 926	197	54 - 917	281	151 - 730

Table 28: Trace element content of leaves of Diplorynchus condylocarpon (ppm).

7. <u>THE DISTRIBUTION OF ELEMENTS IN THE BIOGEOCHEMICAL ENVIRONMENT</u>

Leaf samples of either Diplorynchus condylocarpon or Combretum ghasalense, two common Central African trees, were taken along soil sample traverse lines whenever an appropriate tree was present close to a soil sampling point (figures 14 and 15). Sampling throughout each traverse was confined to one species. Leaf samples were also collected elsewhere over some intrusives, along with nearby soils. There is a general antipathy in the geographical distribution of the two genera, with Diplorynchus growing mainly on hilly and well-drained terrain, and Combretum preferring flat and low-lying ground. Both genera are phreatophytes, and can be expected to take up metals from the soil at considerably greater depths than those reached in soil sampling.

The leaves were dried, ashed and analysed for Ni, Cu, Co, Zn, Cr, Fe and Mn by atomic absorption spectroscopy. For each sample the metal content of the ash was converted to the equivalent concentration of metal in the dry leaf (using the weight percentage ash as a conversion factor) by a computer program PRASH.

Of the elements determined, Cu, Zn, Fe and Mn have long been known to be essential to all plants (Sauchelli, 1969). Copper occurs throughout plant tissue, but is concentrated in leaves. It is vital for growth and reproduction, and its metabolic role appears to be that of an enzyme activator. From 3 to 40 ppm Cu is typical in plant tissues. Zinc is incorporated in various metalloenzymes which catalyze oxidation reactions, control the transformation of carbohydrates, regulate sugar consumption, aid the formation of growth-promoting auxins, decompose carbonic acid and promote water absorption. The usual Zn content of plants is 5 to 40 ppm. Iron is essential in the catalyst employed in chloropyll formation and in the prosthetic group of respiratory enzymes, and between 700 and 2000 ppm Fe is the norm in plant tissues. Manganese is an enzyme activator in respiratory processes such as the oxidation of carbohydrate, in the metabolism of nitrogen, and in the synthesis of chlorophyll. Plants of the same species show considerable variation in Mn content, but 30 to 500 ppm is typical.
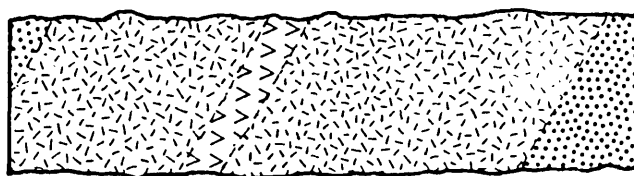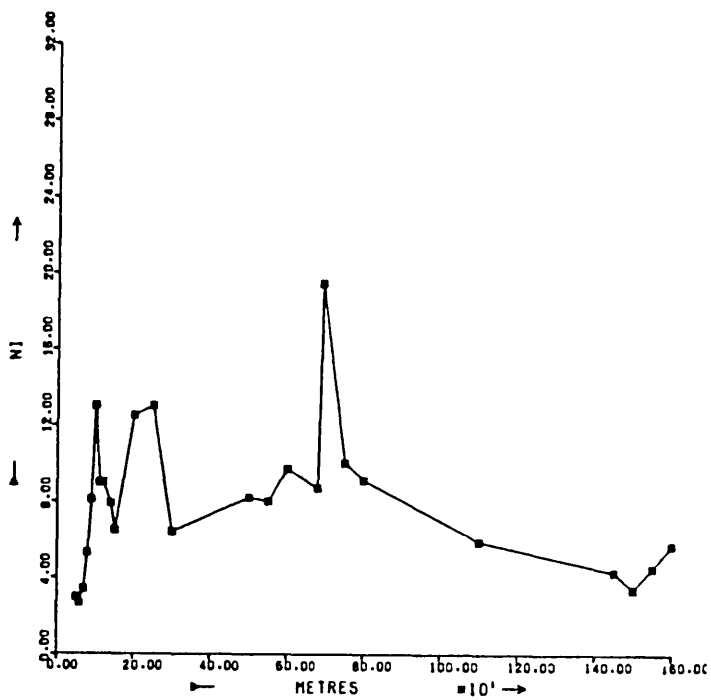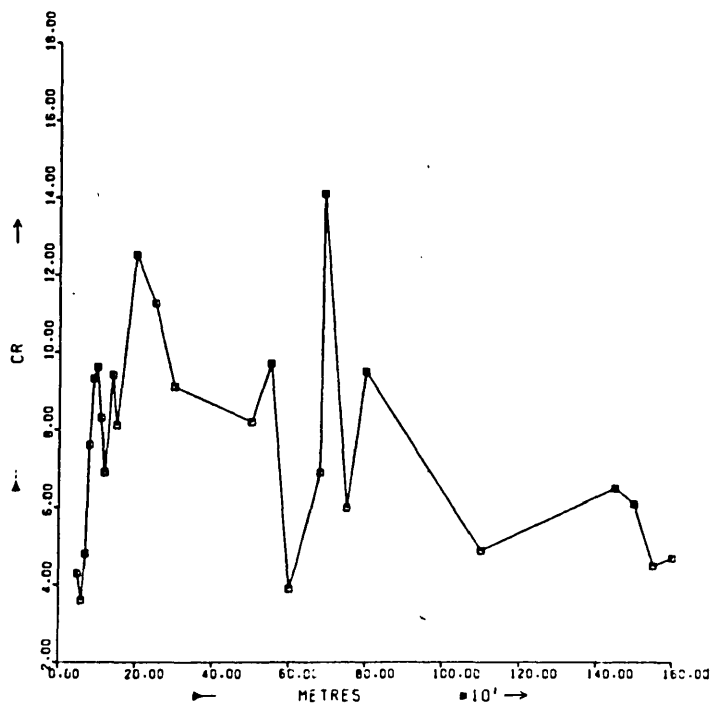
Figure 100: Chitina, distribution of Ni (ppm) and Cr (ppm) along Diplorynchus
biogeochemical traverse line (for geological legend see figure 6).

The essentiality of Co in plant metabolism is not clearly established, but the tissues of many plants contain about 1 ppm. A few ppm of Cr is common in most plants, and may be essential. However, Ni is non-essential to plants, and although most species are found to contain low levels of up to about 5 ppm, high concentrations of Ni are toxic. Indeed, even essential elements are toxic to a plant if taken up in particularly large amounts. A plant obtains trace elements from the soil via the root systems, and, for the most part, it controls the quantity of each element taken up to meet its requirements. Numerous factors contribute to determining the availability of elements in the soil to the plant, but particularly important are pH and the concentration of each element in the soil. All seven metals investigated are relatively mobile in some form, and therefore available for plant uptake, below pH 5.3. Iron (Fe^{2+}), Cr, Cu and Mn tend to be precipitated as hydroxides above about pH 5.5, and Ni and Zn are precipitated above pH 6.7.

The plant restricts its uptake of each element to required or sub-toxic levels by means of an exclusion mechanism (Brooks, 1972). Beyond a certain threshold concentration of an element in the soil, the exclusion mechanism controlling uptake of that element breaks down, and the plant accumulates comparatively large quantities of the element. The plant may immediately suffer the effects of toxicity, or may be able to tolerate unusually high concentrations of the element to some degree, above which poisoning occurs. In this case of limited tolerance the plant is said to operate a partial exclusion mechanism. Therefore, where a partial exclusion mechanism is operated, a species growing in soils with background concentrations of a particular element takes up relatively little of that element, in a controlled manner, while in anomalous soils the threshold is exceeded and specimens of the same species growing there take up comparatively large quantities.
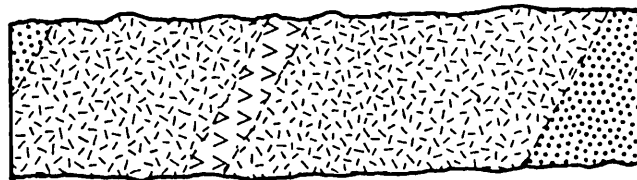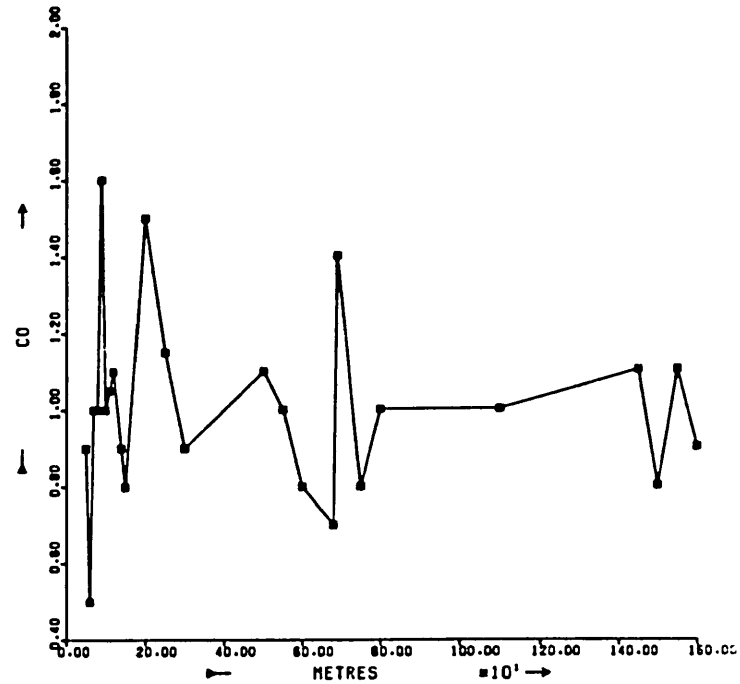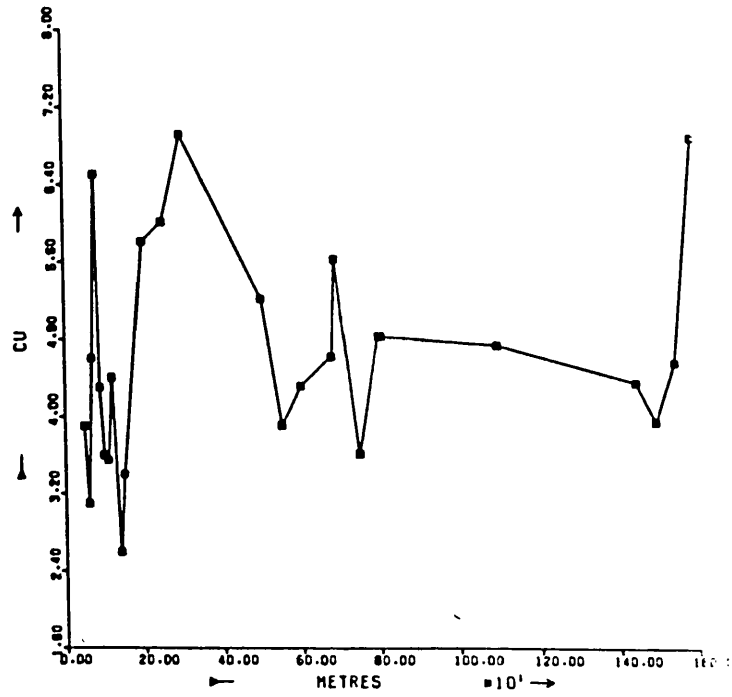
Figure 101: Chitina, distribution of Co (ppm) and Cu (ppm) along Diplorynchus biogeochemical traverse line (for geological legend see figure 6).

For example, most plants limit their Cu uptake to about 10 ppm, provided the soil contains less than 50 ppm, but in soils with a higher Cu content, uptake increases rapidly to as much as 200 ppm (Cole, 1971). The operation of a partial exclusion mechanism is especially useful in prospecting because of the sharp background-to-anomaly contrast that the plant achieves. The trace element contents of Diplorynchus and Combretum leaves, detailed in appendix 2, are appraised with a view to establishing the normal trace element requirements of the two species, the factors which may cause the uptake of anomalous levels, and the significance of such anomalies in nickel prospecting.

7.1   Diplorynchus condylocarpon

Leaf samples of Diplorynchus were obtained over the mineralized Munali and weakly mineralized Kingston intrusives and in the non-mineralized Chitina, King Edward and Musangashi areas (table 28).

7.1.1.   Chitina

At Chitina, 25 leaf samples were collected along the soil traverse line (sample nos. 489-02 to 489-49). They contain from 3 to 19 ppm Ni, and the maximum value occurs in the Ni soil anomaly zone. The highest Cr value of 14 ppm occurs in conjunction with the highest Ni and higher than average Cr in the soil (figure 100). Iron values ranging from 21 to 501 ppm in the leaves reflect the general pattern of Fe distribution in the soil. The Ni, Cr and Fe contents of Chitina leaves appear to be at least somewhat related to the Ni, Cr and Fe concentrations in the soil. The consistently low Co and Cu content of leaves, independent of fluctuations in the Co and Cu levels in the soil, suggests controlled uptake mechanisms for Co and Cu (figure 101). There is only a narrow range of Zn content in the leaves, and Zn uptake is clearly closely controlled. The maximum Zn value of 19 ppm is found in the leaves of a tree growing on soil with 52 ppm Zn, while over the coincident Ni and Zn soil anomaly there is only 14 ppm Zn in the leaves of a tree rooted in soil containing 1300 ppm Zn. There is a fairly wide range of Mn in the leaves, and in almost
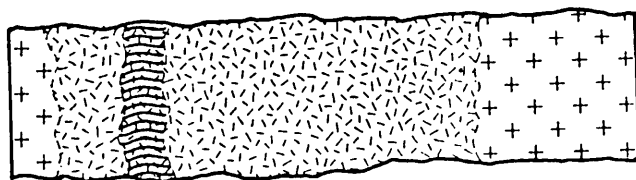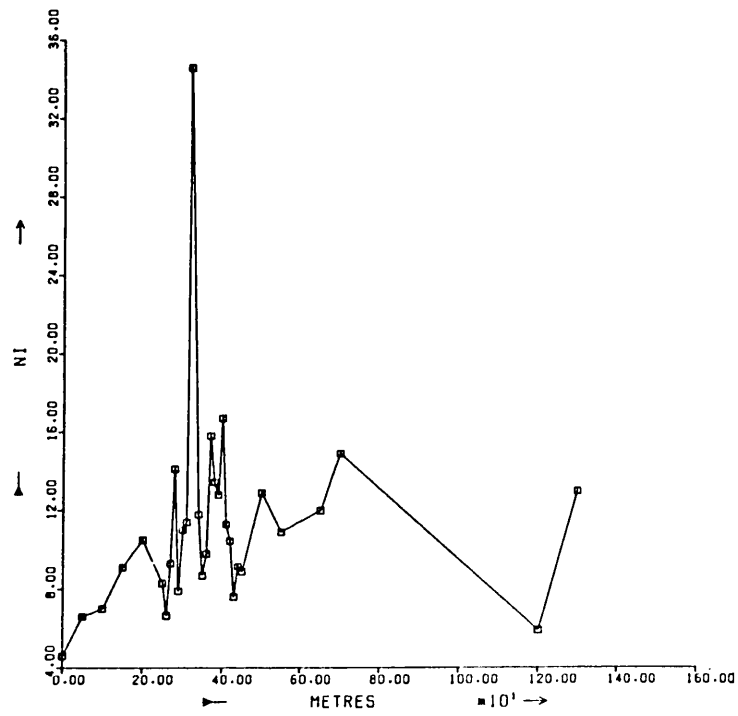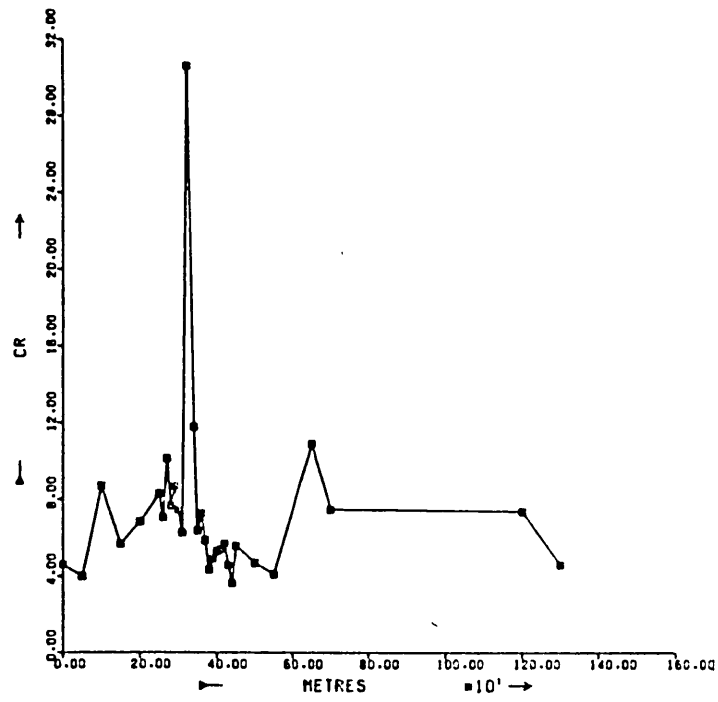
Figure 102:   Musangashi, distribution of Ni (ppm) and Cr (ppm) along Diplorynchus
biogeochemical traverse line   (for geological legend see figure 10).

all leaf samples the level exceeds that in the underlying
soil, suggesting that the plant is concentrating Mn to a
controlled extent in order to meet its requirements. Chitina
soils have a comparatively low mean Mn content of 650 ppm.
The soil pH throughout the Chitina traverse is about 5.1, so
that the metals investigated are probably present in relatively
available forms.

7.1.2. <u>Musangashi</u>

The distribution of elements in the leaf samples
taken along the Musangashi traverse line is similar to Chitina
(sample nos. 689-01 to 689-43). Higher than average Ni values of
up to 35 ppm are associated with the Ni soil anomaly, and the
highest Cr and Fe values in both leaves and soils occur in
conjunction with the highest Ni (figure 102). The correlations
between Ni, Cr and Fe in the leaves are strong. Cobalt, Cu and
Zn levels are again low and variations bear no relationship to
Co, Cu and Zn levels in the soil, confirming that carefully
controlled uptake is the norm for these metals. The soil contains
a mean Mn concentration of 978 ppm, higher than Chitina soils,
and, in contrast to Chitina, the leaves do not concentrate Mn in
excess of soil levels. As the Musangashi soil pH is about 5.1,
the availability of elements in the soil is likely to be much the
same as at Chitina, and this may be a significant factor in
producing similar biogeochemical patterns.

7.1.3. <u>King Edward</u>

At King Edward, 19 Diplorynchus samples were
collected over the southern contact zone of the intrusive where
the principal Ni soil anomaly occurs (sample nos. 599-01 to 599-19).
Soil samples were collected near to each sampled tree (sample nos.
545-01 to 545-96). The Ni mean of the leaves is 15 ppm, but there
are clearly two populations present. The population around 5 ppm
Ni is from trees growing on soils containing approximately 300 ppm
Ni derived from mafic contact rocks, while the remaining leaves
contain around 20 ppm Ni and are from trees on soils containing
some 2000 ppm Ni overlying ultramafic rock. Chromium values
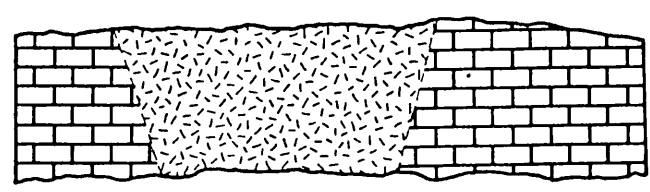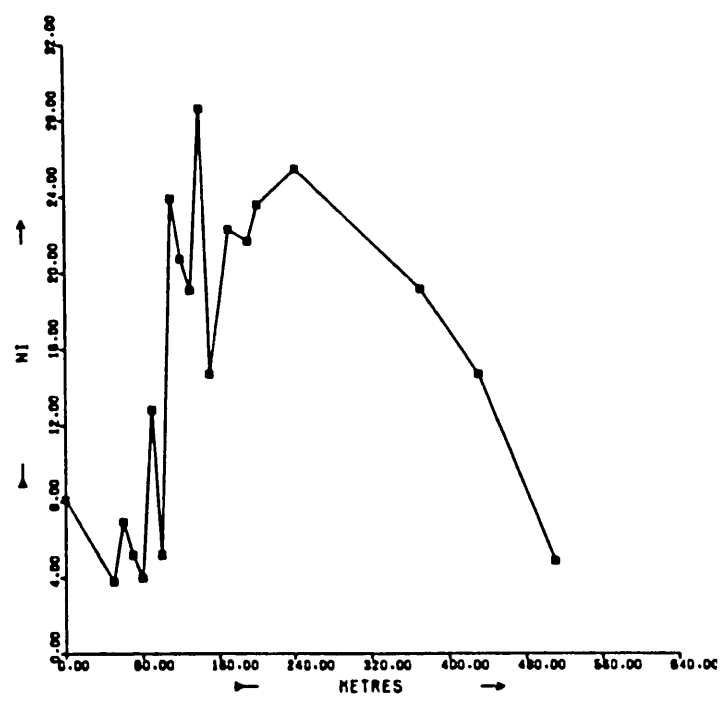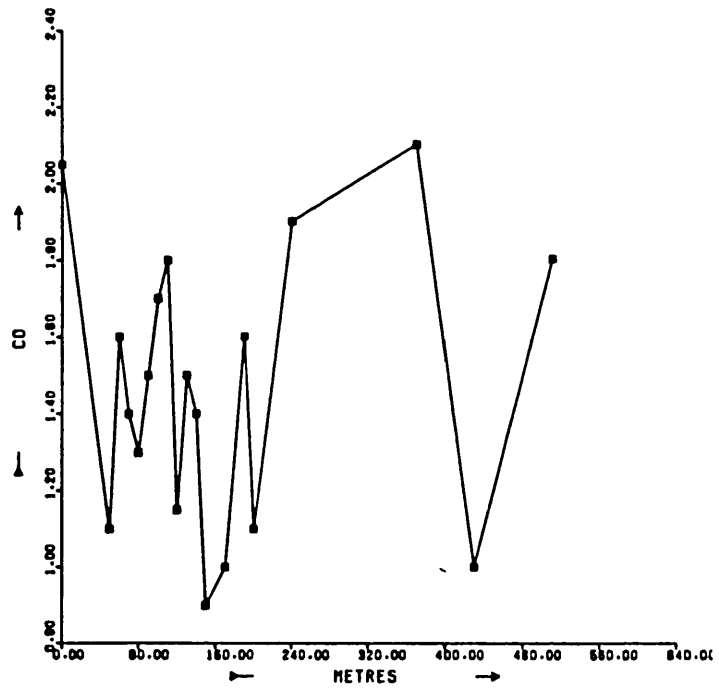
Figure 103: King Edward, distribution of Ni (ppm) and Co (ppm) along Diplorynchus biogeochemical traverse line (for geological legend see figure 8).

are similar to those at Chitina and Musangashi, despite higher Cr
in soils overlying ultramafic rocks, thus suggesting that Cr
uptake is controlled by an exclusion mechanism. The higher pH
of 6.0 in King Edward soils may also contribute to low Cr levels
in leaves by inhibiting Cr mobility. Iron values, also generally
higher in the soils, exhibit a higher mean but narrower range in
the leaves compared with Chitina and Musangashi. Consistently
low Co, Cu and Zn again demonstrate closely controlled uptake,
and Co does not correlate with Ni as it commonly does in rocks
and soils (figure 103). Manganese exhibits a considerable range,
but individual values are not related to soil Mn levels.

7.1.4.   Kingston

At Kingston, leaf samples were collected along the
traverse line near 20 soil sample sites (sample nos. 899-02 to 899-25).
Leaves from trees growing in the weakly mineralized zone have a
high Ni content of up to 154 ppm. Soil Ni values reach 12,500 ppm,
and it seems that the threshold concentration of Ni in the soil has
been exceeded and the partial exclusion principle is operating and
producing a clear biogeochemical Ni anomaly. The soil contains
high Cu, up to 1020 ppm in the mineralized zone, but although leaf
Cu values are slightly elevated to a maximum of 14 ppm, a threshold
does not seem to have been exceeded, and there is no biogeochemical
Cu anomaly comparable with the Ni anomaly (figure 104). Chromium
values in the leaves are unusually low, despite a high soil Cr
level, and this is again tentatively attributed to the high soil
pH of about 6.0, which limits Cr mobility and availability. Iron,
Co, Zn and Mn values are clearly controlled in the usual way (figure
105).

7.1.5.   Munali

Along the Munali soil traverse, the leaf samples
contain around 7 ppm Ni over background gabbro and 14 to 20 ppm Ni
across the mineralized zone (sample nos. 189-01 to 189-34). The
Munali mineralization is massive sulphides, but Ni values in the
leaves of trees rooted in the overlying soil are much lower than
those encountered over weakly disseminated mineralization at Kingston.
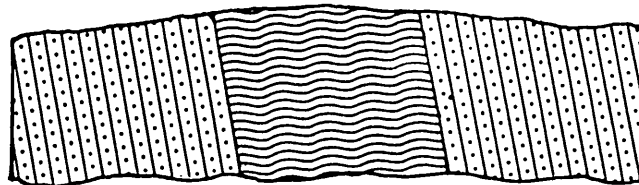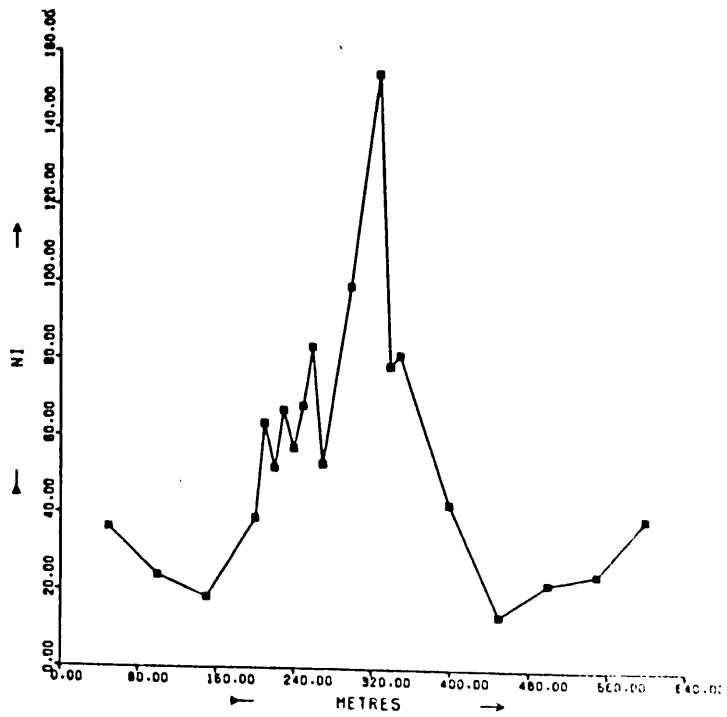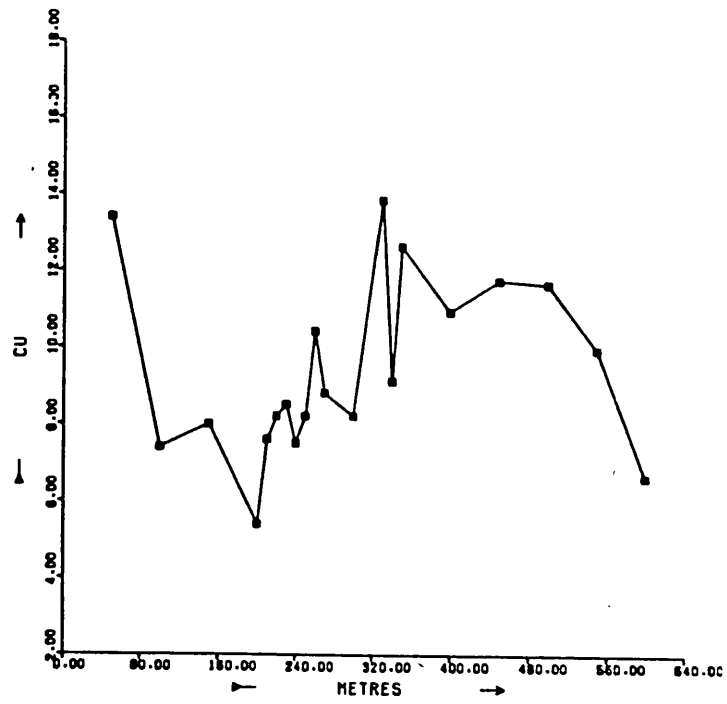
Figure 104: Kingston, distribution of Ni (ppm) and Cu (ppm) along Diplorynchus biogeochemical traverse line (for geological legend see figure 13).

The Ni uptake control mechanism does not break down at Munali, because the Ni threshold in the soil is not exceeded, and perhaps partly because the soil is highly ferruginous. The highest Ni level in the soil of the Munali mineralized zone is 6500 ppm compared with up to 12,500 ppm Ni at Kingston. The Munali soil is slightly more ferruginous with up to 25.5% Fe compared with 21.0% at Kingston, and possibly Ni availability is limited by the extremely high concentrations of secondary Fe oxides in the soils. The leaves contain concentrations of Cr, Fe, Co and Mn found to be typical in the other field areas, showing that the normal uptake control mechanisms for these metals are operative. The Cu content of the leaves over the Munali gabbro and mineralized zone reaches only 5 ppm despite soil Cu levels of up to 940 ppm and a pH range of 5.2 to 6.0 (figure 106). However, in the leaves of trees growing on schist at the northeast end of the Munali traverse, Cu values rise to 10 ppm, reflecting the combination of elevated soil Cu content of up to 1045 ppm and increased Cu availability due to the lower pH of about 4.4. Iron uptake appears to be similarly affected, with less than 200 ppm in the leaves of trees from the ferruginous soils over the mineralized zone, but up to 747 ppm in the soil over schist containing around only 6% Fe (figure 107).

7.1.6. The significance of Diplorynchus biogeochemistry

In the five field areas studied, Diplorynchus leaves contain generally similar amounts of Zn, indicating closely controlled uptake. The Mn content of leaves is relatively variable, but seemingly unrelated to soil Mn content, and equally controlled uptake is inferred. The amount of Fe taken up by individual plants is also subject to significant variation. Chromium uptake is controlled at a low level, and is perhaps influenced by soil pH. However, in view of the poor precision of the Cr biogeochemistry data, little significance is attached to the very limited variation in Cr values seen in Diplorynchus leaves. Cobalt and Cu uptake is generally low, and Cu uptake can be seen to be affected by pH at Munali. In the mineralized soils at Kingston and Munali, anomalous Co and Cu levels are found, but the uptake
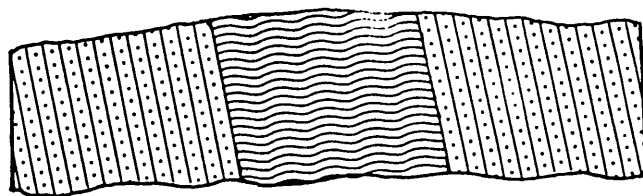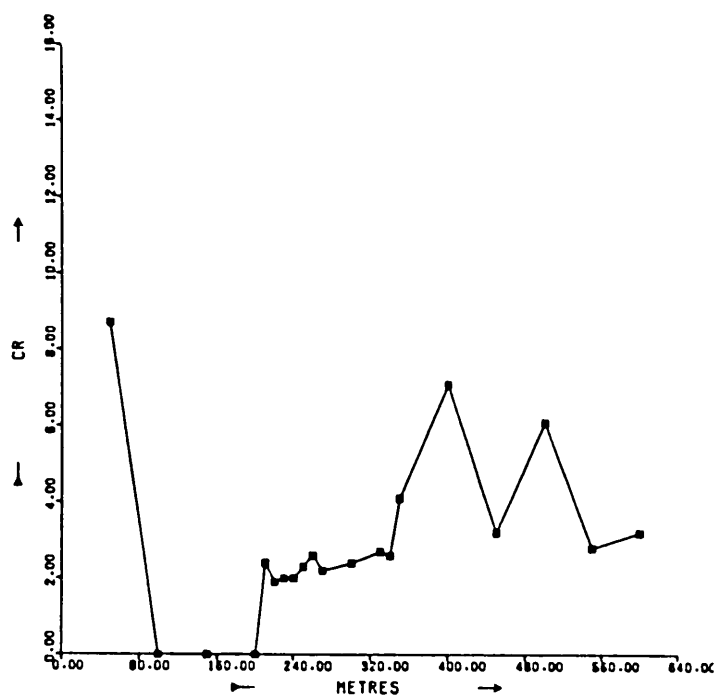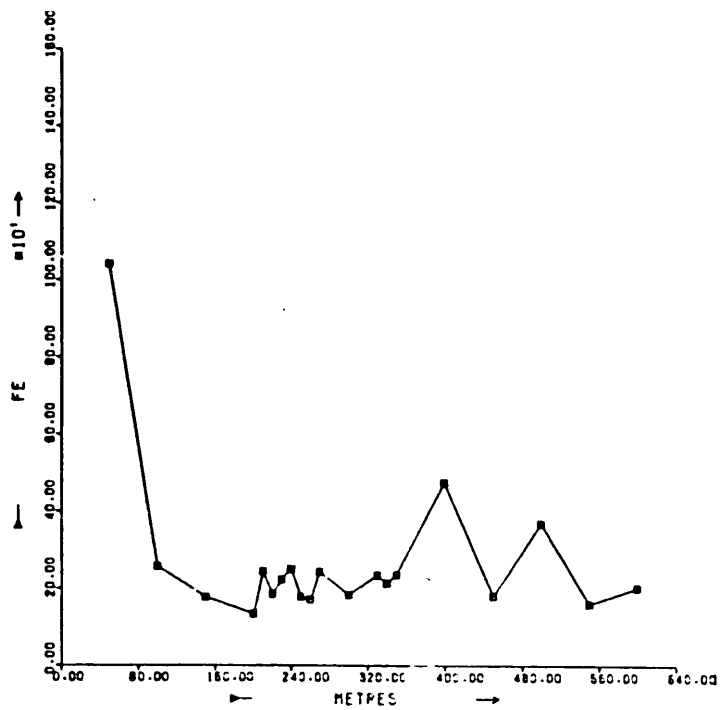
Figure 105: Kingston, distribution of Cr (ppm) and Fe (ppm) along Diplorynchus biogeochemical traverse line (for geological legend see figure 13).

thresholds are not exceeded, and there are no biogeochemical
Co and Cu anomalies. Thus, factors other than the total metal
content of the soil (e.g. Eh, pH, clay mineral content) contribute
to determining metal uptake by plants. Nickel uptake is clearly
not closely controlled because Ni soil anomalies are invariably
reflected by an increased Ni level in leaf samples. At Kingston,
where the soils contain up to 12,500 ppm Ni, the leaves contain
exceptionally high levels of Ni up to 154 ppm. However, over
mineralization at Munali the soils contain up to 6500 ppm Ni,
but leaf Ni content does not exceed 20 ppm. The Ni uptake control
mechanism therefore appears to break down where there is more than
6500 ppm Ni in the soil, subject to variations in soil chemistry.
Highly ferruginous soils appear to restrict the availability of
Ni to Diplorynchus, and this constitutes a serious biogeochemical
prospecting disadvantage,as soils over potentially economic
primary nickel mineralization are usually ferruginous.

7.2. Combretum ghasalense

Combretum leaves were collected over the mineralized
Munali intrusive and the non-mineralized Chombwa and King Edward
intrusives (table 29).

7.2.1. King Edward

At King Edward 33 combretum samples were obtained
along the soil traverse line (sample nos. 589-01 to 589-39). The
leaves of most trees growing over ultramafic rock contain more
than 10 ppm Ni, and the maximum value of 23 ppm occurs on the margin
of a 2500 ppm Ni soil anomaly. Over gabbroic contact rocks and
limestone the leaves contain less than 10 ppm Ni. The highest Cr
in leaves occurs in conjunction with the highest Ni, but not with
the Cr soil anomaly which occurs over the peridotite unit (figure 108).
The mean leaf Cr content is 12 ppm, higher than typical Cr levels
in Diplorynchus, despite a fairly high pH of about 6.0. There is
a wide range of Fe values not closely related to soil Fe content,
and the maximum of 1150 ppm exceeds the highest Fe value found in
Diplorynchus leaves. Similarly the Zn range of 14 to 76 ppm is much
greater than in Diplorynchus, and the mean of 31 ppm is higher,
although Zn uptake still appears to be closely controlled and largely
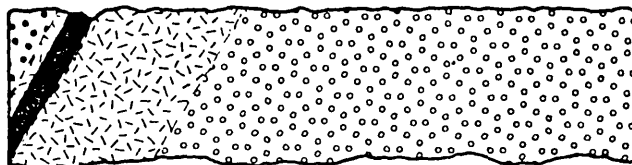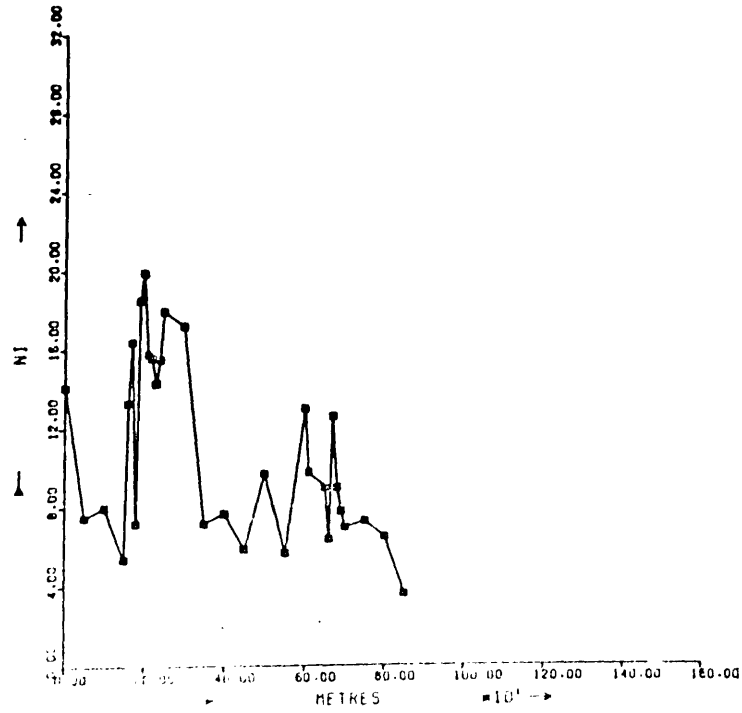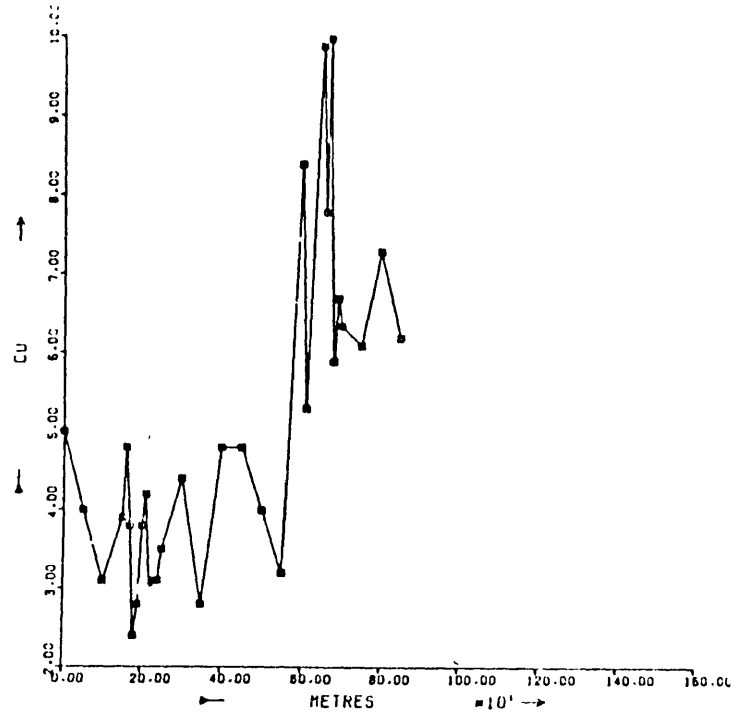
Figure 106: Munali, distribution of Ni (ppm) and Cu (ppm) along Diplorynchus biogeochemical traverse line (for geological legend see figure 9).

independent of soil Zn levels. Manganese uptake is also unrelated
to soil Mn levels, and the range of 59 to 229 ppm in leaves is rather
lower than Mn levels in Diplorynchus. Cobalt and Cu levels are
consistently low, although at 2 ppm the mean Co content of the
leaves is higher than in Diplorynchus.

Over the southern contact zone of the King Edward
intrusive there is the unusual occurrence of Combretum and Diplorynchus
trees growing in close proximity. The trace element content of the
leaves of two adjacent trees was found to reflect the general
observations pertaining to the differences between the two genera,
namely similar Ni and Cu contents, higher Co, Zn, Cr and Fe levels
and a lower Mn concentration in Combretum (table 30).

7.2.2. Chombwa

At Chombwa, 11 Combretum samples were collected
along the soil traverse line (sample nos. 299-01 to 299-25) and a
further 26 were taken elsewhere over gabbro and a Ni soil anomaly
related to a lens of meta-lherzolite (sample nos. 289-01 to 289-30).
Soil samples were taken near trees sampled off the soil traverse
line (sample nos. 235-01 to 235-30). The Ni background in the
leaves is around 7 ppm, and values rise to 24 ppm Ni over the meta-
lherzolite where the soil contains up to 1550 ppm Ni. Over the
dunite lens on the traverse line, where there is a maximum of
3000 ppm Ni in the soil, Ni concentrations in the leaves increase
to a massive 442 ppm, which suggests that the Combretum exclusion
mechanism breaks down at a much lower soil Ni concentration than is
the case with Diplorynchus. In the leaves the highest Cr values
occur in conjunction with high Ni, although the highest soil Cr
concentration occurs elsewhere. As at King Edward, there are higher
Cr, Zn and Fe means and maxima than are usually found in Diplorynchus,
although uptake of these elements appears to be controlled. Manganese
again exhibits a low mean compared with Diplorynchus. The Co content
of leaves is usually less than 2 ppm, but rises sharply to 11 ppm
in conjunction with the highest Ni. There is a more conspicuous Co
anomaly than Ni anomaly over the meta-lherzolite lens (figure 109).
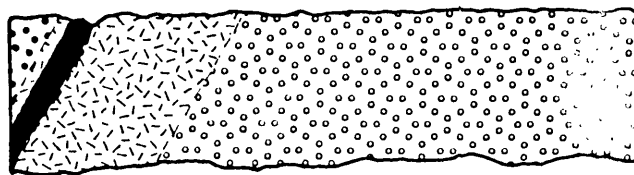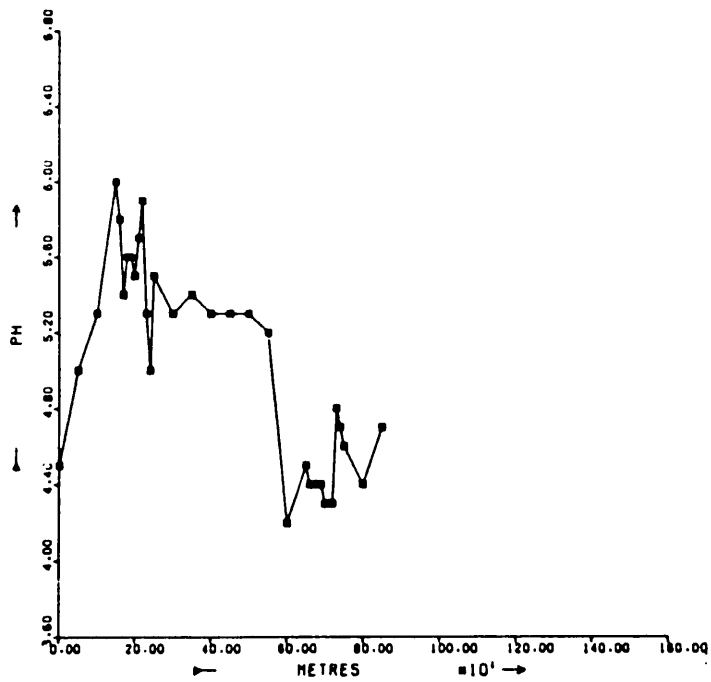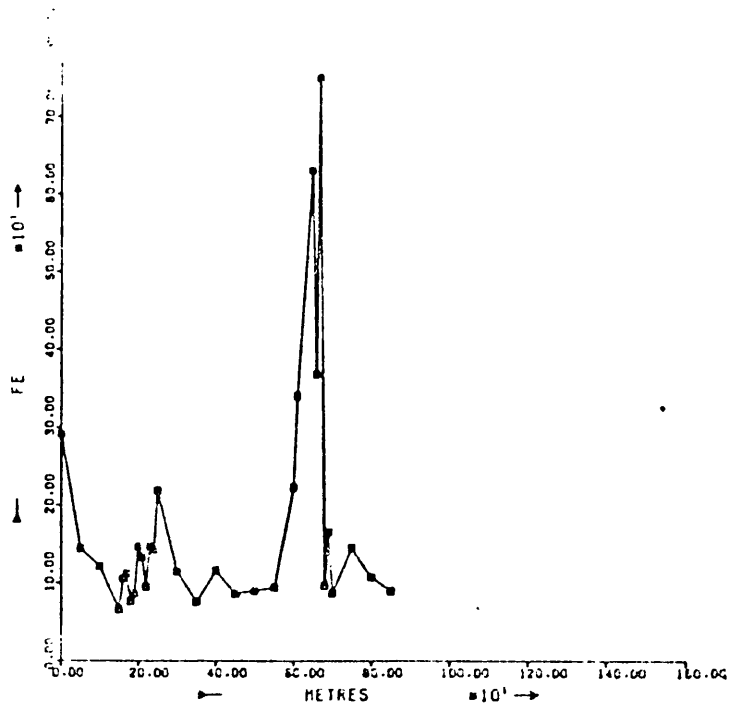
Figure 107: Munali, distribution of soil pH and Fe (ppm) along Diplorynchus biogeochemical traverse line (for geological legend see figure 9).

Copper uptake is typically low, and is apparently unaffected by the drop in soil pH from over 6.0 in the south of the sampled area to less than 5.0 along the traverse further north.

7.2.3. Munali

Over the southeastern part of the Munali gabbro, 22 leaf samples were collected (sample nos. 199-01 to 199-23), along with nearby soils (sample nos. 145-01 to 145-23). The levels of all trace elements are comparable with background levels for Combretum at King Edward and Chombwa and the soil pH ranges from 4.5 to 5.9. Two slightly stunted trees on the edges of a nearby gossan outcrop in the southeastern part of the intrusive were also sampled (sample nos. 199-89 and 199-90). The soil near these trees contains high concentrations of 5000 ppm Ni, 350 ppm Co, 600 ppm Cu and 27.5% Fe (sample no. 145-88). The leaves of the two trees contain high levels of 174 and 205 ppm Ni, indicating substantial Ni uptake despite the high Fe content of the soil. Iron in the leaves is higher than typical for Combretum at 1690 and 2340 ppm, but it is not realistic to assess whether this level represents the breakdown of the Fe exclusion mechanism (figure 110). Cobalt and Cu values are within the normal range, at 7 and 9 ppm Co and 8 and 9 ppm Cu, as are the levels of Zn, Cr and Mn.

7.2.4. The significance of Combretum biogeochemistry

The pattern of trace element uptake in Combretum resembles that for Diplorynchus. In general, however, Combretum takes up slightly higher concentrations of Zn, Cr, Co and Fe, and a little less Mn. Combretum accumulates high concentrations of Ni at relatively low soil Ni levels, suggesting that its Ni exclusion mechanism breaks down at a lower threshold, perhaps about 3000 ppm (in conjunction with the appropriate soil chemistry conditions). However, there is no discrimination between mineralized and non-mineralized locations, since leaves from trees on non-mineralized soil at Chombwa contain up to 442 ppm Ni, compared with a maximum of 205 ppm Ni in leaves from trees near gossan at Munali. In the samples examined, there is no evidence to suggest that thresholds of other metals are exceeded, and only biogeochemical Ni anomalies are encountered.
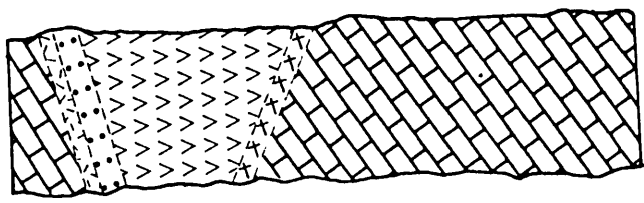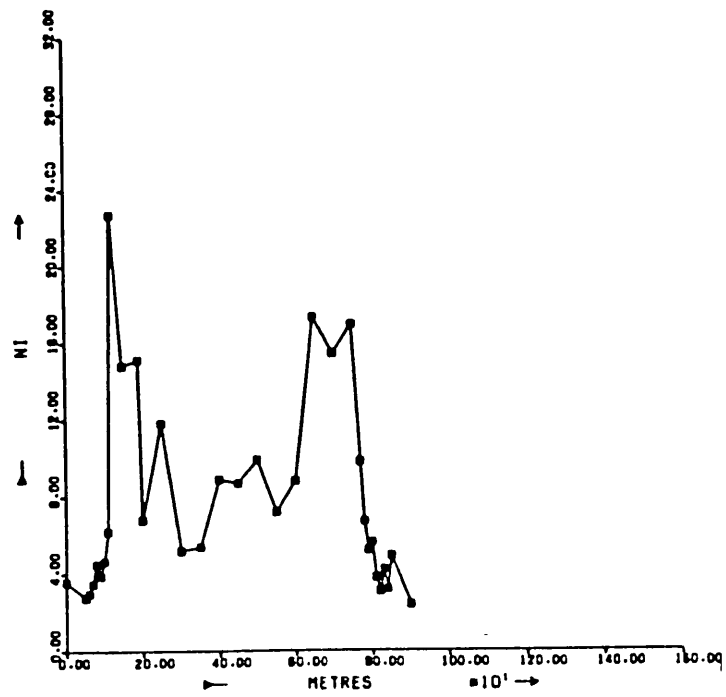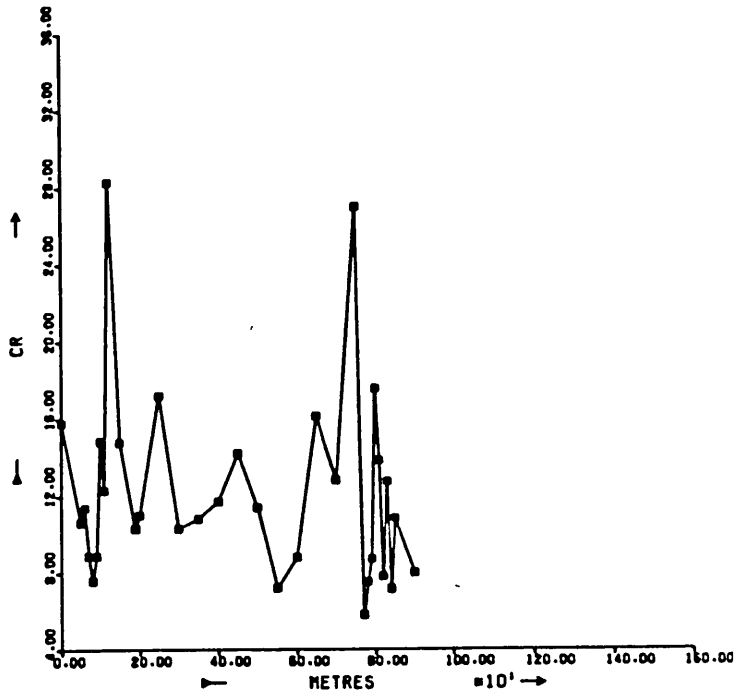
Figure 108: King Edward, distribution of Ni (ppm) and Cr (ppm) along Combretum biogeochemical traverse line (for geological legend see figure 8).

7.3.   Dicoma niccolifera

During fieldwork, general observation of the flora
was maintained in order to identify any vegetation characterstic
of nickel-rich soils. This met with success only at Kingston,
where the small Dicoma niccolifera flower was noted. Species of
Dicoma have also been observed over the Great Dyke of Rhodesia
(Wild, 1970).

Leaves from a specimen of Dicoma were dried and
ashed in the usual manner and yielded 9.9% ash. The leaves contain
2530 ppm Ni, a concentration vastly in excess of levels in nearby
Diporynchus samples which reach a maximum of 154 ppm. The leaves
also contain unusually rich concentrations of 20 ppm Co, 50 ppm Cu
and 91 ppm Cr, though enrichmant of these elements is not as dramatic
as for Ni. The levels of 24 ppm Zn and 248 ppm Mn in the laves are
similar to the concentration of these elements found in Diplorynchus.

Dicoma niccolifera presumably prospers on nickel-rich
soils because it assimilates high concentrations of Ni without toxic
effects. However, its distribution is clearly relatively limited, and
it was not found on almost equally nickel-rich soil overlying
substantially higher grade mineralization at Trojan, a few km away
from Kingston.

7.4.   Discussion

There is little doubt that the optimum biogeochemical
sampling medium was used in the present studies. Other researchers who
have dealt with the biogeochemistry of Ni in recent years have all commended
the use of leaves as the optimum sampling medium. Wilding (1965)
investigated the Ni and Cu content of several Central African trees,
including species of Diplorynchus and Combretum, and states that
leaves generally contain more Ni than twigs or bark, and that the Ni
distribution pattern is a little better defined on the basis of Ni in
leaves than twigs or bark. The biogeochemical results obtained by
Cole (1971) in Rhodesia substantiate Wilding's findings. Hall, Both

	Chombwa 37		King Edward 33		Munali 23	
	Mean	Range	Mean	Range	Mean	Range
% ash	6.0	4.2 - 9.0	7.0	4.7 - 10.8	7.1	3.2 - 9.9
Ni	35	3 - 442	8	2 - 23	7	3 - 14
Cu	5	3 - 11	4	3 - 8	6	3 - 11
Co	2	1 - 11	2	2 - 4	3	1 - 11
Zn	31	15 - 58	31	14 - 76	21	6 - 28
Cr	17	5 - 43	12	6 - 28	10	3 - 15
Fe	379	86 - 1720	477	241 - 1150	883	317 - 1490
Mn	146	22 - 757	129	59 - 229	72	31 - 216

Table 29: Trace element content of leaves of Combretum ghasalense (ppm)

	Diplorynchus	Combretum
Ni	24	23
Cu	4	5
Co	2	3
Zn	16	42
Cr	6	28
Fe	172	850
Mn	694	102

Table 30: Comparative trace element content of leaves of adjacent
Diplorynchus and Combretum trees at King Edward (ppm)

and Smith (1973) determined Ni and Cu in leaves, twigs, bark, wood
and roots of Melaleuca cheathiana in Western Australia and concluded that
leaves were the most satisfactory organ in that the results showed
least background variability and greatest anomaly contrast. The
detection of biogeochemical Ni anomalies in trees rooted in soil and
weathered rock over mineralization has regularly been successful.
Wilding (1965) and Cole (1971) both found up to 1350 ppm Ni in the ash
of leaves of various Combretum species over the Empress orebody in
Rhodesia, and Hall, Both and Smith (1973) found 45 ppm Ni in leaves (dry
weight) of Melaleuca in Western Australia. The same researchers have
met with varying success in distinguishing mineralization from non-
mineralized ultramafic rock on the basis of Ni biogeochemistry. Wilding
(1965) found that leaf ash of some specimens of Diplorynchus and
Brachystegia growing over non-mineralized serpentinite contained more
than 1000 ppm Ni, compared with around 700 ppm Ni in leaf ash from
members of the same species over nearby mineralization. The data
published by Hall, Both and Smith (1973) indicates that Melaleuca leaves
contained 16 to 28 ppm Ni over non-mineralized ultramafic rocks flanking
the mineralization over which they found their biogeochemical anomaly of
45 ppm Ni. Cole (1971), however, was able to show clearly that a 1500
ppm Ni soil anomaly over serpentinized gabbro was a near-surface
phenomenon because the ash of Combretum leaves were contained only
50 ppm Ni compared with up to 1350 ppm Ni over nearby mineralization.

There results exemplify the importance of rooting depth
in the accumulation of Ni by trees. The active roots of phreatophytes
are mainly embedded in the zone of semi-permanent saturation between
high and low water table levels. Within this zone, secondary minerals
constitute a significant source of trace elements available to trees, and
high concentrations of Ni may accumulate in the upper part of this zone
as evidenced by several pit profiles. Although Ni concentrations in primary
mineralization are much higher than in non-mineralized ultramafic rock,
during weathering and oxidation much more Ni is lost in solution due
to the lower pH and hence higher Ni mobility created by the oxidation
of sulphides, and also Ni has an increased tendency to maintain its close
association with Fe and thereby accumulates in the B horizon of the soil.
Weathering non-mineralized ultramafic rock creates a high pH environment
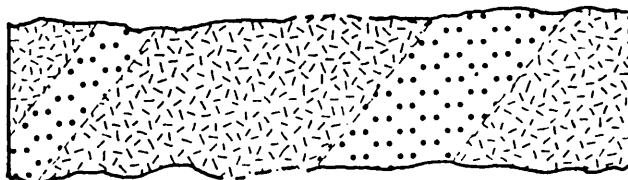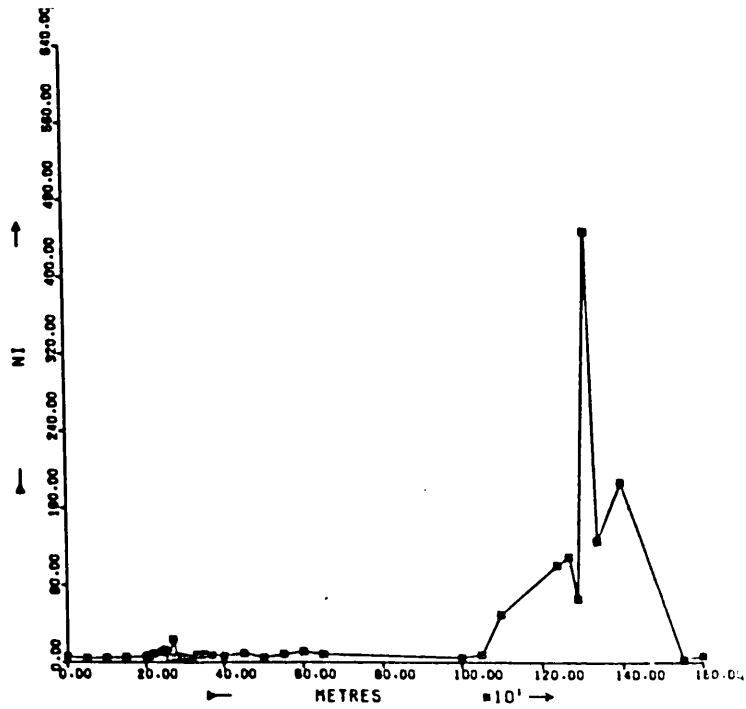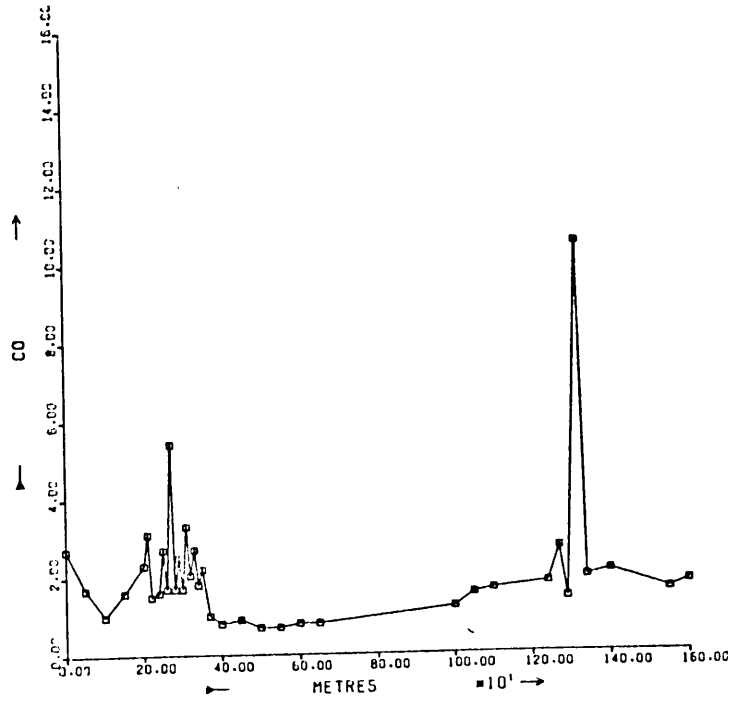
Figure 109: Chombwa, distribution of Ni (ppm) and Co (ppm) along Combretum biogeochemical traverse line (for geological legend see figure 7).

which favours the precipitation and assimulation of Ni. As a result
Ni concentration in the upper C horizon from which trees obtain part of
of their trace element supply, are not necessarily significantly
different over mineralization compared with non-mineralized ultramafic
rock.

For example at Munali and Chombwa, very marked Combretum
Ni anomalies are geographically near to the pit profiles studied in each
area, and it seems reasonable to speculate that the distribution of
Ni observed in the soil profile in the pits is more or less applicable
to the soil in which these Combretum trees are rooted. Over mineralization
at Munali, Combretum leaves contain a maximum of 205 ppm Ni and the
upper C horizon of the nearby soil contains 18,000 ppm Ni; over
non-mineralized peridotite at Chombwa, Combretum leaves contain a
maximum of 442 ppm Ni and the upper C horizon of the nearby soil
contains 15,000 ppm Ni. Thus, high Ni concentrations in the upper C
horizon cause Ni uptake mechanisms in trees to break down, producing
clearly anomalous Ni levels in leaves, but the C horizon Ni
enrichment and hence the biogeochemical anomaly may be derived either from
mineralization or ultramafic rock.

The magnitude of the biogeochemical Ni anomaly will depend
upon the amount of Ni enrichment and density of root in the upper C
horizon. At Chitina, soil anomalies in excess of 400 ppm delineated
during prospecting are underlain by non-mineralized peridotite and the
Chitina pit, sited on one such anomaly, located 6000 ppm Ni in the
upper C horizon. The biogeochemical response to a similar soil anomaly
which was not pitted was a maximum value of 19 ppm Ni in Diplorynchus
leaves. If around 6000 ppm Ni is also present in the upper C horizon in
the immediate vicinity of the biogeochemical anomaly it seems that
this quantity of Ni, perhaps coupled with other soil conditions,
is insufficient to exceed the threshold for exclusion mechanism breakdown
in Diplorynchus. There is a similar weak biogeochemical anomaly of
20 ppm in Diplorynchus leaves over mineralization at Munali
and this again, in the absence of pitting nearby, may be due to insufficient
Ni accumulation in the upper C horizon to effect exclusion mechanism
breakdown. Therefore the accumulation of sufficient Ni in part of the
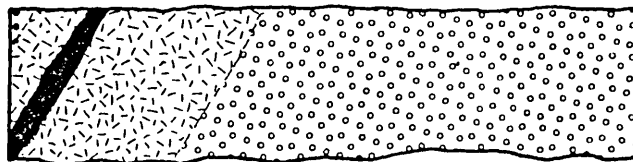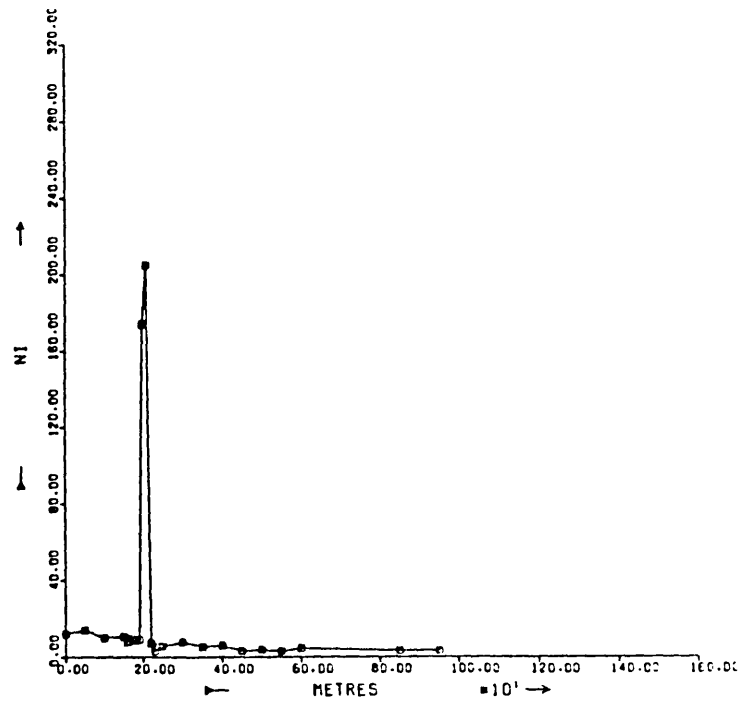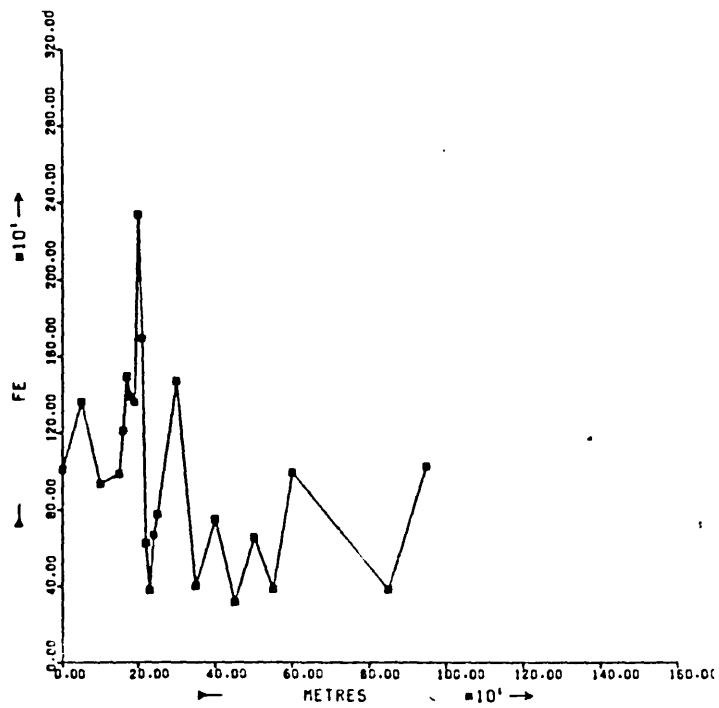
Figure 110: Munali, distribution of Ni (ppm) and Fe (ppm) along Combretum biogeochemical traverse line (for geological legend see figure 9).

rooting zone of the species studied is paramount for effecting
exclusion mechanism breakdown producing anomalous Ni concentrations
in leaves. However this upper C horizon Ni enrichment is not unique
to weathered rock overlying mineralization, and owing to the
higher pH, is often more prevalent over non-mineralized ultramafic
rock.

The concentrations of Cu, Co, Zn, Cr, Fe and Mn in
leaves encountered in this research are normally within the range
considered by Brooks (1972) to be more or less typical. Other Ni
biogeochemistry researchers have not located strongly anomalous
concentrations of these metals in vegtation growing over mineralization
or ultramafic rock. Wilding (1965) found no biogeochemical Cu anomalies in
trees over mineralization or ultramafic rocks in Rhodesia, with Cu
concentrations in leaf ash of about 50 to 300 ppm. Cole (1971) claimed
that over mineralized gabbro, Combretum species contained up to 200
ppm Cu in leaf ash compared with 10 ppm or so over non-mineralized
gabbro and serpentinized gabbro (with anomalous Cu levels in the
overlying soil) in the same vicinity. However, a range of 10 to
200 ppm Cu in Combretum leaf ash probably represents about 0.5 to
10 ppm Cu in the leaf, which is the same range as observed for Combretum
in the current research where values at the top end of the range do not
necessarily come from trees over mineralization. Hall, Both and Smith (1973)
present data which indicate that the Cu, Co and Zn levels are closely
similar in leaves of two Melaleucia trees containing background amounts
of 5 ppm Ni and anomalous amounts of 28 ppm Ni, and Cole (1971a) states
that Eucalyptus and other plants in the vicinity of and over the Kambalda
nickel orebody, Western Australia, do not contain high concentrations of
metals other than Ni.

However, variations within the typical range for these
metals in leaves are clearly related to bedrock geochemistry; the Cr
content of Diplorynchus leaves increases over ultramafic lenses at
Chitina and Musangashi; the Co content of Combretum leaves increases over
peridotite at Chombwa; and Cu and Fe uptake by Diplorynchus increases with

a fall in pH over schist at Munali. Hall, Both and Smith (1973) found the leaves of some specimens of Melaleucia growing in soil over mineralization to contain elevated concentrations of Cu, Zn, Cr Fe and Mn (in addition to anomalous Ni concentrations) compared with other members of the same species in the vicinity, and largely to reflect the soil geochemistry. These variations in essential element biogeochemistry may contribute to the interpretation of biogeochemical Ni anomalies, for example anomalous Ni coupled with high Cr in Diplorynchus leaves at Musangashi suggests ultramafic rock at depth, whereas anomalous Ni with high Fe in Combretum leaves at Munali indicates mineralization.

From the data produced in this work and most of the earlier research, biogeochemistry appears to contribute little to distinguishing Ni anomalies associated with mineralization. Geobotany is useful in locating serpentinites by virtue of the diminution in size and density of species growing on serpentine soils compared with those growing in the surrounding countryside, and this type of geobotanical anomaly is evident at Paulwi. However, the plants growing on soil overlying primary nickel mineralization do not appear to be affected in the same way, possibly because low Ca in serpentine soil, rather than high Ni, is mainly responsible for the morphological changes and reduced density of trees. Specialized floras, including Ni accumulator plants such as Dicoma niccolifera, often abound on ultramafic rocks but are indiscriminate indicators of high Ni concentrations in the soil rather than primary mineralization in particular. Wilding and Cole have both encountered marked reduction in the number of trees over primary nickel mineralization in Central Africa and Australia although none were evident in this investigation. It seems probable that these "clearings" are produced by Cu, rather than Ni, toxicity, because Cu soil anomalies were associated with the nickel mineralizations studied by Wilding and Cole, and "copper clearings" are a very characteristic feature of localities underlain by sedimentary copper mineralization in the Katanga rocks of Central Africa. The geobotanical indicators discussed here are easily taken into account during prospecting but offer no especially useful guide to the presence of nickel mineralization.

Sample no.	Ni	Cu	Co	Zn	Cr	Fe	Ti	Mn	S	pH
525-09	1775	235	175	183	3900	18.0	2450	1260	60	6.4
525-08	2200	178	225	160	2250	16.0	2350	1760	45	6.5
525-07	1750	138	170	125	1400	11.9	2250	1300	135	7.3
525-06	1150	143	110	100	850	11.3	2900	990	170	6.2
525-05	1250	146	135	112	1300	10.8	2350	1360	-	7.1
525-03	135	72	45	45	200	5.6	2050	790	130	6.2
525-01	500	138	70	58	300	6.9	2050	880	50	7.0
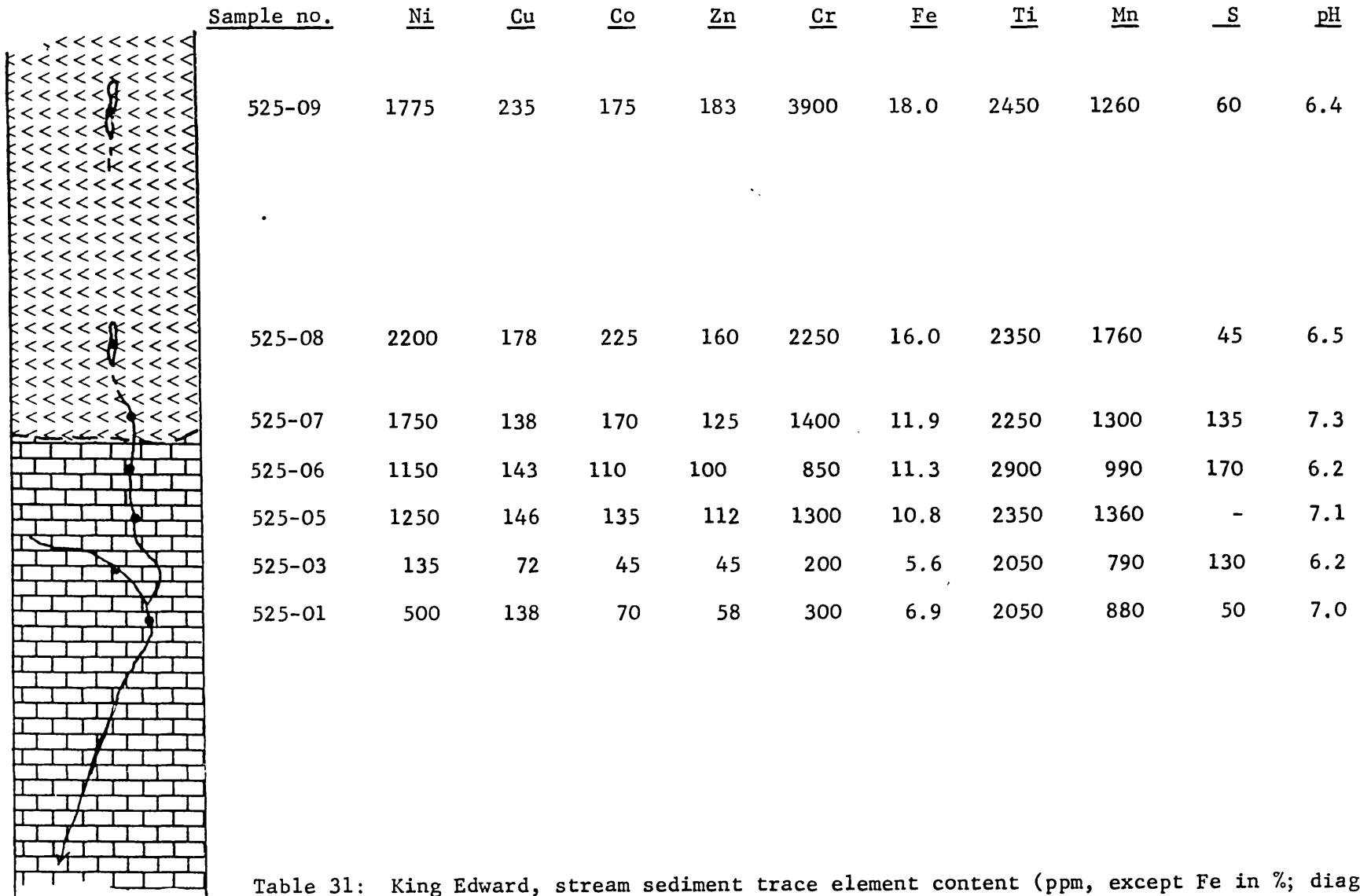
Table 31: King Edward, stream sediment trace element content (ppm, except Fe in %; diagram topologically adjusted, approx. scale 1:12,500; for geological legend see figure 8)

8.   THE DISTRIBUTION OF ELEMENTS IN STREAM SEDIMENTS

Sediment samples were collected at approximately
100 m intervals for some distance along streams draining intrusives
and their coarse and fine fractions were analysed by atomic
absorption spectroscopy for trace metals. The pH and S content
of samples was also determined, using the intermediate and coarse
fractions respectively. The optimum pattern of sampling and analysis
deduced from these detailed studies was applied to regional drainage
reconnaissance. Stream sediment sample analytical results are listed
in appendix 2.

8.1.   Areas of free-flowing stream drainage

Streams which are active during the wet season,
become dry as the water table falls in the dry season, and have
beds of sandy sediment, are found draining the mineralized Munali
and Trojan intrusives, the weakly mineralized Kingston peridotite,
and the non-mineralized Paulwi and King Edward intrusives. The
more conventional fine fraction trace element dispersion patterns
were established along with pH and S data with a view to determining
the optimum combination of elements for distinguishing between mineralized
and non-mineralized localities. The association of these elements with
secondary Fe minerals such as goethite and ferro-manganese coatings,
especially in the coarse fraction,was again examined to ascertain the
relevance of this aspect of dispersion to mineral exploration.

8.1.1.   King Edward

Sediment samples were collected from the single sandy
stream draining the King Edward intrusive (figure 8). Samples from
the upper reaches of the stream come from seepage depressions which
in the wet season overflow to link up with the stream bed proper.
High values of up to 2200 ppm Ni, 225 ppm Co, 3900 ppm Cr and 18.0% Fe
occur in sediments from the stream bed overlying peridotite and high
concentrations of these elements persist for at least 200 m downstream
beyond the limestone contact (table 31). However, these levels fall
sharply below the confluence with a major right bank tributary rising
on limestone to 70 ppm Co, 300 ppm Cr and 6.9% Fe, although evidence
of the ultramafic intrusive is still present due to an elevated Ni
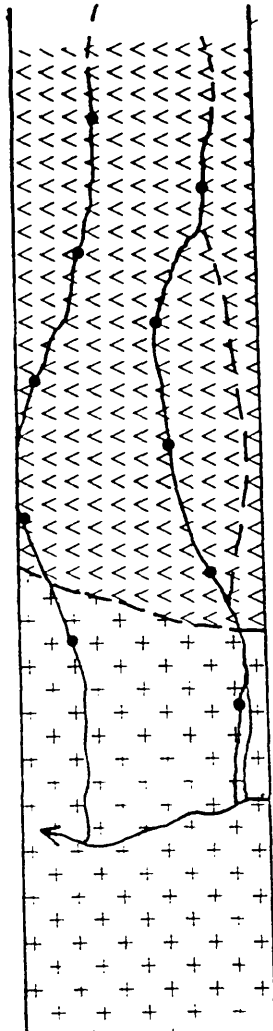
Sample No.	Ni	Cu	Co	Zn	Cr	Fe	Ti	Mn	S	pH
325-01	400	96	65	109	1550	5.8	3650	710	30	6.0
325-06	700	62	75	68	1500	5.7	1700	900	65	6.3
325-02	700	100	85	80	1100	7.2	2550	1000	40	6.3
325-07	700	42	75	71	1900	5.3	1600	850	75	6.6
325-03	600	92	75	97	1100	6.3	2800	1000	30	6.1
325-08	900	62	90	83	2000	7.0	2050	1120	30	6.4
325-04	600	140	100	97	750	10.0	3850	1040	75	5.9
325-09	950	68	105	79	2400	7.0	1650	1120	120	6.5
325-05	400	89	60	100	1100	5.6	3500	760	60	6.1
325-10	450	41	50	77	1250	4.6	2350	830	180	6.5

Table 32: Paulwi, stream sediment trace element content (ppm, except Fe, in %; diagram topologically adjusted, approx. scale 1:12,500; for geological legend see figure 11).

level of 500 ppm. Moderately high Cu concentrations, up to 235 ppm, can also be traced beyond the confluence, whereas evidence of slightly elevated Zn, reaching 183 ppm, is lost. Sulphur values vary erratically between 45 and 170 ppm, while Ti and Mn concentrations remain similar throughout the drainage system at about 2000 and 1000 ppm respectively.

Despite the high pH of the sediments, ranging from 6.2 to 7.3, there is a good downstream dispersion of most elements for at least 200 m below the peridotite-limestone contact. Beyond this distance, tributary dilution causes a substantial drop in the levels of most elements occuring in anomalous concentrations in the stream draining the intrusive, but anomalous Ni values and moderately high Cu values persist below the confluence.

8.1.2.　Paulwi

The sediments of two streams draining pyroxenite at Paulwi were each sampled over a distance of about 400 m (figure 11). The sediments contain high Ni and Cr with maxima of 950 ppm Ni and 2400 ppm Cr (table 32). The Ni level falls to about 400 ppm as the streams flow onto granite gneiss, but this is still likely to be much higher than the Ni content of the granite gneiss, and therefore represents downstream dispersion from the pyroxenite. Cobalt follows the same distribution pattern as Ni. The Zn, Ti, Mn, and S content of the sediments is similar to that at King Edward, but the Cu and Fe content is lower at 41 to 140 ppm Cu and 4.6 to 10.0% Fe. Anomalous concentrations of Ni and Cr are the principal expression of the Paulwi pyroxenite in the stream sediments. Because of the short distance over which the Paulwi streams were sampled little deduction can be made concerning downstream dispersion of trace elements, although all characteristics of the pyroxenite are still evident immediately after the streams pass onto granite gneiss.
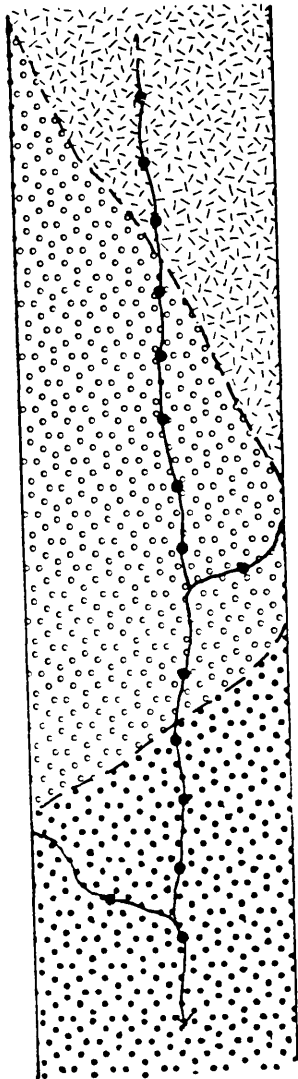
Sample no.	Ni	Cu	Co	Zn	Cr	Fe	Ti	Mn	S	pH
125-05	340	470	70	22	80	14.8	2350	320	70	5.5
125-06	320	290	75	20	100	23.5	2150	230	155	5.5
125-07	285	350	60	18	80	15.5	2550	260	78	5.5
125-08	240	238	55	17	85	19.0	2400	230	195	5.4
125-09	255	180	70	23	80	14.0	2700	440	75	5.1
125-10	170	90	45	19	120	21.0	2400	200	120	5.2
125-11	160	120	40	20	90	17.0	2550	230	80	5.3
125-12	163	110	43	20	90	17.0	2375	200	125	5.4
125-17	800	48	110	24	310	33.5	2400	330	–	6.0
125-19	300	82	80	24	240	30.5	2700	270	190	5.4
125-20	215	69	65	23	105	13.8	3150	380	–	5.6
125-21	190	63	55	19	95	13.5	3050	280	–	5.7
125-22	185	65	60	19	200	24.0	2350	200	–	5.6
125-24	80	290	35	14	60	5.8	2750	280	–	5.2
125-25	135	104	35	15	95	9.4	2400	230	–	5.7

Table 33: Munali, stream sediment trace element content (ppm, except Fe, in % ; diagram topologically adjusted, approx. scale 1:12,500; for geological legend see figure 9).

8.1.3.   <u>Munali</u>

A stream sampled over 1400 m at Munali drains the
northeast corner of the gabbro, and rises near outcrops of ferruginous
gabbro and a diamond drillhole which intersects at depth 0.87% Ni
over 4.20 m (figure 9).   Only the first 300 m or so of the stream
cuts through gabbro, but although the stream then runs on schist
for the remaining 1100 m sampled, a left bank tributary draining
a locally non-mineralized part of the gabbro brings in more material
derived from the gabbro, while a right bank tributary draining the
schist causes dilution of gabbroic sediment.   The stream and all
tributaries are sandy, and the pH of sediments is about 5.5,
rendering most metals reasonably mobile.

Near the headwaters the Ni content is 340 ppm,
accompanied by a high Cu concentration of 470 ppm (table 33).   The
Ni and Cu values decline downstream over 700 m, but Ni values then
rise to 300 ppm below the confluences with the left bank tributary
in which the sediments contain up to 800 ppm Ni (sample nos. 125-13 to
125-17).   However, Cu values decline still further after the
confluence to around 60 ppm, because the Cu content of the sediments
of the left bank tributary is low, at around 60 ppm.   Further down
the main stream Cu values in the sediments increase to 104 ppm and Ni
values fall to 135 ppm below the confluence with the right bank
tributary draining schist and containing up to 290 ppm Cu and 80 ppm Ni
(sample nos. 125-23 and 125-24).   The pattern of Co distribution in
the drainage system is similar to that of Ni.

The Fe and Cr content of the sediments of the left
bank tributary draining the gabbro are (like the Ni and Co content)
much higher than in the headwaters of the main stream, with values
of up to 37.0% Fe and 360 ppm Cr.   Below the confluence, therefore,
the levels of these elements rise to 30.5% Fe and 240 ppm Cr.
Throughout the drainage system the Mn content is low at around 300 ppm,
and there is about 20 ppm Zn and 2500 ppm Ti in most samples.
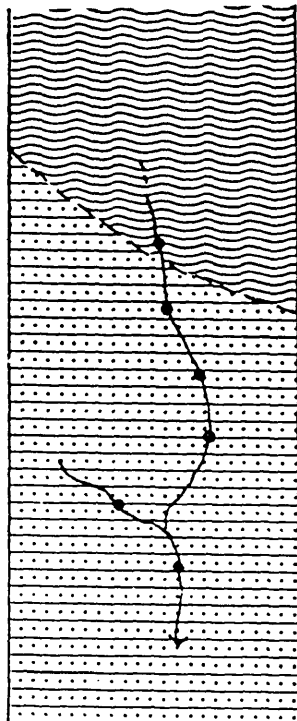
Sample no.	Ni	Cu	Co	Zn	Cr	Fe	Ti	Mn	pH
825-27	3400	90	185	142	7500	16.5	1050	1330	6.5
825-26	3300	137	190	147	7000	16.5	1500	1770	6.5
825-25	3250	124	185	210	7000	16.0	1700	1650	6.2
825-24	2850	113	160	142	5000	12.8	1750	1700	6.8
825-22	260	124	70	260	450	7.2	1800	1630	6.5
825-23	360	90	70	104	280	7.3	1900	1500	6.3

Table 34: Kingston, stream sediment trace element content (ppm, except Fe, in %; diagram topologically adjusted, approx. scale 1:12,500; for geological legend see figure 13).

The S content of the sediments is similar to
that at King Edward and is fairly erratic along the course of the
stream. The highest S value of 195 ppm occurs 400 m downstream
from the headwaters, but the sediment contains 190 ppm S at 1000 m
downstream, below the confluence with the left bank tributary
draining locally non-mineralized gabbro. The higher S values occur
in conjunction with the highest Fe in the sediments, and there
appears to be a significant positive correlation between Fe and S.

High Ni and Cu in Munali stream sediments indicates
the presence of mineralization. Nickel values are not especially
high compared with those encountered in non-mineralized areas, nor
compared with a tributary draining a non-mineralized locality at
Munali. There is fair downstream dispersion of the Ni and Cu
anomaly which can be identified some 500 m or more below source.

8.1.4.   Kingston

In a sandy stream draining weakly mineralized
serpentinite at Kingston there are high values of over 3000 ppm Ni,
16.0% Fe, 185 ppm Co and 7000 ppm Cr in the sediments near the
headwaters, and the concentrations of these elements fall only
slowly downstream as the drainage channel cuts across amphibolite
(figure 13; table 34). However, about 450 m from the headwaters,
the stream is joined by a right bank tributary which rises on
amphibolite and contains 260 ppm Ni, 7.2% Fe, 70 ppm Co and 450 ppm Cr
in the sediments. Below the confluence almost all sign of the Ni
anomaly is lost, with only 360 ppm Ni, 7.3% Fe, 70 ppm Co and 280 ppm Cr
in the stream sediments. The concentrations of other elements
are fairly uniform throughout the drainage system, at about 110 ppm Cu,
150 ppm Zn, 1700 ppm Mn and 1600 ppm Ti. In contrast to the high Cu
content of the stream draining the mineralized locality at Munali,
the Cu level in the Kingston stream is not anomalously high, reflecting
the lower grade of mineralization at Kingston. The very high Cr
levels suggest that silicate minerals in ultramafic rock, rather
than sulphides, may be the principal source of the high Ni concentrations.
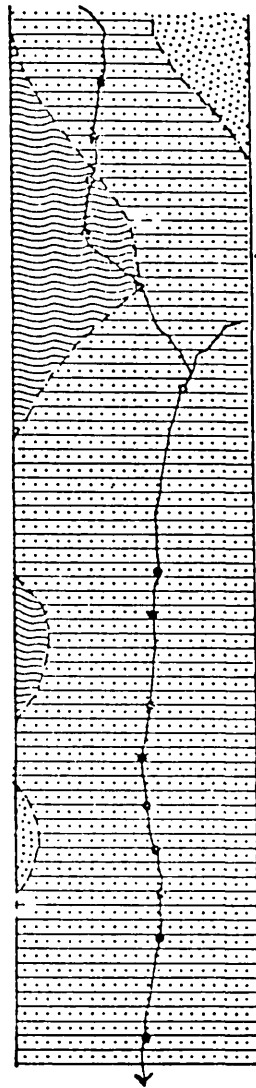
Sample no.	Ni	Cu	Co	Zn	Cr	Fe	Mn	Ti	S	pH
825-01	3300	1100	200	670	1200	7.3	1550	1000	235	6.2
825-02	4750	530	185	265	1605	10.0	1655	800	240	6.5
825-03	5000	830	180	240	1400	8.6	1390	650	305	6.8
825-04	6000	540	180	290	1800	9.8	1180	600	-	7.0
825-05	5000	600	175	420	2000	11.5	1080	700	350	7.0
825-06	1400	390	110	220	900	7.0	1320	1600	130	6.2
825-16	3250	260	135	220	900	7.0	8400	1100	-	-
825-17	2600	220	110	220	1200	7.5	4800	1400	85	7.1
825-19	4500	790	190	400	1200	7.0	9900	1300	-	-
825-20	3400	930	150	330	1150	7.1	2900	1700	-	7.2
825-21	1400	220	105	180	1050	7.0	1050	1500	-	-
825-35	1500	215	95	200	1000	6.8	1700	1650	-	-
825-36	3000	870	280	139	1000	9.3	8000	1500	-	6.7
825-37	1900	430	230	120	800	11.5	5300	1800	-	-
825-39	1425	360	138	137	900	7.3	910	2225	-	6.6

Table 35: Trojan stream sediment trace element content (ppm, except Fe, in %; diagram topologically adjusted, approx scale 1:15,000; for geological legend see figure 12).

Within the 500 m over which the Kingston stream was studied,
tributary dilution, rather than distance from source, is the
chief constraint on downstream dispersion of metals in sediments.

8.1.5. Trojan

The sandy stream draining Trojan Hill offers little
opportunity to assess downstream dispersion because it flows
downslope from or cuts across, the mineralized serpentinite unit
over much of the 850 m of its course prior to joining the vlei (figure
12). The sediments contain exceptionally high values of up to
6000 ppm Ni, 1100 ppm Cu and 670 ppm Zn, while Cr values are low,
at less than 2000 ppm, compared with Kingston sediments (table 35).
At Trojan there are higher S and Zn levels in the sandy sediments
than at Munali, with values of up to 350 ppm S and 670 ppm Zn, but
these are probably derived from the nearby pyritic argillite rather
than the mineralized serpentinite. Pyritic argillite exposed in
a pit at another locality at Trojan contains 1480 ppm S and 570 ppm
Zn (sample no. 855-27). Thus, as at Munali, anomalous concentrations
of Ni and Cu in the stream sediments best characterize the presence
of mineralization at Trojan.

8.1.6. Chinkozia

The stream sampled at Chinkozia drains a low order
Ni soil anomaly (figure 5). The stream runs over intrusive rocks
for most of the 3600 m sampled, but trace element concentrations
are consistently low, simply reflecting the norite parent material.
Nickel values vary from 65 to 190 ppm and show a general correlation
with Cr, which fluctuates between 35 and 180 ppm. Other elements
exhibit a narrower range, with around 40 ppm Cu, 50 ppm Co, 40 ppm Zn,
600 ppm Mn, 1500 ppm Ti and 4% Fe. The relatively close relationship
between Ni and Cr suggests that patches of more ultramafic rock
may be responsible for the elevated values. There is no evidence
of mineralization, and indeed the rather monotonous dispersion
pattern provokes very little comment.
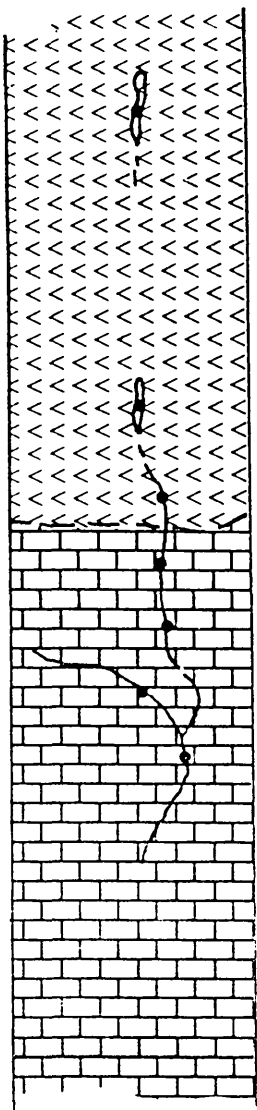
Sample no.	Coarse fraction content				Coarse-to-fine-fraction ratios			
	Ni	Cu	Fe	Mn	Ni	Cu	Fe	Mn
522-07	2000	98	13.8	5250	1.14	0.71	1.16	4.04
522-06	1660	114	16.0	4460	1.44	0.80	1.42	4.51
522-05	1970	110	14.5	6200	1.58	0.75	1.34	4.55
522-01	190	60	5.3	1225	0.38	0.43	0.77	1.39

Table 36: King Edward, stream sediment coarse fraction trace element content (ppm, except Fe in %) and coarse-to-fine size fraction ratios (diagram topologically adjusted, approx. scale 1:12,500; for geological legend see figure 8).

8.1.7.   The significance of multi-element behaviour

                In the field areas studied, the combination of Ni
and Cu stream sediment anomalies represents the most useful guide
to the presence of mineralization, confirming the findings of
previous workers (Coope, 1958). High S values appear to reflect
the presence of sulphide minerals, as at Trojan, but there is
insufficient evidence to affirm that the S content of stream
sediments makes any contribution to nickel prospecting. A
combination of high Ni and Cr concentrations in sediments
characterizes non-mineralized intrusives. There is usually good
downstream dispersion, for at least 500 m from source, of Ni and
Cu, but anomalies can easily be lost below a confluence due to
tributary dilution of the sediment.

8.1.8.   The distribution of ore metals in the coarse fraction

                The coarse fraction of some stream sediments from the
King Edward, Munali, Paulwi and Trojan areas were analysed for Ni,
Cu, Fe and Mn to ascertain whether there was an association of Ni
and Cu with secondary Fe or Mn coatings which could be exploited as
a geochemical guide to mineralization.

                At King Edward the coarse fraction of sediments in
the stream proper draining the peridotite contains higher concentrations
of Fe and much higher concentrations of Mn,compared with the fine
fraction, with maxima of 16.0% Fe and 6200 ppm Mn (table 36). In the
same samples, Ni also shows an enrichment in the coarse fraction with
a maximum value of 2000 ppm compared with 1750 ppm in the fine
fraction, but Cu values are lower in the coarse fraction with up to
114 ppm compared with 146 ppm in the fine fraction. Below the
confluence with the tributary rising on limestone, the trace element
content of the coarse fraction falls sharply to 190 ppm Ni, 60 ppm Cu
and 1225 ppm Mn, and the Ni, Cu and Fe concentrations in the coarse
fraction are lower than in the fine fraction. The stream draining the
peridotite has coarse-to-fine-fraction ratios of up to 1.42 for Fe,
4.55 for Mn, 1.58 for Ni and 0.80 for Cu, suggesting that coarse
fraction particles have conspicuously manganiferous and, to a lesser
extent, ferruginous coatings. A little Ni enrichment but no Cu
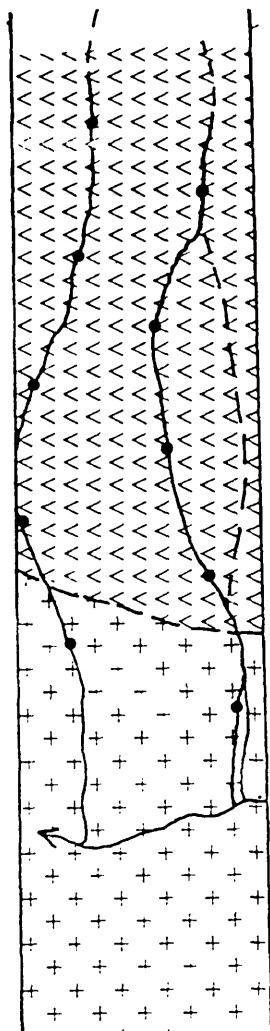
Sample no.	Coarse fraction content				Coarse-to-fine-fraction ratios			
	Ni	Cu	Fe	Mn	Ni	Cu	Fe	Mn
322-01	208	43	3.8	515	0.52	0.45	0.66	0.73
322-06	350	18	2.7	400	0.50	0.29	0.47	0.44
322-02	395	60	5.5	690	0 56	0.60	0.76	0.96
322-07	500	20	3.5	500	0.71	0.48	0 66	0.59
322-03	230	46	4.3	650	0 38	0 50	0.68	0.65
322-08	610	31	4.2	1130	0.68	0.50	0.60	1.01
322-04	305	103	7.0	810	0.51	0.74	0.70	0.78
322-09	525	32	4.3	580	0.55	0.47	0.61	0.52
322-05	180	29	3.3	340	0.45	0.33	0.60	0.48
322-10	225	18	2.6	600	0.50	0.44	0.57	0.72

Table 37: Paulwi, stream sediment coarse fraction trace element content (ppm, except Fe in %) and coarse-to-fine size fraction ratios (diagram topologically adjusted, approx. scale 1:12,500; for geological legend see figure 11).

enrichment appears to be associated with these coarse fractions.
Below the confluence this conspicuous Fe and Mn enrichment in the
coarse fraction disappears, presumably because of changed
deposition characteristics in this stream, and the ratios fall to
0.77 for Fe, 1.39 for Mn, 0.38 for Ni and 0.43 for Cu.

There is little visible evidence of ferruginous
or manganiferous coatings on the surface of coarse fractions of
Paulwi stream sediments. This is confirmed by analytical results
which show that Fe and Mn concentrations in the coarse fraction
range from 2.7% to 7.0% Fe and 340 to 1130 ppm Mn compared with
4.6% to 10.0% Fe and 710 to 1120 ppm Mn in the fine fraction (table
37). Similarly there is from 180 to 610 ppm Ni in the coarse fraction
and 400 to 950 ppm in the fine fraction, and from 18 to 103 ppm Cu
in the coarse fraction compared with 41 to 140 ppm in the fine
fraction. As a result, all coarse-to-fine-fraction ratios are close
to or lower than unity, and range from 0.57 to 0.76 for Fe, 0.44 to
1.01 for Mn, 0.38 to 0.71 for Ni, and 0.29 to 0.74 for Cu. Low ore
metal ratios of this order in stream sediments of a non-mineralized
area conforms with the pattern seen in the non-mineralized soils at
Chombwa.

The coarse fractions of sediment samples covering the
first 800 m of the Munali stream were analysed for Ni, Cu, Fe and
Mn (table 38). There is more Fe in the coarse fractions than the fine
fractions of samples near the headwaters, where ferruginous outcrops
occur. The highest values are 29.0% Fe in the coarse fraction and
23.5% Fe in the fine fraction 200 m downstream from the headwaters.
However, further downstream the position is gradually reversed, and
800 m downstream the coarse fraction contains 6.4% Fe and the fine
fraction 17.0% Fe. There is no evidence of significant Mn enrichment
in the coarse fraction with 155 to 350 ppm Mn compared with 200 to
440 ppm in the fine fraction. The distribution of Ni is roughly linked
to that of Fe, with up to 700 ppm Ni in the coarse fraction compared
with 340 ppm in the fine fraction near the headwaters, and only 125 ppm
Ni in the coarse fraction and 163 ppm in the fine fraction 800 m
downstream. As at King Edward, however, Cu tends to be lower in the
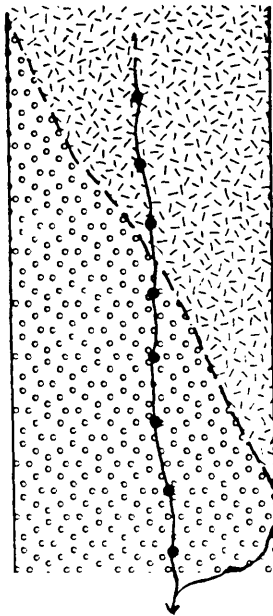
	Sample no.	Coarse fraction content				Coarse-to-fine-fraction ratios			
		Ni	Cu	Fe	Mn	Ni	Cu	Fe	Mn
	122-05	700	290	18.7	215	2.06	0.62	1 27	0.67
	122-06	655	202	29.0	350	2.05	0.70	1.23	1.52
	122-07	525	315	16.8	235	1.84	0.90	1.08	0.90
	122-08	525	150	20.6	240	2.19	0.63	1.08	1.04
	122-09	235	143	13.0	250	0.92	0.79	0.93	0.57
	122-10	395	220	10.5	175	2.32	2.44	0.50	0.88
	122-11	150	118	9.5	155	0.94	0.98	0.56	0.67
	122-12	125	107	6.4	170	0.77	0.97	0.38	0.85

Table 38: Munali, stream sediment coarse fraction trace element content (ppm, except Fe in %) and coarse-to-fine size fraction ratios (diagram topologically adjusted, approx. scale 1:12,500; for geological legend see figure 9).

coarse fraction, with a maximum of 315 ppm compared with 470 ppm
in the corresponding fine fraction near the headwaters, and Cu
concentrations tail off downstream to 107 ppm in the coarse
fraction and 110 ppm in the fine fraction. There are unusually
high Ni and Cu concentrations in the coarse fraction of one sample
at 600 m downstream which contains 395 ppm Ni and 220 ppm Cu, more
than twice as much of each metal than the fine fraction, and no
explanation can be offered for this. In general Ni coarse-to-fine
fraction ratios decline downstream from 2.06 to 0.77 over 800 m,
in close conformity with Fe ratios which fall from 1.27 to 0.38.
The Cu and Mn ratios, in contrast, are low, slightly erratic, and
generally less than unity. Thus there is a very similar pattern
of coarse and fine fraction ore metal relationships in King Edward
and Munali stream sediments, and the only distinctive criterion
identifying the presence of mineralization at Munali appears to be
the high coarse-to-fine-fraction Ni ratios.

The coarse fraction of samples from the sandy stream
draining Trojan Hill are slightly enriched in Fe and Mn, with up to
15.3% Fe and 2100 ppm Mn compared with maxima of 11.5% Fe and
1655 ppm Mn in the fine fraction (table 39). Copper appears to be
co-precipitated with Fe and Mn in view of the clear enrichment of
Cu in the coarse fraction, while Ni concentrations are consistently
higher in the fine fraction. There are coarse-to-fine-fraction ratios
of up to 1.51 for Fe, 1.94 for Mn and 4.06 for Cu, but only 0.76 for
Ni. It is not practical to evaluate downstream dispersion in the
coarse fraction of the Trojan Hill sediment because the sandy stream
joins a vlei after 850 m, and a coarse fraction is not commonly
present in vlei sediment. In the only two samples of coarse sediment
found below the confluence with the vlei, the Ni, Cu and Mn content
is lower than in the corresponding fine fractions, and Fe is only
slightly higher, indicating that ferro-manganese coatings and
accompanying trace element enrichment are not prevalent in any coarse
sediment found in vleis.
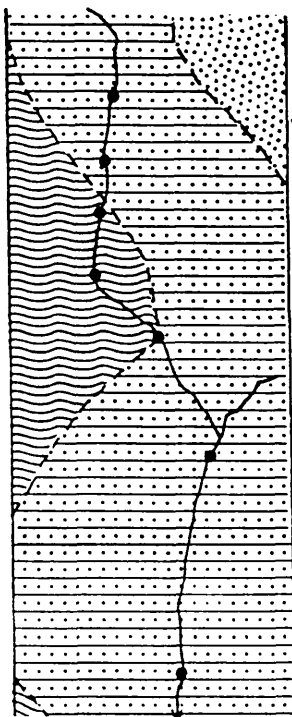
Sample no.	Coarse fraction content				Coarse-to-fine-fraction ratio			
	Ni	Cu	Fe	Mn	Ni	Cu	Fe	Mn
822-01	1835	1225	9.7	2010	0.56	1.11	1.33	1.30
822-02	1880	1000	9.1	1350	0.40	1.89	0.91	0.82
822-03	3820	1940	13.0	2100	0.76	1 73	1.51	1.51
822-04	3060	2190	13 8	1370	0.51	4.06	1 41	1.16
822-05	600	1270	15.3	2100	0 12	2.12	1.33	1.94
822-06	875	280	8.6	1310	0.63	0.72	1.23	0 99
822-16	2450	220	7.6	1790	0.75	0.85	1.09	0.21

Table 39: Trojan, stream sediment coarse fraction trace element content (ppm, except Fe in %) and coarse-to-fine size fraction ratios (diagram topologically adjusted, approx. scale 1:12,500; for geological legend see figure 12).

8.2.   Areas of dambo and vlei drainage

                Broad, fairly flat and almost treeless water courses,
termed dambos in Zambia and vleis in Rhodesia, are common natural
drainage features in Central Africa. In dambos and vleis the water
table is near to ground level much of the time, usually rising
during the wet season to form a temporary swamp, and falling
steadily during the dry season to leave a dry surface in places.
Reducing conditions prevail much of the time, and the sediments
are grey to black, fine grained silt and mud, with a high organic
content. A coarse fraction is not normally found in dambo and vlei
sediments. Dambo drainage characterizes the non-mineralized Chitina
area, and a vlei drains the southern flank of Trojan Hill, where
mineralization occurs.

8.2.1. Chitina

                At Chitina, the upper reaches of a tributary dambo
of the Filanga seem to drain mafic and ultramafic intrusive rocks,
and one sediment sample collected from the dambo during prospecting
drainage reconnaissance contains an anomalous concentration of 230 ppm
Ni. This tributary was sampled for 1200 m downstream from the
headwaters (figure 6). The known Ni anomaly is reflected by a
maximum Ni value of 175 ppm 500 m from the tributary headwaters, and
is accompanied by slightly higher Cu, Co, Zn and Cr concentrations
than are found upstream (table 40). Nickel, Cu and Cr levels fall
quickly downstream from the anomaly, although higher Co and Zn values
are found a further 200 m downstream in conjunction with unusually
high Fe and Mn concentrations. Beyond 900 m from the headwaters
the levels of all elements determined in the sediments drop sharply
as the dambo passes onto granite.
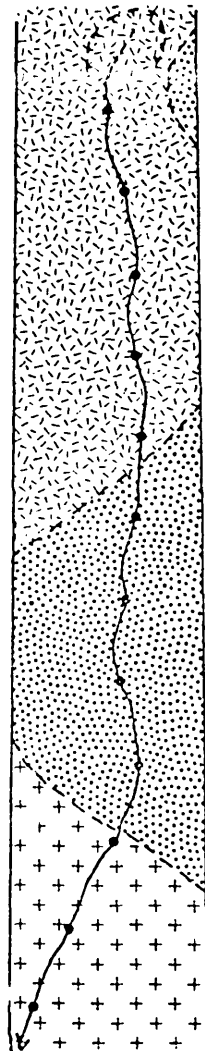
Sample No.	Ni	Cu	Co	Zn	Cr	Fe	Ti	Mn	pH
425-37	155	65	65	120	90	4.3	1100	340	4.5
425-36	125	59	50	86	80	2.8	1150	210	4.2
425-35	160	63	90	117	90	4.1	1950	410	4.6
425-34	145	61	90	122	70	3.6	950	500	4.7
425-33	175	80	75	133	105	3.6	900	350	4.6
425-32	105	44	120	133	80	10.1	450	970	4.5
425-31	120	42	190	147	75	16.5	750	1180	3.9
425-30	55	31	35	80	50	4.1	1500	220	3.9
425-29	85	47	30	94	90	2.2	1200	170	4.0
425-28	25	16	10	31	30	0.5	1050	90	4.2
425-27	25	19	15	33	15	1.5	1050	130	4.4
425-26	20	14	10	27	20	0.5	1300	90	4.3

Table 40: Chitina, dambo sediment trace element content (ppm, except Fe in %; diagram topologically adjusted, approx scale 1:15,000; for geological legend see figure 6).

Downstream dispersion of trace elements appears to be very restricted, probably to 100 or 200 m from source, and certainly to less than 500 m. This seems likely to be due to the fixation of metals as organo-metallic complexes by the organic components of the sediment. The low pH of 3.9 to 4.7 reflects the high organic content of the sediment. The low Eh-pH environment of the dambo does not favour precipitation of Fe and Mn oxides (figure 20). Therefore enrichments of these two metals seen in the sediment are also ascribed to their fixation as organo-metallic complexes.

8.2.2.   Trojan

At Trojan a sandy tributary drains the northeast corner of Trojan Hill and joins a vlei which runs westward along and beyond the south flank of Trojan Hill. These drainage channels, which mainly overlie amphibolite, were sampled over a distance of 2150 m downstream from the headwaters of the sandy tributary (figure 12). The tributary rises downslope from the mineralized zone on Trojan Hill, and intersects the serpentinite intrusive (though not the mineralized zone) over a short distance. The Ni values in the sandy tributary reach 6000 ppm, but then fall sharply as the tributary joins the organic-rich vlei (table 35). Further downstream along the vlei, Ni values are erratic and high in places. This suggests little downstream dispersion, but localized Ni enrichment derived from circulating groundwater. High Cu, Mn and Zn values commonly accompany the high Ni values, and this sporadic enrichment of all four metals is attributed to their fixation by organic sediments. However, Fe, Co and Cr levels fluctuate comparatively little. There is an unusually high pH of 6.2 to 7.2 throughout the vlei, perhaps due to the influence of the mafic rocks over which it flows.

| | Regional | Streams draining mafic-ultramafic intrusive | | | | Streams draining iron-banded quartzite | | | | |
	mean	41005	41019	41020	41047	41092	41091	41090	41075	41069
Ni	67	259	185	179	230	244	221	208	178	210
Fe %	2.9	6.6	4.9	8.0	3.9	9.2	8.6	7.9	2.2	5.2
Cu	42	95	77	85	93	103	44	39	103	70
Zn	127	520	238	199	134	258	69	199	254	268
V	77	244	159	161	145	56	27	37	69	216
Co	32	29	54	28	62	211	273	264	89	50
Cr	199	506	348	396	185	90	36	58	147	266
Ti	9000	6385	7795	7205	4675	2155	1970	4260	5195	14900
Mg %	0.2	1.2	0.6	0.9	0.5	0.2	0.2	0.2	0.3	0.4
Ca %	0.4	0.9	0.7	0.9	0.3	0.6	0.4	0.5	0.3	0.6

Table 41:   Chitina, trace element characteristics of regional stream sediments with anomalous Ni content (ppm, except as stated).

Much higher Ni and Cu concentrations in the
Trojan vlei compared with the Chitina dambo indicate the
presence of mineralization. The dambo and vlei sediments
probably reflect the trace metal content of localized seepages
of circulating groundwater, and substantial dispersion of
soluble metals is achieved in this way. Fixation of elements
by organic-rich sediments, however, severely limits downstream
dispersion along the water courses.

8.3. Regional stream sediment patterns

In view of the paucity of information contributed
to the identification of mineralized intrusives by the ore metal
and S content of the coarse size fraction of stream sediment
samples, it was concluded that the conventional fine fraction of
samples analysed for trace and major elements provides the
optimum data for the evaluation of regional drainage patterns. In
the fine fraction, downstream dispersion of more than 500 m is to
be expected, except beyond stream confluences. The -200 μm fraction
of regional stream sediment samples collected during prospecting
reconnaissance surveys of the Chitina, Munali and Paulwi areas
were analysed by direct-reading emission spectrography. Full
analytical details are given in appendix 2 and those elements
found to be of interest in other aspects of the research are
reviewed for criteria indicating mineralized intrusives.

8.3.1. Chitina

At Chitina, where there is much dambo drainage,
the regional stream sediment suite comprises 114 samples collected
at 500 m intervals along water courses and at confluences, and
covers 140 km^2. Several drainage channels in the east of the
region disect the Chitina mafic-ultramafic complex.

	Regional mean	NE flank of gabbro			NW flank		S-central
		11543	11545	11547	11542	11544	11573
Ni	56	164	197	161	110	168	224
Fe %	4.2	8.2	14.6	19.5	7.2	8.1	9.7
Cu	78	178	83	69	181	74	158
Zn	67	62	96	94	121	157	37
V	185	403	1390	1420	294	230	661
Co	20	30	26	26	25	31	36
Cr	116	153	248	270	171	167	164
Ti %	0.9	1.3	4.5	5.4	1.4	0.9	1.9
Mg %	0.9	1.8	1.3	1.4	2.0	1.1	1.8
Ca %	0.5	0.9	1.7	3.2	1.0	0.6	1.1

Table 42: Munali, trace element characteristics of regional stream sediments with anomalous Ni content (ppm, except as stated).

	Regional mean	Streams draining mafic-ultramafic complex		
		31394	31401	31407
Ni	642	2020	2055	2090
Fe %	6.6	9.0	9.1	15.0
Cu	55	12	41	27
Zn	115	16	23	144
V	160	19	52	89
Co	60	121	140	199
Cr	1265	1485	1645	2795
Ti	11800	70	382	2081
Mg %	4.2	8.0	4.6	7.5
Ca %	2.7	0.4	0.9	1.2

Table 43: Paulwi, trace element characteristics of regional streat sediments with anomalous Ni content (ppm, except as stated).

The Ni mean for the sediments of the region is
67 ppm, but most samples contain less Ni than this and anomalies
stand out clearly. Each of the streams draining the intrusive
reflects the presence of nickel-rich rocks by anomalies of 179
to 259 ppm Ni. There are anomalies of 178 to 244 ppm Ni not
related to mapped intrusive rocks, clustered around the north-
central portion of the sampled area in the headwaters of streams
draining an iron-banded quartzite formation (table 41).

Each of these stream sediment Ni anomaly types
has a characteristic trace element assemblage. In those sediments
derived from mafic and ultramafic rocks, high Ni values are usually
accompanied by moderately high Fe and Cu concentrations and
conspicuously high Zn, V, Cr and Mg values. The sediments derived
from the iron-banded quartzite tend to have very high Fe and Co,
while Cu and Zn values vary from average to high, and V, Cr and
Mg concentrations are distinctly low. Thus high V, Cr and Mg
in the stream sediments distinguish a mafic-ultramafic intrusive
from a nickeliferous iron-banded quartzite, at least in the
Chitina region. Another interesting distinction is that the
anomalous samples derived from the intrusive contain four or
more times as much Ni as they do Co, but the sediments downstream
from the iron-banded quartzite formation contain about equal
concentrations of both metals. Some of the sediment samples
derived from the iron-banded quartzite also contain unusually high
concentrations of Mn.

8.3.2. Munali

The Munali regional drainage suite comprises 101
samples collected at 500 m intervals along mainly free-flowing
streams and at confluences over 60 km^2, including the mineralized
Munali gabbro.

Alluvium

Quartzite

Crystalline limestone

Biotite gneiss

Gabbro

Schist

Granite
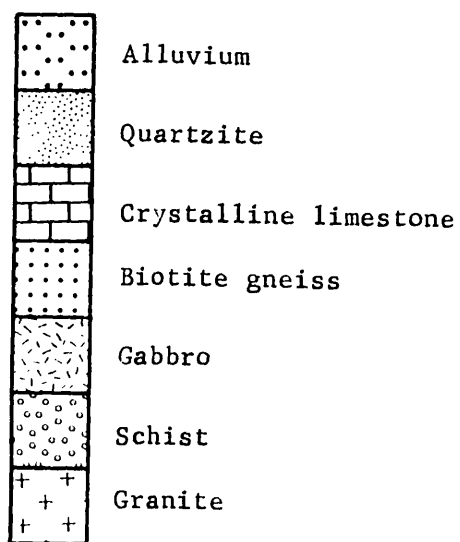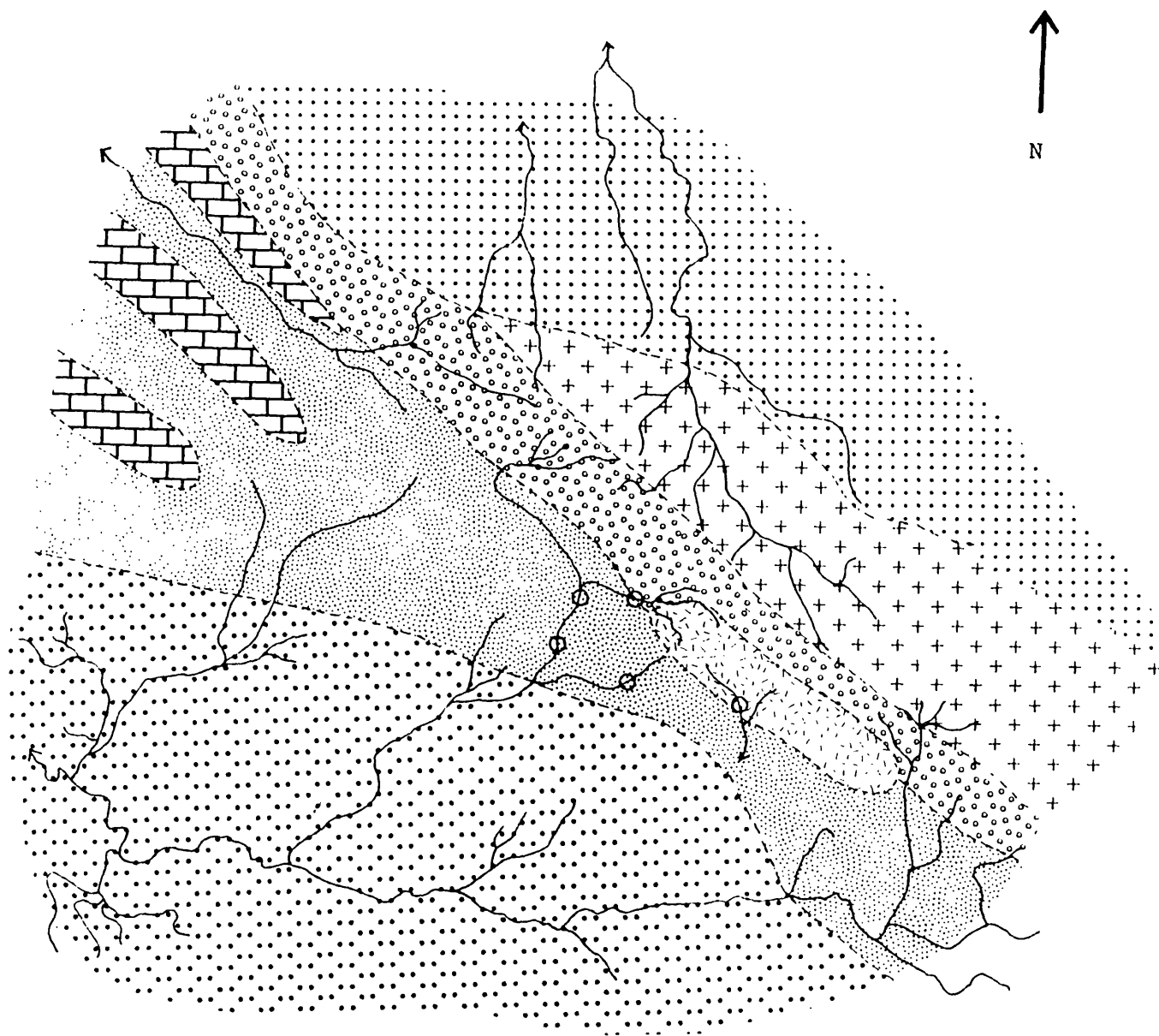
O   Stream sediments with Ni content in excess of $\bar{x}+2\sigma$

Figure 111:   Munali, regional stream sediment reconnaissance Ni anomalies
(approx scale 1:50,000; streams shown sampled at 500 m intervals).

The only Ni anomalies in the region, where the mean Ni content of the sediments is 56 ppm, occur in three streams draining the northeast, northwest and south-central parts of the gabbro (table 42). There is much the same enrichment of other elements in conjunction with the Munali stream sediment Ni anomalies as with those derived from the mafic-ultramafic rocks at Chitina. The Munali Ni anomalies are accompanied by high Fe, Cu, V, Cr and Mg values, and Zn is high in some samples. There are also Ca anomalies near the Munali gabbro, up to 3.2% Ca compared with a mean of 0.5%, but these are attributed to remnants of the limestone formation into which the gabbro was intruded as well as the calcareous nature of parts of the gabbro. High Ti values, attributed to the ilmenite content of the gabbro, are also seen in the sediments with concentrations up to 5.4% Ti. Cobalt levels in the anomalous samples are close to the regional mean, and Ni concentrations are approximately five times Co concentrations.

The geochemical characteristics of the Munali sediments clearly indicate the presence of an intrusive body (as opposed to an iron-rich meta-sedimentary formation) by the association of high Ni, V, Cr and Mg and a high Ni:Co ratio. Compared with sediments in the streams intersecting the Chitina intrusive there are lower Cr values, suggesting a predominantly mafic intrusive at Munali. However, the only characteristics distinguishing the presence of mineralization at Munali are higher Fe and Cu in the Munali sediments than in the Chitina sediments.

8.3.3.   Paulwi

The rugged Paulwi region has a dense network of fast-flowing streams, and a suite of 139 regional drainage samples, taken at 500 m intervals along streams and at confluences, covers only 20 km^2, with many of the streams sampled draining the Paulwi mafic-ultramafic intrusive complex. As a result the Ni mean of the sampled population appears high, at 642 ppm, whereas background Ni concentrations are around 200 ppm; in the higher ranges, 43

Amphibolite

Quartzite

Granite gneiss

Quartz-mica schist

Serpentinite

Pyroxenite

O   Stream sediments with Ni content in excess of $\bar{x}+2\sigma$
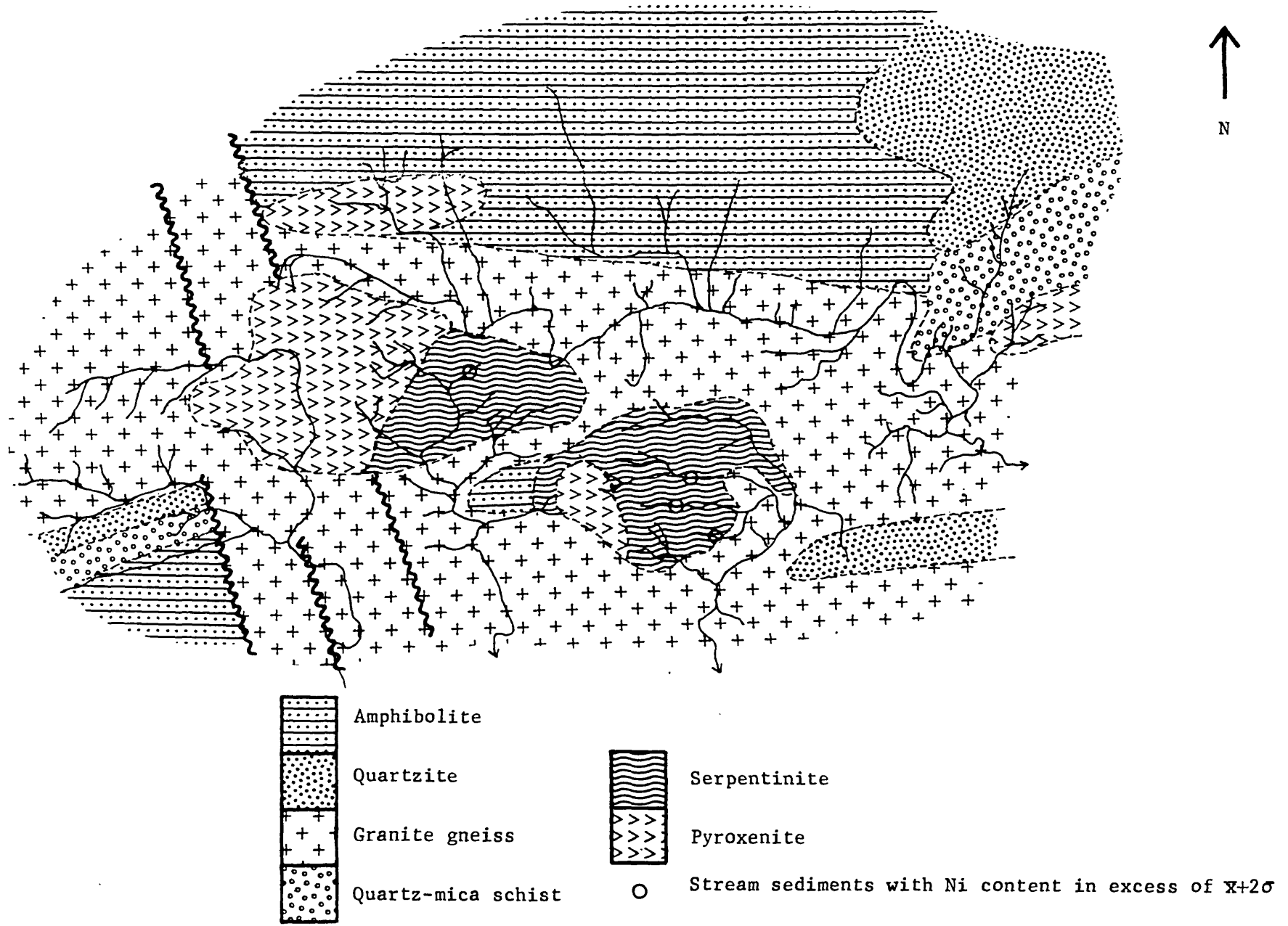
Figure 112:   Pauwli, regional stream sediment reconnaissance Ni anomalies   (approx scale 1:50,000; streams shown sampled at 500 m intervals).

samples contain 1000 to 2000 ppm Ni, and three samples contain
slightly more than 2000 ppm (table 43). High Ni values in
the sediments are accompanied by high Fe, Cr and Mg, and low V
and Ti concentrations. In anomalous samples, Ni levels are
about ten times greater than Co concentrations, while Cu values
are around or lower than the regional mean.

The very high Ni, Cr and Mg concentrations and
high Ni:Co ratios in the Paulwi stream sediments clearly identify
the presence of an intrusive, and along with low V and Ti
concentrations, suggest a mainly ultramafic rock type. The
fairly modest increase in Fe values in the Paulwi sediments
compares with that at Chitina, and cannot,therefore, be regarded
as a mineralization indicator. However, unlike at Chitina and
Munali, the Cu content of Paulwi stream sediments is extremely
low, and this feature in particular suggests that mineralization
is not present at Paulwi.

8.3.4. Summed standard normal deviates

The significant multi-element data in distinguishing
between Ni anomaly types in regional stream sediment patterns is
best evaluated by generating uni-variate summed standard normal
deviates. For each of the three regional drainage suites (taken
separately) standard normal deviates were calculated using GESTAT,
and various combinations of factors were tested using a modified
version of SUMSND. The modified program selected only those
samples with NiZ factors above an arbitrarily-selected threshold
of +2.00, thereby ensuring the inclusion of a significant Ni anomaly
component in Zsums, while excluding samples which contain only
anomalous levels of elements other than Ni. The samples fulfilling
this criterion comprise five samples from streams draining the
Munali intrusive (sample nos. 11543, 11544, 11545, 11547 and
11573), four from streams draining the Paulwi intrusive (sample nos.
31393, 31394, 31401 and 31407; figure 112), and seven samples in
the Chitina region of which three are from streams draining the
intrusive rocks (samples nos. 41005, 41019, and 41047) and four

Legend:

- Gabbro and peridotite
- Schist
- Granite
- Muscovite gneiss
- Quartzite
- Iron-banded quartzite
- ○ Stream sediments with Ni content in excess of $\bar{x}+2\sigma$
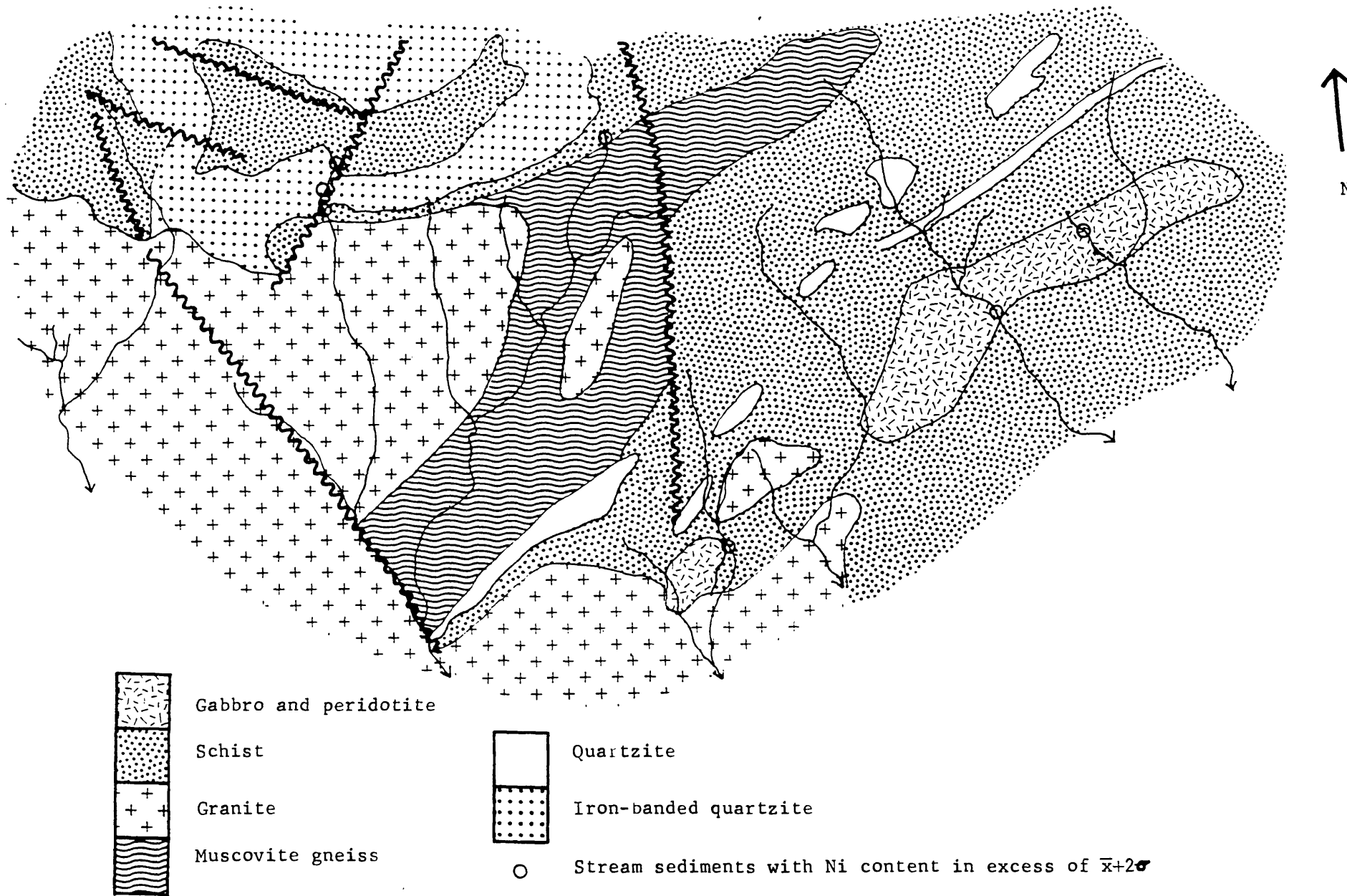
Figure 113: Chitina, regional stream sediment reconnaissance Ni anomalies (approx scale 1:100,000; streams shown sampled at 500 m intervals).

are from the principal stream draining the iron-banded quartzite
formation (sample nos. 41069, 41090, 41091, and 41092; figure 113).

Initially the established concept of coincident
Ni and Cu anomalies as a mineralization indicator was tested
using summed standard normal deviates. When NiZ and CuZ factors
were added the maximum Zsum at Paulwi was +1.77 and the highest
Zsum at Munali was +5.39, suggesting good contrast between
mineralized and non-mineralized intrusives. However, equally
high Zsums up to +5.19 are associated with the Chitina intrusive,
and there are Zsums up to +5.26 in the stream draining the iron-
banded quartzite.

Since particularly high Fe values are found in
the Munali sediments, the NiZ, CuZ and FeZ factors were added,
producing Zsums of up to +8.00 at Munali compared with a maximum
of +3.69 at Paulwi. Contrast between the Munali and Chitina
intrusives is improved slightly, as the highest Zsum for the
streams draining the Chitina intrusive is +6.54, but in the
stream draining the iron-banded quartzite formation the Zsums
reach +7.52.

In order to improve discrimination between the
mineralized and non-mineralized intrusives, Zsums were generated
in which the NiZ, CuZ and FeZ factors were added and either the
CrZ or MgZ factors subtracted, since higher Cr and Mg values in
stream sediments suggest that the source of the Ni anomaly is
ultramafic rock rather than mineralization. In fact, the
subtraction of either CrZ or MgZ factors gave some improvement,
but the better contrast was obtained when subtracting the MgZ
factor, with Zsums up to +7.26 at Munali, +2.37 at Paulwi and
+3.64 near the Chitina intrusive. The MgZ factor made little
difference to the Zsums associated with sediments from the iron-
banded quartzite, which remained as high at +7.37.
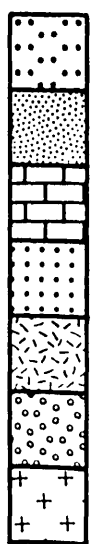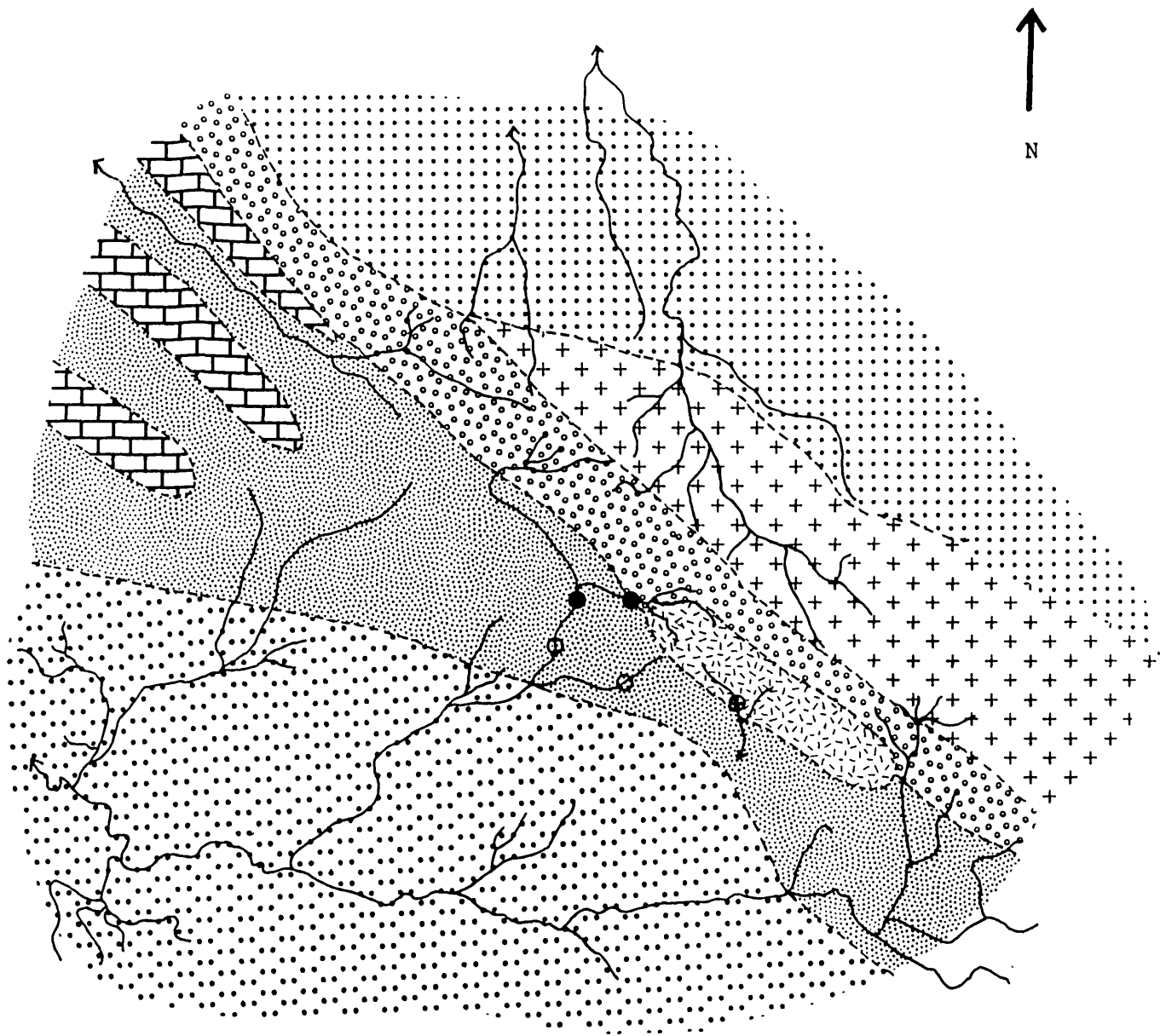
Alluvium

Quartzite

Crystalline limestone

Biotite gneiss

Gabbro

Schist

Granite

O Stream sediments with more
   than $\bar{x}+2\sigma$ Ni but Zsums less
   than +3.50

⊕ Stream sediments with more
   than $\bar{x}+2\sigma$ Ni and Zsums
   between +3.50 and +5.50

● Stream sediments with more
   than $\bar{x}+2\sigma$ Ni and Zsums
   greater than +5.50

Figure 114: Munali, regional stream sediment reconnaissance Zsums   (approx
            scale 1:50,000; streams shown sampled at 500 m intervals).

To cope with this problem, the feature of contrasting Ni:Co ratios in sediments from intrusives and from the iron-banded quartzite was taken into account. When Zsums were generated in which the NiZ, CuZ and FeZ factors were added and the MgZ and CoZ factors substracted, the five Zsums at Munali all exceed +2.47 and the highest Zsums are +5.92 and +6.53 (figure 114). The four sediment samples reflecting the presence of the iron-banded formation at Chitina have Zsums between -1.20 and +3.10, and there is therefore adequate contrast with mineralization at Munali. At Paulwi the Zsums are in the rage -1.35 to +0.54 (figure 115). In sediments from streams draining the Chitina intrusive the Zsums range is +1.09 to +2.93 (figure 116). There is therefore excellent contract between mineralized and non-mineralized intrusives. Thus, this Zsums formula clearly defines Munali as the most promising target for the location of mineralization among the four Ni anomalies originally considered.

8.4. Discussion

In areas of free flowing drainage, stream water flows through the wet season and early dry season, and streams cut channels and small valleys into the rock and soil. Much of the stream water is rainwater run-off, and a lot of sediment is carried into the stream course by bank erosion. Springs and seepages near headwaters bring some ground water into the stream. The trace element load of the drainage system comprises the metal content of the eroded material plus the soluble salts in groundwater. The dispersion patterns formed during weathering and soil formation determine the trace element characteristics of the eroded bank material. The trace element content of the groundwater is probably influenced by the pH of the rocks through which the groundwater circulates: in a high pH environment such as weathering non-mineralized mafic and ultramafic rocks, metals are relatively immobile; in an environment such as oxidizing sulphides in mafic and ultramafic rocks, a low pH prevails and metals are relatively soluble and mobile.

Amphibolite	
Quartzite	Serpentinite
Granite gneiss	Pyroxenite
Quartz-mica schist	O Stream sediments with more than $\bar{x}+2\sigma$ Ni but Zsums less than +3.50
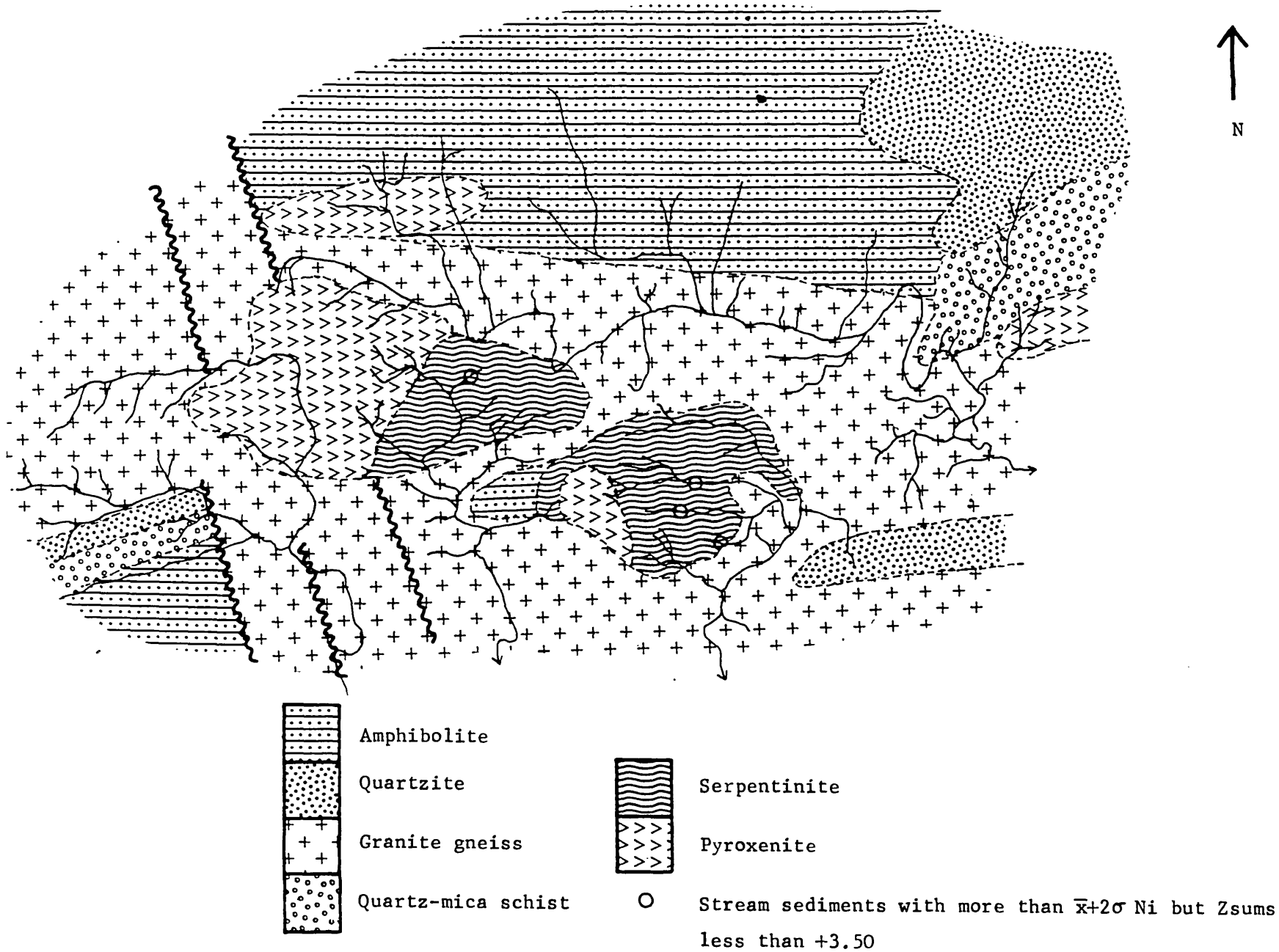
Figure 115: Paulwi, regional stream sediment reconnaissance Zsums (approx scale 1:50,000; streams shown sampled at 500 m intervals).

Within the stream, dispersion of the mechanical load
of eroded material is largely determined by the rate of flow of the
stream. Thus, a fast-flowing stream achieves greater mechnical
dispersion than a slow-flowing stream, and small, light particles of
sediment undergo greater dispersion than large, heavy fragments. In
non-mineralized areas, mechanical transport is thought to be by far the
dominant agent of trace metal dispersion. Metals in solution brought into
the stream may undergo some chemical dispersion in soluble form, but are
always subject to hydrolysis due to increasing pH , absorption by clay
minerals and scavenging by secondary Fe oxides. This latter process
is probably expecially prevalent where the weathering products of
oxidizing sulphide mineralization arc brought into the stream,
although all factors probably interact to some extent. At Munali and
Trojan chemical dispersion is expected to be higher than
elsewhere owing to the presence of mineralization, and the effect
of pH on sustained chemical dispersion along the stream course is
evident in Ni and Cu data. At Munali there is 340 ppm Ni in the
sediment near the headwaters of the stream, and Ni concentration falls to
163 ppm   700 m downstream before a confluence. Due to the lower pH
of hydrolysis of Cu compared with Ni, Cu is precipitated much more
quickly, and Cu levels in the sediment fall from 470 ppm to 110 ppm over
the same distance.   The low pH of the Munali sediments and probably
the stream water is almost certainly instrumental in promoting the chemical
dispersion of Cu and especially Ni. At Trojan the same pattern is
apparent though less clear because of the shorter distance between the
stream headwaters and the first confluence, and the higher pH .

As streams draining both mineralized and non-mineralized
intrusives flow beyond the contact onto country rocks, bank material of
markedly different composition is eroded into the streams and begins
to contribute to the stream sediment. In general this process does not
cause excessive dilution of the stream sediment concentrations of Ni
and Cr, which are normally the two metals most characteristic of the
mafic and ultramafic rocks upstream. This is probably attributable to
high stream flow rates resulting in considerable downstream mechanical
dispersion of the sediment derived from mafic or ultramafic rock.   The

N

Gabbro and peridotite

Schist

Granite

Muscovite gneiss

Quartzite

Iron-banded quartzite

O   Stream sediments with more than $\bar{x}+2\sigma$ Ni but Zsums less than +3.50
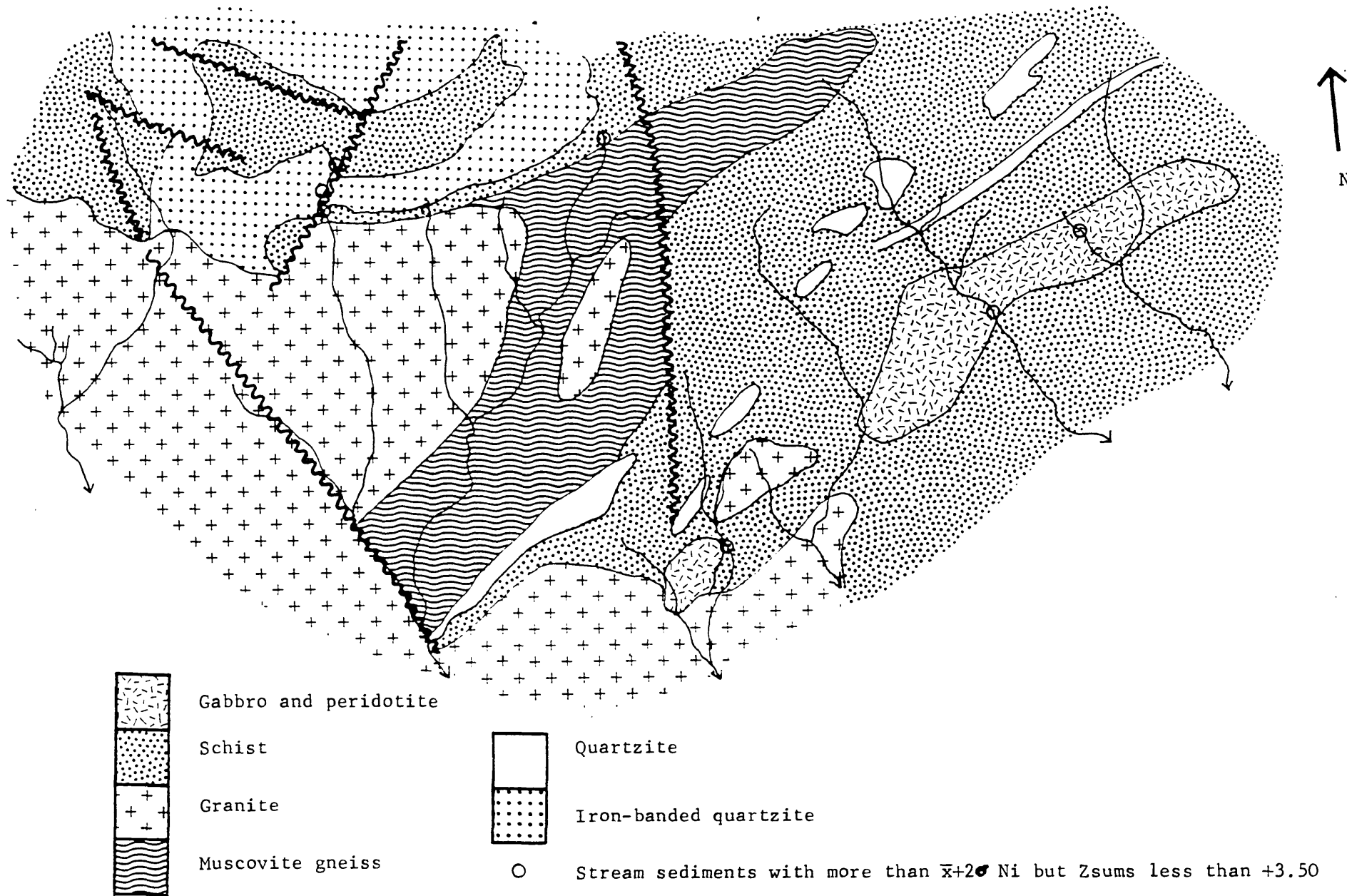
Figure 116:   Chitina, regional stream sediment reconnaissance Zsums   (approx scale 1:100,000; streams shown sampled at 500 m intervals).

nature of the drainage patterns studied in Central Africa did not
afford an opportunity to ascertain the full distance beyond a mafic
or ultramafic intrusive over which the trace element characteristics
of the rock might persist without tributary dilution. Coope (1958)
points out that a Ni drainage train from non-mineralized ultramafic
rock in Sierra Leone was traced downstream for 2.5 miles. At
confluences, dilution of the trace element content of both sediment
and water of each tributary is inversely proportional to the load
it contributes to the stream below the confluence. In the dendritic
systems of Central Aftrica tributary dilution is common and the
sediments with trace elements characteristic of mafic and ultramafic
intrusives soon suffer severe dilution. Thus it is by tributary
dilution, rather than bank dilution along a single stream, that trace
element anomalies related to intrusives tend to be lost.

The accumulation of Fe in the coarse fraction of stream
sediments is ascribed to the presence of nodules and coatings of
secondary Fe oxides, such as goethite. The Fe may be deposited in situ,
or ferruginous particles from the soil B horizon may be washed into
the stream and mechanically transported. A moderate enrichment of Fe
is found in the coarse fraction of sediments from the headwaters of
streams at King Edward, Munali and Trojan. Higher coarse fraction Ni
values, approximately twice the Ni concentration of the fine fraction,
occur in association with Fe enrichment in the stream draining mineralized
gabbro at Munali, but in the stream draining mineralized serpentinite
at Trojan Hill, Ni values are higher in the fine fraction. This
difference may be due to the contrasting low Ni background
produced by the Munali gabbro and the high Ni background furnished
by the Trojan serpentinite, with the result that the Ni content
of ferruginous material accumulating in the coarse fraction remains
conspicuous at Munali, but is camouflaged at Trojan. However,
there is Cu enrichment in the coarse fraction of Trojan sediments,
but not at Munali. The low pH of about 5.5 at Munali favours chemical
dispersion of mobile Cu, and this renders the fine fraction of sediments
relatively rich in Cu. At Trojan the high pH of about 7.0 severely limits
chemical dispersion of Cu, and Cu is found mainly in mechanically
dispersed particles, especially coarse, ferruginous material derived

from mineralization. Downstream dispersion of coarse, lateritic detritus is relatively limited and for example, at Munali, coarse-to-fine-fraction Fe and Ni ratios in excess of unity persist for about 400 m, whereas the fine fraction Ni and Cu anomalies can be traced for over 500 m.

      Much of the Mn found in the coarse fraction of stream sediments may be in the form of secondary Mn oxides coatings, deposited onto particles in the soil or stream. Such coatings are usually made up of a lower layer of Fe oxide which may catalyze the deposition of the Mn from solution as black Mn oxides. These are active scavengers of heavy metals from solution. Black coatings were not noted on the coarse fraction of sediments, but analysis revealed that significant Mn enrichment is found at King Edward, with values of up to 6200 ppm in the coarse fraction compared with 1360 ppm in the corresponding fine fraction. There is a little coarse fraction Mn enrichment at Trojan, but not in other field areas. Thus the existence and degree of Mn accumulation in the coarse fraction of stream sediments varies in different field areas, and is presumably controlled by factors not investigated such as changes in Eh, especially when groundwater reaches the surface environment at seepages or springs, and by surface properties of the natural coarse particles which form a substrate for Fe and Mn oxide deposition (Whitney, 1975). Manganese enrichment clearly declines when traced below the tributary confluence at King Edward, suggesting that the ultramafic rock and mineral detritus which constitutes the coarse fraction of sediments near the stream headwaters provides a high ion exchange capacity substrate favourable to Fe and Mn oxide accumulation. In addition, Ni is enriched in the coarse fraction of King Edward stream sediments, and the Ni is assumed to be associated with ferro-manganese coatings. Copper concentrations are higher in the fine fraction, and this pattern of Ni, but not Cu, enrichment associated with Mn coatings in the coarse fraction of sediments from stream draining non-mineralized areas has been noted elsewhere (Carpenter, Pope and Smith, 1975).

The coarse fraction Fe and Ni enrichment disappears below the confluence, along with the Mn enrichment.

No uniform pattern of ore metal distribution among the coarse and fine size fractions emerges from the stream sediments investigated. Iron enrichment in the coarse fraction occurs in the mineralized Munali and Trojan areas, but also occurs at King Edward. Nickel enrichment accompanies Fe, but is thought to be camouflaged at Trojan, while Cu enrichment in the coarse fraction seems unique to Trojan. Furthermore, these coarse fraction characteristics exhibit less downstream dispersion from source than features seen in the file fraction. Manganese coatings are not a conspicuous feature of Central African stream sediments, and seem unlikely to be an important control in trace element dispersion. Therefore the coarse fraction of stream sediments does not appear to present a relevant sampling medium for nickel prospecting in Central Africa.

The lack of diagnostic S anomalies in stream sediments from mineralized localities is attributed to the very high mobility of the element and its ambiguity in the secondary environment. The modest S anomalies noted in soils and weathered rock overlying mineralization cannot be expected to exhibit as much contrast when eroded into and diluted by stream sediments. Sulphur fixed by plants and micro-organisms and returned to the soil in organic form also finds its way into the stream sediment, and S from this source can furnish non-significant anomalies similar in magnitude to the S content of stream sediments derived from soils overlying mineralization. Groundwaters accumulating part of their soluble load from oxidizing mineralization can contain high concentrations of sulphate anions but on reaching the surface drainage system, sulphate has a strong tendency to remain in solution as evidenced by the fact that sea water contains 884 ppm S, mainly as the sulphate anion . According to Peters (1974), sulphate anions

mainly remain in solution indefinitely and do not contribute significantly
to the S content of stream sediments.

The F⁻anion is also highly moblie, and Boyle (1976) has
identified anomalous F stream sediment dispersion trains associated with
kimberlites, carbonatites and other fluoriferous rocks. It seems
reasonable to speculate that the Munali mineralization and similar
occurences might produce a F stream sediment anomaly. However,
late-stage magmatic injections of nickeliferous sulphides associated
with hydrothermal fluids may contain F enrichments relative to their
mafic or ultramafic host rocks, but many acidic and alkalic country
rocks, such as the Munali schist, normally contain still higher levels
of F. Any stream sediment F anomaly derived from mineralization might
easily be masked by more F from other sources furnishing sediment
and water to the stream beyond the mafic or ultramafic rock contacts.
Thus, although substantial dispersion of F from mineralization may occur
in the drainage system, recognition of a significant F anomaly at a
distance from source realistic for a regional geochemical reconnaissance
survey appears unlikely, and the determination of F in such surveys is
not recommended.

Dambos and vleis occupy shallow depressions
within areas of little topographic expression, and hence receive a
comparatively small amount of their sediment from the erosion of
bank material. On the other hand, the near-surface sediment of these water
courses is saturated by groundwater for much of the year. Thus,
in contrast to free-flowing streams, dambos and vleis receive most
of their heavy metal load via chemical dispersion in circulating
groundwater rather than mechanical dispersion of rock and soil fragments.

The amount of heavy metals transported by the circulating
groundwater is thought to depend largely upon the prevailing pH in the
groundwater system. In areas of weathering non-mineralized mafic and

ultramafic rock as at Chitina, a fairly high pH is to be expected
and this will inhibit the chemical mobility and dispersion of most
metals, including Ni, Cr and Cu. Consequently there are low values
reaching maxima of 175 ppm Ni and 105 ppm Cr in the Chitina dambo
although up to 6000 ppm Ni and 1950 ppm Cr was found in weathered bedrock
exposed in the Chitina pit a few hundred metres away. Conversely in
areas where mafic and ultramafic rock contains oxidizing sulphide
mineralization, as at Trojan, a lower pH prevails, and the
mobility and groundwater dispersion of heavy metals is enhanced.
Where circulating groundwater reaches the surface in the Trojan vlei
sediment contains up to 4500 ppm Ni and 930 ppm Cu. Dambo and vlei
sediments, then, are a sensitive indicator of mineralization because
they reflect the metal content of the circulating groundwater, and this
tends to be high when the pH in weathering bedrock is low, and low
when the pH is high. It should be noted, however, that where groundwater
movement is strongly directional, dambo and vlei sediments will reflect
only the metal content of the weathering rocks through which the
groundwater reaching the dambo or vlei has passed.

Once the metals in solution in the groundwater reach the
dambo or vlei, organic fixation is believed to play a dominant role in
inhibiting downstream dispersion. The erratic distribution of metal
values along the length of these water courses at both Chitina and Trojan
is attributed to a combination of varying metal load in the local
groundwater and varying organic content in the dambo or vlei. This
erratic metal distribution probably persits because of the severely
restricted downstream movement of sediment, which produces a more even
anomaly decay pattern in the sediment of freely flowing streams.

The use of Zsums for interpreting multi-variate regional stream
sediments data has the same merits as their use for soils data.
The Zsum formula for distinguishing regional stream sediment anomalies
reflecting mineralized intrusives from those related to non-mineralized
intrusives may prove to be widely applicable. However, this research
encountered only one problem of interpreting a Ni anomaly from a
different source, namely the nickeliferous iron-banded quartzite at Chitina.

Weathered outcrops of rocks similar to this are particularly difficult
to distinguish from true Ni gossans in Western Australia and Clema
and Stevens-Hoare (1973) devised a method of multi-variable discrimination.
Their discriminant function did not include Co, which proved a useful
factor in the Chitina region, but did include Mn with which Co
usually exhibits a strong affinity in the secondary environment. Clema
and Stevens-Hoare found that high Mn characterized many non-significant
Ni anomalies, and indeed, both Mn and Co are strongly enriched in the
sediments derived from the iron-banded quartzite at Chitina. Sedimentary
formations such as the Chitina iron-banded quartzite are perhaps the
most widespread source and non-significant Ni-Cu anomalies, and their
enrichment in Mn and Co may be typical. If so, this characteristic
must be taken into account in any empirical discrimination function
designed to identify significant Ni anomalies. In fact, Mn may be
the more satisfactory variable to incorporate into Zsums, because
stream sediments derived from mineralized mafic and ultramafic
intrusives often exhibit Co anomalies but not Mn enrichment.

Geochemical dispersion in regional stream sediment
populations was studied using samples collected at 500 m intervals
along drainage courses. This interval was chosen on the basis of
preliminary studies in which sampling was performed at 100 m intervals,
but in this work long dispersion trains without tributory dilution were
not available. After inspection of the dispersion trains seen in the
regional stream sediment populations, it seems that tributory dilution
does indeed play a dominant role in anomaly detection in areas of
free-flowing drainage, such as Munali and Paulwi At Munali the high
Zsums anomaly in the stream draining the mineralized north east corner of
the intrusive persists beyond the first confluence with a major
tributary about one km from the anomaly source, but is finally lost
after another confluence some two km from the anomaly source. At Paulwi
numerous small streams rising on ultramafic rock and sampled just above
confluences, adequately reflect the rock type which they drain by Ni

concentrations around 2000 ppm. Sampling all tributaries just upstream
of confluences, rather than at 500 m intervals, is probably viable
in the stream sediment reconnaissance of regions of free-flowing
dentritic drainage for primary nickel mineralization in Central Africa.
However, the same system cannot be recommended in regions of dambo
or vlei drainage. In the Chitina regional stream sediment there is
virtually no trace element indication of mafic and ultramafic rocks
downstream of the contacts of the intrusive with the country rocks
due to the fixation of metals with organic matter. At Trojan, Ni and
Co are apparently reasonably mobile on the groundwater system by token
of their association with mineralization and the low pH this creates
during oxidation, and this phenomenon obviously aids geochemical
prospecting. Nevertheless, once these metals are fixed by organic
matter in the vlei, there is again little evidence of downstream
dispersion and anomalies are scattered erratically along the vlei.
Thus, while good anomaly contrast is to be expected in dambos and
vleis, organic sediments are not an ideal medium for regional
reconnaissance, because a small sample interval must be adopted to
locate the anomalies which tend to be erratically distributed
in the vicinity of mineralization.

9.   SULPHUR DIOXIDE IN SOIL GAS

Some vapours emitted by orebodies have already proved useful pathfinders, such as radon for uranium, and mercury for base metal and precious metal sulphides. It seems probable that sulphide ores also generate SO_2 during oxidation, and artificial weathering and oxidation of sulphides in the laboratory results in the production of gaseous SO_2 (Rouse and Stevens, 1971). However, the solubility of SO_2 in water is extremely high: approximately 35 ml of SO_2 dissolves in one ml of water at $20^{\circ}C$, and this rises to 70 ml SO_2 per ml of water at $0^{\circ}C$. This suggests that most SO_2 generated in the natural environment initially dissolves in the groundwater. But if the water table falls at some stage as it does annually in areas of alternating wet and dry seasons, the oxidizing rock can be expected to dry with the release of SO_2. In a permeable rock and subsoil, SO_2 will migrate down the concentration gradient, which is normally towards the surface. Thus the level of SO_2 in the near-surface soil pore spaces might adequately reflect the sulphide content of the underlying rock, and a SO_2 anomaly would suggest the presence of mineralization. This type of investigation met with some success in identifying pyrite bodies in Newfoundland (Peters, 1974). The same principles are applicable to nickel sulphides, and so the method was tested and developed for possible use in exploration for primary nickel ore.

9.1.   Orientation sampling and analysis in Britain

Preliminary sampling and analysis was carried out at two locations in England and Wales, with a view to optimizing the method prior to fieldwork in Central Africa. In the first stage of the work, at Parys Mountain, Anglesey, a procedure tested in Newfoundland (Peters, 1974) was closely followed, but many practical aspects of this were modified for the second stage at the Wheal Jane Mine, Cornwall.
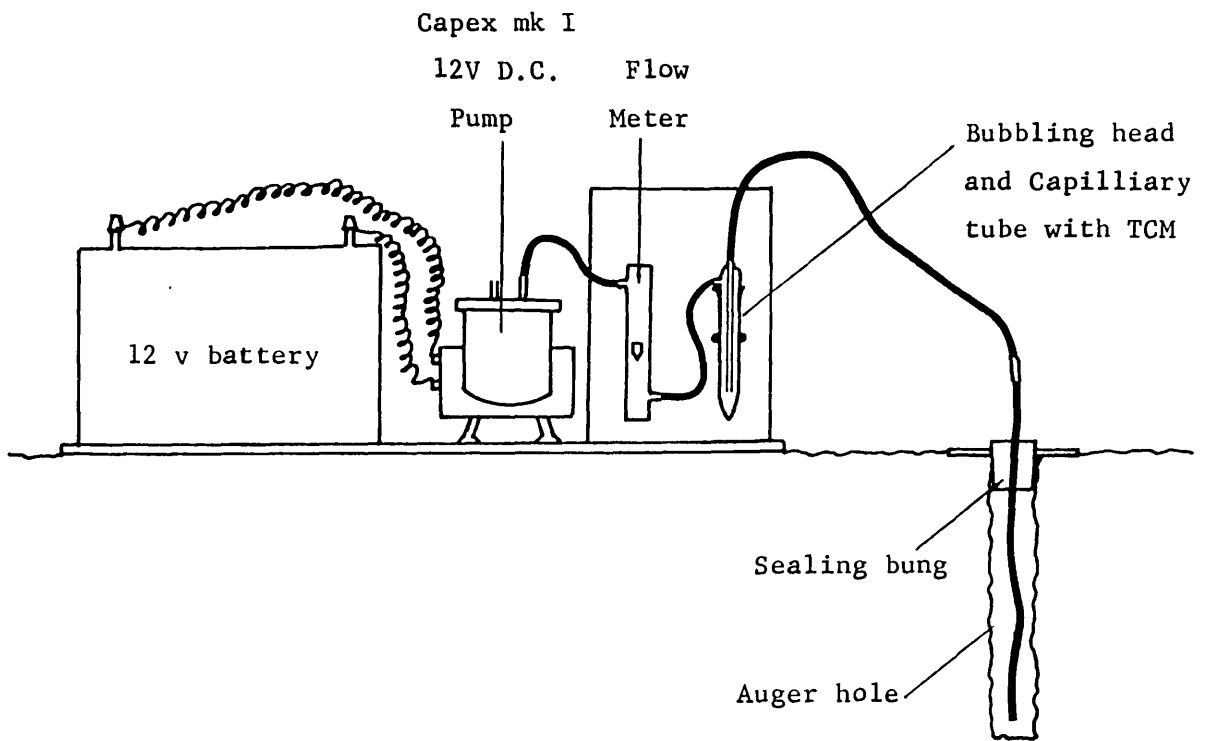
Figure 117: Diagram of apparatus for soil gas SO_2 sampling.

9.1.1.   Sampling and analytical method   '

Samples of soil gas were obtained using a Capex
Mark I 12V pump operating at a selected flow rate of about one
litre per minute and driven by a generator via a transformer,
or a 12V acid battery. Gas was sucked out of an auger hole about
four cm wide and 20 to 30 cm deep, into which was inserted a
cylindrical stainless steel probe four cm in diameter and 15 cm
long with an open base and barrel perforations. Soil gas was
drawn into the probe, along polythene tubing attached to the head
thereof, bubbled through 10 ml of 0.04M potassium tetrachloromercurate
solution (TCM) in a dreschel bottle, and finally past an adjustable
flow rate meter. When the sampling method was modified, the steel
probe was replaced by a probe comprising a 65 mm diameter rubber bung
with a length of semi-rigid polythene tubing fitted tightly through
a single hole; the dreschel bottle was replaced by a centrifuge tube
and a capilliary bubbling head mounted on a small frame; and only
2 ml of TCM was used (figure 117).

After a measured volume of soil gas was passed,
pumping was stopped and the concentration of SO_2 absorbed by the
TCM was subsequently determined colorimetrically. The details
of the colorimetric determination are discussed by King and Pruden
(1969), Scaringelli, Saltzman and Frey (1967) and West and Gaeke
(1956). The quantities and concentrations of the reagents employed
were appropriately adjusted for the method using the reduced
volume of TCM, and the procedure for this method is described. To
the 2 ml of exposed TCM in a centrifuge tube, 1 ml of 0.12%
sulphamic acid was added, and the solutions were mixed and allowed
to stand for 10 minutes to destroy nitrites in solution formed
from oxides of nitrogen in soil gas. Then 1 ml of 0.08% formaldehyde
solution followed by 1 ml of 0.04% HCl-bleached para-rosaniline
hydrochloride (PRA) were added and mixed, and the solution was
allowed to stand for 30 minutes for development of a pink colour.
Finally the absorbance of the solution at 548 μm was determined
spectrophotometrically using a Pye SP600 spectrophotometer or a
Gilford automatic micro-sampling spectrophotometer. According
to Peters (1974), the limit of detection of the colorimetric
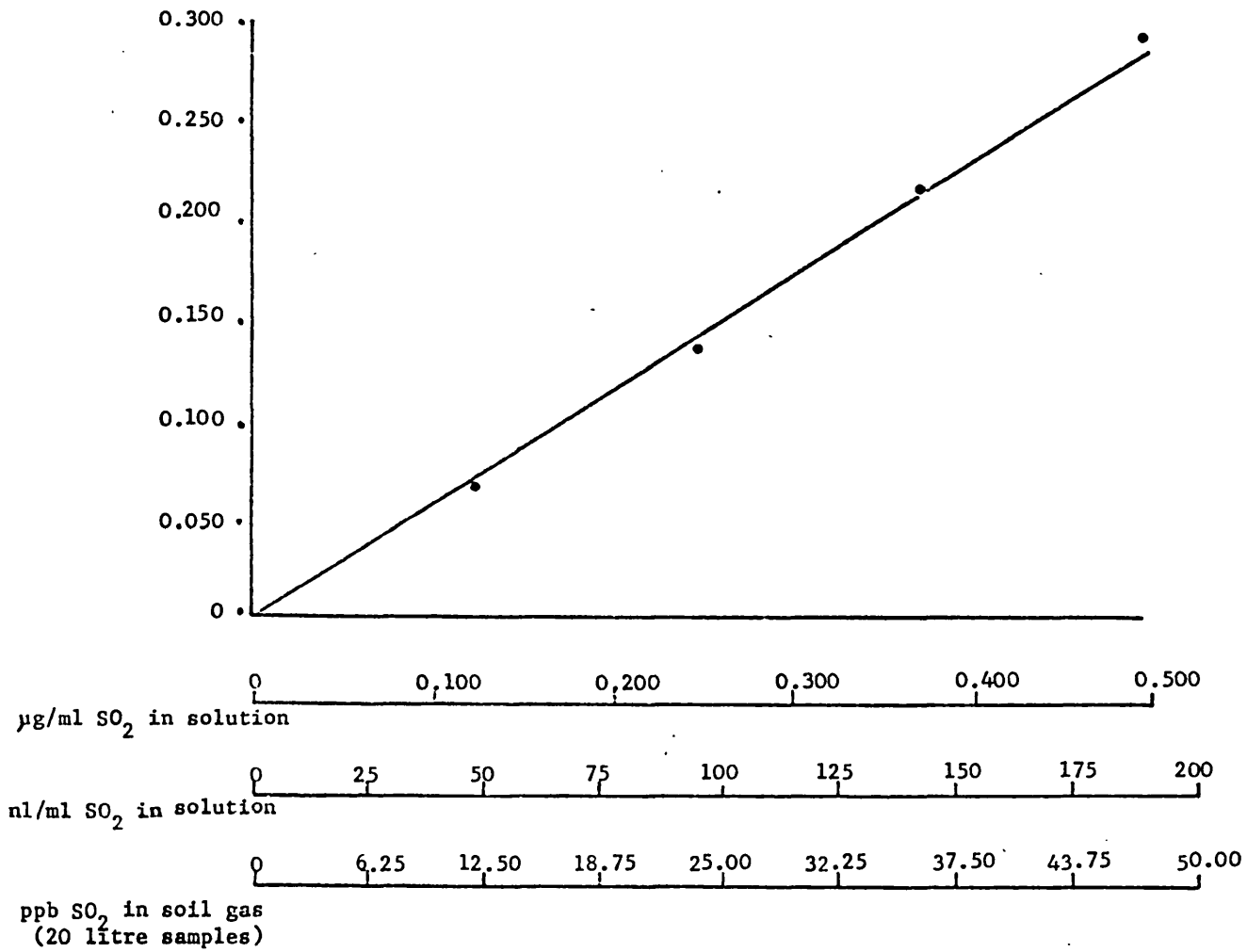
Figure 118: Calibration curve for sulphite standards dyed with PRA and determined spectrophotometrically at 548 µm (Lusaka laboratory calibration).

determination is less than 1 ppb SO_2 for a 20 litre gas sample
in 25 ml of absorbant solution.

9.1.2. Calibration and SO_2 determination

The following procedure was always used for reagent/
spectrophotometer calibration. A solution of approximately 0.1M
sodium thiosulphate was standardized by titration against a
potassium iodate solution of known concentration. The sodium
thiosulphate solution was then used in the titrimetric determination
of the free iodine concentration in an approximately 0.1M solution
of iodine in potassium iodide. Then a second thiosulphate titration
was performed to obtain the free iodine content of an equal volume
mixture of the iodine in potassium iodide solution and a sulphite
solution (prepared by dissolving about 400 mg of hydrous sodium
sulphite in 250 ml of deionized water). The amount of iodine
reduced to iodide by sulphite ions was thus found by difference,
and from this the precise concentration of the sulphite solution
was calculated.

Next, 2 ml of this standard sulphite solution was
diluted to 100 ml with TCM, and aliquots of 0,1,2,3,4 and 5 ml·
of this solution were transferred to 25 ml volumetric flasks. To
each flask was added 5 ml 0.12% sulphamic acid, 5 ml 0.08%
formaldehyde solution, 5 ml PRA and sufficient TCM to bring the
solutions to volume. The flasks were allowed to stand for 30
minutes for colour development, and then absorption at 548 μm was
determined spectrophotometrically. The absorbance of each solution
was graphically plotted against sulphite concentration to provide
a directly linear calibration curve (figure 118).

Samples were analysed by the addition of the same
reagents to exposed TCM solutions and to one or more aliquots of
unexposed TCM to provide reagent blanks. The TCM for samples
and blanks was dispensed at the same time, and solutions maintained
as blanks accompanied the other solutions into the field. In the
spectrophometric determination, samples were read relative to
reagent blanks.

9.1.3.   Sampling and analytical results

To ensure that the initial method was operational prior to fieldwork, laboratory air was sampled several times with fairly consistent and acceptable results around 0.04 ppb SO_2.

Fieldwork was first carried out at the disused Parys Mountain copper mine, Anglesey, north Wales.   Over several days, sampling was done at about 30 sites including mineralized rock dumps, oxidized slimes ponds and pyritic tailings. At each site an auger hole was made, the probe inserted and packed around the lip with soil, 10 ml of TCM was pipetted into the dreschel bottle, and soil gas was pumped for measured times of up to 100 minutes with the battery powered pump. On completion of pumping the exposed TCM was decanted into a 25 ml volumetric flask, and the dreschel bottle and sintered bubbling tube were washed with deionized water. The weather was cold (1 to $2^{o}C$), windy and frequently raining. Samples were analysed the same evening by the addition of colorimetric reagents to the TCM to give a final volume of 25 ml of solution for spectrophotometric determination. However no samples contained detectable SO_2.

No single explanation was available for the failure to detect SO_2 during fieldwork at Parys Mountain. Since maximum analytical sensitivity was essential, the modified bubbling apparatus was devised whereby the pumped soil gas stream was impinged by capilliary tubing and bubbled through 2 ml of TCM in a V-bottomed centrifuge tube, and this was later brought up to 5 ml of final solution for colorimetric determination by the addition of reagents of adjusted concentration. This improved analytical sensitivity by a factor of five times and reduced Peters' reported limit of detection to 0.2 ppm SO_2 for a 20 litre gas sample. This modification also eliminated most of the tedious handling of glassware and solutions previously experienced at each site. Analysis of laboratory air using the modified apparatus continued to give results of about 0.04 ppb SO_2.

In order to eliminate the possibility of unsuitable sample sites in Anglesey, further fieldwork was carried out at the Wheal Jane Mine, Cornwall, southwest England. About 30 samples were taken at several sites on the tailings dam, which contains 0.2 to 0.4% sulphide minerals, and along a soil traverse over copper mineralization adjacent to an old working. Prior to embarking on sampling each day, 20 centrifuge tubes in a rack were filled with 2 ml TCM. At sample sites, auger holes were prepared in the same manner as previously, but steel probe was replaced by a rubber bung with polythene tubing. For each sample a fresh TCM tube was fitted to the capilliary bubbler, and a measured volume of soil gas was pumped by means of a 12V pump powered by a petrol-driven generator, to eliminate fluctuations in flow rate. The weather was cool (5 to $6^{o}C$), mainly dry, with light breezes.

In addition to sampling the soil gas in the routine way, various inducers were tested to promote SO_2 flow in the soil. At different sites, about 50 ml of concentrated solutions of hydrochloric acid, hydrogen peroxide, acidified potassium permanganate and acidified potassium dichromate were poured down the auger hole immediately before the probe was inserted in order to oxidize sulphur-containing compounds. In another test, the hole and surrounding soil was dried and heated to a maximum temperature of $42^{o}C$ with an infrared lamp. Finally, an ultrasonic probe was placed beneath the surface near the sampling hole and ultrasound was generated during sampling in the hope of maximizing pore space and gas flow in the surrounding soil. The exposed solutions were analysed the same evening by the addition of colorimetric reagents and spectrophotometric determination.

Several field days were spent exhaustively testing all alternatives at selected sites, but no SO_2 was found in any of the samples.

9.2. Occurrence of sulphur dioxide in British soils.

Bulk samples of Wheal Jane tailings and soil overlying copper mineralization were taken (in polythene bags to retain moisture) for laboratory study.

An experiment was designed in which a stream of inert gas was passed over a specimen of the undried sample in a LECO induction furnace, and then bubbled through a 2 ml solution of TCM, and SO_2 was determined colorimetrically as before. Fractional thermal analysis of the sample was achieved by increasing the voltage to the furnace in stages and using a different TCM solution for each stage. Despite numerous analyses of damp tailings and soil samples, it proved impossible to obtain reproducible analytical results, but in general, no SO_2 was obtained from samples until the temperature was raised above about $150^{o}C$. Just above this temperature some SO_2 was occasionally recorded, and it was inferred that SO_2 was possibly associated with soil moisture.

To further examine this hypothesis, an experiment was constructed whereby the soil gas and moisture in the pore spaces of a 50 g sample were evacuated using a vacuum desicator, and the water vapour content of the gases so removed was condensed in a cold trap. An aliquot of the liquid which was condensed was analysed for SO_2 by the same method as before. By this procedure the tailings sample was found to contain 40 ppb SO_2, expressed as a function of sample weight. Thus, it seems that SO_2 completely dissolves in the moisture content of damp surface material.

Date ('75)	Area	Sample site	Equilibriation Time (hr)	Pumping Rate (1/min)	Pumping Time (min)	Absorbance 548 mµ	ppb SO$_2$
27.6	Nampundwe Mine Concentrate Dump	40% sulphides	0	1	5	0.061	37.6
			0	1	10	0.084	26.0
			0	1	10	0.052	16.0
			0	1	10	0.074	22.8
			0	1	10	0.094	29.6
			0	1	20	0.084	13.2
			1.5	1	10	0.120	37.6
30.6	Nampundwe Mine Concentrate Dump	4r% sulphides	0	1	10	0.036	12.0
			1.0	1	10	0.068	20.8
			1.0	1	·20	0.063	10.4
2.7	Nampundwe Mine Concentrate Dump	40% sulphides	0.25	1	10	0.014	4.4
			0.5	1	10	0.020	6.4
			1.0	1	10	0.021	6.4
			0.5	1	20	0.029	4.8
			0.5	1	5	0.024	14.4
	/Analysed 3.7/		0.5	1	10	0	0
3.7	Munali	135-11	1.0	1	10	-0.017	-
		135-11	1.0	1	10	-0.016	-
		135-11	1.0.	1	10	-0.017	-
9.7	Munali	135-11	72	0.5	40	0	0
		135-11	120	0.5	40	-0.023	-
		145-88	24	0.5	40	-0.016	-
17.7	Munali Traverse	135-01	72	0.5	40	-0.014	0
		135-02	72	0.5	40	-0.020	0
		135-06	72	0.5	40	-0.017	0
		135-08	72	0.5	40	0.020	3.2
		135-15	72	0.5	40	-0.011	0
		135-17	72	0.5	40	0.004	0.6
21.7	King Edward Traverse	535-01	72	0.5	40	0.001	0
		535-08	72	0.5	40	0.003	0.4
		535-11	72	0.5	40	0.004	0.6
		535-13	72	0.5	40	0.005	0.8
		535-18	72	0.5	40	0.009	1.4
		535-21	72	0.5	40	0.010	1.6
	Lusaka Laboratory Calibration	µg/ml SO$_2$					
		0				0	
		0.123				0.057	
		0.246				0.117	
		0.369				0.187	
		0.492				0.254	

Absorbance read relative to reagent blanks.

Table 44: Soil gas SO$_2$ sampling and analysis in Central Africa.

Any trace quantities of SO_2 derived from the
oxidation of sulphide minerals in the natural environment might
be expected to dissolve in the moisture present in fairly damp
soils. Moisture coats soil particles and is not stripped off by
pumping except under vacuum. Consequently conventional soil gas
sampling was ineffective in detecting SO_2 in the moist soils
encountered in fieldwork in Britain. It was surmised that a
success might be obtained in the comparatively arid soils found
in Central Africa during the dry season, and fieldwork in Zambia
was planned accordingly.

9.3.   Sampling and analysis in Central Africa.

About 960 mm of rain fell in the Zambian field
areas between November 1974 and April 1975. Rainfall ceased in
early April. Fieldwork was carried out during late June and
July 1975, and the soil was found to be dry and friable to a depth
of at least 60 cm; daytime air temperatures were in the range
19 to 26°C. The analytical method remained identical to the
procedure developed in Britain, and spectrophotometric measurements
were made on a Hilger-Watts Uvispec spectrophotometer in the Lusaka
laboratory of the Geological Survey of Zambia.

Initial tests were performed on concentrate tips
containing about 40% sulphide minerals, mainly pyrite and
chalcopyrite, at Nampundwe Mine near Lusaka. On three days samples
were taken to test the sampling variables of hole equilibriation
time, pumping flow rate and pumping time. Sample holes were
augered to the maximum practical depth, usually 50 to 60 cm.

On the first two sampling days, absorbances in the
range 0.036 to 0.120 were recorded representing 10.4 to 37.6 ppb SO_2,
but samples taken on the third day from comparable sites had
absorbances of only 0.014 to 0.029, representing 4.4 to 14.4 ppb SO_2
(table 44). Lower air temperatures experienced on the third sampling
day may account for the difference in magnitude of the results. This
feature aside, the Nampundwe results indicated that the highest SO_2
concentrations are recorded when a sample hole is allowed to
equilibriate with the probe emplaced between excavation and sampling,
and when a relatively small volume of sample is collected.
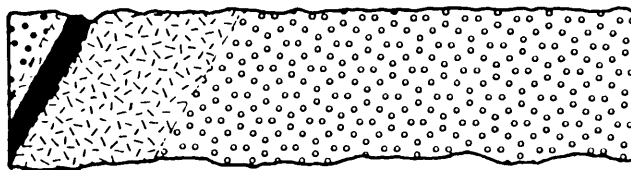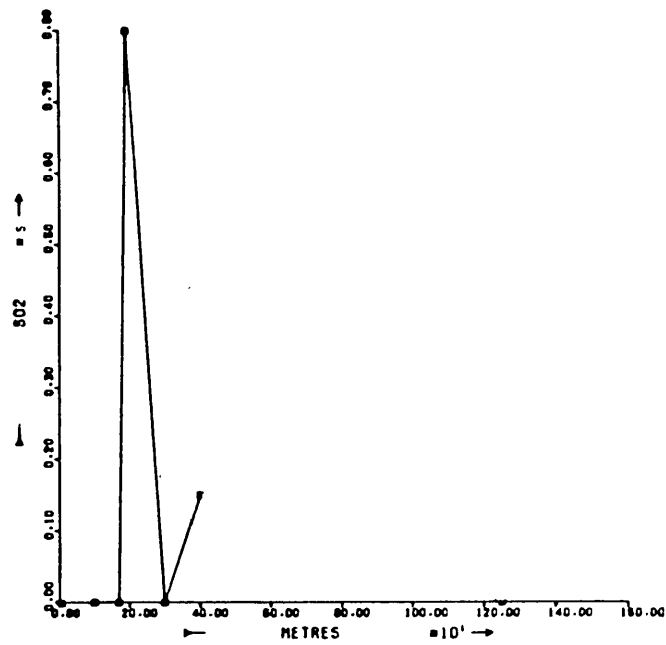
Figure 119: Munali, SO_2 content of soil gas (ppb); for geological legend see figure 9 .

Protracted retention of exposed solutions prior to analysis showed that all SO_2 is lost within 24 hours, thereby rendering same-day sampling and analysis essential.

Based on the Nampundwe findings, fieldwork was planned in the mineralized Munali field area and the non-mineralized King Edward areas, both within 80 km of Lusaka. Since same day sampling and analysis precluded the regular preparation and determination of calibration standards, all absorbance readings for samples from these areas were converted to concentrations of SO_2 using the same calibration curve, compiled from an analysis of standard sulphite solutions prepared in the Lusaka laboratory (figure 112).

Orientation sampling was carried out at Munali. Triplicate samples were taken in the vicinity of suboutcropping mineralization (soil sample no. 135-11), but on analysis gave absorbance readings lower than unexposed blank reagent solutions. Sampling was repeated at this site and at another site over the projected suboutcrop of mineralization (soil sample no. 145-88), with sample site equilibration times increased by a large factor, and sample volume increased slightly. Two of these samples gave absorbance readings lower than the reagent blank, but the third, using a 72 hour site equilibration time and a pumping rate of 0.5 litres per minute for 40 minutes, produced an absorbance of zero. Relative to the negative results produced by other samples, this at least suggested a preferred sampling method. Therefore, a traverse of six soil sample sites was prepared along part of the Munali soil traverse line and allowed to equilibrate for three days (sample nos. 135-01 to 135-17). Sampling was performed at consecutive sites during the course of a morning, and the solutions were analysed the same afternoon. All samples except two were found to have absorbances lower than blanks in the batch, and for these two, the absorbances recorded were 0.020 and 0.004 respectively. The most optimistic, but not necessarily valid, interpretation of this data is furnished by the arbitrary conversion of negative absorbances to zero ppb SO_2, and the calibration curve conversion of positive absorbances. On this basis, all Munali soil gas samples contained zero ppb SO_2 except at soil sample site 135-08, overlying
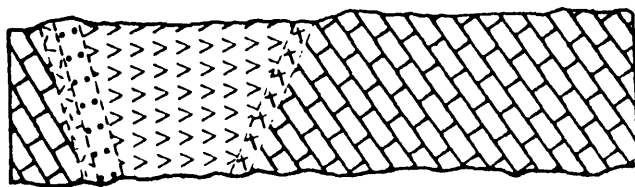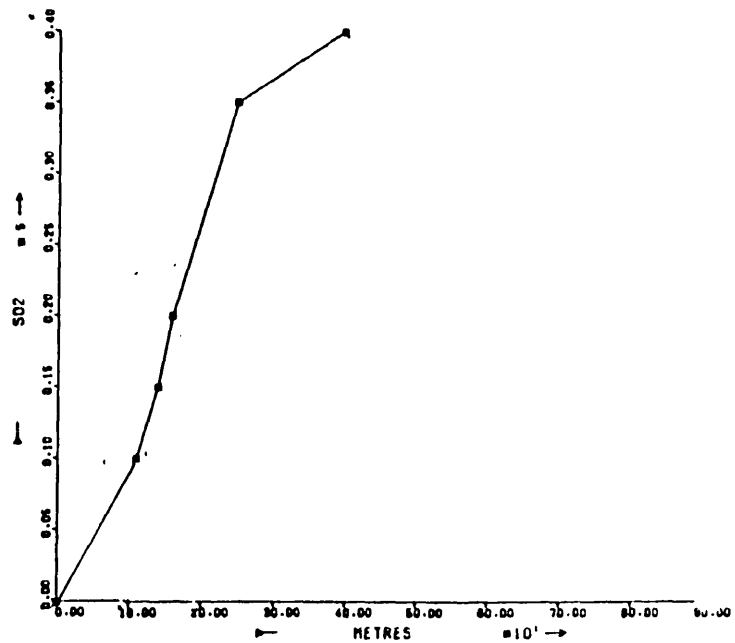
Figure 120: King Edward, SO_2 content of soil gas (ppb); for geological legend see figure 8.

mineralization, there was 3.2 ppb SO_2, while at site
135-17, over non-mineralized gabbro, there was 0.6 ppb SO_2
(figure 119). A similar traverse of six soil gas samples was
carried out over the non-mineralized ultramafic intrusive at
King Edward, along part of the soil traverse line (sample nos.
535-01 to 535-21). The results ranged from zero to 1.6 ppb SO_2,
increasing steadily along the traverse from commencement of
sampling soon after dawn to termination in early afternoon (figure
1.20). All other field areas were too far from the Lusaka
laboratory to permit same day sampling and analysis, and were not
investigated.

Thus, in the arid soils of Central Africa during
the dry season, soil gas SO_2 determination might be regarded as
partially successful in delineating mineralization by a low-
contrast anomaly. This poor contrast is probably a reflection of
the limitations of the method which were noted as the work was
carried out. The loss of SO_2 from exposed TCM over a 24 hour
period suggests that some loss is likely over shorter periods
of sample preservation. This loss is largely attributed to
photocatalytic breakdown of the TCM-SO_2 complex by sunlight
(Scaringelli, Saltzman and Frey, 1967). Testwork at Nampundwe
showed that the highest SO_2 results are recorded after prolonged
site equilibration times and relatively short pumping times,
which indicates that only the gas in the sample hole and immediate
soil pore spaces is sampled before atmospheric air is entrained.
Finally, it is apparent that the amount of SO_2 available in the
soil gas is dependent upon air temperature and the direct
incidence of sunlight on the soil (Rouse and Stevens,1971). This
is seen in the comparison of results for different sampling days
at Nampundwe, and especially along the King Edward traverse.

Furthermore, subsequent statistical analysis on the
variability of blank reagents indicated that absorbance readings
from a number of blanks prepared simultaneously could vary by up
to 0.050 absorbance units (J.S. Lovell, pers.comm.) Thus, the
practical limit of detection is about 10 ppb SO_2 for a 20 litre
gas sample in 5 ml of absorbant solution. Since all results from
the Munali and King Edward soil gas traverses were below this limit

of detection, they must be regarded as having little validity.

9 4.   Discussion

The soil gas SO_2 investigation encountered
and confirmed many of the problems experienced by previous
researchers in this field. It was essential to perform most of
the development work for the method in Britain, but climatic
conditions do not favour vapour dispersion of highly soluble gases
in this country. It was therefore inevitable that certain operational
problems would emerge when arid test areas in Central Africa were
investigated.From the results obtained, it is possible only to state
that the present technique appears inadequate for the detection
of significant concentrations of SO_2 in soil gas, even over sulphide
ore. However, during the course of this research, some literature
has been published which calls into question the relevance of SO_2
in soil gas to sulphide mineral exploration.

Rouse and Stevens (1971) state that SO_2 was generated
during the artifical weathering of sulphides in the laboratory and in
sulphide-rich tailings dumps exposed to the atmosphere. A similar,
albeit slower, process was assumed during the oxidation of sulphide
deposits in situ. A mechanism of repeated SO_2 dissolution and release
with seasonal fluctuations in the water table was suggested as the
means by which gaseous SO_2 could persist in the soil pore space
and migrate to the surface.

However, pollution research by Smith, Bremner and
Tabatabai (1973) has shown that the SO_2 sorption capacity of air-dry
soils ranges from 1.1 to 15.3 mg SO_2 per g of soil, and the same soils
when moist have SO_2 sorption capacities in the range 9.3 to 66.8 mg
SO_2 per g. This relatively small difference between dry and moist soils

indicates that microbial activity does not play a significant role in SO_2 sorption. All soils studied required less than one minute to achieve 95% sorption of SO_2 from air initially containing 100 ppm SO_2. Both the rate and quantity of SO_2 sorption by soils are so great that Smith, Bremner and Tabatabai have suggested that soil is an important natural sink for SO_2 and could be used for the purification of industrial effluent. It therefore seems extremely probable that any minute concentrations of SO_2 evolved from oxidizing sulphide ores in the natural environment might migrate towards the surface in the manner suggested by Rouse and Stevens, but near the surface would be removed from the vapour phase by sorption onto soil. It is likely that this sorbed SO_2 would be oxidized to sulphate and subsequently removed by leaching and plant uptake, thereby rendering the sorption sites in the soil available for further sorption. In this way, a soil would not become saturated with SO_2, and hence little or no SO_2 can be expected to persist in the vapour phase.

Rouse and Stevens (1971) described the detection of SO_2 anomalies in soil gas and the atmosphere over sulphide orebodies. Their sampling and analytical methods, however , were stated to be proprietary, and were not described. According to West and Gaeke (1956) and Scaringelli, Saltzman, and Frey (1967) the reagents used in the present research are highly specific for SO_2, and the principal deleterious effect encountered was temperature variation. It may be the case that Rouse and Stevens were in fact detecting gases other than or in addition to SO_2 and that these produced anomalies over mineralization. Bremner and Banwart (1975) showed that several sulphur-bearing gases in soils are not sorbed by the soil to the same extent as SO_2. Over a period of 15 days, sorption from air initially containing 500 ppm of dimethyl sulphide, dimethyl disulphide, carbonyl sulphide or carbon disulphide by air-dry soil varies from 14 to 140 μg of

gas per g of soil, and by moist soils ranges from 35 to 2340 µg per g. Much higher sorption by moist soils is attributed to the role of micro-organisms in the sorption process. These low sorption rates suggest that dimethyl sulphide, dimethyl disulphide carbonyl sulphide and carbon disulphide may be far more prevalent than SO_2 in soil gas, and may be a source of significant S anomalies in vapour geochemistry.

10.   SUMMARY AND CONCLUSIONS

The extremely fine disseminations of sulphide minerals which are sparingly distributed throughout unweathered mafic and ultramafic intrusive rocks can be selectively analysed for their metal content by attacking a pulverized rock sample with Br in dilute acid solution, and for S, by a rapid combustion technique. The method of determining metals produces some spurious results as a result of the partial attack of silicate minerals by the dilute acid. Nevertheless, high mean concentrations, in suites of non-mineralized random core samples from different intrusives, of S, Co_S, Zn_S and to a lesser extent Fe_S, distinguish those intrusives with which economic or sub-economic mineralization are associated. A substantially higher percentage of Ni_S expressed as total Ni also characterizes mineralized intrusives, and high Cu_S in intrusives with ore of liquid-magmatic origin contrasts with low Cu_S in non-mineralized intrusives of similar silicate mineralogy. High S:Ni and S:Co ratios are found in mineralized intrusives compared with their non-mineralized counterparts of the same rock type, and equally high S:Cu ratios in both mafic and ultramafic rocks indicate the presence of mineralization, compared with lower S:Cu ratios in non-mineralized intrusives.

However, weathering, and the oxidation of sulphide minerals in particular, is generally too intense in Central Africa to allow the preservation of the same patterns in surface exposures of intrusive rocks. Most of the useful discriminant parameters identified in unweathered rocks are not successful when applied to outcrops. This contrasts with good discrimination of mineralized intrusives in the Canadian Shield on the basis of Ni_S, Cu_S, Co_S and S (Cameron, Siddeley and Durham, 1971) but sulphide oxidation in surface outcrops

is clearly less severe in the cool temperate climate of eastern
Canada. In Central Africa, the higher S content of outcrops is
the most promising criterion for distinguishing mineralization;
in the present research dealing with seven mineralized and non-
mineralized intrusives, the two mineralized intrusives are ranked
on S content a close third and fourth. This ranking is improved
by taking into account the visible degree of outcrop weathering
in the different field areas, and any correlation of S with Ni_s
indicating nickeliferous sulphides, or with Fe_s, indicating
pyrite or other non-economic sulphides.

Because weathering is relatively intense in Central
Africa, a thick, mature cover of residual soil is usually developed
and useful geochemical information about the nature of the parent
material and occurrence of primary mineralization can be obtained
from this.

Redistribution of Ni during soil formation depends
upon the mobility of the Ni ion. When Ni is leached from minerals
weathering in the acidic A horizon of the soil, a considerable
proportion of this Ni is carried in solution down the vertical profile
by percolating rainwater. Some Ni coprecipitates with and is
adsorbed by secondary Fe oxides in the B horizon, and more precipitates
by hydrolysis due to increases in pH in the upper C horizon.
Following this complex redistribution, highly anomalous amounts of
Ni may accumulate in the B and upper C horizons of the soil, but
the significance of such anomalies can be equivocal because the
mineralogy of the parent material is not easily perceived, and the
Ni could be derived from primary silicates or sulphides.

Not all elements undergo the same pattern of
redistribution and so multi-element data can assist in Ni anomaly
interpretation. In the C horizon, Ni enrichment derived from
ultramafic rocks is accompanied by high Cr and Mn and low Al, Ti,
V, Li, Ga and F; mafic rocks are characterized by high Al, Ti, V,

Li and Ga, and especially high Ni concentrations with this
association suggest the presence of mineralization. Owing to
the predominantly chalcophile nature of Cu, primary nickel
mineralization, particularly of liquid-magma segregation origin,
is commonly cupriferous, and elevated Cu concentrations characterize
the C horizon of soils overlying mineralization.

Plants rooted in the C horizon of the soil can take
up to their leaves substantial quantities of Ni when the threshold
level of Ni in the soil for a species is exceeded and the exclusion
mechanism, normally operated by the plant to restrict the uptake of
non-essential and toxic elements such as Ni, breaks down. The
accumulation of Ni in the C horizon often produces this biogeochemical
effect, but the provenance of Ni in leaves is no more apparent than
that of the Ni in the C horizon of the soil. Again multi-element
data can contribute to anomaly interpretation, but the uptake of
many elements other than Ni is closely controlled by plants within
a range reflecting their metabolic requirements. However, a
biogeochemical Ni anomaly coupled with Cr concentrations near the
top of a limited range suggests ultramafic rock at depth, while a
biogeochemical Ni anomaly with Cu values slightly above the norm
indicates mineralization.

Iron accumulates in the B horizon of the soil as
secondary Fe oxides, and considerable Fe enrichment can occur here
when a substantial primary source of Fe, such as massive sulphide
mineralization, is available. Elements which are siderophile in
the primary environment seem to retain this characteristic to some
extent in the B horizon of the soil, especially in the presence of
large quantities of Fe. Thus Fe derived from nickeliferous sulphides
accumulates in the B horizon and coprecipitates and adsorbs Ni, Cu
and S. This combination of high Fe, Ni, Cu and S therefore characterizes
mineralization. Where present in high concentrations, as over
mineralization, the secondary Fe oxides tend to accrete and form

nodules, so that compared with soils elsewhere in which the coarse
fraction comprises mainly resistant mineral grains, the soil over
mineralization is particularly enriched in Fe, Ni, Cu and S in the
coarse fraction.

Only low order S anomalies occur over mineralization in the
B horizon of the soil. The S is thought to occur as sulphate groups
which substitute for hydroxyl groups in the polymerization of ferric
hydroxide, but the sulphate ion is extremely soluble and much S is lost
in solution from the soil. Sulphur dioxide derived from the oxidation
of sulphides at depth probably does not occur as a vapour within the
soil because of the ready sorption of SO_2 by soils, and its sub-
sequent oxidation to and possible dissolution as sulphate (Smith,
Bremner and Tabatabai, 1973)

A F soil anomaly over predominantly mafic or ultramafic
rocks may provide another indication of mineralization. Ultramafic
rocks contain only small amounts of F, although during weathering some
F enrichment is brought about by clay minerals in the A and B horizons
of the soil. Mafic rocks have only a slightly higher F content than
ultramafic rocks. The aqueous fluids which are associated with nickel ore
genesis or emplacement are potentially fluoriferous, and hence high
F may occur with primary nickel mineralization, and this is reflected
in the overlying soil.

A substantial quantity of material from the upper horizons
of the soil is carried into the stream courses by rainwater run-off
in areas of free-flowing drainage. The particulate material
which makes up the stream sediment has some characteristics in common
with the B horizon of the soil, of which coincident Ni and Cu anomalies,
and to a lesser extent Fe anomalies,are the most characteristic features
denoting mineralization, and high Mg and Cr suggest ultramafic rocks.
These anomalies are most persistent in the fine fraction of the

sediment, where they are probably enhanced by the precipitation of
Ni and Cu brought into the stream water by springs and groundwater
seepage. The fine fraction anomalies are dramatically reduced
beyond confluences, but in areas of free-flowing dendritic drainage,
sampling every tributary just above the confluence facilitates
definition of all significant and non-significant Ni anomalies on
the basis of the multi-element composition of the samples. Dispersion
of the coarse material in stream sediments is more limited, and
anomalies based on relative enrichment of Ni, Cu and Fe in the
coarse fraction persist only some 400 m from source.

The S content of stream sediments is not a useful
parameter because of the very high mobility and general ubiquity of
moderate quantities of S in the secondary environment. Similarly any
F anomaly derived from Ni mineralization would soon be masked in the
drainage by F derived from still more fluoriferous rock units. The
value of S and F in nickel prospecting lies only in their anomalous
concentrations in soils overlying mineralization when compared with
soils covering the adjacent mafic and ultramafic host rock.

In areas of dambo and vlei drainage, most metals are
derived from circulating groundwater and are fixed by organic sediment.
There is little downstream dispersion compared with areas of free-
flowing drainage, although the same elements are useful in Ni
anomaly interpretation. Metal distribution along dambos and vleis
is erratic and a sampling interval of 100 m or 200 m is probably
desirable for the detection of anomalies.

A choice of techniques is available for the evaluation
of multi-element data relevant to distinguishing Ni anomalies related
to primary mineralization. In this research, the summation of
standard normal deviates of useful elements to produce uni-variate
Zsums was devised. The formula for generating Zsums is flexible so that
those elements found to be useful from orientation surveys and
backwards regression of training sets can be incorporated into the

equation. High Zsums identify promising prospecting targets, although a "threshold" figure is difficult to define and depends partly on the number of elements included in the formula. In Australia, Clema and Stevens-Hoare (1973) devised an evaluation based on the ratios of particular trace metals in samples, but employing closely similar fundamental geochemical principles. Both techniques appear to be applicable to the interpretation of soil and stream sediment data.

10.1   A scheme of prospecting for primary nickel ore in Central Africa

As in all geochemical surveys, when planning a programme of geochemical prospecting for primary nickel mineralization, an orientation survey in the same region is highly desirable. While reiterating this recommendation, it must also be said that this present research is mainly by way of an orientation survey for nickel prospecting in Central Africa (and other regions of similar climate), and so guidelines for commercial operations can be given on the basis of the results obtained.

It is usually possible for a mineral exploration organization undertaking a search for primary nickel ore to select a region within which suitable mafic and ultramafic host rocks are known to occur from geological survey maps or are suspected from aerial photography. The initial reconnaissance of such a region should comprise the collection of samples of the sediment of free-flowing drainage channels a few metres upstream in each tributary at every confluence, and collection of sediment samples along dambos and vleis at 100 m or 200 m intervals. The fine fraction of these samples should be analysed for Ni, Cu, Co, Cr, Mg, Fe and Mn using a rapid and economical method with fair precision (perhaps better than 30% for each element) such as emission spectroscopy or atomic absorption spectroscopy. Coincident Ni, Cu and Fe anomalies are the best indication of mineralization. High Ni associated with Cr and Mg anomalies suggests an ultramafic rock and unusual enrichments of Ni, Fe, Co and Mn are probably derived from ironstone or ferruginous

sedimentary formations. Rapid evaluation of these multi-element
data can be achieved by generating uni-variate Zsums, as described
in this research, or calculating certain ratios of elements taken in
combination, as described by Clema and Stevens-Hoare (1973). A Zsum formula
likely to provide successful discrimination of mineralized intrusives
is the addition of the standard normal deviates of Ni, Cu and Fe and the
subtraction of the Co and Mg standard normal deviates, but in many
cases Mn and Cr could be substituted for Co and Mg. With this
five-element formula, Ni anomalies in excess of the regional Ni means
plus two standard deviations supported by Zsums in excess of +3.50
are indicative of mineralization. However, in any region the results
of an orientation survey would give the best guide to the choice of
elements to be incorporated into the Zsum formula and the magnitude of
a Zsum anomaly associated with mineralization.

The use of outcrop sampling as a means of establishing
mineralization potential of mafic and ultramafic intrusives in Central
Africa is clearly limited by the high degree of weathering. The
selection of the more promising targets among many intrusives might
be attempted by collecting random outcrop samples and analyzing for
S and perhaps Ni_S and Fe_S. Intrusives with the highest S concentrations,
and at least 300 ppm S,represent the favourable areas for further
investigation, and an improved assessment might be achieved by
considering that a fair correlation of Ni_S and S suggests better potential
than a good Fes and S correlation.

The detailed appraisal of an intrusive, considered from
reconnaissance sampling to have some mineralization potential,
is best made by soil geochemistry, provided the soil cover is residual.
In this research, anomalous Ni concentrations were found in the B
horizon of the soil over distances of 60 to 80 m along traverse lines at
right angles to the long axis of the mineralization. Therefore a sample
interval of 30 m is recommended, probably on a square grid covering slightly
more than the area thought to be underlain by intrusive rocks. Soil

profile development should be studied in pits dug for the purpose,
and a sampling depth should be adopted whereby the B horizon of the
soil is sampled consistently. The fine fraction of samples should
be analysed for Ni, Cu, Co, Cr, Fe, V and F and the coarse fraction for
Ni, Cu, Fe and S. Coincident Ni, Cu and S anomalies are a
particularly characteristic expression of mineralization at depth
and concentrations of F in soils overlying mineralization may be
higher than F in soils over adjacent mafic or ultramafic rock if
fluoriferous fluids were associated with ore genesis or emplacement.

These multi-element data required for Ni anomaly
interpretation are conveniently reduced to uni-variate Zsums by adding
the standard normal deviates of these four elements for each soil
sample in the grid. High Zsums, probably those over +6.00, define
significant Ni anomalies. Other favourable indications are the
enrichment of Ni, Cu and Fe in the coarse fraction, especially over
massive sulphides, and Ni values in excess of Cr, or a high Ni:Cr
ratio. The non-significant Ni anomaly found over lenses of
ultramafic rock within a predominantly mafic intrusive is accompanied
by high Cr values, or a low Ni:Cr ratio, a negative V anomaly,
possibly a negative F anomaly, no Cu anomaly and a relative enrichment
of Ni, Cu or Fe in the fine fraction.

A promising soil anomaly should be followed-up by
pitting, trenching, or auger drilling to reach and sample the underlying
C horizon. Considerable enrichment of Ni in the upper C horizon,
perhaps more than 1% Ni, can occur over both mineralization and
ultramafic rock. Wilding (1965) has suggested that increasing Ni
values with depth in the C horizon are a good indication of
mineralization, but this has not been affirmed in the present research.
Once again, multi-element data make the most valuable contribution
to Ni anomaly interpretation, so that Ni enrichment accompanied by
high Cu, S and F suggests mineralization, while high Cr, Mg and low

Al, Ti, V, Li, Ga and F reflect ultramafic rock. Wilding (1965)
states that anomalous concentrations of Ni extracted from
C horizon samples using an ammonium acetate leach (termed
exchangeable nickel, exNi) are indicative of mineralization.

Biogeochemistry offers little advantage in nickel
prospecting in areas of residual soils in Central Africa. Where
Ni thresholds in the soil are exceeded, the partial exclusion
mechanism of those common trees studied in this research breaks
down, and large biogeochemical Ni anomalies result. However, these
anomalies seem to reflect Ni enrichment in the C horizon of the soil,
and do not distinguish between mineralization and ultramafic rock.
Because plants usually control and restrict their uptake of most
metals other than Ni, only slight changes in the leaf content
of these metals occur in trees rooted in soils containing anomalous
coneentrations of the same metals. Hence, multi-element data
interpretation is substantially restricted in biogeochemistry
compared with soil geochemistry.

The determination of SO_2 in soil gas cannot be
recommended on the basis of the results obtained in this research.
Indeed, there is considerable doubt as to the existence of SO_2
in the vapour phase within the soil pore space.

The optimum diamond drilling targets are
therefore defined by B horizon and C horizon multi-element
geochemistry. Where a scout drilling programme fails to produce
conclusive evidence of potentially economic mineralization, an
investigation of primary dispersion patterns in the mafic or
ultramafic rock might be useful. Random core samples of unweathered
non-mineralized mafic and ultramafic rock should be analysed for total
Ni, Cu and Co by emission spectroscopy or atomic absorption
spectroscopy for Ni_S, Cu_S, Co_S and Zn_S using a Br attack and atomic

absorption spectroscopy, and for S using the rapid combustion method. A high percentage of total Ni in the form of Ni_S, high Co_S, Zn_S, Cu_S and S ,high S:Ni, S:Co and S:Cu ratios are good indications of a mineralized intrusive, and a recommendation that drilling should continue. The values obtained could conveniently be compared with the corresponding data obtained in this research, by Cameron, Siddeley and Durham (1971) and by Hausen, Ahlrichs and Odekirk (1973).

10.2.   Recommendations for further research

The more rewarding opportunities for further research into geochemical prospecting for primary nickel ore lie with various aspects of S dispersion, and are therefore also applicable to prospecting for other sulphide ores. Of particular merit is the speciation of S in soils, with a view to the selective determination of S associated with secondary Fe oxides. Similar work was carried out by Peters (1974) using stepwise thermal decomposition of samples and simultaneous emission spectroscopy determination of S evolved at different temperatures. According to Peters, organic S compounds were determined at a sample temperature of about $450°$ C and pyrite broke down with the release of S when the sample temperature was raised to $670°$ C.

Phreatophyte trees take up S in solution by their roots in the C horizon of the soil and weathered bedrock. Thus biogeochemistry may offer a means, largely free of the complications introduced by organic compounds and secondary Fe oxides in the A and B soil horizons, of indicating the S content of bedrock. Sulphur is essential to plants, which contain around 500 ppm according to Brooks (1972), and controlled uptake is therefore to be anticipated. However, in the present research it was noted that the leaf content of several essential trace metals fluctuated somewhat with variations in concentration of the corresponding metal in the underlying soil, and

so low order biogeochemical S anomalies, at the top of the normal S range, may be found to reflect sulphide mineralization at depth.

The S content of soil gas may prove a useful guide to sulphide mineralization, but SO_2 may not be the optimum parameter to measure. Bremner and Banwart (1975) have shown that dimethyl sulphide, dimethyl disulphide, carbonyl sulphide and carbon disulphide are much less readily sorbed than SO_2 by the soil, and are therefore more persistent in the vapour phase. The determination of one of these compounds in soil gas, or the combined S content of several compounds, may constitute a viable prospecting technique. The analysis of soil gas could be particularly useful where soil geochemistry does not furnish a fair reflection of bedrock composition, as in areas of transported overburden.

The value of F in soils as a pathfinder for certain base metals deposit has been reviewed by Boyle (1976) and this element seems a potentially useful guide to some, if not all, occurrences of primary nickel mineralization. A more detailed and widespread investigation is required of the association of fluoriferous gangue minerals with nickel sulphides, and further study is needed of the behaviour of F during the weathering of sulphide deposit and the formation of ferruginous and lateritic soils. In the secondary environment, F is incorporated into clay minerals, and optimum anomaly contrast may be found in the soil horizon and sample size fraction richest in clay minerals. The partial, rather than total, extraction of F from samples may also prove rewarding.

Further research on the selective dissolution and determination of metals in sulphide minerals in mafic and ultramafic rocks as a means of discriminating mineralized and non-mineralized intrusives is not necessarily recommended. This approach was found to be successful by Cameron, Siddeley and Durham (1971), partially successful in the present research, but rejected as ineffective

by Hausen, Ahlrichs and Odekirk (1973). However, in any new work on this technique, samples should be analyzed for Zn_s and the discriminant power of this variable appraised. According to Moeskops (1976), high total Zn in mafic and ultramafic rocks is not a promising indication of mineralization, and in the present research the highest Zn levels are found in the non-mineralized Chitina intrusive. Nevertheless, Zn is highly mobile in the primary environment, and in the presence of S in mafic and ultramafic melts may be incorporated into widely dispersed sulphide minerals.

Finally, this research has emphasized the significance of multi-element data in Ni anomaly interpretation and the value of reducing the useful variables from each sample to a single composite expression. The application and development of such techniques with other appropriate soil and stream sediment geochemistry data sets acquired in connection with primary nickel prospecting will further substantiate and refine the principles of rapid and successful Ni anomaly evaluation.

10.3.   The future demand for primary nickel ore

At present, primary nickel ore constitutes the most attractive source of nickel. Since the oil price increases of 1973, energy costs have become a particularly large component of nickel production costs, and sulphide ore processing consumes far less energy than oxide ore processing (Dasher, 1976).

By 1985, however, ocean-floor mining of manganese nodules seems likely to be a significant source of nickel. The most promising ocean-floor prospect is in the mid-Pacific between Mexico and Hawaii, where there are nodule deposits grading 1.4% Cu and 1.6% Ni. The international legal problems posed by mining the ocean-floor have become the subject of protracted debate, under the auspices of the United Nations, and are as yet unresolved. Meanwhile,

five multi-national consortia have reached an advanced stage of
research in nodule recovery and treatment, and feel that such mining
is economically feasible when based on both copper and nickel
extraction. The USA has taken the lead in pressing for an
international agreement that would permit ocean-floor mining to begin
and has proposed that the output of nickel from this source should
increase at an annual rate of not less than 6% of present nickel
production (Spooner, 1976). During the period 1960 to 1974, world
demand for nickel increased at an annual average rate of 6.5%, and
forecasts for the next decade suggest slightly slower growth in demand.
Hence, if the US proposal is accepted, ocean-floor mining will meet
all additional demand for nickel above current levels and is expected
to furnish 220 million tonnes of nickel per annum, 18% of world
requirements, in 1985 (Sisselman, 1975). Furthermore, the US proposal
places the onus on terrestrial nickel producers to cut their output
in the event of over supply in the market.

The potential of ocean-floor mining along with the
recent business recession and high energy costs, has caused
postponement of the development of some terrestrial nickel projects,
and an economic boom in the near future might cause a nickel shortage
and high prices. As before, this would promote nickel prospecting and
exploration, especially, in view of the cheaper processing costs, for
primary sulphide ore. However, in the long term, the exploitation
of ocean-floor resources and the proposed nickel mining policy
associated with such mining seem likely to diminish the incentive for
terrestrial nickel prospecting, although large, high grade sulphide
deposits may continue to be viable targets.

REFERENCES

Aguilera, N.H. and Jackson, M.L. (1953); Iron oxide removal from soils and clays. Proc. Soil Sci. Soc. of America, vol. 17, no. 4, pp 359-364

Aldous, K.M., Dagnall, R.M., Pratt, S.J. and West, T.S. (1969); Microwave-excited electrodeless discharge tubes containing organo-sulphur and phosphorus compounds. Anal. Chem., vol.41, no. 13, pp 1851-1853

Band, R. (1969); Dispersion of nickel and molybdenum from mineralization in glaciated terrain, southern Norway. Univ. of London, Ph.D. Thesis

Barr, M.W.C. (in print); The geology of the Chongwe River area. Geol. Survey of Zambia, Report

Bowen, N.L. (1956); The evolution of the igneous rocks. Dover Publications Inc., New York

Boyle, D.R. (1976); The geochemistry of fluorine and its application to mineral exploration. Univ. of London, Ph.D. Thesis

Boyle, R.W. and Dass, A.S. (1967); Geochemical prospecting - use of the 'A' horizon in soil surveys. Econ. Geol., vol. 62, no. 2, pp 274-275

Bremner, J.M. and Banwart, W.L. (1975); Sorption of sulphur gases by soils. Soil Biol. Biochem., vol. 8, pp 79-83

Brooks, R.R. (1972); Geobotany and biogeochemistry in mineral exploration. Harper and Row, New York

Buchanan, D.L. (1975); Identification of geological environments in basic and ultrabasic igneous rocks that favour the formation of sulphide segregations. Trans. IMM 858, pp B289-B291

Butt, C.R.M. and Sheppy, N.R. (1975); Geochemical exploration problems in western Australia exemplified by the Mt Keith area. Geochem. Expl. 1974, pp 391-416

Cameron, E.M., Siddeley, G. and Durham, G.G. (1971); Distribution of ore elements in rocks for evaluating ore potential- nickel, copper, cobalt and sulphur in ultramafic rocks of the Canadian Shield. CIM special volume no. 11, pp 298-313

Carpenter, R.H., Pope, T.A. and Smith, R.L. (1975); Fe-Mn oxide coatings in stream sediment geochemical surveys. Jour. of Geochem. Expl., vol. 4, no. 3, pp 349-364

Chamberlain, J.A. (1967); Sulphides in the Muskox Intrusion. Can. Jour. Earth Sci., vol. 4, pp 105-152

Chester, R. and Hughes, M.J. (1967); A chemical technique for the separation of ferro-manganese minerals, carbonate minerals, and absorbed trace elements from pelagic sediments. Chem. Geol. 2, pp-249-262

Clark, T. and Naldrett, A.J. (1972); The distribution of Fe and Ni between synthetic olivine and sulphur at 900°C. Econ. Geol., vol. 67, no. 7, pp 939-952

Clema, J.M. and Stevens-Hoare, N.P. (1973); A method of distinguishing nickel gossans from other ironstones on the Yilgarn Shield, Western Australia. Jour. of Geochem. Ex., vol. 2, no. 4, pp 393-402

Clews, D.R. (1962); The secondary dispersion of copper in the drainage system of the Kilembe Mine area, Uganda. Univ. of London, Ph.D. Thesis

Coates Palgrave, O.M. and K. (1957); Trees of central Africa. National Publications Trust, Rhodesia and Nyasaland, Salisbury

Cole, M.M. (1971); Biogeographical/geobotanical and biogeochemical investigations connected with exploration for nickel-copper ores in the hot, wet summer/dry winter savanna woodland environment. Jour. of S.A. Inst. Min. and Met., May 1971, pp 199-209

Cole, M.M. (1971A); The importance of environment in biogeographical/ geobotanical and biogeochemical investigations. CIM special vol. 11, pp 414-425

Coope, J.A. (1958); Studies in geochemical prospecting for nickel in Bechuanaland and Tanganyika. Univ. of London, Ph.D. Thesis

Cox, R. (1975); Geochemical soil surveys in exploration for nickel-copper sulphides at Pioneer, near Norseman, Western Australia. Geochem. Expl. 1974, pp 437-460

Czamanske, G.K. and Ingamells, C.O. (1970); Selective chemical dissolution of sulphide minerals - a method of mineral separation. Amer. Min., vol. 55, pp 2131-2134

Dasher, J. (1976); The energy picture in nickel production. Min. Mag., vol. 134, no. 5, pp 379-389

Davenport, P.H. and Nichol, I. (1973); Bedrock geochemistry as a guide to areas of base-metal potential in volcano-sedimentary belts of the Canadian Shield. Geochem. Expl. 1972, pp 45-59

Davies, B.E. (1974); Loss on ignition as an estimate of soil organic matter. Proc. Soil Sci. Soc. of Amer., vol. 38, no. 1 pp 150-151

Drysdall, A.R., Johnson, R.L., Moore, T.A. and Thieme, J.G. (1972); Outline of the geology of Zambia. Geologie en Mijnbouw, vol. 51, no. 3, pp 265-276

Ellis, A.J., Tooms, J.S., Webb, J.S. and Bicknell, J.V. (1967); Solution experiments in geochemical prospecting. Trans. IMM 76B, pp B25-B38

Evans, D.S. (1971); Secondary dispersion of mercury and associated elements at Keel, Eire, Univ. of London, Ph.D. Thesis

Fanshawe, D.R. (1968); Fifty common trees of Zambia. Ministry of Natural Resources and Tourism, Zambia, Forest Dept. Bulletin no.5.

Foster, J.R. (1973); The efficiency of various digestion procedures on the extraction of metals from rocks and rock-forming minerals. CIM Bulletin, vol. 66, no. 736, pp 85-92

Garrett, R.G. (1967); A program for the rapid screening of multivariate data from the earth sciences and remote sensing. Northwestern Univ., Illinois,Report no. 11

Ginzburg, I.I. (1960); Principles of geochemical prospecting. Pergamon Press, Oxford

Goldschmidt, V.M. (1954); Geochemistry. Clarendon Press, Oxford

Hall, J.S., Both, R.A. and Smith, F.A. (1973); A comparative study of rock, soil and plant geochemistry in relation to nickel mineralization in the Pioneer area, Western Australia. Proc. Aus. IMM, no.247, pp 11-12

Harden, G. (1962); Geochemical dispersion patterns and their relationship to bedrock geology in the Nyawa area, Northern Rhodesia. Univ. of London, Ph.D. Thesis

Haughton, D.R., Roeder, P.L. and Skinner, B.J. (1969); Solubility of sulphur in mafic magmas. Econ. Geol., vol. 69, no. 4, pp 451-467

Hausen, D.M., Ahlrichs, J.W. and Odekirk, J.R. (1973); Application of sulphur and nickel analysis to geochemical prospecting, Geochem. Expl. 1972, pp 12-24

Hawkes, H.E. and Webb, J.S. (1962); Geochemistry in mineral exploration. Harper and Row, New York

Hem, J.D. (1970); Study and interpretation of the chemical characteristics of natural waters. US Dept. of the Interior, Geol. Survey Water Supply Paper 1473

Howarth, R.J. (1972); Generation of random number tables for randomising sample order prior to submission for analysis. Unpublished computer program

Howarth, R.J. (1973); Fortran IV programs for empirical discriminant classification of spatial data. Geocom. Programs, 7

Keep, F.E. (1929); The geology of the Shabani Mineral Belt. Geol. Survey of Southern Rhodesia, Bulletin no. 12

King, H.G.C. and Pruden, G. (1969); The determination of sulphur dioxide with rosaniline dyes. The Analyst, vol. 94, pp 43-48

Lalonde, J.P. (1974); Research in geochemical prospecting methods for fluorite deposits, Madoc area, Ontario. Geol. Survey Canada, Paper 73-38

Le Riche, H.H. and Weir, A.H. (1963); A method of studying trace elements in soil fractions. Jour. Soil Sci., vol. 14, no. 2, pp 225-235

Le Roex, H.D. (1964); Nickel deposits on the Trojan claims, Bindura district, southern Rhodesia. Some ore deposits of southern Africa, Geol. Soc. S.A., Johannesburg

Loughlan, F.C. (1969); Chemical weathering of the silicate minerals. Elsevier, Netherlands

Lynch, J.J. (1971); The determination of copper, nickel and cobalt in rocks by atomic absorption spectrometry using a cold leach. CIM special volume no. 11, pp 313-314

Mason, B. (1966); Principles of geochemistry. John Wiley and Sons Inc., New York

Mazzucchelli, R.H. (1972); Secondary geochemical dispersion patterns associated with the nickel sulphide deposits at Kambalda, Western Australia. Jour. of Geochem. Ex., vol. 1, no.1, pp 105-115

Mckinstry, H.E. (1948); Mining geology. Prentice-Hall Inc., New Jersey

Mendelsohn, F. (1961); The geology of the Northern Rhodesian Copperbelt. Macdonald and Co., London

Meyer, W.T. and Lam Shang Leen, K.C.Y. (1973); Microwave induced argon plasma emission system for geochemical trace analysis. Geochem. Expl. 1972, pp 325-334

Meyer, W.T. (1973); Development and application of thermally-evolved vapour analysis in exploration geochemistry. Univ. of London, Ph.D. Thesis

Michener, C.E. (1957); Annual Report N.A.O.R.G.S.

Moeskops, P.G. (1976); Yilgarn nickel gossan geochemistry - a review including new data considerations. Abstracts 25th Int. Geol. Congress, pp 449-450

Naldrett, A.J. and Arndt, N.T. (1975); Association of nickel sulphides with rocks of volcanic origin suggests new exploration targets. The Northern Miner, 6 March 1975, pp 39-40

Naldrett, A.J. (1966); The role of sulphurization in the genesis of iron-nickel sulphide deposits of the Porcupine district, Ontario. CIM Bulletin, vol. 59, no. 648, pp 489-497

Peters R.G. (1974); Secondary dispersion of sulphur from sulphide deposits in the Notre Dame Bay area, Newfoundland. Univ. of London, Ph.D. Thesis

Phillips, K.A. (1958); The geology of the metalliferous deposits of the Luiri Hills area (Mumbwa district). Geol. Survey of Northern Rhodesia, Report no. 4

Polferov, D.V. and Suslova, S.I. (1966); Geochemical criteria of the nickeliferous capacity of ultrabasic massifs. Geochem. Int., vol. 3, pp 487-498

Prasad, R. and Vrana, S. (1972); The intrusives of the Chombwa area with special reference to the eclogites. Records of Zambian Geol. Survey, vol. 12

Rouse, G.E. and Stevens, D.N. (1971); The use of sulphur dioxide gas geochemistry in the detection of sulphide deposits. Amer. Inst. of Min. and Met. Engineers

Sauchelli, V. (1969); Trace elements in agriculture. Van Nostrand Reinhold, Princeton, New Jersey

Scaringelli, F.P., Saltzman, B.E. and Frey, S.A. (1967); Spectrophotometric determination of atmospheric sulphur dioxide. Anal. Chem., vol. 39, no. 14, pp 1709-1719

Simpson, J.G. (1967); The geology of the Chinyunyu area. Geol. Survey of Zambia, Report no. 19

Sisselman, R. (1975); Ocean miners take soundings on legal problems, development alternatives. Eng. and Min. Jour., vol. 178, no. 4, pp 75-86

Smith, A.G. (1963); The geology of the country around Mazabuka and Kafue. Geol. Survey of Northern Rhodesia, Report no. 2

Smith, B.H. (1976); Some aspects of the use of geochemistry in the search for base-metal sulphides in lateritic terrain in western Australia. Abstracts 25th Int. Geol. Cong., vol. 2, sect. 10B, pp 458-459

Smith, K.A., Bremner, J.M. and Tabatabai, M.A. (1973); Sorption of atmospheric pollutants by soils. Soil Sci., vol. 116, no. 4, pp 313-319

Spooner, J. (1976); Nickel offshore. Min. Jour., vol. 176, no. 7346, pp1-2

Stillman, C.J. (1965); The geology of the Musofu River and Mkushi areas. Geol. Survey of Zambia, Report no. 12

Stumm, W. and Morgan, J.J. (1962); Chemical aspects of coagulation. Jour. of American Water Works Assoc., Aug 1962, pp 971-992

Stumm, W. and Morgan, J.J. (1970); Aquatic chemistry. Wiley-Interscience, New York

Thompson, M. and Howarth, R.J. (1973); The rapid estimation and control of precision by duplicate determinations. The Analyst, vol. 98, no. 1164, pp 153-160

Thompson, M. and Howarth, R.J. (1976); Duplicate analysis in geochemical practice. The Analyst, vol. 101, pp 690-709

Turner, F.J. and Verhoogen, J. (1960); Igneous and metamorphic petrology. McGraw-Hill, New York

Tyndale-Biscoe, R. (1933); The geology of the central part of the Mazoe valley gold belt. Geol. Survey of Southern Rhodesia, Bulletin no. 22

West, P.W. and Gaeke, G.C. (1956); Fixation of sulphur dioxide as disulphitomercurate and subsequent colorimetric estimation. Anal. Chem., vol. 28, no. 12, pp 1816-1819

Whitney, P.R. (1975); Relationship of manganese-iron oxides and associated heavy metals to grain size in stream sediments. Jour. of Geochem. Expl., vol. 4, no. 2, pp 251-264

Wiik, V.H. (1969); Soil and laterite formation. Geol. Research Unit, RST. Technical Services Limited, Report no. GR/14

Wild, H. (1970); Geobotanical anomalies in Rhodesia, 3, the vegetation of the nickel-bearing soils. Supplement to Kirkia, vol. 7

Wilding, I.G.P. (1965); Investigation of the secondary dispersion of nickel in Rhodesia and Zambia. Univ. of London, Ph.D. Thesis

Wilmshurst, J.R. (1975); The weathering products of nickeliferous sulphides and their associated rocks in western Australia. Geochem. Expl. 1974, pp 417-436

APPENDICES

I. <u>ARGON PLASMA EMISSION SPECTROGRAPHY</u>

Argon plasma emission spectrography facilitates
the analysis of volatile elements by fractional thermal
decomposition of the parent material and emission spectrographic
determination of a single volatile element at a selected wavelength
(Meyer and Lam Shang Leen, 1973). The determination of S in rocks
and soils was initially attempted using an induction furnace
linked to this instrument, and following the method described by

Meyer (1973). The analytical procedure was to pack approximately
20 mg of sample (powdered rock or fine soil) into the conical cavity
of a carbon rod electrode which was then induction heated in a LECO
radio-frequency furnace. The temperature was controlled by adjusting
the voltage to the furnace, and a maximum temperature of about $800^{\circ}C$
was attainable. A stream of argon was passed over the heated sample,
and the volatile components were carried by the gas stream upwards
from the furnace into a plasma induced by microwaves. The emission
from the plasma was dispersed by a plane grating monochromator, and
a suitable wavelength for the determination of S was selected. The
emission intensity at this wavelength was detected by a photomultiplier,
and recorded by pen on a paper chart recorder (figure 121). Up to 20
samples per hour could be analysed, according to the fractional analysis
desired.

To calibrate the instrument, standards containing
50,000 ppm, 20,000 ppm, 10,000 ppm, 5,000 ppm, and 1,000 ppm S were
prepared by grinding together weighed quantities of Analar $Fe_2(SO_4)_3$
and Specpure SiO_2. There were analysed by packing a carbon electrode
cavity with the standard, heating to $800^{\circ}C$ in the argon plasma emission
spectrograph, and noting the emission intensity at S wavelengths. The
results for all five standards were plotted graphically and provided
fair calibration curves in view of the limitations of dry mixing and
the approximate weights taken in analysis. Two atomic sulphur lines,
at $4697\overset{\circ}{A}$ and $1900\overset{\circ}{A}$, were calibrated, and in both cases S concentration
was proportional to the log of emission intensity up to about 10,000 ppm
S, and was directly proportional to emission intensity at higher
concentrations. The $4697\overset{\circ}{A}$ wavelength was the more sensitive but is
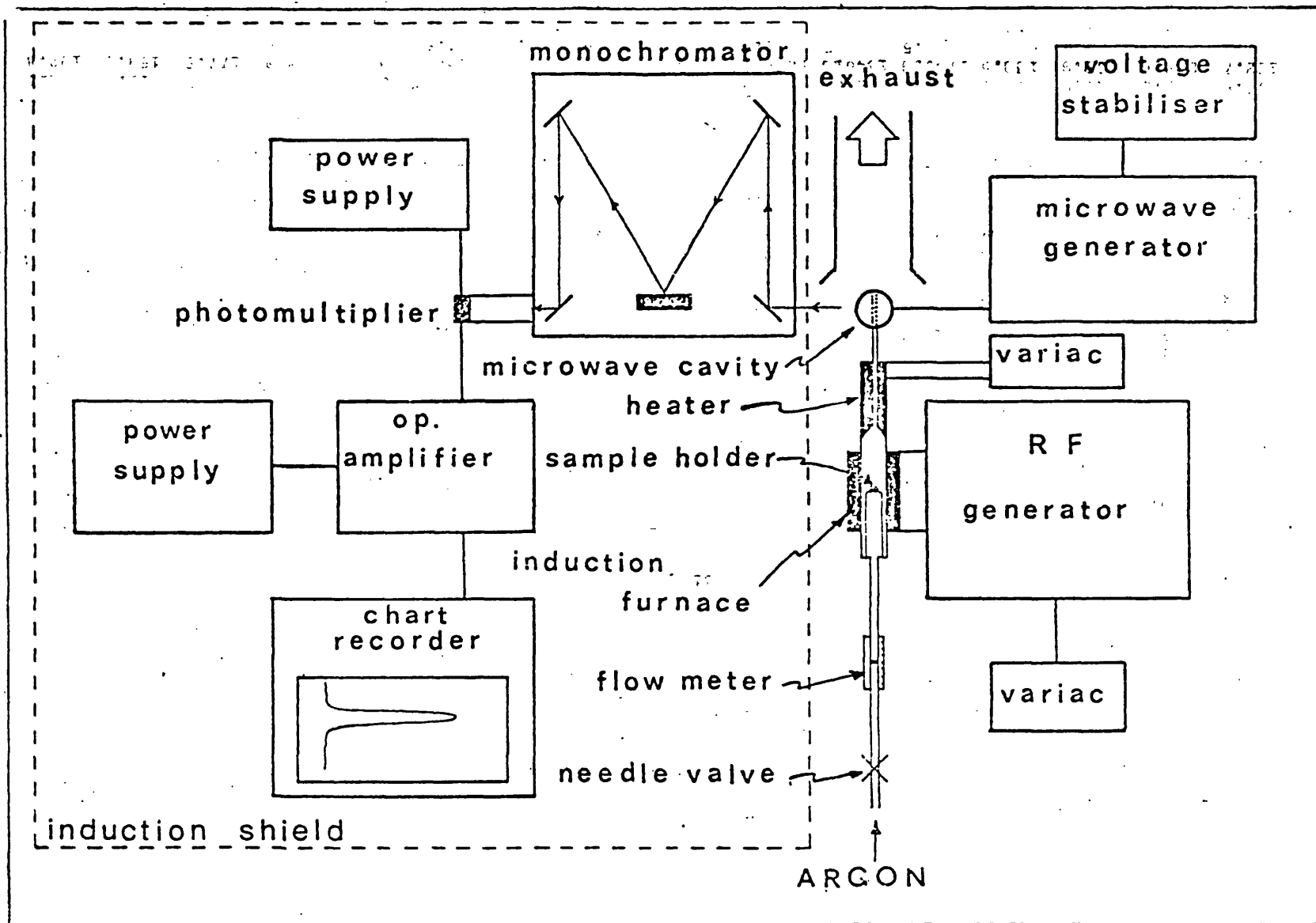
Figure 121:   Schematic diagram of argon plasma emission system (after Meyer, 1973).

known to be subject to possible interference from the molecular carbon Swann bands in that part of the spectrum. However an empty carbon electrode sample holder heated to $800^{o}C$ produced no significant response on the chart recorder.

During calibration the optimum monochromator inlet and outlet slit widths were found to be 0.05 mm, and therefore these widths were used in sample analysis. The inverse dispersion of the monochromator was $25\overset{o}{A}$ (possibly greater below $2000\overset{o}{A}$) and so the operating band pass of the instrument was $25\overset{o}{A}\times0.05$ mm = $1.25\overset{o}{A}$. To cope with any emission intensities beyond the calibrated range of the monochromator the window height at the inlet slit was adjusted.

Two parallel investigations were carried out, one using the $4697\overset{o}{A}$ wavelength for the analysis of diamond drill core samples, which were expected to contain little or no C, and the other using the $1900\overset{o}{A}$ wavelength for the analysis of soils, which would probably contain organic C.

Diamond drillhole core

Core samples were analysed for S present as sulphide minerals by heating to about $750^{o}C$, when pyrite, pyrrhotite and associated sulphides break down. The $4697\overset{o}{A}$ line was selected on the monochromator since C interference was not anticipated. The samples analysed comprised 65 core specimens taken at 5 m intervals along diamond drillhole MH58 at Munali, plus 10 duplicates, occasional calibration standards and blanks. The calibration standards yielded consistent results, duplicate analyses showed the technique to have fair asymptotic precision of the order of 20% to 30% when estimated graphically and blank electrode determinations proved that there was no interference from non-sample material. A computer program KAL was written to convert spectrograph output chart records from peak height values into S concentrations employing the calibration curves from standards.

Argon plasma emission spectrography[*]			Calcimetry		Emission Spec.
S (ppm)	C (ppm)	C (ppm)			
$4697Å$	$2478Å$	$4697Å$	% CO_2	C (ppm)	% Ca

Typical "background" samples

MH58-05	200	200	300	0.0	0	0.0
MH58-10	12,900	7200	2100	1.6	4300	9.1
MH58-45	300	500	400	0.2	500	7.7

Samples with visible sulphide mineralization

MH58-14	60,000	4800	14,900	5.8	15,800	5.6
MH58-17	30,000	1900	4600	2.8	7600	7.0
MH58-30	85,700	4200	24,800	12.7	34,600	16.2

Apparently "anomalous" samples

MH58-19	530,000	89,400	195,200	18.8	51,300	27.9
MH58-61	430,000	110,600	156,800	42.4	119,600	23.7
MH58-62	158,600	53,000	52,700	10.0	27,800	11.6
MH58-63	401,400	101,500	145,900	41.1	112,100	35.7
MH58-64	330,000	101,500	118,500	22.4	61,100	11.1
MH58-65	387,200	89,400	140,400	37.5	102,200	35.7

[*] Figures obtained by converting peak heights to S and C concentrations using appropriate calibration curves.

Table 45: Diamond drillhole MH58, example argon plasma emission spectrography S and C results, calcimetry and Ca results.

In MH58 core samples, the S concentrations determined range from 200 ppm to 530,000 ppm (table 45). However, there is poor correspondence between high S values in MH58 core samples, and visible grains of sulphide mineralization in the core. Samples MH58-19 and MH58-61 through MH58-65 each seemingly contain between 158,600 ppm and 530,000 ppm S, and figures at the high end of this range suggest almost pure sulphide minerals. The core log for the drillhole records only trace quantities of sulphides in the vicinity of these samples, and the log is supported by low analytical results for the ore metals. The maximum visible mineralization in the core was noted in the vicinity of samples MH58-17 and MH58-30, which contain 30,000 ppm and 85,700 ppm S respectively.

The most likely source of analytical error was thought to be interference, probably from the molecular carbon bands in the spectrum around $4697\overset{o}{A}$. An investigation of this hypothesis was made by calibrating both the atomic carbon $2478\overset{o}{A}$ wavelength for C, and the response to C at $4697\overset{o}{A}$. Carbon standards were prepared by grinding together weighed quantities of Analar $CaCO_3$ and Specpure SiO_2 to give 50,000 ppm, 20,000 ppm, 10,000 ppm, 5,000 ppm, and 1,000 ppm C standards. These were analysed using both wavelengths, and calibration curves were obtained showing that C concentration is proportional to the log of emission intensity up to 10,000 ppm C, and above this is directly proportional to emission intensity at both wavelengths.

Analysis of MH58 core samples using the $2478\overset{o}{A}$ wavelength produced peak heights which have a +0.84 correlation with peak heights at $4697\overset{o}{A}$. The computer program KAL was modified to effect conversion of chart record peak heights into C concentrations according to the calibration curves for the appropriate wavelenghts.

Carbon results from the 2478Å and 4697Å wavelengths are somewhat similar for those samples containing little or no visible sulphide mineralization, while the response at 4697Å is enhanced where sulphides are recorded. Therefore, the 4697Å wavelength is indeed sensitive to S, but is prone to C interference.

The source of C in diamond drillhole MH58 was identified by analyzing core samples for carbonate using a Collins gas burette calcimeter. Using this apparatus the evolution of CO_2 upon acid dissolution of sample material is quantitatively measured. The standard practice of sample dissolution in 50% HCl solution was modified by the addition to the acid of 2 g/l $CuCl_2$, which reacts with any acid soluble sulphides in the sample to form insoluble CuS and thereby inhibits the evolution of H_2S. Most of the 65 samples analysed evolved between zero and 2% of sample weight as CO_2, and seven samples, including MH58-19 and MH58-61 through MH58-65, evolved between 10.0% and 42.4% CO_2 (table 45). The C content of samples was calculated at 27% of CO_2 evolved, and ranges from zero to 115,600 ppm. Calcium concentrations of the MH58 core samples, determined by direct-reading-emission spectroscopy, are typically around 7% for most samples and range from 11.1% to 35.7% for the seven samples with a high C content. There is a +0.91 correlation between C determined by argon plasma emission spectrography and at 2478Å and C determined by calcimetry, and a +0.80 correlation between C determined at 2478Å and Ca.

Thus the source of C interference in the analysis of rocks for S by argon plasma emission spectrography is largely the thermal decomposition of $CaCO_3$ into CaO and CO_2. The CO_2 is carried by the argon stream into the plasma, where molecular carbon emissions are detected at 4697Å.

Sample No.	Temp (°C)	Argon plasma emission spectrography (1900Å)		Cum.C (a)	L-O-I C (ppm)	Gravimetry Total C (b)	$\frac{a}{b}$ X 100%
		S (ppm)	C (ppm)				
Munali							
145-84*	450	10909	3787	8612	58500	25170	34.2
	750	12727	4825		4300		
145-88*	450	5011	2332	5687	63500	16707	34.0
	750	10000	3355		0		
145-31	450	630	784	1669	14800	7862	21.2
	750	794	885		7300		
Chombwa							
245-11	450	2511	1662	4255	42700	13399	31.8
	750	6309	2633		16700		
245-17	450	2511	1662	3954	67000	16107	24.5
	750	5011	2332		400		
Chitina							
435-04	450	398	615	1500	15100	5515	27.2
	750	794	885		500		
435-12	450	630	784	1783	47100	9173	18.4
	750	1000	999		6100		
435-49	450	630	784	2615	48400	8353	31.3
	750	3162	1831		0		
Trojan							
835-19*	450	13663	7832	18784	63500	44390	42.3
	750	20000	10952		10300		
835-23	450	1995	1437	4070	62600	18673	21.8
	750	6309	2633		0		

*Sample from mineralized zone.

Table 46: Soil samples, example argon plasma emission spectrography S and C results, loss-on-ignition and gravimetry results.

<u>Soils</u>

Soil samples were analysed by fractional thermal decomposition, first at 450°C to determine S associated with organic matter, and subsequently (using the same sample material) at 750°C for sulphur present as residual sulphides or thermally-decomposable sulphates. Preliminary experiments indicated that S concentrations and probably anomaly contrast are greatest in the fine fraction of samples. A total of 130 fine fraction soil samples from Munali, Chombwa, Chitina, and Trojan were analysed for S using the 1900Å line to avoid C interference from organic matter in the samples. About 20 samples analysed in duplicate at both temperatures, standards checked at 750°C and blanks analysed at intervals gave satisfactory results similar to those achieved with core samples at 4697Å. Sample results in peak heights were again converted to S concentrations using the program KAL.

Analytical results for the 450°C fraction for S associated with organic matter are mainly in the range 300 to 5000 ppm, although Trojan soils are conspicuously enriched with values of 2000 to 13,000 ppm. For the 750°C sulphide and sulphate fraction the typical range is 500 to 8000 ppm S except at Trojan where 3000 to 20,000 ppm is characteristic (table 46). Soil sample results exhibit a curiously high correlation of +0.93 between the 450°C and 750°C peaks, which are usually in the ratio 450°C:750°C = 2:3.

Carbon interference was again considered the likely cause of unusual S results and the C response at 1900Å was evaluated using the C standards. Once again, C concentration is proportional to the log of emission intensity up to 10,000 ppm C, and above this is directly proportional to emission intensity. A modified version of KAL was used to convert sample peak heights into C values, and readings range from a few hundred to several thousand ppm C.

A selection of soil samples was analysed by calcimetry, but no detectable CO_2 was evolved. Direct-reading emission spectrometer analyses showed that most of the soil samples contain less than 2% Ca, and there are non-significant correlations of +0.17 and +0.20 between Ca and peak heights at $450°C$ and $750°C$. The soils therefore probably contain insignificant amounts of carbonate minerals, and it was assumed that C is present mainly in the form of organic matter.

The C content of selected soil samples was determined gravimetrically using a LECO furnace with total C ancilliary equipment. In 10 fine fraction soil samples analysed in this way, total C ranges from 5515 ppm to 44,390 ppm, and is ascribed to organic matter. The sum of C values obtained at $450°C$ and $750°C$ by argon plasma emission spectrography in each of the same 10 samples ranges from 1500 ppm to 18,800 ppm C. Expressed as a percentage of total C determined gravimetrically, the cumulative plasma-determined C represents from 18.4% to 42.3% of total C (table 46). The loss-on-ignition technique was used as a more or less qualitative guide to the fractional C content of these 10 soil samples. Loss-on-Ignition at $450°C$ varied from about 2% to 12% of total dried weight and is attributed to volatilization of organic matter. There is very little additonal loss of weight from samples when ignited at $750°C$ following ignition at $450°C$, a result consistent with the observed absence of carbonate minerals in soils. Carbon is estimated as representing 58% of weight loss at $450°C$.

Gravimetric total C and loss-on-ignition results do not, in themselves, demonstrate that C is the principal component determined in argon plasma emission spectrographic analysis of soils at 1900Å. However, in argon plasma emission spectrography the sample is heated in a stream of inert gas, whereas when C is determined gravimetrically or by loss-on-ignition combustion is in O_2 or air.

It might be expected that only partial volatilization of C would take place in the absence of O_2, accounting for the consistently low C results obtained in argon plasma emission spectrography. To test this hypothesis an experiment was designed to determine volatile C under destructive distillation conditions in an inert atmosphere. A weight of 500 mg of soil sample 245-11 was placed into a fused silica boat, inserted into a silica tube, which also contained a plug of CuO, and both sample and CuO were heated to 750°C in a stream of argon. The gases evolved from the sample were carried in the argon stream through the hot CuO plug, where all volatile C compounds were oxidized to CO_2. The gas stream was then bubbled through a 0.5M NaOH solution in which CO_2 was absorbed. Sample heating was continued for about 10 minutes, after which the CO_2 absorbed was determined by back titration of the NaOH solution with HCl. The C content of the sample was then calculated. The figure so obtained is approximate because any S gases and N_2 evolved by the sample would also be oxidized to acidic gases and react with the NaOH solution; however it was thought that the concentrations of these gases would be small compared with carbon gases. By this technique soil sample 245-11 was found to contain 4380 ppm C volatile under destructive distillation at 750°C. Carbon determined by argon plasma emission spectrography under comparable conditions but in two stages (at 450°C and then at 750°C) totalled 4255 ppm. Following the development of the combustion technique for sulphur analysis (section 3.6.2), sample 245-11 was found to contain 246 ppm S. A number of other soil samples were analysed for C under destructive distillation conditions and yielded results matching those obtained in argon plasma emission spectrography.

Thus when soils are heated in an inert atmosphere as in argon plasma emission spectrography, the organic matter undergoes destructive distillation. If heated in two stages, at 450°C and 750°C, the C content of volatile compounds evolved is in the approximate ratio 450°C: 750°C = 2:3. The sum of the C evolved in these two stages, or in a single stage of destructive distillation at 750°C, represents about 30% of total C in the soil sample.

Conclusions

It was concluded that both the 4697Å and 1900Å atomic sulphur wavelengths, thought to be useful in argon plasma emission spectrography, suffered from C interference. This may have been due to defective intrumentation, and in this respect the monochromator was particularly suspect. Nevertheless, the existence of C interference when using the only available instrument precluded the use of argon plasma emission spectrography for S analysis, and alternative rapid S methods were researched (section 3.6.2.).

II.   ANALYTICAL DATA

This appendix contains all the analytical data generated during the research project. The data most pertinent to arguments used in the text are also presented in the appropriate tables and figures.

Sample numbers

All samples (with the exception of DDH MH58 core) were allocated a five digit number, eg. 86031, in which the first three digits act as codes (table 47). The final two digits are sequential sample identifiers. In regional stream sediments the third digit does not have any sample preparation significance, but is part of a three-digit sample identifier; all regional stream sediment samples are -200 μm fraction. The core from DDH MH58 has only a two-digit sequential sample identifier.

In the text, sample numbers are separated into three leading digits and two trailing digits by a hyphen for clarity of presentation, but in this appendix the hyphen is omitted for ease of computerized handling.

Distances

Horizontal distances are from origins marked with a triangle on figures 5 to 13, and vertical distances are depths below surface.

Element concentrations

Analytical results are in ppm and percent for most sample types, all elements are reported in ppm except Fe, Mg, Ca, K, Al and Si. For leaf samples, Fe is reported in ppm.

The presentation of element concentrations to one decimal place reproduces information obtained in the laboratory, and does not imply analytical precision of this order.

Digit	1st digit=field area	2nd digit=sample type	3rd digit=sample preparation
1	Munali	Regional stream sediment	-
2	Chombwa	Local stream sediment	Coarse fraction
3	Paulwi	Soil	-
4	Chitina	Soil	-
5	King Edward	Pit profile	Fine fraction
6	Musangashi	Outcrop	-
7	Chinkozia	Core	-
8	Trojan/Kingston	Leaves	-
9	-	Leaves	Ash
0	-	-	-

Table 47: Sample numbering scheme

DDH MH58 CORE

	2	3	4	5	6	7	8	9	10	11	12	13	14	15	16	17	18
M	5.0	10.0	15.0	20.0	25.0	30.0	35.0	40.0	45.0	50.0	55.0	60.0	65.0	70.0	75.0	80.0	85.0
NI	65.0	65.0	70.0	50.0	90.0	140.0	55.0	70.0	65.0	65.0	35.0	60.0	300.0	105.0	70.0	40.0	50.0
CU	43.0	45.0	55.0	53.0	66.0	81.0	48.0	49.0	44.0	42.0	27.0	55.0	14.0	60.0	58.0	27.0	41.0
CO	35.0	40.0	35.0	45.0	60.0	80.0	55.0	40.0	30.0	45.0	20.0	50.0	115.0	60.0	40.0	20.0	35.0
ZN	36.0	42.0	16.0	52.0	25.0	22.0	22.0	19.0	16.0	27.0	26.0	37.0	29.0	18.0	17.0	17.0	16.0
CR	75.0	90.0	50.0	60.0	50.0	55.0	45.0	45.0	55.0	40.0	55.0	45.0	25.0	105.0	45.0	45.0	55.0
FE	9.6	9.4	11.0	12.0	11.5	11.5	12.5	12.0	10.5	11.5	14.5	14.0	19.0	14.0	13.5	9.9	13.0
TI	3100.0	2050.0	7500.0	3700.0	4000.0	5500.0	8000.0	5500.0	10000.0	5500.0	6000.0	3500.0	2950.0	11000.0	2100.0	1750.0	8000.0
MN	440.0	390.0	270.0	310.0	220.0	260.0	420.0	280.0	300.0	200.0	170.0	350.0	540.0	410.0	290.0	380.0	230.0
NI S	14.0	24.0	18.0	28.0	54.0	98.0	26.0	48.0	28.0	20.0	20.0	24.0	60.0	58.0	44.0	20.0	24.0
CU S	22.0	32.0	20.0	43.0	56.0	65.0	43.0	48.0	24.0	34.0	23.0	45.0	11.0	51.0	42.0	16.0	32.0
CO S	8.0	8.0	4.0	20.0	34.0	50.0	29.0	22.0	12.0	23.0	10.0	32.0	34.0	26.0	16.0	6.0	16.0
ZN S	5.0	9.0	3.0	22.0	11.0	8.0	7.0	7.0	4.0	3.0	9.0	20.0	6.0	5.0	5.0	5.0	5.0
TI X	12.0	12.0	10.0	16.0	14.0	14.0	16.0	20.0	8.0	10.0	10.0	12.0	4.0	20.0	14.0	12.0	16.0
FE S	1.0	1.2	.6	1.5	1.5	1.8	1.5	1.8	.7	1.2	.9	1.5	1.0	2.0	1.5	1.1	1.2
PB	4.9	10.6	13.1	7.9	10.8	7.0	8.1	9.3	8.3	10.1	10.3	31.3	6.8	9.4	11.4	15.1	9.5
MO	.0	.2	.0	.0	.0	.4	.6	1.1	.2	.0	.1	.7	.0	.0	.2	1.3	.4
V	219.7	290.1	510.2	281.9	428.0	366.5	456.8	468.0	343.4	398.2	381.7	354.9	460.0	318.5	368.0	376.1	137.9

	19	20	21	22	23	24	25	26	27	28	29	30	31	32	33	34	35
M	90.0	95.0	100.0	105.0	110.0	115.0	120.0	125.0	130.0	135.0	140.0	145.0	150.0	155.0	160.0	165.0	170.0
NI	35.0	55.0	85.0	25.0	80.0	50.0	65.0	65.0	40.0	70.0	165.0	600.0	100.0	45.0	35.0	90.0	65.0
CU	14.0	44.0	40.0	46.0	30.0	45.0	28.0	20.0	48.0	99.0	125.0	101.0	30.0	51.0	42.0	40.0	80.0
CO	25.0	35.0	40.0	40.0	115.0	40.0	50.0	20.0	30.0	35.0	90.0	145.0	30.0	30.0	40.0	50.0	75.0
ZN	14.0	18.0	17.0	27.0	14.0	24.0	17.0	24.0	22.0	21.0	21.0	20.0	21.0	22.0	18.0	34.0	16.0
CR	35.0	55.0	30.0	50.0	45.0	45.0	55.0	45.0	60.0	50.0	60.0	35.0	30.0	45.0	50.0	20.0	55.0
FE	2.7	10.5	13.5	11.0	7.3	12.5	12.0	10.5	10.5	17.5	12.5	6.3	13.5	11.0	11.0	9.6	16.0
TI	300.0	3750.0	2800.0	5000.0	4000.0	5000.0	6500.0	4100.0	3700.0	6000.0	7500.0	2900.0	1150.0	3500.0	10000.0	3250.0	10000.0
MN	1100.0	240.0	300.0	220.0	150.0	350.0	160.0	250.0	270.0	450.0	330.0	770.0	510.0	220.0	470.0	560.0	190.0
NI S	20.0	24.0	52.0	13.0	26.0	20.0	16.0	26.0	20.0	52.0	118.0	520.0	42.0	26.0	24.0	22.0	42.0
CU S	10.0	34.0	36.0	37.0	23.0	40.0	23.0	54.0	40.0	86.0	101.0	83.0	20.0	46.0	36.0	32.0	69.0
CO S	12.0	13.0	18.0	20.0	46.0	22.0	36.0	22.0	16.0	16.0	62.0	108.0	18.0	20.0	18.0	14.0	64.0
ZN S	4.0	5.0	5.0	15.0	24.0	59.0	5.0	7.0	7.0	9.0	6.0	7.0	4.0	9.0	7.0	6.0	6.0
TI X	6.0	14.0	12.0	14.0	10.0	14.0	10.0	14.0	14.0	30.0	18.0	6.0	10.0	14.0	20.0	6.0	16.0
FE S	.8	1.4	1.0	1.3	1.6	1.0	.8	1.1	1.4	3.9	2.1	2.6	1.1	1.5	1.0	.7	2.3
PB	9.4	13.1	9.8	11.8	6.7	12.9	11.3	10.0	8.8	14.0	10.6	9.8	15.0	10.5	14.1	14.5	8.5
MO	3.7	1.3	.2	.9	.7	.9	.0	.0	.0	3.3	.1	.0	.2	.3	.2	.3	.6
V	11.4	143.8	413.4	189.7	60.4	463.7	466.6	455.5	314.3	73.9	297.1	179.5	283.9	402.4	225.7	200.7	161.1

DDH MM58 CORE

	36	37	38	39	40	41	42	43	44	45	46	47	48	49	50	51	53
M	175.0	180.0	185.0	190.0	195.0	200.0	205.0	210.0	215.0	220.0	225.0	230.0	235.0	240.0	245.0	250.0	260.0
NI	40.0	45.0	120.0	95.0	50.0	160.0	50.0	80.0	65.0	80.0	95.0	120.0	65.0	120.0	25.0	20.0	55.0
CU	58.0	31.0	95.0	104.0	49.0	55.0	72.0	62.0	52.0	67.0	78.0	50.0	41.0	34.0	22.0	18.0	38.0
CO	40.0	10.0	75.0	75.0	45.0	60.0	50.0	35.0	40.0	85.0	55.0	40.0	40.0	35.0	10.0	10.0	30.0
ZN	24.0	15.0	14.0	17.0	19.0	26.0	24.0	22.0	56.0	44.0	46.0	22.0	48.0	20.0	12.0	12.0	18.0
CR	50.0	35.0	60.0	50.0	50.0	30.0	50.0	55.0	45.0	90.0	90.0	110.0	85.0	65.0	40.0	45.0	55.0
FE	11.0	9.4	10.5	11.5	13.0	17.5	13.0	7.3	10.1	13.0	11.5	11.0	10.5	6.7	4.0	3.3	10.5
TI	6500.0	3400.0	6000.0	9500.0	8500.0	3300.0	10300.0	6510.0	2350.0	8000.0	2600.0	3950.0	2000.0	1600.0	3900.0	2800.0	7000.0
HN	320.0	230.0	210.0	270.0	200.0	390.0	330.0	430.0	380.0	670.0	550.0	230.0	350.0	380.0	130.0	150.0	330.0
NI S	20.0	14.0	74.0	54.0	32.0	98.0	26.0	54.0	46.0	40.0	64.0	92.0	42.0	76.0	16.0	16.0	28.0
CU S	40.0	18.0	71.0	82.0	43.0	54.0	53.0	54.0	47.0	53.0	74.0	44.0	37.0	22.0	17.0	10.0	31.0
CO S	22.0	6.0	34.0	32.0	24.0	20.0	18.0	24.0	22.0	15.0	26.0	26.0	24.0	18.0	6.0	6.0	13.0
ZN S	8.0	3.0	5.0	5.0	5.0	6.0	7.0	7.0	26.0	6.0	14.0	8.0	20.0	4.0	4.0	4.0	3.0
TI X	14.0	6.0	16.0	14.0	12.0	14.0	14.0	16.0	18.0	20.0	38.0	14.0	14.0	10.0	10.0	8.0	12.0
FE S	1.5	.5	1.5	1.4	1.2	1.3	1.4	1.0	2.0	2.0	3.2	1.6	1.5	.9	.7	.6	1.1
PB	11.1	9.3	11.5	6.0	9.8	7.2	7.4	9.6	11.4	3.7	12.1	11.3	8.4	8.8	5.1	7.7	7.0
MO	1.1	.5	.3	.0	.7	.0	.0	.0	.0	.4	.0	.4	.2	.2	.2	.0	1.0
V	371.8	181.0	288.3	284.7	321.5	539.2	292.3	199.9	440.5	331.1	270.2	371.2	321.6	325.0	223.5	242.1	267.1

	54	55	56	57	58	59	60	61	62	63	64	65
M	265.0	270.0	275.0	280.0	285.0	290.0	295.0	300.0	305.0	310.0	315.0	320.0
NI	45.0	40.0	45.0	75.0	60.0	85.0	75.0	85.0	175.0	160.0	140.0	135.0
CU	37.0	19.0	71.0	33.0	29.0	10.0	52.0	8.0	45.0	23.0	39.0	42.0
CO	25.0	25.0	50.0	40.0	15.0	20.0	50.0	40.0	60.0	45.0	25.0	40.0
ZN	15.0	14.0	20.0	17.0	15.0	16.0	49.0	24.0	26.0	45.0	10.0	39.0
CR	55.0	50.0	100.0	120.0	80.0	105.0	35.0	55.0	90.0	30.0	80.0	50.0
FE	6.1	10.5	11.5	14.0	12.5	12.0	12.0	4.1	9.0	4.6	4.3	3.4
TI	2100.0	5000.0	8500.0	8500.0	3800.0	7500.0	4000.0	300.0	3000.0	400.0	600.0	450.0
MN	310.0	160.0	270.0	220.0	170.0	180.0	440.0	127.0	550.0	1290.0	1020.0	1230.0
NI S	26.0	18.0	65.0	32.0	16.0	36.0	52.0	30.0	92.0	66.0	44.0	56.0
CU S	21.0	15.0	64.0	37.0	23.0	340.0	43.0	5.0	67.0	17.0	28.0	29.0
CO S	18.0	12.0	26.0	20.0	6.0	12.0	23.0	12.0	36.0	24.0	12.0	20.0
ZN S	4.0	3.0	5.0	5.0	3.0	4.0	20.0	5.0	9.0	22.0	8.0	13.0
TI X	10.0	8.0	12.0	12.0	12.0	12.0	16.0	10.0	16.0	3.0	8.0	6.0
FE S	.0	.8	1.2	1.1	1.0	1.2	1.7	1.1	1.7	1.8	1.4	1.1
PB	6.2	8.3	9.3	4.7	9.3	6.1	3.1	2.0	9.9	11.8	5.0	15.1
MO	.0	.2	.0	.4	.3	.0	.6	.0	.2	1.2	.4	.0
V	226.3	240.5	294.3	567.5	471.3	340.0	412.9	.3	221.4	2.0	123.4	.3

	2	3	4	5	6	7	8	9	10	11	12	13	14	15	16	17	18
M	5.0	10.0	15.0	20.0	25.0	30.0	35.0	40.0	45.0	50.0	55.0	60.0	65.0	70.0	75.0	80.0	85.0
GA	25.0	34.2	48.6	33.8	41.2	29.4	38.0	37.5	41.3	46.9	43.3	43.8	36.9	38.6	47.6	40.1	45.8
SN	7.1	14.7	22.0	9.6	17.4	9.2	14.4	13.9	15.1	15.2	15.4	18.4	6.6	16.2	19.0	17.5	12.6
BE	0	0	0	0	0	0	0	0	0	0	0	0	0	0	0	0	0
MG	3.6	4.1	6.4	5.0	4.7	2.7	2.6	3.2	3.8	4.5	3.5	5.0	3.9	3.8	4.8	5.3	2.0
CA	5.8	7.2	10.9	6.0	9.2	6.1	4.8	5.6	9.1	7.9	7.3	7.9	5.6	7.1	6.4	7.0	5.3
SR	134.4	181.1	234.6	172.9	192.6	141.8	93.9	137.6	112.2	171.3	175.1	236.8	179.6	158.9	220.4	124.3	151.0
BA	124.3	82.2	71.0	58.8	77.8	42.2	42.2	58.0	45.6	60.2	50.5	111.6	142.4	55.8	89.0	42.2	45.6
K	.4	.3	.7	.5	.5	.3	.5	.6	.5	.5	.4	.9	3.0	.5	.6	.3	.3
LI	2.7	2.7	.2	5.5	.2	.2	3.8	.2	.2	.2	.2	3.9	53.2	4.1	.2	4.6	.2
AL	10.2	10.1	12.4	19.8	11.4	6.5	7.4	8.3	10.9	10.9	7.5	11.5	6.8	10.5	11.1	6.9	9.9
SC	16.2	22.5	31.0	24.8	28.2	20.0	17.8	21.2	21.0	26.8	26.2	30.0	6.1	22.5	26.5	19.1	15.7
SI	19.4	24.7	33.5	17.5	27.3	17.9	24.4	20.7	27.9	26.3	21.3	26.8	7.3	24.2	31.7	31.1	31.5
S	635.0	340.0	335.0	3150.0	5875.0	6310.0	2725.0	2665.0	1710.0	4270.0	545.0	1395.0	3290.0	3300.0	1900.0	250.0	1275.0
CO2	2.5	2.0	.5	0	1.7	.3	.8	.5	2.0	2.0	1.1	2.0	5.8	.1	.6	2.8	1.6

	19	20	21	22	23	24	25	26	27	28	29	30	31	32	33	34	35
M	90.0	95.0	100.0	105.0	110.0	115.0	120.0	125.0	130.0	135.0	140.0	145.0	150.0	155.0	160.0	165.0	170.0
GA	13.5	49.9	44.2	48.0	39.6	48.5	46.3	40.9	39.0	52.8	39.4	43.9	40.1	35.5	46.4	43.4	42.6
SN	9.8	19.7	12.3	15.0	6.4	17.2	19.4	16.8	14.8	17.9	19.2	14.7	19.6	14.4	23.8	20.2	16.3
BE	1.3	0	0	0	0	0	0	0	0	0	0	0	.8	0	0	0	0
MG	8.0	3.3	4.7	3.1	1.2	3.5	4.3	4.0	3.2	1.5	4.4	5.7	7.4	4.0	5.2	7.8	2.5
CA	24.7	3.9	5.9	7.7	3.0	7.6	6.3	5.0	7.0	4.4	7.9	16.2	11.6	6.9	11.7	6.3	7.4
SR	233.7	121.3	208.3	191.7	45.3	203.0	174.5	136.7	220.1	100.3	236.7	237.8	77.5	255.5	376.0	100.0	99.5
BA	50.0	60.2	53.9	82.7	25.5	94.0	50.3	49.5	58.8	49.0	58.3	43.6	44.6	52.4	80.8	104.2	37.8
K	.1	.4	.5	.7	.2	1.0	.4	.5	.6	.5	.5	.2	.5	.4	.5	2.1	.2
LI	24.6	.2	5.4	.5	.2	3.3	.2	.2	.2	.2	.2	13.4	15.6	.2	.2	20.5	.2
AL	0	9.3	10.3	11.0	8.2	8.2	11.4	9.6	9.6	9.0	9.6	10.3	2.2	9.0	13.3	8.6	8.8
SC	1.3	18.9	19.5	23.2	10.9	22.7	22.9	23.2	27.6	23.3	28.1	14.1	5.9	23.0	39.1	19.0	23.9
SI	5.7	36.2	22.3	23.4	37.2	25.7	34.2	32.5	24.2	34.5	25.4	16.7	14.3	25.4	32.7	26.6	26.2
S	70.0	2575.0	1170.0	2335.0	15500.0	2560.0	2190.0	2885.0	2400.0	1645.0	6290.0	7335.0	875.0	2250.0	2165.0	1025.0	1295.0
CO2	18.8	.8	2.0	.1	.6	.5	2.0	.7	.2	.9	0	12.5	5.2	.2	.5	1.7	.5

	36	37	38	39	40	41	42	43	44	45	46	47	48	49	50	51	53
M	175.0	180.0	185.0	190.0	195.0	200.0	205.0	210.0	215.0	220.0	225.0	230.0	235.0	240.0	245.0	250.0	260.0
GA	42.9	45.5	43.3	33.0	40.9	41.5	35.4	35.0	40.5	36.1	38.6	35.2	36.8	36.2	32.9	30.7	42.6
SN	14.3	14.6	18.6	9.9	13.0	11.5	11.7	16.3	21.7	14.3	19.2	18.4	12.5	11.4	5.5	12.9	11.0
BE	0	0	0	0	0	0	0	0	0	0	0	0	0	0	0	.6	0
MG	3.3	2.8	4.3	3.0	3.1	3.4	3.1	4.0	5.1	3.9	4.2	4.7	3.3	3.6	2.8	4.1	2.7
CA	5.6	9.1	7.6	5.7	6.5	4.9	5.1	7.8	8.5	7.7	8.4	7.6	7.4	7.7	6.3	6.9	5.2
SR	199.3	140.1	257.1	118.4	250.0	140.1	169.3	223.2	130.9	151.0	219.8	239.4	229.5	164.1	123.5	78.0	53.2
BA	77.3	42.2	76.9	44.6	52.4	50.3	64.2	90.4	87.1	117.9	107.2	72.0	75.4	129.9	21.1	32.9	37.3
K	.6	.2	.5	.4	.4	1.0	.5	.5	.4	.7	.4	.4	.7	.4	.1	.3	.5
LI	.2	.2	1.0	.2	.2	.2	.4	.2	.2	4.9	.2	.2	2.4	6.8	.2	5.7	
AL	9.3	9.7	11.5	8.9	7.8	7.5	10.1	12.1	12.8	10.8	12.0	10.2	10.4	9.5	5.3	6.7	10.9
SC	22.4	19.9	23.8	21.4	20.5	21.0	23.1	26.4	24.2	24.2	25.5	25.1	25.1	21.3	5.8	13.7	20.9
SI	29.3	32.0	29.8	24.5	27.4	16.0	21.3	27.9	32.0	23.2	25.1	20.8	23.5	24.1	20.4	30.8	25.9
S	2170.0	295.0	5470.0	5255.0	2615.0	2975.0	2590.0	2385.0	1610.0	2495.0	2970.0	2890.0	1960.0	2445.0	270.0	165.0	995.0
CO2	1.2	2.9	.5	.3	0	1.6	0	.4	.3	.2	.9	.2	0	3.8	.6	2.2	.2

DDH MH58 CORE

	54	55	56	57	58	59	60	61	62	63	64	65
M	265.0	270.0	275.0	280.0	285.0	290.0	295.0	300.0	305.0	310.0	315.0	320.0
GA	32.3	44.8	34.0	43.7	39.9	32.5	34.6	23.2	31.6	33.1	22.7	39.8
SN	11.6	12.8	10.5	11.7	13.6	11.1	12.9	9.5	12.3	13.8	3.5	14.0
BF	0	0	0	0	0	0	0	1.8	0	.1	0	1.1
MG	3.3	3.4	3.4	3.9	4.6	3.6	3.4	8.2	5.2	5.8	3.4	5.3
LA	5.9	7.0	6.3	9.1	7.6	5.6	6.7	23.7	11.6	35.7	11.	32.8
SR	91.3	52.0	118.0	184.4	233.7	119.3	154.4	1239.7	364.3	963.6	193.2	822.3
BA	29.5	44.1	56.3	41.5	62.2	56.8	64.9	37.3	77.8	40.5	37.8	71.0
K	.2	.2	.5	.5	.5	.6	.4	.1	.6	.2	.3	.6
LI	.2	.2	.2	.3	.2	.2	.6	48.4	11.3	70.5	16.9	60.7
AL	9.4	11.0	9.3	10.4	9.8	8.9	9.6	0	6.8	.2	4.0	.4
SC	19.3	27.0	22.8	19.4	20.5	20.4	21.9	.0	19.5	13.9	3.7	3.7
SI	28.5	34.2	22.7	20.9	24.7	24.8	20.6	3.9	12.0	4.2	0.5	4.3
S	560.0	605.0	2770.0	1510.0	185.0	6525.0	2575.0	435.0	1775.0	1240.0	75.0	105.0
CO2	2.3	.4	0	1.6	.7	0	0	42.4	10.0	41.1	22.4	37.5

MAFIC AND ULTRAMAFIC CORE AND OUTCROPS

	17002	17003	17004	17005	17006	17007	17008	17010	17011	17012	17013	17014	17015	17016	17017	17019	17020
NI S	160.0	66.0	150.0	12.0	42.0	42.0	8.0	28.0	50.0	90.0	22.0	16.0	54.0	52.0	300.0	54.0	174.0
CU S	59.0	24.0	56.0	5.0	2.0	65.0	1.0	37.0	35.0	38.0	3.0	105.0	40.0	6.0	67.0	17.0	8.0
CO S	36.0	20.0	28.0	6.0	4.0	39.0	4.0	34.0	22.0	26.0	4.0	6.0	20.0	8.0	35.0	8.0	33.0
ZN S	10.0	9.0	27.0	3.0	1.0	9.0	2.0	7.0	14.0	22.0	3.0	7.5	10.0	4.0	9.0	6.0	33.5
FE S	1.4	.4	.8	0	0	1.3	0	1.4	.1	.9	.0	.4	.9	.1	1.5	.8	.2
TI X	40.0	0	60.0	0	60.0	0	0	40.0	0	40.0	0	0	0	0	0	0	0
FE	5.3	8.8	5.9	3.8	5.8	4.5	3.8	5.1	4.7	5.1	6.5	5.8	5.4	5.4	5.8	5.9	18.9
CU	72.3	39.9	76.0	29.0	23.6	95.2	25.0	47.6	50.8	43.5	120.1	126.8	51.7	31.3	81.7	26.3	123.1
PB	15.3	9.8	10.4	5.7	10.5	11.6	6.2	5.6	9.4	10.0	8.8	13.1	6.9	11.2	10.2	8.2	24.9
ZN	59.4	63.3	63.8	17.8	42.2	91.3	6.9	33.9	39.5	31.3	23.6	48.0	33.1	29.1	44.5	49.7	64.8
MO	.0	.0	.0	.0	.0	.0	.0	1.4	1.2	.2	.0	..	.0	.	.5	.0	.0
V	565..	914.3	574.5	347.5	420.6	754.1	566.5	548.2	732.2	399.4	735.0	823.9	612.0	641.7	741.9	527.9	1590.6
CO	40.5	31.0	30.2	6.4	28.7	35.4	23.6	35.3	29.2	35.0	21.2	10.1	33.6	15.2	41.6	29.8	91.3
NI	154.3	127.6	186.1	33.7	315.6	66.3	79.9	75.6	116.6	175.1	131.1	123.1	75.9	131.1	436.8	127.5	920.7
CR	192.3	71.8	30.9	87.9	660.9	100.1	76.4	141.1	207.9	251.5	117.3	70.6	11.4	135.7	264.4	225.6	199.5
GA	24.0	30.8	22.7	21.0	16.5	26.9	16.5	21.2	22.0	14.6	23.2	20.1	23.5	21.4	17.4	17.7	52.0
SN	13.7	9.7	8.7	1.3	3.2	10.2	2.0	2.8	4.0	6.8	6.4	14.9	6.9	10.0	7.8	5.8	27.7
TI	18956.0	16705.4	16383.0	17475.9	4232.5	13776.3	11173.7	13912.5	11931.9	8098.9	10819.8	21157.4	14952.4	12724.2	16216.2	7245.0	25280.8
ZR	0	0	0	0	0	0	0	0	0	0	0	0	0	0	0	0	0
U	4.3	4.0	4.5	1.6	7.0	4.1	2.9	2.5	2.5	4.0	3.8	5.1	3.2	3.3	3.9	4.0	9.7
CA	6.3	6.9	6.1	4.6	5.3	6.3	4.2	4.9	3.4	5.2	6.2	4.6	5.9	7.4	5.0	5.8	.9
SR	223.2	245.6	206.5	177.7	360.0	334.5	118.4	73.4	270.8	173.9	193.5	471.0	141.0	265.1	280.4	224.1	40.9
BA	72.3	59.3	56.8	49.5	110.0	64.9	26.3	45.7	43.3	71.6	48.6	69.3	61.6	66.5	57.3	110.9	30.1
K	.9	.4	.3	.2	1.9	.5	.2	.3	.5	.3	.4	.6	.5	1.0	.5	1.0	.3
LI	.2	.2	.2	.6	19.8	.2	.2	12.3	.5	14.4	.2	.2	.2	.2	.6	8.1	.2
AL	8.7	7.7	8.0	7.1	5.9	10.7	3.9	5.8	5.1	3.2	6.1	8.6	6.7	7.1	7.6	6.8	1.7
SC	29.4	43.1	31.6	16.7	20.9	44.5	15.1	23.5	17.6	18.2	26.6	32.0	24.2	26.6	22.3	25.2	46.5
SI	26.1	12.8	28.1	22.4	15.9	19.7	12.3	15.1	15.5	14.5	17.1	27.2	18.0	11.5	23.7	25.0	10.6
MN	1989.3	1103.1	1655.3	496.7	1137.8	1258.4	476.8	476.5	488.0	1370.2	469.8	720.0	1446.7	799.3	1025.7	1060.7	2020.5
S	4365.0	1440.0	3035.0	10.0	990.0	2690.0	10.0	2280.0	1630.0	535.0	365.0	453.0	2890.0	1550.0	3640.0	1410.0	130.0

MAFIC AND ULTRAMAFIC CORE AND OUTCROPS

		17021	17023	17025	17026	17027	17028	17029	17030	27001	27002	27003	27004	27005	27006	27007	27008	27009
NI	S	54.0	130.0	52.0	33.0	64.0	148.0	28.0	162.0	58.0	91.0	14.0	74.0	8.0	98.0	42.0	82.0	260.0
CU	S	53.0	20.0	32.5	24.5	40.0	25.0	35.0	22.0	38.5	45.5	7.0	0	0	35.0	18.0	62.0	4.0
CO	S	16.0	14.0	32.0	11.0	20.0	20.0	22.0	34.0	41.0	46.0	4.0	4.0	0	10.0	0	12.0	19.0
ZN	S	11.0	7.0	23.0	16.0	43.0	30.0	34.0	39.0	7.5	7.5	5.0	1.0	1.0	4.0	5.0	6.0	5.5
FE	S	1.4	.3	1.2	.4	.3	1.0	.9	.2	3.4	2.6	.2	0	0	1.2	0	1.2	.0
TI	X	40.0	0	40.0	0	0	0	0	0	0	2.0	40.0	0	0	40.0	0	0	0
FE		5.3	13.2	6.3	14.1	5.8	7.3	4.4	2.0	4.3	4.8	4.1	4.5	4.7	4.3	2.2	4.2	5.2
CU		75.3	30.9	37.6	121.3	60.0	28.7	53.2	30.5	47.4	58.6	25.4	5.8	6.7	53.2	50.0	77.8	29.3
PB		11.5	16.0	7.2	12.4	12.8	12.7	6.7	4.8	9.1	9.6	9.8	19.9	23.2	8.0	5.5	7.1	14.7
ZN		71.0	67.4	39.2	69.7	121.7	55.0	73.5	26.2	38.1	52.8	76.2	15.7	26.9	47.9	56.5	55.5	49.2
MO		.3	.8	.0	.0	.0	.0	.8	.8	.0	.0	.0	.0	.0	.0	.0	1.8	1.5
V		505.3	1543.9	604.1	1177.0	459.6	713.1	430.7	412.7	380.7	368.0	430.8	35.6	30.9	149.1	90.6	166.6	95.8
CO		34.4	54.7	35.6	28.5	40.2	35.5	32.5	33.5	33.8	37.5	36.9	89.3	85.7	46.8	37.8	54.5	98.0
NI		96.2	410.6	46.2	153.3	138.7	272.0	63.2	279.5	58.7	64.3	65.9	1818.6	1822.8	444.2	346.9	455.9	1143.2
CR		256.1	87.7	37.0	153.0	603.0	779.0	97.3	782.0	396.0	34.2	226.8	1501.3	1356.6	574.5	402.6	1392.3	1954.5
GA		20.1	41.6	17.7	25.0	17.8	23.7	21.0	13.7	13.7	10.0	14.1	1.4	2.8	12.7	9.8	12.0	6.7
SN		6.5	21.2	4.3	10.0	9.0	12.5	0	0	2.1	5.2	6.3	23.7	13.9	11.1	.3	2.3	17.0
TI		12004.1	15186.7	14096.1	14495.7	6290.0	7944.8	12730.4	2210.3	8445.6	10673.7	7867.7	112.6	56.7	2897.	2906.4	2006.8	1793.5
BE		0	0	0	0	0	0	0	.8	0	0	0	0	0	0	0	0	0
MG		3.5	7.6	3.3	4.5	5.6	5.8	2.1	3.5	3.4	3.3	4.7	11.4	9.3	6.3	5.0	5.7	9.5
CA		6.5	3.6	5.4	4.4	6.1	4.3	4.8	3.4	5.8	5.5	5.6	.2	.9	5.4	4.7	5.7	2.8
SR		208.3	75.6	160.2	191.5	170.2	144.2	153.5	153.0	63.2	68.7	60.0	17.7	33.5	274.4	189.9	240.3	132.7
BA		63.5	271.6	75.2	44.2	90.6	60.7	49.5	21.0	70.7	74.2	161.3	67.1	80.6	147.8	232.1	57.8	73.4
K		.5	3.7	.4	.4	.9	.7	.4	.6	.2	.3	1.5	.9	.0	.8	.6	.6	.3
LI		7.3	1.6	.2	.2	1.8	.2	3.0	24.3	31.1	27.1	32.3	.2	.2	15.3	19.1	27.1	.2
AL		7.0	7.6	7.8	7.4	7.5	5.6	5.9	5.2	7.0	5.9	6.8	0	0	11.8	11.6	8.0	3.6
SC		23.7	26.5	28.8	28.3	21.4	31.0	19.8	12.0	23.0	31.4	24.2	5.2	2.2	9.0	6.4	9.6	10.3
SI		19.1	11.0	20.5	22.7	13.0	11.5	13.6	6.6	17.3	18.1	25.2	1.6	3.9	22.1	12.3	15.8	4.5
MN		1626.0	733.1	2016.1	1198.1	1578.2	1732.3	1348.9	495.6	2133.8	2315.3	2221.6	419.3	430.9	1079.7	660.7	1115.3	1530.4
S		2045.0	1400.0	2570.0	533.0	260.0	325.0	2845.0	920.0	4369.0	5190.0	460.0	10.0	25.0	10.0	525.0	780.0	10.0

MAFIC AND ULTRAMAFIC CORE AND OUTCROPS

	27010	27011	27012	37001	37002	37003	37004	37005	37006	37007	37008	37009	37010	37011	37012	37013	37014
NI S	260.0	126.0	255.0	340.0	161.0	120.0	300.0	246.0	27?.0	15?.?	5?.?	22.?	22.0	96.?	260.?	40?.?	360.0
CU S	18.?	0	11.?	1.?	0	0	72.0	31.0	66.0	1.0	24.0	12.0	46.0	34.5	0	95.0	230.0
CO S	20.0	6.0	30.0	20.0	8.0	6.0	22.0	24.0	18.0	4.0	6.0	6.0	8.0	12.0	10.0	36.0	24.0
ZN S	5.0	2.0	8.0	7.0	2.0	3.0	7.0	14.0	8.5	3.0	7.0	6.0	30.0	11.5	6.0	23.0	18.0
FE S	.2	0	.1	.0	0	0	.4	.0	.4	0	.5	.6	.6	.2	.0	.1	.1
TI X	40.0	0	20.0	?	?	?	?	?	20.0	0	0	0	0	0	40.0	0	60.0
FE	5.2	6.0	5.2	4.4	8.5	7.9	7.2	5.0	9.6	6.6	3.6	2.6	4.9	3.5	7.3	4.6	4.0
CU	32.7	9.6	24.1	24.7	23.0	10.6	78.6	69.8	47.0	46.5	32.8	17.0	53.0	36.9	23.4	121.7	190.4
PB	14.5	14.3	21.0	12.4	26.4	15.9	10.7	16.3	6.3	16.7	12.0	9.1	25.9	11.1	22.1	17.2	6.8
ZN	98.5	32.8	85.4	55.1	62.2	29.8	71.0	45.1	39.2	45.0	57.5	63.2	161.9	68.5	44.0	61.2	59.9
MO	.0	.0	.0	.2	.0	.0	1.1	.0	.5	.0	.6	1.2	.3	.5	.2	.0	.3
V	75.9	70.5	87.3	74.5	35.5	31.0	121.4	118.6	98.1	76.4	91.9	82.0	292.3	109.7	45.7	106.9	173.1
CO	83.5	60.0	88.5	100.9	154.4	157.2	97.8	118.7	98.5	125.6	59.3	59.8	37.1	68.2	145.4	86.6	70.8
NI	1033.2	906.2	1014.0	1503.8	2424.5	2262.5	1445.5	1641.?	1605.?	1982.3	1121.5	971.4	86.9	678.?	2335.1	938.5	912.7
CR	1783.2	1583.7	2016.7	2403.1	2772.8	2528.7	1923.3	2543.5	2023.6	2495.8	1973.9	2114.?	309.0	1952.0	2749.5	2187.6	1867.1
GA	5.3	4.9	8.5	4.7	3.2	4.2	8.1	7.9	5.9	5.1	8.5	6.8	18.8	6.5	4.4	7.2	8.7
SN	15.3	10.9	23.8	13.9	43.1	39.9	8.2	21.5	6.1	24.8	9.1	2.5	9.2	5.5	39.1	15.7	0
TI	1554.5	1008.7	1783.6	504.5	145.6	134.4	845.0	892.8	997.8	476.2	662.7	497.0	14145.6	1195.3	169.4	641.9	1447.5
	0	0	?	?	?		.3	?	.3	?	.7	.2	0	0	0	0	0
MG	10.1	6.3	3.9	8.3	13.2	12.2	6.0	10.0	5.8	3.9	6.4	6.5	1.5	7.5	10.4	9.2	4.6
CA	2.3	2.5	2.8	1.4	.7	.5	1.9	2.1	2.3	1.3	3.5	7.5	2.1	1.0	1.1	1.4	1.3
SR	158.3	111.5	195.1	14.7	28.3	14.2	12.0	40.3	19.9	30.5	329.7	238.1	181.1	21.6	34.5	40.5	20.9
BA	157.3	66.5	160.8	12.7	55.7	9.0	8.0	84.1	5.6	52.4	73.7	221.6	323.5	169.4	38.1	27.4	467.5
K	.4	.2	.3	.1	.2	.3	.1	.6	.1	.3	.3	.2	1.9	.9	.1	.1	3.9
LI	.2	8.1	.2	.2	.2	.2	.2	.2	.2	.2	31.6	35.4	32.4	24.2	.2	.5	58.0
AL	5.0	2.4	4.3	2.1	0	0	2.0	2.5	1.6	1.3	3.5	3.7	9.3	2.1	.1	1.6	3.0
SC	10.3	6.6	8.7	6.7	9.0	5.3	4.7	9.2	4.6	5.8	9.4	9.2	17.6	8.2	3.2	9.0	5.8
SI	12.5	9.3	6.1	12.6	10.6	11.0	9.3	7.1	9.3	9.3	18.9	14.4	36.9	16.6	3.9	13.0	10.6
MN	1769.2	1049.2	1520.4	1018.2	1353.6	415.2	1169.9	1754.3	1069.7	1108.1	1324.3	1228.5	1541.8	1632.2	1047.8	1594.0	876.5
S	215.0	10.0	405.0	240.0	720.0	700.0	425.0	285.0	233.0	280.0	400.0	10.0	720.0	258.0	10.0	265.0	1130.0

MAFIC AND ULTRAMAFIC CORE AND OUTCROPS

		37015	87003	87004	87005	87006	87007	97013	37014	37016	87017	87018	87019	87020	67021	87022	87023	87024
NI	S	420.0	1840.0	2800.0	640.0	12.0	540.0	1100.0	2500.0	-	320.0	1760.0	500.0	940.0	1100.0	80.0	440.0	580.0
CU	S	22.0	35.0	220.0	8.0	0	6.0	15.0	100.0	240.0	2.0	43.0	20.0	34.0	63.0	140.0	1.0	68.0
CO	S	16.0	58.0	104.0	16.0	0	22.0	40.0	106.0	124.0	16.0	60.0	20.0	40.0	66.0	10.0	12.0	28.0
ZN	S	12.0	90.0	51.0	7.0	3.0	68.0	24.0	90.0	43.0	20.0	8.0	30.0	100.0	36.0	70.0	2.0	13.0
FE	S	1.0	1.4	1.0	.0	0	.0	.1	2.3	7.0	.0	.1	.0	.1	3.7	2.4	.0	.5
TI	X	0	40.0	0	0	0	0	0	0	0	0	0	0	0	120.0	0	0	0
FE		7.5	4.6	0.3	6.7	4.3	2.3	5.3	4.6	5.9	3.5	3.0	5.6	4.2	3.7	3.4	5.3	6.3
CU		43.5	107.5	133.6	53.0	61.7	31.6	31.1	97.0	191.3	60.4	55.0	87.2	46.2	72.5	137.7	37.8	94.2
PB		16.3	17.6	21.0	19.4	20.5	22.5	22.3	16.9	15.1	19.1	24.4	18.5	16.6	12.6	26.7	16.0	19.4
ZN		109.3	67.2	50.8	42.1	40.1	133.3	75.7	115.7	169.2	33.4	12.6	72.8	133.9	43.6	175.6	63.2	75.6
MO		1.0	.2	.9	.0	.0	.1	1.2	.6	.0	.3	1.0	.0	.0	.0	2.2	.0	.5
V		75.7	40.1	51.9	42.3	55.5	47.3	60.1	54.4	118.7	52.4	62.2	51.8	55.9	91.0	146.7	52.7	120.5
CO		128.3	92.3	143.2	92.3	92.1	97.4	107.7	107.0	122.2	93.0	130.3	75.1	161.8	64.6	23.9	118.6	88.9
NI		2042.3	2113.0	2523.0	2306.3	1519.9	1893.0	2747.4	2275.6	2265.2	1785.	2295.8	1573.5	2169.2	1344.9	164.3	2089.6	1738.2
CR		3379.7	1270.4	1050.0	1355.2	1431.2	1472.1	1597.9	1279.9	194.0	1162.2	1399.8	1423.4	1490.5	1409.7	216.7	1359.2	1532.7
GA		4.2	1.7	3.8	3.2	4.9	3.4	5.2	3.1	5.8	3.5	3.5	3.8	2.1	4.3	18.9	5.1	9.6
SN		24.9	15.3	16.1	23.6	24.5	31.5	26.3	19.3	17.3	15.9	16.6	30.0	18.9	12.7	4.7	25.8	1.4
TI		298.5	123.7	128.6	169.7	305.9	296.4	204.5	321.0	397.4	321.0	168.2	248.3	199.6	495.0	2303.4	256.1	576.5
BE		.4	0	0	0	0	0	.2	.6	0	0	1.0	0	0	0	0	0	.6
MG		11.3	9.5	7.6	12.5	10.4	14.1	12.5	10.4	11.2	8.7	8.3	9.7	11.2	8.3	2.3	13.0	6.4
CA		.3	.2	.3	.9	2.3	.3	.7	.4	3.2	1.4	.1	.2	.3	5.9	1.8	1.3	3.0
SR		23.0	11.3	7.1	23.8	40.0	8.7	14.3	4.9	21.3	19.0	3.7	8.4	9.9	52.8	100.3	10.2	6.9
BA		19.3	16.0	29.3	196.1	16.7	5.7	.4	.0	26.3	11.1	.4	140.0	11.1	15.1	241.7	2.9	14.3
K		.1	.0	.0	.0	.0	0	0	0	.1	.0	0	.0	.0	.0	2.1	0	.1
LI		.9	.2	.2	.2	.2	.2	1.5	.2	.2	.7	.8	.2	.2	3.2	42.4	2.5	.8
AL		1.1	.2	.6	1.2	2.3	1.5	2.2	1.1	6.0	1.6	.8	.7	.8	1.6	5.6	.8	2.6
SC		6.7	3.6	2.4	5.3	5.3	3.8	4.0	1.8	14.2	3.1	.0	2.8	3.5	5.5	5.3	5.6	4.6
SI		11.0	10.6	9.3	10.6	4.2	12.3	7.9	14.5	10.6	10.6	6.1	9.3	10.6	7.7	29.4	11.0	9.3
MN		1555.4	283.9	393.0	651.4	1025.3	836.7	488.2	403.1	1219.5	1247.7	252.8	635.6	852.8	1283.4	469.6	920.3	1020.1
S		115.0	4208.0	4705.0	200.0	550.0	620.0	300.0	3630.0	11930.0	1160.0	1055.0	805.0	630.0	18870.0	420.0	370.0	1220.0

MAFIC AND ULTRAMAFIC CORE AND OUTCROPS

	87025	87026	87027	87028	87029	97030	16001	16002	16003	16004	16005	16006	16007	16008	16009	16010	16011
NI S	480.0	500.0	54.0	1400.0	220.0	220.0	14.0	14.0	12.0	15.0	10.0	10.0	6.0	12.0	12.0	7.0	12.0
CU S	0	3.0	0	100.0	1.0	0	4.0	11.0	3.0	5.0	2.0	8.0	3.0	4.0	2.5	6.0	8.0
CO S	4.0	16.0	2.0	30.0	2.0	6.0	4.0	8.0	4.0	6.0	4.0	4.0	4.0	2.0	4.0	3.0	2.0
ZN S	2.0	4.0	1.0	6.0	1.0	1.0	3.0	2.0	7.0	2.0	2.0	7.0	5.0	5.0	3.0	2.5	3.0
FE S	.	.0	0	.0	0	0	.1	.4	.0	.0	.0	.1	.0	.0	.1	.3	.4
TI X	0	40.0	0	0	0	40.0	0	0	0	0	0	0	0	0	0	0	0
FE	5.0	6.6	9.6	5.0	3.2	4.1	6.8	6.2	5.1	36.5	5.4	6.5	3.9	3.1	11.1	3.3	4.3
CU	6.2	45.1	326.2	371.2	20.6	56.9	34.4	37.5	46.5	264.5	47.7	37.7	17.6	22.4	16.1	16.8	16.7
PB	12.4	15.9	17.2	15.9	9.9	12.5	9.6	8.6	8.1	5.2	13.9	8.9	8.7	9.7	8.4	5.9	6.5
ZN	11.5	43.2	52.0	55.9	13.2	14.9	18.6	28.6	63.0	43.1	94.2	46.0	26.7	28.0	10.2	27.4	43.3
MO	.0	.0	.0	.0	.0	.0	.0	.0	.0	1.4	.0	.0	.0	.0	.0	.0	.0
V	34.4	43.4	53.1	64.2	36.9	50.1	317.9	305.0	625.4	1131.9	752.5	171.0	412.4	195.3	546.6	723.0	654.8
CO	147.7	101.4	147.1	122.7	102.9	117.0	51.5	23.2	24.8	24.3	29.5	17.5	32.4	23.3	62.8	16.9	18.9
NI	2545.3	1908.7	2166.2	2617.4	2262.5	2231.5	560.8	112.5	42.4	496.8	60.8	42.2	46.8	85.7	421.9	120.6	92.7
CR	1238.7	1491.5	2236.4	2250.9	1327.9	1506.3	1035.2	56.0	26.1	64.9	37.5	44.6	17.0	44.4	674.2	168.6	162.2
GA	1.0	2.4	2.8	6.4	.6	3.2	12.1	14.3	19.2	24.3	30.4	25.4	20.0	30.7	13.9	26.1	21.7
SN	15.5	17.5	30.8	29.4	7.9	13.2	7.5	6.3	8.1		15.3	6.0	3.0	11.6	.4	2.4	3.2
TI	161.3	205.3	235.3	400.8	143.2	174.1	4587.2	21312.2	23594.2	22944.7	20366.4	18613.0	13746.7	21401.5	6000.3	9387.4	6201.0
BE	0	0	0	0	0	0	0	0	0	0	0	0	0	0	0	0	0
MG	9.2	8.8	10.1	12.7	9.0	9.1	6.4	2.7	3.2	.9	3.6	2.0	2.5	3.2	5.6	2.5	3.4
CA	.2	2.0	1.2	2.7	.2	1.4	4.4	8.4	7.0	.8	6.8	5.4	2.8	6.7	3.6	3.3	5.3
SR	4.5	18.0	3.9	11.2	7.3	12.3	103.6	271.5	243.5	47.8	323.0	159.2	87.2	113.1	11.2	88.1	200.7
BA	5.5	19.1	145.8	9.0	9.5	12.4	60.2	325.0	104.1	132.3	321.6	91.6	28.5	40.2	52.4	36.0	56.8
K	0	.1	.1	.0	.0	.0	.4	.4	.3	.2	.6	.4	.2	.1	.1	.4	.4
LI	.2	.2	.2	.2	.2	.2	12.7	.2	.2	.2	.2	.2	.2	.2	.2	1.9	.2
AL	0	.1	.4	1.2	0	.1	5.7	7.3	10.4	.3	13.8	7.8	6.8	9.9	1.1	5.0	9.2
SC	.0	4.5	4.9	8.6	.8	2.0	16.2	27.6	40.8	8.9	37.9	21.9	26.4	24.5	16.9	13.2	24.0
SI	9.3	9.3	9.3	11.0	10.6	3.9	21.1	18.2	21.9	10.0	19.0	31.7	19.7	34.1	9.3	16.4	17.6
MN	1197.7	980.7	1663.2	845.0	813.5	331.4	1099.9	1218.4	2031.6	444.3	1951.9	1403.1	458.1	481.5	497.5	439.0	576.3
S	570.0	285.0	645.0	610.0	400.0	325.0	85.0	405.0	120.0	830.0	56.0	135.0	110.0	120.0	75.0	140.0	200.0

MAFIC AND ULTRAMAFIC CORE AND OUTCROPS

		16012	16013	16014	16015	16016	16017	16018	16019	16020	16021	26001	26002	26003	26004	26005	26006	26007
NI	S	8.0	21.0	5.0	10.0	60.0	26.0	33.0	98.0	42.0	25.0	26.0	52.0	52.0	36.0	240.0	300.0	280.0
CU	S	13.0	17.5	8.0	10.0	87.0	47.0	17.5	60.0	29.0	16.0	22.0	85.0	79.0	94.0	19.0	25.0	35.0
CO	S	2.0	8.0	4.0	4.0	6.0	4.0	2.0	8.0	8.0	4.0	4.0	8.0	8.0	8.0	20.0	24.0	22.0
ZN	S	3.0	3.0	5.0	2.0	6.0	24.0	13.5	4.0	2.0	2.0	9.0	8.0	5.0	4.0	20.0	6.0	7.0
FE	S	.4	.5	.4	.4	.1	.1	.3	.1	.0	.0	.4	.5	.3	.1	.4	.8	.9
TI	X	3	20.0	0	0	0	0	0	0	0	0	0	0	0	0	0	0	0
FE		4.3	5.1	6.3	5.1	21.1	13.0	37.6	23.7	23.8	18.4	4.1	2.9	2.8	2.7	5.2	4.9	3.9
CU		48.3	57.4	24.3	39.9	493.5	433.3	542.9	451.9	433.5	27.9	48.3	123.5	93.2	108.6	36.4	34.5	36.7
PB		9.5	10.7	11.9	13.1	12.6	14.4	8.9	13.8	17.6	17.6	13.8	8.5	6.8	7.6	17.7	13.2	12.7
ZN		36.0	39.3	54.7	44.0	16.7	36.4	33.3	40.8	25.3	31.6	114.7	83.3	46.7	77.5	57.9	92.4	56.7
MO		.0	.0	.0	.0	1.8	.3	3.2	.4	2.4	3.3	.0	.0	.7	.0	.3	.2	1.0
V		708.5	513.5	802.1	473.6	116.2	1018.8	78.4	1822.0	413.6	199.2	142.9	207.3	177.7	217.1	91.6	89.2	117.4
CO		24.5	43.1	31.2	28.5	224.2	87.3	71.3	81.3	215.5	155.7	54.5	35.2	30.0	30.5	94.0	83.7	75.4
NI		115.3	175.7	93.0	117.3	3265.3	1592.6	1368.5	1569.2	2935.3	2474.3	633.7	299.4	269.6	100.6	1112.0	979.0	878.1
CP		278.7	498.7	191.7	142.4	116.9	1170.9	113.3	1181.4	248.7	58.4	1966.5	1556.2	1294.2	300.5	2085.0	1773.3	1528.6
GA		20.3	19.2	25.4	19.3	5.9	25.4	5.1	43.3	10.9	-.6	12.0	1.9	1.6	11.5	8.7	6.4	8.5
SN		4.4	6.6	1.7	11.2	1	11.4	0	5.2	4.9	0.5	12.1	1.9	0	5.9	16.2	10.9	8.6
TI		7630.3	8138.0	10642.1	20881.9	403.7	19016.9	315.6	21994.0	6334.3	1577.9	2776.6	3086.1	2448.2	4964.1	1451.3	1849.6	2429.8
BE		.3	0	0	0	2.5	0	1.3	0	0	.9	0	0	0	0	0	0	0
MG		3.3	4.0	3.9	3.5	2.3	6.3	.6	4.6	5.0	4.9	8.6	5.5	4.3	5.2	8.7	6.9	6.5
CA		4.3	5.3	5.7	6.3	.6	.5	.6	.6	.5	.5	5.5	8.2	7.8	7.5	2.5	2.8	2.5
SR		194.4	132.4	251.1	272.7	33.8	31.3	37.8	24.3	22.0	22.6	266.2	321.3	267.8	362.8	205.4	113.8	220.2
BA		79.5	94.7	227.6	169.1	65.9	246.1	72.3	57.3	41.3	65.6	337.7	116.6	66.0	95.9	106.5	187.4	128.4
K		.5	.4	.6	.5	.1	.2	.2	.2	.2	.2	.7	.4	.3	.4	.3	.2	.3
LI		.2	3.6	.2	.8	.2	.2	.2	.0	.2	.2	14.5	1.2	10.4	.2	2.7	.2	6.1
AL		6.4	7.3	7.8	9.5	.2	7.2	1.2	7.6	.9	.1	10.9	10.1	6.8	8.5	4.2	4.4	4.0
SC		21.1	16.7	28.7	27.2	29.5	58.7	16.9	39.0	31.7	25.0	12.7	23.2	14.7	23.2	7.2	8.1	6.6
SI		21.1	20.3	22.4	13.4	3.3	10.6	3.9	3.9	9.3	3.9	28.9	16.5	13.8	18.8	5.2	10.6	9.3
MN		911.5	1562.8	1067.3	1516.4	225.7	415.4	186.4	1076.7	350.7	394.0	1504.9	1250.7	1069.7	1489.2	1523.5	1439.3	1242.4
S		160.3	420.0	235.0	120.0	725.0	415.0	2620.0	310.0	1010.0	560.0	150.0	420.0	495.0	600.0	370.0	470.0	450.0

MAFIC AND ULTRAMAFIC CORE AND OUTCROPS

		26008	26009	26010	26011	26012	26013	26014	36001	36002	36003	36004	36005	36006	36007	36008	36009	36010
NI	S	240.0	32.0	63.0	22.0	24.0	26.0	260.0	44.0	36.0	52.0	33.0	20.0	36.0	44.0	8.0	28.0	30.0
CU	S	19.3	38.0	75.0	60.0	93.0	81.3	113.0	26.0	5.0	12.0	17.5	30.0	27.0	20.0	4.0	44.0	26.0
CO	S	22.0	6.0	9.0	24.0	2.0	15.0	26.0	6.0	4.0	9.0	4.0	4.0	6.0	6.0	0	6.0	4.0
ZN	S	6.0	21.0	3.0	9.0	9.0	4.0	74.0	5.0	6.0	20.0	4.0	2.0	5.0	4.0	11.0	16.0	6.0
FE	S	.7	.8	.8	1.5	2.0	1.0	1.1	.9	.1	.2	.8	.8	1.7	.5	.2	.5	.4
TI	X	0	0	0	0	0	0	0	0	0	0	0	0	0	0	0	0	0
FE		5.3	3.3	4.4	4.4	7.6	7.0	4.9	3.2	4.0	4.8	2.7	8.3	3.7	4.1	3.2	4.7	4.8
CU		25.9	56.9	100.8	67.4	113.3	90.3	131.5	36.5	23.7	22.9	30.0	83.9	27.4	37.6	18.0	70.2	39.7
PB		10.9	6.5	5.3	13.9	10.6	10.7	17.1	11.1	9.5	6.3	8.5	19.9	11.5	11.8	6.5	13.7	30.2
ZN		71.9	64.6	49.0	152.4	116.1	120.4	54.5	29.8	41.1	23.9	29.6	158.8	50.0	46.2	58.6	101.8	79.9
MO		.5	.7	.0	.6	.0	.6	.0	.0	.2	1.5	.4	.6	.7	.2	.0	.0	.2
V		90.0	188.4	155.2	285.5	411.1	514.4	97.2	156.0	113.0	94.4	133.7	441.1	116.6	184.3	202.1	208.9	241.4
CO		90.3	39.5	46.8	40.4	39.0	46.3	94.8	55.2	79.6	82.0	49.7	41.3	89.7	67.2	62.6	53.1	61.2
NI		1082.1	339.2	363.8	47.4	70.9	44.3	1097.6	569.1	1133.5	743.2	533.4	108.5	718.8	649.7	597.8	409.3	603.4
CR		1828.9	1305.3	1149.4	340.2	409.5	102.9	2073.6	1503.4	2141.3	2170.3	1764.6	289.0	2037.3	2053.2	1800.0	1111.5	1520.4
GA		6.0	14.3	1.3	15.1	14.9	15.1	5.9	4.2	9.1	3.8	4.0	20.9	6.0	5.8	6.3	10.2	12.3
SN		10.9	0	4.3	5.3	9.1	13.3	14.4	7.0	4.4	5.8	2.9	16.3	11.0	17.6	0	7.3	5.4
TI		2229.2	2369.4	1640.2	7083.9	3857.0	14166.9	1736.2	626.2	476.2	560.5	547.7	16281.6	554.8	667.4	1136.7	1620.6	1196.4
BE		0	0	0	0	0	0	0	0	0	.3	0	0	0	0	0	0	0
MG		8.9	4.5	6.3	4.1	3.8	4.5	9.4	6.7	6.2	6.9	6.4	5.3	8.0	8.4	6.4	6.6	6.1
CA		2.3	5.5	6.8	5.9	5.7	8.0	2.1	5.7	1.1	1.3	5.2	9.1	1.3	6.2	5.4	5.7	6.3
SR		111.7	321.9	230.0	128.9	143.9	251.1	341.1	45.6	16.4	8.2	51.5	429.2	17.1	45.0	23.0	105.0	104.8
BA		68.2	83.5	53.9	82.8	139.6	171.0	215.1	64.1	54.9	8.2	68.0	662.4	25.3	156.8	17.6	131.8	172.3
K		.3	.6	.2	.2	.3	.9	.4	.2	.1	.2	.2	1.3	.1	.2	.3	.4	.4
LI		3.7	30.5	.9	.2	.2	25.4	.2	1.8	.2	8.4	5.1	14.8	.2	.2	14.7	.2	20.0
AL		3.9	8.1	7.9	9.5	7.7	9.1	3.9	1.3	2.7	.4	1.9	9.4	.9	2.3	3.0	5.6	4.7
SC		7.2	7.9	12.1	24.8	24.1	32.6	7.9	15.7	5.1	2.7	14.6	28.9	9.6	18.0	19.2	19.3	16.3
SI		10.5	15.2	18.0	19.3	22.6	27.0	10.6	11.8	19.1	13.1	11.2	23.4	13.6	20.1	10.6	21.2	14.9
MN		1281.1	924.5	1350.8	2670.7	3121.1	4156.8	1724.5	1532.6	1111.9	1069.6	1445.9	3127.7	1575.2	2107.1	1266.9	1942.5	1732.3
S		395.0	295.0	415.0	1570.0	895.0	1520.0	330.0	80.0	25.0	165.0	90.0	120.0	90.0	215.0	90.0	205.0	150.0

MAFIC AND ULTRAMAFIC CORE AND OUTCROPS

		36011	36012	36013	36014	36015	36016	36017	36018	36019	36020	36021	3F022	3E023	35024	3E025	36026	36027
NI	S	24.3	66.0	180.0	88.0	76.0	106.0	0	81.0	86.0	98.0	70.0	140.0	26.0	220.0	72.0	18.0	80.0
CU	S	18.0	1.0	-	1.5	1.6	0	5	4.0	.	1.6	0	0	14.0	0	66.0	16.0	0
CO	S	0	0	0	6.0	2.0	6.0	0	3.0	4.0	4.0	0	4.0	4.0	8.0	3.0	4.0	6.0
ZN	S	10.0	1.0	1.0	24.0	1.0	13.0	2.0	12.0	2.0	1.0	0	7.0	3.0	2.0	4.0	4.0	1.0
FE	S	.5	0	0	.0	0	0	0	0	0	0	0	0	.3	0	.9	.4	0
TI	X	0	0	0	0	0	0	0	0	-	0	0	0	0	0	0	0	0
FE		4.4	6.4	6.1	4.7	6.0	6.1	9.1	3.8	6.4	6.8	6.5	6.6	6.2	8.8	3.7	4.6	4.7
CU		77.5	16.1	26.8	5.8	4.2	10.9	48.3	46.6	9.9	7.1	6.8	4.6	41.2	5.9	128.8	48.7	7.8
PB		13.1	98.4	19.5	24.3	8.0	15.9	30.9	16.2	18.8	14.0	16.4	29.9	7.1	20.7	17.5	18.4	9.1
ZN		67.8	50.0	45.0	115.7	12.8	30.9	27.6	68.1	59.7	26.2	59.8	69.2	59.2	87.5	27.8	118.4	10.5
MO		.4	.6	.0	.0	.4	.5	.0	.0	.2	.0	.4	.8	.0	.0	.0	.0	.5
V		200.8	61.4	40.9	53.8	35.0	38.2	49.4	54.3	51.7	37.9	40.6	40.3	193.0	60.2	140.1	222.3	40.6
CO		74.3	137.1	119.1	81.7	113.4	130.8	149.3	129.3	132.2	135.1	125.8	106.7	59.7	146.7	58.3	43.6	109.7
NI		586.3	2352.6	2196.6	2063.7	2175.8	2391.3	2666.9	2034.6	2221.9	2394.0	2117.0	2257.8	349.3	2719.0	765.2	232.0	1980.4
CR		1801.5	3098.5	2939.1	2615.2	2493.6	2358.9	2574.6	2911.9	2715.8	2391.3	2449.3	2797.1	915.7	2744.9	1930.1	866.6	2247.1
GA		9.5	6.7	5.3	3.3	1.7	3.2	3.5	5.0	3.2	1.5	5.9	3.2	0.9	4.0	5.9	14.0	1.1
SN		4.3	29.3	32.0	34.5	11.3	23.4	30.5	33.8	24.7	25.6	24.4	23.2	6.6	34.7	7.2	10.5	13.4
TI		2250.4	225.8	121.7	152.8	67.7	101.8	177.9	183.1	131.2	74.9	129.0	81.6	878.3	193.7	1490.1	2516.4	125.9
BE		0	0	0	0	0	.3	0	0	.6	.	.1	.4	0	.	0	0	.2
MG		6.7	10.7	10.9	12.5	7.1	7.9	9.2	9.6	9.0	9.3	3.3	8.6	7.1	10.2	8.4	6.1	7.5
CA		1.3	.3	.3	.2	.1	.2	.3	.3	.3	.2	.2	.2	7.8	.4	3.5	7.7	.2
SR		39.5	6.9	15.4	12.4	7.3	7.3	15.3	13.0	7.8	16.0	8.6	8.2	81.3	10.9	81.7	212.7	6.6
BA		27.9	4.1	44.0	83.9	22.0	31.2	193.8	49.1	15.3	105.7	20.5	16.2	89.8	50.5	55.7	142.9	5.7
K		.2	0	.2	.0	0	.3	.1	.1	.1	.1	.0	.0	.3	.1	.3	.5	.0
LI		4.3	.2	.2	4.8	2.3	.2	.2	.2	.2	.2	5.6	2.9	.2	8.7	.2	3.5	.2
AL		2.4	0	0	.2	0	0	0	.4	0	0	0	0	7.2	.1	3.9	8.0	0
SC		14.2	3.9	3.5	4.2	.0	.6	3.0	6.3	2.0	1.6	2.1	1.1	21.4	5.3	11.5	21.7	.0
SI		12.4	11.0	5.9	10.6	10.6	9.3	9.3	9.3	3.9	9.3	9.3	3.9	21.4	9.3	12.4	24.9	10.6
MN		1761.0	470.3	1323.2	1241.5	473.9	483.1	477.4	1000.4	497.3	492.1	731.3	399.2	1896.5	1080.1	1530.5	2149.4	433.5
S		1158.3	190.0	130.0	150.0	120.0	90.0	120.0	535.0	50.0	115.0	160.0	70.0	140.0	155.0	245.0	140.0	100.0

MAFIC AND ULTRAMAFIC CORE AND OUTCROPS

		36028	36029	36030	56001	56002	56003	56004	56005	56006	56007	56008	56009	56010	66001	66002	66003	66004
NI	S	188.0	34.0	22.0	300.0	230.0	74.0	89.5	170.0	42.0	25.0	320.0	0.0	128.0	12.0	75.0	57.0	18.0
CU	S	.	0	12.0	3.2	0	2.0	2.0	0	1.0	3.0	0	0	1.0	14.0	60.0	62.0	15.0
CO	S	12.0	-	4.0	15.0	12.0	6.3	4.0	9.0	0	4.0	4.0	0	6.0	6.0	6.0	6.0	3.0
ZN	S	5.0	1.0	19.0	9.5	15.0	3.0	3.0	2.0	0	2.0	2.0	0	3.0	5.0	6.0	6.0	6.0
FE	S	0	0	.4	.0	.0	0	.0	0	0	.0	.1	0	0	.1	.8	1.0	.1
TI	X	0	0	0	0	0	.	.	.	0	.	0	0	0	0	0	0	0
FE		7.3	8.6	3.2	5.7	5.9	5.1	5.5	9.9	4.0	7.1	5.7	5.4	6.1	5.3	4.2	5.0	5.4
CU		13.3	10.4	33.2	16.0	11.8	57.8	12.2	10.7	13.3	29.7	10.6	10.1	49.6	15.4	60.8	96.7	66.5
PB		12.0	15.4	15.2	19.0	14.2	14.0	14.6	12.5	10.1	16.2	15.3	11.6	17.0	6.4	14.9	39.5	13.1
ZN		37.0	65.1	43.0	41.5	20.0	44.8	23.7	27.5	11.9	48.9	27.6	35.6	37.2	41.7	72.5	81.3	64.8
MO		.7	1.2	.0	.0	.0	.3	.3	.0	.5	.	.0	.0	.3	.4	.9	1.0	.4
V		58.1	42.9	208.9	72.6	55.8	52.7	34.9	45.7	33.8	157.2	73.8	46.1	55.0	139.2	150.0	145.9	185.8
CO		173.4	158.6	53.7	83.0	93.4	122.1	101.5	113.3	91.4	94.5	122.8	122.8	120.8	85.5	70.5	83.4	71.5
NI		2778.9	2790.2	397.6	1947.0	1524.7	1616.3	1589.3	1790.3	2101.4	761.3	2330.8	239.3	1666.9	1185.1	738.3	955.4	744.5
CR		2673.2	2693.4	1592.1	1312.7	943.2	1.63.1	1216.9	1114.7	1035.5	216.4	1163.5	936.2	1103.5	1609.3	1469.6	1619.5	1623.0
GA		2.3	3.2	8.4	9.1	4.8	5.3	3.7	4.1	3.4	13.2	4.0	1.4	5.4	7.5	9.2	8.6	8.9
SN		23.5	27.3	10.3	15.2	11.9	17.3	13.7	15.0	9.0	1.4	15.9	8.1	17.1	.2	4.9	5.5	10.6
TI		210.3	99.7	1173.0	1249.9	1085.7	684.5	733.1	514.0	1032.9	5233.1	1175.7	387.7	957.5	853.5	987.4	436.5	1107.5
BE		.5	.5	.	.	0	.	0	0	0	.	0	0	0	.9	0	.4	1.1
MG		9.1	9.8	7.8	8.5	8.0	8.8	9.2	11.8	6.8	6.3	8.0	7.8	8.7	6.9	5.9	6.7	7.5
CA		.2	.3	7.4	1.4	1.1	1.3	.5	1.1	.6	2.9	1.3	.9	1.5	2.3	2.4	4.1	1.5
SR		7.3	9.4	71.1	23.4	22.4	77.1	11.0	13.7	7.1	71.8	16.4	22.5	73.0	12.5	73.7	267.5	10.7
BA		14.3	43.3	63.7	33.6	23.8	35.4	25.2	210.2	18.9	103.6	75.6	63.3	41.3	44.0	65.0	283.4	68.0
K		.0	.1	.2	.1	.1	.2	.1	.0	.0	.2	.0	.0	.2	.0	.4	.4	.1
LI		.2	8.6	.2	.2	.2	.2	.2	.2	.2	.2	.2	.2	.2	2.1	3.0	6.0	28.6
AL		.1	0	4.7	2.3	1.0	.8	1.0	.5	.1	2.7	1.2	.7	1.3	2.2	3.9	4.3	1.8
SC		2.5	2.8	23.2	5.2	3.8	3.2	4.2	7.3	.1	7.3	4.7	2.2	4.6	9.1	8.2	8.4	9.7
SI		10.5	9.3	19.5	4.9	9.3	3.9	10.6	11.0	3.9	9.3	5.5	10.6	3.9	7.6	15.8	13.9	16.3
MN		864.3	1199.9	1924.6	714.1	735.7	1188.4	854.7	794.7	484.4	499.1	1426.9	1062.0	1235.9	1065.6	1522.5	1759.6	2283.1
S		80.0	85.0	50.0	80.0	315.0	330.0	235.0	140.0	135.0	95.0	75.0	170.0	350.0	60.0	125.0	120.0	95.0

MAFIC AND ULTRAMAFIC CORE AND OUTCROPS

	66005	66006	65007	66008	66009	66010	66011	56012	66013	66014	66015	66016	66017	66018	66019	66020	76001
NI S	24.0	33.0	27.0	24.0	27.0	15.0	30.0	30.0	18.0	75.0	84.0	30.0	30.0	36.0	120.0	24.0	15.0
CU S	12.0	0	14.0	23.0	13.0	19.0	33.0	12.0	11.0	70.0	53.0	131.0	139.0	85.0	345.0	18.0	54.0
CO S	9.0	3.0	0	6.0	6.0	9.0	3.0	6.0	0	6.0	9.0	9.0	6.0	6.0	18.0	3.0	3.0
ZN S	9.0	1.0	5.0	3.0	8.0	4.0	7.0	5.0	5.0	5.	5.5	5.0	11.0	9.0	8.1	4.0	6.0
FE S	.1	0	.1	.8	.1	.4	1.5	.2	.1	.6	1.0	.4	.6	.5	.7	.3	.6
TI X	2	0	0	0	0	0	0	0	60.0	0	0	0	0	0	0	60.0	0
FE	4.3	4.3	5.7	4.1	7.0	4.4	5.1	7.0	5.0	5.5	4.5	3.8	3.3	3.0	4.2	5.5	3.5
CU	13.3	52.4	17.8	46.1	12.9	43.5	35.8	15.1	9.2	71.9	52.1	141.8	146.2	89.0	237.7	22.4	43.7
PB	13.4	12.6	16.7	9.4	9.2	11.0	14.5	11.6	29.7	11.7	76.4	11.9	76.4	8.1	7.5	8.1	17.9
ZN	90.5	91.8	93.3	62.6	49.6	59.4	74.2	55.8	92.7	109.2	67.4	74.6	88.8	50.6	68.4	33.7	65.9
MO	.5	.1	.5	.1	.0	.2	.6	.0	.5	2.2	.5	.9	.6	.0	1.7	.0	.0
V	100.3	109.1	128.6	169.3	153.3	235.4	174.3	158.6	186.1	177.2	166.6	214.8	178.9	202.4	158.3	160.1	137.4
CO	83.3	112.6	83.0	55.7	33.7	21.7	73.1	95.3	73.3	79.9	63.8	57.9	43.0	47.7	58.8	90.1	42.2
NI	1116.4	2007.5	1231.3	515.9	1135.3	114.2	792.3	1112.6	927.1	720.0	711.3	117.0	117.0	256.5	374.4	1093.8	369.6
CR	1359.3	1477.9	1771.0	1445.7	1660.8	77.2	1719.4	1585.7	1465.5	1591.3	1204.7	149.1	169.1	473.5	374.2	1511.3	679.3
GA	6.2	7.3	6.1	8.3	5.3	17.3	6.7	5.2	6.6	9.9	13.1	16.5	15.4	17.7	14.3	6.7	10.0
SN	6.2	13.5	12.3	4.1	3.6	10.5	7.0	2.3	3.0	12.6	8.2	2	1.2	1.3	0	0	5.9
TI	766.5	819.6	739.3	1154.6	813.9	2642.3	1936.4	849.5	555.2	1744.4	532.0	1093.0	796.6	665.1	468.9	1194.7	367.3
BE	.1	0	.1	0	0	0	0	.7	.4	0	0	.7	0	0	.9	0	0
MG	7.7	9.7	9.4	6.2	6.6	4.3	7.4	7.2	5.8	13.3	7.3	3.1	3.8	4.2	3.5	5.8	5.7
CA	1.3	2.0	.9	2.2	1.5	8.4	2.1	.9	.4	2.9	4.9	4.2	5.1	5.3	4.9	2.8	6.9
SR	24.5	54.8	29.3	83.5	16.2	379.3	77.6	15.8	22.7	61.5	154.1	119.2	167.8	126.3	105.7	25.2	202.1
BA	259.2	152.0	137.1	109.5	166.2	574.1	88.9	112.4	1030.8	70.0	93.6	166.6	232.5	45.6	93.1	231.1	112.4
K	.1	0	.1	.3	.1	.4	.3	.1	.1	.4	.3	.5	.6	.3	.3	.1	.2
LI	.2	6.4	1.8	7.3	.2	.2	7.1	7.0	1.0	.2	4.3	10.3	25.6	7.0	18.5	.2	6.2
AL	3.3	3.2	4.1	3.6	1.9	11.5	3.7	1.9	.0	3.4	6.7	6.1	6.9	8.7	6.7	2.3	9.2
SC	10.5	11.6	15.3	13.8	10.9	39.1	14.0	16.5	11.9	15.1	8.3	8.4	10.5	9.6	6.0	10.1	15.1
SI	10.5	11.6	16.3	17.0	12.1	25.3	15.7	11.2	14.8	19.1	15.0	18.5	17.5	19.1	18.0	9.3	22.9
MN	1432.0	2111.6	2024.5	1515.0	1307.3	1433.1	1859.9	2073.2	1777.3	1685.8	1391.3	1475.3	1720.0	1168.4	1243.2	816.2	1442.9
S	115.0	50.0	320.0	95.0	35.0	610.0	135.0	80.0	230.0	13.0	150.0	470.0	3.5.0	345.0	1090.0	110.0	65.0

MAFIC AND ULTRAMAFIC CORE AND OUTCROPS

		76002	76003	76004	76005	76006	76007	76008	76009	76010	76011	76012	76013	76014	76015	76016	76017	76018
NI	S	18.0	27.0	15.0	21.0	33.0	12.0	24.0	12.0	9.0	27.0	54.0	27.0	45.0	30.0	6.0	36.0	18.0
CU	S	45.0	30.0	24.0	13.0	37.0	48.0	49.0	26.0	23.0	39.0	123.0	42.0	67.0	81.0	12.0	53.0	38.0
CO	S	6.0	6.0	3.0	5.0	3.0	3.0	9.0	6.0	5.0	6.0	15.0	6.1	9.0	3.	12.0	9.0	9.0
ZN	S	5.0	5.0	5.0	6.0	6.0	9.	11.0	4.0	5.0	7.0	7.0	6.0	7.0	5.0	6.0	8.0	8.0
FE	S	.5	.3	.3	.2	.6	.4	.8	.4	.1	.4	.6	.7	.6	.2	.1	.7	.4
TI	X	0	0	0	0	0	0	0	0	0	0	0	60.0	0	0	0	0	0
FE		3.3	3.6	2.0	4.1	3.5	1.9	5.2	5.2	3.4	3.7	4.6	3.8	3.9	3.4	3.9	3.8	3.0
CU		78.5	103.9	62.9	61.9	52.1	49.0	84.3	73.6	83.0	74.2	144.2	73.4	87.3	166.2	30.8	75.6	65.7
PB		8.5	8.5	5.4	3.0	3.7	6.1	14.5	7.3	11.1	3.5	9.4	9.1	8.0	7.0	8.8	11.5	15.3
ZN		59.5	88.9	87.8	109.8	100.3	62.4	127.7	95.4	117.6	83.7	56.6	69.4	99.3	106.8	49.3	88.2	101.7
MO		.3	.0	.0	.2	.0	1.4	.0	.0	.3	.4	.5	.4	.0	.0	.0	.0	.0
V		273.2	211.1	152.6	193.2	252.2	159.4	336.4	239.3	244.0	212.6	328.7	263.4	242.8	213.8	644.9	248.0	376.9
CO		45.1	53.3	37.3	44.9	40.9	5.9	38.4	51.4	45.6	47.6	47.3	44.9	43.1	45.3	52.4	40.9	23.9
NI		332.0	319.7	171.4	271.1	171.4	33.2	132.6	256.3	270.5	230.7	213.6	239.1	213.6	312.8	9.6	165.6	53.7
CR		332.0	440.7	237.4	513.5	414.4	115.1	182.3	368.5	455.1	401.9	536.7	399.0	386.3	338.0	24.8	366.1	110.8
GA		14.3	13.6	12.8	15.2	13.0	25.2	16.6	14.3	14.3	12.9	14.2	16.7	12.6	11.8	20.1	18.5	23.7
SN		0	1.4	0	2.0	2.6	0	5.7	3.8	1.8	2.2	.8	4.1	1.5	.6	0	6.1	.4
TI		840.5	783.5	923.8	1003.9	3123.9	1774.9	4234.4	1233.6	1907.3	1632.9	2166.5	1509.5	2600.3	977.2	10085.8	2046.6	5096.7
GE		.0	0	0	0	0	.1	0	0	0	0	0	.2	0	0	0	0	0
MG		3.2	3.9	3.2	4.2	3.9	.4	3.4	4.6	3.9	4.2	3.4	4.2	3.7	3.9	2.2	4.0	1.4
CA		4.4	4.6	3.9	6.7	4.6	5.4	4.7	5.7	4.3	5.1	4.9	5.1	4.7	4.6	5.2	5.7	4.4
SR		237.5	217.4	273.9	325.1	231.3	382.1	251.3	212.4	293.4	224.0	197.6	253.3	254.8	225.9	300.6	338.7	359.9
BA		209.3	175.4	165.6	223.8	139.3	329.1	304.2	158.6	134.6	176.5	193.3	193.2	250.0	143.8	198.0	247.8	551.4
K		.4	.6	.5	.6	.7	1.0	1.4	.6	1.1	.7	1.0	.7	.9	.6	.5	.9	2.0
LI		10.0	10.6	6.5	8.9	8.7	5.9	6.7	7.7	14.2	15.6	19.3	15.7	16.1	11.4	17.2	10.9	27.1
AL		7.4	7.3	9.4	7.8	7.1	11.7	7.5	8.4	8.6	7.6	6.4	6.9	8.6	8.0	7.2	9.3	8.8
SC		12.3	12.4	13.3	13.5	17.6	4.2	13.6	16.5	15.7	15.1	15.3	13.6	18.1	17.5	24.7	12.4	12.9
SI		14.3	19.2	16.5	20.6	18.4	25.5	24.7	23.6	21.8	21.8	19.6	21.9	23.5	22.4	7.2	22.5	22.1
MN		1019.9	1532.7	1026.3	1496.2	1560.1	375.7	1691.0	1391.3	1710.8	1535.8	1522.5	1678.9	1634.2	1379.0	1198.4	1684.4	1116.8
S		50.0	75.0	100.0	90.0	873.0	160.0	1195.0	95.0	125.0	335.0	1330.0	145.0	790.0	100.0	96.0	1015.0	635.0

MAFIC AND ULTRAMAFIC CORE AND OUTCROPS

		76019	76020	76021	76022	76023	76024	76025	76026	76027	86001	86002	86003	86004	86005	86006	86007	86008
NI	S	18.0	54.0	18.0	102.0	15.0	45.0	15.0	42.0	15.0	460.0	420.0	158.0	0	140.0	175.0	76.0	216.0
CU	S	38.0	52.0	50.0	63.0	34.0	42.0	25.0	86.0	34.0	34.0	120.0	10.0	0	12.0	39.0	17.0	77.0
CO	S	9.0	15.0	6.0	12.0	9.0	15.0	6.0	9.0	9.0	12.0	22.0	6.0	0	8.0	7.0	4.0	8.0
ZN	S	12.0	8.0	9.0	6.0	16.0	22.0	17.0	5.0	15.0	0.0	6.0	2.0	2.0	3.0	3.0	6.0	4.0
FE	S	.5	.5	.5	.7	1.3	1.6	.8	.3	.5	.1	.1	.1	0	.0	.1	.1	.0
TI	X	0	0	0	0	0	0	0	0	0	0	0	0	0	0	0	0	0
FE		4.5	3.8	3.3	4.9	6.2	4.8	4.7	7.0	3.0	6.5	4.6	7.9	9.4	5.5	9.7	6.1	5.9
CU		65.3	51.0	64.2	222.0	51.0	49.2	25.0	81.9	50.4	175.5	203.5	75.3	32.4	44.2	195.7	61.4	365.5
PB		13.4	12.3	20.1	9.3	19.2	18.5	29.1	11.1	23.8	14.9	15.6	3.1	6.2	7.6	8.0	8.8	14.7
ZN		117.5	100.9	113.9	58.6	151.1	138.1	180.0	85.2	122.6	48.6	23.3	15.0	23.5	18.2	20.3	29.1	111.7
MO		.0	.0	2.0	.1	.0	.0	2.4	.5	1.2	.3	.6	.8	.3	.2	.7	.0	.9
V		417.3	233.1	214.2	207.0	289.5	385.0	135.1	191.1	231.6	70.4	58.2	44.5	49.4	36.5	60.1	63.5	71.2
CO		29.1	36.2	29.4	201.6	22.9	24.9	14.1	30.4	16.1	126.0	126.0	119.1	94.3	119.9	76.1	83.4	110.6
NI		44.5	218.3	86.8	1669.8	22.0	22.5	12.1	141.2	10.1	3383.6	2719.9	2818.0	2729.1	2252.5	2617.9	2016.7	2840.5
CR		104.1	559.3	262.2	290.0	154.4	167.5	123.2	323.0	90.3	1574.6	1573.5	1403.6	1255.7	1 67.5	1719.6	1639.7	2466.4
GA		20.2	14.4	21.4	11.7	16.9	22.3	18.5	19.0	16.5	4.9	3.0	4.6	1.3	.3	3.5	2.4	4.6
SN		1.7	4.1	.8	3.5	7.4	4.3	6.0	2.1	3.2	14.8	15.6	7.8	4.0	4.2	7.3	9.2	18.0
TI		8282.9	2660.1	3100.3	2935.1	13862.8	14056.9	10657.8	2791.5	10358.2	275.8	164.8	103.2	98.6	111.5	148.7	225.3	380.2
BE		0	0	.6	0	0	0	0	0	0	.3	.5	0	0	0	0	0	1.0
MG		1.7	4.1	1.4	3.2	1.6	1.5	.9	3.1	.8	8.9	10.1	10.2	9.1	8.6	8.5	10.2	8.7
CA		5.0	5.5	2.2	5.3	5.7	5.2	2.6	3.8	2.3	.7	.2	.2	.1	.1	.1	.1	.2
SR		419.5	220.5	225.7	261.9	484.6	493.3	281.9	290.4	268.0	6.8	4.8	4.1	4.3	7.1	2.8	7.8	4.6
BA		822.3	315.8	230.2	221.7	1195.0	1109.8	999.9	776.1	370.7	29.3	8.2	1.6	7.5	8.4	4.4	28.5	23.1
K		2.0	.8	2.6	.5	3.0	2.1	3.2	1.1	2.9	.1	.0	0	.0	.0	.0	.0	.0
LI		16.1	14.1	36.8	6.4	3.7	6.9	18.0	16.5	8.0	.2	.2	.2	.2	.2	.2	.2	.2
AL		9.3	8.3	5.8	5.7	10.8	7.8	7.5	7.9	6.9	.9	.7	0	.1	0	.5	.3	1.6
SC		20.3	14.6	7.5	7.9	25.7	21.0	15.3	8.0	13.2	2.7	.5	1.6	1.7	.8	1.3	2.5	4.3
SI		20.7	21.9	26.8	14.7	27.0	27.3	36.2	23.0	32.2	4.7	7.3	11.0	9.3	10.6	4.0	10.6	13.7
MN		1336.3	1708.8	837.5	837.7	1672.3	1788.9	1693.5	1395.1	1279.6	1022.5	428.6	255.3	172.2	383.2	339.8	305.5	850.9
S		1065.0	935.0	595.0	600.0	945.0	2190.0	610.0	680.0	715.0	120.0	350.0	75.0	355.0	360.0	170.0	-	155.0

MAFIC AND ULTRAMAFIC CORE AND OUTCROPS

	86009	86010	86011	86012	86013	86014	86015	86016	86017	86018	86019	86020	86021	86022	86023	86024	86025
NI S	140.0	425.0	116.0	135.0	168.0	135.0	85.0	620.0	540.0	4.0	380.0	300.0	280.0	75.0	360.0	560.0	320.0
CU S	56.0	63.0	9.0	14.0	3.0	73.0	15.5	1.0	1.0	1.0	8.0	2.0	0	43.0	10.0	1.0	1.0
CO S	12.0	20.0	6.0	5.0	9.0	16.0	5.0	10.0	9.0	0	8.0	14.0	0	6.0	10.0	10.0	4.0
ZN S	6.0	6.0	2.0	3.0	4.0	17.0	12.0	2.0	1.0	1.0	4.0	2.0	2.0	21.0	5.0	5.0	2.0
FE S	.0	.0	.0	.1	.0	.0	.0	.0	.0	.	.0	.0	0	.4	.1	0	0
TI X	0	0	0	0	0	0	0	0	0	0	0	0	0	0	0	0	0
FE	10.2	3.8	6.0	5.4	5.0	7.4	4.0	4.8	5.1	5.2	5.5	5.8	5.6	1.6	3.0	3.7	6.4
CU	293.7	285.5	227.3	70.3	52.8	243.4	114.0	16.7	16.1	77.4	96.1	34.0	15.9	79.7	21.5	9.9	21.7
PB	9.2	12.5	14.4	3.2	13.6	15.1	8.2	12.7	15.4	19.6	17.8	14.1	13.8	19.4	17.0	16.3	10.3
ZN	66.2	22.0	39.0	16.2	39.8	176.7	37.3	26.0	29.4	17.3	55.5	102.6	22.1	75.1	36.1	41.2	32.1
MO	1.3	.1	.3	.4	.0	.3	1.0	.5	1.0	.0	.0	.0	.0	7.0	.3	.0	.0
V	43.3	47.3	63.7	47.8	57.5	61.0	54.4	50.3	40.8	2.3	51.1	52.3	30.8	48.8	36.3	15.6	64.5
CO	132.1	127.4	203.4	90.7	105.3	185.1	82.9	100.6	133.6	152.8	122.3	114.2	150.2	11.9	94.0	134.3	145.1
NI	2621.1	2900.7	3135.3	2463.8	2731.2	3356.9	2123.2	2338.2	2841.1	4642.7	3512.0	1860.8	3453.4	297.1	2226.5	3645.4	2808.8
CR	2311.3	1738.6	1803.0	840.4	1721.7	1609.3	1716.7	1342.5	1322.0	1243.4	2372.8	1733.5	1361.6	262.8	1147.4	1095.9	1700.7
GA	1.3	1.3	3.9	1.3	1.7	3.7	2.6	2.6	7.1	1.7	3.8	2.5	2.5	14.1	2.9	4.7	6.0
SN	8.9	8.1	12.3	0	13.9	13.8	0	3.9	21.2	10.5	26.1	15.5	13.6	.1	19.1	21.0	13.3
TI	154.0	158.3	213.7	135.1	137.4	125.3	56.7	160.0	175.0	77.5	282.8	433.1	45.2	1750.2	35.2	85.7	154.8
BE	1.2	0	.3	0	0	.2	1.1	0	0	0	0	0	0	.3	.0	0	0
MG	9.4	7.6	9.0	8.7	12.5	8.6	6.6	8.0	11.0	9.6	11.9	10.4	9.0	.6	8.9	9.8	10.3
CA	.1	.2	.2	.0	.2	.2	.1	.2	.3	.2	.2	1.2	.2	.1	.2	.1	.3
SR	.3	9.2	7.8	.3	7.8	3.3	.8	3.8	5.7	1.5	9.9	10.8	6.2	41.9	10.9	5.2	11.0
BA	6.3	111.2	27.4	.4	11.1	9.2	9.3	9.0	11.1	2.7	22.0	21.4	22.1	12.7	18.9	11.6	18.5
K	.3	.0	.1	0	.0	.3	0	.0	.0	.0	.0	.0	.0	0	.0	0	.0
LI	.2	.2	.2	.2	.2	.2	.6	1.4	.2	.2	.2	.2	.2	.2	.2	.2	.2
AL	.5	.3	1.1	.7	.5	.5	0	0	.3	0	1.0	1.4	0	5.9	.0	0	.2
SC	.5	.0	3.3	.0	2.8	2.2	.0	.6	2.6	.0	5.9	7.2	.0	.0	2.1	.0	1.9
SI	10.5	10.6	4.3	10.6	10.6	9.5	3.9	9.3	11.0	9.3	15.3	10.6	12.6	40.3	28.6	10.6	11.0
MN	457.1	444.7	997.5	270.4	231.6	667.7	452.1	442.2	473.5	779.6	1259.9	1243.8	1102.3	128.2	1015.0	991.1	448.4
S	140.0	190.0	240.0	120.0	65.0	255.0	85.0	200.0	315.0	260.0	335.0	235.0	125.0	333.0	170.0	165.0	190.0

MAFIC AND ULTRAMAFIC CORE AND OUTCROPS

		86025	86027	86028	86029	86030	86031	86032
NI	S	360.0	180.0	204.0	64.0	480.0	100.0	4900.0
CU	S	0	0	0	0	1.0	90.0	3200.0
CO	S	0	4.0	0	0	4.0	14.0	230.0
ZN	S	1.0	0	0	1.0	4.0	6.0	16.0
FE	S	0	0	0	0	0	.1	.4
TI	X	0	0	0	0	0	0	0
FE		4.0	4.3	4.3	6.7	4.8	5.1	7.8
CU		15.4	57.1	0.2	13.0	5.5	115.3	600.6
PB		9.1	13.4	14.4	15.5	12.2	11.7	17.5
ZN		7.3	9.5	31.6	24.5	30.4	71.9	36.6
MO		1.0	.1	.0	.0	.0	.0	.5
V		31.0	31.9	55.1	56.7	39.3	147.1	39.9
CO		118.5	88.3	122.9	132.1	134.4	56.9	353.7
NI		2783.5	2120.0	3012.4	2705.7	3472.0	463.1	3429.3
CR		1196.1	1099.2	1610.4	1355.1	1275.1	1798.4	2222.9
GA		4.3	3.3	6.0	1.8	0	6.5	2.5
SN		11.4	12.4	14.5	18.9	13.6	11.2	21.6
TI		59.2	132.1	69.2	113.8	52.3	905.4	263.6
BE	0	0	0	0	0	0	0	0
MG		8.3	7.0	9.1	9.8	11.3	7.3	8.6
CA		.2	.1	.1	.2	.2	2.6	.4
SR		7.3	3.4	5.7	6.9	8.7	12.9	6.4
BA		29.4	2.2	13.0	24.4	22.5	19.9	5.7
K		0	0	.0	.0	.0	.1	.0
LI		.2	.2	.2	.2	.2	.2	.2
AL		0	0	0	0	0	1.5	0
SC		.0	.0	.0	2.2	2.0	10.0	3.7
SI		11.0	9.3	5.4	9.3	10.6	13.9	10.6
MN		1203.3	498.0	783.1	836.4	1112.2	1960.6	379.5
S		180.0	225.0	80.0	155.0	345.0	1540.0	9390.0

PIT PROFILES

	15509	15510	15511	15512	15513	15514	15515	15516	15517	15518	15519	15520	15521	15522	15523	25513
CM	7.3	20.0	35.0	50.0	1J0.0	200.0	350.0	7.0	20.0	35.0	50.0	100.0	200.0	300.0	400.0	7.0
NI	140.0	170.0	175.0	230.0	245.0	205.0	197.5	2900.0	3000.0	3550.0	9500.0	4600.0	9500.0	18000.0	7500.0	2550.0
CU	205.0	235.0	275.0	250.0	228.0	36.0	36.5	400.0	500.0	560.0	800.0	1050.0	1510.0	720.0	540.0	64.0
CO	50.0	60.0	65.0	70.0	70.0	20.0	25.0	205.0	200.0	205.0	600.0	450.0	500.0	900.0	500.0	175.0
ZN	14.0	19.0	17.0	14.0	16.0	11.0	18.5	27.0	29.0	22.0	29.0	21.0	37.0	26.0	41.0	90.0
CR	80.0	150.0	75.0	175.0	55.0	5.0	25.0	280.0	395.0	300.0	405.0	300.0	65.0	105.0	350.0	3200.0
FE	10.7	10.0	10.4	11.0	10.7	4.4	7.4	27.0	31.5	32.0	25.0	36.0	18.0	20.0	19.0	15.0
TI	4200.0	3200.0	3850.0	3400.0	3300.0	3050.0	2450.0	2400.0	1750.0	2400.0	1900.0	1650.0	3450.0	1950.0	2500.0	2250.0
MN	220.0	240.0	290.0	220.0	310.0	190.0	300.0	555.0	390.0	410.0	540.0	370.0	350.0	535.0	700.0	1345.0
PB	6.4	8.1	5.1	6.9	7.5	3.9	6.4	10.1	13.2	12.1	7.5	14.1	8.3	7.6	10.7	11.5
MO	.3	.1	.0	1.3	.6	.0	.0	.8	2.4	1.6	.0	1.3	.0	.2	.2	.8
V	458.0	473.1	414.5	469.7	482.2	165.9	420.0	619.5	734.3	469.1	444.5	361.3	336.9	382.2	504.5	232.3
GA	22.7	33.0	27.6	24.5	33.2	32.9	23.8	27.7	28.9	25.1	18.3	22.3	32.2	20.7	36.5	30.0
SN	13.7	17.2	14.7	13.1	11.0	3.9	9.9	12.4	9.4	6.0	16.1	6.7	14.7	3.4	11.5	16.8
BE	?	0	0	0	0	.2	2.3	2.2	7.7	2.3	3.5	3.4	.7	5.3	2.1	0
MG	0	1.1	0	0	0	1.8	3.3	3.3	1.7	2.5	3.7	4.3	6.9	3.3	6.3	.0
CA	.9	.8	.6	.7	.8	3.1	3.4	1.6	1.1	1.1	1.4	1.0	2.0	1.1	2.9	.8
SR	38.4	35.9	23.3	26.0	32.0	53.6	80.6	50.8	26.1	39.5	27.7	25.5	26.8	24.0	118.5	19.3
BA	206.3	238.6	173.4	187.3	222.3	81.0	70.4	131.7	81.5	101.5	58.2	64.6	95.0	57.3	75.1	112.3
K	1.7	2.2	1.7	2.0	1.6	.8	.5	.8	.5	.4	.1	.2	.3	.2	.2	.8
LI	4.2	6.1	7.3	10.0	9.6	.5	.5	7.3	8.6	13.5	8.6	.2	10.9	10.9	14.7	23.8
AL	10.9	13.2	9.7	12.2	15.7	8.9	7.2	10.5	7.9	10.9	7.9	4.1	7.2	7.1	10.4	19.4
SC	13.3	19.0	13.9	16.7	22.0	12.5	13.0	18.7	20.5	25.6	18.8	23.0	11.0	13.5	15.6	28.5
SI	30.3	41.4	32.0	33.9	32.1	32.6	28.3	17.3	15.5	11.8	11.8	12.2	16.8	15.6	16.2	31.1
S	-	-	-	-	-	-	-	390.0	465.0	525.0	335.0	390.0	310.0	240.0	160.0	115.0
F	-	-	-	-	-	-	-	266.0	447.0	352.0	247.0	323.0	2280.0	974.0	400.0	475.0
PH	-	-	-	-	-	-	-	5.5	5.1	5.3	5.6	5.5	5.8	6.1	7.5	4.9

	25514	25515	25516	25517	25518	25519	25520	25521	45533	45534	45535	45536	45537	45538	45539	55513	55514
CM	20.0	35.0	50.0	100.0	200.0	300.0	400.0	500.0	7.0	20.0	35.0	50.0	100.0	200.0	300.0	7.0	20.0
NI	2500.0	2650.0	2650.0	2650.0	2900.0	3750.0	15000.0	8000.0	650.0	950.0	1200.0	1800.0	1100.0	1200.0	6000.0	2000.0	2100.0
CU	64.0	68.0	66.0	67.0	68.0	73.0	17.0	11.0	51.0	62.0	70.0	73.0	68.0	70.0	83.0	340.0	350.0
CO	160.0	150.0	165.0	155.0	190.0	230.0	350.0	450.0	60.0	95.0	95.0	145.0	175.0	140.0	350.0	155.0	185.0
ZN	88.0	85.0	90.0	81.0	83.0	95.0	160.0	190.0	400.0	380.0	440.0	410.0	410.0	450.0	520.0	130.0	135.0
CR	3300.0	2400.0	3300.0	2650.0	2800.0	3150.0	4500.0	10500.0	700.0	1450.0	1400.0	2000.0	850.0	1150.0	1950.0	3500.0	3750.0
FE	16.5	16.0	17.5	17.0	19.0	19.5	10.3	13.0	5.8	7.5	9.9	11.5	8.0	8.3	14.0	16.0	18.0
TI	2250.0	2200.0	2000.0	2100.0	2150.0	2250.0	400.0	350.0	1350.0	1250.0	1000.0	1200.0	1150.0	1050.0	300.0	2900.0	3500.0
MN	1120.0	1090.0	1110.0	1050.0	1245.0	2000.0	3400.0	4200.0	630.0	770.0	660.0	1020.0	1700.0	1330.0	4000.0	1400.0	1440.0
PB	11.0	8.3	8.9	7.8	4.2	12.6	9.4	9.7	53.5	64.2	53.5	57.6	140.6	77.7	16.6	8.9	15.2
MO	1.1	1.0	.8	.8	.0	1.2	.0	.0	.2	.6	.9	.5	.4	.0	.0	.0	.5
V	214.5	231.0	273.2	223.5	109.7	236.4	65.9	71.4	119.4	128.3	127.4	122.9	137.7	116.5	67.9	131.7	182.0
GA	33.3	30.1	27.7	20.5	19.9	38.8	3.9	3.4	14.1	18.2	15.6	16.1	17.1	10.8	1.2	16.7	20.9
SN	6.3	3.1	6.5	8.0	0	17.9	11.6	21.8	13.3	6.5	2.1	9.4	4.9	5.1	4.3	3.4	9.5
BE	2.0	2.2	3.7	1.1	2.8	0	3.0	3.6	.6	3.0	3.8	4.1	2.7	3.0	2.9	0	.2
MG	.3	.0	.0	.0	.0	.0	7.1	6.0	4.8	5.5	4.3	5.2	4.4	5.8	6.5	3.8	4.1
CA	.5	.5	.6	.6	.3	.8	.6	.8	.5	.4	.3	.4	.4	.4	.4	2.2	2.5
SR	10.4	10.2	21.1	13.1	4.9	15.1	7.2	6.4	12.3	14.1	8.0	15.8	12.4	10.8	8.2	64.8	82.7
BA	77.8	72.4	119.0	75.8	53.5	87.3	97.2	100.4	148.8	128.4	97.2	143.6	169.9	99.8	159.8	121.1	150.8
K	.3	.7	.7	.6	.5	.8	.1	.1	.5	.5	.4	.5	.5	.4	.1	.6	.6
LI	34.5	33.0	39.5	28.0	33.6	35.1	.2	.2	24.5	35.4	38.3	35.8	32.8	28.0	1.5	23.3	24.0
AL	16.3	17.5	23.3	16.4	12.5	20.9	1.4	1.4	8.2	9.9	8.8	10.8	9.4	7.3	1.8	6.0	5.8
SC	22.1	22.4	34.5	25.1	15.9	27.5	5.3	6.9	9.8	10.3	8.4	13.2	11.6	9.8	6.5	12.0	15.9
SI	27.0	23.2	31.4	24.2	15.5	30.6	12.5	14.2	41.1	34.5	22.4	28.4	33.7	26.7	15.3	17.6	18.4
S	120.0	115.0	120.0	95.0	120.0	105.0	75.0	80.0	10.0	40.0	140.0	240.0	10.0	40.0	10.0	150.0	120.0
F	247.0	447.0	285.0	459.0	355.0	285.0	133.0	109.7	143.0	117.0	95.0	95.0	95.0	83.0	38.0	190.0	117.0
PH	4.9	4.8	4.8	4.9	5.0	5.2	6.2	6.2	5.2	5.3	5.3	5.5	5.7	6.0	6.2	6.2	6.3

	13501	13502	13503	13504	13505	13506	13507	13508	13509	13510	13511	13512	13513	13514	13515	13516	13517
M	3	50.0	100.0	150.0	160.0	170.0	180.0	190.0	200.0	210.0	220.0	230.0	240.0	250.0	300.0	350.0	400.0
NI	80.0	57.5	37.5	300.0	675.0	2000.0	3900.0	5150.0	4200.0	2550.0	6500.0	6000.0	1050.0	1450.0	230.0	260.0	180.0
CU	17.0	6.0	6.0	25.0	57.0	177.0	340.0	535.0	325.0	290.0	940.0	650.0	132.0	164.0	22.0	37.0	484.0
CO	25.0	22.5	22.5	35.0	52.5	130.0	225.0	392.5	275.0	215.0	420.0	450.0	60.0	85.0	55.0	45.0	57.5
ZN	12.0	11.5	7.5	3.0	11.0	15.0	24.0	25.0	40.0	3.0	32.0	17.0	0.0	2.0	15.0	11.0	13.5
CR	55.0	37.5	32.5	55.0	35.0	140.0	245.0	380.0	500.0	230.0	380.0	240.0	115.0	110.0	75.0	70.0	60.0
FE	5.3	4.4	4.1	3.8	5.5	8.3	14.5	19.3	13.3	17.5	21.5	25.5	8.9	9.5	9.8	8.1	7.9
TI	2400.0	1725.0	1475.0	1150.0	1625.0	1750.0	2000.0	1550.0	1200.0	700.0	750.0	900.0	2300.0	1650.0	4000.0	2900.0	2625.0
MN	280.0	290.0	335.0	550.0	440.0	530.0	590.0	895.0	745.0	145.0	53.0	44.0	13.0	160.0	230.0	310.0	265.0
PB	10.4	12.3	11.6	7.9	9.4	13.5	6.5	7.0	9.5	11.3	9.9	10.9	0.9	30.5	7.7	5.2	8.6
MO	1.4	.6	.8	.6	1.0	1.3	.0	.4	.6	.5	.2	.5	.3	.4	1.4	.5	.6
V	185.3	181.0	123.7	201.4	297.1	363.7	635.0	429.2	365.8	550.9	498.0	514.1	318.4	502.1	705.0	485.7	574.6
GA	15.5	14.1	12.3	11.8	14.8	20.3	26.5	20.3	23.6	22.5	13.2	20.3	35.2	32.3	32.8	30.5	30.4
SN	14.3	18.1	15.9	10.0	11.1	11.3	8.6	4.4	5.3	9.9	9.2	7.4	9.6	5.7	9.8	5.0	15.5
BE	3	0	.9	1.1	0	0	0	0	0	4.6	2.4	2.5	1.9	0	0	0	0
MG	.5	1.0	.7	.5	1.3	2.3	3.9	3.9	5.4	5.5	4.1	4.9	3.6	3.2	2.9	1.5	1.4
CA	.3	.6	.4	.4	.6	1.0	1.4	.9	.8	.6	.8	.8	2.5	2.4	5.0	2.9	1.9
SR	21.8	36.5	25.5	26.7	30.4	41.0	50.7	36.9	44.5	16.5	29.9	32.5	127.9	71.4	135.9	177.4	88.3
BA	347.1	624.4	453.9	434.2	412.1	366.1	198.0	161.8	167.3	53.6	98.5	66.8	74.7	106.1	108.4	124.2	255.5
K	1.3	1.6	1.4	1.2	1.4	1.2	.5	.3	.3	.2	.3	.3	.4	.3	.6	.4	1.4
LI	9.7	9.7	3.9	6.3	4.6	9.1	5.4	3.2	2.8	.2	.2	.2	5.6	7.0	5.0	7.4	4.8
AL	7.2	10.1	8.2	5.3	9.9	12.1	7.6	8.3	9.4	3.1	6.0	5.9	10.9	13.0	17.5	13.0	13.3
SC	7.7	16.5	16.1	5.8	9.1	12.3	12.1	11.6	12.2	10.8	10.6	16.1	15.8	14.5	16.3	19.8	18.2
SI	40.3	43.9	42.5	37.3	37.4	35.3	15.2	12.9	12.9	12.2	10.8	10.8	29.5	18.8	29.5	20.3	27.8
S	50.0	65.0	30.0	50.0	45.0	290.0	405.0	255.0	60.0	90.0	535.0	340.0	125.0	170.0	55.0	110.0	65.0
F	200.0	247.0	204.0	285.0	285.0	475.0	998.0	779.0	64.0	176.0	247.0	266.0	247.0	285.0	204.0	133.0	204.0
PH	4.5	5.0	5.3	6.0	5.3	5.4	5.6	5.6	5.5	5.7	5.9	5.3	5.0	5.5	5.3	5.4	5.3

	13518	13519	13520	13521	13522	13523	13524	13525	13526	13527	13528	13529	13530	13531	13532	13533	13534
M	1150.0	500.0	550.0	600.0	650.0	660.0	670.0	680.0	690.0	700.0	710.0	720.0	730.0	740.0	750.0	800.0	850.0
NI	200.0	160.0	130.0	152.5	135.0	15.0	110.0	125.0	95.0	85.0	125.0	105.0	67.5	65.0	82.5	70.0	40.0
CU	44.0	38.0	51.0	710.0	800.0	840.0	890.0	920.0	970.0	930.0	920.0	780.0	1045.0	920.0	975.0	255.0	185.0
CO	60.0	40.0	62.5	62.5	55.0	60.0	60.0	55.0	60.0	60.0	70.0	65.0	55.0	60.0	62.5	55.0	60.0
ZN	20.0	18.0	24.0	7.5	8.0	5.0	10.0	8.0	10.0	34.0	15.0	8.0	3.5	5.5	7.0	6.0	7.0
CR	120.0	120.0	130.0	50.0	40.0	55.0	50.0	40.0	45.0	5.0	51.0	55.0	35.0	45.0	47.5	60.0	40.0
FE	11.5	12.9	13.0	5.9	5.8	6.3	6.2	5.1	6.2	5.8	6.3	6.4	6.3	5.8	6.6	6.4	5.3
TI	4800.0	3400.0	2100.0	2275.0	2400.0	2550.0	2200.0	2200.0	3000.0	2700.0	2850.0	2750.0	2500.0	2725.0	3100.0	2400.0	2300.0
MN	400.0	390.0	415.0	200.0	160.0	180.0	170.0	150.0	180.0	160.0	170.0	150.0	95.0	140.0	135.0	90.0	100.0
PB	6.2	5.3	7.4	9.5	5.4	22.7	4.6	31.6	6.8	5.0	3.1	4.9	5.5	5.0	4.2	6.8	5.9
MO	.5	.2	.5	.9	5.5	1.3	.5	.5	1.4	.1	.6	.5	.5	.5	1.0	1.4	2.4
V	603.1	711.4	429.1	342.7	353.5	403.6	237.3	93.7	232.5	219.7	232.3	192.6	212.4	171.3	143.8	191.5	166.2
GA	35.0	33.7	33.5	28.6	34.0	16.3	25.9	12.3	31.5	29.0	27.5	26.2	31.7	28.3	31.0	34.5	28.1
SN	4.3	3.9	7.3	13.6	0	0	5.6	14.8	10.7	3.3	12.4	7.8	8.4	8.3	6.6	9.8	0
BE	0	1.1	0	0	1.7	2.3	.1	0	.1	.8	.9	.3	.9	1.4	1.2	0	0
MG	1.3	1.5	1.5	2.0	1.2	12.3	1.2	4.4	2.2	1.6	2.2	2.5	2.3	1.8	2.4	2.3	1.2
CA	2.3	2.4	2.8	.6	0	3.3	.2	1.3	.4	.3	.4	.4	.3	.3	.2	.3	0
SR	53.1	66.9	68.3	22.5	.8	705.5	12.7	24.8	16.4	15.7	16.6	19.0	19.1	14.7	12.4	14.7	.8
BA	74.3	85.5	113.4	224.6	272.6	633.8	194.0	117.7	263.7	239.3	271.8	261.7	316.0	228.8	337.6	223.0	215.7
K	.4	.3	.5	3.1	3.7	3.2	2.9	.4	3.7	3.4	7.5	3.4	5.0	3.9	4.1	3.5	3.3
LI	7.7	1.9	3.8	14.4	.2	645.3	22.4	17.3	22.4	24.3	21.5	21.4	30.3	19.1	33.9	32.0	149.3
AL	13.3	9.7	13.0	10.3	9.3	6.9	6.0	7.1	11.0	7.8	10.6	12.5	9.8	8.3	13.2	11.4	8.4
SC	18.8	19.6	25.2	13.9	15.7	6.0	6.7	8.5	11.1	8.6	8.9	9.0	9.5	8.8	5.9	11.6	9.0
SI	18.4	17.4	22.4	38.1	43.9	23.0	24.7	19.5	25.4	30.2	36.0	32.1	24.4	34.0	26.4	29.6	43.9
S	130.0	140.0	65.0	45.0	35.0	10.0	80.0	65.0	50.0	130.0	62.0	60.0	75.0	75.0	75.0	75.0	55.0
F	380.0	168.0	119.0	475.0	374.0	551.0	602.0	583.0	475.0	501.0	750.0	805.0	1046.0	950.0	1365.0	1425.0	570.0
PH	5.3	5.3	5.2	4.2	4.5	4.4	4.4	4.4	4.4	4.3	4.3	4.3	4.8	4.7	4.6	4.4	4.7

PIT PROFILES

	55515	55516	55517	55518	55519	65501	65502	65503	65504	65505	65506	65507	65508	85501	85502	85503	85504
CM	35.0	50.0	100.0	200.0	300.0	7.0	20.0	35.0	50.0	100.0	200.0	300.0	400.0	7.0	20.0	35.0	50.0
NI	2650.0	2750.0	2300.0	1900.0	1400.0	900.0	1000.0	1100.0	1150.0	1500.0	1300.0	1600.0	900.0	8500.0	8000.0	9000.0	8500.0
CU	330.0	233.0	116.0	101.0	70.0	63.0	67.0	72.0	120.0	60.0	52.0	79.0	84.0	340.0	360.0	400.0	420.0
CO	180.0	190.0	225.0	180.0	160.0	80.0	95.0	105.0	65.0	200.0	140.0	100.0	80.0	400.0	350.0	350.0	285.0
ZN	130.0	117.0	130.0	97.0	110.0	78.0	67.0	63.0	88.0	54.0	66.0	55.0	54.0	220.0	200.0	190.0	137.0
CR	4000.0	2500.0	950.0	400.0	550.0	1750.0	2500.0	1800.0	950.0	1750.0	1850.0	550.0	600.0	2450.0	2600.0	2100.0	2650.0
FE	19.0	18.5	12.0	8.9	9.8	10.8	13.0	14.0	11.0	13.0	10.6	7.5	7.3	17.0	16.0	17.0	15.0
TI	3600.0	2700.0	2250.0	1300.0	1200.0	2250.0	2250.0	2250.0	1700.0	2050.0	1750.0	1350.0	1100.0	1000.0	700.0	1000.0	600.0
MN	1435.0	1470.0	1400.0	1350.0	1270.0	945.0	930.0	1070.0	700.0	3050.0	2100.0	1260.0	860.0	1800.0	1600.0	1370.0	920.0
PB	11.1	13.4	10.5	11.5	11.0	16.7	14.8	14.4	13.6	19.7	11.0	32.0	31.1	22.5	36.1	19.1	15.6
MO	.3	.0	.0	.0	.0	.6	.6	1.1	.1	.9	.0	.0	.0	.4	.0	.3	.0
V	118.1	93.5	64.9	53.0	58.8	207.0	163.8	158.9	178.9	123.0	101.4	84.8	67.2	68.9	80.1	88.5	46.2
GA	17.0	15.7	11.2	11.4	9.9	21.8	19.8	19.5	15.8	20.5	15.6	12.8	11.0	12.6	11.3	9.4	5.0
SN	3.1	4.1	7.0	11.1	6.0	3.9	6.1	0	.9	9.4	1.5	1.4	0	10.2	7.8	9.3	6.9
BE	.2	0	1.1	.6	1.1	.	0	1.8	.5	2.4	2.2	2.2	1.8	.5	1.5	2.6	2.1
MG	3.3	5.9	6.4	9.6	9.6	2.7	2.0	1.7	1.4	4.9	3.8	3.5	4.0	4.5	5.4	5.5	5.5
CA	2.1	1.8	1.6	2.1	1.6	.7	.5	.4	.4	1.9	1.7	1.2	1.4	.9	.8	.7	.4
SR	66.1	54.8	51.3	100.7	89.6	23.3	13.5	11.0	10.9	33.7	21.6	33.5	32.4	40.5	47.8	33.7	17.8
BA	94.4	86.8	75.1	98.9	110.6	142.3	98.1	91.8	122.7	227.7	92.8	124.7	90.7	182.0	226.6	164.0	77.8
K	.4	.4	.2	.2	.2	.9	.7	.7	.6	.4	.3	.3	.2	1.1	1.1	.9	.6
LI	26.5	22.9	12.6	22.3	18.6	15.6	14.5	20.6	20.9	7.4	4.2	7.7	7.6	.2	.2	.2	.2
AL	6.7	6.1	3.9	3.9	3.7	14.9	11.4	13.2	11.0	14.1	7.9	6.8	8.1	5.2	7.2	6.4	4.7
SC	14.2	11.5	5.2	4.8	2.8	25.6	21.1	20.6	19.9	34.9	19.5	8.9	9.3	12.0	17.0	14.0	9.7
SI	12.1	13.1	12.7	11.5	10.0	30.0	26.5	21.3	20.3	27.3	23.1	23.5	19.8	24.8	26.3	23.0	14.5
S	95.0	50.0	20.0	10.0	30.0	240.0	140.0	40.0	80.0	120.0	100.0	60.0	160.0	10.0	80.0	80.0	180.0
F	68.0	60.0	60.0	60.0	95.0	119.0	109.0	109.0	95.0	95.0	60.0	76.0	60.0	53.0	78.0	90.0	109.0
PH	6.4	6.6	6.8	7.0	7.2	-	-	-	-	-	-	-	-	6.1	6.0	5.9	5.9

	85516	85517	85518	85519	85520	85521	85522	85523	85524	85525	85526	85527
CM	100.0	7.0	20.0	35.0	50.0	100.0	200.0	7.0	20.0	35.0	50.0	100.0
NI	9000.0	6500.0	6500.0	7500.0	9000.0	11500.0	9500.0	750.0	700.0	650.0	600.0	460.0
CU	270.0	81.0	81.0	86.0	84.0	52.0	85.0	104.0	155.0	190.0	220.0	420.0
CO	195.0	300.0	260.0	300.0	270.0	350.0	350.0	55.0	55.0	55.0	50.0	50.0
ZN	76.0	120.0	105.0	93.0	85.0	75.0	75.0	240.0	220.0	250.0	200.0	570.0
CR	950.0	1650.0	2000.0	1500.0	1000.0	350.0	300.0	600.0	700.0	550.0	600.0	500.0
FF	13.0	13.0	13.5	14.0	12.5	9.4	8.8	9.3	15.0	14.0	12.5	28.0
TI	350.0	550.0	600.0	750.0	200.0	100.0	300.0	1000.0	1050.0	1150.0	950.0	500.0
MN	840.0	1750.0	1360.0	1240.0	1330.0	1900.0	1510.0	2900.0	1640.0	1435.0	930.0	975.0
PB	15.2	15.5	10.6	8.7	7.7	5.9	10.9	26.2	65.0	50.1	59.5	76.6
MO	.0	.0	.0	.0	.0	.0	.0	.0	.9	1.0	2.4	2.1
V	43.2	48.2	49.0	55.7	25.0	19.8	24.1	44.1	72.6	67.7	76.7	78.2
GA	4.0	5.5	8.0	5.2	1.8	.8	1.0	12.1	22.5	17.9	22.4	30.4
SN	6.3	11.6	6.4	5.2	1.9	3.2	12.3	7.3	18.5	14.4	13.8	6.9
BE	1.7	1.5	2.1	2.1	1.6	1.9	1.8	1.5	1.7	2.9	2.3	4.0
MG	7.1	7.3	5.6	5.4	4.8	5.0	7.0	3.7	3.3	2.8	1.5	1.3
CA	.4	.9	.6	.6	.4	.3	.4	1.0	.8	.6	.4	.6
SR	13.1	27.4	13.9	12.9	8.0	5.9	9.6	44.9	27.5	29.8	11.1	18.6
BA	49.2	119.3	75.1	62.4	36.3	23.9	35.0	303.2	226.4	235.8	131.5	192.1
K	.3	.6	.5	.4	.2	.1	.1	1.1	1.5	1.5	1.6	2.4
LI	.2	.2	.2	.2	.2	.2	.2	7.1	4.5	4.0	7.2	7.6
AL	2.0	1.9	2.7	1.7	.6	.6	.2	9.4	13.3	12.0	7.6	10.6
SC	7.3	12.6	8.4	8.1	5.1	4.2	5.0	8.8	13.9	15.4	9.3	14.9
SI	13.5	34.7	33.5	32.4	28.5	33.0	33.4	31.5	41.2	34.8	33.0	18.0
S	280.0	10.0	20.0	10.0	20.0	40.0	120.0	680.0	-	1000.0	-	1480.0
F	119.0	15.0	15.0	43.0	30.0	30.0	32.0	228.0	-	176.0	-	493.0
PH	5.3	6.2	6.1	6.1	6.3	6.4	6.5	6.2	-	6.1	-	6.2

	34523	34529	34530	34531	34532	34533	34534	34535	34536	34537	34538	34539	34540	34541	43501	43502	43503
M	405.0	420.0	435.0	450.0	465.0	480.0	495.0	510.0	525.0	540.0	555.0	570.0	585.0	600.0	0	50.0	60.0
NI	6500.0	7000.0	7000.0	7750.0	7000.0	8250.0	5400.0	4650.0	7300.0	4900.0	8000.0	7500.0	6000.0	4250.0	40.0	20.0	50.0
CU	18.5	15.0	18.0	16.0	33.0	16.0	14.0	12.0	36.0	53.5	20.0	20.0	12.0	12.0	28.0	22.0	26.0
CO	385.0	380.0	395.0	422.5	365.0	415.0	370.0	325.0	375.0	317.5	375.0	380.0	400.0	315.0	20.0	10.0	15.0
ZN	190.0	200.0	170.0	165.0	150.0	117.5	129.0	135.0	161.0	93.5	123.0	131.0	139.0	92.0	59.0	37.0	38.0
CR	15250.0	16000.0	13500.0	13250.0	1250.0	9250.0	9000.0	7300.0	12500.0	4975.0	11500.0	11000.0	1250.0	7900.0	40.0	25.0	45.0
FE	21.5	21.5	20.5	21.0	13.5	19.3	18.0	13.5	13.5	14.0	19.0	20.0	20.5	14.0	2.6	1.2	1.5
TI	650.0	700.0	600.0	650.0	750.0	525.0	500.0	500.0	1400.0	2950.0	950.0	1000.0	700.0	550.0	1400.0	1200.0	900.0
MN	2255.0	2170.0	2300.0	2500.0	2100.0	2500.0	2420.0	2050.0	2100.0	2055.0	2000.0	1820.0	2130.0	1790.0	300.0	210.0	250.0
PB	13.5	19.8	18.4	13.0	15.9	22.5	12.6	28.6	17.5	34.1	16.1	13.6	14.9	13.5	21.7	15.5	14.8
MO	.2	.3	.7	.?	.3	.?	.4	.3	.3	.0	.0	.1	.5	.0	1.1	.5	1.1
V	60.0	58.7	69.9	63.3	33.8	239.6	41.4	361.0	91.6	60.2	73.8	54.2	107.5	39.1	97.9	53.1	47.6
GA	9.3	11.1	10.3	8.0	8.0	0	5.9	0	17.4	9.1	10.5	12.6	11.4	4.7	18.6	15.3	15.4
SN	29.4	31.6	33.0	30.2	22.7	0	25.2	0	23.0	22.1	32.5	17.9	15.1	24.7	11.1	10.0	5.0
BE	2.3	2.1	.4	2.4	1.9	2.?	2.4	2.3	?	?	2.3	2.0	1.4	1.9	0	.6	.4
MG	5.3	8.5	6.3	6.0	7.3	2.7	6.2	16.3	9.1	10.2	7.1	6.9	3.9	9.7	.3	.4	.3
CA	1.3	1.5	1.5	1.3	1.4	4.3	.8	5.3	1.6	1.5	1.1	.6	.6	.6	.2	.3	.2
SR	53.1	63.4	43.0	33.8	57.6	380.9	27.2	1154.8	30.9	21.5	21.7	17.4	19.4	22.7	11.9	12.7	12.2
BA	201.7	196.1	133.9	113.4	141.2	108.2	95.7	280.0	118.5	174.5	67.8	69.4	113.8	74.1	239.7	258.7	227.2
K	.5	.9	.6	.7	.8	9.?	.4	5.4	.5	.3	.4	.4	.3	.3	1.9	2.0	1.8
LI	.2	.?	.2	.2	.2	8048.1	.2	5649.2	.2	6.9	.2	.7	5.0	.2	5.4	5.3	6.6
AL	4.4	3.9	4.4	3.6	2.9	.3	1.5	5.7	4.6	3.1	2.8	3.7	5.5	1.8	8.7	9.1	11.3
SC	17.7	20.4	13.8	12.8	16.7	.0	10.9	.0	17.2	12.5	13.7	13.7	13.1	10.1	7.2	4.7	3.5
SI	8.7	13.2	10.5	3.5	9.8	1.8	7.7	2.9	10.9	11.2	8.2	7.0	24.7	10.4	43.9	43.9	37.3
S	-	-	-	-	-	-	-	-	-	-	-	-	-	-	60.0	75.0	65.0
F	-	-	-	-	-	-	-	-	-	-	-	-	-	-	-	-	-
PH	-	-	-	-	-	-	-	-	-	-	-	-	-	-	4.6	4.9	-

	43504	43505	43506	43507	43508	43509	43510	43511	43512	43513	43514	43515	43516	43517	43518	43519	43520
M	70.0	80.0	90.0	100.0	110.0	120.0	130.0	140.0	150.0	200.0	250.0	300.0	350.0	400.0	450.0	500.0	550.0
NI	40.0	50.0	65.0	130.0	147.5	110.0	190.0	240.0	225.0	345.0	265.0	250.0	245.0	185.0	200.0	210.0	265.0
CU	20.0	25.0	25.0	27.0	20.0	26.0	43.0	45.0	46.0	41.0	54.0	63.0	73.0	72.0	69.0	72.0	92.0
CO	5.0	20.0	15.0	30.0	35.0	20.0	40.0	45.0	40.0	50.0	60.0	50.0	60.0	50.0	50.0	50.0	65.0
ZN	46.0	50.0	52.0	71.0	62.0	60.0	80.0	72.0	74.0	110.0	150.0	190.0	180.0	190.0	190.0	170.0	190.0
CR	45.0	65.0	75.0	120.0	165.0	130.0	190.0	220.0	275.0	320.0	190.0	235.0	150.0	200.0	140.0	305.0	185.0
FE	1.3	2.8	3.1	3.0	3.1	2.8	4.6	5.0	5.1	5.8	6.7	6.4	.6	6.8	6.2	6.0	.7
TI	1050.0	800.0	1100.0	900.0	1350.0	1400.0	1200.0	1150.0	1250.0	1150.0	1150.0	1150.0	900.0	1250.0	750.0	1500.0	1250.0
MN	190.0	220.0	300.0	370.0	425.0	390.0	490.0	500.0	580.0	600.0	800.0	670.0	830.0	500.0	470.0	650.0	1060.0
PB	13.3	20.8	17.6	16.2	15.8	10.3	16.7	12.2	10.8	19.3	33.1	22.4	44.3	47.3	44.9	46.3	37.0
MO	.3	1.5	.9	.7	1.0	.6	.8	.7	.6	.2	1.4	.7	1.5	1.5	.4	1.0	.0
V	54.1	68.4	80.1	90.0	81.5	99.3	118.2	113.2	125.8	172.3	175.2	264.6	316.0	342.7	315.9	215.8	221.4
GA	12.3	14.5	13.6	13.3	13.9	11.4	17.1	15.0	15.8	14.1	22.9	22.8	27.9	31.3	19.4	25.9	16.6
SN	5.3	4.2	7.0	7.9	8.1	5.3	9.2	3.1	2.4	5.4	4.6	1.8	8.4	9.0	7.2	6.2	2.4
BE	0	0	0	0	0	0	0	0	0	1.3	.3	0	0	0	0	0	0
MG	.3	.3	.6	1.3	1.6	.6	1.0	.8	.4	1.1	.5	.2	.3	.4	.5	.4	.4
CA	.1	.2	.3	.2	.3	.2	.5	.5	.2	.3	.4	.6	.8	.7	1.3	1.2	1.3
SR	9.5	12.2	20.8	9.1	12.9	16.0	27.4	24.6	10.9	9.8	26.7	26.2	43.4	35.8	77.0	138.4	69.3
BA	190.3	139.3	257.4	158.3	148.8	203.9	196.1	199.9	106.3	94.0	154.9	149.7	210.8	152.1	192.5	239.8	175.2
K	1.3	1.4	1.8	1.1	.9	.7	1.0	.?	.5	.4	.4	.6	.4	.4	.5	.4	.3
LI	6.0	5.2	3.9	7.4	8.6	7.5	11.1	16.3	19.1	19.2	26.7	39.7	53.9	38.3	27.9	23.3	16.5
AL	6.3	10.7	12.4	6.2	10.4	6.6	15.6	15.1	3.7	4.3	11.4	16.9	14.2	13.6	16.7	14.1	12.3
SC	2.7	5.2	7.3	4.0	5.8	4.9	12.1	10.0	6.9	6.8	12.1	11.0	16.5	17.5	12.4	22.9	11.1
SI	33.5	32.6	34.3	37.2	37.5	38.6	37.1	26.6	29.0	31.0	35.2	32.3	39.4	41.5	35.4	34.8	25.3
S	70.0	95.0	60.0	110.0	70.0	80.0	75.0	60.0	70.0	175.0	115.0	165.0	125.0	55.0	185.0	150.0	170.0
F	-	-	-	-	-	-	-	-	-	-	-	-	-	-	-	-	-
PH	-	-	-	4.7	-	-	-	-	4.7	5.0	5.2	5.7	5.4	4.9	5.4	5.2	5.8

SOIL TRAVERSE LINES

	24501	24502	24503	24504	24505	24506	24507	24508	24509	24510	24511	24512	24513	24514	24515	24516	24517
M	0	50.0	100.0	150.0	200.0	210.0	220.0	231.5	241.0	250.0	260.0	270.0	280.0	290.0	300.0	310.0	320.0
NI	160.0	435.0	1450.0	2050.0	2500.0	2800.0	3000.0	2700.0	2500.0	3000.0	3000.0	2750.0	2800.0	2500.0	2350.0	2000.0	2250.0
CU	59.0	54.0	72.0	77.0	65.0	79.0	70.0	71.0	67.0	72.0	71.0	64.0	66.0	62.0	64.0	64.0	61.0
CO	45.0	50.0	165.0	160.0	140.0	165.0	160.0	160.0	145.0	155.0	155.0	150.0	145.0	170.0	155.0	155.0	150.0
ZN	16.0	40.0	80.0	110.0	98.0	96.0	94.0	98.0	83.0	88.0	100.0	87.0	85.0	86.0	8.0	90.0	74.0
CR	430.0	1700.0	3600.0	4350.0	4000.0	3750.0	3850.0	3900.0	3400.0	3900.0	3650.0	3700.0	3400.0	3250.0	3200.0	3200.0	3050.0
FE	5.3	6.4	10.5	13.5	14.0	16.5	15.0	15.0	14.5	16.0	16.5	15.5	14.0	15.0	14.5	13.5	14.0
TI	1400.0	1350.0	1750.0	1750.0	1750.0	1900.0	1750.0	1800.0	1650.0	2000.0	2000.0	2000.0	1650.0	2000.0	1900.0	1800.0	2300.0
MN	570.0	640.0	810.0	1100.0	1000.0	1150.0	1140.0	1060.0	1180.0	1150.0	1180.0	1180.0	1060.0	1170.0	1150.0	1230.0	1110.0
PB	9.1	9.0	9.1	10.9	13.0	11.1	15.0	7.6	10.8	7.1	11.6	9.1	5.7	3.9	58.6	11.8	12.1
MO	2.0	.9	.1	.6	1.4	1.4	1.6	.4	1.0	.2	1.0	1.4	.7	.0	.0	1.2	1.2
V	223.4	133.3	135.5	201.8	222.6	191.1	248.1	198.5	237.9	192.7	252.4	200.4	131.6	205.3	635.9	228.2	275.2
GA	20.7	16.5	22.1	27.2	33.0	34.2	37.8	22.4	29.6	20.0	32.8	25.3	21.9	19.4	0	33.9	33.9
SN	12.2	11.0	9.3	11.0	15.9	6.1	13.7	9.8	8.8	7.9	11.2	6.8	.6	1.5	0	8.5	16.4
BE	0	0	0	0	.4	2.5	.2	3.1	1.8	2.2	1.1	1.6	2.6	1.5	1.8	0	0
MG	.4	1.3	.8	.7	.6	.5	.9	.6	.5	.6	.6	.5	.5	.4	20.4	.6	1.0
CA	.4	.6	.4	.5	.5	.4	.6	.5	.4	.5	.5	.4	.3	.3	5.8	.5	.7
SR	22.7	38.3	14.8	15.2	15.5	10.4	16.5	15.2	10.2	13.2	13.5	13.7	13.0	7.0	2020.8	16.2	23.8
BA	110.8	179.4	83.6	79.0	87.2	58.4	103.1	97.0	73.3	105.2	75.4	94.6	97.4	67.6	555.8	92.2	120.1
K	.5	.7	.7	.8	.7	.7	.9	.7	.6	.7	.8	.6	.6	.6	6.1	.8	.9
LI	13.1	17.2	28.8	31.7	34.6	42.5	38.0	32.1	39.7	29.3	36.8	35.5	33.5	30.3	439.3	36.1	42.0
AL	9.5	15.9	11.5	16.6	14.8	14.6	19.7	16.7	15.5	16.4	17.0	14.9	16.8	12.4	5.8	17.2	22.4
SC	11.7	14.7	14.5	20.4	25.2	21.5	27.8	22.2	20.3	28.7	24.3	25.0	23.3	15.3	.0	27.5	36.3
SI	37.7	38.0	23.1	29.0	34.7	19.8	33.7	22.3	25.0	19.7	25.7	20.9	14.5	17.4	2.4	25.6	34.5
S	135.0	155.0	170.0	260.0	185.0	170.0	240.0	240.0	335.0	360.0	130.0	430.0	225.0	260.0	225.0	150.0	190.0
F	447.0	352.0	390.0	285.0	285.0	285.0	285.0	285.0	229.0	119.0	143.0	190.0	204.0	247.0	352.0	285.0	243.0
PH	4.7	4.7	4.7	4.2	4.9	4.3	4.6	4.6	4.8	4.6	4.8	4.6	4.8	4.8	4.7	4.8	4.8

	24518	24519	24520	24521	24522	24523	24524	24525	34501	34505	34509	34513	34517	34521	34525	34526	34527
M	330.0	340.0	350.0	400.0	450.0	500.0	550.0	600.0	0	60.0	120.0	180.0	240.0	300.0	360.0	375.0	390.0
NI	2300.0	2200.0	2100.0	1150.0	330.0	157.5	125.0	115.0	4300.0	5500.0	3500.0	5400.0	6000.0	5500.0	5000.0	6000.0	6000.0
CU	63.0	67.5	66.5	49.0	37.0	33.0	32.0	36.0	8.0	24.0	70.0	21.5	20.0	18.0	15.0	15.0	18.0
CO	145.0	155.0	170.0	120.0	35.0	67.5	75.0	60.0	300.0	410.0	225.0	422.5	380.0	430.0	380.0	375.0	375.0
ZN	75.0	75.0	77.5	60.0	37.0	33.0	37.0	30.0	150.0	240.0	160.0	215.0	132.0	150.0	240.0	132.0	160.0
CR	3300.0	3155.0	2850.0	2000.0	900.0	250.0	115.0	100.0	13000.0	17300.0	9000.0	13750.0	7000.0	10000.0	19500.0	8000.0	12500.0
FE	14.0	13.8	14.3	11.0	7.7	8.1	10.5	11.0	15.0	18.5	13.0	23.8	23.5	21.5	17.5	17.5	19.0
TI	1750.0	1825.0	1850.0	1900.0	1750.0	2175.0	1650.0	2000.0	400.0	950.0	1800.0	900.0	600.0	600.0	550.0	450.0	700.0
MN	1060.0	1055.0	1100.0	940.0	690.0	935.0	900.0	1000.0	2000.0	2600.0	1640.0	2900.0	2400.0	2900.0	2200.0	2000.0	2250.0
PB	7.5	13.9	12.2	75.8	7.3	6.3	8.2	5.7	11.3	3.5	27.4	13.0	12.2	11.9	10.6	11.1	8.7
MO	.5	1.7	1.8	.0	.5	.3	1.0	.5	.2	.0	1.0	.3	.0	.0	.0	.0	.0
V	240.0	301.0	251.2	391.2	326.7	363.3	491.8	413.7	51.8	230.2	125.0	54.1	42.0	43.0	63.2	32.8	48.4
GA	28.2	39.0	31.2	0	22.4	19.0	37.9	37.1	6.9	21.0	31.0	6.8	3.6	4.5	7.2	3.8	4.9
SN	6.2	11.1	6.8	0	9.3	8.6	9.7	6.6	30.2	6.1	11.5	12.7	18.4	10.1	17.8	19.3	11.4
BE	0	0	0	2.0	0	0	0	0	0.9	.2	2.6	2.0	2.2	1.7	2.7	1.9	2.5
MG	.5	.5	.7	36.9	.5	.4	.4	.3	7.0	1.7	2.6	4.3	6.1	6.0	4.8	6.0	4.5
CA	.5	.5	.6	6.8	.6	.5	.8	.9	.6	.3	1.7	.9	.8	.8	.9	.8	.9
SR	12.7	12.4	17.7	1644.7	20.1	36.3	34.2	37.1	19.2	16.0	59.4	55.4	25.0	25.7	33.4	24.5	24.8
BA	72.7	85.5	101.9	178.1	79.2	233.2	72.1	82.1	52.1	249.5	134.2	143.6	87.1	91.3	102.0	77.5	97.0
K	.7	.8	.8	6.8	.6	.6	.6	.5	.3	2.9	1.8	.7	.4	.4	.5	.3	.5
LI	37.4	43.3	40.7	7357.8	25.5	22.2	40.4	43.0	.2	17.6	25.6	.2	.2	.2	.2	.2	.2
AL	17.7	16.8	22.5	5.4	9.3	10.0	17.0	15.2	.8	9.1	11.4	2.4	1.2	2.4	1.9	1.0	1.7
SC	23.5	24.0	24.8	.0	16.1	21.7	31.3	32.0	8.1	7.3	11.0	10.6	11.1	9.4	10.0	10.2	8.5
SI	23.0	31.9	27.6	2.3	33.5	26.7	31.0	28.7	12.2	23.1	21.5	9.6	6.9	7.2	8.2	11.8	7.0
S	240.0	185.0	200.0	165.0	170.0	240.0	180.0	150.0	-	-	-	-	-	-	-	-	-
F	247.0	247.0	323.0	266.0	150.0	113.0	323.0	228.0	-	-	-	-	-	-	-	-	-
PH	4.3	4.3	4.9	5.4	5.2	4.9	5.0	5.5	-	-	-	-	-	-	-	-	-

	53505	53507	53508	53509	53510	53511	53512	53513	53514	53515	53516	53517	53518	53519	53520	53521	53522
M	90.0	100.0	110.0	120.0	130.0	140.0	150.0	160.0	170.0	180.0	190.0	200.0	250.0	300.0	350.0	400.0	450.0
NI	1000.0	1400.0	1600.0	1700.0	2150.0	2350.0	2500.0	3350.0	2800.0	2700.0	2575.0	2500.0	2700.0	2600.0	1900.0	1700.0	2100.0
CU	88.0	98.0	92.0	125.0	102.0	62.0	66.0	57.0	60.0	57.0	93.5	96.0	227.0	289.0	323.0	460.0	340.0
CO	75.0	100.0	127.0	125.0	15.0	140.0	163.0	161.0	155.0	160.0	150.0	155.0	200.0	185.0	190.0	145.0	180.0
ZN	48.0	57.0	49.0	59.0	43.5	41.0	20.0	83.0	52.0	65.0	66.0	66.0	154.0	220.0	150.0	122.0	127.0
CR	2350.0	2750.0	2800.0	2750.0	2925.0	2350.0	2200.0	1530.0	1501.0	1500.0	2400.0	3100.0	3950.0	6500.0	5000.0	4000.0	4000.0
FE	17.0	20.0	20.5	19.5	16.0	18.0	17.5	16.0	15.0	15.5	19.5	20.0	21.5	24.0	17.5	16.5	18.0
TI	1050.0	1050.0	850.0	1150.0	875.0	750.0	850.0	750.0	750.0	750.0	975.0	125.0	191.0	2250.0	2400.0	3400.0	2850.0
MN	800.0	750.0	700.0	870.0	670.0	530.0	600.0	690.0	620.0	600.0	725.0	910.0	1460.0	1490.0	1500.0	1320.0	1410.0
PB	11.7	19.0	13.2	15.8	14.2	14.2	11.9	16.2	10.8	12.3	11.6	13.7	17.3	10.4	10.4	15.4	10.6
MO	.2	21.9	.8	.9	.1	.7	.0	.4	.0	.1	.4	.6	.2	.3	.0	.6	.0
V	196.3	419.0	134.2	135.2	101.7	103.0	104.7	85.3	71.8	76.4	96.7	119.9	66.0	129.8	146.7	194.6	191.8
GA	13.3	25.4	13.1	14.1	10.1	11.7	11.9	10.2	3.9	3.7	11.2	11.8	12.2	13.8	13.4	22.2	14.7
SN	11.1	0	9.6	10.1	13.3	15.7	12.3	15.9	8.3	7.0	9.3	14.4	20.4	9.4	4.3	5.8	9.5
BE	0	24.1	0	0	0	0	.1	.1	.3	.9	.2	0	1.0	0	0	0	0
MG	4.4	3.2	4.9	5.5	7.1	7.8	6.3	8.3	5.5	0.8	5.7	7.1	6.1	5.3	4.1	3.4	4.1
CA	2.0	2.0	1.8	2.0	2.8	3.0	3.3	3.1	2.2	1.7	2.3	2.5	1.2	2.5	2.4	2.7	2.5
SR	31.3	.9	24.4	22.6	21.9	21.0	19.8	33.9	24.4	22.4	24.3	25.9	30.6	65.4	73.9	121.0	70.7
BA	135.7	101.9	135.3	132.6	34.5	67.4	148.7	59.7	56.4	49.0	53.0	69.5	117.2	120.0	138.6	205.5	132.4
K	1.1	1.2	.7	.9	.6	.4	.4	.3	.3	.3	.3	.3	1.1	.5	.4	.6	.5
LI	56.3	.2	28.1	27.6	7.7	2.5	.2	.2	1.6	.2	.2	.2	6.0	14.1	17.9	35.5	19.6
AL	4.5	4.5	5.1	6.5	5.1	3.4	3.5	3.7	3.9	3.4	4.3	4.3	5.1	7.5	6.0	9.2	6.5
SC	10.3	34.8	10.3	9.6	9.9	13.8	13.7	13.0	8.1	8.7	12.6	13.4	6.6	14.9	12.7	17.7	15.8
SI	21.2	34.2	13.1	13.4	12.7	11.8	9.3	9.9	7.6	7.1	7.9	10.0	11.9	11.4	12.5	16.2	13.2
S	135.0	140.0	80.0	95.0	70.0	55.0	60.0	60.0	80.0	130.0	70.0	60.0	65.0	115.0	130.0	90.0	110.0
F	-	-	-	-	-	-	-	-	-	-	-	-	-	-	-	-	-
PH	6.4	6.1	6.0	5.8	5.8	6.1	5.9	6.0	5.4	6.1	5.7	6.2	6.2	6.4	6.2	5.9	6.2

	53523	53524	53525	53526	53527	53528	53529	53530	53531	53532	53533	53534	53535	53536	53537	53538	53539
M	500.0	550.0	600.0	650.0	700.0	750.0	760.0	770.0	780.0	790.0	800.0	810.0	820.0	830.0	840.0	850.0	900.0
NI	1800.0	1500.0	1100.0	1575.0	1700.0	1300.0	850.0	600.0	600.0	650.0	465.0	375.0	320.0	220.0	190.0	165.0	100.0
CU	410.0	450.0	330.0	435.0	340.0	154.0	118.0	104.0	109.0	121.0	110.0	102.0	100.0	90.0	92.0	115.5	70.0
CO	155.0	140.0	120.0	145.0	155.0	110.0	80.0	75.0	70.0	80.0	60.0	50.0	55.0	50.0	50.0	42.5	30.0
ZN	125.0	112.0	95.0	143.0	121.0	32.0	87.0	74.0	82.0	79.0	75.0	69.0	70.0	63.0	63.0	71.0	58.0
CR	3650.0	3000.0	2250.0	2800.0	2300.0	1630.0	1150.0	900.0	1000.0	950.0	700.0	650.0	440.0	270.0	210.0	160.0	115.0
FE	16.5	16.0	13.5	18.0	16.5	1.5	10.5	9.8	9.8	10.0	9.0	7.8	7.7	7.3	7.0	6.9	5.4
TI	3300.0	3300.0	3000.0	2900.0	1900.0	1900.0	2000.0	1900.0	1900.0	2000.0	2000.0	1900.0	1900.0	2200.0	2000.0	1700.0	1800.0
MN	1300.0	1350.0	1140.0	1345.0	1220.0	1150.0	910.0	930.0	860.0	830.0	725.0	720.0	900.0	860.0	690.0	810.0	430.0
PB	11.9	11.2	15.2	20.8	25.3	16.1	18.4	15.1	12.4	11.5	19.6	10.6	11.6	16.8	11.9	34.0	11.9
MO	.0	.3	1.1	.0	.5	.5	1.1	.5	.5	.0	.6	.4	.6	1.0	.8	.0	.9
V	223.3	216.4	194.4	534.1	202.0	159.4	197.3	186.7	161.6	695.1	211.6	267.0	241.2	251.3	221.8	569.6	151.8
GA	16.3	18.7	25.9	0	21.3	21.3	25.3	14.7	18.9	0	19.6	18.2	21.8	25.7	25.0	0	20.5
SN	8.4	8.0	6.6	0	15.5	6.1	11.5	12.7	7.6	0	19.5	6.8	8.0	19.4	10.0	0	8.2
BE	0	0	0	0	0	0	0	0	0	2.0	0	0	0	0	0	0	0
MG	3.3	4.0	3.3	1.7	4.7	3.0	2.6	2.5	2.3	21.9	2.4	1.6	1.2	2.3	1.0	27.7	1.0
CA	2.1	2.7	1.8	3.3	1.4	.9	.9	1.3	1.1	4.6	1.5	.9	.9	1.1	.7	4.3	.7
SR	82.3	109.3	94.2	114.1	49.3	24.6	31.2	35.6	33.2	757.3	35.5	20.6	25.9	28.8	22.3	1752.4	29.1
BA	141.3	217.5	216.6	191.6	173.4	149.7	170.6	206.8	139.1	194.5	156.2	104.7	115.1	174.4	128.0	384.5	228.6
K	.5	.8	1.0	6.9	.8	1.2	1.6	1.5	1.3	4.0	1.6	1.4	1.4	2.1	2.1	3.5	2.5
LI	26.1	49.7	78.6	5790.9	707.9	42.5	45.5	33.1	43.0	5543.5	50.5	45.3	56.9	60.6	60.5	6290.2	48.0
AL	6.3	11.5	14.6	0	7.2	9.4	10.4	9.4	10.3	6.4	9.5	9.9	7.2	13.8	10.7	6.9	16.6
SC	14.2	17.5	14.9	.0	16.4	11.8	13.3	11.5	6.7	.0	11.9	6.5	6.6	12.1	11.2	.0	9.6
SI	15.4	20.8	25.2	1.6	23.9	22.1	31.4	34.5	27.4	2.6	33.1	27.4	24.8	43.7	31.5	2.8	29.0
S	65.0	95.0	35.0	95.0	55.0	70.0	70.0	70.0	80.0	75.0	110.0	95.0	85.0	90.0	95.0	130.0	105.0
F	-	-	-	-	-	-	-	-	-	-	-	-	-	-	-	-	-
PH	6.1	6.1	5.7	5.9	6.0	5.8	-	-	-	-	6.0	-	-	-	-	5.8	5.4

SOIL TRAVERSE LINES

	43521	43522	43523	43524	43525	43526	43527	43528	43529	43530	43531	43532	43533	43534	43535	43536	43537
M	600.0	650.0	660.0	670.0	680.0	690.0	700.0	710.0	720.0	730.0	740.0	750.0	800.0	850.0	900.0	950.0	1000.0
NI	600.0	700.0	900.0	800.0	950.0	1150.0	1250.0	1250.0	1200.0	1150.0	800.0	760.0	460.0	550.0	475.0	425.0	360.0
CU	100.0	109.0	119.0	132.0	148.0	144.0	160.0	155.0	112.0	126.0	109.0	117.0	100.0	104.0	104.5	95.0	68.0
CO	70.0	70.0	90.0	70.0	100.0	85.0	35.0	97.5	80.0	85.0	70.0	84.0	74.0	90.0	70.0	70.0	60.0
ZN	160.0	210.0	360.0	230.0	190.0	200.0	191.0	190.0	180.0	190.0	166.0	200.0	200.0	260.0	300.0	220.0	200.0
CR	500.0	850.0	1050.0	950.0	1400.0	1300.0	1550.0	1225.0	1450.0	530.0	900.0	900.0	440.0	525.0	510.0	700.0	750.0
FE	8.3	8.3	9.6	.9	10.5	9.4	9.8	1.5	11.0	9.5	8.9	9.1	6.6	8.2	9.5	7.8	8.1
TI	1600.0	1450.0	1500.0	1200.0	1350.0	1350.0	1300.0	1125.0	1500.0	950.0	1500.0	1550.0	1550.0	1450.0	1375.0	1300.0	1700.0
MN	540.0	800.0	700.0	720.0	800.0	620.0	640.0	740.0	660.0	750.0	690.0	630.0	780.0	1500.0	835.0	670.0	870.0
PB	28.4	34.2	43.2	23.6	34.0	24.5	49.1	42.3	44.9	39.1	35.0	47.0	39.0	65.4	34.3	46.3	49.0
MO	1.5	1.3	1.4	.0	.5	.6	1.4	.9	.4	.3	..	.9	.5	.3	.2	.7	12.7
V	260.5	314.7	258.8	500.2	255.8	345.1	270.4	235.7	297.8	265.0	249.0	235.0	217.0	291.5	202.5	286.7	437.7
GA	27.4	29.5	27.5	0	20.2	0	26.9	27.1	30.5	30.8	24.1	30.1	24.2	22.4	17.8	31.7	37.7
SN	4.1	13.9	1.7	0	0	0	10.4	5.2	10.8	2.3	4.6	5.9	3.8	13.5	2.7	6.6	0
BE	0	0	0	2.0	0	2.0	0	.0	0	0	0	0	0	0	.1	0	9.4
MG	.9	1.2	1.1	28.6	.6	26.4	1.8	1.2	1.6	.9	.9	1.0	.6	1.2	.6	1.0	.5
CA	.5	.9	6.0	6.0	.5	7.2	1.2	.6	.9	.6	.7	.7	.7	1.1	.8	.7	0
SR	23.1	51.2	67.6	1267.8	41.4	1154.3	151.2	86.9	63.4	59.8	52.8	63.4	58.2	64.3	140.1	75.0	37.9
BA	95.7	151.0	138.1	585.7	114.9	890.3	256.4	168.1	166.6	111.7	131.6	168.1	213.7	188.2	305.4	220.4	342.0
K	.3	.5	.4	5.5	.2	6.3	.4	.3	.4	.3	.4	.5	.3	.3	.4	.6	.9
LI	36.0	32.3	38.3	3678.0	39.3	1265.1	42.5	41.9	43.3	47.7	34.4	17.8	25.5	37.3	28.7	48.3	.2
AL	15.2	15.7	22.6	7.3	14.3	7.1	20.9	17.4	18.0	15.4	14.3	21.1	15.5	12.9	14.1	18.4	14.9
SC	12.2	23.5	18.4	.0	11.9	.0	30.9	27.2	24.2	16.9	14.2	20.6	17.4	13.5	18.6	19.5	39.3
SI	31.6	43.9	27.8	2.5	17.3	2.5	32.1	25.8	33.0	25.0	31.2	30.4	27.8	32.5	24.1	34.4	43.9
S	60.0	110.0	75.0	130.0	90.0	65.0	105.0	90.0	80.0	95.0	110.0	110.0	150.0	100.0	85.0	30.0	120.0
F	-	-	-	-	-	-	-	-	-	-	-	-	-	-	-	-	-
PH	4.3	5.0	5.0	4.9	5.1	4.9	5.2	5.3	5.1	5.2	5.4	5.6	5.3	5.7	5.6	5.1	5.5

	43538	43539	43540	43541	43542	43543	43544	43545	43546	43547	43548	43549	53501	53502	53503	53504	53505
M	1050.0	1100.0	1150.0	1200.0	1250.0	1300.0	1350.0	1400.0	1450.0	1500.0	1550.0	1600.0	0	50.0	60.0	70.0	80.0
NI	320.0	260.0	285.0	370.0	275.0	270.0	210.0	195.0	140.0	125.0	110.0	85.0	220.0	300.0	295.0	390.0	650.0
CU	84.0	78.0	76.0	96.0	85.0	107.0	102.0	100.0	62.0	59.0	61.0	60.0	115.0	100.0	96.0	82.0	76.0
CO	55.0	60.0	45.0	50.0	50.0	8.0	75.0	75.0	55.0	55.0	60.0	45.0	40.0	40.0	50.0	45.0	60.0
ZN	260.0	230.0	290.0	330.0	310.0	360.0	320.0	280.0	180.0	190.0	150.0	117.0	43.0	37.0	43.0	40.0	54.0
CR	375.0	305.0	280.0	225.0	225.0	245.0	295.0	100.0	140.0	115.0	95.0	65.0	445.0	700.0	850.0	1100.0	2000.0
FE	7.4	5.7	5.4	6.6	5.8	7.7	10.1	8.3	5.3	4.7	5.0	4.1	11.0	9.4	9.5	11.0	16.5
TI	700.0	1250.0	1200.0	1150.0	1200.0	1100.0	1150.0	1450.0	1350.0	1150.0	1250.0	1750.0	1050.0	1100.0	1250.0	1000.0	1150.0
MN	660.0	940.0	690.0	430.0	580.0	750.0	960.0	890.0	680.0	730.0	780.0	690.0	1640.0	900.0	900.0	770.0	780.0
PB	29.8	91.0	62.3	32.8	60.4	59.0	47.2	43.8	24.6	30.8	20.7	22.9	13.9	14.7	17.9	12.2	13.2
MO	.4	1.0	2.0	.8	1.7	1.5	.8	1.5	1.1	.7	.6	1.3	.8	1.0	.8	.4	.8
V	238.3	223.6	225.7	149.2	215.9	203.6	213.3	233.7	157.9	196.4	151.5	145.9	287.6	245.5	264.8	231.3	192.3
GA	21.5	29.9	27.7	28.5	36.2	36.8	23.9	29.4	24.7	27.7	22.4	23.4	17.8	18.3	15.7	14.4	14.1
SN	4.0	11.7	6.4	4.4	9.9	5.9	1.9	33.7	4.9	11.0	9.8	11.6	10.0	10.1	18.4	11.8	10.1
BE	0	0	0	1.3	0	0	0	0	0	0	0	0	0	0	0	0	0
MG	.5	.7	.4	.4	.3	.4	.3	.3	.2	.3	.3	.3	1.9	1.8	4.5	3.6	3.4
CA	.7	1.2	.7	.4	.5	.4	.4	.4	.3	.4	.4	.5	.8	.8	1.1	1.6	1.5
SR	53.3	101.0	39.6	35.1	23.6	14.4	13.4	14.6	7.0	12.2	16.2	15.6	43.4	34.9	27.4	30.1	41.4
BA	197.5	426.8	214.2	215.9	152.8	170.2	144.4	176.1	131.1	168.0	247.5	234.2	504.5	148.6	148.4	112.7	151.5
K	.5	.5	.5	.6	.7	.5	.5	.6	.5	.7	1.0	1.0	1.4	1.6	1.5	1.2	1.1
LI	33.0	40.0	44.5	61.0	64.3	53.1	31.7	35.8	26.7	20.3	23.1	23.4	112.4	88.6	91.0	98.6	75.3
AL	19.2	19.4	17.0	17.0	17.8	22.0	18.3	17.0	13.0	13.7	13.8	19.8	10.1	7.1	6.1	4.4	4.7
SC	15.5	22.1	13.3	14.7	17.6	17.9	14.3	15.3	8.2	12.1	10.7	10.2	11.4	11.4	8.4	7.5	8.6
SI	32.5	38.7	40.3	24.9	35.2	34.8	22.3	30.9	33.8	43.9	36.2	40.9	24.5	28.9	39.5	27.0	20.1
S	155.0	100.0	125.0	95.0	130.0	95.0	90.0	55.0	85.0	100.0	95.0	115.0	150.0	440.0	123.0	225.0	205.0
F	-	-	-	-	-	-	-	-	-	-	-	-	-	-	-	-	-
PH	5.3	5.5	5.2	4.9	4.8	4.6	5.0	5.2	4.7	4.7	4.6	5.1	6.1	5.5	6.4	6.6	6.2

	63501	63502	63503	63504	63505	63506	63507	63508	63509	63510	63511	63512	63513	63514	63515	63516	63517
M	0	50.0	100.0	150.0	200.0	250.0	260.0	270.0	280.0	290.0	300.0	310.0	320.0	330.0	340.0	350.0	360.0
NI	25.0	45.0	82.5	450.0	500.0	725.0	700.0	700.0	900.0	500.0	1500.0	1000.0	1000.0	1100.0	850.0	1050.0	1050.0
CU	6.0	10.0	26.5	80.0	67.0	61.0	64.0	66.0	66.0	28.0	69.0	47.0	68.0	68.0	64.0	67.0	61.0
CO	15.0	35.0	20.0	65.0	40.0	55.0	90.0	8.0	80.0	7.0	450.0	12.0	11.0	11.0	95.0	100.0	100.0
ZN	24.0	24.0	29.0	53.0	52.0	69.5	55.0	64.0	79.0	3.0	45.0	59.0	77.0	75.0	85.0	80.0	74.0
CR	30.0	50.0	600.0	900.0	1200.0	1500.0	1750.0	1200.0	1750.0	1550.0	3700.0	1950.0	2000.0	1650.0	1900.0	1700.0	2200.0
FE	.9	1.3	2.8	8.0	8.9	9.1	9.5	9.0	9.5	0.0	13.5	11.0	12.5	12.5	11.0	12.0	13.0
TI	1350.0	1250.0	1550.0	1450.0	1725.0	1950.0	1500.0	2200.0	1650.0	1200.0	1250.0	1500.0	2000.0	2200.0	2600.0	2100.0	2200.0
MN	300.0	370.0	95.0	73.0	265.0	51.0	970.0	740.0	1070.0	820.0	6100.0	1240.0	1100.0	1130.0	1030.0	920.0	840.0
PB	44.5	55.2	29.0	22.3	34.9	14.9	17.7	19.0	23.5	16.7	59.5	11.0	21.3	13.6	13.9	13.4	20.1
MO	1.3	1.4	.9	1.3	.0	1.1	.7	.9	.9	.9	1.1	.0	1.6	.4	.7	1.5	.0
V	62.2	80.7	134.6	133.3	517.8	189.0	188.8	186.9	119.9	165.9	253.0	136.5	194.2	146.4	182.7	183.1	625.7
GA	16.5	18.5	17.7	31.8		19.6	17.6	22.4	23.7	14.1	19.1	12.3	22.5	19.1	18.2	17.6	0
SN	8.3	8.3	4.9	2.0	0	7.5	9.6	9.7	9.4	16.0	16.3	2.0	9.2	0	1.1	1.7	0
BE	0	0	0	.7	1.1	0	.6	0	.8	0	.3	.5	1.7	.4	0	0	2.0
MG	.3	.4	1.2	.8	12.9	3.3	3.4	4.1	4.0	6.3	5.5	4.3	2.6	1.9	2.2	2.1	9.0
CA	.4	.4	.2	.3	5.1	.6	.6	.6	.7	.8	.8	.4	.6	.4	.5	.5	5.6
SR	68.0	56.4	25.9	15.2	1930.1	16.6	28.3	21.2	41.4	15.4	22.7	10.1	37.8	12.6	13.8	14.4	1336.6
PA	427.3	385.9	167.1	132.2	310.7	123.8	160.6	150.2	276.3	80.0	313.9	87.6	192.6	105.2	117.2	107.7	271.6
K	3.4	3.3	2.0	.6	3.6	.7	.5	.8	.6	.5	.7	.6	.7	.7	.8	.8	6.3
LI	7.5	6.1	15.3	40.6	1893.9	21.6	22.0	20.9	22.0	15.5	39.6	9.0	19.0	19.8	15.7	14.7	5205.9
AL	10.4	8.4	7.2	17.7	5.1	10.8	13.1	10.0	12.7	5.1	8.6	7.1	17.0	15.1	13.0	15.6	3.9
SC	4.3	4.8	5.0	16.4	.0	17.5	23.8	21.4	32.9	12.8	22.4	11.6	44.7	20.5	18.8	20.0	.0
SI	40.1	39.0	29.3	24.5	2.2	29.8	23.9	29.0	24.4	26.5	18.8	15.7	25.8	18.5	22.9	22.5	1.9
S	30.0	55.0	20.0	40.0	45.0	75.0	85.0	100.0	90.0	60.0	65.0	70.0	55.0	30.0	45.0	60.0	40.0
F	-	-	-	-	-	-	-	-	-	-	-	-	-	-	-	-	-
PH	4.3	4.6	4.3	4.7	5.3	5.3	5.5	5.4	5.2	5.8	5.7	5.6	5.4	5.4	5.4	5.4	5.4

	63518	63519	63520	63521	63522	63523	63524	63525	63526	63527	63528	63529	63530	63531	63532	63533	63534
M	370.0	380.0	390.0	400.0	410.0	420.0	430.0	440.0	450.0	500.0	550.0	600.0	650.0	700.0	750.0	800.0	850.0
NI	1000.0	1000.0	850.0	830.0	650.0	500.0	500.0	550.0	500.0	550.0	650.0	550.0	650.0	600.0	600.0	500.0	275.0
CU	66.0	66.0	56.0	54.0	59.0	42.0	40.0	43.0	38.0	39.0	50.0	52.0	60.0	65.0	120.0	42.0	105.0
CO	100.0	90.0	85.0	110.0	85.0	90.0	80.0	80.0	60.0	125.0	80.0	85.0	65.0	85.0	85.0	85.0	35.0
ZN	81.0	83.0	91.0	73.0	63.0	46.0	55.0	58.0	59.0	59.0	74.0	62.0	71.0	73.0	53.0	52.0	37.0
CR	1850.0	1850.0	1750.0	1900.0	1600.0	1250.0	1150.0	1350.0	1150.0	1100.0	1500.0	1600.0	1700.0	1250.0	1250.0	1250.0	850.0
FE	12.5	12.5	10.5	10.5	8.6	6.5	6.7	7.3	6.9	6.0	10.0	8.8	9.3	9.4	6.1	6.8	6.3
TI	2200.0	2200.0	1900.0	1800.0	1800.0	1400.0	1600.0	1500.0	1550.0	1500.0	1750.0	1500.0	1650.0	1500.0	1450.0	1400.0	1400.0
MN	1010.0	940.0	1210.0	1180.0	850.0	970.0	830.0	940.0	690.0	1760.0	880.0	850.0	990.0	1.6.0	940.0	95.0	240.0
PB	18.9	12.0	19.3	17.9	12.6	.7	14.8	24.7	16.0	19.4	11.6	13.0	16.2	23.9	51.4	10.2	18.6
MO	.3	.3	.9	.7	.3	.0	1.0	.7	3.6	.8	.5	.7	.0	1.1	.9	.4	1.4
V	218.3	138.4	153.9	178.5	150.9	.3	138.8	139.0	113.9	142.5	161.1	155.5	140.4	166.9	212.4	136.2	194.8
GA	20.0	13.8	19.0	16.8	13.7	0	13.4	14.8	18.9	14.7	16.1	14.9	14.4	19.3	22.8	13.1	15.7
SN	5.1	.2	7.7	3.5	.6	0	5.6	14.2	0	13.4	.0	8.6	5.4	12.7	4.4	2.2	6.9
BE	.4	.3	.2	0	.1	2.0	0	.0	4.9	0	.9	1.4	.6	0	0	0	0
MG	1.8	2.3	3.0	3.7	3.2	9.9	3.9	4.7	3.1	4.9	2.3	3.9	2.9	3.6	.6	2.3	1.5
CA	.5	.5	.6	.6	.5	5.2	.6	.8	0	.9	.4	.7	.7	.7	1.6	.4	.6
SR	17.3	17.4	34.9	16.8	14.2	157.1	16.1	28.2	.8	31.5	19.7	26.9	35.1	25.3	87.6	12.8	17.5
BA	121.2	125.6	223.6	163.4	143.7	25.1	113.5	174.4	123.1	207.4	97.4	150.8	306.7	176.3	208.7	122.8	81.8
K	.3	.6	.9	.8	.6	7.7	.7	.8	.7	.8	.6	.6	.7	.9	.4	.4	.4
LI	14.5	13.2	15.6	16.1	19.6	1265.0	18.0	19.1	33.9	20.3	26.0	30.9	21.5	19.7	21.9	16.7	13.0
AL	11.2	13.8	11.9	10.4	6.8	3.7	8.2	8.4	7.7	7.2	7.7	9.1	7.7	8.9	15.4	11.0	13.0
SC	24.0	22.3	26.8	16.5	12.5	..	12.1	15.4	21.6	17.6	14.9	20.9	18.1	26.8	14.4	14.5	15.8
SI	24.2	19.3	25.2	24.2	18.9	2.0	28.1	31.3	43.9	33.0	19.7	23.4	25.5	31.6	30.1	27.2	35.7
S	15.0	65.0	100.0	90.0	75.0	70.0	75.0	70.0	65.0	90.0	40.0	40.0	30.0	85.0	40.0	100.0	25.0
F	-	-	-	-	-	-	-	-	-	-	-	-	-	-	-	-	-
PH	5.4	5.4	5.5	5.5	-	-	-	-	-	5.1	5.2	5.2	5.3	5.3	5.4	5.1	5.1

	63535	63536	63537	63538	63539	63540	63541	63542	63543	83501	83502	83503	83504	83505	83506	83507	83508
M	900.0	950.0	1000.0	1050.0	1100.0	1150.0	1200.0	1250.0	1300.0	0	50.0	100.0	150.0	200.0	210.0	220.0	230.0
NI	300.0	275.0	130.0	110.0	200.0	262.5	300.0	350.0	235.0	950.0	1050.0	1200.0	1800.0	2450.0	4450.0	4500.0	6000.0
CU	94.5	114.0	109.0	40.0	66.0	53.0	59.0	57.0	43.0	82.0	204.0	410.0	290.0	230.0	240.0	260.0	250.0
CO	142.5	110.0	50.0	22.5	35.0	62.5	35.0	30.0	25.0	70.0	100.0	150.0	130.0	140.0	250..	250..	285.0
ZN	36.5	39.0	4.0	25.0	36.0	31.5	36.0	36.0	41.0	270.0	80.0	520.0	1900.0	270.0	280.0	270.0	240.0
CR	475.0	480.0	230.0	322.5	370.0	4925.0	750.0	650.0	425.0	1150.0	3200.0	1850.0	1800.0	900.0	1700.0	1700.0	1750.0
FE	6.3	6.2	5.1	3.3	5.6	5.4	6.6	6.8	5.3	11.0	19.0	9.1	9.3	6.8	9.5	11.5	12.0
TI	1375.0	1400.0	2200.0	1300.0	1750.0	1400.0	1400.0	1400.0	1400.0	900.0	750.0	1050.0	1000.0	1100.0	850.0	800.0	700.0
MN	3100.0	1850.0	560.0	200.0	230.0	345.0	310.0	140.0	260.0	390.0	1520.0	145.0	130.0	1360.0	1600.0	1900.0	1880.0
PB	22.5	17.0	22.6	16.2	10.2	13.2	8.5	9.0	9.1	19.3	50.3	70.9	28.8	31.9	22.9	27.6	24.9
MO	.5	.6	1.1	.3	1.3	.6	.4	.6	.0	.0	.0	1.2	.4	1.5	.1	.8	.6
V	173.3	193.6	214.4	153.4	123.8	152.4	144.0	165.2	153.9	.3	513.7	175.9	121.5	67.1	73.8	77.3	92.3
GA	15.9	16.7	13.5	13.4	14.5	15.3	15.9	13.8	14.9	13.5	.7	19.7	15.4	20.3	9.3	11.8	12.2
SN	11.5	3.2	7.9	2.9	3.8	7.3	2.5	4.3	3.3	.0	.0	24.8	8.6	.0	7.5	11.2	8.4
BE	.0	.0	.0	0	0	.0	0	.7	0	1.9	0	.1	.6	1.5	.3	.1	1.0
MG	1.0	.7	.6	1.2	1.0	1.9	1.8	1.5	.9	2.0	4.1	4.9	5.5	2.1	4.3	6.6	3.7
CA	.5	.6	.7	.4	.5	.5	.5	.4	.4	0	5.8	.8	1.4	0	.8	1.3	.8
SR	23.8	15.1	26.1	9.2	22.1	16.8	24.3	13.9	39.6	.8	1457.6	20.6	17.4	.8	28.5	57.8	40.8
BA	302.5	179.4	123.5	44.5	87.6	172.0	179.9	105.8	263.0	127.5	256.7	150.4	135.8	214.2	183.6	313.1	168.6
K	.3	.2	.3	.2	.3	.3	.5	.5	.7	1.5	10.3	1.1	1.0	1.8	1.1	1.2	1.1
LI	7.5	12.7	8.4	13.7	12.2	14.4	23.6	26.9	18.4	428.4	6119.3	2.1	6.3	166.6	.2	.2	.2
AL	8.3	12.2	8.4	4.8	15.4	9.7	13.3	11.3	15.8	5.1	1.3	5.8	7.4	1.0	5.4	9.7	4.5
SC	17.5	11.8	12.5	5.4	14.4	14.7	13.3	12.6	12.5	.0	.0	11.0	8.9	5.9	7.2	13.3	9.3
SI	38.2	28.3	37.5	28.4	30.7	37.3	26.4	30.0	28.1	37.1	1.8	32.5	21.9	43.9	24.3	31.0	23.0
S	80.0	30.0	25.0	30.0	20.0	25.0	20.0	25.0	20.0	50.0	100.0	610.0	225.0	25.0	120.0	70.0	70.0
F	-	-	-	-	-	-	-	-	-	162.0	119.0	114.0	149.0	76.0	43.0	95.0	43.0
PH	5.5	5.2	4.9	4.8	-	-	-	-	-	5.0	5.9	6.1	6.2	5.9	5.9	6.0	6.5

	83509	83510	83511	83512	83513	83514	83515	83516	83517	83518	83519	83520	83521	83522	83523	83524	84501
M	240.0	250.0	260.0	270.0	280.0	290.0	300.0	350.0	400.0	450.0	500.0	550.0	600.0	650.0	700.0	750.0	0
NI	7500.0	8200.0	5000.0	7300.0	6300.0	6900.0	6000.0	4200.0	3200.0	2300.0	2200.0	1850.0	2500.0	1600.0	1100.0	1000.0	2500.0
CU	300.0	350.0	375.0	520.0	470.0	460.0	400.0	420.0	320.0	290.0	280.0	209.0	147.0	136.0	89.0	79.0	120.0
CO	375.0	400.0	340.0	350.0	230.0	325.0	280.0	280.0	185.0	160.0	115.0	125.0	105.0	80.0	65.0	100.0	155.0
ZN	280.0	220.0	215.0	530.0	180.0	530.0	400.0	630.0	950.0	640.0	470.0	470.0	320.0	220.0	90.0	81.0	50.0
CR	2300.0	2550.0	2425.0	2430.0	2250.0	2000.0	2200.0	2300.0	2150.0	1950.0	1950.0	2350.0	2100.0	1750.0	1350.0	1750.0	2850.0
FE	13.5	15.5	14.0	13.5	13.0	12.5	14.0	12.5	11.0	10.2	8.4	9.3	9.2	8.9	8.0	6.7	20.0
TI	700.0	800.0	725.0	750.0	1000.0	650.0	800.0	900.0	950.0	1000.0	950.0	950.0	1250.0	1250.0	900.0	1050.0	1700.0
MN	2000.0	1820.0	1725.0	1500.0	1420.0	1780.0	1600.0	1750.0	1420.0	1150.0	960.0	1070.0	950.0	670.0	390.0	1100.0	1640.0
PB	23.3	24.2	19.7	49.7	47.5	30.3	35.7	44.2	34.5	29.2	31.4	15.8	21.0	15.9	12.7	9.5	13.5
MO	1.2	.9	.4	1.4	1.4	.0	.5	.5	.1	.3	.4	1.0	.7	.4	.2	.0	.3
V	30.5	91.7	82.8	74.9	114.8	105.6	99.6	137.3	110.5	122.9	101.5	145.9	118.4	138.1	118.8	134.4	179.1
GA	12.7	12.0	8.2	14.6	13.8	9.7	15.9	16.9	11.8	14.0	15.7	16.4	13.6	14.1	13.1	11.4	15.3
SN	.0	6.7	5.9	15.6	10.5	11.1	22.3	25.8	17.9	24.5	14.1	6.6	1.4	13.1	6.7	7.9	11.1
BE	3.2	1.0	1.4	.5	1.0	.7	.5	.7	.4	0	0	0	0	0	0	0	0
MG	1.3	3.6	2.8	4.0	5.6	3.6	6.8	6.2	5.5	.5	6.5	4.1	5.3	7.1	7.3	7.4	4.2
CA	0	.6	.7	.8	1.4	1.2	1.4	2.0	1.7	2.1	2.3	.7	1.5	1.9	2.1	2.9	1.3
SR	.8	33.2	58.2	47.9	43.9	38.8	48.2	95.7	71.4	37.5	48.2	17.0	31.2	21.0	17.4	24.3	20.4
BA	157.4	161.8	158.1	169.7	172.1	142.4	181.5	253.5	164.1	184.3	213.8	112.1	123.3	95.6	67.1	123.3	110.5
K	1.2	1.1	.8	1.0	.9	.3	1.1	.9	.8	.6	.6	.6	.5	.3	.3	.5	.5
LI	130.3	.2	.2	.7	.2	.2	.2	.2	1.5	7.8	13.3	21.1	15.5	11.0	15.1	16.7	6.2
AL	4.2	5.2	2.9	5.3	3.2	4.3	7.5	7.5	6.2	7.9	8.0	10.1	5.8	7.0	8.7	7.4	6.2
SC	6.1	10.5	8.2	12.6	11.9	9.1	16.5	15.9	9.2	12.1	14.1	17.3	11.8	14.1	16.9	14.0	13.8
SI	33.3	21.9	16.1	17.2	24.9	15.3	22.1	29.0	22.7	22.2	19.9	31.2	15.8	23.9	20.5	21.2	20.0
S	140.0	120.0	75.0	185.0	90.0	70.0	40.0	40.0	95.0	40.0	130.0	125.0	30.0	125.0	55.0	20.0	40.0
F	48.0	173.0	113.0	124.0	35.0	119.0	30.0	15.0	53.0	70.0	53.0	53.0	53.0	30.0	34.0	15.0	23.0
PH	6.5	6.3	6.3	6.2	6.4	5.5	6.5	6.9	6.2	5.9	6.2	5.8	6.5	6.3	6.5	5.5	5.9

OFF-LINE SOILS

	14501	14502	14503	14504	14505	14506	14507	14508	14509	14510	14511	14512	14513	14514	14515	14516	14517
M	J	50.7	100.0	150.0	160.0	170..	180.(	190.0	200.0	210.0	220.0	23.0	240.0	250.0	300.0	350.0	400.0
NI	160.0	135.0	195.0	205.0	190.0	200.0	250.0	275.0	450.0	230.0	200.0	155.0	230.0	210.0	170.0	200.0	110.0
CU	47.0	41.0	54.0	55.0	52.0	55.0	63.0	71.0	80.0	50.0	60.0	50.0	58.0	72.0	69.0	83.0	114.0
CO	30.0	25.0	40.0	35.0	35.0	40.0	50.0	50.0	110.0	40.0	40.0	35.0	40.0	45.0	60.0	50.0	40.0
ZN	21.0	19.0	25.0	17.0	18.0	25.0	24.0	23.0	25.0	19.0	26.0	27.0	22.0	22..	27.0	22.0	26.0
CR	40.0	30.0	50.0	40.0	45.0	50.0	50.0	60.0	65.0	45.0	50.0	45.0	50.0	45.0	40.0	55.0	45.0
FE	4.3	4.3	6.2	5.0	5.2	6.3	7.5	7.1	7.2	5.0	6.0	5.8	7.6	7.2	9.3	15.0	7.8
TI	1800.0	1600.0	1900.0	1850.0	1950.0	2250.0	2200.0	2000.0	2400.0	1900.0	1750.0	1850.0	1950.0	1950.0	2200.0	2200.0	1900.0
MN	200.0	160.0	260.0	250.0	260.0	260.0	330.0	340.0	340.0	250.0	290.0	230.0	270.0	280.0	330..	24...	240.0
PB	9.8	3.8	8.6	6.9	7.2	9.1	4.3	19.6	4.3	5.7	11.1	10.8	45.5	5.7	5.1	37.3	9.7
MO	.7	.2	.9	.5	.8	.1	.0	.0	.3	.0	1.0	1.5	.0	.1	.4	.0	1.0
V	284.3	185.1	337.2	275.1	317.0	67.0	349.7	154.9	285.8	291.9	364.9	467.3	513.1	350.0	372.1	514.5	444.1
GA	19.3	14.7	21.7	22.8	23.6	0	17.0	0	22.5	16.4	27.2	20.7	0	20.3	24.7	0	27.7
SN	13.3	6.1	14.9	14.2	10.5	.	15.7	.	5.6	11.4	17.6	17.0	0	11.2	6.5	0	14.6
BE	0	0	0	0	0	2.0	0	1.0	0	0	0	0	0	0	0	2.0	0
MG	.7	.6	1.3	1.0	1.0	34.2	1.3	65.2	1.1	1.1	1.3	.6	115.4	.9	.9	147.9	.7
CA	.5	.4	1.1	.8	.8	6.3	1.1	8.3	.6	.8	.9	.9	9.0	.6	.9	10.1	.8
SR	39.3	35.2	59.3	71.8	45.7	511.2	46.5	907.2	40.0	75.9	60.5	73.5	1693.2	50.5	60.7	1655.3	49.6
BA	295.0	312.7	454.2	369.3	287.6	133.1	277.4	927.0	262.1	352.2	376.1	424.4	162.7	355.2	333.1	809.2	253.5
K	2.7	2.1	2.8	2.8	2.7	2.5	2.3	3.5	2.5	2.5	3.1	2.7	4.1	2.4	1.9	3.7	2.2
LI	10.5	8.9	6.4	7.8	5.4	2943.3	7.2	1544.2	13.4	4.0	6.4	2.3	6184.8	9.6	6.2	1147.7	4.7
AL	9.3	10.1	15.4	11.5	11.7	7.7	11.0	9.7	13.6	11.0	10.9	11.2	12.3	10.7	16.3	12.9	9.3
SC	6.5	6.1	11.2	13.2	3.2	.0	8.3	.0	8.3	11.7	13.7	11.5	.0	9.4	14.0	.0	14.9
SI	28.4	23.4	32.3	24.1	27.5	1.8	25.4	1.3	20.8	20.5	35.3	36.5	1.8	22.4	21.5	1.9	32.7
PH	4.3	5.3	5.5	5.5	5.1	5.2	5.4	5.5	5.3	5.1	5.1	5.4	5.4	5.0	5.2	5.0	5.3

	14518	14519	14520	14521	14522	14523	14538	23501	23502	23503	23504	23505	23506	23507		23509	23510
M	450.0	500.0	550.0	600.0	850.0	950.0	190.0	0	50.0	100.0	150.0	200.0	210.0	220.0		240.0	250.0
NI	110.0	120.0	70.0	95.0	75.0	70.0	5000.0	270.0	300.0	500.0	525.0	650.0	750.0	750.0		850.0	1550.0
CU	135.0	240.0	260.0	330.0	600.0	580.0	600.0	120.0	88.0	45.0	36.0	57.0	45.0	38.0		40.0	40.0
CO	50.0	65.0	50.0	60.0	80.0	65.0	350.0	70.0	60.0	60.0	75.0	95.0	110.0	90.0		105.0	190.0
ZN	40.0	24.0	27.0	16.0	22.0	16.0	43.0	41.0	39.0	36.0	38.0	57.0	70.0	78.0		79.0	73.0
CR	60.0	60.0	35.0	55.0	45.0	50.0	205.0	850.0	1150.0	400.0	455.0	1450.0	1850.0	4500.0		4500.0	4600.0
FE	8.0	7.2	5.0	6.0	2.0	4.8	27.5	6.1	5.3	5.0	5.4	6.4	7.2	6.8		7.9	10.5
TI	2250.0	2450.0	1950.0	2400.0	3200.0	3300.0	1600.0	2000.0	1800.0	1550.0	1900.0	1500.0	1800.0	2000.0		2000.0	1900.0
MN	310.0	30.0	20.0	20.0	10.0	10.0	690.0	700.0	590.0	500.0	745.0	920.0	950.0	860.0		1000.0	2120.0
PB	8.7	14.4	33.8	6.9	7.6	4.9	8.1	4.8	5.3	5.1	4.6	10.6	9.0	10.9		13.3	11.9
MO	1.1	.0	.0	1.0	.2	.3	.4	.0	.8	.1	.2	.6	.0	.2		.5	.1
V	362.1	495.8	343.0	325.8	261.6	209.9	882.9	255.4	173.9	121.0	120.9	182.1	163.5	223.1		145.8	168.9
GA	22.3	0	0	27.1	29.3	36.2	32.6	2.1	23.5	17.4	16.6	21.9	14.0	19.8		18.9	18.7
SN	10.7	0	0	11.9	14.7	9.7	7.7	2.3	1.6	5.4	1.0	11.0	11.0	23.8		20.0	18.5
BE	0	2.0	0	0	0	1.1	0	0	0	.5	0	0	0	0		0	0
MG	1.0	53.5	31.2	1.6	1.8	1.6	3.6	.9	1.4	5.4	3.2	3.5	3.1	3.7		3.7	5.0
CA	1.4	7.4	5.6	.6	.3	.2	1.3	1.2	1.2	7.2	1.0	1.9	1.9	2.0		1.7	2.0
SR	80.4	1983.4	1476.6	29.5	21.4	12.3	40.7	31.4	47.0	31.7	26.1	41.7	40.9	52.2		46.0	54.4
BA	341.0	261.5	140.5	209.6	231.3	242.5	99.0	81.5	73.2	130.2	53.2	126.5	93.1	97.4		116.9	92.7
K	2.2	3.2	2.4	3.0	2.7	3.3	.5	.3	.3	.4	.3	.3	.3	.4		.4	.4
LI	9.2	5367.3	5626.0	13.7	21.2	30.5	5.7	5.0	20.5	27.0	20.4	12.8	7.5	5.7		7.3	3.5
AL	15.2	9.5	7.8	12.3	9.9	9.3	9.2	13.4	17.4	14.0	13.6	20.6	10.9	14.1		14.4	9.4
SC	11.3	.0	.0	6.1	9.8	6.1	24.1	17.2	14.1	6.1	5.0	14.2	7.7	11.5		12.0	11.4
SI	25.5	2.0	1.9	26.3	26.1	27.0	14.6	26.0	28.3	23.4	21.7	34.4	24.1	29.9		34.0	19.5
PH	5.9	4.8	5.2	5.3	4.7	4.7	5.6	5.0	5.5	5.5	5.5	6.0	7.3	6.2		6.0	6.1

SOIL TRAVERSE LINES

	84502	84503	84504	84505	84506	84507	84508	84509	84510	84511	84512	84513	84514	84515	84516	84517	84518
M	50.0	100.0	150.0	200.0	210.0	220.0	230.0	240.0	250.0	260.0	270.0	280.0	290.0	300.0	310.0	320.0	330.0
NI	1600.0	950.0	1050.0	5100.0	4500.0	8900.0	8000.0	8300.0	10300.0	9500.0	7500.0	10000.0	12500.0	11900.0	11500.0	2000.0	8250.0
CU	123.0	106.0	90.0	132.0	260.0	60.0	69.0	144.0	300.0	540.0	330.0	500.0	405.0	310.0	236.0	680.0	535.0
CO	105.0	90.0	95.0	260.0	265.0	300.0	270.0	275.0	275.0	380.0	360.0	330.0	400.0	300.0	310.0	300.0	305.0
ZN	68.0	120.0	102.0	116.0	320.0	116.0	103.0	90.0	85.0	78.0	78.0	50.4	91.0	87.5	86.0	80.0	78.5
CR	15.0	950.0	1750.0	2500.0	1800.0	2750.0	2300.0	2450.0	4000.0	1950.0	1700.0	2450.0	2250.0	2650.0	2500.0	4000.0	4475.0
FE	12.5	9.6	8.4	15.0	10.0	16.5	17.0	16.5	15.5	17.0	17.0	10.0	18.0	19.0	17.0	16.5	17.8
TI	2400.0	2200.0	2000.0	850.0	950.0	500.0	500.0	550.0	450.0	400.0	450.0	350.0	400.0	450.0	450.0	500.0	450.0
MN	1680.0	1760.0	1500.0	1980.0	1700.0	1800.0	1400.0	1310.0	1300.0	1440.0	1420.0	1540.0	1290.0	1420.0	1380.0	1450.0	1650.0
PB	16.5	15.6	11.2	12.6	5.5	6.5	11.6	96.9	11.9	9.7	9.5	35.2	13.2	25.1	9.0	9.2	12.0
MO	1.2	.6	.0	.0	.0	.2	.0	.0	.0	.0	.2	.0	.4	.0	.0	.0	.2
V	346.1	228.7	203.7	87.0	67.5	152.8	52.5	500.1	61.3	52.1	43.5	370.2	53.4	291.1	53.7	73.8	67.8
GA	32.3	26.4	19.2	10.1	6.6	20.3	7.1	0	6.4	4.0	5.7	0	6.2	0	4.5	7.5	7.6
SN	9.3	16.1	32.4	11.7	.6	11.5	5.4	0	11.4	7.6	4.2	0	8.3	0	2.8	10.1	11.8
BE	0	0	0	0	1.6	0	1.2	1.9	1.1	1.1	1.4	.5	1.5	.2	1.7	1.7	2.1
MG	2.3	3.9	4.3	7.2	4.4	2.2	5.9	2.8	6.4	5.1	5.8	3.5	5.3	2.6	5.6	7.0	5.7
CA	1.3	2.7	2.3	.7	.4	1.0	.6	4.6	.8	1.0	1.8	5.5	1.2	4.2	.7	.6	.6
SR	32.3	77.1	37.7	23.6	8.2	29.1	13.5	2484.7	10.1	13.0	11.9	1124.0	12.5	1278.8	8.7	9.7	11.3
BA	214.2	327.5	235.4	147.6	59.7	78.1	72.4	371.5	94.9	67.2	68.1	146.3	51.2	163.9	46.0	50.8	58.1
K	.4	.6	.7	.6	.2	.3	.4	5.7	.5	.3	.3	7.5	.3	5.6	.2	.3	.3
LI	20.2	11.7	12.9	.2	.3	8.5	.2	2032.1	.2	.2	.2	3452.8	.2	6205.3	.2	.2	.2
AL	15.7	15.6	9.0	4.6	2.6	8.6	2.8	.4	2.7	1.5	2.1	.5	2.4	.5	1.4	1.9	2.7
SC	22.7	28.8	14.4	12.4	7.8	7.1	9.5	.3	8.8	7.7	9.0	.4	10.3	.0	6.9	10.8	9.6
SI	24.8	31.8	29.8	16.4	11.4	23.1	10.9	1.6	17.1	10.2	11.0	1.6	9.8	1.6	12.9	20.5	13.2
S	70.0	60.0	60.0	60.0	15.0	15.0	30.0	35.0	20.0	50.0	25.0	60.0	75.0	50.0	40.0	50.0	40.0
F	73.0	570.0	124.0	70.0	72.0	62.0	48.0	43.0	67.0	35.0	37.0	83.0	76.0	38.0	15.0	15.0	53.0
PH	5.9	6.0	5.7	6.0	6.0	6.2	6.2	6.0	6.1	6.0	6.1	6.1	5.9	6.1	6.0	5.9	6.0

	84519	84520	84521	84522	84523	84524	84525
M	340.0	350.0	400.0	450.0	500.0	550.0	600.0
NI	8500.0	5000.0	3200.0	650.0	420.0	1100.0	3850.0
CU	1020.0	360.0	225.0	170.0	104.0	143.0	34.0
CO	400.0	250.0	182.5	70.0	90.0	105.0	175.0
ZN	82.0	85.0	100.0	84.0	95.0	106.0	118.0
CR	5200.0	4100.0	3750.0	1050.0	1200.0	2400.0	5000.0
FE	21.0	17.0	15.8	9.4	6.0	6.9	15.5
TI	650.0	600.0	1100.0	1300.0	2500.0	1550.0	800.0
MN	1560.0	1440.0	1515.0	1100.0	1530.0	1390.0	1140.0
PB	11.1	15.5	7.8	12.1	10.2	10.3	11.4
MO	.0	.4	.3	.4	.5	.1	.1
V	93.5	89.1	100.5	267.5	231.0	274.8	102.3
GA	6.5	8.0	9.7	25.6	21.7	20.5	8.5
SN	16.7	19.0	3.4	3.3	3.8	7.7	13.1
BE	1.8	1.9	1.4	0	0	0	1.0
MG	7.3	7.3	3.9	2.2	1.3	1.7	5.9
CA	.8	.9	.6	1.2	1.4	2.3	1.3
SR	12.2	22.2	13.2	30.1	63.7	62.2	15.4
BA	146.5	102.6	100.8	137.9	393.8	108.5	76.9
K	.2	.4	.3	.5	.7	.3	.5
LI	.2	.2	.2	.4	.2	.2	.2
AL	2.2	3.5	2.7	14.6	13.1	10.6	2.8
SC	13.2	10.6	8.2	23.8	25.9	20.8	13.8
SI	8.1	18.6	11.8	36.5	32.3	28.5	22.4
S	23.0	60.0	30.0	80.0	60.0	5.0	50.0
F	48.0	49.0	52.0	60.0	15.0	30.0	29.0
PH	6.1	6.3	5.7	6.1	6.0	6.0	6.0

	23511	23512	23513	23514	23515	23516	23517	23518	23519	23520	23522	23525	23526	23527	23528	23529	23530
M	260.0	270.0	230.0	29?.?	3?0.?	31?.?	?2?.?	330.?	34?.?	?5?.?	37?.?	4?.??	45?.?	5?1.?	55?.?	600.0	650.0
NI	1000.0	800.0	900.0	950.0	1100.0	950.0	1200.0	900.0	1100.0	1200.0	1100.0	1000.0	650.0	650.0	550.0	600.0	400.0
CU	38.0	32.0	38.0	34.0	38.0	37.0	38.0	29.0	39.0	38.0	41.0	40.0	33.0	40.0	41.0	56.0	61.0
CO	145.0	110.0	125.0	130.0	135.0	140.0	140.0	105.0	125.0	125.0	110.0	110.0	65.0	75.0	75.0	85.0	70.0
ZN	91.0	92.0	77.0	105.0	102.0	110.0	89.0	103.0	86.0	9?.5	91.?	88.0	64.0	47.?	41.?	45.0	34.0
CR	4700.0	6500.0	3750.0	6?.0.0	4700.0	6100.0	3750.0	6000.0	3750.0	3575.0	2725.0	3050.0	1850.0	1150.0	900.0	650.0	490.0
FE	8.2	8.0	8.4	3.0	8.8	7.5	9.3	7.8	9.6	9.6	9.8	9.6	7.5	8.3	8.3	9.0	8.0
TI	2350.0	2500.0	2050.0	2000.0	2100.0	2050.0	2200.0	2100.0	2350.0	1950.0	2950.0	2500.0	1850.0	2000.0	1900.0	1900.0	2000.0
MN	1390.0	1380.0	1140.0	1350.0	1450.0	1460.0	1440.0	960.0	1290.0	1255.0	1025.0	1020.0	530.0	730.0	820.6	1036.0	760.0
PB	12.1	11.9	12.2	15.2	11.5	11.8	13.0	9.2	15.9	7.7	14.1	12.4	7.6	7.8	38.8	6.5	9.1
MO	.3	.6	.0	.1	.2	.3	.5	.1	.1	.1	.1	.9	.5	1.0	.0	.7	.5
V	211.2	198.1	164.0	63.4	165.8	165.1	207.6	176.0	174.6	150.4	196.0	150.8	174.6	182.6	242.1	169.6	185.6
GA	20.5	23.4	16.2	6.5	17.4	22.6	21.2	20.1	20.6	14.3	23.5	23.1	18.9	22.9	0	20.7	22.6
SN	24.4	19.2	23.7	17.2	12.6	15.4	16.1	16.3	9.9	6.7	19.3	11.8	6.7	7.8	0	5.6	11.9
BE	.?	0	0	1.4	0	0	0	0	0	0	0	0	0	0	1.7	0	0
MG	4.2	3.7	3.4	3.8	3.4	4.3	3.4	2.9	2.3	2.2	4.1	3.2	.8	.8	41.5	.6	.7
CA	1.5	1.5	1.6	.9	1.6	1.8	1.5	1.2	.8	.9	1.4	.9	.6	.7	5.9	.6	.6
SR	49.0	54.9	49.1	17.8	39.5	51.8	41.8	26.9	19.6	20.2	32.2	23.3	22.2	26.7	1477.1	15.1	19.8
BA	116.9	99.1	116.9	86.1	120.9	119.5	142.8	74.2	86.6	77.4	204.5	192.4	119.5	176.6	231.1	147.4	189.5
K	.4	.3	.4	.4	.4	.5	.4	.4	.2	.2	.2	.3	.4	.9	1.4	1.2	1.3
LI	1.3	4.7	4.5	.2	3.8	5.5	6.0	4.0	10.0	3.8	7.5	13.0	10.6	13.3	5320.6	14.4	14.9
AL	12.5	13.5	11.9	3.1	12.5	11.3	14.1	10.2	9.5	9.0	16.6	14.6	14.0	19.8	8.5	17.6	16.3
SC	14.5	12.8	11.9	13.9	11.0	12.4	12.6	9.8	9.7	9.5	19.0	15.3	11.6	13.1	.0	12.3	14.2
SI	29.5	27.1	30.9	17.3	28.9	27.1	27.3	24.3	24.2	19.5	36.3	32.6	29.9	32.4	2.1	29.4	34.1
PH	6.3	6.2	6.0	6.1	6.2	6.3	6.2	6.1	6.0	6.0	5.8	6.1	5.5	6.0	5.5	5.6	5.7

	54501	54502	54503	54504	54505	54506	54507	54508	54509	54510	54511	54512		54513	54514	54515	54516
M	0	50.0	60.0	70.0	80.0	90.0	100.0	110.0	120.0	130.0	140.0	150.0		170.0	190.0	200.0	240.0
NI	350.0	297.5	280.0	290.0	285.0	365.0	800.0	1700.0	1800.0	1500.0	1750.0	1950.0		2250.0	2350.0	2700.0	2900.0
CU	153.0	119.0	115.0	147.0	236.0	169.0	176.0	203.0	183.0	170.0	150.0	135.0		95.0	112.0	124.0	87.0
CO	80.0	50.0	50.0	50.0	50.0	55.0	70.0	130.0	165.0	135.0	135.0	140.0		155.0	175.0	215.0	210.0
ZN	49.0	41.0	37.0	46.0	190.3	73.0	69.0	72.0	69.0	64.0	62.0	61.5		47.0	46.0	46.0	53.0
CR	500.0	650.0	490.0	650.0	5500.0	850.0	1550.0	2750.0	2850.0	2800.0	3400.0	3400.0		2750.0	2400.0	2000.0	2000.0
FE	9.7	9.4	8.3	8.5	9.4	9.6	17.5	18.5	18.5	19.0	21.0	21.0		20.0	21.0	20.0	19.5
TI	1450.0	1200.0	1450.0	1300.0	1150.0	1100.0	1100.0	950.0	1100.0	1150.0	950.0	1050.0		800.0	900.0	850.0	1000.0
MN	1480.0	800.0	870.0	800.0	960.0	940.0	770.0	780.0	830.0	800.0	720.0	765.0		690.0	810.0	950.0	1060.0
PB	17.5	9.2	19.4	23.7	57.7	13.0	15.2	32.2	16.7	19.6	20.7	17.0		40.7	13.9	13.5	12.3
MO	1.5	.8	2.6	.0	1.7	.5	.7	.9	.3	.3	.7	.9		.0	.3	.6	.0
V	341.5	304.5	624.8	83.0	263.4	232.6	211.7	141.8	139.1	135.0	149.7	148.2		424.5	112.8	117.2	142.5
GA	25.7	22.5	31.9	0	28.5	18.1	14.6	17.6	13.1	11.4	13.3	13.4		0	9.4	12.1	10.4
SN	11.1	6.3	21.0	0	9.4	13.7	9.7	15.0	12.6	13.0	21.1	12.3		0	16.3	11.8	12.9
BE	0	0	0	0	0	0	0	0	0	0	0	0		.2	0	0	0
MG	2.7	1.7	2.6	36.4	2.0	3.3	2.9	6.8	5.5	6.0	7.2	5.2		12.8	5.9	5.6	5.4
CA	1.1	1.6	1.2	8.6	1.2	2.3	1.6	2.5	2.2	2.5	2.3	2.0		5.8	2.4	2.1	1.8
SR	43.4	45.3	43.1	996.8	29.5	37.9	32.6	32.6	22.5	30.3	32.6	22.0		1237.7	19.0	16.4	12.9
BA	189.2	286.6	352.9	844.4	327.0	191.7	163.6	129.3	103.1	139.1	146.3	114.7		973.8	82.7	106.5	70.6
K	2.3	2.3	3.5	5.0	3.7	1.3	1.4	.8	.7	.8	.8	.7		4.6	.6	.5	.4
LI	78.5	56.5	78.2	145.1	93.4	50.9	43.3	39.4	21.6	13.5	16.4	20.6		2961.0	8.4	13.5	6.1
AL	12.3	7.3	12.9	8.4	9.5	9.0	5.2	6.3	4.5	5.0	0.4	4.7		4.0	7.8	4.8	4.0
SC	13.1	8.7	17.0	.0	8.9	8.5	7.7	14.0	9.5	10.9	13.5	9.0		.0	10.2	10.0	9.8
SI	29.3	20.2	39.7	3.4	22.3	27.5	24.6	13.3	11.2	14.2	16.4	13.1		2.1	10.7	9.4	10.1
PH	-	-	-	-	-	-	-	-	-	-	-	-		-	-	-	-

OFF-LINE SOILS

	54517	54518	54519	83587	83538	83583	83590	83591	33592
M	370.0	430.0	510.0	220.0	230.0	240.0	250.0	260.0	277.0
NI	2300.0	1350.0	175.0	7500.0	10000.0	9500.0	9500.0	11000.0	11000.0
CU	71.0	82.0	60.0	850.0	1000.0	750.0	620.0	590.0	720.0
CO	170.0	110.0	50.0	400.0	450.0	350.0	350.0	500.0	450.0
ZN	67.0	45.0	120.0	142.0	250.0	230.0	170.0	130.0	154.0
CR	2400.0	1900.0	110.0	5150.0	6500.0	5550.0	3850.0	4000.0	3500.0
FE	21.0	16.0	19.0	19.0	23.0	20.5	17.5	19.0	19.0
TI	950.0	1000.0	500.0	700.0	650.0	750.0	550.0	350.0	550.0
MN	1060.0	840.0	460.0	2140.0	1960.0	1820.0	1740.0	1600.0	1440.0
PB	10.9	11.6	8.6	24.7	19.2	14.8	25.5	26.9	19.1
MO	.0	.8	.3	.7	1.2	.7	.0	1.1	.0
V	91.0	110.5	61.5	106.2	37.8	91.5	159.4	89.8	40.0
GA	9.4	11.0	6.9	15.0	13.0	8.4	0	14.9	0
SN	10.2	6.3	0	15.1	7.8	4.8	0	18.5	0
BE	0	0	.6	:	1.3	1.0	1.6	1.1	2.0
MG	7.1	5.1	1.1	4.2	4.3	3.9	5.2	6.6	3.5
CA	2.2	.9	15.3	1.5	1.0	.7	5.7	.7	5.1
SR	28.9	21.4	62.8	79.3	44.0	33.6	958.0	50.1	850.6
BA	72.7	87.6	103.0	303.8	176.0	140.4	403.3	251.5	773.0
K	.5	.6	.9	1.3	.9	.3	9.8	.8	7.8
LI	.8	43.0	45.1	.2	.2	.2	3621.3	.2	1924.2
AL	4.0	4.3	3.0	7.1	6.1	5.3	1.7	7.1	1.2
SC	9.5	6.7	2.1	13.3	14.6	11.1	.2	21.0	.2
SI	10.4	15.6	3.6	17.3	13.1	11.9	1.7	21.1	1.7
PH	-	-	-	6.1	6.4	5.4	5.9	5.9	5.8

PIT PROFILE AND SOIL TRAVERSE COARSE FRACTIONS

	15216	15217	15218	15219	15220	15221	15222	15223	25213	25214	25215	25216	25217	25218	25219	25220	25221
M	7.0	20.0	35.0	50.0	100.0	200.0	300.0	400.0	7.0	20.0	35.0	50.0	100.0	200.0	300.0	400.0	500.0
NI	2500.0	2650.0	3200.0	10000.0	4600.0	9000.0	7000.0	3000.0	1950.0	2150.0	2150.0	2400.0	1900.0	2700.0	3250.0	13000.0	8000.0
CU	550.0	670.0	610.0	1080.0	1000.0	1410.0	470.0	120.5	49.0	55.0	52.0	56.0	52.0	61.0	66.0	18.0	12.0
FE	50.5	50.3	50.0	33.0	40.0	19.0	18.0	11.5	13.0	14.5	13.5	14.0	12.5	14.5	16.5	10.0	9.6
MN	360.0	290.0	230.0	440.0	350.0	310.0	720.0	640.0	1190.0	1220.0	1320.0	1310.0	1310.0	1500.0	1640.0	960.0	1000.0

	13201	13202	13203	13204	13205	13206	13207	13208	13209	13210	13211	13212	13213	13214	13215	13216	13217
M	0	50.0	100.0	150.0	160.0	170.0	180.0	190.0	200.0	210.0	220.0	230.0	240.0	250.0	300.0	350.0	400.0
NI	40.0	15.0	35.0	80.0	225.0	290.0	550.0	5150.0	3100.0	175.0	830.0	6500.0	1850.0	1950.0	185.0	200.0	212.5
CU	15.0	4.0	3.0	7.0	20.0	221.0	650.0	640.0	250.0	225.0	1580.0	860.0	255.0	230.0	17.0	31.5	50.5
FE	4.4	4.0	2.8	3.1	4.4	14.5	38.5	36.5	30.5	19.5	36.0	31.5	24.5	20.0	16.5	12.3	20.5
MN	210.0	130.0	200.0	180.0	190.0	290.0	530.0	720.0	460.0	410.0	700.0	520.0	180.0	160.0	210.0	375.0	340.0

	13218	13219	13220	13221	13222	13223	13224	13225	13226	13227	13228	13229	13230	13231	13232	13233	13234
M	450.0	500.0	550.0	600.0	650.0	660.0	670.0	680.0	690.0	700.0	710.0	720.0	730.0	740.0	750.0	800.0	850.0
NI	220.0	167.5	160.0	167.5	160.0	170.0	125.0	130.0	82.5	75.0	130.0	77.5	65.0	52.5	65.0	55.0	25.0
CU	46.0	33.0	44.5	625.0	650.0	760.0	750.0	780.0	805.0	66.0	640.0	55.0	1020.0	235.0	990.0	154.0	49.0
FE	18.5	17.5	19.5	10.3	10.0	8.9	8.6	10.0	5.4	5.0	6.3	5.0	6.3	5.8	7.0	4.8	2.0
MN	410.0	395.0	405.0	205.0	150.0	180.0	160.0	160.0	155.0	105.0	130.0	135.0	160.0	130.0	650.0	60.0	30.0

	24201	24202	24203	24204	24205	24206	24207	24208	24209	24210	24211	24212	24213	24214	24215	24216	24217
M	0	50.0	100.0	150.0	200.0	210.0	220.0	230.0	240.0	250.0	260.0	270.0	280.0	290.0	300.0	310.0	320.0
NI	110.0	325.0	1100.0	1575.0	2050.0	2200.0	2300.0	2750.0	2100.0	2450.0	2350.0	2150.0	2100.0	2050.0	1925.0	1712.5	2000.0
CU	42.0	41.0	55.0	61.5	58.0	60.0	61.0	73.0	58.0	60.0	58.5	55.0	55.0	56.0	55.0	51.5	60.0
FE	4.3	5.2	8.8	9.8	10.8	11.0	12.5	13.0	12.0	12.0	11.8	12.0	12.5	13.0	12.0	11.1	13.0
MN	395.0	480.0	720.0	2325.0	1900.0	2150.0	1170.0	3400.0	1470.0	2500.0	2375.0	1670.0	1550.0	1220.0	1120.0	1065.0	1070.0

	24218	24219	24220	24221	24222	24223	24224	24225
M	330.0	340.0	350.0	400.0	450.0	500.0	550.0	600.0
NI	1850.0	1450.0	1400.0	730.0	300.0	145.0	125.0	110.0
CU	51.0	49.0	51.0	32.0	36.0	34.0	38.0	34.0
FE	11.5	10.0	11.0	7.5	5.5	7.9	12.0	10.5
MN	1080.0	830.0	940.0	610.0	550.0	720.0	910.0	920.0

DIPLORYNCHUS AND COMBRETUM LEAVES

	18901	18902	18903	18904	18905	18906	18907	18903	18909	18910	18911	18912	18913	18914	18915	18916	18917
M	0	50.0	100.0	150.0	160.0	170.0	180.0	190.0	200.0	210.0	220.0	.3 ..	240.0	250.00	300.0	350.0	400.0
NI	14.1	7.5	9.0	5.4	13.3	16.4	7.2	18.5	13.9	15.9	15.6	14.3	15.5	18.0	17.2	7.2	7.7
CU	5.3	4.0	3.1	3.9	4.8	3.3	2.4	2.8	3.8	4.2	3.0	3.1	3.1	3.5	4.4	2.8	4.8
CO	1.4	1.4	.8	.9	1.2	1.3	1.0	1.2	1.4	1.0	1.1	1.0	1.0	2.5	.6	.9	1.0
ZN	8.7	9.0	12.6	9.3	12.1	9.7	10.5	11.0	13.9	10.0	14.5	12.6	13.4	9.7	11.5	9.9	14.5
CR	9.1	5.8	4.2	5.3	6.1	5.1	5.2	5.9	5.6	6.2	7.6	6.4	9.5	8.3	5.7	3.8	4.8
FE	291.5	144.6	121.6	66.1	105.1	112.6	76.9	86.5	145.9	132.9	95.3	146.8	143.1	210.6	114.8	76.0	116.1
MN	683.2	925.7	775.6	349.8	545.6	307.0	191.5	353.6	361.3	203.5	194.4	104.6	169.7	235.3	160.8	193.7	121.0

	18918	18919	18920	18921	18922	18926	18927	18928	18929	18930	18931	18932	18933	18934	48902	48903	48904
M	450.0	500.0	550.0	600.0	610.0	650.0	660.0	670.0	680.0	690.0	700.0	750.0	800.0	850.0	50.0	60.0	70.0
NI	5.3	9.7	5.7	13.0	3.8	9.0	6.4	12.6	9.0	7.3	7.0	7.3	6.5	3.6	3.0	2.7	3.4
CU	4.3	4.0	3.2	8.4	5.3	9.9	7.8	10.0	5.9	6.7	6.3	6.1	7.3	6.2	3.9	3.1	4.6
CO	.3	.9	.9	.9	1.0	1.3	.8	1.6	.9	.7	.8	1.4	1.3	.5	.9	.5	1.0
ZN	12.7	16.2	19.6	11.9	9.1	8.2	6.4	8.2	6.3	5.7	10.1	7.6	8.1	8.8	10.4	12.3	11.6
CR	4.5	6.7	3.8	3.7	5.1	4.2	4.5	7.0	4.5	5.9	4.4	5.6	5.4	4.0	4.3	3.6	4.8
FE	86.4	89.6	94.4	222.8	339.3	629.1	367.2	747.4	97.0	165.4	87.1	145.1	107.6	89.9	100.0	65.1	92.1
MN	150.1	238.0	302.1	222.9	407.2	545.2	255.4	467.1	277.4	459.4	175.1	122.8	484.2	111.3	739.1	470.5	726.7

	48905	48906	48907	48908	48909	48911	48912	48913	48914	48915	48919	48920	48921	48925	48926	48932	48933
M	80.0	90.0	100.0	110.0	120.0	140.0	150.0	200.0	250.0	300.0	500.0	550.0	600.0	680.0	690.0	750.0	800.0
NI	5.3	8.1	13.0	9.0	9.0	7.9	6.5	12.5	13.0	6.4	8.2	8.0	9.7	8.7	19.4	10.0	9.1
CU	6.5	4.3	3.6	3.5	4.4	2.6	3.4	5.8	6.0	6.9	5.2	3.9	4.3	4.6	5.6	3.6	4.8
CO	1.0	1.6	1.0	1.0	1.1	.9	.8	1.5	1.1	.9	1.1	1.0	.8	.7	1.4	.8	1.0
ZN	9.5	18.6	9.4	14.6	12.0	10.5	12.1	12.0	11.5	13.7	14.3	12.6	11.7	10.1	14.6	9.6	11.4
CR	7.5	9.3	9.6	8.3	6.9	9.4	8.1	12.5	11.3	9.1	8.2	9.7	3.9	6.9	14.1	6.0	9.5
FE	70.5	21.1	36.4	144.3	129.7	176.2	121.1	5.1.	341.0	261.3	131.9	33.8	128.2	110.0	297.2	159.6	147.8
MN	654.3	1178.2	699.2	1250.7	1241.4	973.4	1029.0	1250.3	727.2	525.2	357.2	678.3	854.8	146.7	844.8	678.2	524.3

	48939	48946	48947	48948	48949	58901	58902	58903	58904	58905	58906	58907	58908	58909	58912	58916	58917
M	1100.0	1450.0	1500.0	1550.0	1600.0	0	50.0	60.0	70.0	80.0	90.0	100.0	110.0	120.0	150.0	190.0	200.0
NI	5.3	4.3	3.4	4.5	5.7	3.6	2.8	7.0	3.5	4.5	3.9	4.7	6.2	22.7	14.8	15.1	6.8
CU	4.7	4.3	3.9	4.5	5.8	4.3	3.4	3.4	3.5	4.2	3.6	4.2	3.7	4.8	3.6	4.1	2.7
CO	1.3	1.1	.8	1.1	.9	2.4	2.6	1.9	1.8	2.3	2.1	2.5	2.5	3.4	3.3	2.5	1.9
ZN	11.3	14.8	12.2	13.1	15.1	23.7	14.1	18.3	21.3	21.2	14.2	23.0	17.3	41.3	50.9	41.3	23.0
CR	4.3	6.5	6.1	4.5	4.7	15.6	10.6	11.4	8.9	7.6	8.9	14.9	12.3	28.3	14.8	10.3	11.0
FE	106.2	104.2	55.8	91.3	110.9	395.4	263.6	274.3	364.8	295.0	314.6	440.0	369.9	850.3	335.6	260.1	241.1
MN	335.1	694.4	892.8	1715.5	943.7	229.3	157.4	194.5	175.3	159.2	53.4	89.2	129.5	102.0	77.2	135.1	109.6

	88991	88992	89902	89903	89904	33905	89906	89907	89008	89909	89910	89911	89912	89915	89918	89919	89920
M	260.0	270.0	50.0	100.0	150.0	200.0	210.0	220.0	230.0	240.0	250.0	260.0	270.0	300.0	330.0	340.0	350.0
NI	217.3	196.0	36.4	24.0	13.4	38.9	63.4	51.9	56.8	57.0	67.9	83.2	53.0	98.9	154.2	76.2	81.1
CU	77.3	66.5	13.4	7.4	8.0	5.4	7.5	5.2	8.5	7.5	8.2	10.4	8.8	8.2	13.8	9.1	12.6
CO	8.5	6.9	3.5	1.8	1.1	1.2	1.7	1.1	1.4	1.4	1.4	1.3	1.3	1.4	2.1	1.8	2.8
ZN	16.2	18.7	15.6	14.8	3.3	5.4	7.8	6.9	7.5	5.5	5.9	5.7	6.4	5.2	7.2	7.8	11.4
CR	5.0	4.3	3.7	0	0	0	2.4	1.9	2.0	2.0	2.3	2.6	2.2	2.4	2.7	2.6	4.1
FE	547.3	451.6	1039.5	253.3	173.3	134.3	243.7	185.3	222.5	250.3	178.0	171.7	243.1	183.7	204.0	213.8	235.2
MN	506.3	204.5	294.5	243.1	136.3	237.4	536.0	151.9	194.2	183.1	190.0	179.5	163.6	202.6	335.1	229.4	730.0

	89921	89922	89923	89924	89925		19901	19902	19903	19904	19905	19906	19907	19908	19909	19910	19911
M	400.0	450.0	500.0	550.0	600.0		0	50.0	100.0	150.0	160.0	170.0	180.0	190.0	200.0	210.0	220.0
NI	42.5	14.0	22.3	24.3	39.2		12.1	14.1	10.1	10.8	8.0	9.7	8.8	9.1	7.0	7.9	7.4
CU	10.3	11.7	11.6	9.3	5.6		5.7	5.6	5.5	3.9	6.1	7.1	4.4	6.8	6.1	3.8	4.6
CO	2.1	1.0	2.1	1.4	1.9		2.8	3.3	2.3	3.0	2.2	3.1	2.5	3.0	2.9	2.0	1.7
ZN	6.1	7.6	9.5	7.7	10.7		21.0	16.9	17.1	25.6	20.9	16.7	18.9	22.7	21.8	25.4	16.3
CR	7.1	3.2	6.1	2.3	3.2		12.1	14.1	11.7	14.8	11.0	13.2	9.5	11.3	9.6	10.2	7.2
FE	473.3	180.7	367.2	160.0	202.2		1009.8	1362.1	935.0	186.0	1211.4	1491.9	1387.9	1761.9	1194.0	717.6	624.6
MN	354.5	183.9	336.1	215.2	568.0		76.7	43.3	95.7	118.3	71.6	79.0	69.4	93.2	64.0	66.0	38.4

	19912	19913	19914	19915	19916	19917	19918	19919	19920	19921	19922	19923	19989	19990	28901	28902	28903
M	230.0	240.0	250.0	300.0	350.0	400.0	450.0	500.0	550.0	600.0	850.0	950.0	200.0	210.0	0	50.0	100.0
NI	3.2	5.5	5.5	7.8	5.4	6.2	3.2	3.7	3.0	4.6	3.2	3.3	173.7	204.5	5.8	4.2	4.6
CU	2.7	7.8	4.4	5.5	3.5	6.9	4.3	5.6	4.5	10.6	6.3	7.7	9.0	8.3	4.1	3.1	2.8
CO	.9	1.8	1.9	3.7	2.3	2.3	2.5	1.9	3.2	4.1	11.4	8.1	9.3	6.7	2.7	1.7	1.0
ZN	15.8	20.6	27.7	16.5	23.1	41.2	25.0	16.2	17.9	20.7	6.3	8.3	26.4	38.3	43.9	32.3	19.4
CR	4.7	6.1	5.5	3.2	11.6	10.1	7.5	9.4	11.1	16.5	3.2	6.6	9.3	9.6	10.3	5.6	12.8
FE	379.3	667.0	775.3	1469.6	410.7	745.7	317.3	654.0	382.3	992.4	380.6	1321.2	2335.6	1693.7	425.3	333.7	281.3
MN	31.7	30.6	55.4	50.5	215.8	34.3	60.0	71.7	67.4	76.5	69.8	69.2	149.7	300.4	137.2	108.4	27.1

	28904	28905	28906	28907	28909	28910	28911	28912	28917	28914	28915	28916	28917	28918	28919	28920	28922
M	150.0	200.0	210.0	220.0	240.0	250.0	260.0	270.0	280.0	290.0	300.0	310.0	320.0	330.0	340.0	350.0	370.0
NI	5.1	6.3	6.2	3.8	10.8	13.1	5.3	23.5	5.8	5.8	4.2	3.6	3.3	7.6	7.4	8.3	7.1
CU	4.1	3.3	5.1	4.0	5.1	6.3	4.3	4.0	4.6	5.4	3.5	3.6	3.7	3.0	3.2	3.6	10.6
CO	1.5	2.3	3.1	1.5	1.6	2.7	1.7	5.4	1.7	2.5	1.7	3.3	2.0	2.7	1.8	2.2	1.0
ZN	31.7	21.1	22.6	23.5	53.6	33.4	33.3	32.2	29.0	19.8	15.3	52.4	32.0	28.8	27.1	47.7	32.4
CR	9.5	16.4	14.0	12.6	9.6	20.3	13.3	145.5	20.3	12.4	17.3	16.4	11.1	19.0	14.7	14.1	12.7
FE	387.3	381.6	1445.3	222.3	235.5	775.1	266.2	1723.3	389.3	404.1	267.2	173.7	256.1	273.3	217.6	258.6	233.2
MN	31.7	139.2	159.4	125.6	92.3	95.4	133.1	152.2	145.2	37.1	28.5	235.9	79.8	79.7	37.1	44.4	43.1

DIPLORYNCHUS AND COMBRETUM LEAVES

	58918	58919	58920	58921	58922	58923	58924	58925	58926	58927	58928	58930	58931	58932	58933	58934	58935
M	250.0	300.0	350.0	470.0	450.0	500.0	550.0	600.0	650.0	700.0	750.0	770.0	780.0	790.0	800.0	810.0	820.0
NI	11.9	5.2	5.4	8.9	8.7	9.9	7.2	6.8	17.3	15.4	16.9	9.8	6.7	5.2	5.6	3.8	3.1
CU	4.0	4.1	3.5	4.2	4.7	4.6	4.3	7.5	5.1	4.8	4.6	3.2	3.7	3.5	4.2	3.8	4.3
CO	2.0	1.8	2.2	1.9	2.8	2.3	2.0	3.1	2.7	2.9	3.8	2.9	2.6	2.2	2.5	1.7	2.4
ZN	25.2	18.6	19.4	15.9	29.8	24.3	28.8	29.8	37..	25.0	29.2	34.5	38.9	43.5	35.0	36.3	58.1
CR	17.2	10.3	10.8	11.7	14.2	11.4	7.2	8.6	16.1	12.8	26.9	5.8	7.5	8.7	17.5	13.8	7.8
FE	745.5	439.0	323.0	562.8	444.3	429.3	367.1	482.6	1015.0	671.9	1151.1	287.8	373.0	286.9	766.9	461.7	415.9
MN	91.9	108.5	102.3	89.1	120.7	83.5	129.6	114.1	149.3	140.8	107.4	149.7	119.3	69.5	98.1	82.7	219.7

	58936	58937	58938	58939	63901	68902	66903	68904	68905	68906	68907	68908	68909	68910	68911	68912	68913
M	830.0	840.0	850.0	900.0	0	50.0	100.0	150.0	200.0	250.0	260.0	270.0	280.0	290.0	300.0	310.0	320.0
NI	4.2	3.2	4.9	2.4	4.6	5.6	7.0	9.1	10.5	8.3	6.7	9.3	14.1	7.9	11.0	11.4	34.6
CU	4.7	3.8	4.3	4.4	3.2	6.8	6.1	2.8	2.9	2.9	4.9	4.0	3.8	3.3	3.8	2.5	2.5
CO	2.5	2.0	2.7	2.8	.7	.5	.7	.6	.7	.8	.9	1.2	1.0	.7	1.0	.8	1.8
ZN	44.1	42.8	34.7	76.3	13.0	13.6	17.4	11.4	13.5	13.3	12.8	21.5	18.5	15.7	11.0	7.6	15.3
CR	12.7	7.2	10.8	8.0	4.6	4.0	8.7	5.7	6.6	8.3	7.1	10.1	7.7	8.7	7.5	6.3	30.6
FE	933.2	431.8	406.1	401.8	97.2	71.8	108.8	64.4	80.2	104.1	123.2	126.4	143.6	115.8	82.7	71.5	662.4
MN	114.5	149.8	140.8	225.0	370.1	578.6	208.8	140.2	239.7	83.3	66.3	184.5	266.6	91.	190.4	84.1	917.2

	68915	68916	68917	68918	68919	68920	68921	68922	68923	68924	68925	68926	68927	68928	68930	68931	68941
M	340.0	350.0	360.0	370.0	380.0	390.0	400.0	410.0	420.0	430.0	440.0	450.0	500.0	550.0	650.0	700.0	1200.0
NI	11.8	8.7	9.8	15.8	13.4	12.8	16.7	11.3	10.4	7.6	9.1	8.9	12.9	10.9	12.0	14.9	5.9
CU	2.2	2.2	3.2	2.8	2.8	3.2	5.1	5.7	3.1	4.6	3.5	2.4	3.1	3.5	4.4	3.7	3.4
CO	.3	.6	1.0	.3	.6	1.0	1.1	.8	.9	.7	.7	.6	.7	.6	1.4	1.0	1.0
ZN	7.5	8.4	9.1	11.0	9.5	7.9	21.3	9.2	12.1	13.9	12.1	7.4	8.2	13.2	16.4	12.9	11.8
CR	11.8	6.4	7.3	5.9	4.3	4.9	5.3	5.4	5.7	4.6	3.7	5.6	4.7	4.1	10.9	7.5	7.4
FE	149.0	77.1	91.6	100.4	73.3	83.5	90.4	86.9	92.4	60.2	60.8	55.6	75.2	80.2	145.0	69.6	73.8
MN	168.7	176.6	195.8	212.6	165.9	122.7	159.5	53.9	94.7	111.2	85.1	122.3	70.5	98.7	103.9	323.1	142.8

	68943	88902	88906	88908	88909	88910	88911	88914	88915	88917	88918	88919	88924	88987	88988	88989	88990
M	130.0	50.0	210.0	230.0	240.0	250.0	260.0	290.0	300.0	400.0	450.0	500.0	750.0	220.0	230.0	240.0	250.0
NI	13.0	492.8	137.1	207.6	152.1	237.4	131.4	172.6	174.9	156.6	213.5	211.7	329.3	311.3	360.4	360.8	248.1
CU	5.5	261.8	72.8	112.1	62.5	87.5	53.8	76.7	67.3	72.8	155.9	98.8	186.1	129.4	137.0	108.2	92.2
CO	.7	16.9	6.2	7.9	6.4	9.4	5.7	7.6	6.7	7.0	9.8	9.2	15.7	9.7	12.6	11.3	8.9
ZN	12.0	49.3	19.7	23.3	19.7	22.5	16.1	21.6	18.2	30.5	33.8	21.2	20.8	25.3	31.5	15.5	19.5
CR	4.5	7.7	0	4.2	5.8	6.2	5.7	5.4	0	0	8.9	7.1	14.3	0	0	0	0
FE	106.4	903.6	415.8	456.7	428.3	574.5	445.6	507.5	443.9	516.7	622.9	832.8	1288.5	671.3	684.8	627.1	638.1
MN	291.5	415.8	231.1	298.9	453.0	243.9	331.4	435.9	753.2	297.5	427.1	197.6	257.7	544.8	630.8	1070.9	726.7

	12505	12506	12507	12508	12509	12510	12511	12512	12513	12514	12515	12516	12517	12518	12519	12520	12521
M	100.0	200.0	300.0	400.0	500.0	600.0	700.0	800.0	400.0	500.0	600.0	700.0	800.0	900.0	1000.0	1100.0	1200.0
NI	340.0	320.0	285.0	240.0	255.0	170.0	160.0	162.5	750.0	650.0	450.0	700.0	800.0	170.0	300.0	215.0	190.0
CU	470.0	290.0	350.0	239.0	130.0	90.0	120.0	170.5	66.0	75.0	48.5	4.0	48.1	69.0	62.0	69.0	63.0
CO	70.0	75.0	60.0	55.0	70.0	45.0	40.0	42.5	90.0	95.0	72.5	110.0	110.0	37.5	80.0	65.0	55.0
ZN	22.0	20.0	18.0	17.0	23.0	19.0	20.0	19.5	23.0	24.0	26.5	29.0	24.0	20.0	24.0	23.0	19.0
CR	80.0	100.0	30.0	85.0	30.0	120.0	90.0	90.0	360.0	160.0	260.0	340.0	310.0	122.5	240.0	105.0	95.0
FE	14.3	23.5	15.5	13.0	14.0	21.0	17.0	17.0	19.5	12.5	25.0	37.0	37.5	14.9	30.5	13.8	13.5
TI	2350.0	2150.0	2550.0	2400.0	2700.0	2400.0	2550.0	2375.0	2100.0	2200.0	2100.0	2500.0	2400.0	2350.0	2700.0	3150.0	3050.0
MN	320.0	230.0	260.0	230.0	440.0	200.0	230.0	260.0	870.0	360.0	410.0	330.0	330.0	150.0	270.0	380.0	280.0
S	70.0	155.0	78.0	195.0	75.0	120.0	30.0	125.0	-	-	-	-	-	-	190.0	-	-
PH	5.5	5.5	5.5	5.4	5.1	5.2	5.3	5.4	5.6	5.0	5.7	6.1	6.0	5.7	5.4	5.6	5.7

	12522	12523	12524	12525	32501	32502	32503	32504	32505	32506	32507	32508	32509	32510	42526	42527	42528
M	1300.0	1200.0	1300.0	1400.0	100.0	130.0	260.0	140.0	420.0	100.0	160.0	220.0	280.0	400.0	1200.0	1100.0	1000.0
NI	185.0	47.5	30.0	135.0	400.0	700.0	600.0	600.0	450.0	700.0	700.0	900.0	950.0	450.0	20.0	25.0	25.0
CU	65.0	100.0	290.0	104.0	35.0	100.0	92.0	14.0	80.0	62.0	42.0	62.0	68.0	41.0	14.0	19.0	16.0
CO	60.0	20.0	35.0	35.0	65.0	95.0	75.0	100.0	65.0	75.0	75.0	90.0	105.0	50.0	10.0	15.0	10.0
ZN	19.0	11.5	14.0	15.0	133.0	80.0	97.0	97.0	102.0	68.0	71.0	83.0	79.0	77.0	27.0	33.0	31.0
CR	200.0	77.5	50.0	95.0	1550.0	1100.0	1100.0	750.0	1100.0	1500.0	1900.0	2000.0	2400.0	1250.0	20.0	15.0	30.0
FE	24.0	7.4	5.8	9.4	5.4	7.2	6.3	10.0	5.6	5.7	5.3	7.0	7.0	4.6	.5	1.5	.5
TI	2350.0	2950.0	2750.0	2400.0	3650.0	2550.0	2800.0	3350.0	3500.0	1700.0	1500.0	2050.0	1650.0	2350.0	1300.0	1050.0	1050.0
MN	200.0	140.0	280.0	230.0	710.0	1000.0	1000.0	1040.0	760.0	900.0	550.0	1120.0	1120.0	630.0	90.0	130.0	90.0
S	-	-	-	-	30.0	40.0	30.0	75.0	60.0	65.0	75.0	36.0	120.0	180.0	-	-	-
PH	5.5	5.2	5.2	5.7	6.0	6.3	6.1	5.9	6.1	6.3	6.6	6.4	6.5	6.5	4.3	4.4	4.2

	42523	42530	42531	42532	42533	42534	42535	42536	42537	52509	52508	52507	52506	52505	52503	52501	72501
M	900.0	800.0	700.0	600.0	500.0	400.0	300.0	200.0	100.0	100.0	450.0	600.0	700.0	800.0	700.0	900.0	100.0
NI	85.0	55.0	120.0	105.0	175.0	145.0	160.0	125.0	155.0	1775.0	2200.0	1750.0	1150.0	1250.0	135.0	500.0	145.0
CU	47.0	31.0	42.0	44.0	30.0	62.0	63.0	59.0	65.0	235.0	175.0	138.0	143.0	146.0	72.0	136.0	28.0
CO	30.0	35.0	190.0	120.0	75.0	90.0	90.0	50.0	65.0	175.0	225.0	170.0	110.0	135.0	45.0	70.0	55.0
ZN	94.0	80.0	147.0	133.0	133.0	122.0	117.0	85.0	120.0	192.5	160.0	125.0	100.0	112.0	45.0	58.0	30.0
CR	90.0	50.0	75.0	80.0	105.0	70.0	90.0	80.0	90.0	3700.0	2250.0	1400.0	850.0	1300.0	200.0	300.0	70.0
FE	2.2	4.1	16.5	11.1	3.6	3.6	4.1	2.8	4.3	19.0	16.0	11.9	11.5	10.8	5.6	6.9	2.4
TI	1200.0	1500.0	750.0	450.0	900.0	950.0	1950.0	1150.0	1100.0	2450.0	2350.0	2250.0	2900.0	2350.0	2050.0	2050.0	750.0
MN	170.0	220.0	1180.0	970.0	350.0	500.0	410.0	210.0	340.0	1260.0	1760.0	1300.0	990.0	1360.0	790.0	680.0	960.0
S	-	-	-	-	-	-	-	-	-	60.0	45.0	135.0	170.0	-	130.0	50.0	-
PH	4.0	3.9	3.9	4.5	4.6	4.7	4.6	4.2	4.5	6.4	6.5	7.3	6.2	7.1	6.2	7.0	6.4

	72506	72508	72509	72510	72511	72512	72513	72516	72519	72519	72520	72521	72522	72523	72525	72527	72547
M	600.0	800.0	900.0	1000.0	1100.0	1200.0	1300.0	1500.0	1600.0	1900.0	2000.0	2100.0	2200.0	2300.0	300.0	2700.0	3000.0
NI	140.0	175.0	170.0	140.0	115.0	175.0	150.0	165.0	190.0	150.0	190.0	155.0	135.0	125.0	125.0	120.0	90.0
CU	40.0	64.0	54.0	36.0	29.0	57.5	40.0	46.0	57.0	38.0	52.0	45.0	37.0	32.5	34.0	33.0	28.0
CO	50.0	45.0	50.0	40.0	35.0	52.5	55.0	55.0	60.0	5.0	62.0	45.0	45.0	45.0	45.0	45.0	40.0
ZN	30.0	40.0	30.0	32.0	26.0	34.5	33.0	40.0	47.0	43.0	49.0	46.0	38.0	42.0	41.0	43.0	46.0
CR	70.0	80.0	90.0	80.0	40.0	92.5	95.0	115.0	55.0	190.0	140.0	110.0	80.0	77.5	80.0	90.0	45.0
FE	2.4	3.0	2.8	2.3	2.0	2.8	2.8	3.8	4.1	6.1	4.5	4.1	3.5	3.5	3.9	4.2	3.1
TI	750.0	700.0	600.0	750.0	650.0	650.0	900.0	950.0	950.0	1000.0	1150.0	1600.0	1200.0	1375.0	1150.0	1650.0	2100.0
MN	710.0	730.0	770.0	640.0	530.0	695.0	730.0	780.0	360.0	630.0	900.0	620.0	590.0	635.0	590.0	630.0	560.0
S	-	-	-	-	-	-	-	-	-	-	-	-	-	-	-	-	-
PH	-	-	-	6.5	-	-	-	-	-	-	-	7.4	-	-	-	7.3	7.7

DIPLORYNCHUS AND COMBRETUM LEAVES

	28925	28926	28927	28928	28929	28930	29901	29902	29903	29909	29912	29914	29917	29919	29921	29924	29925
M	400.0	450.0	500.0	550.0	600.0	650.0	0	50.0	100.0	240.0	270.0	290.0	320.0	340.0	400.0	550.0	600.0
NI	6.5	9.5	4.9	9.5	11.1	8.5	4.7	7.7	49.0	93.4	107.8	65.5	441.6	124.2	184.1	3.3	6.4
CU	9.2	5.9	10.1	6.5	10.9	9.6	4.7	8.1	2.7	4.5	4.0	6.3	5.7	3.3	2.6	6.3	5.3
CO	.8	.9	.7	.7	.8	.4	1.2	1.5	1.6	1.8	2.7	1.4	10.5	2.2	2.1	1.6	1.8
ZN	27.1	28.4	25.7	20.6	27.9	26.7	19.3	27.4	23.1	31.3	34.3	35.6	43.2	26.7	57.6	27.9	33.3
CR	8.1	3.9	7.4	3.0	5.6	8.0	11.8	22.0	16.4	15.1	17.8	11.7	43.0	12.8	21.2	4.7	6.0
FE	92.1	85.7	172.9	171.3	133.7	272.6	316.1	685.8	283.9	379.6	411.7	234.0	465.6	226.9	302.1	274.8	500.0
MN	21.7	27.8	49.4	26.9	47.4	50.8	117.9	119.1	370.4	361.5	377.9	168.5	521.5	186.4	122.7	139.7	757.5

	59901	59902	59903	59904	59905	59906	59907	59908	59909	59910	59911	59912	59913	59914	59915	59916	59917
M	0	50.0	60.0	70.0	80.0	90.0	100.0	110.0	120.0	130.0	140.0	150.0	170.0	190.0	200.0	240.0	370.0
NI	8.1	3.8	6.9	5.2	4.0	12.8	5.2	23.9	29.3	19.1	28.5	14.7	22.3	17.7	23.6	25.5	19.2
CU	5.3	4.2	4.4	3.6	5.9	3.0	6.6	4.3	2.3	2.2	2.6	3.3	3.7	2.5	3.7	2.7	4.3
CO	2.0	1.1	1.6	1.4	1.3	1.5	1.7	1.8	1.1	1.5	1.4	.9	1.0	1.6	1.1	1.9	2.1
ZN	20.5	14.3	12.5	16.5	15.1	13.5	18.0	15.9	15.4	15.5	9.5	14.4	7.4	10.6	15.8	18.6	14.2
CR	7.4	6.5	10.9	6.2	5.4	11.3	17.9	5.1	4.3	11.2	5.7	7.1	8.3	12.4	10.5	11.6	14.2
FE	215.5	138.7	272.0	186.9	290.7	240.1	297.7	171.6	223.6	194.7	171.9	152.6	169.4	199.7	244.2	231.9	224.2
MN	410.0	273.2	641.0	335.3	188.4	255.1	363.1	673.9	252.9	220.9	194.8	134.3	330.5	347.7	220.5	247.4	291.8

	59918	59919
M	430.0	510.0
NI	14.7	4.9
CU	3.3	6.6
CO	1.0	1.8
ZN	12.2	15.9
CR	7.6	8.8
FE	217.7	265.1
MN	227.9	379.9

COARSE FRACTIONS OF SEDIMENTS OF STREAMS DRAINING INTRUSIVES

	12205	12206	12207	12208	12209	12210	12211	12212	32201	32202	32203	32204	32205	32206	32207	32208	32209
M	100.0	200.0	300.0	400.0	500.0	600.0	700.0	800.0	100.0	180.0	260.0	340.0	420.0	100.0	160.0	220.0	280.0
NI	700.0	655.0	525.0	525.0	235.0	335.0	150.0	125.0	207.5	395.0	230.0	3.5	18.0	350.0	500.0	610.0	525.0
CU	290.0	202.0	305.0	15	143.0	220.0	118.0	137.0	43.0	60.0	46.0	103.0	29.0	13.0	20.0	31.0	32.0
FE	18.7	29.0	16.8	20.6	13.0	10.5	9.5	6.4	3.8	5.5	4.3	7.0	3.3	2.7	3.5	4.2	4.3
MN	215.0	350.0	235.0	240.0	250.0	175.0	155.0	170.0	515.0	690.0	650.0	810.0	340.0	400.0	500.0	1130.0	580.0

	32210	52201	52215	52216	52217	82211	82212	82213	82214	82215	82216
M	400.0	900.0	800.0	700.0	600.0	200.0	300.0	400.0	500.0	800.0	850.0	1150.0
NI	225.0	190.0	1970.0	1660.0	2000.0	1835.0	1800.0	3320.0	3060.0	600.0	875.0	2450.0
CU	18.0	60.0	110.0	114.0	98.0	1225.0	1000.0	1340.0	2190.0	1270.0	280.0	220.0
FE	2.6	5.3	14.5	16.0	13.9	9.7	9.1	13.0	13.8	15.3	9.6	7.6
MN	600.0	1225.0	6200.0	4460.0	5250.0	2010.0	1350.0	2100.0	1370.0	2100.0	1310.0	1790.0

SEDIMENTS OF STREAMS DRAINING INTRUSIVES

	72549	72550	72552	72553	82501	82502	82503	82504	82505	82506	82516	82517	82519	82520	82521	82535	82536
M	3100.0	3300.0	3500.0	3600.0	200.0	300.0	400.0	500.0	600.0	450.0	1150.0	1250.0	1450.0	1550.0	1650.0	1750.0	1850.0
NI	85.0	75.6	85.0	65.0	330.0	475.0	500.0	6300.0	50.0	141.0	3750.0	2600.0	4500.0	3400.0	1400.0	1500.0	3000.0
CU	39.0	23.0	29.0	15.0	1100.0	530.0	833.0	540.0	600.0	790.0	460.0	220.0	790.0	930.0	220.0	215.0	870.0
CO	70.0	35.0	35.0	30.0	200.0	185.0	180.0	190.0	175.0	110.0	135.0	110.0	190.0	150.0	105.0	95.0	280.0
ZN	64.0	37.0	48.0	35.0	670.0	265.0	240.0	290.0	420.0	220.0	220.0	220.0	460.0	330.0	180.0	200.0	139.0
CR	35.0	90.0	45.0	85.0	1200.0	1005.0	1400.0	1800.0	2100.0	900.0	900.0	1200.0	1200.0	1350.0	1150.0	1000.0	1000.0
FE	6.5	4.4	3.4	3.7	7.3	10.0	8.6	9.8	11.5	7.0	7.0	7.5	7.9	7.1	7.0	6.8	9.3
TI	2500.0	1900.0	2350.0	2200.0	1000.0	800.0	650.0	500.0	700.0	1600.0	1100.0	1400.0	1300.0	1700.0	1500.0	1650.0	1500.0
MN	420.0	500.0	570.0	330.0	1550.0	1655.0	1390.0	1180.0	1040.0	122.0	8400.0	4800.0	9900.0	2900.0	1650.0	1700.0	8000.0
S	-	-	-	-	235.0	240.0	305.0	-	350.0	130.0	-	85.0	-	-	-	-	-
PH	-	-	-	-	6.2	6.5	6.8	7.0	7.0	6.2	-	7.1	-	7.2	-	-	6.7

	82537	82539				82522	82523	82524	82525	82526	82527
M	1950.0	2150.0				400.0	500.0	400.0	300.0	200.0	110.0
NI	1900.0	1425.0				260.0	300.0	2550.0	3250.0	3300.0	3400.0
CU	430.0	360.0				124.0	90.0	113.0	124.0	137.0	90.0
CO	230.0	137.5				70.0	70.0	160.0	195.0	190.0	185.0
ZN	120.0	136.5				260.0	104.0	142.0	210.0	147.0	142.0
CR	800.0	900.0				450.0	280.0	5.0	7000.0	7000.0	7500.0
FE	11.5	7.3				7.3	7.3	12.8	16.0	16.5	16.5
TI	1900.0	2225.0				1800.0	1900.0	1750.0	1700.0	1500.0	1050.0
MN	5300.0	910.0				1630.0	1500.0	1700.0	1650.0	1770.0	1330.0
S	-	-				-	-	-	-	-	-
PH	-	6.6				6.5	6.3	6.8	6.2	6.5	6.5

REGIONAL STREAM SEDIMENTS

	11429	11430	11431	11432	11433	11434	11435	11436	11437	11438	11439	11440	11441	11540	11541	11542	11543
FE	1.3	1.5	1.6	1.5	2.0	1.1	1.4	1.1	1.2	1.7	1.4	1.9	4.6	4.0	4.4	7.2	8.2
CU	20.9	28.1	23.1	25.9	31.9	23.0	26.9	17.4	21.1	20.7	28.9	22.5	1.3.3	126.5	78.7	18..6	177.5
PB	6.3	6.9	7.0	8.1	11.3	5.2	6.3	5.5	8.6	7.9	6.3	9.8	11.4	12.5	17.1	12.2	10.9
ZN	12.3	22.3	28.3	37.6	27.3	12.3	21.0	13.1	19.5	17.0	21.2	22.5	57.7	113.1	110.7	121.0	61.5
MO	.7	2.2	2.0	1.4	1.7	1.7	2.3	1.2	14.4	1.7	1.4	.6	1.6	.4	.6	1.6	.4
V	52.3	62.4	63.9	72.7	78.9	50.8	60.9	43.0	69.5	66.8	56.8	73.4	234.4	231.9	199.1	294.2	462.5
CO	7.5	6.8	8.9	3.5	7.1	7.1	10.8	6.4	9.6	5.7	3.7	12.5	32.3	27.9	25.8	24.6	30.1
NI	12.1	14.3	15.6	15.5	17.6	15.1	20.1	15.7	14.8	13.9	14.6	14.4	33.5	108.8	68.1	110.3	163.8
CR	27.5	33.6	33.2	37.7	43.8	29.3	40.2	26.9	26.8	19.7	23.9	26.9	51.4	159.4	135.9	170.5	153.1
GA	14.1	9.7	11.4	14.8	13.8	13.9	13.1	11.3	14.1	12.1	15.4	15.3	16.8	23.9	25.4	22.0	25.4
SN	13.0	9.5	8.1	12.9	18.2	7.1	9.6	9.6	15.4	1.0	13.5	20.4	16.6	6.7	9.7	14.0	17.7
TI	4178.3	5194.4	6564.1	6734.4	4585.0	3469.7	3105.3	1743.5	6466.7	3811.0	4873.8	4572.7	11465.3	7377.0	7268.2	14139.2	13224.7
BE	1.0	.6	0	0	1.2	1.2	2.3	2.9	0	2.8	.8	4.1	0	2.3	.9	0	0
MG	.4	.3	.6	.0	.4	.4	.5	0	.4	.4	.0	.6	2.7	1.4	1.2	2.0	1.8
CA	.2	.2	.2	.4	.3	.2	.2	.1	.3	.2	.2	.5	.5	.4	.4	1.0	.9
SR	36.3	47.5	57.4	77.7	45.6	35.3	36.2	17.1	35.0	23.4	38.3	54.5	37.2	28.2	36.6	51.9	35.2
BA	236.7	311.3	461.2	423.6	331.9	243.9	253.5	173.9	256.5	226.6	276.2	313.7	306.3	295.2	276.9	286.6	196.6
K	3.5	2.7	3.4	3.3	3.4	3.2	3.4	2.5	3.0	3.3	3.3	4.2	4.2	2.7	2.6	2.4	2.2
LI	.7	.2	.2	2.3	.2	1.6	2.5	2.6	1.7	1.5	3.7	1.6	6.1	60.1	64.2	29.2	19.7
AL	8.3	7.2	7.5	13.4	7.6	7.3	6.9	5.3	6.6	5.8	6.4	8.3	9.0	12.6	11.3	13.0	10.7
SC	3.7	4.2	3.7	4.6	5.7	2.9	3.7	2.0	3.8	5.1	3.2	5.2	13.3	8.9	7.2	14.8	12.1
SI	38.3	37.8	33.9	36.1	43.9	32.5	35.0	33.9	35.3	41.0	30.7	39.9	39.5	26.0	23.9	31.7	38.3
MN	70.4	145.4	138.5	124.7	122.2	97.9	111.9	60.6	113.0	96.6	108.1	138.6	374.9	461.2	442.6	424.9	438.6

	11544	11545	11546	11547	11548	11549	11553	11554	11555	11556	11557	11558	11559	11560	11561	11562	11563
FE	8.1	14.6	11.4	19.5	4.5	5.5	2.9	3.8	4.4	4.7	2.5	2.1	1.4	1.6	2.5	1.6	1.7
CU	73.7	92.8	195.1	69.0	137.0	118.7	94.1	80.8	263.9	270.5	165.3	135.3	19.3	59.9	82.2	59.8	20.8
PB	15.5	10.7	9.7	13.9	5.6	4.8	7.1	11.0	9.1	6.6	9.4	7.3	4.6	8.1	13.5	8.1	6.4
ZN	157.2	95.7	71.5	94.0	23.3	28.2	30.9	36.4	57.9	28.6	43.8	18.0	6.7	23.5	30.9	16.3	9.2
MO	2.0	.7	5.3	.3	21.6	.5	.9	2.7	.6	.6	2.1	.9	1.1	1.8	.9	1.3	1.2
V	229.7	1338.1	315.2	1422.1	168.6	193.1	128.4	114.3	140.2	159.4	92.0	105.3	42.5	56.5	95.5	64.3	65.1
CO	30.8	25.6	25.4	25.9	22.3	18.9	20.2	19.0	29.3	33.9	16.2	25.1	7.7	8.3	13.1	9.5	7.8
NI	168.3	197.1	113.9	161.0	75.3	65.5	29.9	36.0	46.9	43.6	20.5	30.5	16.9	16.6	17.2	14.7	12.7
CR	166.5	248.3	167.6	270.2	141.2	159.7	86.8	99.0	117.7	133.5	60.8	82.3	34.7	55.2	64.8	55.1	51.1
GA	18.5	43.9	27.5	40.4	22.1	19.0	15.1	12.7	21.7	17.8	14.9	15.6	9.8	11.8	14.7	10.5	10.9
SN	11.5	11.9	12.9	22.9	11.6	7.7	10.5	16.6	19.7	18.3	15.6	13.2	14.9	1.5	21.5	9.5	9.9
TI	8775.3	44935.5	11813.3	75435.1	5926.8	8294.4	11890.2	8416.1	7293.7	9915.4	9970.5	5480.8	4164.3	3938.9	6252.1	4152.4	5251.4
BE	2.0	0	0	0	.5	.5	0	0	.1	0	0	.2	1.0	1.5	0	1.0	.0
MG	1.1	1.3	1.7	1.4	2.0	1.5	1.3	1.5	1.7	1.5	.9	1.0	0	.3	.4	.3	.4
CA	.5	.6	3.2	.4	.5	.5	.6	.4	.3	.3	.2	.2	.3	.2	.2		
SR	37.2	71.1	25.6	38.2	27.5	23.3	34.1	16.4	20.1	20.7	27.5	26.4	13.8	21.8	21.1	19.0	29.3
BA	347.1	328.3	223.6	236.6	211.7	146.9	266.6	219.4	312.7	243.5	380.1	300.1	203.8	274.5	250.4	242.8	343.5
K	2.0	1.6	2.2	1.0	1.9	1.5	2.3	2.0	2.5	2.4	3.0	2.6	2.6	3.3	3.3	2.6	3.6
LI	24.1	.2	20.0	.2	34.1	74.5	9.0	2.7	19.2	10.4	2.6	11.8	2.1	.3	.5	.2	.2
AL	12.4	10.6	11.7	9.6	11.5	8.9	9.5	9.4	11.7	9.5	13.2	7.8	4.9	6.6	7.4	6.2	7.2
SC	12.2	29.2	14.3	34.0	8.9	7.5	8.3	9.2	12.1	8.3	7.2	4.8	1.3	4.3	5.6	4.1	4.6
SI	43.9	14.4	33.8	11.3	27.4	30.4	33.0	45.7	36.5	33.7	37.9	27.7	31.1	38.0	43.9	36.3	31.8
MN	847.7	463.0	399.5	1702.1	413.6	436.7	299.4	237.6	290.4	205.1	207.7	318.9	95.3	98.7	171.9	137.6	90.2

REGIONAL STREAM SEDIMENTS

	11014	11015	11016	11017	11018	11019	11020	11021	11022	11023	11024	11025	11026	11027	11028	11029	11030
FE	2.7	4.6	5.2	5.5	4.8	4.4	3.3	4.5	5.1	4.3	3.3	5.1	5.7	6.1	5.1	4.1	2.7
CU	28.3	42.9	79.9	54.2	67.9	47.4	51.5	49.0	64.5	39.8	45.0	57.3	124.5	118.0	110.3	52.6	43.7
PB	16.9	15.6	15.4	17.3	19.8	20.0	16.7	19.2	25.1	15.6	19.5	27.9	17.9	11.1	14.5	21.0	16.4
ZN	81.2	89.6	69.7	129.8	195.8	153.3	80.8	114.5	171.3	97.8	114.6	206.0	130.7	72.2	96.8	98.7	78.0
MO	1.0	.8	1.1	.8	1.5	1.7	.9	.7	1.0	1.2	1.1	2.2	1.0	.6	.8	1.3	1.2
V	116.3	175.9	223.2	167.2	233.6	182.7	158.8	145.5	191.6	146.8	156.4	249.9	250.8	231.0	214.3	173.9	195.7
CO	13.5	17.9	23.5	21.0	27.5	21.6	18.4	17.6	40.3	15.3	18.8	25.1	28.8	22.1	23.7	25.6	21.0
NI	32.3	51.6	82.7	65.1	62.3	59.1	54.6	46.5	79.6	41.5	58.1	68.0	92.3	95.1	84.3	39.7	31.3
CR	93.7	127.1	133.2	114.8	119.4	114.4	107.9	107.8	136.2	90.2	103.0	155.5	146.4	144.7	141.9	117.5	156.7
GA	14.1	14.7	16.1	18.7	22.2	19.2	18.4	17.6	25.8	14.6	16.9	23.2	25.9	24.1	19.8	18.9	24.8
SN	14.7	11.0	13.2	3.1	13.0	16.1	9.0	9.7	11.6	12.9	10.8	21.0	16.0	8.2	10.3	11.7	10.6
TI	5995.7	11900.1	10726.5	6731.2	13133.3	12673.0	8824.5	6318.5	7072.3	10059.3	7647.2	15034.9	11781.0	11046.5	8494.6	8890.2	3958.1
BE	.7	0	0	.2	0	0	0	1.1	2.2	0	0	0	0	0	1.6	0	3.6
MG	.3	.3	.3	.6	1.3	1.2	1.3	.8	1.4	.4	1.0	1.2	1.6	1.2	1.1	.8	.4
CA	.7	.8	.6	.6	.3	.3	.6	.6	.5	.9	.6	.9	.6	.4	.5	.5	.3
SR	53.3	47.4	38.1	32.5	52.6	56.0	43.1	65.9	29.7	49.6	37.7	58.7	37.5	24.8	36.0	31.9	22.2
BA	183.4	244.1	315.0	192.9	317.9	257.1	237.3	271.9	242.8	242.4	186.1	316.6	314.8	246.3	340.9	257.3	275.7
K	1.3	1.7	2.3	1.6	2.4	2.0	2.3	2.4	2.9	1.3	1.9	2.9	2.4	2.3	2.4	2.6	2.8
LI	17.2	18.9	35.5	27.8	24.3	24.4	26.7	32.1	52.0	16.0	27.9	31.1	36.4	39.2	36.7	17.6	19.2
AL	9.3	9.9	10.9	9.6	14.3	10.7	10.6	12.3	12.7	10.8	9.4	13.4	13.9	12.1	11.8	9.7	11.0
SC	6.3	7.6	8.9	6.2	12.1	8.9	7.7	8.6	9.9	9.0	6.5	9.8	12.0	9.4	11.9	9.1	4.8
SI	41.3	31.4	40.9	34.6	39.3	39.5	39.5	43.8	49.1	45.9	35.1	36.2	38.7	32.4	38.8	33.8	30.0
MN	298.3	388.6	453.1	381.9	453.3	461.4	399.8	435.1	1032.1	405.2	391.7	477.9	1049.9	394.5	442.9	450.5	1048.4

	11031	11032	11033	11034	11035	11036	11037	11038	11039	11040	11041	11042	11418	11419	11420	11421	11422
FE	3.1	3.3	5.4	4.3	5.3	5.3	4.5	5.4	5.2	3.3	3.2	6.2	2.1	1.6	2.2	.7	.9
CU	53.9	52.2	72.7	43.1	53.8	47.8	52.5	46.4	79.2	66.2	53.9	73.9	30.1	16.6	24.9	14.2	16.7
PB	20.5	14.9	16.5	15.4	15.5	16.7	10.7	15.4	13.3	8.6	8.7	15.4	7.5	8.2	8.9	5.7	5.7
ZN	98.3	61.1	95.8	85.1	121.3	97.1	85.6	109.8	97.4	49.6	33.3	91.2	27.9	15.4	30.9	19.3	11.3
MO	1.3	.4	.2	.9	1.2	.8	.8	1.7	.8	.2	.6	.3	1.5	.6	1.5	1.2	.9
V	161.2	154.3	241.2	165.2	195.6	171.1	180.2	155.3	215.3	161.7	145.1	221.7	90.6	77.6	89.0	42.7	50.4
CO	16.5	20.0	23.9	13.6	25.9	22.7	21.2	21.6	22.9	16.6	18.2	20.3	13.7	5.2	12.2	5.2	7.2
NI	37.3	44.5	72.7	42.7	61.6	49.8	51.9	48.1	73.1	51.8	53.5	71.6	21.5	13.1	17.7	12.1	13.3
CR	121.3	111.3	103.0	122.0	156.9	137.7	142.1	134.6	154.3	123.1	114.1	159.3	46.2	28.7	40.8	21.1	23.2
GA	15.2	17.5	26.2	14.7	24.9	16.7	18.6	21.4	25.3	20.0	12.8	28.8	15.0	11.0	13.3	11.1	12.0
SN	13.5	8.6	15.0	9.6	11.0	17.3	5.5	10.5	8.9	4.3	8.7	8.6	11.5	12.3	11.8	7.1	10.3
TI	11355.5	7250.8	7921.8	7737.6	7350.0	8815.8	6516.4	7473.8	6199.0	5335.7	5737.0	8573.1	7262.4	2926.3	6929.9	3974.9	3126.1
BE	.3	.3	.5	1.9	.3	0	2.6	1.4	1.6	2.3	.3	.1	.7	1.6	0	.7	1.6
MG	.7	.6	.9	.5	.0	.3	.6	.6	.0	.8	.0	1.4	.6	.3	.0	.3	.4
CA	.3	.5	.5	.6	.5	.8	.4	.5	.3	.3	.4	.6	.3	.3	.3	.2	.2
SR	68.1	37.2	30.5	43.2	34.0	54.5	26.9	24.0	22.3	27.1	30.6	43.3	45.9	53.5	54.8	42.4	34.2
BA	222.1	229.4	285.5	289.3	321.8	323.6	294.5	256.8	261.5	275.6	156.1	39..7	355.0	319.7	407.5	243.9	218.9
K	2.0	1.8	2.5	1.5	2.3	1.3	2.0	1.9	2.3	2.2	1.1	3.1	3.4	3.6	3.6	3.1	2.9
LI	27.3	29.5	37.9	23.0	53.4	27.5	45.4	32.8	69.4	58.1	23.0	70.3	3.9	.2	3.5	.2	1.1
AL	9.3	10.2	13.2	9.5	12.8	12.4	10.9	11.6	17.2	11.3	6.6	13.2	9.4	7.5	10.3	6.6	6.3
SC	7.3	9.6	10.2	3.6	3.2	12.1	6.7	3.6	7.3	7.8	5.4	9.6	4.7	4.4	5.9	3.4	2.6
SI	34.5	31.4	37.1	45.9	29.0	43.3	30.2	34.2	25.5	22.1	27.4	31.5	36.8	42.4	46.7	32.3	33.4
MN	373.2	382.7	453.2	451.1	463.1	476.5	435.1	423.1	375.8	316.8	308.2	493.2	152.2	164.9	166.7	58.6	106.2

REGIONAL STREAM SEDIMENTS

	31144	31145	31146	31147	31148	31149	31158	31159	31161	31162	31163	31164	31165	31166	31167	31168	31169
FE	3.3	4.9	4.9	4.5	4.3	4.0	4.7	6.2	7.3	6.5	3.8	4.2	2.7	4.7	3.5	3.1	10.7
CU	52.3	58.5	54.9	37.6	35.9	45.6	54.3	25.6	49.2	61.0	46.2	63.7	38.8	68.4	29.7	46.7	45.7
PB	25.4	26.8	29.4	29.0	13.8	28.7	16.2	7.8	10.6	16.1	31.0	31.6	25.7	29.2	32.1	41.5	30.6
ZN	70.5	122.6	145.8	136.7	35.7	144.3	88.2	45.3	96.0	89.5	169.6	134.8	79.4	194.4	133.6	90.5	257.2
MO	.7	1.4	1.3	1.1	.0	1.4	.3	.0	.0	.1	2.2	1.5	.8	1.5	2.1	.6	.0
V	164.3	234.6	225.1	179.4	166.6	168.5	117.9	77.2	127.3	152.1	184.2	156.4	125.2	167.1	203.1	97.5	215.3
CO	14.3	20.3	17.7	27.3	59.2	21.3	48.4	76.4	71.4	7..7	20.2	20.5	18.5	23.6	21.3	16.2	65.6
NI	42.3	43.4	63.7	216.4	807.2	93.8	603.4	1037.5	733.9	696.3	122.2	61.6	149.7	133.2	123.1	48.2	827.3
CR	122.3	158.9	429.9	663.2	1475.3	369.4	1557.6	1849.4	1955.8	1740.9	918.9	186.9	539.1	439.1	475.8	226.5	2939.9
GA	15.3	18.2	19.3	21.2	9.6	18.2	15.2	5.4	17.8	13.9	17.9	19.9	14.4	21.9	15.7	24.0	21.9
SN	7.5	9.5	24.5	13.5	2.2	9.4	11.3	13.6	16.7	26.5	14.7	7.0	6.8	8.4	11.4	10.5	54.0
TI	18734.9	20007.5	36300.9	16154.6	4058.5	15029.5	7916.8	1570.7	13137.3	12145.8	34793.3	15533.0	13569.0	15600.9	15147.3	7177.1	12631.1
BE	0	0	0	0	.3	0	0	1.3	0	0	0	0	0	0	0	0	0
MG	1.4	1.5	2.0	3.3	4.4	2.1	4.8	8.5	7.3	5.2	2.8	1.3	2.4	2.2	2.2	.9	4.7
CA	2.3	2.8	5.5	2.4	1.0	2.8	1.5	1.1	2.1	2.4	6.2	2.3	2.9	2.8	2.4	1.3	3.1
SR	231.3	136.1	338.9	135.4	51.9	187.7	77.1	15.9	36.5	64.7	414.9	193.5	181.8	139.6	151.2	136.9	135.7
BA	631.3	533.7	633.1	503.8	263.6	605.4	242.9	53.2	143.1	233.3	753.0	528.5	516.8	576.8	471.5	406.4	257.1
K	.3	3.4	2.9	3.7	2.3	3.4	2.2	.4	.6	1.0	2.8	2.9	3.1	3.1	3.4	3.8	2.4
LI	8.4	6.7	.2	2.1	4.7	7.3	9.5	.2	.2	.2	.2	10.5	6.7	15.1	1.2	26.4	3.2
AL	11.2	10.5	11.4	3.3	3.3	10.7	5.9	1.1	5.0	6.2	13.7	11.5	8.5	12.1	8.4	12.8	13.0
SC	10.3	11.2	15.6	13.9	5.1	12.0	6.2	5.3	15.3	17.6	21.3	10.3	9.0	11.0	10.1	7.0	10.7
SI	23.0	30.3	23.6	33.3	26.1	30.3	19.0	16.9	18.9	21.0	26.0	28.5	22.9	32.4	34.9	24.6	26.5
MN	478.5	955.1	1914.6	923.5	850.7	1031.5	1185.7	1211.3	1939.6	2356.9	1472.9	1162.3	467.3	928.2	484.2	426.6	1581.5

	31173	31172	31173	31174	31175	31176	31238	31289	31290	31291	31292	31293	31294	31295	31296	31297	31298
FE	7.2	8.1	5.1	3.6	5.5	4.3	4.3	3.1	5.1	3.8	3.5	3.2	2.8	7.1	5.1	3.7	3.9
CU	48.5	63.3	59.7	57.5	71.3	43.4	73.9	46.5	99.5	51.7	33.6	48.5	36.6	116.2	164.9	44.1	70.7
PB	28.3	17.0	26.7	33.7	33.2	25.3	33.4	44.6	35.3	36.6	32.3	36.9	39.9	33.2	29.4	37.7	33.4
ZN	177.5	109.6	135.6	87.6	149.0	92.1	144.2	89.6	127.5	109.3	65.9	111.8	104.4	159.7	186.9	153.0	110.4
MO	.4	.2	.4	.3	.8	.7	.2	1.3	1.5	.3	.2	1.2	1.5	.6	1.7	2.2	1.6
V	249.5	109.6	175.9	125.4	148.6	139.8	134.4	144.7	145.7	119.5	142.3	161.8	165.2	212.1	187.5	156.1	173.4
CO	22.3	91.3	23.5	21.1	19.6	23.5	19.9	15.6	23.0	16.2	15.4	16.3	15.7	30.5	22.9	17.2	21.7
NI	111.3	1340.6	197.8	115.5	77.8	125.4	122.9	27.5	85.7	49.5	31.3	30.0	31.4	80.1	58.2	33.8	51.4
CR	1157.0	2184.4	1656.8	469.0	223.3	650.5	757.3	21.5	203.2	209.1	96.6	88.5	109.8	190.4	152.1	145.5	151.2
GA	26.5	14.2	17.7	19.7	23.2	19.6	26.3	21.5	26.6	24.0	18.9	20.9	24.8	29.6	24.6	20.9	27.8
SN	30.9	14.1	23.8	9.7	11.1	11.2	11.2	7.7	6.2	9.1	7.7	7.4	6.5	17.0	12.5	11.2	15.0
TI	42655.3	2761.9	30719.0	9538.2	12426.7	19756.3	12333.8	15294.5	11015.9	15407.9	14460.6	11779.3	8068.7	15889.0	14340.1	18702.5	16709.2
BE	0	1.9	0	0	0	0	0	5	0	0	0	0	1.4	0	0	0	.0
MG	5.0	4.9	3.2	2.2	2.7	2.3	2.9	.6	1.6	1.7	1.0	1.0	.6	2.0	2.0	1.5	1.7
CA	9.7	1.4	5.4	1.3	3.3	3.5	2.8	1.9	2.1	3.8	2.1	1.8	1.1	2.8	2.7	3.1	2.9
SR	488.3	61.2	232.0	174.4	171.8	201.5	329.5	162.2	145.6	255.7	163.5	166.1	119.1	141.9	182.6	271.3	220.7
BA	798.3	139.6	584.5	393.0	441.3	438.6	790.1	527.3	423.7	524.8	411.0	565.1	410.0	419.0	557.1	645.6	620.2
K	2.3	1.5	2.4	3.0	3.9	3.3	3.4	3.6	3.1	3.5	3.4	3.9	3.8	3.5	3.3	3.5	3.3
LI	.2	6.2	4.8	31.4	43.3	4.3	30.2	17.9	61.9	27.2	6.2	10.9	23.3	36.5	32.5	17.1	27.5
AL	14.5	4.2	12.5	13.5	12.9	10.3	14.8	11.7	13.3	13.6	9.8	16.3	12.2	12.4	14.3	13.4	14.4
SC	25.2	4.5	17.0	7.9	12.1	11.2	10.9	7.0	9.0	11.9	7.6	8.1	6.0	12.4	13.2	13.3	10.3
SI	27.3	14.5	22.6	27.5	33.0	32.4	29.3	30.6	23.1	26.4	27.1	30.2	31.5	29.9	29.2	27.3	27.3
MN	2366.2	1007.0	1726.6	457.3	1143.3	1093.8	1057.9	483.0	946.0	459.0	429.3	485.7	482.4	1618.2	1316.4	479.5	1217.9

REGIONAL STREAM SEDIMENTS

	11564	11565	11566	11567	11568	11569	11570	11571	11572	11573	11574	11575	11576	11577	11578	11579	11580
FE	2.2	3.6	5.2	1.8	3.0	3.5	5.0	4.1	6.6	9.7	6.1	4.8	4.5	3.4	3.8	2.5	1.6
CU	47.3	30.6	71.7	39.1	52.8	48.7	50.1	68.8	123.1	158.4	132.9	81.5	100.6	114.5	73.4	61.3	53.6
PB	11.3	9.2	17.0	7.3	5.8	15.5	15.8	12.1	9.7	6.9	9.1	9.3	8.2	11.7	13.4	11.4	6.7
ZN	44.5	70.5	222.6	43.4	61.9	131.3	179.0	116.0	63.3	36.6	66.1	111.6	69.3	48.4	78.0	76.9	34.7
MO	1.7	.3	1.4	1.0	1.3	1.5	1.2	.9	2.4	.8	.4	.8	1.9	.2	1.5	.8	.6
V	72.4	131.1	170.6	92.1	117.4	142.3	165.6	157.2	212.1	661.1	406.4	155.8	143.8	142.8	174.2	132.9	160.4
CO	9.2	14.7	23.2	17.9	15.4	16.6	21.6	19.6	20.0	36.0	27.3	24.4	25.3	24.4	18.8	24.3	14.7
NI	28.1	36.6	54.9	21.5	34.8	42.2	56.3	43.2	51.5	224.0	130.1	47.9	48.8	42.3	75.8	55.6	55.8
CR	88.3	99.9	122.0	67.1	93.4	109.1	146.3	117.0	189.6	165.5	125.3	123.2	110.5	107.4	103.6	87.7	75.1
GA	9.3	15.8	20.4	12.4	13.8	19.9	21.9	15.6	20.0	26.5	22.5	21.2	22.0	20.9	19.0	14.3	10.5
SN	13.2	9.2	13.2	5.8	4.3	7.6	7.7	6.7	14.4	11.1	14.5	9.2	15.9	14.5	12.1	8.0	2.1
TI	5119.2	10443.4	8093.3	9190.0	6837.8	6450.5	7612.0	6229.5	11553.0	19256.2	15674.0	7984.1	5810.5	6206.5	13133.3	6989.3	11558.0
BE	.0	0	0	0	.1	1.0	.8	2.6	0	0	0	0	1.4	.9	0	0	.0
MG	.4	.8	1.0	.6	.7	.9	1.2	1.1	1.8	1.8	1.7	1.4	1.3	1.3	.9	.7	.9
CA	.3	.4	.6	.3	.4	.4	.4	.5	.5	1.1	1.0	.4	.6	.5	.7	.6	.6
SR	14.0	37.0	46.7	24.1	34.4	27.3	30.8	46.3	26.2	53.0	52.3	32.3	29.6	39.2	46.1	42.2	52.9
BA	145.8	267.8	355.7	189.8	295.2	205.0	245.7	322.3	214.3	315.0	365.2	292.3	329.5	350.7	344.6	289.3	359.5
K	.3	1.9	2.0	1.7	2.1	2.0	2.2	2.4	2.6	1.8	2.6	2.3	2.8	3.5	2.7	2.3	1.7
LI	2.8	18.5	42.1	12.4	19.7	36.3	48.7	32.3	16.6	4.0	8.9	32.7	29.1	21.3	22.7	16.6	14.5
AL	5.1	13.5	11.6	5.8	8.0	10.0	13.1	11.7	12.0	14.2	13.5	12.4	12.1	10.6	10.9	9.4	9.0
SC	5.0	7.9	9.3	5.3	5.4	9.1	8.6	11.6	11.7	10.4	14.0	7.6	7.0	7.4	10.0	7.8	11.5
SI	39.4	41.8	40.9	32.8	31.6	34.6	34.5	34.8	35.2	37.0	31.4	30.9	31.6	35.2	32.9	32.6	20.6
MN	350.5	430.2	495.2	298.5	357.7	365.0	428.5	393.9	325.6	465.7	435.4	451.7	402.0	424.7	312.4	390.8	358.1

	11581	11582	11586	11587	11588	11589	11590	11591	11592	11593	11594	11595	11596	11597	11599	11600	31143
FE	4.4	4.6	4.9	4.6	4.4	5.3	5.3	4.7	5.0	5.2	6.8	2.3	5.6	3.3	3.4	2.9	3.3
CU	98.8	102.1	113.3	187.5	157.3	296.3	228.2	60.0	167.6	101.1	17.5	21.9	127.2	22.5	56.1	24.9	50.5
PB	15.0	15.1	5.0	6.9	5.6	9.2	9.6	9.1	9.7	6.4	9.5	7.4	7.9	5.5	8.5	8.4	22.0
ZN	115.2	120.8	17.9	30.7	39.9	28.3	54.8	56.5	56.4	29.1	23.6	13.9	63.8	14.8	23.1	35.5	78.1
MO	1.7	2.0	1.0	1.2	.8	1.4	1.6	1.0	1.9	.8	.9	.5	.5	.9	.7	2.1	.6
V	214.5	182.5	202.3	233.5	152.9	220.7	181.3	135.6	181.6	185.0	297.6	105.8	169.1	118.8	139.0	130.0	202.5
CO	31.0	24.3	31.7	32.2	28.3	46.5	36.8	27.3	20.5	21.4	3.1	6.6	25.3	6.6	18.5	4.2	15.9
NI	95.0	86.3	103.6	99.1	85.5	65.8	130.1	36.0	85.9	90.7	13.4	20.8	78.4	26.1	98.7	20.6	34.9
CR	142.3	129.3	243.3	232.8	172.4	193.8	223.0	125.5	215.7	213.3	187.8	92.0	164.9	97.6	330.9	80.7	126.9
GA	22.7	21.9	22.0	21.6	21.0	18.1	24.2	14.6	20.9	22.7	13.3	10.5	19.0	11.5	13.9	11.1	14.7
SN	11.3	11.0	10.3	10.9	11.1	15.1	15.0	12.2	15.0	2.7	29.1	15.3	16.8	18.1	15.7	18.5	10.1
TI	5885.4	7263.1	6097.0	7687.2	5229.3	12273.0	7628.5	9320.5	9578.8	7997.5	19715.2	8306.1	6475.2	8199.5	7899.3	14866.7	23097.8
BE	4.4	2.7	.2	2.7	1.0	0	0	0	.2	0	0	0	.7	0	0	0	0
MG	1.0	1.1	2.2	1.5	2.2	1.0	1.4	.8	1.8	1.8	.0	.5	2.0	.0	1.5	.5	1.7
CA	.4	.5	.3	.4	.4	.7	.7	.8	.4	.5	.5	.3	.6	.3	.4	.4	4.3
SR	31.5	31.5	19.8	24.8	23.0	32.7	30.5	46.3	34.9	38.0	41.7	36.7	31.6	26.0	31.6	51.9	236.4
BA	392.5	291.5	112.3	143.2	184.3	193.9	218.0	260.8	345.6	256.9	212.5	218.8	236.5	203.4	276.2	229.4	535.1
K	3.0	2.7	1.5	2.0	1.8	1.5	2.2	1.3	2.9	3.2	1.9	2.0	2.5	2.0	3.0	1.5	2.7
LI	35.0	39.3	36.5	37.0	34.3	14.4	31.2	15.5	20.1	21.0	.2	.2	18.5	1.4	10.8	.2	1.5
AL	12.3	12.1	9.1	8.9	10.2	9.4	10.1	11.2	11.6	5.9	7.2	7.3	11.3	6.9	7.2	8.7	10.0
SC	9.2	10.0	5.0	6.2	5.8	8.9	8.0	11.2	10.0	9.3	10.3	5.1	8.6	5.1	8.0	6.2	13.6
SI	33.7	35.3	27.5	28.9	30.1	35.2	33.5	41.8	43.9	35.7	31.2	42.9	42.1	39.5	46.7	39.5	23.3
MN	430.3	393.1	1323.1	415.9	444.6	368.0	1078.5	433.3	445.8	292.2	99.4	157.0	473.9	79.5	158.6	80.6	485.3

REGIONAL STREAM SEDIMENTS

	31384	31385	31386	31387	31388	31389	31390	31391	31392	31393	31394	31395	31396	31397	31398	31399	31400
FE	4.8	3.5	5.6	2.6	6.4	2.3	8.1	9.7	11.3	10.8	9.0	14.1	10.2	11.3	10.1	10.7	13.6
CU	37.1	39.0	32.4	35.3	52.1	63.5	36.1	40.7	39.3	31.9	11.5	35.2	24.7	26.7	22.9	33.8	27.0
PB	14.4	32.3	21.0	33.1	17.5	25.4	9.6	13.3	15.9	12.6	8.7	15.7	10.4	13.5	8.6	10.5	12.9
ZN	67.8	95.0	73.9	75.2	113.3	68.9	207.4	40.7	124.4	81.6	15.9	80.9	81.3	74.1	70.6	111.7	154.6
MO	.2	.6	.0	.7	.2	.7	.6	.0	.3	.0	.0	.0	.0	.0	.1	.1	.1
V	79.2	111.2	95.8	90.8	115.1	124.2	112.3	115.5	117.2	75.6	19.0	104.8	66.9	195.3	103.9	76.0	190.7
CO	57.7	33.2	53.3	27.6	62.0	27.9	89.3	126.1	122.7	169.1	121.0	155.3	104.5	128.4	125.3	143.4	130.0
NI	1066.3	451.7	950.8	333.3	828.7	143.5	1358.0	1728.7	1711.2	1939.2	2619.8	1937.8	1401.6	1515.9	1616.6	1729.6	1183.1
CR	1759.7	1323.9	1970.1	1641.2	233.8	499.0	24.1.4	2301.3	2615.1	2373.9	1463.7	2821.4	2135.6	3122.0	2454.9	2444.9	2725.8
GA	10.5	21.3	14.8	19.0	17.7	21.5	12.5	7.6	10.4	9.5	0	6.6	6.5	12.0	9.1	10.3	15.7
SN	2.3	6.1	15.7	1.1	15.7	6.0	24.0	23.0	33.5	31.0	6.0	35.7	26.2	51.1	25.9	23.4	67.0
TI	1909.0	4992.1	3773.7	5180.0	5034.2	5963.4	2902.9	1255.8	1830.3	994.7	70.1	1093.8	1628.4	1909.1	1192.6	1213.4	2919.7
BE	2.3	1.7	1.1	1.1	1.2	0	1.1	1.6	2.4	0.7	2.1	5.0	2.9	4.7	3.2	3.0	6.3
MG	5.4	1.9	6.4	1.5	5.2	2.1	4.9	7.0	7.3	7.2	3.0	6.3	7.1	7.5	4.8	5.4	5.7
CA	1.2	1.1	1.1	1.2	1.6	1.6	1.5	2.3	1.9	1.2	.4	1.1	1.2	1.7	1.0	1.0	1.6
SR	62.2	145.9	60.4	150.2	31.3	159.1	37.1	23.6	37.4	28.2	6.8	25.7	44.2	30.4	21.7	33.8	27.5
BA	219.3	248.0	132.9	363.2	171.5	268.4	82.6	63.5	110.4	59.3	19.4	77.7	75.9	65.8	52.1	81.1	64.8
K	2.2	3.5	2.7	3.5	2.9	2.6	.6	.4	.6	.2	.1	.6	.6	.7	.5	.5	.6
LI	7.3	13.5	3.9	17.0	8.4	21.3	7.7	.2	.2	.2	.2	.2	.2	.2	.2	2.6	.2
AL	3.3	9.5	4.0	9.6	5.7	9.4	4.1	1.9	3.3	2.1	0	1.6	2.6	3.5	1.3	3.3	2.8
SC	4.0	4.8	5.6	5.3	5.9	5.5	6.3	5.8	4.3	5.4	1.2	6.6	5.8	6.6	2.9	4.9	6.8
SI	18.5	27.9	25.3	27.5	19.3	22.5	8.6	9.4	13.3	5.3	6.5	10.8	8.1	13.3	6.3	8.4	7.0
MN	668.5	436.5	863.0	452.5	474.9	1020.3	432.2	1240.2	1523.9	1441.2	468.9	1372.9	463.5	1116.6	435.9	1166.1	445.1

	31401	31402	31403	31404	31405	31406	31407	31408	31409	31410	31411	31412	31413	31414	31415	31416	31417
FE	9.1	7.3	8.4	9.6	7.4	6.3	15.0	6.3	5.2	6.4	8.9	4.4	5.5	9.3	10.0	7.3	4.2
CU	41.3	34.9	41.8	30.6	35.0	28.7	26.9	24.5	51.5	26.3	34.9	32.4	28.4	30.9	34.3	28.3	75.3
PB	9.5	9.9	10.0	15.4	13.8	7.6	15.9	7.1	13.3	8.5	15.1	9.5	7.7	10.1	18.2	15.8	35.9
ZN	23.1	44.7	55.5	53.6	77.9	37.3	143.5	71.7	74.1	83.0	125.8	37.0	45.1	107.1	143.4	105.5	157.4
MO	.1	.0	.0	.0	.0	.0	.5	.0	.1	.1	.0	.0	.0	.0	.0	.0	.6
V	52.3	81.1	85.1	57.8	64.0	51.0	69.0	89.7	89.0	44.9	90.9	125.2	86.5	165.1	160.2	116.7	114.7
CO	140.3	103.0	112.2	161.9	111.4	124.3	198.9	121.5	72.9	110.1	120.6	59.4	99.6	79.0	97.7	91.5	24.1
NI	2055.5	1569.0	1561.9	1351.7	1513.9	1563.4	2090.1	1503.4	1148.4	1596.3	1328.6	572.0	1257.6	669.5	1200.6	1394.7	107.7
CR	1644.3	2155.8	2243.4	2100.5	2148.1	2035.4	2797.4	2141.6	1607.7	1791.5	2328.1	156.6	1890.3	2379.4	2654.7	2531.0	791.1
GA	5.4	7.2	5.4	6.4	7.6	6.2	10.4	7.3	13.8	3.5	16.3	8.0	6.3	11.1	15.8	11.2	25.7
SN	5.3	16.9	12.1	36.8	16.8	14.6	59.6	20.0	4.2	8.8	26.7	7.8	12.8	32.4	36.7	31.2	10.9
TI	382.2	866.5	857.0	1356.3	862.6	456.8	2091.3	5096.5	4431.8	3285.1	8006.1	3032.0	2526.3	12965.3	7757.3	3063.0	8427.2
BE	2.3	2.4	3.9	2.0	3.6	2.6	3.4	.0	0	1.3	0	0	.7	0	.4	1.7	0
MG	4.5	6.7	5.9	3.1	8.2	5.5	7.5	5.4	4.3	5.4	4.6	5.9	5.3	8.0	6.1	6.7	1.5
CA	.9	1.4	1.1	1.3	1.2	.3	1.2	1.0	1.4	.9	2.0	2.3	1.1	3.5	1.5	1.3	1.4
SR	21.5	23.3	23.3	35.3	37.2	19.3	25.2	24.5	64.0	25.4	67.8	33.5	18.4	43.0	54.7	50.2	88.3
BA	49.3	44.5	45.3	106.2	34.2	48.8	73.3	84.3	202.5	80.9	89.9	100.2	89.1	101.0	175.6	158.6	270.4
K	.5	.7	.5	.4	.7	.4	.4	.5	1.8	.7	1.1	.5	.3	.6	1.9	1.6	3.5
LI	1.1	.2	.2	.2	.2	.2	.2	.2	12.1	10.4	19.1	4.7	.2	.2	1.0	1.4	28.3
AL	.5	1.9	1.6	1.9	3.4	1.7	2.7	1.3	5.9	2.9	5.4	7.9	1.4	4.6	5.6	4.7	11.6
SC	2.2	3.4	4.3	5.7	6.3	2.9	8.4	5.8	5.4	4.4	8.5	11.8	5.5	12.4	7.0	5.0	6.5
SI	12.3	11.4	11.7	7.5	10.5	4.9	7.9	10.3	16.8	6.9	9.4	12.9	8.7	21.3	18.1	15.7	35.3
MN	480.3	755.3	637.3	1689.4	487.1	455.3	2769.2	493.7	1026.1	477.2	1775.7	497.0	1326.8	1869.2	879.0	1056.3	1019.6

REGIONAL STREAM SEDIMENTS

	31299	31300	31330	31331	31332	31333	31335	31336	31337	31338	31339	31340	31361	31362	31363	31364	31365
FE	6.5	4.1	2.1	2.6	3.2	1.4	4.1	4.9	7.3	2.0	1.9	3.1	4.1	3.3	6.0	8.9	29.4
CU	74.2	43.3	19.5	32.9	29.7	18.7	19.0	19.0	32.3	17.6	19.9	23.0	35.5	41.6	48.3	57.8	33.7
PB	34.8	32.2	28.5	20.5	26.5	17.0	27.5	25.3	27.5	28.8	27.1	30.6	31.3	27.0	14.4	13.1	27.0
ZN	126.4	105.3	51.4	83.3	86.2	20.5	125.9	145.5	104.0	64.1	94.7	65.9	116.4	82.1	114.6	53.2	461.4
MO	.7	1.2	1.0	1.2	1.3	.5	1.6	.8	.9	1.1	1.4	1.1	.4	.2	.2	.0	.4
V	211.9	173.2	86.0	117.1	171.9	105.2	161.2	197.3	173.5	90.5	97.2	132.1	166.5	150.0	103.8	121.1	319.2
CO	26.3	16.3	12.6	12.1	11.1	9.8	16.8	23.1	17.4	9.4	12.5	12.0	19.7	20.9	58.0	120.9	203.3
NI	75.1	26.2	84.3	40.1	20.4	13.1	94.7	78.5	48.6	22.5	26.7	17.4	114.9	180.2	838.6	1713.7	1594.9
CR	295.1	80.0	474.3	123.6	51.5	40.3	291.4	773.7	382.7	81.3	71.8	43.2	667.2	923.7	2155.7	2497.6	3691.9
GA	26.7	21.3	11.2	19.2	22.2	14.4	18.7	17.1	20.5	16.3	15.6	15.3	19.1	17.2	15.1	8.4	22.9
SN	16.5	11.1	4.0	8.1	20.5	8.5	9.0	12.0	17.0	7.5	6.7	7.6	15.4	13.2	10.4	32.7	144.5
TI	16956.1	18029.0	4262.0	16373.2	23103.7	9093.9	13688.3	11222.0	19694.4	7039.6	5219.6	8917.1	20713.7	22544.0	5007.3	1429.4	5812.0
BE	.5	0	1.8	0	0	.0	.0	0	0	0	1.2	0	0	0	0	2.4	11.3
MG	1.9	1.3	.7	1.1	1.0	.5	1.5	2.1	1.3	.6	.5	.6	2.4	2.2	4.7	7.6	9.5
CA	2.5	2.3	1.0	3.3	4.5	2.4	2.1	2.8	3.2	1.4	1.3	1.1	4.1	3.7	1.4	1.5	2.6
SR	171.5	230.4	110.8	259.5	409.4	227.3	162.3	146.6	346.5	214.8	205.2	161.9	208.5	218.2	64.9	27.5	47.0
BA	496.3	480.3	445.1	509.8	624.7	424.5	472.7	370.0	597.0	696.3	582.0	472.4	502.8	453.5	188.6	76.1	110.3
K	3.4	3.2	3.2	3.0	3.2	2.7	3.1	2.7	3.2	4.1	3.7	3.5	3.4	3.5	1.7	.7	.7
LI	24.3	4.9	1.8	12.1	8.0	7.3	5.1	2.6	3.6	.2	2.8	1.3	1.9	4.3	12.7	.2	.2
AL	12.5	11.1	7.8	9.9	11.7	7.0	8.8	8.4	10.2	8.8	9.2	9.6	9.8	8.6	5.6	2.7	6.9
SC	10.5	9.3	4.3	3.8	10.1	4.1	9.0	8.2	9.1	6.7	5.9	6.0	10.4	9.2	4.2	5.2	16.9
SI	32.3	31.0	38.6	26.7	25.0	21.6	35.0	30.8	27.7	39.4	38.8	40.7	29.2	22.4	18.8	8.8	9.3
MN	1337.9	456.1	331.6	392.0	455.6	337.3	1019.7	865.1	493.4	410.4	349.4	414.0	1238.5	443.5	494.4	1188.3	2411.4

	31365	31367	31368	31369	31370	31371	31372	31373	31374	31375	31377	31378	31379	31380	31381	31382	31383
FE	8.2	15.0	12.5	13.0	9.9	10.4	5.9	16.9	4.6	4.2	5.7	4.4	3.9	9.3	2.3	2.3	4.2
CU	77.9	44.7	34.2	51.0	47.6	35.8	67.1	43.9	37.9	39.0	50.6	47.6	34.8	31.3	39.4	38.1	45.9
PB	22.3	18.7	16.2	24.4	15.0	14.4	22.7	22.1	31.9	35.4	19.9	19.7	13.7	13.8	29.1	24.2	18.1
ZN	114.2	265.2	165.6	241.7	150.6	175.5	140.4	276.1	83.3	123.6	142.3	122.4	42.9	99.1	89.5	73.0	97.1
MO	1.2	.3	.0	.1	.0	.2	.3	.0	1.4	1.3	.3	.6	1.4	.5	.6	.8	.0
V	154.7	207.7	184.2	164.2	128.3	159.4	129.6	326.6	193.2	152.6	136.8	124.6	62.0	99.7	129.1	121.3	164.8
CO	76.5	119.1	131.2	111.2	35.6	97.1	39.5	139.0	20.8	17.8	42.9	36.9	59.8	106.1	15.4	15.9	20.2
NI	1084.5	1338.1	1632.6	1530.7	1231.2	1206.8	500.9	1224.9	152.2	115.5	427.3	412.4	1097.2	1503.0	69.9	49.5	122.6
CR	2325.9	3036.6	2736.7	2874.6	2335.6	2553.4	1402.0	3179.0	1176.0	459.9	1903.0	1761.3	1492.9	2443.6	297.5	270.2	549.6
GA	16.5	15.8	19.4	19.1	15.5	13.3	21.2	22.4	20.0	22.0	19.0	17.4	11.5	6.6	21.2	19.5	20.7
SN	13.2	46.1	59.3	56.7	32.7	21.0	10.6	90.4	9.7	10.1	9.4	7.3	2.0	20.7	11.3	7.9	9.4
TI	5643.3	11251.8	5025.6	9062.3	6587.0	5392.3	8349.1	14692.7	24039.7	14245.8	9401.7	5264.6	965.5	11040.1	16236.9	10911.9	15118.6
BE	1.8	.9	1.4	0	.7	2.4	0	0	0	0	0	0	2.2	4.5	0	0	0
MG	4.7	7.2	6.7	3.8	7.2	5.5	5.7	6.5	2.0	1.7	3.8	3.6	4.5	7.9	1.1	.8	1.6
CA	1.5	2.0	1.6	3.5	1.8	1.6	2.0	2.7	3.5	3.5	2.2	2.7	.8	1.4	2.5	1.7	3.3
SR	57.1	49.8	37.7	63.3	54.7	51.4	117.4	77.0	335.1	256.6	118.4	146.4	46.3	35.2	319.6	375.9	236.1
BA	178.2	116.1	96.9	127.0	107.3	130.7	296.3	143.1	688.9	642.3	272.5	301.8	154.8	89.1	521.5	500.7	577.5
K	2.5	1.3	1.3	1.5	1.5	1.6	3.3	1.6	3.3	.2	2.7	2.5	2.2	.9	3.2	3.3	2.9
LI	12.1	.2	.2	.2	.2	2.6	10.1	.2	3.5	9.1	16.3	24.8	10.1	.2	8.9	9.9	9.0
AL	5.5	6.1	5.0	6.4	5.2	4.3	8.9	5.4	12.0	12.9	8.4	7.2	3.6	2.4	9.9	10.7	10.2
SC	7.3	10.2	7.7	9.2	8.0	7.3	9.9	9.6	11.5	10.0	7.4	6.0	1.8	5.5	7.1	5.9	10.1
SI	21.8	17.2	15.5	13.8	17.5	13.5	33.6	12.2	33.1	45.1	24.8	21.4	15.6	12.1	25.6	25.4	26.6
MN	1149.2	1655.0	1557.5	2133.2	1313.6	1027.2	1084.3	1394.3	1112.2	713.7	491.7	423.7	424.7	947.3	466.5	452.8	1061.4

REGIONAL STREAM SEDIMENTS

	31635	31637	41001	41002	41003	41004	41005	41006	41007	41008	41009	41010	41011	41012	41014	41015	41016
FE	8.1	4.4	5.7	4.5	3.0	2.7	6.6	4.8	2.4	3.2	2.2	2.8	4.1	2.9	3.4	3.9	1.3
CU	82.5	68.1	65.3	59.5	35.4	47.4	94.7	71.3	46.6	71.5	31.3	31.9	32.3	38.8	42.5	40.2	20.2
PB	13.4	11.3	22.3	27.4	16.2	20.6	91.4	22.7	17.4	22.8	13.3	12.2	20.5	14.5	26.9	20.3	10.3
ZN	151.3	71.2	205.4	307.2	153.4	180.3	520.3	190.4	197.3	185.3	69.8	141.3	142.3	172.2	100.9	148.6	63.5
MO	.7	.7	.5	2.5	.6	1.3	.9	1.1	.8	.8	.7	1.6	1.1	1.5	.7	1.1	.6
V	307.3	254.8	169.4	139.3	93.0	99.1	243.6	143.0	89.5	149.6	68.8	66.1	89.5	75.1	122.8	113.3	96.7
CO	21.3	15.5	33.6	29.2	21.5	22.9	24.8	32.2	20.5	36.9	12.?	15.5	14.4	17.4	17.1	16.6	7.2
NI	41.0	31.5	92.2	90.5	60.0	72.1	258.9	73.4	37.5	101.7	25.2	27.8	30.1	29.8	45.6	42.3	36.3
CR	174.8	130.2	193.8	203.2	162.3	152.7	506.1	150.3	102.7	207.8	76.5	67.9	123.2	68.3	119.8	111.4	106.1
GA	20.5	18.5	21.9	15.2	1.7	15.1	16.9	21.2	15.5	17.4	10.1	12.4	19.4	16.0	11.9	14.6	13.5
SN	16.3	13.9	9.4	12.7	10.3	6.9	2.4	10.6	10.3	8.8	13.6	5.2	12.3	8.6	10.4	5.6	7.2
TI	24283.2	19454.6	8016.9	11107.3	10376.5	6705.0	6333.7	7753.3	7903.3	7362.1	6751.2	8366.7	6709.1	10033.8	10478.3	11378.5	8419.2
BE	0	0	.6	0	0	0	3.7	0	0	0	0	0	.5	0	0	0	0
MG	1.3	1.0	.1	.5	.0	.0	1.2	.0	.3	.5	.0	.3	.3	.4	.0	.5	.2
CA	3.1	1.7	.6	.9	.3	.8	.9	.0	.6	.5	.4	.4	.3	.6	1.3	1.0	.4
SR	183.5	203.1	22.0	46.2	38.0	39.0	52.3	27.3	31.6	36.4	22.1	25.0	19.3	25.7	65.9	58.7	30.5
BA	500.3	344.0	377.4	592.9	342.2	368.2	256.4	426.6	420.8	410.0	281.5	427.6	339.3	497.1	365.9	381.5	254.7
K	2.3	1.2	1.8	1.5	.9	1.1	1.1	1.8	1.3	1.4	1.1	1.1	2.3	1.1	1.3	1.4	1.3
LI	16.4	14.8	55.7	25.2	17.1	26.3	51.3	40.6	26.0	39.5	13.3	21.2	14.9	13.3	10.2	10.7	12.2
AL	11.7	8.0	12.1	11.3	7.8	8.9	11.7	11.7	10.1	11.6	6.4	9.0	11.3	8.3	10.6	12.2	9.3
SC	17.3	11.3	8.4	14.1	7.6	8.2	8.4	7.2	6.9	8.8	7.2	6.3	8.2	8.4	9.6	9.2	8.1
SI	28.8	26.2	36.9	43.3	43.0	36.0	35.0	35.8	49.1	34.1	43.2	40.1	43.9	43.9	46.7	39.1	38.8
MN	1423.5	425.9	446.0	1062.3	471.4	438.4	431.6	487.4	453.6	452.3	373.1	427.1	373.4	806.6	499.9	1096.9	311.7

	41017	41018	41019	41020	41021	41022	41023	41024	41025	41026	41027	41028	41029	41030	41032	41033	41034
FE	1.4	2.1	4.9	8.0	3.3	4.3	2.0	2.4	3.2	3.2	1.6	2.1	3.7	3.2	3.8	1.6	1.6
CU	26.1	43.3	76.8	84.8	45.9	46.5	25.8	33.1	47.9	40.4	24.3	28.2	41.5	38.8	52.3	32.3	27.6
PB	18.4	15.3	51.3	47.9	27.7	51.2	31.3	21.4	33.6	27.4	18.2	17.8	21.6	21.5	20.0	15.9	13.4
ZN	77.3	130.1	237.7	199.1	199.0	205.1	202.8	123.2	162.1	150.4	95.8	115.5	140.1	88.9	166.2	115.5	117.7
MO	1.1	1.1	.5	.3	.7	1.9	.9	.3	1.6	1.7	.8	1.0	.8	1.0	1.1	1.2	1.4
V	61.3	84.1	153.3	161.6	139.4	146.4	70.6	79.3	121.5	119.8	69.3	75.8	104.4	117.2	94.1	75.2	66.2
CO	9.1	38.0	54.3	23.3	31.8	22.0	18.9	21.5	16.3	19.0	14.5	21.0	24.2	22.9	15.6	24.3	13.1
NI	33.3	97.5	184.5	178.9	63.7	152.6	48.9	54.0	75.1	73.4	37.4	53.3	67.8	68.2	65.1	43.6	37.1
CR	109.2	144.6	348.2	395.4	160.6	311.4	145.4	135.8	196.7	182.2	118.7	135.2	173.8	183.1	158.1	105.0	99.3
GA	10.8	21.5	28.1	21.9	14.6	12.6	9.9	12.7	15.9	14.1	10.3	12.2	15.6	11.9	19.1	13.8	9.6
SN	9.1	6.9	7.1	0	25.5	16.3	10.9	8.5	10.1	12.7	5.8	3.9	12.7	5.8	6.9	5.9	3.5
TI	9606.7	5855.4	7733.5	7203.7	11854.9	12943.3	14350.8	8357.8	11999.9	12327.7	9510.4	7574.2	9147.8	9072.4	8649.9	8693.3	8754.2
BE	0	1.2	0	0	0	0	0	0	0	0	0	0	0	0	0	0	0
MG	.1	.3	.6	.3	.4	.0	.4	.3	.0	.0	.3	.3	.0	.3	.0	.3	.3
CA	.2	.4	.7	.9	1.6	.7	.9	.6	.5	.6	.5	.4	.6	.4	.3	.3	.4
SR	15.2	25.5	41.9	47.2	67.8	44.7	57.5	37.0	36.8	42.2	37.0	27.1	33.5	24.5	19.3	2.1	28.1
BA	238.0	222.7	255.7	280.0	211.7	182.5	179.6	241.1	309.8	332.3	184.0	199.0	347.2	246.9	296.2	270.5	287.9
K	1.2	.9	1.0	.5	.6	.5	.5	.8	1.6	1.3	.9	.9	1.4	1.1	1.5	1.1	.8
LI	22.4	57.7	64.9	43.0	23.8	31.0	19.4	22.1	41.2	29.4	11.9	2.2	26.5	25.7	38.7	27.2	24.0
AL	9.3	13.6	15.5	16.9	9.5	11.1	8.1	9.8	15.7	13.3	3.6	8.8	12.5	9.8	13.4	8.7	8.6
SC	9.3	8.4	9.4	11.0	3.2	11.1	7.2	8.5	11.1	12.0	7.5	5.2	10.2	8.2	8.8	6.2	6.2
SI	46.7	26.9	33.7	23.3	43.9	46.7	43.9	37.0	49.7	46.7	39.7	36.6	41.1	43.9	35.8	31.9	37.8
MN	260.7	406.9	1036.2	437.0	1099.3	447.5	1049.8	442.7	390.8	462.1	384.7	444.1	727.1	417.7	312.1	413.8	314.8

REGIONAL STREAM SEDIMENTS

	31418	31419	31420	31421	31422	31423	31424	31425	31426	31427	31428	31429	31430	31431	31433	31434	31435
FE	9.?	13.7	9.9	12.5	7.7	7.8	4.0	6.4	5.8	6.8	5.3	8.3	4.5	7.2	6.2	4.8	5.2
CU	61.9	30.6	05.5	56.2	47.0	36.4	70.9	80.8	112.5	131.3	89.4	145.9	142.2	160.3	238.7	172.6	94.1
PB	11.4	17.8	12.9	18.9	18.1	12.9	20.5	22.1	24.3	16.4	11.9	23.9	13.5	24.0	20.9	12.1	15.1
ZN	117.4	146.5	157.4	146.7	120.9	69.7	95.9	177.5	222.9	147.3	95.1	210.0	126.3	282.7	183.7	113.1	123.2
MO	.?	.0	.0	.0	.0	.2	.3	.0	1.7	.4	1.0	.0	.0	2.6	.4	.0	.0
V	147.4	175.2	124.4	104.5	115.8	53.4	203.0	205.4	104.0	195.2	277.5	325.6	356.6	469.0	561.1	361.1	138.5
CO	125.1	128.4	93.8	134.2	85.7	125.1	33.7	39.9	24.4	42.6	34.0	43.3	27.5	27.9	37.8	33.0	18.4
NI	1533.5	1563.8	1461.4	1689.8	1120.2	1940.5	257.9	321.0	132.1	352.9	91.2	209.1	111.8	93.7	118.9	97.7	13.2
CR	2476.5	3101.7	2437.4	2597.1	2403.1	2129.4	1352.5	1240.9	396.1	1062.1	387.2	599.2	345.6	365.7	374.0	140.1	18.0
GA	13.4	13.6	15.8	12.8	12.0	7.9	17.1	16.0	27.3	21.6	23.4	27.9	23.5	29.3	22.9	19.6	22.6
SN	24.1	63.5	20.0	54.8	21.0	19.5	17.4	23.9	3.7	11.8	9.6	26.4	17.3	25.7	29.8	13.4	12.4
TI	6359.3	5816.3	12526.5	3044.9	5652.8	1128.5	16376.8	23629.1	10809.8	13206.4	23737.2	30598.8	22139.8	41131.5	36199.1	20521.3	29594.1
BE	?	1.7	?	1.6	1.7	2.1	?	?	?	?	0	0	0	0	0	0	0
MG	5.8	7.5	6.5	9.7	6.5	7.4	4.9	7.2	1.7	4.2	2.5	5.3	3.3	4.1	4.9	3.7	3.2
CA	1.8	1.6	2.5	2.2	1.7	.9	2.6	3.8	1.3	2.2	4.9	6.5	5.2	9.0	10.1	6.4	10.3
SR	33.5	47.7	64.7	43.3	154.2	26.7	92.0	112.8	65.9	72.4	165.5	233.4	196.0	340.9	291.8	164.4	367.9
BA	97.1	184.3	189.2	75.4	336.1	8.2	327.8	340.9	342.3	291.4	294.1	540.7	564.8	578.7	385.5	191.6	537.8
K	.5	1.7	.6	.5	1.8	.8	2.7	2.2	3.3	2.8	1.6	2.7	2.4	2.2	1.7	1.3	1.8
LI	1.8	.2	.2	.2	8.0	.4	5.2	6.4	47.7	19.6	17.5	19.3	21.4	12.2	14.6	16.6	8.7
AL	5.0	5.1	8.5	5.0	6.6	2.1	9.6	10.3	13.5	8.9	8.8	13.7	12.1	14.7	13.8	10.6	13.1
SC	7.3	7.6	12.4	8.4	9.0	3.8	8.9	12.6	8.7	9.2	16.7	21.2	16.5	28.5	23.1	16.2	27.3
SI	12.1	17.4	12.7	12.6	13.8	10.6	31.3	31.7	29.3	26.0	19.0	28.8	21.6	24.6	21.4	18.0	25.3
MN	1269.0	1278.1	1435.5	1764.4	491.1	1213.9	1330.2	1774.1	1210.3	1305.9	490.6	2039.8	1447.3	1965.7	1919.0	1168.9	1395.5

	31435	31437	31438	31439	31440	31441	31442	31443	31444	31628	31629	31630	31631	31632	31633	31634	31635
FE	5.5	4.1	6.8	7.2	6.6	5.3	6.8	6.5	6.3	9.5	10.9	4.6	5.0	8.1	6.8	8.2	6.4
CU	63.9	43.7	44.0	46.1	40.0	32.7	35.9	49.0	28.9	84.4	108.6	65.7	131.3	111.0	144.1	140.4	93.9
PB	10.2	9.9	9.7	10.8	11.1	10.4	11.0	9.7	9.7	16.5	23.2	8.9	8.9	23.7	14.1	23.1	17.9
ZN	72.3	57.5	93.6	59.7	98.5	60.2	65.1	76.2	78.1	105.0	242.1	86.7	55.8	196.7	149.0	165.7	135.4
MO	.3	.2	.0	.0	.1	.0	.0	.0	.0	.0	1.6	.0	.0	1.4	1.6	4.6	1.9
V	138.4	203.3	221.4	152.9	99.4	103.0	104.2	116.9	101.5	316.1	332.1	174.9	197.9	373.1	289.8	394.0	352.5
CO	52.3	52.2	52.8	74.3	66.4	70.6	71.4	79.4	77.2	39.7	29.0	29.9	36.3	31.0	37.5	26.7	18.5
NI	390.3	399.5	387.9	713.3	633.7	674.3	628.1	723.3	721.1	136.1	89.9	113.1	131.9	82.2	165.5	21.6	19.8
CR	1139.0	1276.9	1148.7	1703.7	1649.1	1723.1	1660.1	1729.6	1723.7	293.3	222.8	189.5	263.4	223.1	344.3	123.4	119.9
GA	15.0	11.1	11.4	9.5	8.8	5.3	7.9	7.8	7.2	19.7	26.7	18.5	18.9	26.8	19.5	32.8	27.0
SN	6.9	4.0	10.1	13.5	5.3	9.2	18.6	5.9	13.4	25.2	29.1	7.5	7.7	33.3	8.8	30.4	22.3
TI	8633.2	5702.7	6464.2	6906.1	6327.1	3755.9	5485.6	3599.9	4947.9	21509.3	33259.3	7990.1	7846.1	30499.6	16211.9	40997.4	38694.9
BE	0	0	0	0	0	0	0	.4	0	0	0	0	0	0	0	0	0
MG	5.2	5.4	7.4	5.8	6.6	7.1	8.6	6.7	7.9	5.5	4.9	3.9	3.0	3.5	2.7	2.6	2.2
CA	2.5	3.6	5.7	2.1	1.4	1.5	2.0	1.7	1.2	7.2	7.8	4.1	3.2	5.4	3.1	6.2	5.9
SR	59.?	49.0	61.3	31.2	23.1	24.5	20.3	21.5	18.2	94.2	226.9	93.4	78.6	241.5	147.1	510.2	336.5
BA	158.4	113.9	140.2	120.1	113.2	118.3	91.7	162.9	110.7	227.7	327.8	133.4	171.7	353.9	373.5	935.5	484.9
K	1.3	.8	.9	.6	.5	.4	.3	.4	.4	1.4	1.9	1.1	1.1	2.0	1.5	2.3	2.0
LI	9.2	8.7	5.2	1.9	.5	.2	.2	.8	.2	6.8	13.2	13.8	16.3	16.9	16.0	17.8	10.4
AL	4.9	4.9	5.2	3.7	3.2	1.7	2.5	3.1	1.6	7.2	12.9	7.0	8.1	12.2	10.2	15.6	12.4
SC	14.0	13.6	13.6	12.5	14.6	11.0	11.2	13.0	9.5	16.2	24.7	11.6	10.6	18.8	15.2	29.9	28.5
SI	18.4	18.1	21.8	26.5	19.4	16.3	20.6	20.1	18.5	25.4	23.9	20.1	20.1	33.3	27.2	34.1	21.5
MN	1577.1	1125.0	1727.7	1594.2	1532.7	1531.9	1995.3	1823.2	1569.3	2123.3	2150.5	494.3	1125.9	2193.5	1492.6	2503.9	1720.9

	41069	41070	41071	41072	41073	41074	41075	41076	41077	41078	41079	41080	41081	41082	41083	41084	41085
FE	5.2	.5	.7	2.3	2.4	.6	2.2	1.8	2.8	1.1	1.2	1.3	1.0	1.8	3.2	1.2	1.0
CU	70.0	12.1	22.2	61.4	94.8	13.1	103.0	52.6	73.4	19.3	8.8	20.6	25.2	21.8	30.5	25.2	22.2
PB	72.3	18.4	23.5	54.0	35.1	12.0	26.2	29.0	35.5	10.9	17.8	10.2	12.9	12.4	19.2	13.8	14.3
ZN	267.8	69.1	95.4	129.2	132.1	36.1	253.6	137.7	162.9	53.7	73.3	63.4	82.9	131.1	159.8	85.2	110.2
MO	1.4	1.5	.9	1.4	.6	.5	1.9	2.0	1.3	1.1	1.1	.8	.7	.8	1.0	1.4	1.6
V	215.5	27.6	46.4	83.5	112.4	37.3	69.1	64.0	83.5	29.0	47.2	31.0	44.4	35.8	42.9	63.6	41.3
CO	49.3	6.3	9.0	76.5	24.4	4.3	89.3	59.4	52.7	8.4	12.8	28.6	32.9	56.1	118.2	23.0	17.9
NI	209.9	9.2	34.7	117.0	43.0	13.6	177.8	107.6	117.8	5.8	23.3	42.8	59.8	61.1	135.1	24.9	39.4
CR	266.1	94.1	115.1	123.3	109.3	63.3	146.9	112.5	117.2	26.5	49.3	44.8	64.7	67.9	70.7	66.7	70.3
GA	26.1	4.8	11.4	22.0	18.6	6.9	31.9	20.2	28.4	7.9	14.7	11.3	13.2	12.2	13.7	12.2	10.4
SN	14.5	5.9	13.3	7.0	7.1	10.4	2.6	5.8	6.0	6.4	4.8	2.0	7.0	7.6	19.3	3.5	7.2
TI	14913.0	18367.4	15775.6	9960.7	15157.6	10484.3	5193.2	7399.2	7725.6	17639.5	11349.7	5121.2	6471.0	5415.5	5699.1	8451.4	9976.6
BE	3	(	(	(	(	.	4.2	.6	.7	u	0	0	u	0	0	0	0
MG	.4	.2	.2	.2	.0	0	.3	.2	.0	.0	.2	.2	.0	.0	.0	.3	.2
CA	.5	.2	.3	.3	.6	.2	.4	.4	.3	.3	.4	.3	.4	.3	.5	.4	.3
SR	24.8	15.0	15.6	11.4	29.1	9.5	11.4	20.0	10.6	19.9	26.9	20.9	22.7	22.7	26.9	31.5	21.3
BA	350.3	166.5	155.5	171.6	224.2	159.6	372.5	315.7	198.1	242.4	314.2	230.6	218.1	253.7	568.8	357.4	219.1
K	1.0	.4	.5	.5	.5	.5	.3	.7	.8	.7	0	.6	.7	.6	.9	.9	.6
LI	63.0	.2	9.2	43.3	20.5	4.0	81.6	51.5	67.9	1.3	16.6	14.5	20.6	18.2	11.9	13.6	15.1
AL	20.9	3.4	7.4	15.0	13.2	5.3	20.3	14.9	19.2	5.9	10.8	7.4	8.8	7.9	7.3	9.2	7.9
SC	16.5	3.3	5.7	9.1	9.5	3.2	6.4	8.4	6.8	2.5	4.3	2.2	4.4	3.2	4.3	4.6	5.2
SI	46.7	43.9	43.9	41.8	29.5	43.3	43.9	42.3	46.7	35.8	42.4	37.7	38.2	38.1	43.9	34.3	43.9
MN	383.5	221.2	219.3	340.6	387.1	39.4	269.8	403.6	300.6	421.0	310.4	343.7	338.3	2605.7	4366.0	486.3	318.4

	41086	41087	41088	41089	41090	41091	41092	41093	41094	41095	41096	41097	41098	41099	41100	41101	41102
FE	.3	2.1	.9	1.0	7.9	6.6	9.2	.7	1.1	8.8	2.5	1.0	1.0	3.0	3.3	2.7	.6
CU	14.4	22.9	16.6	17.1	38.9	43.8	103.4	10.3	19.3	76.4	41.7	18.5	10.8	43.9	56.2	33.7	3.6
PB	14.2	19.0	11.0	14.7	17.8	13.3	24.0	9.0	14.5	24.1	15.0	18.8	7.8	14.0	30.0	20.9	.0
ZN	80.3	170.3	77.1	91.2	133.8	68.7	257.6	58.5	75.8	230.8	143.0	102.8	49.5	128.6	172.6	144.8	11.8
MO	.5	.9	1.2	1.3	.0	.0	1.7	1.3	.7	1.3	.6	1.4	.9	.8	1.3	1.4	.1
V	25.3	51.6	29.6	31.8	37.2	26.7	55.7	24.7	36.0	115.2	62.5	67.0	24.3	39.0	55.6	59.6	2.6
CO	11.4	30.0	9.8	13.1	264.3	272.7	210.8	4.3	21.0	43.7	26.3	7.8	14.8	26.2	52.1	33.9	5.4
NI	14.7	44.1	24.2	19.0	237.7	220.7	244.2	6.7	17.7	60.3	44.8	17.9	9.9	160.6	128.2	70.8	8.6
CR	54.5	74.1	51.2	59.7	58.2	38.4	89.6	35.2	48.7	128.1	90.0	64.8	29.2	176.8	140.7	90.4	12.7
GA	8.3	11.7	6.1	7.3	8.2	4.9	13.4	5.5	10.0	21.3	14.3	17.9	5.6	26.1	36.6	27.5	2.8
SN	9.4	14.9	5.8	6.0	16.3	11.1	3.4	4.7	10.0	10.1	9.2	7.1	3.0	0	3.5	4.0	0
TI	11946.1	10806.9	9306.6	10440.0	4257.9	1971.5	2156.6	9051.1	8264.1	4580.6	5260.2	8186.1	6678.9	2794.7	6091.7	5202.0	588.5
BE	0	0	0	0	.2	1.2	9.1	0	0	4.2	.6	0	0	4.6	1.9	2.7	4.3
MG	.2	.2	.2	.2	.2	.2	.2	.2	.2	.4	.0	.3	.2	.3	.3	.2	.4
CA	.3	.4	.2	.3	.5	.4	.6	.2	.3	.5	1.2	.2	.2	.2	.4	.3	0
SR	18.8	22.2	10.9	18.0	29.1	21.3	43.9	13.9	23.4	34.6	74.3	26.5	19.4	6.7	15.9	12.1	.8
BA	132.7	229.6	159.9	139.5	1763.9	1546.3	1234.2	121.2	219.9	460.7	536.7	389.5	138.8	177.5	153.0	192.8	36.9
K	.3	.6	.3	.4	.5	.5	1.5	.6	.9	2.0	1.5	1.7	.4	.4	.6	.7	.1
LI	17.3	23.2	7.1	17.3	4.3	.2	27.4	11.1	11.6	43.0	34.2	17.6	7.6	44.3	65.0	43.1	11.1
AL	4.3	7.0	4.4	5.0	5.6	3.3	7.6	4.9	6.6	15.1	10.1	13.7	4.6	17.4	20.4	18.9	1.6
SC	3.8	5.3	3.2	4.5	5.7	3.1	10.3	3.8	5.2	7.8	6.2	6.6	3.1	2.6	6.6	5.7	.0
SI	40.1	43.9	43.9	43.9	43.9	32.0	20.8	42.9	42.2	37.6	43.9	43.2	39.8	31.7	35.2	43.0	15.4
MN	342.7	487.2	172.6	387.2	4852.3	4654.2	4853.3	127.5	377.1	1275.9	492.5	156.9	305.3	118.3	386.1	275.8	41.2

REGIONAL STREAM SEDIMENTS

	41035	41036	41037	41038	41039	41040	41041	41042	41043	41044	41045	41046	41047	41048	41049	41050	41051
FE	16.8	3.8	4.7	.3	3.3	8.9	4.2	1.6	.8	1.6	.4	1.5	3.9	5.8	.7	1.4	1.2
CU	55.8	45.7	55.2	12.6	119.4	93.4	77.7	31.3	30.4	21.3	10.4	29.8	92.7	50.6	17.5	31.3	13.4
PB	20.3	20.3	17.4	17.7	25.4	30.0	32.2	21.0	19.2	17.8	9.3	21.2	21.1	11.6	10.6	15.0	7.9
ZN	153.3	215.9	65.8	19.0	236.6	171.4	240.9	149.2	83.1	172.3	35.8	73.0	133.6	51.7	51.6	100.1	43.1
MO	.3	3.4	.3	.1	1.2	.5	1.2	1.3	.8	.0	.7	.3	.3	.0	1.2	.5	.5
V	115.1	94.2	92.9	26.0	157.3	175.3	151.3	74.0	66.7	48.2	33.6	89.9	144.5	88.3	39.9	62.1	33.5
CO	58.3	29.5	46.3	3.3	43.7	63.8	47.1	16.6	12.1	10.9	5.9	18.5	61.8	57.2	6.1	12.5	8.2
NI	170.5	83.4	85.5	7.1	155.3	155.7	168.0	63.7	59.3	32.4	17.1	52.7	230.3	90.6	16.3	34.9	14.8
CR	278.3	139.0	153.9	34.6	215.3	2.6.7	229.7	132.6	152.5	114.9	45.6	1'2.4	185.1	113.3	45.2	77.4	42.5
GA	13.3	15.3	13.8	6.6	25.0	31.9	37.1	19.0	16.5	12.3	7.3	15.0	30.8	15.8	11.4	14.2	6.4
SN	1.7	6.3	2.4	3.5	6.1	7.8	5.5	11.2	3.6	12.8	7.1	6.4	5.0	.2	7.4	10.4	5.7
TI	4184.3	7372.1	4754.4	8024.3	10423.2	5691.3	6025.2	9660.3	8393.8	11345.5	8517.1	8493.2	4675.3	3321.0	8673.4	5935.8	5429.0
BE	3.2	.9	2.3	0	1.4	4.5	4.7	0	0	0	r	r	4.8	3.2	r	6	.0
MG	.5	.2	.3	.2	.4	.4	.0	.2	.2	.0	0	.2	.5	.2	.2	.3	.2
CA	.5	.3	.3	.2	.4	.4	.4	.2	.2	.3	.2	.3	.3	.2	.2	.3	.2
SR	36.7	20.5	31.0	13.7	27.6	21.5	17.8	16.9	11.4	14.1	9.9	17.1	13.9	13.1	16.3	21.1	13.4
BA	323.7	308.4	445.9	152.6	372.0	314.8	356.3	252.1	169.5	139.2	113.2	302.0	335.6	260.8	222.4	243.9	135.9
K	.3	1.1	1.7	.7	1.6	2.1	2.4	1.2	1.0	.6	.5	1.2	2.0	1.7	1.2	1.4	.8
LI	38.5	38.5	51.1	3.7	73.6	85.1	95.6	42.3	40.9	34.4	16.6	41.2	102.2	54.7	16.3	20.2	6.8
AL	11.3	11.4	10.2	5.0	16.2	17.0	21.9	13.3	10.8	7.9	4.7	9.7	16.2	9.7	7.8	8.9	4.7
SC	9.7	8.0	8.2	2.8	9.7	7.3	8.1	8.2	5.6	7.2	3.1	6.8	6.0	5.4	3.8	6.4	3.8
SI	32.4	43.9	31.6	35.3	35.6	30.2	40.9	42.7	36.3	43.9	32.0	36.1	31.0	22.1	43.9	43.9	43.9
MN	405.3	403.0	463.0	82.3	426.7	1792.1	437.0	265.5	169.7	266.2	120.9	306.9	378.6	351.6	217.2	301.8	251.1

	41052	41053	41054	41055	41056	41057	41058	41059	41060	41061	41062	41063	41064	41065	41066	41067	41068
FE	6.1	6.6	1.4	.8	1.1	2.0	1.7	2.5	1.5	1.0	1.6	1.2	1.5	.5	.5	2.7	1.2
CU	62.1	72.9	33.6	12.4	21.9	43.5	48.4	60.9	45.4	72.4	-7.2	26.5	39.9	17.3	11.5	32.6	15.6
PB	16.7	14.8	25.5	13.1	30.9	31.8	17.1	41.3	29.4	43.6	51.7	25.2	25.5	12.8	12.9	24.7	25.1
ZN	218.0	213.8	115.2	53.0	66.2	84.7	67.7	230.7	103.6	136.8	105.5	94.6	74.4	43.1	35.5	78.9	52.3
MO	1.5	.6	.7	.9	1.1	1.7	.8	1.5	.7	1.5	.6	1.0	.8	.6	1.3	.8	1.1
V	104.5	121.5	54.1	48.5	46.3	85.3	99.4	85.8	69.5	122.3	68.7	61.8	65.5	40.3	37.5	77.6	50.5
CO	43.5	61.3	13.1	5.1	6.2	24.6	28.6	50.2	15.6	11.4	25.5	8.4	19.9	6.8	3.5	14.2	13.6
NI	101.3	104.6	38.2	12.3	13.1	64.3	95.5	95.6	75.4	26.3	62.8	28.5	44.1	13.1	10.0	31.9	11.6
CR	175.5	149.1	127.3	47.3	147.4	161.6	155.9	153.9	185.9	98.9	142.5	128.7	157.2	62.4	62.3	119.3	108.3
GA	19.2	24.8	13.9	8.8	11.9	17.1	17.5	24.8	14.5	17.0	20.4	9.9	13.0	8.3	7.8	9.8	7.7
SN	7.0	2.2	9.5	6.4	4.5	6.1	6.8	5.5	8.6	11.5	7.6	9.2	10.4	8.9	5.3	5.2	6.4
TI	7884.5	4135.4	18859.4	6627.0	25387.8	10205.5	6753.7	11323.5	13974.0	13346.8	7744.3	15454.4	10924.4	13210.2	15192.5	14454.8	16706.2
BE	.9	5.1	0	0	0	0	.3	0	0	0	0	0	0	0	0	0	0
MG	.3	.3	.0	.2	.2	.2	.3	.4	.0	.3	.3	.2	.0	.2	.2	.0	.2
CA	.4	.3	.6	.3	.5	.3	.3	.5	.4	.7	.5	.5	.4	.3	.2	.6	.4
SR	25.3	12.1	35.3	27.6	41.0	15.3	24.5	47.5	17.9	39.7	36.9	35.4	26.6	16.0	11.8	38.7	28.8
BA	489.0	244.0	235.8	353.7	233.8	307.6	275.9	342.3	206.4	323.1	275.3	375.4	203.4	211.5	133.4	243.7	171.8
K	1.5	1.5	.9	1.8	.8	1.0	1.2	1.0	.7	.8	1.4	.8	.6	.8	.5	.5	.4
LI	43.3	77.4	17.1	10.6	8.8	35.2	47.1	34.7	15.7	7.0	29.1	5.3	16.0	4.8	3.3	11.7	1.1
AL	15.5	14.3	9.0	7.8	7.7	13.5	11.1	16.5	9.5	14.3	10.3	9.3	9.6	5.6	4.7	7.8	6.3
SC	11.2	5.6	4.6	5.5	3.3	8.9	7.0	8.4	5.6	11.8	4.0	7.8	5.6	3.8	2.7	4.8	4.3
SI	43.9	29.0	36.4	46.7	31.9	41.8	31.1	37.5	37.1	43.9	37.6	43.9	36.8	41.4	43.9	33.4	43.9
MN	1125.0	443.3	332.4	23.8	416.4	219.5	364.2	426.3	306.3	447.9	317.0	283.6	345.8	195.5	166.5	351.0	369.3

REGIONAL STREAM SEDIMENTS

	41103	41104	41105	41106	41107	41108	41109	41110	41111	41112	41114	41115	41116	41117
FE	1.3	1.5	.7	1.2	.6	.4	16.3	3.1	6.1	5.1	4.0	1.3	1.2	1.3
CU	25.5	21.6	14.6	21.6	14.3	18.6	145.5	77.1	113.1	68.4	78.1	27.6	15.7	21.5
PB	10.3	10.2	11.6	12.3	6.2	7.9	16.7	14.8	72.8	22.1	18.1	11.6	11.3	14.1
ZN	53.5	55.3	51.0	56.9	24.2	24.3	303.6	117.2	191.7	119.2	159.2	46.9	65.8	73.4
MO	.7	.5	.7	.4	.4	.9	.4	1.1	1.2	1.1	1.2	.8	.8	1.0
V	60.5	43.2	23.3	31.2	19.1	36.3	59.7	62.6	113.7	92.5	93.6	41.1	31.5	79.3
CO	11.3	11.3	6.6	31.6	3.5	4.7	30.0	20.5	115.7	20.3	38.7	18.9	18.5	15.2
NI	25.4	14.8	7.2	16.0	4.6	11.3	55.3	34.7	94.1	47.0	63.8	18.5	15.3	14.6
CR	81.3	30.4	29.5	37.5	24.0	33.7	51.3	72.4	110.6	93.5	115.8	53.9	44.2	46.6
GA	17.1	11.5	6.9	6.2	4.3	5.0	12.5	17.0	22.3	15.1	26.0	9.1	8.8	9.5
SN	2.5	4.9	12.5	13.2	5.3	4.3	1.9	5.0	6.5	7.6	5.7	4.1	9.9	13.2
TI	4753.5	7550.6	13100.8	6704.4	10755.6	92...3	1986.4	8593.2	4937.3	7.68.4	3446.9	5553.5	9466.5	10167.1
BE	.9	0	0	0	0	.3	5.7	0	4.2	.3	4.1	0	0	0
MG	.1	.0	.2	.2	0	.2	.3	.3	.4	.0	.2	.2	.0	.2
CA	.2	.3	.3	.5	.2	.2	.6	.4	.5	.4	.3	.2	.3	.4
SR	15.4	21.7	14.6	20.9	11.0	13.0	22.2	32.3	34.5	22.7	16.7	23.1	21.9	31.8
BA	215.3	228.1	110.3	234.1	88.4	175.8	459.9	418.0	497.1	343.9	256.1	230.1	186.0	196.6
K	1.3	.6	.3	.4	.2	.5	1.0	1.1	1.5	1.1	.9	.9	.6	.6
LI	14.3	8.4	2.5	1.5	.2	8.0	21.9	36.2	66.2	52.0	48.5	13.4	9.8	8.6
AL	11.3	7.9	4.5	5.6	3.9	5.4	8.3	15.5	14.4	14.4	13.9	6.8	6.0	6.1
SC	3.7	2.5	3.3	5.0	1.8	3.6	7.2	4.7	9.9	7.6	4.4	4.3	4.0	5.9
SI	31.2	36.9	42.9	43.9	39.0	41.5	37.5	34.0	46.0	46.7	37.8	36.4	41.0	43.9
MN	201.3	289.7	305.7	1011.0	292.9	127.7	433.1	302.5	3047.5	315.1	265.2	315.6	283.9	342.2

III.   <u>ANALYTICAL ERROR</u>

            The results of duplicate analyses were used to
evaluate analytical precision, and this is discussed in Chapter
3. Other features of the analytical systems used in the research
are illustrated by processing duplicate data with a computer
program PRESIZN, which generates the contigency tables presented
in this appendix. These contingency tables are interpreted by
reference to simulation studies (Thompson and Howarth, 1976). Six
types of error can be recognized in simulated contingency tables:
round-off error; setting negative results to zero; systematic
bias on one of two duplicate measurements; log-normal error; mixtures
of two analytical systems; and a non-linear system. Most of the
analytical systems used in the research exhibit no quantifiable error;
a few systems show round-off error and non-linearity.

<u>Round-off error</u>

            In the analytical systems used, round-off error is
apparent for Ag, Be, Cd, Li and Mo determined by emission spectrography
Ni and Co determined by atomic absorption spectroscopy in London, and
Cr in leaves determined by atomic absorption spectroscopy in Lusaka.
Emission spectrography results were rounded-off prior to duplicate
processing and round-off to the nearest 0.1 ppm becomes significant
for Ag, Be, Cd, Li and Mo because most values are very low. For
Cr in leaves the round-off error was introduced by the atomic
absorption spectrophotometer operator, who reported instrument
readings to the nearest 50 ppm because of the use of an unstable Cr
lamp. The source of Ni, Cu and Co round-off error in atomic absorption
spectroscopy is less obvious, but is again attributed to the instrument
reading practice of the operator.

<u>Non-linear systems</u>

            Non-linearity is less obvious than round-off error,
but the contingency tables suggest that non-linear systems may
occur in emission spectrography results for Ni in atomic absorption
spectroscopy results for Fe determined in London, and in Ni and Cu
in leaves determined by atomic absorption spectroscopy in Lusaka,
and perhaps in S analysis. Possible sources of non-linearity are

different sample types, varying instrument operating characteristics
on different days and varying efficiency of batch sample preparations.

Other errors

Systematic bias was not tested because this requires
a comparison of positive and negative differences, and absolute
differences were used throughout. The identification of log-normal
error requires much larger data sets than those used in the research.
Finally, mixed analytical systems are almost certainly present in
the data, but not immediately apparent in the contingency tables,
perhaps because any differences in analytical response between
systems are not acute.

CONTINGENCY TABLE FOR SI DETERMINED BY EMISSION SPECTROGRAPHY

REGRESSION OF STANDARD DEVIATION ON CONCENTRATION

INTERCEPT	-.812457	STANDARD ERROR	.680031	T-VALUE	-1.194735
COEFFICIENT	.186253	STANDARD ERROR	.027602	T-VALUE	6.747736
OBSERVATIONS	11				

TEST ADEQUACY OF EQUATION

CELL EXPECTATION FOR MODEL 1.2

DECILE	CONCENTRATION RANGE		DIFFERENCE DECILE FOR MODEL									
			1	2	3	4	5	6	7	8	9	10
1	1.8000E+00	7.5500E+00	6	0	2	0	0	0	0	0	1	3
2	9.3200E+00	1.0955E+01	7	1	0	2	1	0	0	0	1	0
3	1.0980E+01	1.4480E+01	1	1	3	3	1	1	0	0	1	1
4	1.4535E+01	2.0155E+01	0	1	1	1	1	1	1	0	1	5
5	2.0175E+01	2.2250E+01	0	0	2	7	0	1	1	3	0	2
6	2.2320E+01	2.4810E+01	2	1	0	1	0	1	2	1	1	3
7	2.4920E+01	2.9430E+01	1	0	4	0	2	1	0	1	2	1
8	2.9415E+01	3.2390E+01	1	0	1	1	0	2	2	3	1	1
9	3.2400E+01	3.6045E+01	0	1	1	1	4	3	0	1	1	0
10	3.6935E+01	4.2210E+01	0	1	2	3	4	1	0	1	0	0
	COLUMN TOTALS		18	6	16	15	17	11	6	10	9	16

CONTINGENCY TABLE FOR BA DETERMINED BY EMISSION SPECTROGRAPHY

REGRESSION OF STANDARD DEVIATION ON CONCENTRATION

INTERCEPT	-3.192258	STANDARD ERROR	5.304020	T-VALUE	-.601856
COEFFICIENT	.185440	STANDARD ERROR	.026748	T-VALUE	6.932914
OBSERVATIONS	11				

TEST ADEQUACY OF EQUATION

CELL EXPECTATION FOR MODEL   1.2

DECILE	CONCENTRATION RANGE		DIFFERENCE DECILE FOR MODEL									
			1	2	3	4	5	6	7	8	9	10
1	9.3500E-01	4.4465E+01	5	0	1	0	0	0	0	0	1	4
2	4.4600E+01	5.4885E+01	0	0	2	1	0	2	1	2	2	2
3	5.5080E+01	9.1695E+01	1	2	0	0	0	1	1	1	4	2
4	9.2300E+01	1.0651E+02	1	0	0	1	2	0	3	0	2	3
5	1.0773E+02	1.2616E+02	1	1	1	2	1	1	1	1	0	3
6	1.2626E+02	1.5693E+02	2	1	2	1	0	2	0	0	0	4
7	1.5809E+02	1.8201E+02	2	2	1	0	1	1	2	0	1	2
8	1.8600E+02	2.4628E+02	2	1	0	1	3	3	1	0	0	1
9	2.4700E+02	3.1575E+02	0	4	1	2	0	1	1	0	2	1
10	3.4000E+02	5.1551E+02	2	0	2	0	1	2	2	0	3	0
	COLUMN TOTALS		17	11	10	5	8	13	12	4	15	22

CONTINGENCY TABLE FOR K DETERMINED BY EMISSION SPECTROGRAPHY

REGRESSION OF STANDARD DEVIATION ON CONCENTRATION

INTERCEPT	.00974	STANDARD ERROR	.014758	T-VALUE	.063270
COEFFICIENT	.100004	STANDARD ERROR	.011506	T-VALUE	8.691517
OBSERVATIONS	11				

TEST ADEQUACY OF EQUATION

CELL EXPECTATION FOR MODEL   1.2

DECILE	CONCENTRATION RANGE		DIFFERENCE DECILE FOR MODEL									
			1	2	3	4	5	6	7	8	9	10
1	0	1.8000E-01	1	0	0	0	0	0	0	2	3	6
2	1.8500E-01	3.1500E-01	1	0	1	0	1	2	1	2	1	3
3	3.2500E-01	4.0000E-01	1	1	1	1	1	2	1	1	1	2
4	4.0500E-01	5.0000E-01	1	2	1	1	2	1	0	0	2	2
5	5.1000E-01	5.9500E-01	1	1	1	0	2	2	1	1	1	2
6	5.9500E-01	7.5000E-01	0	1	1	3	1	1	1	1	1	2
7	7.5000E-01	1.0100E+00	2	3	1	1	0	1	1	0	2	1
8	1.0500E+00	1.4650E+00	1	0	1	1	2	1	0	1	2	3
9	1.5000E+00	2.3400E+00	2	2	3	1	1	0	2	0	0	1
10	2.3750E+00	3.2600E+00	1	2	0	0	3	1	1	2	0	2
	COLUMN TOTALS		11	12	10	8	13	11	8	10	13	24

CONTINGENCY TABLE FOR AL DETERMINED BY EMISSION SPECTROGRAPHY

REGRESSION OF STANDARD DEVIATION ON CONCENTRATION

INTERCEPT   .159519   STANDARD ERROR   .260561   T-VALUE   .612215
COEFFICIENT   .141413   STANDARD ERROR   .027269   T-VALUE   5.185883
OBSERVATIONS   11

TEST ADEQUACY OF EQUATION

CELL EXPECTATION FOR MODEL   1.2

DECILE	CONCENTRATION RANGE		DIFFERENCE DECILE FOR MODEL									
			1	2	3	4	5	6	7	8	9	10
1	0	1.1350E+00	5	0	0	2	0	1	0	0	0	4
2	1.2700E+00	3.6710E+00	2	0	0	1	1	1	2	1	2	2
3	3.6800E+00	5.1000E+00	1	2	1	1	3	1	2	0	0	1
4	5.1750E+00	6.6100E+00	2	1	1	0	2	0	1	1	2	2
5	6.6400E+00	7.7900E+00	1	0	1	3	1	2	1	1	1	1
6	8.3150E+00	9.5100E+00	0	1	1	2	1	1	2	0	2	2
7	9.5450E+00	1.1230E+01	1	3	3	1	1	0	1	1	1	0
8	1.1250E+01	1.2350E+01	0	0	1	3	2	1	0	1	1	3
9	1.2925E+01	1.5000E+01	2	0	3	2	2	1	0	1	0	1
10	1.5020E+01	1.7740E+01	1	2	1	0	1	1	2	2	0	2
	COLUMN TOTALS		15	9	12	15	14	9	11	8	9	18

CONTINGENCY TABLE FOR SC DETERMINED BY EMISSION SPECTROGRAPHY

REGRESSION OF STANDARD DEVIATION ON CONCENTRATION

INTERCEPT	1.197299	STANDARD ERROR	.669273	T-VALUE	1.788955
COEFFICIENT	.098690	STANDARD ERROR	.048848	T-VALUE	2.020365
OBSERVATIONS	11				

TEST ADEQUACY OF EQUATION

CELL EXPECTATION FOR MODEL   1.2

DECILE	CONCENTRATION RANGE		DIFFERENCE DECILE FOR MODEL									
			1	2	3	4	5	6	7	8	9	10
1	7.0000E-02	3.7250E+00	3	2	0	1	0	0	2	1	1	2
2	7.7250E+00	6.5300E+00	1	1	2	2	2	2	1	0	0	2
3	6.5650E+00	7.8100E+00	0	2	2	0	0	0	2	1	1	4
4	8.0650E+00	8.7200E+00	1	2	1	3	0	3	2	0	0	0
5	8.7500E+00	1.0290E+01	2	3	2	0	1	1	1	0	2	0
6	1.0525E+01	1.2540E+01	1	0	2	0	1	1	3	4	0	0
7	1.2625E+01	1.5080E+01	1	1	2	1	0	1	3	1	1	1
8	1.5015E+01	1.9375E+01	1	1	1	3	0	0	2	0	3	1
9	1.8715E+01	2.1525E+01	1	1	2	0	1	0	1	0	0	3
10	2.1650E+01	2.5225E+01	3	0	0	3	0	1	1	3	0	1
		COLUMN TOTALS	14	15	14	13	5	9	18	10	8	14

CONTINGENCY TABLE FOR GA DETERMINED BY EMISSION SPECTROGRAPHY

REGRESSION OF STANDARD DEVIATION ON CONCENTRATION

INTERCEPT	-.276978	STANDARD ERROR	.609778	T-VALUE	-.454227
COEFFICIENT	.151095	STANDARD ERROR	.032202	T-VALUE	5.002626
OBSERVATIONS	11				

TEST ADEQUACY OF EQUATION

CELL EXPECTATION FOR MODEL   1.2

DECILE	CONCENTRATION RANGE		DIFFERENCE DECILE FOR MODEL									
			1	2	3	4	5	6	7	8	9	10
1	0	4.5350E+00	6	0	0	0	1	1	0	0	0	4
2	4.6250E+00	8.5150E+00	1	0	0	1	2	1	1	0	1	5
3	8.6650E+00	1.1605E+01	0	1	0	2	1	2	2	1	1	2
4	1.1810E+01	1.3840E+01	0	1	1	0	2	0	2	4	1	1
5	1.3925E+01	1.6145E+01	2	1	0	2	2	2	1	0	1	1
6	1.6900E+01	1.7845E+01	4	0	3	1	0	1	1	0	1	1
7	1.7990E+01	2.0855E+01	2	2	1	2	4	0	1	0	0	0
8	2.0920E+01	2.2410E+01	3	0	1	2	4	0	0	0	2	0
9	2.2930E+01	2.9430E+01	2	2	0	4	0	0	2	1	0	1
10	3.0070E+01	3.7550E+01	1	1	1	1	0	2	4	0	2	0
	COLUMN TOTALS		21	9	7	15	16	9	14	6	9	15

CONTINGENCY TABLE FOR LI DETERMINED BY EMISSION SPECTROGRAPHY

REGRESSION OF STANDARD DEVIATION ON CONCENTRATION

INTERCEPT	1.210510	STANDARD ERROR	.552467	T-VALUE	2.191099
COEFFICIENT	.052868	STANDARD ERROR	.023398	T-VALUE	2.259545
OBSERVATIONS	11				

TEST ADEQUACY OF EQUATION

CELL EXPECTATION FOR MODEL   1.2

DECILE	CONCENTRATION RANGE		DIFFERENCE DECILE FOR MODEL									
			1	2	3	4	5	6	7	8	9	10
1	1.5000E-01	1.5000E-01	12	0	0	0	0	0	0	0	0	0
2	1.5000E-01	1.5000E-01	12	0	0	0	0	0	0	0	0	0
3	1.5000E-01	6.4000E-01	8	1	0	2	1	0	0	0	0	0
4	3.2000E-01	3.8650E+00	0	0	0	0	1	1	1	2	4	3
5	4.745E+00	9.310E+00	1	0	0	1	0	1	0	2	1	6
6	9.3950E+00	1.4045E+01	3	3	1	1	1	0	1	0	1	1
7	1.4425E+01	2.1700E+01	0	0	0	1	3	1	0	0	1	6
8	2.3065E+01	2.9045E+01	0	0	1	2	1	1	2	2	2	1
9	2.9425E+01	4.2770E+01	1	3	0	2	1	0	2	0	1	2
10	4.5260E+01	5.8430E+01	2	1	2	1	2	0	3	1	0	0
	COLUMN TOTALS		39	8	4	10	10	4	9	7	10	19

CONTINGENCY TABLE FOR BE DETERMINED BY EMISSION SPECTROGRAPHY

REGRESSION OF STANDARD DEVIATION ON CONCENTRATION

INTERCEPT	.070930	STANDARD ERROR	.058716	T-VALUE	1.208087
COEFFICIENT	.272335	STANDARD ERROR	.066374	T-VALUE	4.110564
OBSERVATIONS	11				

TEST ADEQUACY OF EQUATION

CELL EXPECTATION FOR MODEL   1.2

DECILE	CONCENTRATION RANGE		DIFFERENCE DECILE FOR MODEL									
			1	2	3	4	5	6	7	8	9	10
1	0	0	12	0	0	0	0	0	0	0	0	0
2	0	0	12	0	0	0	0	0	0	0	0	0
3	0	0	12	0	0	0	0	0	0	0	0	0
4	0	0	12	0	0	0	0	0	0	0	0	0
5	0	0	12	0	0	0	0	0	0	0	0	0
6	0	0	12	0	0	0	0	0	0	0	0	0
7	0	2.9500E-01	3	0	0	0	0	0	0	2	1	6
8	7.5500E-01	7.9000E-01	0	0	1	2	0	0	2	0	1	6
9	8.1000E-01	1.5900E+00	1	1	1	0	1	1	1	0	2	4
10	1.6950E+00	2.9100E+00	4	1	0	3	1	0	1	0	2	0
	COLUMN TOTALS		80	2	2	5	2	1	4	2	6	16

CONTINGENCY TABLE FOR CA DETERMINED BY EMISSION SPECTROGRAPHY

REGRESSION OF STANDARD DEVIATION ON CONCENTRATION

INTERCEPT	.035928	STANDARD ERROR	.063565	T-VALUE	.565227
COEFFICIENT	.161876	STANDARD ERROR	.025526	T-VALUE	6.341594
OBSERVATIONS	11				

TEST ADEQUACY OF EQUATION

CELL EXPECTATION FOR MODEL   1.2

DECILE	CONCENTRATION RANGE		DIFFERENCE DECILE FOR MODEL									
			1	2	3	4	5	6	7	8	9	10
1	1.5500E-01	3.1000E-01	3	0	1	1	6	0	0	0	1	0
2	3.1500E-01	4.2500E-01	0	1	2	2	1	2	4	0	0	0
3	4.3000E-01	5.0500E-01	3	1	1	0	2	1	1	2	1	0
4	5.1500E-01	7.1000E-01	2	1	2	0	0	2	2	0	1	2
5	7.2000E-01	1.2050E+00	1	1	1	3	1	3	0	0	1	1
6	1.2500E+00	1.5800E+00	0	2	1	2	2	1	2	1	0	1
7	1.6050E+00	1.9500E+00	1	2	2	1	0	1	2	2	0	1
8	1.9650E+00	2.7300E+00	1	0	2	1	1	1	3	2	1	0
9	2.8350E+00	5.0200E+00	1	1	1	1	1	2	0	1	0	4
10	5.2000E+00	6.7400E+00	1	1	1	1	1	3	0	2	0	2
		COLUMN TOTALS	13	10	14	12	15	16	14	10	5	11

CONTINGENCY TABLE FOR MG DETERMINED BY EMISSION SPECTROGRAPHY

REGRESSION OF STANDARD DEVIATION ON CONCENTRATION

INTERCEPT	.037777	STANDARD ERROR	.092081	T-VALUE	.416264
COEFFICIENT	.200087	STANDARD ERROR	.020625	T-VALUE	9.701170
OBSERVATIONS	11				

TEST ADEQUACY OF EQUATION

CELL EXPECTATION FOR MODEL   1.2

DECILE	CONCENTRATION RANGE		1	2	3	4	5	6	7	8	9	10
							DIFFERENCE DECILE FOR MODEL					
1	5.0000E-03	2.1500E-01	7	4	0	0	0	0	0	0	0	1
2	2.2000E-01	5.6000E-01	4	4	2	0	2	0	0	0	0	0
3	7.6500E-01	9.7500E-01	0	2	2	2	2	1	0	1	0	2
4	9.9500E-01	1.6700E+00	0	2	3	0	1	2	1	0	2	1
5	1.6950E+00	2.8450E+00	3	1	1	1	2	0	0	1	1	2
6	3.0250E+00	3.9250E+00	0	0	2	2	1	0	2	1	2	2
7	3.9350E+00	4.8800E+00	1	0	1	1	1	2	1	4	1	0
8	4.8900E+00	5.8200E+00	1	0	0	1	3	4	1	0	1	1
9	5.9500E+00	8.0410E+00	1	4	0	0	1	0	3	0	3	0
10	8.1050E+00	9.8900E+00	2	0	1	2	3	2	1	0	0	1
	COLUMN TOTALS		19	17	12	9	16	11	9	7	10	10

CONTINGENCY TABLE FOR SP DETERMINED BY EMISSION SPECTROGRAPHY

REGRESSION OF STANDARD DEVIATION ON CONCENTRATION

INTERCEPT	-1.058024	STANDARD ERROR	2.148293	T-VALUE	-.492495
COEFFICIENT	.189093	STANDARD ERROR	.020886	T-VALUE	9.053387
OBSERVATIONS	11				

TEST ADEQUACY OF EQUATION

CELL EXPECTATION FOR MODEL   1.2

DECILE	CONCENTRATION RANGE		1	2	3	4	5	6	7	8	9	10
			DIFFERENCE DECILE FOR MODEL									
1	3.3050E+00	1.1450E+01	2	0	0	0	1	1	0	0	0	8
2	1.2585E+01	1.5410E+01	1	0	1	1	0	1	2	1	1	4
3	1.5605E+01	1.9975E+01	0	2	1	0	0	0	3	1	2	3
4	2.0920E+01	2.4405E+01	1	1	1	3	1	2	1	0	1	1
5	2.4470E+01	3.3460E+01	1	0	2	1	1	1	1	1	1	3
6	3.4210E+01	4.4960E+01	1	2	2	2	1	1	3	0	0	0
7	4.5105E+01	6.3605E+01	2	0	1	0	1	0	0	3	3	2
8	6.4730E+01	9.6905E+01	1	4	1	0	2	0	2	1	0	1
9	1.0101E+02	2.0072E+02	0	2	2	3	1	1	0	3	0	0
10	2.0154E+02	2.9256E+02	2	0	0	1	2	0	4	0	1	2
	COLUMN TOTALS		11	11	11	11	10	7	16	10	9	24

CONTINGENCY TABLE FOR MN DETERMINED BY EMISSION SPECTROGRAPHY

REGRESSION OF STANDARD DEVIATION ON CONCENTRATION

INTERCEPT	79.277446	STANDARD ERROR	102.172485	T-VALUE	.775918
COEFFICIENT	.165375	STANDARD ERROR	.097073	T-VALUE	1.703611
OBSERVATIONS	11				

TEST ADEQUACY OF EQUATION

CELL EXPECTATION FOR MODEL , 1.2

DECILE	CONCENTRATION RANGE		DIFFERENCE DECILE FOR MODEL									
			1	2	3	4	5	6	7	8	9	10
1	2.0000E-02	2.7157E+02	5	1	3	1	0	2	0	0	0	0
2	2.8387E+02	3.9119E+02	3	6	0	1	1	0	1	0	0	0
3	3.9169E+02	4.4299E+02	6	2	3	1	0	0	0	0	0	0
4	4.4541E+02	6.1547E+02	7	2	1	0	0	0	1	1	0	0
5	6.3638E+02	7.5529E+02	0	0	0	0	0	1	0	1	3	7
6	7.5743E+02	1.0257E+03	0	1	0	0	0	1	1	0	0	9
7	1.0267E+03	1.2159E+03	3	1	1	1	0	0	0	0	1	5
8	1.2359E+03	1.4439E+03	1	3	1	2	0	3	1	0	1	0
9	1.4585E+03	1.7021E+03	2	1	1	3	2	2	1	0	0	0
10	1.7089E+03	2.1071E+03	2	1	0	1	2	1	3	1	1	0
	COLUMN TOTALS		29	18	10	10	5	10	8	3	6	21

CONTINGENCY TABLE FOR SN DETERMINED BY EMISSION SPECTROGRAPHY

REGRESSION OF STANDARD DEVIATION ON CONCENTRATION

INTERCEPT	1.573211	STANDARD ERROR	.965859	T-VALUE	1.628822
COEFFICIENT	.222681	STANDARD ERROR	.080329	T-VALUE	2.772113
OBSERVATIONS	11				

TEST ADEQUACY OF EQUATION

CELL EXPECTATION FOR MODEL 1.2

DECILE	CONCENTRATION RANGE		DIFFERENCE DECILE FOR MODEL									
			1	2	3	4	5	6	7	8	9	10
1	0	2.0750E+00	7	3	1	0	0	1	0	0	0	0
2	2.1550E+00	4.2700E+00	0	0	0	0	1	0	1	6	1	3
3	4.2900E+00	6.2000E+00	0	1	0	0	2	3	1	1	2	2
4	5.2200E+00	7.7050E+00	1	2	1	3	0	1	2	0	2	0
5	7.8350E+00	9.8200E+00	1	1	1	0	1	2	0	2	3	1
6	9.8400E+00	1.0715E+01	2	2	0	2	1	1	0	2	2	0
7	1.0760E+01	1.2455E+01	2	2	1	2	0	1	1	1	0	2
8	1.2485E+01	1.4855E+01	1	1	4	1	0	0	1	2	2	0
9	1.5110E+01	1.8530E+01	2	2	0	2	0	2	0	2	1	1
10	1.9180E+01	2.7965E+01	2	2	2	0	1	0	1	2	0	2
	COLUMN TOTALS		18	16	10	10	6	11	7	18	13	11

CONTINGENCY TABLE FOR TI DETERMINED BY EMISSION SPECTROGRAPHY

REGRESSION OF STANDARD DEVIATION ON CONCENTRATION

INTERCEPT	201.465735	STANDARD ERROR	267.421359	T-VALUE	.753364
COEFFICIENT	.149106	STANDARD ERROR	.029117	T-VALUE	5.120855
OBSERVATIONS	11				

TEST ADEQUACY OF EQUATION

CELL EXPECTATION FOR MODEL   1.2

DECILE	CONCENTRATION RANGE		DIFFERENCE DECILE FOR MODEL									
			1	2	3	4	5	6	7	8	9	10
1	9.0000E-02	6.6738E+02	6	3	3	0	0	0	0	0	0	0
2	7.9917E+02	1.6497E+03	7	3	2	0	2	0	1	1	0	0
3	1.7193E+03	3.0450E+03	3	0	4	0	2	1	0	1	1	0
4	3.0630E+03	5.4856E+03	1	1	2	2	0	2	2	1	0	1
5	5.5811E+03	6.6520E+03	1	1	2	1	0	1	0	1	2	3
6	5.7537E+03	7.9992E+03	2	1	3	0	0	1	0	1	2	2
7	8.0169E+03	8.9823E+03	1	3	1	1	0	0	1	0	3	2
8	9.1473E+03	1.1215E+04	2	0	1	0	4	0	1	1	3	0
9	1.1223E+04	1.6021E+04	1	2	0	0	1	2	2	1	0	3
10	1.6167E+04	1.9756E+04	1	1	2	2	0	0	3	0	1	2
		COLUMN TOTALS	21	15	20	6	9	7	10	7	12	13

CONTINGENCY TABLE FOR CR DETERMINED BY EMISSION SPECTROGRAPHY

REGRESSION OF STANDARD DEVIATION ON CONCENTRATION

INTERCEPT	16.213972	STANDARD ERROR	9.024489	T-VALUE	1.796664
COEFFICIENT	.062151	STANDARD ERROR	.007725	T-VALUE	8.045595
OBSERVATIONS	11				

TEST ADEQUACY OF EQUATION

CELL EXPECTATION FOR MODEL   1.2

DECILE	CONCENTRATION RANGE		DIFFERENCE DECILE FOR MODEL									
			1	2	3	4	5	6	7	8	9	10
1	3.5000E-01	4.8715E+01	5	3	2	1	1	0	0	0	0	0
2	5.1145E+01	1.0431E+02	3	2	2	2	2	0	0	0	0	1
3	1.0528E+02	1.5210E+02	3	2	1	4	1	0	1	0	0	0
4	1.5274E+02	2.6436E+02	1	0	5	0	2	2	1	0	1	0
5	2.7017E+02	6.8026E+02	1	0	1	1	0	1	1	2	2	3
6	7.0530E+02	1.1594E+03	0	1	1	0	2	1	1	1	1	4
7	1.1925E+03	1.3772E+03	2	1	2	0	2	1	2	0	1	1
8	1.3917E+03	1.5746E+03	2	0	2	1	2	0	1	1	3	0
9	1.5766E+03	2.0208E+03	2	1	0	0	2	1	2	0	1	3
10	2.0532E+03	2.5449E+03	1	1	2	1	3	1	3	0	0	0
	COLUMN TOTALS		20	11	18	10	17	7	12	4	9	12

CONTINGENCY TABLE FOR CO DETERMINED BY EMISSION SPECTROGRAPHY

REGRESSION OF STANDARD DEVIATION ON CONCENTRATION

INTERCEPT	.221137	STANDARD ERROR	1.043339	T-VALUE	.211952
COEFFICIENT	.091881	STANDARD ERROR	.012843	T-VALUE	7.154094
OBSERVATIONS	11				

TEST ADEQUACY OF EQUATION

CELL EXPECTATION FOR MODEL   1.2

DECILE	CONCENTRATION RANGE		DIFFERENCE DECILE FOR MODEL									
			1	2	3	4	5	6	7	8	9	10
1	3.5000E-01	1.6615E+01	3	2	2	1	0	1	0	1	1	1
2	1.7770E+01	2.2920E+01	0	3	2	0	1	1	0	0	3	2
3	2.3110E+01	2.8650E+01	0	4	0	0	3	0	2	1	0	2
4	2.9840E+01	3.9205E+01	2	2	0	0	2	0	1	2	0	3
5	3.9295E+01	5.5455E+01	2	0	0	0	3	3	0	0	2	2
6	5.6750E+01	7.1380E+01	1	1	2	1	1	3	1	1	0	1
7	7.4690E+01	9.7655E+01	0	0	1	1	2	1	4	0	1	2
8	9.7740E+01	1.0493E+02	2	2	1	0	2	1	2	2	0	0
9	1.0639E+02	1.2574E+02	2	1	2	1	0	1	1	2	0	2
10	1.2595E+02	1.9363E+02	1	1	0	2	1	0	2	2	1	2
	COLUMN TOTALS		13	16	10	6	15	11	13	11	8	17

CONTINGENCY TABLE FOR NI DETERMINED BY EMISSION SPECTROGRAPHY

REGRESSION OF STANDARD DEVIATION ON CONCENTRATION

INTERCEPT	22.080123	STANDARD ERROR	13.931972	T-VALUE	1.584853
COEFFICIENT	.043402	STANDARD ERROR	.013640	T-VALUE	3.182097
OBSERVATIONS	11				

TEST ADEQUACY OF EQUATION

CELL EXPECTATION FOR MODEL   1.2

DECILE	CONCENTRATION RANGE		1	2	3	4	5	6	7	8	9	10
1	1.4020E+01	5.8110E+01	6	6	0	0	0	0	0	0	0	0
2	5.8145E+01	9.4090E+01	4	3	0	4	0	0	0	1	0	0
3	9.4960E+01	1.2522E+02	1	2	2	4	1	0	1	0	1	0
4	1.2541E+02	1.9776E+02	2	4	1	3	0	1	0	0	0	1
5	2.1830E+02	4.1064E+02	3	2	1	0	1	0	1	0	1	3
6	4.3682E+02	6.8954E+02	2	0	1	3	1	2	1	0	1	4
7	5.7366E+02	1.1120E+03	1	1	0	1	0	0	1	1	1	6
8	1.1536E+03	1.4201E+03	0	2	2	1	0	0	1	1	1	4
9	1.5033E+03	1.7397E+03	1	1	0	1	0	1	4	2	1	1
10	1.7472E+03	2.7333E+03	3	2	0	2	0	1	0	1	2	1
	COLUMN TOTALS		23	23	7	16	3	5	9	6	8	20

CONTINGENCY TABLE FOR IO DETERMINED BY EMISSION SPECTROGRAPHY

REGRESSION OF STANDARD DEVIATION ON CONCENTRATION

INTERCEPT	.139454	STANDARD ERROR	.082918	T-VALUE	1.681821
COEFFICIENT	.335285	STANDARD ERROR	.105393	T-VALUE	3.181279
OBSERVATIONS	11				

TEST ADEQUACY OF EQUATION

CELL EXPECTATION FOR MODEL 1.2

DECILE	CONCENTRATION RANGE		DIFFERENCE DECILE FOR MODEL									
			1	2	3	4	5	6	7	8	9	10
1	2.0000E-02	2.0000E-02	12	0	0	0	0	0	0	0	0	0
2	2.0000E-02	2.0000E-02	12	0	0	0	0	0	0	0	0	0
3	2.0000E-02	1.7000E-01	3	3	2	0	1	0	1	2	0	0
4	2.3000E-01	3.3500E-01	0	0	2	1	0	0	0	0	5	4
5	3.4000E-01	5.0000E-01	1	1	1	1	2	0	1	0	0	5
6	5.1500E-01	5.5000E-01	3	1	0	1	0	0	0	1	3	2
7	5.6000E-01	7.6500E-01	2	0	1	1	2	1	1	2	0	2
8	7.6500E-01	9.7500E-01	1	1	2	1	2	0	1	1	1	2
9	1.0550E+00	1.3100E+00	1	2	0	3	2	3	1	0	0	0
10	1.3700E+00	2.0000E+00	2	1	0	2	1	1	1	1	1	2
	COLUMN TOTALS		37	9	8	10	10	5	6	7	10	18

CONTINGENCY TABLE FOR V DETERMINED BY EMISSION SPECTROGRAPHY

REGRESSION OF STANDARD DEVIATION ON CONCENTRATION

INTERCEPT	2.554173	STANDARD ERROR	5.490605	T-VALUE	.466039
COEFFICIENT	.100825	STANDARD ERROR	.025933	T-VALUE	3.887846
OBSERVATIONS	11				

TEST ADEQUACY OF EQUATION

CELL EXPECTATION FOR MODEL   1.2

DECILE	CONCENTRATION RANGE		DIFFERENCE DECILE FOR MODEL									
			1	2	3	4	5	6	7	8	9	10
1	3.1000E-01	5.3650E+01	4	2	1	3	1	0	0	0	1	0
2	5.4435E+01	6.9490E+01	2	1	1	3	0	0	1	0	1	3
3	7.0400E+01	8.3540E+01	4	0	1	2	2	1	1	0	1	0
4	9.5120E+01	1.1614E+02	0	0	2	1	2	1	2	1	2	1
5	1.1647E+02	1.5152E+02	0	1	3	0	1	3	1	1	2	0
6	1.5205E+02	1.6590E+02	0	2	3	1	0	0	2	1	2	1
7	1.6941E+02	1.9729E+02	4	0	1	0	0	3	0	0	3	1
8	1.9845E+02	2.3309E+02	0	1	4	1	1	3	0	1	0	1
9	2.3500E+02	3.2503E+02	2	1	0	1	1	0	0	2	0	5
10	3.2663E+02	6.1689E+02	0	2	2	0	0	2	2	1	0	3
	COLUMN TOTALS		16	10	18	12	8	13	9	7	12	15

CONTINGENCY TABLE FOR AG DETERMINED BY EMISSION SPECTROGRAPHY

REGRESSION OF STANDARD DEVIATION ON CONCENTRATION

INTERCEPT	-.012666	STANDARD ERROR	.013585	T-VALUE	-.932294
COEFFICIENT	.480228	STANDARD ERROR	.041023	T-VALUE	11.706217
OBSERVATIONS	11				

TEST ADEQUACY OF EQUATION

CELL EXPECTATION FOR MODEL   1.2

DECILE	CONCENTRATION RANGE		DIFFERENCE DECILE FOR MODEL									
			1	2	3	4	5	6	7	8	9	10
1	5.0000E-02	5.0000E-02	12	0	0	0	0	0	0	0	0	0
2	5.0000E-02	5.0000E-02	12	0	0	0	0	0	0	0	0	0
3	5.0000E-02	5.0000E-02	12	0	0	0	0	0	0	0	0	0
4	5.0000E-02	5.0000E-02	12	0	0	0	0	0	0	0	0	0
5	5.0000E-02	5.0000E-02	12	0	0	0	0	0	0	0	0	0
6	5.0000E-02	5.0000E-02	12	0	0	0	0	0	0	0	0	0
7	5.0000E-02	5.0000E-02	12	0	0	0	0	0	0	0	0	0
8	5.0000E-02	5.0000E-02	12	0	0	0	0	0	0	0	0	0
9	5.0000E-02	2.4000E-01	3	1	1	0	0	0	0	0	1	6
10	2.5500E-01	1.7950E+00	1	0	1	1	0	0	1	1	0	7
	COLUMN TOTALS		100	1	2	1	0	0	1	1	1	13

CONTINGENCY TABLE FOR CO DETERMINED BY EMISSION SPECTROGRAPHY

REGRESSION OF STANDARD DEVIATION ON CONCENTRATION

INTERCEPT	.071764	STANDARD ERROR	.152152	T-VALUE	.471659
COEFFICIENT	.766469	STANDARD ERROR	.109667	T-VALUE	6.989053
OBSERVATIONS	11				

TEST ADEQUACY OF EQUATION

CELL EXPECTATION FOR MODEL   1.2

DECILE	CONCENTRATION RANGE		DIFFERENCE DECILE FOR MODEL									
			1	2	3	4	5	6	7	8	9	10
1	0	1.6000E-01	7	0	0	1	0	0	3	1	0	0
2	1.6000E-01	1.6000E-01	12	0	0	0	0	0	0	0	0	0
3	1.6000E-01	1.6000E-01	12	0	0	0	0	0	0	0	0	0
4	1.6000E-01	1.6000E-01	12	0	0	0	0	0	0	0	0	0
5	1.6000E-01	4.9500E-01	2	2	0	0	2	0	4	2	0	0
6	5.0000E-01	8.5000E-01	0	0	0	3	1	0	1	7	3	0
7	8.9000E-01	1.2500E+00	2	0	3	1	0	0	1	2	1	2
8	1.3300E+00	1.7950E+00	0	2	0	2	3	0	1	1	3	0
9	1.9350E+00	2.6550E+00	2	0	1	0	1	2	2	2	0	2
10	2.6900E+00	3.5900E+00	1	4	0	0	1	4	1	0	0	1
	COLUMN TOTALS		50	9	4	4	8	6	13	15	7	5

CONTINGENCY TABLE FOR ZN DETERMINED BY EMISSION SPECTROGRAPHY

REGRESSION OF STANDARD DEVIATION ON CONCENTRATION

INTERCEPT	-10.990376	STANDARD ERROR	5.144557	T-VALUE	-2.118817
COEFFICIENT	.451932	STANDARD ERROR	.030348	T-VALUE	14.891800
OBSERVATIONS	11				

TEST ADEQUACY OF EQUATION

CELL EXPECTATION FOR MODEL   1.2

DECILE	CONCENTRATION RANGE		DIFFERENCE DECILE FOR MODEL									
			1	2	3	4	5	6	7	8	9	10
1	1.9750E+00	3.0320E+01	7	0	0	0	0	0	0	0	0	5
2	3.1275E+01	4.7980E+01	0	0	1	0	1	0	1	2	1	6
3	4.8640E+01	5.8245E+01	2	0	1	0	1	3	0	2	1	2
4	5.8310E+01	7.2495E+01	1	1	0	0	0	1	1	3	2	3
5	7.3435E+01	8.9490E+01	0	2	1	0	1	3	4	0	1	0
6	9.0500E+01	1.0424E+02	3	3	1	1	1	1	1	0	1	0
7	1.0549E+02	1.2318E+02	1	3	1	2	0	1	1	1	1	1
8	1.2355E+02	1.4554E+02	2	1	2	1	0	1	2	2	0	1
9	1.4807E+02	2.3297E+02	0	5	0	1	1	1	1	0	1	2
10	2.5068E+02	7.1726E+02	2	0	1	0	1	2	1	1	2	2
		COLUMN TOTALS	18	15	8	5	6	13	12	11	10	22

CONTINGENCY TABLE FOR P3 DETERMINED BY EMISSION SPECTROGRAPHY

REGRESSION OF STANDARD DEVIATION ON CONCENTRATION

INTERCEPT	1.098176	STANDARD ERROR	.577941	T-VALUE	1.900153
COEFFICIENT	.127912	STANDARD ERROR	.027141	T-VALUE	4.712946
OBSERVATIONS	11				

TEST ADEQUACY OF EQUATION

CELL EXPECTATION FOR MODEL   1.2

DECILE	CONCENTRATION RANGE		DIFFERENCE DECILE FOR MODEL									
			1	2	3	4	5	6	7	8	9	10
1	8.7500E-01	8.0700E+00	1	2	2	0	1	2	2	1	0	1
2	8.1850E+00	9.0300E+00	2	0	1	2	2	1	2	1	1	0
3	9.1500E+00	1.0415E+01	0	1	1	2	0	2	2	1	2	1
4	1.0490E+01	1.1675E+01	2	1	1	3	1	0	1	1	2	0
5	1.1635E+01	1.3855E+01	0	2	3	1	0	1	3	1	0	1
6	1.3955E+01	1.5945E+01	3	1	2	1	1	0	1	0	3	0
7	1.6010E+01	1.7495E+01	2	0	1	1	1	1	2	1	2	1
8	1.7595E+01	2.1035E+01	0	1	2	2	1	1	0	1	1	3
9	2.1615E+01	2.9415E+01	2	0	2	1	0	1	1	2	1	2
10	3.1040E+01	5.8950E+01	0	1	2	1	4	0	0	0	2	2
	COLUMN TOTALS		12	9	17	14	11	9	14	9	14	11

CONTINGENCY TABLE FOR CU DETERMINED BY EMISSION SPECTROGRAPHY

REGRESSION OF STANDARD DEVIATION ON CONCENTRATION

INTERCEPT	2.388362	STANDARD ERROR	.932039	T-VALUE	2.562512
COEFFICIENT	.051332	STANDARD ERROR	.008833	T-VALUE	5.811164
OBSERVATIONS	11				

TEST ADEQUACY OF EQUATION

CELL EXPECTATION FOR MODEL 1.2

DECILE	CONCENTRATION RANGE		DIFFERENCE DECILE FOR MODEL									
			1	2	3	4	5	6	7	8	9	10
1	5.9400E+00	2.4680E+01	1	3	1	2	2	1	1	0	1	0
2	2.5490E+01	3.6420E+01	2	0	1	0	2	0	2	3	1	1
3	3.7590E+01	4.4970E+01	2	4	0	0	1	1	1	1	0	2
4	4.5170E+01	5.2055E+01	0	1	1	2	2	3	2	0	0	1
5	5.2835E+01	6.6645E+01	0	2	3	1	2	2	0	0	2	0
6	6.6990E+01	7.8630E+01	1	4	1	0	0	2	0	4	0	0
7	7.8985E+01	9.5505E+01	1	1	1	1	1	2	1	1	2	1
8	9.7020E+01	1.2457E+02	0	2	0	1	0	3	2	2	1	1
9	1.2682E+02	1.4435E+02	3	2	1	0	1	1	0	0	1	3
10	1.7552E+02	2.8645E+02	1	0	1	1	2	1	2	0	2	2
	COLUMN TOTALS		11	19	10	8	13	16	11	11	10	11

CONTINGENCY TABLE FOR FE DETERMINED BY EMISSION SPECTROGRAPHY

REGRESSION OF STANDARD DEVIATION ON CONCENTRATION

INTERCEPT	.044519	STANDARD ERROR	.179272	T-VALUE	.248333
COEFFICIENT	.211218	STANDARD ERROR	.024849	T-VALUE	8.499905
OBSERVATIONS	11			

TEST ADEQUACY OF EQUATION

CELL EXPECTATION FOR MODEL   1.2

DECILE	CONCENTRATION RANGE		DIFFERENCE DECILE FOR MODEL									
			1	2	3	4	5	6	7	8	9	10
1	9.1000E-01	2.1350E+00	0	2	1	1	2	0	2	2	0	2
2	2.3450E+00	3.8900E+00	2	2	1	1	2	2	0	2	0	0
3	4.0150E+00	4.8750E+00	0	1	2	0	2	2	0	3	1	1
4	4.8300E+00	5.2500E+00	2	0	1	0	2	1	1	2	1	2
5	5.6350E+00	6.1400E+00	0	0	1	1	4	3	0	1	0	2
6	6.1950E+00	6.8450E+00	1	3	2	1	2	1	1	1	0	0
7	7.0900E+00	7.8450E+00	3	0	2	0	1	1	3	2	0	0
8	7.9600E+00	9.3100E+00	0	1	0	2	0	4	2	1	2	0
9	9.3450E+00	1.0690E+01	0	2	0	1	1	3	1	2	0	2
10	1.0700E+01	1.3755E+01	1	0	1	3	4	0	0	2	0	1
	COLUMN TOTALS		0	11	11	10	20	17	10	18	4	10

CONTINGENCY TABLE FOR Hg DETERMINED BY ATOMIC ABSORPTION SPECTROSCOPY (LUSAKA)

REGRESSION OF STANDARD DEVIATION ON CONCENTRATION

INTERCEPT	-1.167213	STANDARD ERROR	1.484835	T-VALUE	-.786090
COEFFICIENT	.104629	STANDARD ERROR	.008378	T-VALUE	12.488523
OBSERVATIONS	6				

TEST ADEQUACY OF EQUATION

CELL EXPECTATION FOR MODEL   .3

DECILE	CONCENTRATION RANGE		DIFFERENCE DECILE FOR MODEL									
			1	2	3	4	5	6	7	8	9	10
1	3.0600E+01	4.4400E+01	1	0	0	1	1	0	0	0	0	0
2	5.0900E+01	6.9200E+01	1	0	0	0	0	1	0	0	0	1
3	7.6500E+01	8.5050E+01	0	0	0	2	0	0	0	1	0	0
4	8.7450E+01	9.4700E+01	0	0	0	0	1	1	0	1	0	0
5	1.1910E+02	1.3450E+02	0	0	1	0	0	1	0	0	1	0
6	1.4980E+02	1.5690E+02	1	0	0	0	1	1	0	0	0	0
7	1.5735E+02	1.6595E+02	0	0	0	1	0	1	0	0	0	1
8	1.7505E+02	1.8450E+02	0	0	0	0	0	2	0	0	0	1
9	1.8640E+02	2.3530E+02	1	1	0	0	0	1	0	0	0	0
10	2.3970E+02	2.6035E+02	0	1	0	0	0	1	0	0	0	1
	COLUMN TOTALS		4	2	1	4	3	9	0	2	1	4

CONTINGENCY TABLE FOR FE DETERMINED BY ATOMIC ABSORPTION SPECTROSCOPY (LUSAKA)

REGRESSION OF STANDARD DEVIATION ON CONCENTRATION

INTERCEPT	6.253136	STANDARD ERROR	1.611890	T-VALUE	3.879382
COEFFICIENT	.046199	STANDARD ERROR	.005592	T-VALUE	8.261614
OBSERVATIONS	3				

TEST ADEQUACY OF EQUATION

CELL EXPECTATION FOR MODEL .3

DECILE	CONCENTRATION RANGE		DIFFERENCE DECILE FOR MODEL									
			1	2	3	4	5	6	7	8	9	10
1	5.0750E+01	7.3600E+01	1	0	1	0	0	1	0	0	0	0
2	8.0200E+01	8.7200E+01	0	0	0	0	1	1	0	0	0	1
3	9.0450E+01	1.2315E+02	1	0	0	0	1	0	0	1	0	0
4	1.2640E+02	1.4440E+02	1	1	0	0	0	0	0	0	1	0
5	1.5260E+02	2.1875E+02	0	0	0	0	1	0	0	1	1	0
6	2.2055E+02	2.5610E+02	0	1	1	0	0	0	0	0	0	1
7	2.5860E+02	2.7200E+02	1	0	0	0	1	1	0	0	0	0
8	2.8390E+02	3.4100E+02	0	0	1	0	0	0	1	0	0	1
9	3.6480E+02	4.1135E+02	0	1	0	0	0	1	0	1	0	0
10	4.3180E+02	4.4605E+02	0	1	0	0	1	1	0	0	0	0
	COLUMN TOTALS		4	4	3	0	5	5	1	3	2	3

CONTINGENCY TABLE FOR CU DETERMINED BY ATOMIC ABSORPTION SPECTROSCOPY (LUSAKA)

REGRESSION OF STANDARD DEVIATION ON CONCENTRATION

INTERCEPT	.038427	STANDARD ERROR	.090903	T-VALUE	.422726
COEFFICIENT	.053431	STANDARD ERROR	.023041	T-VALUE	2.318970
OBSERVATIONS	3				

TEST ADEQUACY OF EQUATION

CELL EXPECTATION FOR MODEL   .3

DECILE	CONCENTRATION RANGE		DIFFERENCE DECILE FOR MODEL									
			1	2	3	4	5	6	7	8	9	10
1	1.9500E+00	2.6500E+00	0	0	0	1	0	0	0	0	0	2
2	2.7500E+00	2.9000E+00	1	0	1	0	0	1	0	0	0	0
3	3.1000E+00	3.3000E+00	1	0	0	0	0	0	0	0	0	2
4	3.4000E+00	3.5000E+00	1	0	0	0	1	0	1	0	0	0
5	3.5000E+00	3.5500E+00	0	0	0	0	1	0	0	1	0	1
6	3.6000E+00	3.7500E+00	2	0	0	0	0	0	1	0	0	0
7	3.8000E+00	4.0000E+00	2	0	0	0	0	0	1	0	0	0
8	4.0000E+00	4.3500E+00	2	0	0	0	0	1	0	0	0	0
9	4.4000E+00	4.6500E+00	1	0	0	1	0	1	0	0	0	0
10	4.9500E+00	5.3500E+00	0	0	0	0	0	0	0	1	0	2
	COLUMN TOTALS		10	0	1	2	2	3	3	2	0	7

CONTINGENCY TABLE FOR NI DETERMINED BY ATOMIC ABSORPTION SPECTROSCOPY (LUSAKA)

REGRESSION OF STANDARD DEVIATION ON CONCENTRATION

INTERCEPT	.032763	STANDARD ERROR	.047637	T-VALUE	.687880
COEFFICIENT	.049713	STANDARD ERROR	.005615	T-VALUE	8.853779
OBSERVATIONS	3				

TEST ADEQUACY OF EQUATION

CELL EXPECTATION FOR MODEL　　　　.3

DECILE	CONCENTRATION RANGE		DIFFERENCE DECILE FOR MODEL									
			1	2	3	4	5	6	7	8	9	10
1	2.8000E+00	3.2000E+00	0	0	0	1	0	0	0	0	1	1
2	3.2000E+00	3.3000E+00	3	0	0	0	0	0	0	0	0	0
3	3.5000E+00	4.6500E+00	0	0	0	0	0	1	0	0	0	2
4	5.5000E+00	6.0500E+00	1	0	0	1	1	0	0	0	0	0
5	6.2000E+00	6.6500E+00	0	0	0	0	0	0	0	0	0	3
6	6.9000E+00	7.5000E+00	1	0	1	0	0	0	0	0	0	1
7	7.6500E+00	8.3000E+00	1	0	0	0	1	0	0	1	0	0
8	8.7000E+00	9.1500E+00	0	0	1	0	0	0	0	0	0	2
9	9.3000E+00	1.0500E+01	1	0	0	0	0	1	0	0	0	1
10	1.1650E+01	1.3450E+01	2	0	0	0	0	0	0	0	1	0
	COLUMN TOTALS		9	0	2	2	2	2	0	1	2	10

CONTINGENCY TABLE FOR CO DETERMINED BY ATOMIC ABSORPTION SPECTROSCOPY (LUSAKA)

REGRESSION OF STANDARD DEVIATION ON CONCENTRATION

INTERCEPT	.088104	STANDARD ERROR	.183826	T-VALUE	.466587
COEFFICIENT	.075739	STANDARD ERROR	.109430	T-VALUE	.692119
OBSERVATIONS	3				

TEST ADEQUACY OF EQUATION

CELL EXPECTATION FOR MODEL   .3

DECILE	CONCENTRATION RANGE		1	2	3	4	5	6	7	8	9	10
			DIFFERENCE DECILE FOR MODEL
1	6.5000E-01	7.0000E-01	1	0	0	1	0	0	1	0	0	0
2	7.0000E-01	9.0000E-01	1	0	0	0	0	0	2	0	0	0
3	9.0000E-01	1.0000E+00	1	0	0	0	0	0	0	0	1	1
4	1.0500E+00	1.1500E+00	0	0	0	1	0	0	0	1	0	1
5	1.1500E+00	1.2000E+00	2	0	0	0	0	0	0	1	0	0
6	1.5500E+00	1.6500E+00	1	0	1	0	0	0	1	0	0	0
7	1.7500E+00	1.8000E+00	1	0	1	0	0	0	0	0	0	1
8	1.9500E+00	2.0500E+00	0	0	0	0	0	0	1	0	2	0
9	2.0500E+00	2.4500E+00	0	0	0	0	0	1	1	1	0	0
10	2.5000E+00	2.6000E+00	3	0	0	0	0	0	0	0	0	0
	COLUMN TOTALS		10	0	2	2	0	1	6	3	3	3

CONTINGENCY TABLE FOR ZN DETERMINED BY ATOMIC ABSORPTION SPECTROSCOPY (LUSAKA)

REGRESSION OF STANDARD DEVIATION ON CONCENTRATION

INTERCEPT	-.204347	STANDARD ERROR	2.549898	T-VALUE	-.080335
COEFFICIENT	.136295	STANDARD ERROR	.135462	T-VALUE	1.006148
OBSERVATIONS	3				

TEST ADEQUACY OF EQUATION

CELL EXPECTATION FOR MODEL   .3

DECILE	CONCENTRATION RANGE		DIFFERENCE DECILE FOR MODEL									
			1	2	3	4	5	6	7	8	9	10
1	8.2500E+00	9.0000E+00	1	0	1	0	1	0	0	0	0	0
2	9.5000E+00	1.0100E+01	0	3	0	0	0	0	0	0	0	0
3	1.1300E+01	1.2150E+01	0	0	1	1	0	0	0	0	1	0
4	1.2150E+01	1.2800E+01	1	0	0	0	0	0	0	0	1	1
5	1.3450E+01	1.4050E+01	0	0	1	0	1	0	0	0	0	1
6	1.4350E+01	1.5400E+01	0	0	0	0	0	0	0	1	1	1
7	1.7850E+01	2.0610E+01	1	0	1	0	0	0	0	1	0	0
8	2.0700E+01	2.1500E+01	0	0	0	0	0	0	1	1	1	0
9	2.2650E+01	2.4950E+01	0	0	1	0	0	0	1	0	1	0
10	2.6700E+01	2.8050E+01	0	0	1	0	1	0	0	0	1	0
	COLUMN TOTALS		3	3	6	1	3	0	2	3	6	3

CONTINGENCY TABLE FOR CR DETERMINED BY ATOMIC ABSORPTION SPECTROSCOPY (LUSAKA)

REGRESSION OF STANDARD DEVIATION ON CONCENTRATION

INTERCEPT	-1.251624	STANDARD ERROR	2.592989	T-VALUE	-.482695
COEFFICIENT	.371869	STANDARD ERROR	.273469	T-VALUE	1.338912
OBSERVATIONS	3				

TEST ADEQUACY OF EQUATION

CELL EXPECTATION FOR MODEL .3

DECILE	CONCENTRATION RANGE		DIFFERENCE DECILE FOR MODEL									
			1	2	3	4	5	6	7	8	9	10
1	3.6500E+00	4.3500E+00	0	2	0	0	0	0	0	0	0	1
2	4.4000E+00	5.7000E+00	1	0	0	0	0	0	0	0	0	2
3	6.0000E+00	6.6000E+00	3	0	0	0	0	0	0	0	0	0
4	6.9500E+00	7.1000E+00	1	0	0	0	0	0	0	0	1	1
5	7.1500E+00	7.5000E+00	2	0	1	0	0	0	0	0	0	0
6	7.6500E+00	8.3000E+00	1	0	1	0	0	0	0	1	0	0
7	3.9000E+00	1.0150E+01	0	0	0	0	0	1	0	1	1	0
8	1.0250E+01	1.0950E+01	0	0	0	0	0	1	0	1	1	0
9	1.1100E+01	1.1250E+01	0	0	0	0	1	0	0	0	0	0
10	1.2300E+01	1.4000E+01	1	0	0	0	1	1	0	0	0	0
	COLUMN TOTALS		11	2	2	0	2	3	0	3	3	4

CONTINGENCY TABLE FOR FE DETERMINED BY ATOMIC ABSORPTION SPECTROSCOPY (LONDON)

REGRESSION OF STANDARD DEVIATION ON CONCENTRATION

INTERCEPT	.011103	STANDARD ERROR	.141432	T-VALUE	.078502
COEFFICIENT	.035895	STANDARD ERROR	.012007	T-VALUE	2.989451
OBSERVATIONS	10				

TEST ADEQUACY OF EQUATION

CELL EXPECTATION FOR MODEL   1.2

DECILE	CONCENTRATION RANGE		DIFFERENCE DECILE FOR MODEL									
			1	2	3	4	5	6	7	8	9	10
1	1.1250E+00	3.3000E+00	5	0	2	0	0	2	1	1	0	1
2	3.3250E+00	5.5000E+00	1	0	1	2	1	1	1	1	0	4
3	5.6250E+00	6.9000E+00	1	0	1	0	2	1	1	2	0	4
4	6.9000E+00	8.4000E+00	2	1	0	1	1	1	3	0	0	3
5	8.7500E+00	9.9750E+00	2	1	0	1	2	0	3	2	1	0
6	1.0000E+01	1.2250E+01	5	0	0	1	0	1	3	0	1	1
7	1.2250E+01	1.4250E+01	7	0	0	0	0	3	0	0	1	1
8	1.4500E+01	1.8500E+01	4	0	0	0	1	0	2	1	1	3
9	1.8750E+01	2.1500E+01	2	0	0	5	0	0	3	0	0	2
10	2.1500E+01	5.0250E+01	3	1	2	1	0	1	1	0	0	3
		COLUMN TOTALS	32	3	6	11	7	10	18	7	4	22

CONTINGENCY TABLE FOR MN DETERMINED BY ATOMIC ABSORPTION SPECTROSCOPY (LONDON)

REGRESSION OF STANDARD DEVIATION ON CONCENTRATION

INTERCEPT	4.062469	STANDARD ERROR	7.321253	T-VALUE	.554887
COEFFICIENT	.030675	STANDARD ERROR	.007424	T-VALUE	4.131980
OBSERVATIONS	10				

TEST ADEQUACY OF EQUATION

CELL EXPECTATION FOR MODEL   1.2

DECILE	CONCENTRATION RANGE		DIFFERENCE DECILE FOR MODEL									
			1	2	3	4	5	6	7	8	9	10
1	9.5000E+01	2.0000E+02	5	0	0	0	0	1	4	0	0	2
2	2.0000E+02	2.9500E+02	1	0	0	0	2	1	0	3	2	3
3	3.0000E+02	3.8500E+02	3	0	0	2	0	1	4	1	1	0
4	3.9500E+02	5.1000E+02	5	0	0	2	0	1	0	1	2	1
5	5.1500E+02	6.7000E+02	4	1	1	0	1	0	1	1	0	3
6	6.9000E+02	8.3500E+02	1	1	3	1	0	3	0	2	0	1
7	9.4500E+02	1.1200E+03	1	3	0	1	0	0	3	1	1	2
8	1.1275E+03	1.5150E+03	2	4	2	0	0	2	0	0	0	2
9	1.5150E+03	2.3250E+03	2	1	1	2	1	0	1	2	0	2
10	2.375E+03	2.0110E+04	2	0	0	2	0	3	1	0	2	2
	COLUMN TOTALS		26	10	7	10	4	12	14	11	8	19

CONTINGENCY TABLE FOR CU DETERMINED BY ATOMIC ABSORPTION SPECTROSCOPY (LONDON)

REGRESSION OF STANDARD DEVIATION ON CONCENTRATION

INTERCEPT	.753869	STANDARD ERROR	.623891	T-VALUE	1.232376
COEFFICIENT	.021200	STANDARD ERROR	.002924	T-VALUE	7.249512
OBSERVATIONS	10				

TEST ADEQUACY OF EQUATION

CELL EXPECTATION FOR MODEL   1.2

DECILE	CONCENTRATION RANGE		DIFFERENCE DECILE FOR MODEL									
			1	2	3	4	5	6	7	8	9	10
1	6.0000E+00	2.6000E+01	7	0	0	0	1	0	0	1	0	3
2	2.6500E+01	3.8000E+01	2	0	0	3	1	0	2	0	2	2
3	3.9000E+01	5.0500E+01	6	0	1	2	0	1	0	0	0	2
4	5.0500E+01	5.9000E+01	1	0	3	0	0	3	0	3	2	6
5	5.9500E+01	6.9000E+01	1	0	3	0	1	1	3	2	0	1
6	6.9000E+01	1.0450E+02	0	0	1	1	1	1	1	1	2	4
7	1.0950E+02	1.6400E+02	1	4	1	0	1	0	2	0	1	2
8	1.6950E+02	3.6750E+02	3	1	1	1	1	1	1	1	0	2
9	3.7500E+02	6.1000E+02	4	0	0	0	3	3	0	0	0	2
10	6.2500E+02	1.0800E+03	1	0	3	2	0	0	2	1	1	2
		COLUMN TOTALS	26	5	13	9	9	10	11	9	8	20

CONTINGENCY TABLE FOR NI DETERMINED BY ATOMIC ABSORPTION SPECTROSCOPY (LONDON)

REGRESSION OF STANDARD DEVIATION ON CONCENTRATION

INTERCEPT	-4.431260	STANDARD ERROR	5.920066	T-VALUE	-.748515
COEFFICIENT	.046214	STANDARD ERROR	.003160	T-VALUE	14.626121
OBSERVATIONS	10				

TEST ACCURACY OF EQUATION

CELL EXPECTATION FOR MODEL   1.2

DECILE	CONCENTRATION RANGE		DIFFERENCE DECILE FOR MODEL									
			1	2	3	4	5	6	7	8	9	10
1	4.500E+01	8.000E+01	12	0	0	0	0	0	0	0	0	0
2	8.000E+01	1.250E+02	10	0	0	0	0	0	0	0	0	2
3	1.475E+02	1.750E+02	3	0	0	0	0	0	0	4	2	3
4	1.900E+02	4.075E+02	4	0	0	2	0	3	0	0	0	3
5	4.500E+02	1.075E+03	6	0	0	0	0	1	0	1	2	2
6	1.075E+03	1.575E+03	4	0	0	1	2	1	0	0	2	2
7	1.675E+03	2.120E+03	0	1	1	4	0	1	1	0	3	1
8	2.150E+03	3.125E+03	7	0	1	0	1	2	1	2	1	1
9	3.200E+03	5.000E+03	1	3	1	2	0	0	1	1	1	2
10	5.150E+03	1.275E+04	5	0	0	0	2	0	5	0	0	0
	COLUMN TOTALS		46	4	3	9	5	8	8	9	11	16

CONTINGENCY TABLE FOR CD DETERMINED BY ATOMIC ABSORPTION SPECTROSCOPY (LONDON)

REGRESSION OF STANDARD DEVIATION ON CONCENTRATION

INTERCEPT	3.459603	STANDARD ERROR	1.865729	T-VALUE	1.854290
COEFFICIENT	.014784	STANDARD ERROR	.012657	T-VALUE	1.168044
OBSERVATIONS	10				

TEST ADEQUACY OF EQUATION

CELL EXPECTATION FOR MODEL   1.2

DECILE	CONCENTRATION RANGE		DIFFERENCE DECILE FOR MODEL									
			1	2	3	4	5	6	7	8	9	10
1	2.0000E+01	3.2500E+01	2	0	0	0	0	0	9	0	0	1
2	3.5000E+01	4.7500E+01	5	0	0	0	0	0	5	0	0	1
3	4.7500E+01	6.0000E+01	4	0	0	0	0	5	1	0	0	2
4	6.2500E+01	7.2500E+01	2	0	0	0	0	8	0	0	1	1
5	7.5000E+01	1.0250E+02	7	0	0	0	0	3	0	0	2	0
6	1.0500E+02	1.4750E+02	4	0	0	0	3	1	0	1	0	3
7	1.4750E+02	1.7500E+02	3	0	1	0	4	0	0	3	0	1
8	1.7750E+02	2.2750E+02	1	0	0	1	3	0	0	6	0	1
9	2.3500E+02	3.4000E+02	4	0	0	3	0	0	2	0	1	2
10	3.8500E+02	7.2500E+02	4	0	1	0	0	1	0	0	0	6
	COLUMN TOTALS		37	0	2	4	10	18	17	10	4	18

REGRESSION OF STANDARD DEVIATION ON CONCENTRATION

INTERCEPT	17.957327	STANDARD ERROR	15.254951	T-VALUE	1.118150
COEFFICIENT	.031960	STANDARD ERROR	.010654	T-VALUE	2.999886
OBSERVATIONS	10				

TEST ADEQUACY OF EQUATION

CELL EXPECTATION FOR MODEL   1.2

DECILE	CONCENTRATION RANGE		DIFFERENCE DECILE FOR MODEL									
			1	2	3	4	5	6	7	8	9	10
1	1.0000E+01	4.0000E+01	2	4	1	5	0	0	0	0	0	0
2	4.5000E+01	8.0000E+01	1	4	3	0	0	2	0	0	1	1
3	8.5000E+01	1.3500E+02	2	3	4	0	0	1	2	0	0	0
4	1.6500E+02	3.1500E+02	2	2	4	0	1	2	0	0	1	0
5	3.2250E+02	4.7500E+02	1	0	1	2	1	2	1	3	0	1
6	5.0000E+02	1.0250E+03	2	0	0	2	0	2	1	1	1	3
7	1.1000E+03	1.8750E+03	2	0	0	1	2	0	2	2	0	3
8	1.9250E+03	2.4250E+03	2	0	0	1	0	1	1	3	4	0
9	2.5000E+03	3.5750E+03	3	0	3	0	1	0	0	1	0	4
10	7.7500E+03	3.0000E+04	2	2	0	0	2	1	0	1	2	2
	COLUMN TOTALS		19	15	16	11	7	11	7	11	9	14

CONTINGENCY TABLE FOR ZN DETERMINED BY ATOMIC ABSORPTION SPECTROSCOPY (LONDON)

REGRESSION OF STANDARD DEVIATION ON CONCENTRATION

INTERCEPT	2.981171	STANDARD ERROR	.795558	T-VALUE	3.747270
COEFFICIENT	.004997	STANDARD ERROR	.011641	T-VALUE	.429257
OBSERVATIONS	10				

TEST ADEQUACY OF EQUATION

CELL EXPECTATION FOR MODEL   1.2

DECILE	CONCENTRATION RANGE		DIFFERENCE DECILE FOR MODEL									
			1	2	3	4	5	6	7	8	9	10
1	2.5000E+00	1.2000E+01	0	3	0	3	0	1	0	2	0	3
2	1.2500E+01	2.0000E+01	2	4	0	2	0	2	0	2	0	0
3	2.0000E+01	2.4500E+01	1	3	0	3	0	3	0	1	0	1
4	2.5000E+01	3.3500E+01	1	6	0	1	1	0	2	1	0	0
5	3.4500E+01	4.5500E+01	0	1	0	3	1	0	3	1	0	3
6	4.6000E+01	5.7500E+01	1	1	0	1	1	0	1	1	3	3
7	6.0000E+01	6.9500E+01	4	1	0	1	1	0	1	1	1	2
8	7.1000E+01	1.0000E+02	1	0	0	1	2	0	0	4	1	3
9	1.0000E+02	1.9000E+02	3	1	2	0	1	1	3	0	0	1
10	1.9000E+02	1.7400E+03	2	0	0	0	0	0	1	0	2	7
	COLUMN TOTALS		15	20	2	15	7	7	11	13	7	23

CONTINGENCY TABLE FOR TI DETERMINED BY ATOMIC ABSORPTION SPECTROSCOPY (LONDON)

REGRESSION OF STANDARD DEVIATION ON CONCENTRATION

INTERCEPT	23.956476	STANDARD ERROR	45.656772	T-VALUE	.524577
COEFFICIENT	.082632	STANDARD ERROR	.028268	T-VALUE	2.923164
OBSERVATIONS	10				

TEST ADEQUACY OF EQUATION

CELL EXPECTATION FOR MODEL   1.2

DECILE	CONCENTRATION RANGE		DIFFERENCE DECILE FOR MODEL									
			1	2	3	4	5	6	7	8	9	10
1	2.0000E+02	6.5000E+02	3	0	0	1	2	0	1	0	1	4
2	6.5000E+02	9.7500E+02	2	0	1	2	0	2	1	1	0	3
3	9.7500E+02	1.1000E+03	3	0	1	0	3	1	0	2	1	1
4	1.1000E+03	1.3750E+03	3	0	2	0	2	1	1	0	2	1
5	1.3750E+03	1.5500E+03	7	2	1	3	0	1	1	0	1	0
6	1.5500E+03	1.8250E+03	3	0	0	1	0	0	2	1	2	3
7	1.8500E+03	2.0500E+03	1	2	2	0	2	1	0	1	1	2
8	2.0750E+03	2.2750E+03	1	3	0	0	0	3	1	0	1	3
9	2.3000E+03	2.6250E+03	4	1	0	1	2	1	0	0	1	2
10	2.6750E+03	4.3700E+03	2	1	1	1	2	0	1	1	0	3
		COLUMN TOTALS	25	9	8	9	13	10	8	6	10	22

CONTINGENCY TABLE FOR S DETERMINED BY MODIFIED COMBUSTION METHOD

REGRESSION OF STANDARD DEVIATION ON CONCENTRATION

INTERCEPT	-6.857720	STANDARD ERROR	2.619706	T-VALUE	-2.621561
COEFFICIENT	.067538	STANDARD ERROR	.002136	T-VALUE	31.613062
OBSERVATIONS	3				

TEST ADEQUACY OF EQUATION

CELL EXPECTATION FOR MODEL   .4

DECILE	CONCENTRATION RANGE		DIFFERENCE DECILE FOR MODEL									
			1	2	3	4	5	6	7	8	9	10
1	7.0000E+01	1.5800E+02	2	0	0	0	0	0	1	0	0	1
2	1.8500E+02	2.6800E+02	0	0	0	0	1	1	1	0	0	1
3	2.7000E+02	3.3500E+02	0	0	2	0	0	0	0	0	0	2
4	3.4000E+02	4.4000E+02	1	1	0	0	1	0	0	1	0	0
5	4.5300E+02	5.3500E+02	0	1	0	0	0	2	0	0	0	1
6	8.7800E+02	1.5200E+03	1	0	0	0	1	0	0	1	-1	0
7	1.5400E+03	1.8950E+03	1	1	0	1	0	0	0	0	0	1
8	2.1800E+03	2.6150E+03	0	0	0	0	1	0	1	1	0	1
9	3.3000E+03	5.2550E+03	1	0	2	0	0	0	0	0	0	1
10	6.1000E+03	1.5500E+04	0	0	1	0	1	0	0	1	0	1
		COLUMN TOTALS	6	3	5	1	5	3	3	4	1	9

REGRESSION OF STANDARD DEVIATION ON CONCENTRATION

INTERCEPT	23.196649	STANDARD ERROR	6.311372	T-VALUE	3.675373
COEFFICIENT	.119238	STANDARD ERROR	.025605	T-VALUE	4.656820
OBSERVATIONS	3				

TEST ADEQUACY OF EQUATION

CELL EXPECTATION FOR MODEL   .4

DECILE	CONCENTRATION RANGE		DIFFERENCE DECILE FOR MODEL									
			1	2	3	4	5	6	7	8	9	10
1	2.4000E+01	3.7000E+01	1	0	1	1	0	0	1	0	0	0
2	3.8000E+01	5.5000E+01	0	0	1	0	1	0	1	1	0	0
3	6.2000E+01	6.5000E+01	0	1	0	0	2	0	1	0	0	0
4	6.8000E+01	1.2400E+02	0	1	1	1	0	1	0	0	0	0
5	1.5000E+02	2.0000E+02	0	0	0	0	0	2	0	1	0	1
6	2.4300E+02	2.9500E+02	0	0	0	1	0	0	1	1	0	1
7	3.1400E+02	4.0000E+02	1	0	0	0	0	1	2	0	0	0
8	4.2000E+02	4.9300E+02	0	0	1	0	1	0	1	0	1	0
9	5.7700E+02	7.4100E+02	2	0	0	1	0	0	0	0	1	0
10	9.5000E+02	2.3750E+03	0	0	0	0	1	0	2	0	1	0
	COLUMN TOTALS		4	2	4	4	5	4	9	3	3	2